MycoKeys

MycoKeys 115: 1–18 (2025)
DOI: 10.3897/mycokeys.115.138252

Research Article

Non-lichenized *Cytosporella*, including *C. fuligomixta* sp. nov., and related plant-associated and fungicolous genera are close to foliicolous, lichenized fungi (Ascomycota, Graphidales)

Marcin Piątek[1], Monika Stryjak-Bogacka[1], Paweł Czachura[1]

[1] *W. Szafer Institute of Botany, Polish Academy of Sciences, Lubicz 46, PL-31-512 Kraków, Poland*
Corresponding author: Marcin Piątek (m.piatek@botany.pl)

Academic editor: Pradeep Divakar
Received: 30 September 2024
Accepted: 15 February 2025
Published: 6 March 2025

Citation: Piątek M, Stryjak-Bogacka M, Czachura P (2025) Non-lichenized *Cytosporella*, including *C. fuligomixta* sp. nov., and related plant-associated and fungicolous genera are close to foliicolous, lichenized fungi (Ascomycota, Graphidales). MycoKeys 115: 1–18. https://doi.org/10.3897/mycokeys.115.138252

Abstract

The genus *Cytosporella* includes non-lichenized, plant associated fungi producing eustromatic conidiomata, phialidic conidiophores and hyaline, ellipsoid conidia. Of the 69 names assigned to this genus in Index Fungorum, only three species are associated with sequence data. In this study, a new species: *Cytosporella fuligomixta* is described based on a strain isolated from the sooty mould community on *Quercus robur* leaves in Poland. The phylogenetic analyses including sequences of two loci (LSU, mtSSU) showed that *Cytosporella* species, together with members of four other non-lichenized, plant associated or fungicolous genera, namely *Cladosterigma*, *Neoacrodontiella*, *Nothoramularia* and *Vanderaaea*, form a sister group to lichenized and lichenicolous fungi from the family Gomphillaceae and order Graphidales. Previously, *Cladosterigma* was resolved as a member of Gomphillaceae using multi-locus (mtSSU, SSU, LSU, ITS, *rpb2*, *tef1*) and two-locus (LSU, mtSSU) sequence analyses, while *Cytosporella*, *Neoacrodontiella*, *Nothoramularia* were shown to belong to this family using LSU sequence analyses. However, none of them resolved these genera as a sister group to lichenized members of Gomphillaceae. The placement of the genus *Vanderaaea* within Gomphillaceae is shown here for the first time. Due to phylogenetic, morphological and ecological characteristics a new subfamily Cladosterigmoideae is described for these five non-lichenized genera.

Key words: Ascomycota, Graphidales, Gomphillaceae, one new species, one new subfamily, sooty mould communities, taxonomy

Introduction

The genus *Cytosporella* includes non-lichenized, plant associated fungi producing eustromatic conidiomata, phialidic conidiophores and hyaline, ellipsoid conidia (Sutton 1980; Crous et al. 2019b; Li et al. 2020). Index Fungorum (2024) includes 69 names assigned to *Cytosporella* but DNA sequence data are available only for three species: *Cytosporella calamagrostidis*, *C. chamaeropis* and *C. juncicola*. The type species is *Cytosporella sycina* (Clements and Shear 1931; Sutton 1980; Li et al. 2020). It has been described from branches of *Ficus carica* in France (Saccardo 1880) but not sequenced yet, making current taxonomy of the genus tentative. The species of *Cytosporella* are saprobic or parasitic on different hosts, mostly on branches of deciduous trees (Li et al. 2020; species data in Index Fungorum 2024). During our surveys of sooty mould communities on ornamental woody plants in southern Poland a new species of *Cytosporella* (described here as *Cytosporella fuligomixta*) was isolated from a sooty mould colony on leaves of *Quercus robur* (Fagaceae).

The sequenced species of *Cytosporella* were shown to be related to three non-lichenized, plant associated or fungicolous genera: *Neoacrodontiella*, *Nothoramularia* and *Vanderaaea*, and altogether they were assigned to the family Acarosporaceae and order Acarosporales (Crous et al. 2019a, 2019b, 2021, 2023). This order and family contain saxicolous and terricolous lichenized fungi in the subclass Acarosporomycetidae of the Lecanoromycetes (Reeb et al. 2004; Miadlikowska et al. 2014; Westberg et al. 2015). Our initial query of sequences of *Cytosporella* (including new species *C. fuligomixta*), *Neoacrodontiella*, *Nothoramularia* and *Vanderaaea* in GenBank showed that most closely related sequences belong to members of the lichenized family Gomphillaceae. Also, non-lichenized, fungicolous *Cladosterigma clavariellum*, which was recently included in Gomphillaceae (Guterres et al. 2020), was amongst the resultant related sequences. This family includes mostly foliicolous lichens and is included either in Graphidales or Ostropales within subclass Ostropomycetidae of the Lecanoromycetes (Baloch et al. 2010; Miadlikowska et al. 2014; Kraichak et al. 2018). Indeed, a recent phylogenetic tree, based on LSU sequences, published in Crous et al. (2024), placed *Cladosterigma*, *Cytosporella*, *Neoacrodontiella* and *Nothoramularia* inside the family Gomphillaceae. The genus *Vanderaaea* was not included in these analyses. Similarly, multi-locus (using mtSSU, SSU, LSU, ITS, *rpb2* and *tef1* sequences) and two-locus (using LSU and mtSSU sequences) trees, published by Guterres et al. (2020), placed *Cladosterigma* inside the family Gomphillaceae with *Vezdamyces vulgaris* (syn. *Gyalideopsis vulgaris*) being the most basal species. However, in these cases (based on GenBank accession numbers of sequences included by Guterres et al. 2020 in their tables), sequences of “*Gyalideopsis vulgaris*” used in the multi-locus tree belonged to *Gyalidea praetermissa* that is a member of Gyalectaceae (Ertz et al. 2021), while LSU sequence used in two-locus tree belonged to other species (closest hits in GenBank are species of Eurotiomycetes) that could have been responsible for such a result.

In this study, we describe and illustrate a new species of *Cytosporella* isolated from a sooty mould colony on leaves of *Quercus robur*. Additionally, based on publicly available sequences, we reassess phylogenetic placement of species of *Cladosterigma*, *Cytosporella*, *Neoacrodontiella*, *Nothoramularia* and *Vanderaaea* using two-locus (LSU, mtSSU) sequence analyses.

Materials and methods

Strain and morphological analyses

The strain was obtained from sooty mould communities during the study of sooty moulds on ornamental woody plants cultivated in municipal greenery in southern Poland (Piątek et al. 2023). Macroscopic features of cultures were documented using 2-week-old colonies grown on malt extract agar (MEA – Blakeslee’s formula), potato dextrose agar (PDA) and oatmeal agar (OA) at 6 °C, 15 °C and 25 °C. Growth at different temperatures was assessed by measuring the colony diameter after 2 weeks and 4 weeks. Microscopic features were studied using colonies grown on MEA and OA at 15 °C after 7 weeks and 6 weeks, respectively. The characteristics of hyphae were observed on MEA and characteristics of conidiomata, conidiophores and conidia were studied on OA. Hyphae taken from the edge of the colony and mature conidiomata were mounted in lactic acid (80%) on microscope slides and analysed under Nikon Eclipse 80i light microscope. Microscopic structures were measured and photographed using NIS-Elements BR 3.0 imaging software. Holotype is a dried specimen obtained from culture and is stored in the fungal collection of the W. Szafer Institute of Botany, Polish Academy of Sciences, Kraków (KRAM F). Culture is deposited in the culture collection of the Westerdijk Fungal Biodiversity Institute (CBS) and in the W. Szafer Institute of Botany, Polish Academy of Sciences, Kraków.

DNA isolation, amplification and sequencing

Genomic DNA was extracted from four-week-old MEA culture using DNeasy® Plant Mini Kit (Qiagen, Germany), according to the manufacturer's protocol. A total of five loci were amplified: ITS1-5.8S-ITS2 rRNA (= ITS), partial large subunit rRNA (28S D1–D2 = LSU), small subunit mtRNA (=mtSSU), partial DNA-directed RNA polymerase II second largest subunit (*rpb2*) and translation elongation factor 1-alpha (*tef1*). To amplify the regions of ITS, LSU, mtSSU, *rpb2* and *tef1*, five different primer pairs were used, namely ITS1–ITS4 (White et al. 1990), LSU1Fd–LR5 (Vilgalys and Hester 1990; Crous et al. 2009), mrSSU1–mrSSU3R (Zoller et al. 1999), fRPB2-5F–fRPB2-7cR (Liu et al. 1999) as well as EF1-983F and EF1-2218R (Rehner and Buckley 2005), respectively. Polymerase chain reaction mixtures were performed in a total volume of 25 µL as explained in Piątek et al. (2023). Amplification conditions for ITS and LSU were described in Czachura et al. (2021), while conditions for subsequent loci were set as follows: an initial denaturation at 94 °C for 3 min, followed by 35 cycles (mtSSU, *rpb2*) or 40 cycles (*tef1*) of denaturation at 94 °C for 60 sec (mtSSU, *rpb2*) or 30 sec (*tef1*); annealing at 52 °C (mtSSU) or 54 °C (*rpb2*) or 55 °C (*tef1*) for 60 sec (mtSSU) or 90 sec (*rpb2*) or 50 sec (*tef1*); and extension at 72 °C for 1 min (mtSSU, *tef1*) or 2 min (*rpb2*). The process was finished with the final extension at 72 °C for 7 min (mtSSU) or 10 min (*rpb2*, *tef1*). PCR amplifications were confirmed on 1% agarose electrophoresis gels stained with SimplySafe (EURx, Poland). Amplicons were enzymatically cleaned using Exo-BAP Mix (EURx, Poland). The same primers as given above were used in sequencing reactions which were carried out by Macrogen Europe B.V. (Amsterdam, The Netherlands). Obtained sequences were assembled and trimmed in Geneious Prime 2020.0.4. Consensus sequences were deposited in the NCBI's GenBank nucleotide database (https://www.ncbi.nlm.nih.gov/genbank/).

Phylogenetic analyses

The affinities of obtained *Cytosporella* sequences and sequences of related genera and species were determined in the NCBIs GenBank nucleotide database using the megablast search tool (Zhang et al. 2000). For the phylogenetic analyses only LSU and mtSSU sequences were used due to limited sampling of reference sequences available for members of Gomphillaceae. The assembled concatenated LSU-mtSSU alignment contained available sequences of all sequenced species of *Cladosterigma*, *Cytosporella*, *Neoacrodontiella*, *Nothoramularia* and *Vanderaaea*, and sequences of selected members of Gomphillaceae and members of its most closely related family Graphidaceae used as an outgroup (Table 1). In the case of problematic sequences of *Vezdamyces vulgaris* (syn. *Gyalideopsis vulgaris*) used by Guterres et al. (2020), the correct sequences obtained from two different specimens were taken following Xavier-Leite et al. (2022).

Sequence reads which we obtained were checked for quality and assembled. The complete LSU and mtSSU sequences were separately aligned for each single-gene dataset using MAFFT algorithm (Katoh et al. 2005) in Geneious 11.1.5. Phylogenetic trees were constructed by using the Maximum likelihood (ML) and Bayesian inference (BI) analysis. For both ML and BI analyses, the model of DNA evolution that best fitted the dataset was determined using the ModelTest-NG v. 0.2.0 under the Bayesian Information Criterion (BIC) (Darriba et al. 2020). Maximum likelihood (ML) analyses were performed using the RAxML-NG v. 1.1.1 (Kozlov et al. 2019). Branch support was inferred with 1000 bootstrap replicates. Bayesian analyses were conducted using a MrBayes v. 3.2.6 (Ronquist et al. 2012). One million generations were run, sampling every 100 generations. Four parallel chains, one cold and three heated, were used. A consensus tree was generated after discarding the first 25% of trees as burn-in. Average standard deviations of split frequencies dropped below 0.01 at the end of the runs. The final phylogenetic trees were graphically visualised using FigTree v.1.4.3.

Results

Phylogenetic analyses

The concatenated LSU-mtSSU alignment contained sequences belonging to 41 species. The alignment comprised a total of 1779 characters (LSU: 969, mtSSU: 810), including alignment gaps. The best matching substitution models selected for single locus alignments in the ML analysis were as follows: TIM2+I+G4 for LSU and TPM3uf+I+G4 for mtSSU. The BI analysis was performed with the following substitution model: GTR+I+G4 for LSU and mtSSU. ML and BI analyses resulted in similar tree topologies. The best scoring maximum likelihood phylogenetic tree is shown on Fig. 1. Maximum likelihood bootstrap (MLB) support values above 70% and Bayesian posterior probabilities (BPP) above 0.95 are shown at the nodes.

Representatives of the family Gomphillaceae formed strongly supported monophyletic lineage (MLB/BPP = 100/1). The strain of the new *Cytosporella* species clustered with members of the genus *Cytosporella* as sister to *C. chamaeropis* and *C. juncicola* (MLB/BPP = 98/1). Representatives of the genera *Cladosterigma*, *Cytosporella*, *Neoacrodontiella*, *Nothoramularia* and *Vanderaaea* formed a well-supported clade (MLB/BPP = 73/1) as a sister group to the well-supported clade (MLB/BPP = 78/1) of the remaining Gomphillaceae that contained lichenized species and two non-lichenized lichenicolous genera (*Corticifraga*, *Taitaia*).

Table 1. List of species, with country of origin, host/substrate, strain/voucher, GenBank accession numbers and references, used in phylogenetic analyses.

Species	Country	Host/substrate	Strain/voucher	GenBank acc. no.		References
				LSU	mtSSU	
Aderkomyces heterellus	Brazil	–	Cáceres & Aptroot 11953	KF833330	KF833342	I. Schmitt, T. Lumbsch, E. Kraichak (unpubl.)
Asterothyrium longisporum	Costa Rica	–	Lücking s.n., F sample no. 4	AY341349	AY341363	Lücking et al. 2004
Aulaxina quadrangula	Costa Rica	–	Lücking s.n., F sample no. 66	AY341350	AY341364	Lücking et al. 2004
Aulaxinella minuta	Costa Rica	–	E. Baloch HK2 (GZU)	–	AY648887	Grube et al. 2004
Chroodiscus defectus	Thailand	–	Papong 5118	FJ708490	FJ708497	–
Cladosterigma clavariellum	Brazil	*Phyllachora* sp. on leaves of *Eugenia florida*	UB 23227	MK933757	MK910849	Guterres et al. 2020
Cladosterigma clavariellum	Brazil	*Phyllachora* sp. on leaves of *Eugenia florida*	UB 23228	MK933758	MK910850	Guterres et al. 2020
Clandestinotrema stylothecium	Nicaragua	–	Lücking 28636	JX421470	HQ639597	Rivas Plata et al. 2011, 2013
Corticifraga peltigerae	Luxembourg	*Peltigera* cf. *rufescens*	Marson 2015-05-02-1	KY462801	–	H.-O. Baral, G. Marson (unpubl.)
Corticifraga peltigerae	India	*Peltigera elisabethae*	Zhurbenko 1353 (LE 260537)	KY661661	KY661684	Pino-Bodas et al. 2017
Cruentotrema thailandicum	Thailand	–	Lumbsch 19955d	JF828975	JF828960	Rivas Plata and Lumbsch 2011
Cytosporella calamagrostidis	Netherlands	*Calamagrostis arenaria*	CPC 46236	PP791461	–	Crous et al. 2024
Cytosporella fuligomixta	Poland	sooty mould community on *Quercus robur* leaves	G107 = CBS 152343	PQ001665	PP999744	this study
Cytosporella juncicola	USA	*Juncus effusus*	CPC 38040	MN567660	–	Crous et al. 2019b
Cytosporella chamaeropis	Italy	*Chamaerops humilis*	CBS 355.71	MH871929	–	Vu et al. 2019
Dyplolabia afzelii	USA	–	Lücking 26509a	JX421483	JX421027	Rivas Plata et al. 2013
Echinoplaca sp.	Nicaragua	–	Lücking 28550	KF833328	KF833340	I. Schmitt, T. Lumbsch, E. Kraichak (unpubl.)
Fissurina comparimuralis	El Salvador	–	Lücking 28103	JX421492	JX421042	Rivas Plata et al. 2013
Fissurina marginata	Thailand	–	Lücking 24122	JX421493	HQ639613	Rivas Plata et al. 2011, 2013
Fissurina rufula	Fiji	–	Lumbsch 20521l	JX421497	JX421053	Rivas Plata et al. 2013
Gomphillus calycioides	UK (Scotland)	–	Lumbsch 20100d (F)	KF833329	KF833341	I. Schmitt, T. Lumbsch, E. Kraichak (unpubl.)
Gomphillus ophiosporus	Costa Rica	–	Will-Wolf 10006a (F)	AY341357	AY341371	Lücking et al. 2004
Graphis scripta	Germany	–	Staiger 982	DQ431937	AY648904	–
Gyalectidium catenulatum	Costa Rica	–	Lücking 032b	KF833323	KF833335	I. Schmitt, T. Lumbsch, E. Kraichak (unpubl.)
Gyalectidium imperfectum	Costa Rica	–	Lücking s.n., F sample no. 2	AY341358	AY341372	Lücking et al. 2004
Gyalidea fritzei	Sweden	–	Nordin 6022 (UPS)	HM244767	HM244744	Baloch et al. 2010
Gyalidea hyalinescens	Costa Rica	–	AFTOL-ID 332	DQ973046	DQ972996	Miadlikowska et al. 2006
Monocalenia monospora	Costa Rica	–	Lücking 032h	KF833327	KF833339	I. Schmitt, T. Lumbsch, E. Kraichak (unpubl.)
Monocalenia monospora	Costa Rica	–	Lücking 032e	KF833325	KF833337	I. Schmitt, T. Lumbsch, E. Kraichak (unpubl.)

Species	Country	Host/substrate	Strain/voucher	GenBank acc. no.		References
				LSU	mtSSU	
Myriotrema olivaceum	Australia	–	Lumbsch 19113f	EU075627	EU075579	–
Neoacrodontiella eucalypti	Malaysia	*Eucalyptus urophylla*	CBS 145561	MK876437	–	Crous et al. 2019a
Nothoramularia ragnhildianicola	Germany	*Ragnhildiana ferruginea* on leaves of *Artemisia vulgaris*	CBS 149076	OQ990069	–	Crous et al. 2023
Ocellularia oculata	Australia	–	Mangold 33a	EU075613	EU075564	–
Phaeographis lobata	Bermuda	–	Berger 19598	DQ431944	DQ431984	–
Psorotheciopsis cf. *premneella*	Cuba	–	Lücking et al. 41885b	MZ851727	–	Xavier-Leite et al. 2022
Pycnotrema pycnoporellum	USA	–	Lücking 26545	HQ639658	HQ639584	Rivas Plata et al. 2011
Rolueckia aggregata	Brazil	–	Cáceres & Aptroot 28665a	MZ851690	–	Xavier-Leite et al. 2022
Rolueckia conspersa	Brazil	–	Xavier-Leite et al. 2803	MZ851644	–	Xavier-Leite et al. 2022
Taitaia aurea	Kenya	*Crocodia* cf. *clathrata*	Kirika 5103 (EA)	MF372797	MF372799	Suija et al. 2018
Taitaia aurea	Kenya	*Crocodia* cf. *aurata*	Rikkinen 16259	MF509277	–	Suija et al. 2018
Thelotrema subtile	Australia	–	Mangold 3j (F)	EU075651	EU075607	Mangold et al. 2008
Thelotrema suecicum	Turkey	–	Palice (ESS 21521)	AY300867	AY300917	Lumbsch et al. 2004
Tricharia longispora	Costa Rica	–	Lücking 033a	KF833326	KF833338	I. Schmitt, T. Lumbsch, E. Kraichak (unpubl.)
Tricharia longispora	Costa Rica	–	Lücking s.n., F sample no. 37	AY341360	AY341374	Lücking et al. 2004
Vanderaaea ammophilae	Netherlands	dead leaves of *Ammophila arenaria*	CBS 886.68	MH878416	–	Crous et al. 2021
Vezdamyces vulgaris	Brazil/Costa Rica	–	Xavier-Leite 1476/ AFTOL ID 105	MZ851481	AY584618	Lutzoni et al. 2004; Xavier-Leite et al. 2022

Taxonomy

Gomphillaceae Walt. Watson ex Hafellner, Beih. Nova Hedwigia 79: 280. 1984

Gomphilloideae Rivas Plata, Lücking & Lumbsch, Fungal Diversity 52(1): 108. 2012

Notes. Nominative subfamily includes current members of the family Gomphillaceae, excluding *Cladosterigma*, *Cytosporella*, *Neoacrodontiella*, *Nothoramularia* and *Vanderaaea*. The development of hyphophores with their diahyphae is a unique feature of this subfamily. Hyphophores with diahyphae are present in many, though not all, members of this lineage (Ferraro 2004; Lücking et al. 2004; Xavier-Leite et al. 2022, 2023).

Cladosterigmoideae Piątek, Stryjak-Bogacka & Czachura, subfam. nov.

MycoBank No: 857024

Etymology. Named after the genus *Cladosterigma*.

Description. Non-lichenized, plant associated or fungicolous fungi. Conidiomata sporodochial, synnematal, eustromatic or conidiophores arising directly from hyphae. Conidiophores hyaline, smooth, subcylindrical,

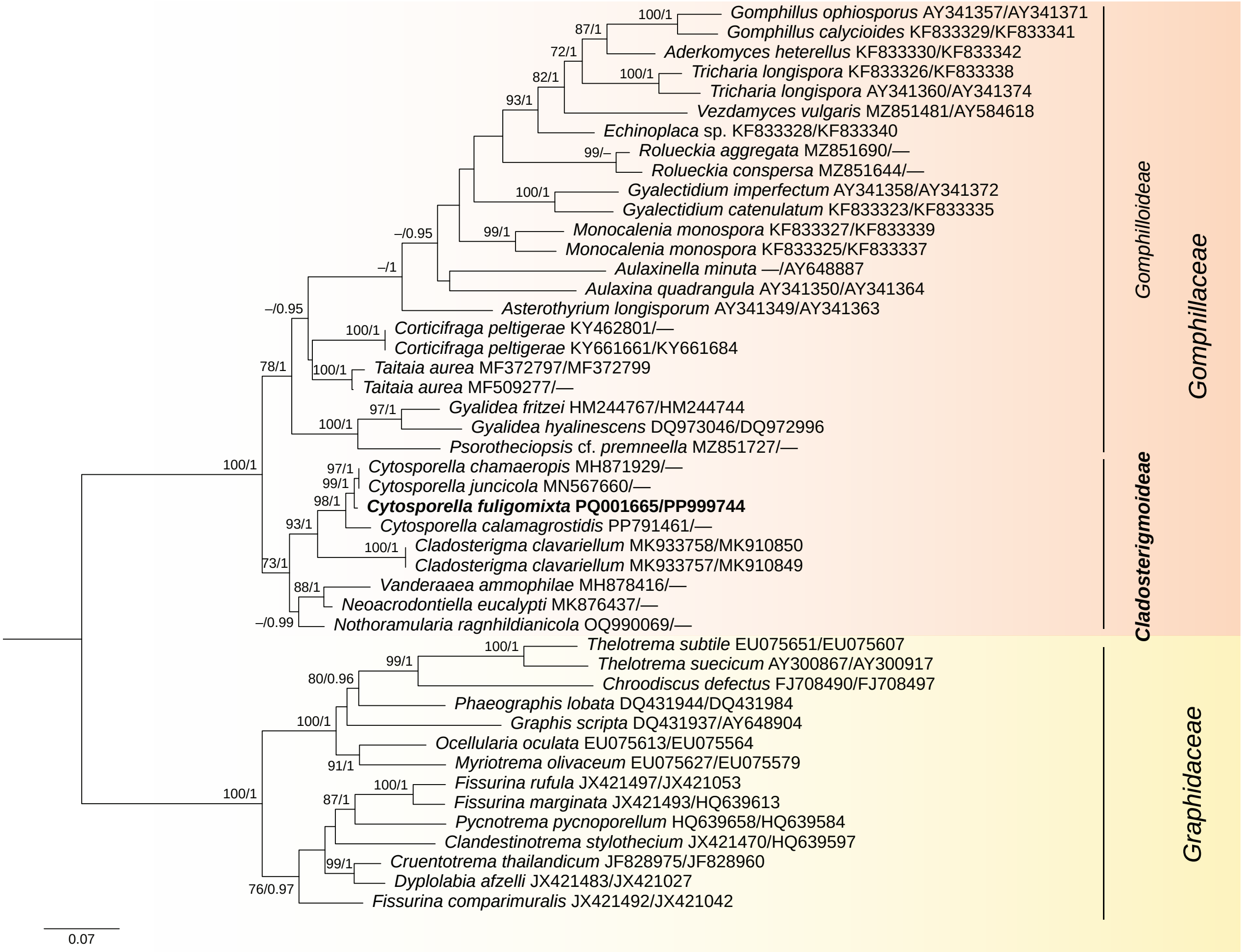

Figure 1. Phylogenetic tree of selected representatives of Gomphillaceae, including all sequenced species of *Cladosterigma*, *Cytosporella*, *Neoacrodontiella*, *Nothoramularia* and *Vanderaaea*, obtained from a maximum likelihood analysis of the combined two-locus alignment (LSU, mtSSU). Representatives of Graphidaceae are used as an outgroup. The positions of *Cytosporella fuligomixta* sp. nov. and Cladosterigmoideae subfam. nov. are indicated in bold. GenBank accession numbers (LSU/mtSSU) are given after species name. Numbers above branches indicate maximum likelihood bootstrap (MLB) support values > 70% and Bayesian posterior probabilities (BPP) > 0.95, respectively (MLB/BPP). The scale bar represents the expected number of changes per site.

conical, ampulliform or subglobose, branched or not, with terminal and/or intercalary conidiogenous cells, sometimes reduced to conidiogenous cells. Conidia solitary or rarely in chains, hyaline, smooth, 0–1-septate, ellipsoid, fusoid or subcylindrical. Sexual morph undetermined [based on generic descriptions in Sutton 1980; Guterres et al. 2020; Crous et al. 2019a, 2021, 2023].

Type genus. *Cladosterigma* Pat.

Notes. This subfamily includes genera *Cladosterigma*, *Cytosporella*, *Neoacrodontiella*, *Nothoramularia* and *Vanderaaea*. Members of this subfamily are different morphologically (absence of hyphophores with diahyphae), phylogenetically (distinct, sister lineage in molecular analyses) and ecologically (non-lichenized and non-lichenicolous species) from representatives of the nominative subfamily.

Cytosporella fuligomixta **Piątek, Stryjak-Bogacka & Czachura, sp. nov.**

MycoBank No: 857025
Figs 2–4

Etymology. Name refers to the isolation of this fungus from sooty mould communities.

DNA barcodes. ITS (PQ001666), LSU (PQ001665), mtSSU (PP999744), *rpb2* (PP997507) and *tef1* (PP997508).

Typus. Poland • Małopolska Province, Kraków County: Kraków-Czyżyny (Park Lotników), municipal greenery (city park), isolated from sooty mould community on *Quercus robur* leaves, 10 Oct. 2018, leg. M. Piątek, W. Bartoszek & P. Czachura (holotype KRAM F-59995; culture ex-type G107 = CBS 152343).

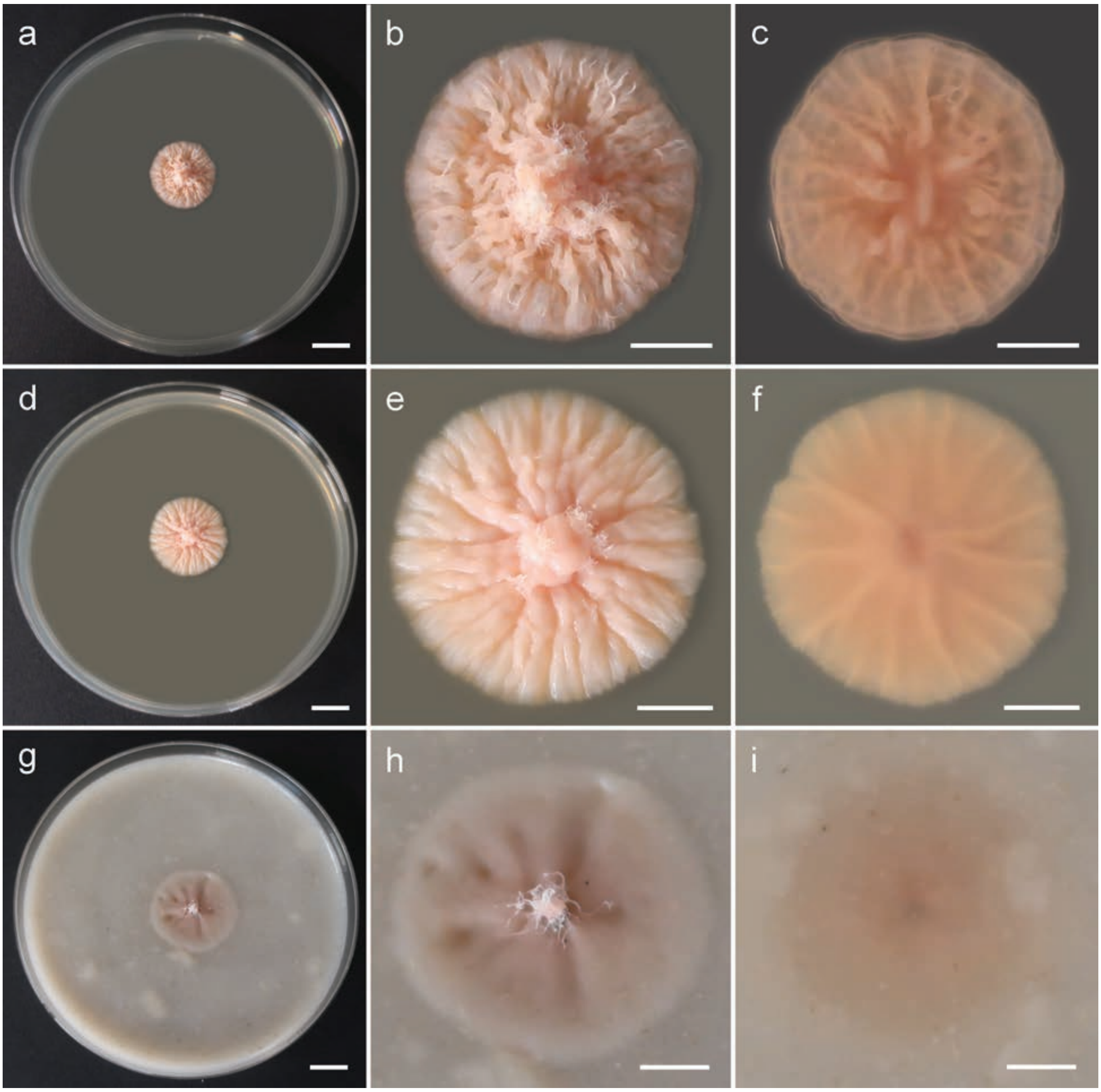

Figure 2. Morphology of cultures of *Cytosporella fuligomixta* (strain G107 = CBS 152343) after 4 weeks of growth at 15 °C: **a–c** general view, upper side and reverse side of colony on MEA **d–f** general view, upper side and reverse side of colony on PDA **g–i** general view, upper side and reverse side of colony on OA. Scale bars: 10 mm (a, d, g); 5 mm (**b, c, e, f, h, i**).

Description. Mycelium composed of sparsely branched, septate, hyaline, straight to curved, thin-walled hyphae, 1.0–1.5 µm wide; sometimes with swellings, 2.0–3.0 µm wide. Hyphae sometimes anastomose, intertwine or form fascicles [description on MEA]. Conidiomata flat, erumpent, separate, eustromatic, brown, disintegrating at the top during maturation, up to 500 µm diam, exuding a creamy conidial mass, partly enclosed by a wall of greenish-olive textura angularis. Conidiophores reduced to conidiogenous cells lining the inner cavity, hyaline, smooth, ampulliform or subcylindrical, phialidic, 3.5–8 × 3–5 µm. Conidia solitary, aseptate, hyaline, smooth, cylindrical, rarely slightly allantoid, apex obtuse, base bluntly rounded, (4–)5–8.5 × 2–2.5(–3) µm [description on OA].

Culture characteristics. Colonies on MEA erumpent, spreading, convex, rosaceous, reaching 4 mm diam after 2 weeks at 6 °C, 9 mm diam after 2 weeks at 15 °C and 6 mm diam after 2 weeks at 25 °C, reaching 6 mm diam after 4 weeks at 6 °C, 18 mm diam after 4 weeks at 15 °C and 8 mm diam after 4 weeks at 25 °C, surface cerebriform, with sparse aerial mycelium, margin finely crenate. Reverse rosaceous. Colonies on PDA erumpent, spreading, umbonate, slimy rosaceous, reaching 4 mm diam after 2 weeks at 6 °C, 11 mm diam after 2 weeks at 15 °C and 4 mm diam after 2 weeks at 25 °C, reaching 7 mm diam after 4 weeks at 6 °C, 20 mm diam after 4 weeks at 15 °C and 7 mm diam after 4 weeks at 25 °C, surface with radial furrows starting from centre towards margin, with sparse aerial

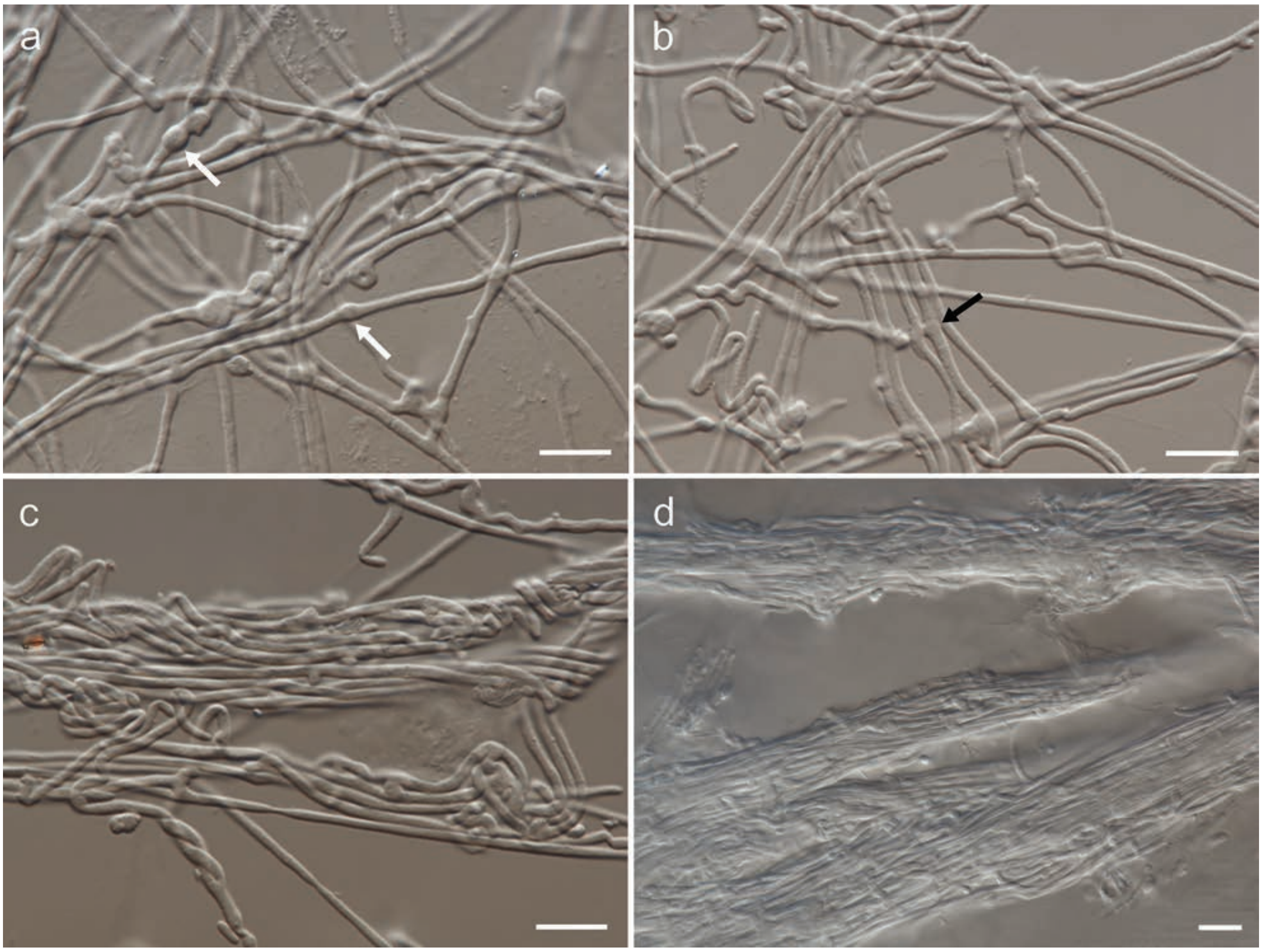

Figure 3. Morphology of *Cytosporella fuligomixta* on MEA (strain G107 = CBS 152343): **a, b** hyphae, white arrows show swellings and black arrow shows anastomosing hyphae **c** intertwined hyphae **d** hyphal fascicles. Scale bars: 10 µm.

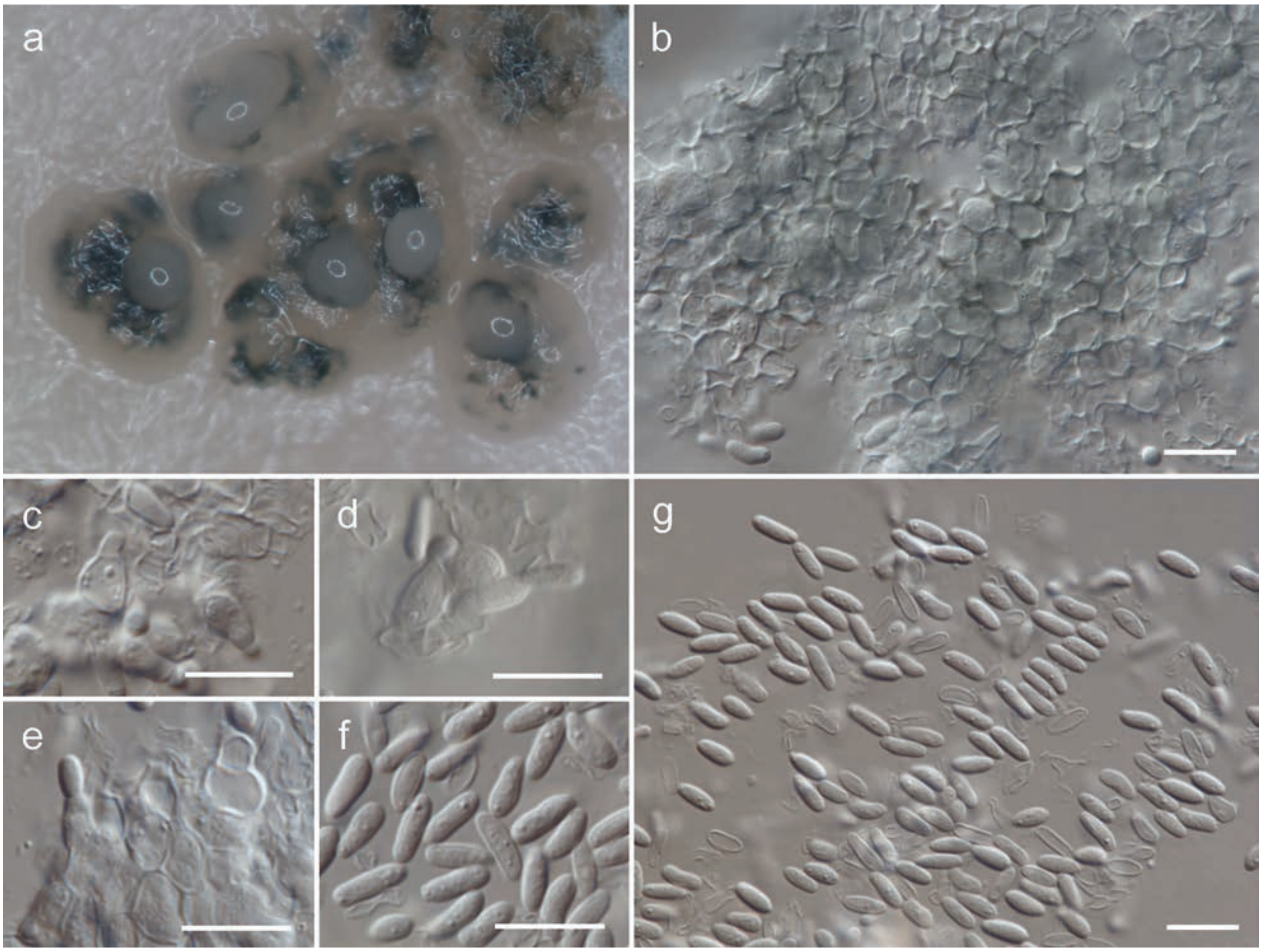

Figure 4. Morphology of *Cytosporella fuligomixta* on OA (strain G107 = CBS 152343): **a** conidiomata **b** wall of textura angularis **c–e** conidiophores **f, g** conidia. Scale bars: 10 µm.

mycelium, margin finely crenate. Reverse rosaceous. Colonies on OA spreading, flat, rosaceous, reaching 4 mm diam after 2 weeks at 6 °C, 10 mm diam after 2 weeks at 15 °C and 5 mm diam after 2 weeks at 25 °C, reaching 8 mm diam after 4 weeks at 6 °C, 22 mm diam after 4 weeks at 15 °C and 5 mm diam after 4 weeks at 25 °C, surface with indistinct radial furrows starting from the centre towards the margin, without aerial mycelium, margin entire. Reverse rosaceous.

Notes. *Cytosporella fuligomixta* is well delimited morphologically and ecologically from four other *Cytosporella* species described on *Quercus* hosts. These are *Cytosporella mendax*, *C. pisiformis*, *C. quercus* and *C. sphaerosperma*. All of them were described from branches or wood of *Quercus* sp. or *Quercus robur* and differ from *C. fuligomixta* in shape and sizes of conidia. The conidia are globose-ellipsoid, hyaline, 4–5 × 3.5–4 µm in *C. mendax* (Saccardo 1884; Saccardo and Roumeguère 1884), globose, yellowish, 3–4 µm in *C. pisiformis* (Saccardo 1884), perfectly globose, hyaline, 9–12 µm in *C. quercus* (Saccardo and Sydow 1902), and globose and hyaline in *C. sphaerosperma* (Saccardo 1884).

Other than being phylogenetically distinct, *Cytosporella fuligomixta* differs also morphologically from three sequenced species of this genus: *C. calamagrostidis*, *C. chamaeropis* and *C. juncicola* (Crous et al. 2019b, 2024). *Cytosporella calamagrostidis* described from old leaves of *Calamagrostis arenaria* has slightly shorter conidia, (5–)6–7 µm long (Crous et al. 2024), *C. chamaeropis* described from rotten *Chamaerops humilis* has globose conidia (Passerini 1888) and *C. juncicola* described from culms of *Juncus effusus* has slightly shorter and narrower conidia, (4–)5–6(–7) × 2 µm (Crous et al. 2019b).

Discussion

Cytosporella is an understudied genus without modern revision and only with few available DNA sequence data (Sutton 1980; van der Aa et al. 2001; Crous et al. 2019b, 2024; Li et al. 2020). The type species *Cytosporella sycina* has not been sequenced yet, making current taxonomy of the genus tentative. However, all sequenced species of *Cytosporella* form monophyletic lineage. All species assigned to this genus in Index Fungorum (2024) are described from different host plants or differ morphologically if described from the same host plant, which suggests that *Cytosporella* species might be host specific. Currently, sparse DNA sequence data does not exclude host specialization of members of this genus. *Cytosporella fuligomixta* described here from the sooty mould community on *Quercus robur* leaves is well delimited morphologically and ecologically from four other species described on *Quercus* hosts.

The phylogenetic analyses including sequences of two loci (LSU, mtSSU) showed that sequenced species of *Cytosporella*, together with four other non-lichenized, plant associated or fungicolous genera, namely *Cladosterigma*, *Neoacrodontiella*, *Nothoramularia* and *Vanderaaea*, form sister group to lichenized and lichenicolous fungi in the family Gomphillaceae. Thus, these five genera belong to the family Gomphillaceae and order Graphidales and not to the family Acarosporaceae and order Acarosporales where they were previously included in most studies (Crous et al. 2019a, 2019b, 2021, 2023). The placement of *Cladosterigma* inside the Gomphillaceae was previously reported by Guterres et al. (2020). Recently, Crous et al. (2024) in a phylogenetic tree based on LSU sequences showed placement of these genera (except *Vanderaaea* that was not included in their analyses) inside the Gomphillaceae that was assigned to Ostropales. Most lichenized clades within Ostropales s.l. are also recognised as distinct orders (Graphidiales, Gyalectales, Odontotrematales, Ostropales s.str. and Thelenellales) (Kraichak et al. 2018; Lücking 2019). Therefore, if that concept is accepted, *Cladosterigma*, *Cytosporella*, *Neoacrodontiella*, *Nothoramularia* and *Vanderaaea* belong to the family Gomphillaceae and order Graphidales. Moreover, the current analyses showed for the first time that they form distinct, sister lineage to remaining, mostly lichenized genera and species.

Biologically and ecologically, the above mentioned lineage of Gomphillaceae represents a coherent group of non-lichenized species occurring on plants or other fungi. The genus *Cladosterigma* contains only one species *Cladosterigma clavariellum* that is fungicolous hyphomycete (hyperarasite) occurring on *Phyllachora* species infecting *Eugenia* species (Myrtaceae) in Paraguay and Brazil (Seifert and Bandoni 2001; Guterres et al. 2020). *Cytosporella*, as stated above, includes species forming eustromatic conidiomata and is associated with diverse host plants. The genus *Neoacrodontiella* is typified with *Neoacrodontiella eucalypti* that produces conidiophores aggregated in sporodochia and occurs on leaves of *Eucalyptus urophylla* (Myrtaceae) in Malaysia (Crous et al. 2019a). The only known species in the genus *Nothoramularia*, namely *Nothoramularia ragnhildianicola*, is a fungicolous hyphomycete (hyperparasite) occurring on cercosporoid *Ragnhildiana ferruginea*, which in turn is parasitic on *Artemisia vulgaris* (Asteraceae) in Germany (Crous et al. 2023). *Vanderaaea* is typified with *Vanderaaea ammophilae* that forms sporodochial conidiomata with curved, 0-1-septate conidia and occurs on dead leaves of *Ammophila arenaria* (Poaceae) in the Netherlands (Crous et al. 2021).

So far, the family Gomphillaceae included mostly foliicolous lichenized fungi, which are predominantly known from the tropics (Xavier-Leite et al. 2022, 2023, 2024). Lichenized fungi from this family are unique in that they form a special type of asexual conidiomata called hyphophores, which produce diahyphae (Ferraro 2004; Lücking et al. 2004; Xavier-Leite et al. 2022, 2023). The family also contained three lichenicolous genera *Corticifraga*, *Paragyalideopsis* and *Taitaia* (Pino-Bodas et al. 2017; Suija et al. 2018; Lücking and Kalb 2002; Xavier-Leite et al. 2022, 2024; Diederich et al. 2024). Current confirmation or inclusion of non-lichenized, plant associated or fungicolous genera *Cladosterigma*, *Cytosporella*, *Neoacrodontiella*, *Nothoramularia* and *Vanderaaea* enlarge the concept of this predominantly lichenized family Gomphillaceae. Due to phylogenetic, morphological (notably: absence of hyphophores with diahyphae) and ecological characteristics a new subfamily Cladosterigmoideae is described for these five non-lichenized genera. It is worthy to note that within Graphidales a very similar situation is found in the lichenized family Graphidaceae, where two non-lichenized genera (*Furcaspora*, *Rubikia*) are now included therein as subfamily Rubikioideae (Cáceres et al. 2020), Additionally, non-lichenized genus *Papilionovela* is a member of the core Graphidaceae (Cáceres et al. 2020). Thus, Gomphillaceae and Graphidaceae, along with still other families of the subclass Ostropomycetidae (e.g. Stictidaceae), constitute good models to study transitions between lichenized and non-lichenized lifestyles.

Acknowledgements

We are grateful to Wacław Bartoszek (Kraków, Poland) for help in the field work.

Additional information

Conflict of interest

The authors have declared that no competing interests exist.

Ethical statement

No ethical statement was reported.

Funding

This study was funded by the National Science Centre, Poland, under the project 2017/27/B/NZ9/02902.

Author contributions

MP: conceptualization, investigation, formal analyses, visualisation, writing – original draft preparation; MSB: investigation, formal analyses, visualisation, writing – review and editing; PC: investigation, writing – review and editing. All authors have read and approved the final version of the manuscript.

Author ORCIDs

Marcin Piątek https://orcid.org/0000-0002-4968-2861
Monika Stryjak-Bogacka https://orcid.org/0000-0003-2845-9975
Paweł Czachura https://orcid.org/0000-0002-3562-8776

Data availability

The data that support the findings of this study are available in GenBank (https://www.ncbi.nlm.nih.gov/genbank/) and in culture collections and fungal herbarium, as shown in Table 1 and the text.

References

Baloch E, Lücking R, Lumbsch HT, Wedin M (2010) Major clades and phylogenetic relationships between lichenized and non-lichenized lineages in Ostropales (Ascomycota: Lecanoromycetes). Taxon 59(5): 1483–1494. https://doi.org/10.1002/tax.595013

Cáceres MES, Lücking R, Schumm F, Aptroot A (2020) A lichenized family yields another renegade lineage: *Papilionovela albothallina* is the first non-lichenized, saprobic member of Graphidaceae subfam. Graphidoideae. The Bryologist 123(2): 144–154. https://doi.org/10.1639/0007-2745-123.2.144

Clements RE, Shear CL (1931) The Genera of Fungi, 2nd edn. H.W. Wilson, New York.

Crous PW, Schoch CL, Hyde KD, Wood AR, Gueidan C, de Hoog GS, Groenewald JZ (2009) Phylogenetic lineages in the Capnodiales. Studies in Mycology 64: 17–47S7. https://doi.org/10.3114/sim.2009.64.02

Crous PW, Carnegie AJ, Wingfield MJ, Sharma R, Mughini G, Noordeloos ME, Santini A, Shouche YS, Bezerra JDP, Dima B, Guarnaccia V, Imrefi I, Jurjević Ž, Knapp DG, Kovács GM, Magistà D, Perrone G, Rämä T, Rebriev YA, Shivas RG, Singh SM, Souza-Motta CM, Thangavel R, Adhapure NN, Alexandrova AV, Alfenas AC, Alfenas RF, Alvarado P, Alves AL, Andrade DA, Andrade JP, Barbosa RN, Barili A, Barnes CW, Baseia IG, Bellanger JM, Berlanas C, Bessette AE, Bessette AR, Biketova AY, Bomfim FS, Brandrud TE, Bransgrove K, Brito ACQ, Cano-Lira JF, Cantillo T, Cavalcanti AD, Cheewangkoon R, Chikowski RS, Conforto C, Cordeiro TRL, Craine JD, Cruz R, Damm U, de Oliveira RJV, de Souza JT, de Souza HG, Dearnaley JDW, Dimitrov RA, Dovana F, Erhard A, Esteve-Raventós F, Félix CR, Ferisin G, Fernandes RA, Ferreira RJ, Ferro LO, Figueiredo CN, Frank JL, Freire KTLS, García D, Gené J, Gęsiorska A, Gibertoni TB, Gondra RAG, Gouliamova DE, Gramaje D, Guard F, Gusmão LFP, Haitook S, Hirooka Y, Houbraken J, Hubka V, Inamdar A, Iturriaga T, Iturrieta-González I, Jadan M, Jiang N, Justo A, Kachalkin AV, Kapitonov VI, Karadelev M, Karakehian J, Kasuya T, Kautmanová I, Kruse J, Kušan I, Kuznetsova TA, Landell MF, Larsson KH, Lee HB, Lima DX, Lira CRS, Machado AR, Madrid H, Magalhães OMC, Majerova H, Malysheva EF, Mapperson RR, Marbach PAS, Martín MP, Martín-Sanz A, Matočec N, McTaggart AR, Mello JF, Melo RFR, Mešić A, Michereff SJ, Miller AN, Minoshima A, Molinero-Ruiz L, Morozova OV, Mosoh D, Nabe M, Naik R, Nara K, Nascimento SS, Neves RP, Olariaga I, Oliveira RL, Oliveira TGL, Ono T, Ordoñez ME, Ottoni AM, Paiva LM, Pancorbo F, Pant B, Pawłowska J, Peterson SW, Raudabaugh DB, Rodríguez-Andrade E, Rubio E, Rusevska K, Santiago ALCMA, Santos ACS, Santos C, Sazanova NA, Shah S, Sharma J, Silva BDB, Siquier JL, Sonawane MS, Stchigel AM, Svetasheva T, Tamakeaw N, Telleria MT, Tiago PV, Tian CM, Tkalčec Z, Tomashevskaya MA, Truong HH, Vecherskii MV, Visagie CM, Vizzini A, Yilmaz N, Zmitrovich IV, Zvyagina EA, Boekhout T, Kehlet T, Læssøe T, Groenewald JZ (2019a) Fungal Planet description sheets: 868–950. Persoonia 42: 291–473. https://doi.org/10.3767/persoonia.2019.42.11

Crous PW, Wingfield MJ, Lombard L, Roets F, Swart WJ, Alvarado P, Carnegie AJ, Moreno G, Luangsaard J, Thangavel R, Alexandrova AV, Baseia IG, Bellanger JM, Bessette AE, Bessette AR, De la Peña-Lastra S, García D, Gené J, Pham THG, Heykoop M, Malysheva E, Malysheva V, Martín MP, Morozova OV, Noisripoom W, Overton BE, Rea AE, Sewall BJ, Smith ME, Smyth CW, Tasanathai K, Visagie CM, Adamčík S, Alves A, Andrade JP, Aninat MJ, Araújo RVB, Bordallo JJ, Boufleur T, Baroncelli R, Barreto RW, Bolin J, Cabero J, Caboň M, Cafà G, Caffot MLH, Cai L, Carlavilla JR, Chávez R, de Castro RRL, Delgat L, Deschuyteneer D, Dios MM, Domínguez LS, Evans HC, Eyssartier G, Ferreira BW, Figueiredo CN, Liu F, Fournier J, Galli-Terasawa LV, Gil-Durán C, Glienke C, Gonçalves MFM, Gryta H, Guarro J, Himaman W, Hywel-Jones N, Iturrieta-González I, Ivanushkina NE, Jargeat P, Khalid AN, Khan J, Kiran M, Kiss L, Kochkina GA, Kolařík M, Kubátová A, Lodge DJ, Loizides M, Luque D, Manjón JL, Marbach PAS, Massola Jr NS, Mata M, Miller AN, Mongkolsamrit S, Moreau PA, Morte A, Mujic A, Navarro-Ródenas A, Németh MZ, Nóbrega TF, Nováková A, Olariaga I, Ozerskaya SM, Palma MA, Petters-Vandresen DAL, Piontelli E, Popov ES, Rodríguez A, Requejo Ó, Rodrigues ACM, Rong IH, Roux J, Seifert KA, Silva BDB, Sklenář F, Smith JA, Sousa JO, Souza HG, De Souza JT, Švec K, Tanchaud P, Tanney JB, Terasawa F, Thanakitpipattana D, Torres-Garcia D, Vaca I, Vaghefi N, van Iperen AL, Vasilenko OV, Verbeken A, Yilmaz N, Zamora JC, Zapata M, Jurjević Ž, Groenewald JZ (2019b) Fungal Planet description sheets: 951–1041. Persoonia 43(1): 223–425. https://doi.org/10.3767/persoonia.2019.43.06

Crous PW, Braun U, McDonald BA, Lennox CL, Edwards J, Mann RC, Zaveri A, Linde CC, Dyer PS, Groenewald JZ (2021) Redefining genera of cereal pathogens: *Oculimacula*, *Rhynchosporium* and *Spermospora*. Fungal Systematics and Evolution 7(1): 67–98. https://doi.org/10.3114/fuse.2021.07.04

Crous PW, Akulov A, Balashov S, Boers J, Braun U, Castillo J, Delgado MA, Denman S, Erhard A, Gusella G, Jurjević Ž, Kruse J, Malloch DW, Osieck ER, Polizzi G, Schumacher RK, Slootweg E, Starink-Willemse M, van Iperen AL, Verkley GJM, Groenewald JZ (2023) New and interesting fungi. 6. Fungal Systematics and Evolution 11(1): 109–156. https://doi.org/10.3114/fuse.2023.11.09

Crous PW, Jurjević Z, Balashov S, De la Peña-Lastra S, Mateos A, Pinruan U, Rigueiro-Rodríguez A, Osieck ER, Altés A, Czachura P, Esteve-Raventós F, Gunaseelan S, Kaliyaperumal M, Larsson E, Luangsa-ard JJ, Moreno G, Pancorbo F, Piątek M, Sommai S, Somrithipol S, Asif M, Delgado G, Flakus A, Illescas T, Kezo K, Khamsuntorn P, Kubátová A, Labuda R, Lavoise C, Lebel T, Lueangjaroenkit P, Maciá-Vicente JG, Paz A, Saba M, Shivas RG, Tan YP, Wingfield MJ, Aas T, Abramczyk B, Ainsworth AM, Akulov A, Alvarado P, Armada F, Assyov B, Avchar R, Avesani M, Bezerra JL, Bhat JD, Bilański P, Bily DS, Boccardo F, Bozok F, Campos JC, Chaimongkol S, Chellappan N, Costa MM, Dalecká M, Darmostuk V, Daskalopoulos V, Dearnaley J, Dentinger BTM, De Silva NI, Dhotre D, Carlavilla JR, Doungsa-ard C, Dovana F, Erhard A, Ferro LO, Gallegos SC, Giles CE, Gore G, Gorfer M, Guard FE, Hanson S-A, Haridev P, Jankowiak R, Jeffers SN, Kandemir H, Karich A, Kisło K, Kiss L, Krisai-Greilhuber I, Latha KPD, Lorenzini M, Lumyong S, Manimohan P, Manjón JL, Maula F, Mazur E, Mesquita NLS, Młynek K, Mongkolsamrit S, Morán P, Murugadoss R, Nagarajan M, Nalumpang S, Noisripoom W, Nosalj S, Novaes QS, Nowak M, Pawłowska J, Peiger M, Pereira OL, Pinto A, Plaza M, Polemis E, Polhorský A, Ramos DO, Raza M, Rivas-Ferreiro M, Rodriguez-Flakus P, Ruszkiewicz-Michalska M, Sánchez A, Santos A, Schüller A, Scott PA, Şen İ, Shelke D, Śliwa L, Solheim H, Sonawane H, Strašiftáková D, Stryjak-Bogacka M, Sudsanguan M, Suwannarach N, Suz LM, Syme K, Taşkın H, Tennakoon DS, Tomka P, Vaghefı N, Vasan V, Vauras J, Wiktorowicz D, Villarreal M, Vizzini A, Wrzosek M, Yang X, Yingkunchao W, Zapparoli G, Zervakis GI, Groenewald JZ (2024) Fungal Planet description sheets: 1614–1696. Fungal Systematics and Evolution 13: 183–439. https://doi.org/10.3114/fuse.2024.13.11

Czachura P, Owczarek-Kościelniak M, Piątek M (2021) *Salinomyces polonicus*: A moderately halophilic kin of the most extremely halotolerant fungus *Hortaea werneckii*. Fungal Biology 125(6): 459–468. https://doi.org/10.1016/j.funbio.2021.01.003

Darriba D, Posada D, Kozlov AM, Stamatakis A, Morel B, Flouri T (2020) ModelTest-NG: A new and scalable tool for the selection of DNA and protein evolutionary models. Molecular Biology and Evolution 37(1): 291–294. https://doi.org/10.1093/molbev/msz189

Diederich P, Ertz D, Berger F, Suija A (2024) *Taitaia*. In: Diederich P, Ertz D, Braun U (Eds) Flora of Lichenicolous Fungi 2. Hyphomycetes. Luxembourg: National Museum of Natural History, Luxembourg, 478–479.

Ertz D, Sanderson N, Lebouvier M (2021) *Thelopsis* challenges the generic circumscription in the Gyalectaceae and brings new insights to the taxonomy of *Ramonia*. Lichenologist (London, England) 53(1): 45–61. https://doi.org/10.1017/S002428292000050X

Ferraro LI (2004) Morphological diversity in the hyphophores of Gomphillaceae (Ostroplaes, lichenized Ascomycetes). Fungal Diversity 15: 153–169.

Grube M, Baloch E, Lumbsch HT (2004) The phylogeny of Porinaceae (Ostropomycetidae) suggests a neotenic origin of perithecia in Lecanoromycetes. Mycological Research 108(10): 1111–1118. https://doi.org/10.1017/S0953756204000826

Guterres DC, Dos Santos MDDM, Silva RAFD, Souza ESDC, Soares WRO, Pinho DB, Dianese JC (2020) *Cladosterigma*: An enigmatic fungus, previously considered a basidiomycete, now revealed as an ascomycete member of the Gomphillaceae. Mycologia 112(4): 829–846. https://doi.org/10.1080/00275514.2020.1781501

Index Fungorum (2024) Index Fungorum. www.indexfungorum.org [Accessed 31 July 2024]

Katoh K, Kuma K, Toh H, Miyata T (2005) MAFFT version 5: Improvement in accuracy of multiple sequence alignment. Nucleic Acids Research 33(2): 511–518. https://doi.org/10.1093/nar/gki198

Kozlov AM, Darriba D, Flouri T, Morel B, Stamatakis A (2019) RAxML-NG: A fast, scalable and user-friendly tool for maximum likelihood phylogenetic inference. Bioinformatics (Oxford, England) 35(21): 4453–4455. https://doi.org/10.1093/bioinformatics/btz305

Kraichak E, Huang JP, Nelsen M, Leavitt SD, Lumbsch HT (2018) A revised classification of orders and families in the two major subclasses of Lecanoromycetes (Ascomycota) based on a temporal approach. Botanical Journal of the Linnean Society 188: 233–249. https://doi.org/10.1093/botlinnean/boy060

Li WJ, McKenzie EHC, Liu JK, Bhat DJ, Dai DQ, Camporesi E, Tian Q, Maharachchikumbura SSN, Luo ZL, Shang QJ, Zhang JF, Tangthirasunun N, Karunarathna SC, Xu JC, Hyde KD (2020) Taxonomy and phylogeny of hyaline-spored coelomycetes. Fungal Diversity 100(1): 279–801. https://doi.org/10.1007/s13225-020-00440-y

Liu YJ, Whelen S, Hall BD (1999) Phylogenetic relationships among ascomycetes: Evidence from an RNA polymerase II subunit. Molecular Biology and Evolution 16(12): 1799–1808. https://doi.org/10.1093/oxfordjournals.molbev.a026092

Lücking R (2019) Stop the abuse of time! Strict temporal banding is not the future of rank-based classifications in Fungi (including lichens) and other organisms. Critical Reviews in Plant Sciences 38(3): 199–253. https://doi.org/10.1080/07352689.2019.1650517

Lücking R, Kalb K (2002) New species and further additions to the foliicolous lichen flora of Kenya (East Africa), including the first lichenicolous *Aulaxina* (Ostropales: Gomphillaceae). Botanical Journal of the Linnean Society 139(2): 171–180. https://doi.org/10.1046/j.1095-8339.2002.00058.x

Lücking R, Stuart BL, Lumbsch HT (2004) Phylogenetic relationships of Gomphillaceae and Asterothyriaceae: Evidence from a combined Bayesian analysis of nuclear and mitochondrial sequences. Mycologia 96(2): 283–294. https://doi.org/10.1080/15572536.2005.11832978

Lumbsch HT, Schmitt I, Palice Z, Wiklund E, Ekman S, Wedin M (2004) Supraordinal phylogenetic relationships of Lecanoromycetes based on a Bayesian analysis of combined nuclear and mitochondrial sequences. Molecular Phylogenetics and Evolution 31(3): 822–832. https://doi.org/10.1016/j.ympev.2003.11.001

Lutzoni F, Kauff F, Cox CJ, McLaughlin D, Celio G, Dentinger B, Padamsee M, Hibbett D, James TY, Baloch E, Grube M, Reeb V, Hofstetter V, Schoch C, Arnold AE, Miadlikowska J, Spatafora J, Johnson D, Hambleton S, Crockett M, Shoemaker R, Sung GH, Lücking R, Lumbsch T, O'Donnell K, Binder M, Diederich P, Ertz D, Gueidan C, Hansen K, Harris RC, Hosaka K, Lim YW, Matheny B, Nishida H, Pfister D, Rogers J, Rossman A, Schmitt I, Sipman H, Stone J, Sugiyama J, Yahr R, Vilgalys R (2004) Assembling the fungal tree of life: Progress, classification, and evolution of subcellular traits. American Journal of Botany 91(10): 1446–1480. https://doi.org/10.3732/ajb.91.10.1446

Mangold A, Martin MP, Lücking R, Lumbsch HT (2008) Molecular phylogeny suggests synonymy of Thelotremataceae within Graphidaceae (Ascomycota: Ostropales). Taxon 57: 476–486.

Miadlikowska J, Kauff F, Hofstetter V, Fraker E, Grube M, Hafellner J, Reeb V, Hodkinson BP, Kukwa M, Lücking R, Hestmark G, Otalora MG, Rauhut A, Büdel B, Scheidegger C, Timdal E, Stenroos S, Brodo I, Perlmutter GB, Ertz D, Diederich P, Lendemer JC, May P, Schoch CL, Arnold AE, Gueidan C, Tripp E, Yahr R, Robertson C, Lutzoni F (2006) New insights into classification and evolution of the Lecanoromycetes (Pezizomycotina, Ascomycota) from phylogenetic analyses of three ribosomal RNA- and two protein-coding genes. Mycologia 98(6): 1088–1103. https://doi.org/10.1080/15572536.2006.11832636

Miadlikowska J, Kauff F, Högnabba F, Oliver JC, Molnár K, Fraker E, Gaya E, Hafellner J, Hofstetter V, Gueidan C, Otálora MA, Hodkinson B, Kukwa M, Lücking R, Björk C, Sipman HJ, Burgaz AR, Thell A, Passo A, Myllys L, Goward T, Fernández-Brime S, Hestmark G, Lendemer J, Lumbsch HT, Schmull M, Schoch CL, Sérusiaux E, Maddison DR, Arnold AE, Lutzoni F, Stenroos S (2014) A multigene phylogenetic synthesis for the class Lecanoromycetes (Ascomycota): 1307 fungi representing 1139 infrageneric taxa, 317 genera and 66 families. Molecular Phylogenetics and Evolution 79: 132–168. https://doi.org/10.1016/j.ympev.2014.04.003

Passerini G (1888) Diagnosi di funghi nuovi. Nota III. Rendiconti della Reale Accademia dei Lincei Ser. 4 4(2): 95–105.

Piątek M, Stryjak-Bogacka M, Czachura P, Owczarek-Kościelniak M (2023) The genus *Rachicladosporium*: Introducing new species from sooty mould communities and excluding cold adapted species. Scientific Reports 13(1): 22795. https://doi.org/10.1038/s41598-023-49696-9

Pino-Bodas R, Zhurbenko MP, Stenroos S (2017) Phylogenetic placement within Lecanoromycetes of lichenicolous fungi associated with *Cladonia* and some other genera. Persoonia 39(1): 91–117. https://doi.org/10.3767/persoonia.2017.39.05

Reeb V, Lutzoni F, Roux C (2004) Contribution of RPB2 to multilocus phylogenetic studies of the euascomycetes (Pezizomycotina, Fungi) with special emphasis on the lichen-forming Acarosporaceae and evolution of polyspory. Molecular Phylogenetics and Evolution 32(3): 1036–1060. https://doi.org/10.1016/j.ympev.2004.04.012

Rehner SA, Buckley E (2005) A *Beauveria* phylogeny inferred from nuclear ITS and EF1-alpha sequences: Evidence for cryptic diversification and links to *Cordyceps* teleomorphs. Mycologia 97(1): 84–98. https://doi.org/10.1080/15572536.2006.11832842

Rivas Plata E, Lumbsch HT (2011) Parallel evolution and phenotypic divergence in lichenized fungi: a case study in the lichen-forming fungal family Graphidaceae (Ascomycota: Lecanoromycetes: Ostropales). Molecular Phylogenetics and Evolution 61(1): 45–63. https://doi.org/10.1016/j.ympev.2011.04.025

Rivas Plata E, Hernández MJE, Lücking R, Staiger B, Kalb K, Cáceres MES (2011) *Graphis* is two genera: A remarkable case of parallel evolution in lichenized Ascomycota. Taxon 60(1): 99–107. https://doi.org/10.1002/tax.601009

Rivas Plata E, Parnmen S, Staiger B, Mangold A, Frisch A, Weerakoon G, Hernández MJE, Cáceres MES, Kalb K, Sipman HJM, Common RS, Nelsen MP, Lücking R, Lumbsch HT (2013) A molecular phylogeny of Graphidaceae (Ascomycota, Lecanoromycetes, Ostropales) including 428 species. MycoKeys 6: 55–94. https://doi.org/10.3897/mycokeys.6.3482

Ronquist F, Teslenko M, van der Mark P, Ayres DL, Darling A, Höhna S, Larget B, Liu L, Suchard MA, Huelsenbeck JP (2012) MrBayes 3.2: Efficient Bayesian phylogenetic inference and model choice across a large model space. Systematic Biology 61(3): 539–542. https://doi.org/10.1093/sysbio/sys029

Saccardo PA (1880) Fungi Gallici lecti a cl. viris P. Brunaud, Abb. Letendre, A. Malbranche, J. Therry, vel editi in Mycotheca Gallica C. Roumeguèri. Series II. Michelia 2(6): 39–135.

Saccardo PA (1884) Sylloge Fungorum 3. P.A. Saccardo, Italy, Padua, i–ii, 1–860.

Saccardo PA, Roumeguère C (1884) Reliquiae mycologicae Libertianae. IV. Revue Mycologique 6: 26–39.

Saccardo PA, Sydow P (1902) Sylloge Fungorum 16. P.A. Saccardo, Patavii, Italy, i–viii, 1–1291.

Seifert KA, Bandoni RJ (2001) Revisiones generum obscurorum hyphomycetum: *Phacellula* Sydow and *Cladosterigma* Pat. Sydowia 53: 156–166.

Suija A, Kaasalainen U, Kirika PM, Rikkinen J (2018) *Taitaia*, a novel lichenicolous fungus in tropical montane forests in Kenya (East Africa). Lichenologist (London, England) 50(2): 173–184. https://doi.org/10.1017/S0024282918000026

Sutton BC (1980) The Coelomycetes. Fungi imperfecti with pycnidia, acervuli and stromata. Commonwealth Mycological Institute, Kew, 1–69. https://doi.org/10.1079/9780851984469.0000

van der Aa HA, Vanev S, Mel'nik VA, Stephenson SL (2001) A new species of *Cytosporella* (Coelomycetes, Deuteromycotina) from subantarctic Campbell Island (New Zealand). New Zealand Journal of Botany 39(3): 543–545. https://doi.org/10.1080/0028825X.2001.9512756

Vilgalys R, Hester M (1990) Rapid genetic identification and mapping of enzymatically amplified ribosomal DNA from several *Cryptococcus* species. Journal of Bacteriology 171(8): 4238–4246. https://doi.org/10.1128/jb.172.8.4238-4246.1990

Vu D, Groenewald M, de Vries M, Gehrmann T, Stielow B, Eberhardt U, Al-Hatmi A, Groenewald JZ, Cardinali G, Houbraken J, Boekhout T, Crous PW, Robert V, Verkley GJM (2019) Large-scale generation and analysis of filamentous fungal DNA barcodes boosts coverage for kingdom fungi and reveals thresholds for fungal species and higher taxon delimitation. Studies in Mycology 92(1): 135–154. https://doi.org/10.1016/j.simyco.2018.05.001

Westberg M, Millanes AM, Knudsen K, Wedin M (2015) Phylogeny of the Acarosporaceae (Lecanoromycetes, Ascomycota, Fungi) and the evolution of carbonized ascomata. Fungal Diversity 73(1): 145–158. https://doi.org/10.1007/s13225-015-0325-x

White TJ, Bruns T, Lee S, Taylor J (1990) Amplification and direct sequencing of fungal ribosomal RNA genes for phylogenetics. In: Innis MA, Gelfand DH, Sninsky JJ, White TJ (Eds) PCR protocols, a guide to methods and applications. Academic Press Inc., San Diego, CA and London, UK, 315–322. https://doi.org/10.1016/B978-0-12-372180-8.50042-1

Xavier-Leite AB, Cáceres MES, Aptroot A, Moncada B, Lücking R, Goto BT (2022) Phylogenetic revision of the lichenized family Gomphillaceae (Ascomycota: Graphidales) suggests post-K–Pg boundary diversification and phylogenetic signal in asexual reproductive structures. Molecular Phylogenetics and Evolution 168: 107380. https://doi.org/10.1016/j.ympev.2021.107380

Xavier-Leite AB, Goto BT, Lücking R, Cáceres MES (2023) New genera in the lichenized family Gomphillaceae (Ascomycota: Graphidales) focusing on neotropical taxa. Mycological Progress 22(12): 88. https://doi.org/10.1007/s11557-023-01933-1

Xavier-Leite AB, Goto BT, Cáceres MES, Lücking R (2024) Reclassification of species in the lichenized family Gomphillaceae Walt. Watson ex Hafellner (Ascomycota: Graphidales) using morphology-based phylogenetic binning. Cryptogamie. Mycologie 45(8): 83–99. https://doi.org/10.5252/cryptogamie-mycologie2024v45a8

Zhang Z, Schwartz S, Wagner L, Miller W (2000) A greedy algorithm for aligning DNA sequences. Journal of Computational Biology 7(1–2): 203–214. https://doi.org/10.1089/10665270050081478

Zoller S, Scheidegger C, Sperisen C (1999) PCR primers for the amplification of mitochondrial small subunit ribosomal DNA of lichen-forming ascomycetes. Lichenologist (London, England) 31(5): 511–516. https://doi.org/10.1006/lich.1999.0220

MycoKeys 115: 19–42 (2025)
DOI: 10.3897/mycokeys.115.139963

Research Article

Introducing *Melanocucurbitaria uktampratovii* sp. nov. and the sexual morph of *Melanocamarosporioides ugamica* in Melanommataceae (Dothideomycetes, Pleosporales)

Dhandevi Pem[1,2], Rajesh Jeewon[3,4], Yusufjon Gafforov[5], Islomjon Urinboev[6], Abdulwahed Fahad Alrefaei[4], Indunil C. Senanayake[7], Alijon Esankulov[8], Kevin David Hyde[1,2,9]

1 *School of Science, Mae Fah Luang University, Chiang Rai 57100, Thailand*
2 *Center of Excellence in Fungal Research, Mae Fah Luang University, Chiang Rai 57100, Thailand*
3 *Faculty of Medicine and Health Sciences, University of Mauritius, Moka, Mauritius*
4 *Department of Zoology, College of Science, King Saud University, P.O. Box 2455, Riyadh 11451, Saudi Arabia*
5 *Central Asian Center of Development Studies, New Uzbekistan University, Tashkent, 100007, Uzbekistan*
6 *Department of Ecological Monitoring, National University of Uzbekistan, Tashkent, 100174, Uzbekistan*
7 *Germplasm Bank of Wild Species & Yunnan Key Laboratory for Fungal Diversity and Green Development, Kunming Institute of Botany, Chinese Academy of Sciences, Kunming, 650201, China*
8 *Scientific-Research Institute of Horticulture, Viticulture and Winemaking named after Academician M. Mirzaev, Tashkent, Uzbekistan*
9 *Department of Botany and Microbiology, College of Science, King Saud University, P.O. Box 22452, Riyadh 11495, Saudi Arabia*
Corresponding authors: Rajesh Jeewon (r.jeewon@uom.ac.mu); Kevin David Hyde (kdhyde3@gmail.com)

Abstract

Most species of Melanommataceae are saprobic on decayed parts of various plants in tropical and temperate terrestrial habitats. During a survey of microfungi associated with terrestrial plants in Uzbekistan, two melanommataceous taxa were collected from dead branches of *Rosa ecae* (Rosaceae) and *Salvia karelinii* (Lamiaceae). This study introduces a new species, *Melanocucurbitaria uktampratovii*, and provides a new host and sexual morph record for *Melanocamarosporioides ugamica*, based on morphological observations and multi-gene phylogenetic analyses of concatenated LSU, SSU, ITS, and TEF-1 sequence data. *Melanocucurbitaria uktampratovii* is the second species described within this genus and differs from the type species of *Melanocucurbitaria* in having smaller ascomata, smaller asci, smaller ascospores, and a different number of septa. The sexual morph of *Melanocamarosporioides ugamica* is characterized by globose to ovoid ascomata, cylindrical-clavate asci, ellipsoidal, muriform ascospores with 5–7 transversely septate, and 5–11 vertical septa. Illustrations and descriptions are provided, along with ecological and morphological comparisons of similar species within their respective genera.

Key words: 1 new species, Central Asia, DNA, host, morphology, phylogeny, record, sequence

This article is part of:
Exploring the Hidden Fungal Diversity: Biodiversity, Taxonomy, and Phylogeny of Saprobic Fungi
Edited by Samantha C. Karunarathna, Danushka Sandaruwan Tennakoon, Ajay Kumar Gautam

Academic editor:
Samantha C. Karunarathna
Received: 22 October 2024
Accepted: 9 January 2025
Published: 7 March 2025

Introduction

Over the past 20 years, extensive research on members of Melanommataceae has yielded numerous taxonomic findings (36 genera, 337 species), largely attributed to advancements in DNA sequencing technology (Pem et al. 2019b;

Citation: Pem D, Jeewon R, Gafforov Y, Urinboev I, Alrefaei AF, Senanayake IC, Esankulov A, Hyde KD (2025) Introducing *Melanocucurbitaria uktampratovii* sp. nov. and the sexual morph of *Melanocamarosporioides ugamica* in Melanommataceae (Dothideomycetes, Pleosporales). MycoKeys 115: 19–42. https://doi.org/10.3897/mycokeys.115.139963

Hongsanan et al. 2020; Gao et al. 2023; Hyde et al. 2024a; Tennakoon et al. 2024). Species within Melanommataceae are classified based on morphological traits, such as the shape of fruiting bodies (conical or round), the type of peridium (cephalothecioid or non-cephalothecioid), the structure of pseudoparaphyses (cellular or trabeculate), the characteristics of asci (with short or furcate pedicels), and the nature of ascospores (monomorphic or dimorphic), along with the presence or absence of gelatinous sheaths, guttules, and germ pores (Wijayawardene et al. 2012; Almeida et al. 2017; Hyde et al. 2018; Dong et al. 2020). However, identifying species based solely on morphology can be challenging, as many species exhibit similar traits, leading to potential confusion. Consequently, modern fungal classification now commonly integrates both DNA-based phylogenetic analysis and morphological assessment coupled with consensus among mycologists for a better classification scheme (Hyde et al. 2023; Kularathnage et al. 2023; Tang et al. 2023; Dong et al. 2024; Sui et al. 2024; Tian et al. 2024).

The primary molecular markers employed in phylogenetic analyses of Melanommataceae (Pleosporales) include the 28S large subunit (LSU), 18S small subunit (SSU), internal transcribed spacers (ITS1–5.8S–ITS2), translation elongation factor 1 gene (TEF-1), and RNA polymerase second largest subunit (rpb2) (Tennakoon et al. 2018; Pem et al. 2019b). Melanommataceae is one of the highly diverse families within Dothideomycetes (Tian et al. 2015; Hongsanan et al. 2020; Pem et al. 2024). The family was introduced by Winter (1885), with *Melanomma* designated as the type genus for species characterized by globose to subglobose ascomata, clavate to nearly cylindrical asci, and fusoid to ellipsoidal or muriform ascospores. Members of Melanommataceae, which belong to Pleosporales, are found in various ecosystems and are known to thrive on a wide range of hosts globally (Gafforov 2017; Li et al. 2017; Pem et al. 2019b; Kularathnage et al. 2023). The cosmopolitan nature of Melanommataceae is underscored by the numerous new genera and species discovered in recent years (Li et al. 2016; Tennakoon et al. 2024). Despite being considered polyphyletic, the taxonomy of Melanommataceae remains unclear, as several genera lack sequence data (Zhang et al. 2012). Several researchers have advocated the inclusion of DNA sequence data with additional sample collections to genera that have insufficient data and for clarifying the confusion between sexual and asexual morphs to stabilize taxonomy (Shenoy et al. 2007; Shenoy et al. 2010; Karunarathna et al. 2017; Hongsanan et al. 2020). To date, there are 26 genera exhibiting sexual morphs and 10 genera exhibiting asexual morphs within Melanommataceae (Hongsanan et al. 2020; Pem et al. 2024). Gao et al. (2023) identified a pleomorphic genus, *Dematiomelanomma*, from grassland vegetation in Yunnan, China, emphasizing the importance of pleomorphism in Melanommataceae. Tennakoon et al. (2024) highlighted the host associations and geographical distribution of *Melanommataceous* species.

Most Melanommataceae species are reported from Western regions, including Europe and North America (Tennakoon et al. 2024). Targeting underexplored regions such as Central Asia, including Uzbekistan, might be helpful for the discovery of new fungi (Gafforov 2017; Kan et al. 2017; Hyde et al. 2019; Cheek et al. 2020; Hyde et al. 2024b; Gafforov et al. 2025). Recent studies have led to the discovery of several new genera and species of ascomycetes in arid regions, particularly from Uzbekistan, Central Asia (Gafforov and Hoshino 2015; Gafforov and Rakhimov 2017; Pem et al. 2018, 2019a, 2019b; Gafforov et al. 2019; Abdurazakov et al. 2021; Appadoo et al. 2021; Htet et al. 2021; Lestari et al. 2021; Aluthmuhandiram et al. 2022; Dong et al. 2023; Senwanna et al. 2024). *Melanocamarosporoides* and *Melanocucurbitaria* were first discovered from Uzbekistan (Wanasinghe et al. 2018; Pem et al. 2019b). However, the two genera are still poorly known worldwide. The aim of the present study was to clarify the taxonomic position of a new species and new record of *Melanocucurbitaria* and *Melanocamarosporioides* and to identify new taxa through multigene phylogeny and morphological examination.

Materials and methods

Sample collection, morphological examination and isolation

Fresh fungal specimens were collected from dead trunks and branches in the Surkhandarya and Tashkent provinces of Uzbekistan, and the important collection information was noted (Rathnayaka et al. 2024). The samples were transported to the laboratory in zip-lock plastic bags and incubated for 24 hours in plastic containers lined with wet tissue paper. The micromorphological characters were examined following the methods described by Pem et al. (2019b). Vertical sections of the ascomata were made using a razor blade and mounted in distilled water on a glass slide. A stereomicroscope (Motic series SMZ-171) was used to observe the surface morphology of fungal fruiting bodies. Micro-morphological structures were examined under a Nikon Eclipse 80i compound microscope, and photographs were captured with a Canon 600D digital camera fitted to the compound microscope using differential interference contrast (DIC) microscopy. The micro-morphological features, including shape, structure, and color, were meticulously recorded. Asci were stained with Melzer's reagent to assess the reactions of the apical ring, while ascospores were stained with Indian ink to evaluate the presence of gelatinous sheaths surrounding them. All measurements, including the height and width of ascomata, asci, ascospores, peridium, and pseudoparaphyses, were made using the Tarosoft® Image Framework program. Photo plates were created using Adobe Photoshop CS3 Extended Version 10.0 (Adobe Systems, USA). Single spore isolation was conducted following the method described by Senanayake et al. (2020). Germinated spores were transferred to malt extract agar (MEA) plates and incubated at 16 °C under daylight, as outlined by Liu et al. (2010). Colony color and other characters were observed, and growth rates were measured after one week and at subsequent weekly intervals. The holotype specimen was deposited in the Tashkent Mycological Herbarium (TASM) at the Institute of Botany, Academy of Sciences of the Republic of Uzbekistan, while an isotype specimen was deposited in the Mae Fah Luang University Herbarium (MFLU) in Chiang Rai, Thailand. Living cultures were submitted to the Culture Collection at Mae Fah Luang University (MFLUCC). The Faces of Fungi (FoF) and Index Fungorum (IF) numbers were provided as outlined by Jayasiri et al. (2015) and Index Fungorum (2024). New taxon and species identification were based on the recommendations of Jeewon and Hyde (2016), Aime et al. (2021), Chethana et al. (2021), and Pem et al. (2021).

DNA extraction, PCR amplification, and sequencing

Genomic DNA was extracted from fresh fungal mycelium using a DNA extraction kit (E.Z.N.A Fungal DNA Mini Kit, D3390-02, Omega Bio-Tek) following the manufacturer's protocol. The DNA product was kept at 4 °C for DNA amplification, and duplicates were maintained at -20 °C for long-term storage. The primers LR0R/LR5 were used to amplify the 28S large subunit rDNA (LSU) (Vilgalys and Hester 1990), NS1/NS4 for 18S small subunit ribosomal RNA (SSU) (White et al. 1990), ITS4/ITS5 for the 5.8S nrRNA gene with the two flanking internal transcribed spacers (ITS) (White et al. 1990), and EF1-983F/EF1-2218R primers for the partial translation elongation factor 1-alpha (TEF-1) (Rehner 2001).The amplification reactions were achieved in a total reaction volume of 25 µl, which comprised 9.5 µ l of sterilized distilled water, 12.5 µl of 2 × Power Taq PCR MasterMix (a ready- to-use mixture, including DNA polymerase, the NH_4^+ buffer system, dNTPs, magnesium chloride, and an inactive red dye and stabilizer) (Bioteke Co., China), 1 µl of each forward and reverse primer and 1 µl of DNA template. The polymerase chain reaction (PCR) thermal cycle program for LSU, SSU, ITS and TEF-1 gene regions was followed as detailed by Pem et al. (2019b). The quality of the PCR products was checked with 1% agarose gel electrophoresis containing the SafeView™. The purified PCR products were sequenced at Sangon Biotech (Shanghai) Co., Ltd., China. Generated nucleotide sequence data were deposited in GenBank, and accession numbers were recorded (Table 1).

Sequence alignment and phylogenetic analyses

The contigs (forward and reverse sequences) were merged using SeqMan (version 7.0.0; DNASTAR, Madison, WI, USA). Assembled sequences were put through a BLAST search in GenBank to find highly similar strains (https://blast.ncbi.nlm.nih.gov/). The other sequences used in the analyses were obtained from recent publications (Gao et al. 2023, Tennakoon et al. 2024). The combined dataset comprised 68 isolates, including *Cyclothyriella rubronotata* (CBS 121892, CBS 141486) as the outgroup taxa. Single gene sequences were aligned using the online MAFFT v.7.526 program (https://mafft.cbrc.jp/alignment/software/) (Katoh and Standley 2013) and improved manually where necessary. Single-gene alignments were combined using BioEdit v.7.2.5 (Hall 1999). Maximum Likelihood (ML) and Bayesian Inference (BI) were performed to analyze the concatenated aligned dataset. Maximum Likelihood analysis was performed using the CIPRES Science Gateway v. 3.3 online platform, with RAxML-HPC v.8 on XSEDE (8.2.12) software, employing the GTR+I+G nucleotide evolution model (Stamatakis et al. 2008; Miller et al. 2010; Stamatakis 2014). The best-fit nucleotide substitution models for individual barcodes were determined with MrModelTest v. 2.3 (Nylander 2004) based on the Akaike Information Criterion (AIC). The Bayesian Inference phylogeny was carried out using MrBayes 3.2.1 (Ronquist et al. 2012), with four chains of 2,000,000 generations and sampling trees every 100th generation. The first 20% of the sampled data was removed as burn-in. The phylograms were viewed with the FigTree v.1.4.0 program (Rambaut et al. 2018) and rearranged in Adobe Illustrator® CS3 (Version 15.0.0, Adobe®, San Jose, CA). The alignments and sequences were submitted to TreeBASE (http://www.treebase.org/) and GenBank (https://www.ncbi.nlm.nih.gov/).

Table 1. Culture collection code and GenBank accession numbers of fungal strains used for phylogenetic analysis in this study.“*” Denotes ex-type, ex-isotype, ex-paratype or ex-epitype strains. “^{T}” Denotes type species. Newly generated sequences are displayed in bold. NA: sequence data is not available.

Taxon	Strain/ Culture accession no	GenBank accession No.			
		ITS	LSU	SSU	TEF-1
Alpinaria rhododendri ^{T}	KT 2520	LC203335	LC203360	LC203314	LC203388
Alpinaria rhododendri ^{T}	MFLU 20-0278	MT229210	MT229208	MT229209	MT254066
Aposphaeria corallinolutea	MFLU 15-2752	KY554202	KY554197	KY554200	KY554205
Aposphaeria corallinolutea	MFLU 16-2412	MT177916	MT177943	MT177971	NA
Bertiella ellipsoidea	MFLUCC 17-2015	MG543922	MG543913	NA	MG547226
Bertiella fici	NCYU 19-0073*	NA	MW063224	MW079352	MW183787
Beverwykella pulmonaria ^{T}	CBS 283.53*	MH857201	MH868739	NG_061258	NA
Byssosphaeria macarangae	MFLUCC 17-2655*	MH389782	MH389778	MH389780	MH389784
Byssosphaeria taiwanense	MFLUCC 17-2643*	MH389783	MH389779	MH389781	MH389785
Camposporium dulciaquae	MFLU 21-0015*	MT864352	MT860430	MW485612	MW537104
Camposporium septatum	MFLUCC 19-0483*	MN758892	MN759023	MN758958	MN784096
Cyclothyriella rubronotata ^{T}	CBS 121892	KX650541	NA	NA	KX650516
Cyclothyriella rubronotata ^{T}	CBS 385.39	MH856047	JX681121	AY642521	NA
Dematiomelanomma yunnanense ^{T}	KUNCC 23-12728*	OQ225528	OQ360647	OQ360651	OQ413238
Dematiomelanomma yunnanense ^{T}	KUNCC 23-12730	OQ225529	OQ360648	OQ360652	OQ413239
Dematiomelanomma yunnanense ^{T}	CGMCC 3.23744	OQ225530	OQ360649	OQ360653	OQ413240
Dematiomelanomma yunnanense ^{T}	KUNCC 22-12677	OQ225531	OQ360650	OQ360654	OQ413241
Fusiconidium mackenziei ^{T}	MFLUCC 14-0434*	NA	KX611112	KX611114	KX611118
Gemmamyces piceae	C251	KY189977	NA	NA	KY190012
Gemmamyces piceae	C209	KY189976	NA	KY190006	KY190011
Herpotrichia juniperi	CBS 200.31	NA	DQ678080	DQ678029	DQ677925
Herpotrichia macrotricha	GKM 196N	NA	GU385176	NA	GU327755
Herpotrichia xiaokongense	KUMCC 21-0004*	NA	MZ408889	MZ408891	MZ394066
Marjia tianshanica ^{T}	TASM 6121*	MG828910	MG829020	MG829127	MG829207
Marjia uzbekistanica	TASM 6122*	MG828911	MG829021	MG829128	MG829208
Melanocamarosporium galiicola ^{T}	MFLUCC 13-0545*	NA	OR206417	OR206407	NA
Melanocamarosporioides ugamica ^{T}	MFLU 17-0064*	MH000192	MH000190	MH000191	MH006610
Melanocamarosporioides ugamica ^{T}	**TASM 6175**	**PQ453019**	**PQ453821**	**PQ433587**	
Melanocucurbitaria uzbekistanica ^{T}	MFLUCC 17-0829*	MG828912	MG829022	MG829129	MG829209
Melanocucurbitaria uktampratovii ^{T}	**TASM 6176**	**PQ453018**	**PQ453820**		**PQ441826**
Melanodiplodia tianschanica ^{T}	MFLUCC 17-0805*	MG828913	MG829023	MG829130	MG829210
Melanodiplodia tianschanica ^{T}	TASM 6111*	MG828914	MG829024	MG829131	MG829211
Melanodiplodia tianschanica ^{T}	TASM 6112	MG828915	MG829025	MG829132	MG829212
Melanomma japonicum	MAFF 239634*	LC203321	LC203339	LC203293	LC203367
Melanomma japonicum	KT 3425*	LC203320	LC203338	LC203292	LC203366
Melanomma pulvis-pyrius ^{T}	CBS 124080*	MH863349	GU456323	GU456302	GU456265
Monoseptella rosae ^{T}	MFLUCC 17-0815*	MG828916	MG829026	MG829133	MG829213
Muriformistrickeria rosae ^{T}	MFLU 16-0227*	MG828918	MG829028	MG829135	MG829215
Muriformistrickeria rubi ^{T}	MFLUCC 17-2550	MG828919	MG829029	MG829136	MG829216
Muriformistrickeria rubi ^{T}	MFLUCC 15-0681*	NA	KT934253	KT934257	KT934261
Neobyssosphaeria clematidis ^{T}	MFLUCC 17-0794*	NA	MT214566	MT408594	NA
Petrakia echinata ^{T}	L54	NA	NA	KY190007	KY190015
Petrakia echinata ^{T}	CBS 133070	JQ691628	LC203352	LC203306	LC203380
Phragmocephala atra	MFLUCC 15-0021	KP698721	KP698725	KP698729	NA
Phragmotrichum chailletii ^{T}	CPC 33263*	MN313812	MN317293	NA	MN313858
Phragmotrichum chailletii ^{T}	CPC 33341	MN313813	MN317294	NA	MN313859

Taxon	Strain/ Culture accession no	GenBank accession No.			
		ITS	LSU	SSU	TEF-1
Phragmocephala garethjonesii	MFLUCC 15-0018*	KP698722	KP698726	KP698730	NA
Pleotrichocladium opacum ^{T}	AU-BD04	JN995638	JN941370	JN938733	NA
Pleotrichocladium opacum ^{T}	FMR 12416*	KY853462	KY853523	NA	NA
Praetumpfia obducens ^{T}	C2	KY189982	NA	NA	KY190017
Praetumpfía obducens ^{T}	C54	KY189984	NA	KY190008	KY190019
Pseudobyssosphaeria bambusae ^{T}	MFLU 18-0151*	MG737556	MG737555	NA	MG737557
Pseudodidymella minima	KT 2918*	LC203333	LC203358	LC203312	LC203386
Pseudodidymella fagi ^{T}	H 2579*	LC150787	LC203356	LC203310	LC203384
Pseudostrickeria ononidis	MFLUCC 14-0949*	NA	KT934255	KT934259	KT934263
Pseudostrickeria rosae	MFLUCC 17-0643*	MG828954	MG829065	MG829169	MG829234
Pseudotrichia mutabilis	SMH 1541	NA	GU385209	NA	NA
Pseudotrichia mutabilis	WU 36923	KY189988	NA	NA	KY190022
Sarimanas pseudofluviatile	KT760*	LC001717	LC001714	LC001711	NA
Sarimanas shirakamiense ^{T}	HHUF 30454*	NR_138017	NG_059803	NG_061263	NA
Seifertia alpina	ZT Myc 59953*	MK502003	MK502026	MK502037	MK502083
Seifertia azaleae ^{T}	ZT Myc 59954	MK502004	MK502028	MK502038	MK502085
Tumularia aquatica	CBS 212.46*	MH856165	MH867689	NA	NA
Tumularia tuberculata ^{T}	CBS 256.84	NA	GU301851	NA	GU349006
Uzbekistanica rosae-hissaricae ^{T}	MFLUCC 17-0819*	MG828975	MG829087	MG829187	MG829242
Uzbekistanica yakutkhanika ^{T}	MFLUCC 17-0842*	MG828978	MG829090	MG829190	MG829245
Uzbekistanica pruni ^{T}	MFLU 17-2136*	MN758893	MN759024	NA	MN784097
Uzbekistanica vitis-viniferae ^{T}	CPC 35793*	MT223867	MT223938	NA	NA
Xenostigmina zilleri^{T}	CBS 115685	FJ839638	FJ839674	LC203316	LC203390
Xenostigmina zilleri^{T}	CBS 115686	GU269841	FJ839676	LC203317	LC203391

Results

Phylogenetic analyses

Single and multi-gene analyses of LSU, SSU, ITS, and TEF-1 were conducted on all accessible sequences of Melanommataceae species to compare tree topology and clade stability (data not shown). Based on these analyses and BLAST results, 68 isolates, including outgroup taxa, were selected for the combined gene analysis (Table 1). The phylogenetic analyses incorporated 3,030 characters, including gaps, from the combined LSU, SSU, ITS, and TEF-1 sequences. The RAxML analysis of the combined data set generated the best scoring tree (Fig. 1). The final ML optimization likelihood value was -14235.344070. There were 22.81% undetermined characters or gaps and 853 distinct alignment patterns. Estimated base frequencies were A = 0.249838, C = 0.234863, G = 0.267108, T = 0.248191; substitution rates AC = 2.297893, AG = 3.198741, AT = 1.875479, CG = 1.160970, CT = 13.099544, GT = 1.0; proportion of invariable sites I = 0.612009; gamma distribution shape parameter α = 0.532932. The Bayesian analysis has resulted in 20,000 trees after 2,000,000 generations. All analyses (ML and BYPP) showed similar topologies and agreed with previous studies (Gao et al. 2023; Tennakoon et al. 2024). According to the multi-gene phylogeny, TASM 6176 groups in a sister clade to *Melanocucurbitaria uzbekistanica* (MFLUCC 17-0829) with 90% ML and 1.00 BYPP statistical support. Our isolate MFLUCC 24-0466 clusters with *Melanocamarosporioides ugamica* (MFLUCC 17-2314) with 99% ML and 1.00 BYPP statistical support.

Figure 1. Phylogram generated from maximum likelihood analysis based on combined LSU, SSU, ITS and TEF-1 sequence data for Melanommataceae. The tree is rooted with *Cyclothyriella rubronotata* (CBS 121892, CBS 141486). The new isolates are in red and ex-type strains and are shown in boldface. Bootstrap support values for maximum likelihood (ML) equal to or greater than 70% and Bayesian posterior probabilities (BYPP) equal to or greater than 0.90 are given above the nodes, respectively.

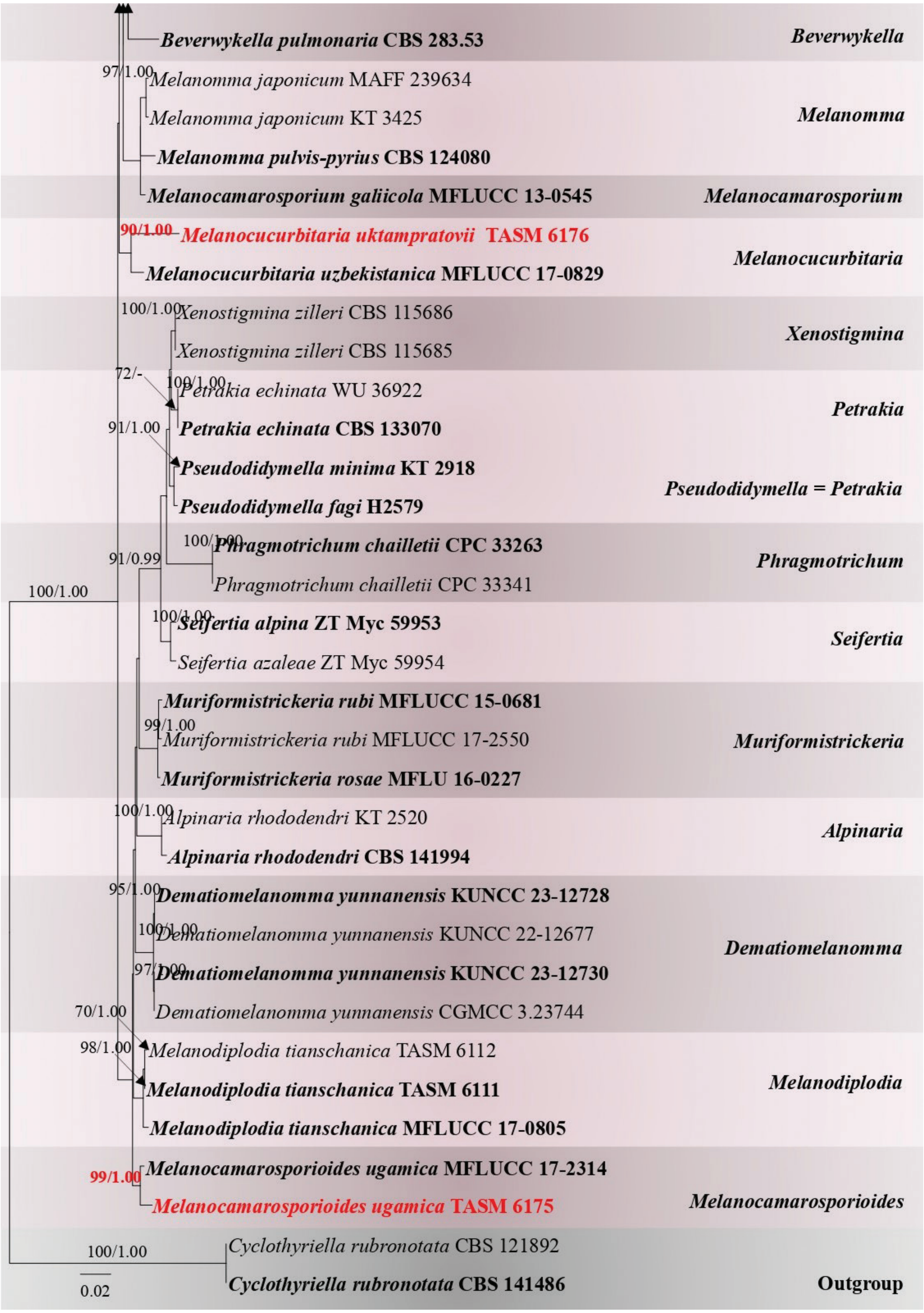

Figure 1. Continued.

Taxonomy

Melanocucurbitaria uktampratovii D. Pem, R. Jeewon, Gafforov & K. D. Hyde, sp. nov.

Index Fungorum: IF902644
Facesoffungi Number: FoF16743
Fig. 2

Etymology. uktam-pratovii (Lat.) in honor of Uzbek scientist, Prof. Uktam Pratovich Pratov (1934–2018), for his contribution to the botanical research in Central Asian countries.

Description. ***Saprobic*** on dead branches of *Salvia karelinii* J. B. Walker. ***Sexual morph*****:** ***Ascomata*** 200–500 μm wide, 250–400 μm high scattered to gregarious, immersed or semi erumpent, carbonaceous, dark brown to black, globose to subglobose, papillate. ***Ostiole*** indistinct, with a small papilla. ***Peridium*** 25–35 μm, 3–5 layers, inner layers composed of subhyaline to light brown cells of *textura angularis*, outer layer composed of irregular, thick-walled, highly pigmented dark-brown cells of *textura angularis*. ***Hamathecium*** 1.5–2.0 μm (n = 10) wide, comprising numerous, filamentous, branched, anastomosing, septate, hyaline, pseudoparaphyses. ***Asci*** 160–175 × 13–14 μm ($\bar{x}$ = 164.0 × 13.6 μm, n = 10), 8-spored, bitunicate, fissitunicate, cylindrical, pedicellate, apically rounded, with an ocular chamber. ***Ascospores*** 18–25 × 7–9 μm ($\bar{x}$ = 20.8 × 7.7 μm, n = 10), uniseriate, ellipsoidal, muriform, 4–6 transverse septa, with 3–7 longitudinal septa, slightly constricted at the septa, more at the middle septum, at first hyaline turning golden brown to dark-brown at maturity, obtuse at the ends, lacking a mucilaginous sheath, smooth and thick-walled. ***Asexual morph*****:** Undetermined.

Culture characteristics. Colonies on MEA, reaching 20–25 mm diam. after 3 weeks at 25 °C, medium dense in middle, medium sparse at the edges, irregular, umbonate, velvety to floccose, undulated edges, smooth.

Known distribution (based on molecular data). Uzbekistan (Wanasinghe et al. 2018; this study).

Confirmed hosts (based on molecular data). *Acer pubescens* Franch (Sapindaceae) (Wanasinghe et al. 2018), *Salvia karelinii* (Lamiaceae) (this study).

Material examined. UZBEKISTAN • Surkhandarya Province, Baysun District, Omonxona Village, South-Western Hissar Mountains, on dead branches of *Salvia karelinii* (Lamiaceae), 13 May 2016, Y. Gafforov, I. Urinboev, YG-S29-3 (TASM 6176, holotype; MFLU 17-0071, isotype), ex-type living culture MFLUCC 17-1953.

GenBank numbers. LSU: PQ453820, ITS: PQ453018, TEF-1: PQ441826.

Notes. The morphology of our collection (TASM 6176) resembles the type species *Melanocucurbitaria uzbekistanica* (TASM 6109) in its scattered to gregarious, dark brown to black, globose to subglobose, papillate ascomata, cylindrical, pedicellate asci and ellipsoidal, muriform ascospores (Wanasinghe et al. 2018). Our collection is different from the type species *M. uzbekistanica* in having smaller ascomata (200–400 × 250–400 μm vs. 500–700 × 550–750 μm), smaller asci (160–175 × 13–14 μm vs. 280–300 × 19–23 μm), smaller ascospores (18–25 × 7–9 μm vs. 37–47 × 17–19 μm) and number of septa (4–6 transverse septa, 3–7 longitudinal septa vs. 6–8 transverse septa, 3–4 longitudinal septa) (Wanasinghe et al. 2018). *Melanocucurbitaria uzbekistanica* also differs from *M. uktampratovii* in having black, semi-immersed ascomata,

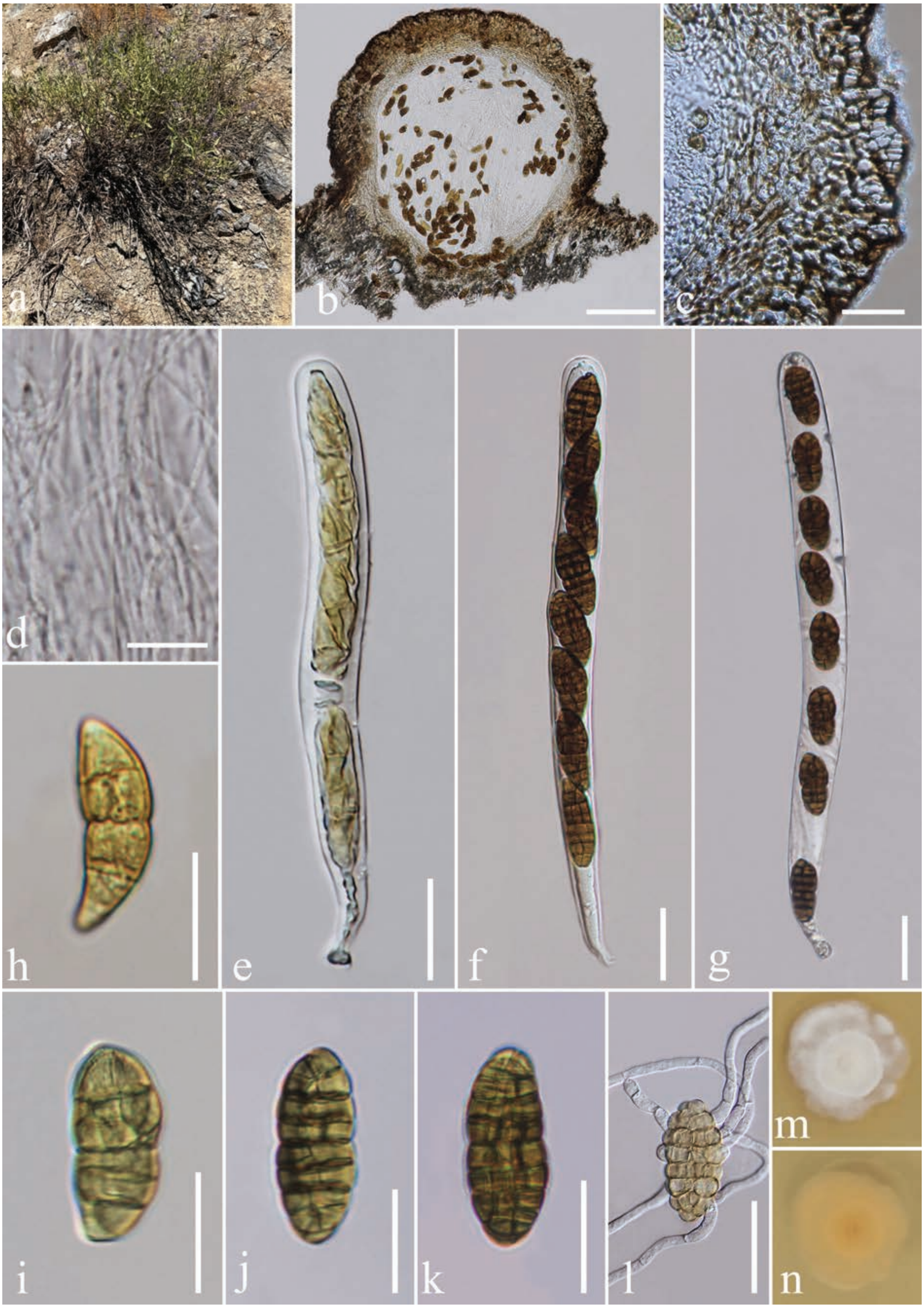

Figure 2. *Melanocucurbitaria uktampratovii* sp. nov. (TASM 6176, holotype) **a** habitat **b** section of ascoma **c** peridium **d** pseudoparaphyses **e–g** asci **h–k** ascospores **l** germinated ascospore **m, n** culture characteristics on MEA (**m** above view, **n** reverse view). Scale bars: 100 µm (**b**); 20 µm (**c, e–l**); 10 µm (**d**).

ostiole filled with brown cells, ascospores which are pale brown at maturity, broadly rounded at the ends, surrounded by a mucilaginous sheath when immature while *M. uktampratovii* has immersed or semi erumpent ascomata, indistinct ostiole, with a small papilla, ascospores which are dark brown at maturity, obtuse at the ends and lacking a mucilaginous sheath. According to the multi-gene phylogeny, our collection clusters with the isolate of *Melanocucurbitaria uzbekistanica* (MFLUCC 17-0829) in 90% ML and 1.00 BYPP supported clade. The nucleotide base comparison of LSU, ITS and TEF-1 regions showed that our strain (TASM 6176) differs from the type strain of *M. uzbekistanica* (MFLUCC 17-0829) by 23/865 bp (2.65%), 15/439 bp (3.41%) and 20/571 bp (3.5%), respectively. Therefore, we introduce our collection as a new species based on morphology and phylogeny. The phylogenetic placement of our strain (TASM 6176) is shown in Fig. 1.

Melanocamarosporioides ugamica **D. Pem, R. Jeewon, Gafforov & K. D. Hyde, in Pem et al. Mycol. Progr. 18(3): 474 (2019)**

Index Fungorum: IF554297
Facesoffungi Number: FoF04363
Fig. 3

Description. ***Saprobic*** on dead branches of *Rosa ecae* Aitch. ***Sexual morph*****:** ***Ascomata*** 145–335 µm wide, 70–195 µm high, solitary to gregarious, flattened, semi-immersed to superficial, dark brown to black, globose to ovoid, carbonaceous, papillate. ***Peridium*** 15–20 µm, two layered, inner layers composed of hyaline to subhyaline cells of *textura prismatica*, outer layer composed of irregular, thick-walled, brown cells of *textura angularis*. ***Hamathecium*** comprising numerous, 1.3–2.5 µm (n = 10) wide, filamentous, branched, anastomosing, septate, hyaline, pseudoparaphyses. ***Asci*** 90–120 × 14.5–16.7 µm (x̄ = 104.9 × 15.5 µm, n = 10), 8-spored, bitunicate, fissitunicate, cylindrical-clavate, pedicellate, apically rounded, with a minute ocular chamber. ***Ascospores*** 19.2–25.0 × 7.9–10.0 µm (x̄ = 21.8 × 8.7 µm, n = 10), uni to biseriate, ellipsoidal, muriform, 5–7 transversely septate, with 5–11 vertical septa, slightly constricted at the septa, dark brown, broadly rounded at the ends, smooth and thick-walled. ***Asexual morph*****:** Undetermined.

Culture characteristics. Colonies on MEA, reaching 25–30 mm diam. after 3 weeks at 25 °C, medium dense, circular, flattened to slightly raised, smooth surface, with edge entire, cottony, mycelium composed of septate, branched hyphae, colony from above whitish, reverse whitish gray to reddish brown in center gradually becoming white towards the edges from the below.

Known distribution (based on molecular data). Uzbekistan (Pem et al. 2019b, this study).

Confirmed hosts (based on molecular data). *Lonicera altmannii* (Caprifoliaceae) (Pem et al. 2019b), *Rosa ecae* (this study).

Material examined. Uzbekistan • Tashkent Province, Bostanlik District, Ugam-Chatkal National Nature Park, Charvak Reservoir, Chimyon in Western Tien Shan Mountain, on dead branches of *Rosa ecae*, 21 July 2019, Y. Gafforov, A. Esankulov, YG-S2-2 (TASM 6175), living culture MFLUCC 24-0466.

GenBank numbers. LSU: PQ453821, SSU: PQ433587, ITS: PQ453019.

Figure 3. *Melanocamarosporioides ugamica* (TASM 6175, new host record and sexual morph) **a, b** appearance of ascomata on the host surface **c** pseudoparaphyses **d–g** asci **h, i** ascospores **j** germinated ascospore **k, l** culture characteristics on MEA (**k** above view, **l** reverse view). Scale bars: 500 μm (**a, b**); 5 μm (**c**); 20 μm (**d–g, j**); 10 μm (**h, i**).

Notes. Our new isolate MFLUCC 24-0466 is morphologically and phylogenetically related to *Melanocamarosporioides ugamica* (MFLUCC 17-2314) but collected from a different host. *Melanocamarosporioides ugamica* was reported from

Uzbekistan on dead trunk and branches of *Lonicera altmannii* (Caprifoliaceae) (Pem et al. 2019b), while our collection was found on dead branches of *Rosa ecae*. *Melanocamarosporioides ugamica* (TASM 6133) is characterized by an asexual morph, namely black, globose, superficial conidiomata and large conidia, which are multiseptate and distinctively dark brown, while our collection (TASM 6175) is in its sexual state, characterized by globose to ovoid, dark brown to black ascomata, cylindrical asci, and dark brown, ellipsoidal, muriform ascospores. Multi-gene phylogeny (LSU, SSU, ITS, and TEF-1) shows that our collection groups with *Melanocamarosporioides ugamica* (MFLUCC 17-2314) in a 99% ML and 1.00 BYPP supported clade. With regard to DNA sequence data comparison, there is a difference of 0.69% (6 out of 865), 0.84% (9 out of 1067), and 0% (0 out of 470) in nucleotide variations within the LSU, SSU, and ITS genes, respectively. Hence, we introduce our collection as a new host record of *Melanocamarosporioides* from *Rosa ecae*. This is also the first sexual morph report in *Melanocamarosporioides*. The phylogenetic placement of our strain TASM 6175 is shown in Fig. 1.

Discussion

During surveys on saprobic fungi associated with flowering plants in Uzbekistan, we found two taxa, which belong to Melanommataceae. The newly described taxon is *Melanocucurbitaria uktampratovii*, which exhibits distinct characteristics compared to the type species *M. uzbekistanica*. *Melanocucurbitaria uktampratovii* is characterized by scattered to gregarious, globose to subglobose, dark brown to black ascomata; cylindrical, pedicellate asci with an ocular chamber; ellipsoidal, muriform ascospores with 4–6 transverse septa and 3–7 longitudinal septa. *Melanocucurbitaria uzbekistanica* is characterized by larger ascomata, asci, and ascospores with 6–8 transverse septa and 3–4 longitudinal septa compared to *M. uktampratovii*, which has 4–6 transverse septa and 3–7 longitudinal septa. In our phylogeny, *Melanocucurbitaria uktampratovii* is closely related to *M. uzbekistanica. Melanocucurbitaria uzbekistanica* is characterized by larger ascomata, asci, and ascospores compared to *M. uktampratovii*. *Melanocucurbitaria uktampratovii* bears morphological resemblance to the type species of *Gemmamyces*, *Melanocamarosporoides*, *Muriformistrickeria*, *Praetumpfia*, *Pseudostrickeria*, and *Uzbekistanica* in having muriform ascospores (Wanasinghe et al. 2018; Gao et al. 2023), but *M. uktampratovii* is distinctly separated from these genera in phylogenetic analysis. In addition, a comparison of nucleotides across several genes also supports that our new taxon is sufficiently distinct to warrant its establishment as a new species.

Melanocamarosporoides ugamica is the type species of *Melanocamarosporoides*. Pem et al. (2019b) introduced the asexual morph of *Melanocamarosporioides* collected on dead trunks and branches of *Lonicera altmannii* (Caprifoliaceae) in Uzbekistan. *Melanocamarosporioides* is distinct from other genera in Melanommataceae based on its multiseptate, large, dark-brown conidia (Pem et al. 2019b). Up to now, the sexual state has not been observed. In this study, we found the sexual morph of *Melanocamarosporoides ugamica* isolated for the first time from dead branches of *Rosa ecae* in Uzbekistan. So far, there is only one species in this genus, and its relationships were not well resolved in previous studies. In our study, multigene phylogeny shows a strong relationship with *Melanodiplodia tianschanica* and *Dematiomelanomma yunnanense*, but *Melanocamarosporioides ugamica* (TASM 6175) can be differentiated based on various morphological features. *Melanodiplodia* produces diplodia-like conidia (Wanasinghe et al. 2018), *Dematiomelanomma* has camarographium-like conidia, whereas *Melanocamarosporioides* forms camarosporium-like conidia (Pem et al. 2019b). Furthermore, the sexual morph of *Melanocamarosporioides ugamica* and *Dematiomelanomma yunnanense* are different in their asci (cylindrical vs. cylindrical-clavate) and ascospore (5–7 transversely septate, with 5–11 vertical septa, lacking a sheath vs. 3–7 transversely septate, and 1–3 vertical septa with a mucilaginous sheath) characteristics. Further sampling is necessary to improve our knowledge of the diversity and ecology of Melanommataceae species on flowering plants in arid and semi-arid habitats.

Conclusion

This study describes a new species in *Melanocucurbitaria* and provides a new record of the sexual morph in *Melanocamarosporioides*, using both morphological and molecular data. To date, there are 25 sexual and 10 asexual morph genera within Melanommataceae (Hongsanan et al. 2020; Pem et al. 2024). In addition to the description of new species, it is essential to elucidate the relationships between sexual and asexual morphs to fully understand the life cycles of microfungi and enhance fungal taxonomy (Lücking et al. 2020; Zhou and May 2022). This understanding will aid in accurately estimating the total number of fungal species worldwide, as previous global estimates relied heavily on the ratio of fungi to their occurrences on hosts (Wu et al. 2019; Niskanen et al. 2023). Numerous ascomycete and basidiomycetous fungi have been discovered in Uzbekistan, and it is likely that many more species await identification in this region. Therefore, conducting comprehensive mycological research in this Central Asia region is essential to uncover its full fungal diversity.

Acknowledgements

Kevin D. Hyde and Rajesh Jeewon acknowledge the financial support provided by the Distinguished Scientist Fellowship Program (DSFP), King Saud University, Kingdom of Saudi Arabia. Yusufjon Gafforov thanks the Innovative Development Agency, State Scientific and Technical Program of Institute of Botany of Uzbekistan Academy of Sciences (2021–2024). Indunil Chinthani Senanayake thanks the research funding program of Kunming Institute of Botany, Chinese Academy of Science. Dhandevi Pem thanks Dhanushka N. Wanasinghe for assistance.

Additional information

Conflict of interest

The authors have declared that no competing interests exist.

Ethical statement

No ethical statement was reported.

Funding

No funding was reported.

Author contributions

Conceptualization: KDH, RJ Data curation: DP, IU, AE Formal analysis: DP, ICS Funding acquisition: KDH, RJ, YG, AAF Investigation: DP Methodology: DP, KDH, RJ Project administration: KDH Supervision: KDH, RJ Writing - original draft: DP, ICS, RJ, YG, KDH Writing - review and editing: DP, ICS, RJ, YG, KDH.

Author ORCIDs

Dhandevi Pem https://orcid.org/0000-0003-1831-9266
Rajesh Jeewon https://orcid.org/0000-0002-8563-957X
Yusufjon Gafforov https://orcid.org/0000-0003-3076-4709
Islomjon Urinboev https://orcid.org/0009-0009-1653-000X
Abdulwahed Fahad Alrefaei https://orcid.org/0000-0002-3761-6656
Indunil C. Senanayake https://orcid.org/0000-0002-7165-2394
Alijon Esankulov https://orcid.org/0009-0000-1862-7555
Kevin David Hyde https://orcid.org/0000-0002-2191-0762

Data availability

All of the data that support the findings of this study are available in the main text.

References

Abdurazakov AA, Bulgakov TS, Kholmuradova TN, Gafforov YS (2021) Powdery mildew fungi (Erysiphaceae) of the Fergana Valley (within Uzbekistan): A first annotated checklist. Novosti sistematiki nizshikh rastenii 55: 55–78. https://doi.org/10.31111/nsnr/2021.55.1.55

Aime MC, Miller AN, Aoki T, Bensch K (2021) How to publish a new fungal species, or name, version 3.0. IMA Fungus 12: 11. https://doi.org/10.1186/s43008-021-00063-1

Almeida DAC, Gusmão LFP, Miller AN (2017) A new species of *Bertiella* (Melanommataceae) from Brazil and a key to accepted species. Mycosphere 8: 392–396. https://doi.org/10.5943/mycosphere/8/4/1

Aluthmuhandiram JVS, Wanasinghe DN, Chethana KWT, Gafforov Y, Saichana N, Li XH, Yan J, Mamarakhimov OM (2022) Lophiostomataceae (Dothideomycetes): Introducing *Lophiostoma khanzadakirgizbaeva* sp. nov. and *Paucispora xishanensis* sp. nov. Phytotaxa 559: 247–262. https://doi.org/10.11646/phytotaxa.559.3.3

Appadoo MA, Wanasinghe DN, Gafforov Y, Chethana KT, Abdurazakov A, Hyde KD, Li Q (2021) Morphological and phylogenetic insights reveal *Cucurbitaria berberidicola* (Cucurbitariaceae, Pleosporales) as a new species from Uzbekistan. Phytotaxa 518: 1–13. https://doi.org/10.11646/phytotaxa.518.1.1

Cheek M, Lughadha EN, Kirk PM, Lindon H, Carretero J, Looney B, Douglas B, Haelewaters D, Gaya E, Llewellyn T, Ainsworth AM, Gafforov Y, Hyde KD, Crous P, Hughes M, Walker BE, Forzza RC, Wong KM, Niskanen T (2020) New scientific discoveries: Plants and fungi. Plants, People, Planet 2: 371–388. https://doi.org/10.1002/ppp3.10148

Chethana KWT, Manawasinghe IS, Hurdeal VG, Bhunjun CS, Appadoo MA, Gentekaki E, Raspé O, Promputtha I, Hyde KD (2021) What are fungal species and how to delineate them? Fungal Diversity 109: 1–25. https://doi.org/10.1007/s13225-021-00483-9

Dong W, Wang B, Hyde KD, McKenzie EHC, Raja HA, Tanaka K, Abdel-Wahab MA, Abdel-Aziz FA, Doilom M, Phookamsak R, Hongsanan S, Wanasinghe DN, Yu XD, Wang GN, Yang H, Yang J, Thambugala KM, Tian Q, Luo ZL, Yang JB, Miller AN, Fournier J, Boonmee S, Hu DM, Nalumpang S, Zhang H (2020) Freshwater Dothideomycetes. Fungal Diversity 105: 319–575. https://doi.org/10.1007/s13225-020-00463-5

Dong W, Hyde KD, Jeewon R, Liao CF, Zhao HJ, Kularathnage ND, Li H, Yang YH, Pem D, Shu YX, Gafforov Y, Manawasinghe IS, Doilom M (2023) Mycosphere notes 449–468: Saprobic and endophytic fungi in China, Thailand, and Uzbekistan. Mycosphere 14: 2208–2262. https://doi.org/10.5943/mycosphere/14/1/26

Dong JH, Li Q, Yuan Q, Luo YX, Zhang XC, Dai YF, Zhou Q, Liu XF, Deng YL, Zhou HM, Muhammad A, Zhao CL (2024) Species diversity, taxonomy, molecular systematics and divergence time of wood-inhabiting fungi in Yunnan-Guizhou Plateau, Asia. Mycosphere 15: 1110–1293. https://doi.org/10.5943/mycosphere/15/1/10

Gafforov YS (2017) A preliminary checklist of ascomycetous microfungi from Southern Uzbekistan. Mycosphere 8: 660–696. https://doi.org/10.5943/mycosphere/8/4/12

Gafforov Y, Hoshino T (2015) Remarks on *Typhula* sp. in Uzbekistan. Mycoscience 56: 109–113. https://doi.org/10.1016/j.myc.2014.04.003

Gafforov Y, Rakhimov D (2017) *Diplodia* and *Dothiorella* species (Botryosphaeriaceae, Ascomycota) from Uzbekistan. Journal of the Botanical Research Institute of Texas 11: 455–467. https://doi.org/10.17348/jbrit.v11.i2.1083

Gafforov Y, Phookamsak R, Jiang HB, Wanasinghe DN, Juliev M (2019) *Ophiobolus hydei* sp. nov. (Phaeosphaeriaceae, Ascomycota) from *Cirsium* and *Phlomoides* in Uzbekistan. Botany 97: 671–680. https://doi.org/10.1139/cjb-2019-0118

Gafforov Y, Yarasheva M, Wang X-W, Rašeta M, Rakhimova Y, Kyzmetova L, Bavlankulova K, Rapior S, Chen J-J, Langer E, Munnavarov B, Aslonov Z, Bakokhoja B, Zhou L-W (2025) Annotated Checklist of Poroid Hymenochaetoid Fungi in Central Asia: Taxonomic Diversity, Ecological Roles, and Potential Distribution Patterns. Journal of Fungi 11(1): 37. https://doi.org/10.3390/jof11010037

Gao Y, Zhong T, Bhat JD, Gomes de Farias AR, Dawoud TM, Hyde KD, Xiong W, Li Y, Gui H, Yang X, Wu S, Wanasinghe DN (2023) Pleomorphic *Dematiomelanommayunnanense* gen. et sp. nov. (Ascomycota, Melanommataceae) from grassland vegetation in Yunnan, China. MycoKeys 98: 273–297. https://doi.org/10.3897/mycokeys.98.107093

Hall TA (1999) BioEdit: A user-friendly biological sequence alignment editor and analysis program for Windows 95/98/NT. Nucleic Acids Symposium Series 41: 95–98. https://doi.org/10.14601/Phytopathol_Mediterr-14998u1.29

Hongsanan S, Hyde KD, Phookamsak R, Wanasinghe DN, McKenzie EHC, Sarma VV, Boonmee S, Lücking R, Bhat DJ, Liu NG, Tennakoon DS, Pem D, Karunarathna A, Jiang SH, Jones EBG, Phillips AJL, Manawasinghe IS, Tibpromma S, Jayasiri SC, Sandamali DS, Jayawardena RS, Wijayawardene NN, Ekanayaka AH, Jeewon R, Lu YZ, Dissanayake AJ, Zeng XY, Luo ZL, Tian Q, Phukhamsakda C, Thambugala KM, Dai DQ, Chethana KWT, Samarakoon MC, Ertz D, Bao DF, Doilom M, Liu JK, Pérez-Ortega S, Suija A, Senwanna C, Wijesinghe SN, Konta S, Niranjan M, Zhang SN, Ariyawansa HA, Jiang HB, Zhang JF, Norphanphoun C, de Silva NI, Thiyagaraja V, Zhang H, Bezerra JDP, Miranda-González R, Aptroot A, Kashiwadani H, Harishchandra D, Sérusiaux E, Aluthmuhandiram JVS, Abeywickrama PD, Devadatha B, Wu HX, Moon KH, Gueidan C, Schumm F, Bundhun D, Mapook A, Monkai J, Chomnunti P, Suetrong S, Chaiwan N, Dayarathne MC, Yang J, Rathnayaka AR, Bhunjun CS, Xu JC, Zheng JS, Liu G, Feng Y, Xie N (2020) Refined families of Dothideomycetes: Dothideomycetidae and Pleosporomycetidae. Mycosphere 11: 1553–2107. https://doi.org/10.5943/mycosphere/11/1/13

Htet ZH, Mapook A, Gafforov Y, Chethana KT, Lumyong S, Hyde KD (2021) Molecular phylogeny and diversity of *Laburnicola* (Didymosphaeriaceae): A new species from Uzbekistan. Phytotaxa 527: 177–190. https://doi.org/10.11646/phytotaxa.527.3.2

Hyde KD, Chaiwan N, Norphanphoun C, Boonmee S, Camporesi E, Chethana KWT, Dayarathne MC, de Silva NI, Dissanayake AJ, Ekanayaka AH, Hongsanan S, Huang SK, Jayasiri SC, Jayawardena R, Jiang HB, Karunarathna A, Lin CG, Liu JK, Liu NG, Lu YZ, Luo ZL, Maharachchimbura SSN, Manawasinghe IS, Pem D, Perera RH, Phukhamsakda C, Samarakoon MC, Senwanna C, Shang QJ, Tennakoon DS, Thambugala KM, Tibpromma S, Wanasinghe DN, Xiao YP, Yang J, Zeng XY, Zhang JF, Zhang SN, Bulgakov TS, Bhat DJ, Cheewangkoon R, Goh TK, Jones EBG, Kang JC, Jeewon R, Liu ZY, Lumyong S, Kuo CH, McKenzie EHC, Wen TC, Yan JY, Zhao Q (2018) Mycosphere notes 169–224. Mycosphere 9: 271–430. https://doi.org/10.5943/mycosphere/9/2/8

Hyde KD, Xu J, Rapior S, Jeewon R, Lumyong S, Niego AGT, Abeywickrama PD, Aluthmuhandiram JVS, Brahamanage RS, Brooks S, Chaiyasen A, Chethana KWT, Chomnunti P, Chepkirui C, Chuankid B, de Silva NI, Doilom M, Faulds C, Gentekaki E, Gopalan V, Kakumyan P, Harishchandra D, Hemachandran H, Hongsanan S, Karunarathna A, Karunarathna SC, Khan S, Kumla J, Jayawardena RS, Liu JK, Liu N, Luangharn T, Macabeo APG, Marasinghe DS, Meeks D, Mortimer PE, Mueller P, Nadir S, Nataraja KN, Nontachaiyapoom S, O'Brien M, Penkhrue W, Phukhamsakda C, Ramanan US, Rathnayaka AR, Sadaba RB, Sandargo B, Samarakoon BC, Tennakoon DS, Siva R, Sriprom W, Suryanarayanan TS, Sujarit K, Suwannarach N, Suwunwong T, Thongbai B, Thongklang N, Wei D, Wijesinghe SN, Winiski J, Yan J, Yasanthika E, Stadler M (2019) The amazing potential of fungi, 50 ways we can exploit fungi industrially. Fungal Diversity 97: 1–36. https://doi.org/10.1007/s13225-019-00430-9

Hyde KD, Abdel-Wahab MA, Abdollahzadeh J, Abeywickrama PD, Absalan S, Afshari N, Ainsworth AM, Akulov OY, Aleoshin VV, Al-Sadi AM, Alvarado P, Alves A, Alves-Silva G, Amalfi M, Amira Y, Amuhenage TB, Anderson J, Antonín V, Aouali S, Aptroot A, Apurillo CCS, Araújo JPM, Ariyawansa HA, Armand A, Arumugam E, Asghari R, Assis DMA, Atienza V, Avasthi S, Azevedo E, Bahkali AH, Bakhshi M, Banihashemi Z, Bao DF, Baral HO, Barata M, Barbosa F, Barbosa RN, Barreto RW, Baschien C, Belamesiatseva DB, Bennett Reuel M, Bera I, Bezerra JDP, Bezerra JL, Bhat DJ, Bhunjun CS, Bianchinotti MV, Błaszkowski J, Blondelle A, Boekhout T, Bonito G, Boonmee S, Boonyuen N, Bregant C, Buchanan P, Bundhun D, Burgaud G, Burgess T, Buyck B, Cabarroi-Hernández M, Cáceres MES, Caeiro MF, Cai L, Cai MF, Calabon MS, Calaça FJS, Callalli M, Camara MPS, Cano-Lira JF, Cantillo T, Cao B, Carlavilla JR, Carvalho A, Castañeda-Ruiz RF, Castlebury L, Castro-Jauregui O, Catania MDV, Cavalcanti LH, Cazabonne J, Cedeño-Sanchez ML, Chaharmiri-Dokhaharani S, Chaiwan N, Chakraborty N, Chaverri P, Cheewangkoon R, Chen C, Chen CY, Chen KH, Chen J, Chen Q, Chen WH, Chen YP, Chethana KWT, Coleine C, Condé TO, Corazon-Guivin MA, Cortés-Pérez A, Costa-Rezende DH, Courtecuisse R, Crouch JA, Crous PW, Cui BK, Cui YY, da Silva DKA, da Silva GA, da Silva IR, da Silva RMF, da Silva Santos AC, Dai DQ, Dai YC, Damm U, Darmostuk V Daroodi Zoha, Das K, Das K, Davoodian N, Davydov EA, Dayarathne MC, Decock C, de Groot MD, De Kesel A, dela Cruz TEE, De Lange R, Delgado G, Denchev CM, Denchev TT, de Oliveira NT, de Silva NI, de Souza FA, Dentinger B, Devadatha B, Dianese JC, Dima B, Diniz AG, Dissanayake AJ, Dissanayake LS, Doğan HH, Doilom M, Dolatabadi S, Dong W, Dong ZY, Dos Santos LA, Drechsler-Santos ER, Du TY, Dubey MK, Dutta AK, Egidi E, Elliott TF, Elshahed MS, Erdoğdu M, Ertz D, Etayo J, Evans HC, Fan XL, Fan YG, Fedosova AG, Fell J, Fernandes I, Firmino AL, Fiuza PO, Flakus A, Fragoso de Souza CA, Frisvad JC, Fryar SC, Gabaldón T, Gajanayake AJ, Galindo LJ, Gannibal PB, García D, García-Sandoval SR, Garrido-Benavent I, Garzoli L, Gautam AK, Ge ZW, Gené DJ, Gentekaki E, Ghobad-Nejhad M, Giachini AJ, Gibertoni TB, Góes-Neto A, Gomdola D, Gomes de Farias AR, Gorjón SP, Goto BT, Granados-Montero MM, Griffith GW, Groenewald JZ, Groenewald M, Grossart HP, Gueidan C, Gunarathne A, Gunaseelan S, Gusmão LFP, Gutierrez AC, GuzmánDávalos L, Haelewaters D, Halling R, Han YF, Hapuarachchi KK, Harder CB, Harrington TC, Hattori T, He MQ, He S, He SH, Healy R, Herández-Restrepo M, Heredia G, Hodge KT, HolgadoRojas M, Hongsanan S, Horak E, Hosoya T, Houbraken J, Huang SK, Huanraluek N, Hur JS, Hurdeal VG, Hustad VP, Iotti M, Iturriaga T, Jafar E, Janik P, Jayalal RGU, Jayasiri SC, Jayawardena RS, Jeewon R, Jerônimo GH, Jesus AL, Jin J, Johnston PR, Jones EBG, Joshi Y, Justo A, Kaishian P, Kakishima M, Kaliyaperumal M, Kang GP, Kang JC, Karimi O, Karpov SA, Karunarathna SC, Kaufmann M, Kemler M, Kezo K, Khyaju S, Kirchmair M, Kirk PM, Kitaura MJ, Klawonn I, Kolarik M, Kong A, Kuhar F, Kukwa M, Kumar S, Kušan I, Lado C, Larsson KH, Latha KPD, Lee HB, Leonardi M, Leontyev DL, Lestari AS, Li CJY, Li DW, Li H, Li HY, Li L, Li QR, Li WL, Li Y, Li YC, Liao CF, Liimatainen K, Lim YW, Lin CG, Linaldeddu BT, Linde CC, Linn MM, Liu F, Liu JK, Liu NG, Liu S, Liu SL, Liu XF, Liu XY, Liu XZ, Liu ZB, Lu L, Lu YZ, Luangharn T, Luangsaard JJ, Lumbsch HT, Lumyong S, Luo L, Luo M, Luo ZL, Ma J, Machado AR, Madagammana AD, Madrid H, Magurno F, Magyar D, Mahadevan N, Maharachchikumbura SSN, Maimaiti Y, Malosso E, Manamgoda DS, Manawasinghe IS, Mapook A, Marasinghe DS, Mardones M, Marin-Felix Y, Márquez R, Masigol H, Matočec N, May T, McKenzie EHC, Meiras-Ottoni A, Melo RFR, Mendes ARL, Mendieta S, Meng QF, Menkis A, Menolli Jr N, Mešić A, Meza Calvo JG, Mikhailov KV, Miller SL, Moncada B, Moncalvo JM, Monteiro JS, Monteiro M, Mora-Montes HM, Moreau PA, Mueller GM, Mukhopadyay S, Murugadoss R, Nagy LG, Najafiniya M, Nanayakkara CM, Nascimento CC, Nei Y, Neves MA, Neuhauser S, Niego AGT, Nilsson RH, Niskanen T, Niveiro N, Noorabadi MT, Noordeloos ME, Norphanphoun C, Nuñez Otaño NB, O'Donnell RP, Oehl F, Olariaga I, Orlando FP, Pang KL, Papp V, Pawłowska J, Peintner U, Pem D, Pereira OL, Perera RH, Perez-Moreno J, Perez-Ortega S, Péter G, Phillips AJL, Phonemany M, Phukhamsakda, Phutthacharoen K, Piepenbring M, Pires-Zottarelli CLA, Poinar G, Pošta A, Prieto M, Promputtha I, Quandt CA, Radek R, Rahnama K, Raj KNA, Rajeshkumar KC, Rämä T, Rambold G, Ramírez-Cruz V, Rasconi S, Rathnayaka AR, Raza M, Ren GC, Robledo GL, Rodriguez-Flakus P, Ronikier A, Rossi W, Ryberg M, Ryvarden LR, Salvador-Montoya CA, Samant B, Samarakoon BC, Samarakoon MC, Sánchez-Castro I, Sánchez-García M, Sandoval-Denis M, Santiago ALCMA, Santamaria B, Santos ACS, Sarma VV, Savchenko A, Savchenko K, Saxena RK, Scholler M, Schoutteten N, Seifollahi E, Selbmann L, Selcuk F, Senanayake IC, Shabashova TG, Shen HW, Shen YM, SilvaFilho AGS, Simmons DR, Singh R, Sir EB, Song Chang-Ge, Souza-Motta CM Sruthi OP, Stadler M, Stchigel AM, Stemler J, Stephenson SL, Strassert JFH, Su HL Su L, Suetrong S, Sulistyo B, Sun YF, Sun YR, Svantesson Sten, Sysouphanthong P, Takamatsu S, Tan TH, Tanaka K, Tang AMC, Tang X, Tanney JB, Tavakol NM, Taylor JE, Taylor PWJ, Tedersoo L, Tennakoon DS, Thamodini GK, Thines M, Thiyagaraja V, Thongklang N, Tiago PV, Tian Q, Tian WH, Tibell L, Tibell S, Tibpromma S, Tkalčec Z, Tomšovský M, Toome-Heller M, Torruella G, Tsurykau A, Udayanga D, Ulukapi M, Untereiner WA, Uzunov BA, Valle LG, Van Caenegem W, Van den Wyngaert S, Van Vooren N, Velez P, Verma RK, Vieira LC, Vieira WAS, Vizzini A, Walker A, Walker AK, Wanasinghe DN, Wang CG, Wang K, Wang SX, Wang XY, Wang Y, Wannasawang N, Wartchow F, Wei DP, Wei XL, White JF, Wijayawardene NN, Wijesinghe SN, Wijesundara DSA, Wisitrassameewong K, Worthy FR, Wu F, Wu G, Wu HX, Wu N, Wu WP, Wurzbacher C, Xiao YP, Xiong YR, Xu LJ, Xu R, Xu RF, Xu RJ, Xu TM, Yakovchenko L, Yan JY, Yang H, Yang J, Yang ZL, Yang YH,Yapa N, Yasanthika E, Youssef NH, Yu FM, Yu Q, fD, Yu YX, Yu ZF, Yuan HS, Yuan Y, Yurkov

A, Zafari D, Zamora JC, Zare R, Zeng M, Zeng NK, Zeng XY, Zhang F, Zhang H, Zhang JF, Zhang JY, Zhang QY, Zhang SN, Zhang W, Zhang Y, Zhang YX, Zhao CL, Zhao H, Zhao Q, Zhao RL, Zhou LW, Zhou M, Zhurbenko MP, Zin HH, Zucconi L (2023) Global consortium for the classification of fungi and fungus-like taxa. Mycosphere 14: 1960–2012. https://doi.org/10.5943/mycosphere/14/1/23

Hyde KD, Noorabadi MT, Thiyagaraja V, He MQ, Johnston PR, Wijesinghe SN, Armand A, Biketova AY, Chethana KWT, Erdoğdu M, Ge ZW, Groenewald JZ, Hongsanan S, Kušan I, Leontyev DV, Li DW, Lin CG, Liu NG, Maharachchikumbura SSN, Matočec N, May TW, McKenzie EHC, Mešić A, Perera RH, Phukhamsakda C, Piątek M, Samarakoon MC, Selcuk F, Senanayake IC, Tanney JB, Tian Q, Vizzini A, Wanasinghe DN, Wannasawang N, Wijayawardene NN, Zhao RL, Abdel-Wahab MA, Abdollahzadeh J, Abeywickrama PD, Abhinav, Absalan S, Acharya K, Afshari N, Afshan NS, Afzalinia S, Ahmadpour SA, Akulov O, Alizadeh A, Alizadeh M, Al-Sadi AM, Alves A, Alves VCS, Alves-Silva G, Antonín V, Aouali S, Aptroot A, Apurillo CCS, Arias RM, Asgari, B, Asghari R, Assis DMA, Assyov B, Atienza V, Aumentado HDR, Avasthi S, Azevedo E, Bakhshi M, Bao DF, Baral HO, Barata M, Barbosa KD, Barbosa RN, Barbosa FR, Baroncelli R, Barreto GG, Baschien C, Bennett RM, Bera I, Bezerra JDP, Bhunjun CS, Bianchinotti MV, Błaszkowski J, Boekhout T, Bonito GM, Boonmee S, Boonyuen N, Bortnikov FM, Bregant C, Bundhun D, Burgaud G, Buyck B, Caeiro MF, Cabarroi-Hernández M, Cai M Feng, Cai L, Calabon MS, Calaça FJS, Callalli M, Câmara MPS, Cano-Lira J, Cao B, Carlavilla JR, Carvalho A, Carvalho TG, Castañeda-Ruiz RF, Catania MDV, Cazabonne J, Cedeño-Sanchez M, Chaharmiri-Dokhaharani S, Chaiwan N, Chakraborty N, Cheewankoon R, Chen C, Chen J, Chen Q, Chen YP, Chinaglia S, Coelho-Nascimento CC, Coleine C, CostaRezende DH, Cortés-Pérez A, Crouch, JA, Crous PW, Cruz RHSF, Czachura P, Damm U, Darmostuk V, Daroodi Z, Das K, Das K, Davoodian N, Davydov EA, da Silva GA, da Silva IR, da Silva RMF, da Silva Santos AC, Dai DQ, Dai YC, de Groot Michiel D, De Kesel A, De Lange R, de Medeiros EV, de Souza CFA, de Souza FA, dela Cruz TEE, Decock C, Delgado G, Denchev CM, Denchev TT, Deng YL, Dentinger BTM, Devadatha B, Dianese JC, Dima B, Doilom M, Dissanayake AJ, Dissanayake DMLS, Dissanayake LS, Diniz AG, Dolatabadi S, Dong JH, Dong W, Dong ZY, Drechsler-Santos ER, Druzhinina IS, Du TY, Dubey MK, Dutta AK, Elliott TF, Elshahed MS, Egidi E, Eisvand P, Fan L, Fan X, Fan XL, Fedosova AG, Ferro LO, Fiuza PO, Flakus A, W. Fonseca EO, Fryar SC, Gabaldón T, Gajanayake AJ, Gannibal PB, Gao F, GarcíaSánchez D, García-Sandoval R, Garrido-Benavent I, Garzoli L, Gasca-Pineda J, Gautam AK, Gené J, Ghobad-Nejhad M, Ghosh A, Giachini AJ, Gibertoni TB, Gentekaki E, Gmoshinskiy VI, GóesNeto A, Gomdola D, Gorjón SP, Goto BT, Granados-Montero MM, Griffith GW, Groenewald M, Grossart H-P, Gu ZR, Gueidan C, Gunarathne A, Gunaseelan S, Guo SL, Gusmão LFP, Gutierrez AC, Guzmán-Dávalos L, Haelewaters D, Haituk H, Halling RE, He SC, Heredia G, HernándezRestrepo M, Hosoya T, Hoog SD, Horak E, Hou CL, Houbraken J, Htet ZH, Huang SK, Huang WJ, Hurdeal VG, Hustad VP, Inácio CA, Janik P, Jayalal RGU, Jayasiri SC, Jayawardena RS, Jeewon R, Jerônimo GH, Jin J, Jones EBG, Joshi Y, Jurjević Ž, Justo A, Kakishima M, Kaliyaperumal M, Kang GP, Kang JC, Karimi O, Karunarathna SC, Karpov SA, Kezo K, Khalid AN, Khan MK, Khuna S, Khyaju S, Kirchmair M, Klawonn I, Kraisitudomsook N, Kukwa M, Kularathnage ND, Kumar S, Lachance MA, Lado C, Latha KPD, Lee HB, Leonardi M, Lestari AS, Li C, Li H. Li J, Li Q, Li Y, Li YC, Li YX, Liao CF, Lima JLR, Lima JMS, Lima NB, Lin L, Linaldeddu BT, Linn MM, Liu F, Liu JK, Liu JW, Liu S, Liu SL, Liu XF, Liu XY, Longcore JE, Luangharn T, Luangsa-ard JJ, Lu L, Lu YZ, Lumbsch HT, Luo L, Luo M, Luo ZL, Ma J, Madagammana AD, Madhushan A, Madrid H, Magurno F, Magyar D, Mahadevakumar S, Malosso E, Malysh JM, Mamarabadi

M, Manawasinghe IS, Manfrino RG, Manimohan P, Mao N, Mapook A, Marchese P, Marasinghe DS, Mardones M, Marin-Felix Y, Masigol H, Mehrabi M, MehrabiKoushki M, Meiras-Ottoni A de, Melo RFR, Mendes-Alvarenga RL, Mendieta S, Meng QF, Menkis A, Menolli Jr N, Mikšík M, Miller SL, Moncada B, Moncalvo JM, Monteiro JS, Monteiro M, Mora-Montes HM, Moroz EL, Moura JC, Muhammad U, Mukhopadhyay S, Nagy GL, Najam ul Sehar A, Najafiniya M, Nanayakkara CM, Naseer A, Nascimento ECR, Nascimento SS, Neuhauser S, Neves MA, Niazi AR, Nie Yong, Nilsson RH, Nogueira PTS, Novozhilov YK, Noordeloos M, Norphanphoun C, Nuñez Otaño N, O'Donnell RP, Oehl F, Oliveira JA, Oliveira Junior I, Oliveira NVL, Oliveira PHF, Orihara T, Oset M, Pang KL, Papp V, Pathirana LS, Peintner U, Pem D, Pereira OL, Pérez-Moreno J, Pérez-Ortega S, Péter G, Pires-Zottarelli CLA, Phonemany M, Phongeun S, Pošta A, Prazeres JFSA, Quan Y, Quandt CA, Queiroz MB, Radek R, Rahnama K, Raj KNA, Rajeshkumar KC, Rajwar Soumyadeep, Ralaiveloarisoa AB, Rämä T, Ramírez-Cruz V, Rambold G, Rathnayaka AR, Raza M, Ren GC, Rinaldi AC, Rivas-Ferreiro M, Robledo GL, Ronikier A, Rossi W, Rusevska K, Ryberg M, Safi A, Salimi F, Salvador-Montoya CA, Samant B, Samaradiwakara NP, Sánchez-Castro I, Sandoval-Denis M, Santiago ALCMA, Santos ACDS, Santos LA dos, Sarma VV, Sarwar S. Savchenko A, Savchenko K, Saxena RK, Schoutteten N, Selbmann L, Ševčíková H, Sharma A, Shen HW, Shen YM, Shu YX, Silva HF, Silva-Filho AGS, Silva VSH, Simmons DR, Singh R, Sir EB, Sohrabi M, Souza FA, Souza-Motta CM, Sriindrasutdhi V, Sruthi OP, Stadler M, Stemler J, Stephenson SL, Stoyneva-Gaertner MP, Strassert JFH, Stryjak-Bogacka M, Su H, Sun YR, Svantesson S, Sysouphanthong P, Takamatsu S, Tan TH, Tanaka K, Tang C, Tang X, Taylor JE, Taylor PWJ, Tennakoon DS, Thakshila SAD, Thambugala KM, Thamodini GK, Thilanga D, Thines M, Tiago PV, Tian XG, Tian WH, Tibpromma S, Tkalčec Z, Tokarev YS, Tomšovský M, Torruella G, Tsurykau A, Udayanga D, Ulukapı M, Untereiner WA, Usman M, Uzunov BA, Vadthanarat S, Valenzuela R, Van den Wyngaert S, Van Vooren N, Velez P, Verma RK, Vieira LC Vieira WAS, Vinzelj JM, Tang AMC, Walker A, Walker AK, Wang QM, Wang Y, Wang XY, Wang ZY, Wannathes N, Wartchow F, Weerakoon G, Wei DP, Wei X, White JF, Wijesundara DSA, Wisitrassameewong K, Worobiec G, Wu HX, Wu N, Xiong YR, Xu B, Xu JP, Xu R, Xu RF, Xu RJ, Yadav S, Yakovchenko LS, Yang HD, Yang X, Yang YH, Yang Y, Yang YY, Yoshioka R, Youssef Noha H, Yu FM, Yu ZF, Yuan LL, Yuan Q, Zabin DA, Zamora JC, Zapata CV, Zare R, Zeng M, Zeng XY, Zhang JF, Zhang JY, Zhang S, Zhang XC, Zhao CL, Zhao H, Zhao Q, Zhao H, Zhao HJ, Zhou HM, Zhu XY, Zmitrovich IV, Zucconi L, Zvyagina E (2024a) The 2024 Outline of fungi and fungus-like taxa. Mycosphere 15: 5146–6239. https://doi.org/10.5943/mycosphere/15/1/25

Hyde KD, Baldrian P, Chen Y, Thilini Chethana KW, De Hoog S, Doilom M, de Farias ARG, Gonçalves MFM, Gonkhom D, Gui H, Hilário S, Hu Y, Jayawardena RS, Khyaju S, Kirk PM, Kohout P, Luangharn T, Maharachchikumbura SSN, Manawasinghe IS, Mortimer PE, Niego AGT, Phonemany M, Sandargo B, Senanayake IC, Stadler M, Surup F, Thongklang N, Wanasinghe DN, Bahkali AH, Walker A (2024b) Current trends, limitations and future research in the fungi. Fungal Diversity 125: 1–71. https://doi.org/10.1007/s13225-023-00532-5

Index Fungorum (2024) Index Fungorum. http://www.indexfungorum.org [accessed on 10 August 2024]

Jayasiri SC, Hyde KD, Ariyawansa HA, Bhat J, Buyck B, Cai L, Dai YC, Abd-Elsalam K, Ertz D, Hidayat I, Jeewon R, Jones EBG, Bahkali AH, Karunarathna SC, Liu JK, Luangsa-ard JJ, Lumbsch TH, Maharachchikumbura SSN, McKenzie EHC, Moncalvo JM, Ghobad-Nejhad M, Nilsson H, Pang K, Pereira OL, Phillips AJL, Raspé O, Rollins AW, Romero AI, Etayo J, Selçuk F, Stephenson SL, Suetrong S, Taylor JE, Tsui CKM, Vizzini

A, Abdel-Wahab MA, Wen TC, Boonmee S, Dai DQ, Daranagama DA, Dissanayake AJ, Ekanayaka AH, Fryar SC, Hongsanan S, Jayawardena RS, Li WJ, Perera RH, Phookamsak R, de silva NI, Thambugala KM, Tian Q, Wijayawardene NN, Zhao RL, Zhao Q, Kang JC, Promputtha I (2015) The Faces of Fungi database: fungal names linked with morphology, phylogeny and human impacts. Fungal Diversity 74: 3–18. https://doi.org/10.1007/s13225-015-0351-8

Jeewon R, Hyde KD (2016) Establishing species boundaries and new taxa among fungi: Recommendations to resolve taxonomic ambiguities. Mycosphere 7: 1669–1677. https://doi.org/10.5943/mycosphere/7/11/4

Kan, YH, Gafforov Y, LiT, Zhou LW (2017) *Hyphodontia zhixiangii* sp. nov. (Schizoporaceae, Basidiomycota) from Uzbekistan. Phytotaxa 299(2): 273–279. https://doi.org/10.11646/phytotaxa.299.2.12

Karunarathna A, Papizadeh M, Senanayake IC, Jeewon R, Phookamsak R, Goonasekara ID, Wanasinghe DN, Wijayawardene NN, Amoozegar MA, Shahzadeh Fazeli SA, Camporesi E, Hyde KD, Weerahewa HLD, Lumyong S, McKenzie EHC (2017) Novel fungal species of Phaeosphaeriaceae with an asexual/sexual morph connection. Mycosphere 8: 1818–1834. https://doi.org/10.5943/mycosphere/8/10/8

Katoh K, Standley DM (2013) MAFFT multiple sequence alignment software version 7: Improvements in performance and usability. Molecular Biology and Evolution 30: 772–780. https://doi.org/10.1093/molbev/mst010

Kularathnage ND, Tennakoon DS, Zhu X, Zhou J, Su B, Xie Y, Chen Q, Calabon MS, Kirk PM, Senanayake IC, Doilom M, Xu B, Dong W, Song J (2023) Reinstating *Dyfrolomyces* and introducing *Melomastia pyriformis* sp. nov. (Pleurotremataceae, Dyfrolomycetales) from Guangdong Province, China. Current Research in Environmental & Applied Mycology 13: 426–438. https://doi.org/10.5943/cream/13/1/16

Lestari A, Wanasinghe D, Gafforov Y, Tennakoon D, Kandawatte T, Abdurazzakov A, Promputtha I, Hyde KD (2021) Taxonomy and phylogenetic appraisal of *Leptosphaeria chatkalica* sp. nov. (Leptosphaeriaceae, Pleosporales) from Uzbekistan. Phytotaxa 520: 155–168. https://doi.org/10.11646/phytotaxa.520.2.3

Li J, Phookamsak R, Mapook A, Boonmee S, Bhat JD, Hyde KD, Lumyong S (2016) *Seifertia shangrilaensis* sp. nov. (Melanommataceae), a new species from Southwest China. Phytotaxa 273: 34–42. https://doi.org/10.11646/phytotaxa.273.1.3

Li J, Jeewon R, Luo ZL, Phookamsak R, Bhat DJ, Mapook A, Phukhamsakda C, Erio C, Lumyong S, Hyde KD (2017) Morphological characterization and DNA based taxonomy of *Fusiconidium* gen. nov. with two novel taxa within Melanommataceae (Pleosporales). Phytotaxa 308: 206–218. https://doi.org/10.11646/phytotaxa.308.2.2

Liu AR, Chen SC, Wu SY, Xu T, Guo LD, Jeewon R, Wei JG (2010) Cultural studies coupled with DNA based sequence analyses and its implication on pigmentation as a phylogenetic marker in *Pestalotiopsis* taxonomy. Molecular Phylogenetics and Evolution 57: 528–535. https://doi.org/10.1016/j.ympev.2010.07.017

Lücking R, Aime MC, Robbertse B, Miller AN, Ariyawansa HA, Aoki T, Cardinali G, Crous PW, Druzhinina IS, Geiser DM, Hawksworth DL, Hyde KD, Irinyi L, Jeewon R, Johnston PR, Kirk PM, Malosso E, May TW, Meyer W, Öpik M, Robert V, Stadler M, Thines M, Vu D, Yurkov AM, Zhang N, Schoch CL (2020) Unambiguous identification of fungi: Where do we stand and how accurate and precise is fungal DNA barcoding? IMA Fungus 11: 14. https://doi.org/10.1186/s43008-020-00033-z

Miller MA, Pfeiffer W, Schwartz T (2010) Creating the CIPRES Science Gateway for inference of large phylogenetic trees. 2010 Gateway Computing Environments Workshop (GCE):1–8. https://doi.org/10.1109/GCE.2010.5676129

Niskanen T, Lücking R, Dahlberg A, Gaya E, Suz L, Mikryukov V, Liimatainen K, Druzhinina I, Westrip J, Mueller G, Martins da Cunha K, Kirk P, Tedersoo L, Antonelli A (2023) Pushing the frontiers of biodiversity research: Unveiling the global diversity, distribution, and conservation of fungi. Annual Review of Environment and Resources 48: 149–176. https://doi.org/10.1146/annurev-environ-112621-090937

Nylander JAA (2004) MrModeltest 2.0. Program distributed by the author. Evolutionary Biology Centre, Uppsala University, Uppsala.

Pem D, Gafforov Y, Jeewon R, Hongsanan S, Promputtha I, Doilom M, Hyde KD (2018) Multigene phylogeny coupled with morphological characterization reveal two new species of *Holmiella* and taxonomic insights within Patellariaceae. Cryptogamie. Mycologie 39: 193–209. https://doi.org/10.7872/crym/v39.iss2.2018.193

Pem D, Jeewon J, Bulgakov T, Gafforov Y, Hongsanan S, Phookamsak R, XU JC, Promputtha I, Doilom M, Hyde KD (2019a) Taxonomy and molecular phylogeny of *Thyrostroma ephedricola* sp. nov. (Dothidotthiaceae) and proposal for *Thyrostroma jaczewskii* comb. nov. Phytotaxa 416: 243–256. https://doi.org/10.11646/phytotaxa.416.4.3

Pem D, Jeewon R, Gafforov Y, Hongsanan S, Phukhamsakda C, Promputtha I, Doilom M, Hyde KD (2019b) *Melanocamarosporioides ugamica* gen. et sp. nov., a novel member of the family Melanommataceae from Uzbekistan. Mycological Progress 18: 471–481. https://doi.org/10.1007/s11557-018-1448-8

Pem D, Jeewon R, Chethana KW, Hongsanan S, Doilom M, Suwannarach N, Hyde KD (2021) Species concepts of Dothideomycetes: Classification, phylogenetic inconsistencies and taxonomic standardization. Fungal Diversity 109: 283–319. https://doi.org/10.1007/s13225-021-00485-7

Pem D, Hyde KD, McKenzie EHC, Hongsanan S, Wanasinghe DN, Boonmee S, Darmostuk V, Bhat JD, Tian Q, Htet ZH, Senanayake IC, Niranjan M, Sarma VV, Doilom M, Dong W (2024) A comprehensive overview of genera in Dothideomycetes. Mycosphere 15: 2175–4568. https://doi.org/10.5943/mycosphere/15/1/18

Rambaut A, Drummond AJ, Xie D, Baele G, Suchard MA (2018) Posterior summarization in Bayesian phylogenetics using Tracer 1.7. Systematic Biology 67: 901–904. https://doi.org/10.1093/sysbio/syy032

Rathnayaka AR, Tennakoon DS, Jones GE, Wanasinghe DN, Bhat DJ, Priyashantha AH, Stephenson SL, Tibpromma S, Karunarathna SC (2024) Significance of precise documentation of hosts and geospatial data of fungal collections, with an emphasis on plant-associated fungi. New Zealand Journal of Botany: 1–28. https://doi.org/10.1080/0028825X.2024.2381734

Rehner SA (2001) Primers for Elongation Factor 1-α (EF1-α). http://ocid.NACSE.ORG/research/deephyphae/EF1primer.pdf

Ronquist F, Teslenko M, van der Mark P, Ayres DL, Darling A, Höhna S, Larget B, Liu L, Suchard MA, Huelsenbeck JP (2012) MrBayes 3.2: Efficient Bayesian phylogenetic inference and model choice across a large model space. Systematic Biology 61: 539–542. https://doi.org/10.1093/sysbio/sys029

Senanayake IC, Rathnayaka AR, Marasinghe DS, Calabon MS, Gentekaki E, Lee HB, Hurdeal VG, Pem D, Dissanayake LS, Wijesinghe SN, Bundhun D, Nguyen TT, Goonasekara ID, Abeywickrama PD, Bhunjun CS, Jayawardena RS, Wanasinghe DN, Jeewon R, Bhat DJ, Xiang MM (2020) Morphological approaches in studying fungi: Collection, examination, isolation, sporulation and preservation. Mycosphere 11: 2678–2754. https://doi.org/10.5943/mycosphere/11/1/20

Senwanna C, Hongsanan S, Khuna S, Kumla J, Yarasheva M, Gafforov Y, Abdurazakov A, Suwannarach N (2024) Insights into the molecular phylogeny and morphology of three novel *Dothiora* species, along with a worldwide checklist of *Dothiora*. Frontiers in Cellular and Infection Microbiology 14: e1367673. https://doi.org/10.3389/fcimb.2024.1367673

Shenoy BD, Jeewon R, Hyde KD (2007) Impact of DNA sequence-data on the taxonomy of anamorphic fungi. Fungal Diversity 26: 1–54.

Shenoy BD, Jeewon R, Wang H, Amandeep K (2010) Sequence data reveals phylogenetic affinities of fungal anamorphs *Bahusutrabeeja*, *Diplococcium*, *Natarajania*, *Paliphora*, *Polyschema*, *Rattania* and *Spadicoides*. Fungal Diversity 44: 161–169. https://doi.org/10.1007/s13225-010-0059-8

Stamatakis A (2014) RAxML version 8: A tool for phylogenetic analysis and post-analysis of large phylogenies. Bioinformatics 30: 1312–1313. https://doi.org/10.1093/bioinformatics/btu033

Stamatakis A, Hoover P, Rougemont J (2008) A rapid bootstrap algorithm for the RAxML web servers. Systematic Biology 57: 758–771. https://doi.org/10.1080/10635150802429642

Sui XN, Guo MJ, Wang QT, Wang HQ, Zhou H, Huang XB, Yu ZF, Hou CL (2024) Taxonomy and phylogeny of *Colletotrichum* on important forest plants in China. Mycosphere 15: 4569–4743. https://doi.org/10.5943/mycosphere/15/1/19

Tang X, Jeewon R, Lu YZ, Alrefaei AF, Jayawardena RS, Xu RJ, Ma J, Chen XM, Kang JC (2023) Morpho phylogenetic evidence reveals four new fungal species within Tetraplosphaeriaceae (Pleosporales, Ascomycota) from tropical and subtropical forest in China. MycoKeys 100: 171–204. https://doi.org/10.3897/mycokeys.100.113141

Tennakoon D, Phookamsak R, Kuo CH, Goh TK, Jeewon R, Hyde KD (2018) Morphological and phylogenetic evidence reveal *Fissuroma taiwanense* sp. nov. (Aigialaceae, Pleosporales) from *Hedychium coronarium*. Phytotaxa 338: 265–275. https://doi.org/10.11646/phytotaxa.338.3.4

Tennakoon D, Thambugala K, de Silva N, Song HY, Suwannarach N, Chen FS, Hu DM (2024) An overview of Melanommataceae (Pleosporales, Dothideomycetes): Current insight into the host associations and geographical distribution with some interesting novel additions from plant litter. MycoKeys 106: 43–96. https://doi.org/10.3897/mycokeys.106.125044

Tian Q, Liu JK, Hyde KD, Wanasinghe DN, Boonmee S, Jayasiri SC, Luo ZL, Taylor JE, Phillips AJL, Bhat DJ, Li WJ, Ariyawansa H, Thambugala KM, Jones EBG, Chomnunti P, Bahkali AH, Xu JC (2015) Phylogenetic relationships and morphological reappraisal of Melanommataceae (Pleosporales). Fungal Diversity 74: 267–324. https://doi.org/10.1007/s13225-015-0350-9

Tian WH, Liu JW, Jin Y, Chen YP, Zhou YF, Wu K, Su PW, Guo XY, Wanasinghe DN, Hyde KD, Liu JK, Maharachchikumbura SSN (2024) Morphological and phylogenetic studies of Ascomycota from gymnosperms in Sichuan Province, China. Mycosphere 15: 1794–1900. https://doi.org/10.5943/mycosphere/15/1/16

Vilgalys R, Hester M (1990) Rapid genetic identification and mapping of enzymatically amplified ribosomal DNA from several *Cryptococcus* species. Journal of Bacteriology 172: 4238–4246. https://doi.org/10.1128/jb.172.8.4238-4246.1990

Wanasinghe DN, Phukhamsakda C, Hyde KD, Jeewon R, Lee HB, Gareth Jones E, Tibpromma S, Tennakoon DS, Dissanayake AJ, Jayasiri SC, Gafforov Y, Camporesi E, Bulgakov TS, Ekanayake AH, Perera RH, Samarakoon MC, Goonasekara ID, Mapook A, Li W, Senanayake IC, Li J, Norphanphoun C, Doilom M, Bahkali AH, Xu J, Mortimer PE, Tibell L, Tibell S, Karunarathna SC (2018) Fungal diversity notes 709–839: Taxonomic and phylogenetic contributions to fungal taxa with an emphasis on fungi on Rosaceae. Fungal Diversity 89: 1–236. https://doi.org/10.1007/s13225-018-0395-7

White T, Bruns T, Lee S, Taylor J (1990) Amplification and direct sequencing of fungal ribosomal RNA genes for phylogenetics. In: Innis MA, Gelfand DH, Sninsky JJ, White TJ (Eds) PCR Protocols: A Guide to Methods and Applications, Academic Press, New York, 315–322. https://doi.org/10.1016/B978-0-12-372180-8.50042-1

Wijayawardene NN, McKenzie EHC, Hyde KD (2012) Towards incorporating anamorphic fungi in a natural classification checklist and notes. Mycosphere 2: 1–88. https://doi.org/10.5943/mycosphere/3/2/5

Winter HG (1885) GL Rabenhorst's Kryptogamen-Flora von Deutschland, Oesterreich und der Schweiz. Volume 1. Pilze–Ascomyceten. Verlag von Eduard Kummer; Leipzig, 65–528. https://doi.org/10.5962/bhl.title.1356

Wu B, Hussain M, Zhang W, Stadler M, Liu X, Xiang M (2019) Current insights into fungal species diversity and perspective on naming the environmental DNA sequences of fungi. Mycology 10: 127–140. https://doi.org/10.1080/21501203.2019.1614106

Zhang Y, Crous PW, Schoch CL, Hyde KD (2012) Pleosporales. Fungal Diversity 53: 1–221. https://doi.org/10.1007/s13225-011-0117-x

Zhou LW, May TW (2022) Fungal taxonomy: Current status and research agendas for the interdisciplinary and globalization era. Mycology 14: 52–59. https://doi.org/10.1080/21501203.2022.2103194

MycoKeys 115: 43–66 (2025)
DOI: 10.3897/mycokeys.115.139757

Research Article

Morphology and multi-gene phylogeny reveal three new species of *Clonostachys* and two combinations of *Sesquicillium* (Bionectriaceae, Hypocreales) from Xizang, China

Shucheng He[1,2], Vinodhini Thiyagaraja[1], Chitrabhanu S. Bhunjun[2], Putarak Chomnunti[2], Lakmali S. Dissanayake[3,4], Ruvishika S. Jayawardena[2], Hongde Yang[1,2], Yun Wei Zhao[1,5], Fatimah Al-Otibi[6], Qi Zhao[1], Kevin D. Hyde[1,2,6]

1 *State Key Laboratory of Phytochemistry and Natural Medicines, Kunming Institute of Botany, Chinese Academy of Sciences, Kunming, Yunnan 650201, China*
2 *Center of Excellence in Fungal Research, Mae Fah Luang University, Chiang Rai 57100, Thailand*
3 *Center for Mountain Futures, Kunming Institute of Botany, Chinese Academy of Sciences, Honghe County 654400, China*
4 *Department of Economic Plants and Biotechnology, Yunnan Key Laboratory for Wild Plant Resources, Kunming Institute of Botany, Chinese Academy of Sciences, Kunming 650201, Yunnan, China*
5 *State Key Laboratory for Conservation and Utilization of Bio-Resources in Yunnan, Yunnan University, Kunming, Yunnan, 650091, China*
6 *Department of Botany and Microbiology, College of Science, King Saud University, P.O. Box 22452, Riyadh 11495, Saudi Arabia*
Corresponding author: Kevin D. Hyde (kdhyde3@gmail.com)

Academic editor: Danny Haelewaters
Received: 20 October 2024
Accepted: 23 January 2025
Published: 11 March 2025

Citation: He S, Thiyagaraja V, Bhunjun CS, Chomnunti P, Dissanayake LS, Jayawardena RS, Yang H, Zhao YW, Al-Otibi F, Zhao Q, Hyde KD (2025) Morphology and multi-gene phylogeny reveal three new species of Clonostachys and two combinations of Sesquicillium (Bionectriaceae, Hypocreales) from Xizang, China. MycoKeys 115: 43–66. https://doi.org/10.3897/mycokeys.115.139757

Abstract

Clonostachys and *Sesquicillium* are genera in Bionectriaceae, and known in sexual perithecial ascomata and hyphomycetous asexual morphs. In their asexual morph, both genera share similar morphology in conidiophores and conidiogenous cell characteristics but differ in the development of conidiophores. The members of *Clonostachys* are distributed worldwide with the majority occurring in the tropics and the species are commonly reported as soil-borne fungi but also reported as endophytes, epiphytes, and saprotrophs. During a microfungi survey in Xizang, China, six collections of fresh and healthy *Ageratina adenophora* and *Houttuynia cordata* leaves were obtained. The taxonomy of these collections was investigated through a combination of morphological analysis and multigene phylogenetic analysis using Maximum likelihood and Bayesian inference. The newly generated sequences were clustered within *Clonostachys* and *Sesquicillium*, showing hyphomycetes asexual morph. The results revealed three new *Clonostachys* species viz, *Clonostachys linzhiensis*, *C. motuoensis*, and *C. yadongensis*. This research sheds light on the overlooked fungal diversity in Xizang, China, expanding the known fungal biodiversity in the region. Additionally, two new combinations, *Sesquicillium aquaticum* and *S. shanghaiense* for *C. aquatica* and *C. shanghaiensis*, and one synonymy, *C. viticola* for *C. swietenia* are established, respectively.

Key words: Asexual morph, endophytes, Hyphomycetes, new taxa, taxonomy

Introduction

Clonostachys (Bionectriaceae, Hypocreales) was established by Corda (1839). The genus was typified by *C. araucaria* (Corda 1839), which was later synonymized under *C. rosea* (Rossman et al. 2013). The genus was considered as the asexual morph of *Bionectria* and both genera were also considered as conspecific in several studies (Luo and Zhuang 2007, 2010; Dong et al. 2023). *Bionectria* was described by Spegazzini (1918). Based on the One Fungus = One Name (1F = 1N) concept, mycologists propose the protection of the older asexual morph-typified name *Clonostachys* for this genus (Rossman et al. 2013; Dong et al. 2023). Members of *Clonostachys* occur as endophytes, entomopathogens, epiphytes, plant pathogens, soil-borne fungi, and saprotrophs, typically found on herbicolous, corticolous, lichenicolous, fungicolous, coprophilous habitats as well as on nematodes and insects (Mazen et al. 2022; Dong et al. 2023; Wang et al. 2023; Zhao et al. 2023). They are distributed globally and commonly occur in tropical regions (Schroers 2001). The sexual morph is characterized by ascomata that do not change colour in 3% Potassium Hydroxide (KOH) or 100% Lactic Acid (LA) (Luo and Zhuang 2007, 2010), perithecial or cleistothecial ascomata that are superficial on the substrate or embedded in the stroma. Ascomata are solitary or densely aggregated, subglobose to pyriform; clavate or cylindrical, sessile or short pedicellate asci, smooth or striated, aseptate to multi-septate, globose, fusiform, ellipsoid or broadly ellipsoid ascospores (Hyde et al. 2020a). The asexual members are characterized by penicillate, sporodochial and dimorphic conidiophores (primary and secondary conidiophores) with phialidic conidiogenous cells, hyaline, smooth, broadly ellipsoidal conidia with ends that are broadly rounded (Bao et al. 2023; Chen et al. 2023; Dong et al. 2023; He et al. 2023; Liu et al. 2023; Perera et al. 2023). Primary conidiophores are mononematous, either verticillium-like or narrowly penicillate, whereas the secondary conidiophores produce imbricate conidial chains that can collapse to slimy masses, particularly on sporodochia (Zhao et al. 2023).

Morphology-based identification of *Clonostachys* is challenging (Schroers et al. 1999; Abreu et al. 2014) and many species were previously placed in various genera such as *Acrostalagmus*, *Clonostachyopsis*, *Dendrodochium*, *Gliocladium*, *Gliocladochium*, *Myrothecium*, *Sesquicillium*, *Spicaria*, *Verticilliodochium*, or *Verticillium* (Schroers 2001). Rossman et al. (2001) first conducted the initial molecular investigation of *Clonostachys*/*Bionectria*, employing large subunit rDNA sequences, and proposed the monophyletic status. Subsequently, DNA sequences from multi-genes including ITS, 28S, *rpb*1, *rpb*2, and *tef*1 have been extensively employed to address the taxonomy of *Clonostachys* (Bao et al. 2023; Chen et al. 2023; Perera et al. 2023; Zhao et al. 2023). Wijayawardene et al. (2022) accepted 78 species under *Clonostachys*, while this was 50 species in Hyde et al. (2024). Zhao et al. (2023) investigated the species diversity within a collection of 420 strains of *Clonostachys* from the culture collection and personal collections at the Westerdijk Fungal Biodiversity Institute in Utrecht, the Netherlands, and identified 19 species based on phylogenetic and morphological analyses. In China, 19 *Clonostachys* species have been reported from different hosts and substrates (Bao et al. 2023; Dong et al. 2023; Perera et al. 2023; Piombo et al. 2023; Wang et al. 2023).

During the microfungi survey in China (He et al. 2024a, b, c; Thiyagaraja et al. 2024), we investigated several isolates from the leaves of *Ageratina adenophora* and *Houttuynia cordata* from Xizang, China. Multigene phylogenetic analyses combining 28S, *tef*1, *rpb*2, ITS, and *tub*2 sequences, along with morphological analyses, support the establishment of three new species: *Clonostachys linzhiensis*, *C. motuoensis* and *C. yadongensis*. The introduction of these new species follows the protocols outlined in Chethana et al. (2021) and Maharachchikumbura et al. (2021). The new species are established based on detailed morphological characterization, and illustrations, along with multigene analyses of maximum likelihood (ML) and Bayesian inference (BI). In addition, through phylogenetic analysis of *Clonostachys*, we suggest that *C. aquatica*, *C. shanghaiensis*, and *C. swieteniae* be synonymous with *Sesquicillium aquaticum*, *S. shanghaiense*, and *C. viticola*, respectively.

Materials and methods

Sample collection, isolation, and morphological characterization

Fresh and healthy leaves of *Ageratina adenophora* and *Houttuynia cordata* were collected from Medog County, Linzhi City, Xizang Autonomous Region, China from October 2021 to July 2023, and information on collection was recorded according to the Rathnayaka et al. (2024). The healthy part of the leaves was initially cleaned and cut into small pieces (5 × 5 mm). The leaf fragments were briefly soaked in a 75% ethanol solution for 30 s, followed by a 2.5% sodium hypochlorite solution for the same duration (Bhunjun et al. 2021). Afterward, they were washed thrice with sterile distilled water for 30 s. Once sterilized, the tissue fragments were allowed to air-dry on sterile filter paper and then transferred to potato dextrose agar (PDA) (Senanayake et al. 2020). The PDA plates were cultured at 25 °C for 2–5 days. Single hyphae were carefully selected from the periphery of the growing colonies and inoculated onto new PDA plates. Following 1–2 weeks of purification, a pure culture was obtained. Sporulation was induced on water agar (WA) medium. The mycelia were mounted on a slide in water using a sterile needle. A NIKON ECLIPSE Ni-U compound microscope was used to examine conidiophores and conidia of a small mass of mycelia. Micro-morphological images were captured with a DS-Ri2 camera attached to the compound microscope. The photoplates used for the figure were processed with Adobe Photoshop. The pure cultures were deposited in the Kunming Institute of Botany, the Chinese Academy of Sciences (KUNCC), Kunming, China. Specimens were deposited in the Herbarium of Cryptogams, Kunming Institute of Botany, Academia Sinica (KUN-HKAS), Kunming, China. Facesoffungi and Index Fungorum numbers were registered following the protocols outlined in Jayasiri et al. (2015) and Index Fungorum, respectively.

DNA extraction, PCR amplification and sequencing

The mycelia growing on a PDA plate were used to extract DNA using the Trilief™ Plant Genomic DNA Kit (Tsingke Biological Technology Co., Ltd in Beijing, China), following the manufacturer's instructions. The primer pairs ITS5/ITS4 (White et al. 1990), LR0R/LR5 (Vilgalys and Hester 1990), T1/T22 (Research & Service 1997), EF1-983F/EF1-2218R (Carbone and Kohn 1999), and fRPB2-5F/fRPB2-7cR (Liu et al. 1999) were used for amplification of the internal transcribed spacer region ITS1-5.8S-ITS2 (ITS), large subunit rDNA (28S), beta-tubulin (*tub*2), translation elongation factor 1-α (*tef*1) gene and RNA polymerase II second-largest subunit (*rpb*2), respectively. The PCR was performed in a 25 μL reaction volume, comprising 21 μL PCR Mix (2 × Rapid Taq Master Mix, Vazyme Biotech Co., Ltd., Nanjing, China), 1 μL of each primer, 2 μL of DNA template. For PCR amplification conditions see Table 1. The PCR products were visualized using agarose gel electrophoresis, and those with the targeted bands were sent to Sangon Biotech Co. Ltd., Kunming, China, for sequencing. The newly generated sequences were submitted to GenBank to obtain accession numbers.

Table 1. Loci, primers, and PCR amplification conditions used in this study.

Locus	Primers	PCR amplification conditions	Reference
ITS	ITS5/ITS4	95 °C: 5 min, (95 °C: 15s, 55 °C: 15s, 72 °C: 15s) × 40 cycles	White et al. (1990); Vilgalys and Hester (1990)
28S	LR0R/LR5		
*tef*1	EF1-983F/EF1-2218R	95 °C: 5 min, (95 °C: 45s, 52 °C: 45s, 72 °C: 70s) × 35 cycles	Carbone and Kohn (1999)
*tub*2	T1/T22	95 °C: 5 min, (95 °C: 45s, 50 °C: 45s, 72 °C: 90s) × 35 cycles	Research and Service (1997)
*rpb*2	fRPB2-5F/fRPB2-7cR	95 °C: 5 min, (95 °C: 45s, 55 °C: 120s, 72 °C: 50s) × 35 cycles	Liu et al. (1999)

Sequence alignment and phylogenetic analyses

The sequences were assembled using Sequencing Project Management (SeqMan) software (Clewley 1995). The assembled sequences were compared with the data in GenBank to determine their close relatives. The results indicate that our specimens were closely related to species of *Clonostachys*. Reference sequences for *Clonostachys* were obtained following recent studies (Bao et al. 2023; Liu et al. 2023; Perera et al. 2023; Piombo et al. 2023; Wang et al. 2023; Zhang et al. 2023; Zhao et al. 2023) (Table 2). Each gene matrix was separately aligned using MAFFT v. 6.8 (Katoh et al. 2018). The aligned datasets were manually edited using BioEdit v. 7.0.9 (Hall 1999) and then combined using SequenceMatrix v1.7.8 (Vaidya et al. 2011). The combined alignment was utilized for ML and BI analyses.

A rapid phylogenetic analysis was performed utilizing OFPT (Zeng et al. 2023) according to its standard protocol. The final phylogenetic analyses were carried out on the CIPRES Science Gateway platform (https://www.phylo.org), employing RAxML-HPC v.8 on XSEDE (8.2.12) for maximum likelihood (ML) estimation and MrBayes on XSEDE (3.2.7a) for Bayesian inference (BI). Phylogenetic results were represented by ML bootstrap values (MLB) equal to or greater than 70% and a posterior probability in Bayesian statistics (BYPP) equal to or exceeding 0.90. These values were displayed above each node in all resulting trees. For visualization purposes, the resulting phylograms were displayed using the FigTree v1.4.0 program. The final reorganization was accomplished using Adobe Illustrator 2020.

Results

Phylogenetic analyses

The combined 28S, *tef*1, *rpb*2, ITS, and *tub*2 dataset comprised 104 taxa. *Fusarium acutatum* (CBS 402.97) and *Nectria cinnabarina* (CBS 279.48) were selected as outgroup taxa (Prasher and Chauhan 2017; Lechat et al. 2020). The dataset consisted of 3146 total characters, including gaps (28S: 1–784 bp; *tef*1: 785–1596; *rpb*2: 1597–2349; ITS: 2350–2826; *tub*2: 2827–3828). The matrix had 1079 distinct alignment patterns, with 41.89% of undetermined characters or gaps. Estimated base frequencies were as follows: A = 0.229764, C = 0.268281, G = 0.268313, T = 0.233642; substitution rates: AC = 1.37920, AG = 4.09491, AT = 1.37920, CG = 0.794178, CT = 8.784537, GT = 1.00000; gamma distribution shape parameter α = 0.494958. The best-scoring RAxML tree with a final likelihood value of -23046.167770 is presented in (Fig. 1). Our specimens *Clonostachys linzhiensis* (HKAS 133179 & HKAS 133180) and *C. motuoensis* (HKAS 133181 & HKAS 133182) formed distinct monophyletic clades with *C. aranearum* with support value of (75% ML) and (85% ML), indicating they are closely related. The two specimens HKAS 133183 and HKAS 133184 formed a sister clade to *C. krabiensis* with high support (100 ML/0.91 PP).

Table 2. Names, voucher numbers, and corresponding GenBank accession numbers of the taxa used in the phylogenetic analyses in this study.

Taxa	Voucher no.	GenBank accession numbers					Reference
		ITS	28S	*tub2*	*tef1*	*rpb2*	
Clonostachys agrawalii	**CBS 533.81**	**AF358241**	N/A	**AF358187**	N/A	N/A	Schroers (2001)
C. ambigua	**PAD S00003**	**MT554898**	N/A	**N/A**	N/A	N/A	Forin et al. (2020)
C. apocyni	**CBS 130.87**	**AF210688**	N/A	**AF358168**	N/A	N/A	Schroers (2001)
C. aranearum	**QLS 0625**	**NR_164542**	N/A	**KU212400**	N/A	N/A	Chen et al. (2016)
C. artemisiae	**MHZU 23-0116**	**OR365451**	N/A	**OR700206**	N/A	N/A	Dong et al. (2023)
C. aurantiaca	CBS:124757	OQ910531	OQ910890	N/A	OQ944545	OQ927609	Zhao et al. (2023)
C. aureofilvella	CBS 195.93	AF358226	N/A	AF358181	N/A	N/A	Schroers (2001)
C. australiana	**CBS:102421**	**OQ910540**	**OQ910899**	**OQ982584**	**OQ944554**	**OQ927618**	Zhao et al. (2023)
C. bambusae	**CBS:139411**	**OQ910542**	**OQ910901**	**OQ982586**	**OQ944556**	**OQ927620**	Zhao et al. (2023)
C. buxicola	**CBS:102419**	**OQ910544**	**OQ910903**	**OQ982588**	**OQ944558**	**OQ927622**	Zhao et al. (2023)
C. byssicola	**CBS 364.78**	**MH861151**	**MH872912**	**AF358153**	N/A	N/A	Vu et al. (2019)
C. capitata	**CBS 218.93**	**AF358240**	**MH874054**	**AF358188**	N/A	N/A	Schroers (2001)
C. catenulata	**CBS 154.27**	**NR_165993**	**NG_063969**	N/A	**OQ944810**	**OQ927866**	Zhao et al. (2023)
C. chlorina	**CBS 287.90**	**NR_137651**	**MH873895**	**OQ982590**	**OQ944560**	**OQ927624**	Schroers (2001)
C. chloroleuca	**CBS:141588**	**OQ910549**	**OQ910908**	N/A	**OQ944563**	**OQ927627**	Zhao et al. (2023)
C. chongqingensis	**HMAS 290894**	**OP205475**	N/A	**OP205324**	N/A	N/A	Zeng and Zhuang (2022)
C. compactiuscula	CBS:123759	OQ910563	OQ910922	OQ982603	OQ944576	OQ927640	Zhao et al. (2023)
C. compactiuscula	**CBS 913.97**	**AF358245**	N/A	**AF358194**	N/A	N/A	Schroers (2001)
C. cylindrica	**CBS:101113**	**OQ910569**	**OQ910928**	N/A	**OQ944582**	**OQ927646**	Zhao et al. (2023)
C. divergens	**CBS 967.73**	**NR_137532**	**OQ910934**	**AF358191**	**OQ944587**	N/A	Schroers (2001)
C. ellipsoidea	**CBS 175.76**	**OQ910580**	**OQ910939**	**OQ982617**	**OQ944592**	**OQ927655**	Zhao et al. (2023)
C. epichloe	**CBS 101037**	**AF210675**	**OQ910940**	**AF358209**	**OQ944593**	**OQ927656**	Schroers (2001)
C. eriocamporesiana	**MFLU 18-2713**	**MN699132**	**N/A**	**MN699965**	**MN699964**	N/A	Hyde et al. (2020b)
C. eriocamporesii	**MFLU 19-0486**	**MN699133**	**NG_068919**	**OQ982619**	N/A	N/A	Hyde et al. (2020b)
C. farinosa	CBS 914.97	AF358252	N/A	AF358151	N/A	N/A	Schroers (2001)
C. flava	**CBS 915.97**	**OQ910619**	**OQ910978**	**OQ982654**	**OQ944631**	**OQ927690**	Zhao et al. (2023)
C. fujianensis	**CBS:127474**	**OQ910620**	**OQ910979**	**OQ982655**	**OQ944632**	**OQ927691**	Zhao et al. (2023)
C. fusca	**CBS 207.93**	**OQ910622**	**OQ910981**	**OQ982657**	**OQ944634**	**OQ927693**	Zhao et al. (2023)
C. garysamuelsii	**CBS:123964**	**OQ910624**	**OQ910983**	**OQ982658**	**OQ944636**	**OQ927695**	Zhao et al. (2023)
C. grammicospora	**CBS 209.93**	**NR_137650**	**NG_064165**	**AF358206**	**OQ944637**	N/A	Forin et al. (2020)
C. grammicosporopsis	CBS 102834	AF358256	OQ910985	OQ982660	OQ944638	OQ927697	Vu et al. (2019)
C. granuligera	**PAD S00011**	**MT554904**	N/A	N/A	N/A	N/A	Forin et al. (2020)
C. hongkongensis	**CBS:115291**	**OQ910630**	**OQ910989**	**OQ982663**	**OQ944642**	**OQ927700**	Zhao et al. (2023)
C. impariphialis	HMAS 275560	KX096609	KX096606	N/A	N/A	N/A	Zeng and Zhuang (2022)
C. indica	**RKV2015**	**KT291441**	N/A	N/A	N/A	N/A	Prasher and Chauhan (2017)
C. intermedia	**CBS 508.82**	**NR_137652**	**OQ910991**	**AF358205**	**OQ944644**	N/A	Schroers (2001)
C. kowhai	**CBS 461.95**	**NR_154748**	**OQ910992**	**AF358170**	**OQ944645**	**OQ927702**	Schroers (2001)
C. krabiensis	**MFLU 16-0254**	**NR168189**	**MH376707**	N/A	N/A	N/A	Tibpromma et al. (2018)
C. krabiensis	CBS 192.96	OQ910634	OQ910993	OQ982666	OQ944646	OQ927703	Zhao et al. (2023)
C. kunmingensis	**YFCC: 898**	**MW199069**	**MW199058**	**MW201676**	**MW295969**	N/A	Wang et al. (2023)
C. leptoderma	**HMAS 255834**	**OP205474**	N/A	**OP205323**	N/A	N/A	Zeng and Zhuang (2022)
C. leucaenae	MFLU 20-0008	ON230050	ON230058	N/A	N/A	N/A	Perera et al. (2023)
C. levigata	CBS 948.97	AF210680	N/A	AF358196	N/A	N/A	Schroers (2001)
C. linzhiensis	**HKAS 133179**	**PQ522504**	**PQ634391**	**PQ650459**	**PQ650477**	N/A	present study
C. linzhiensis	HKAS 133180	PQ522505	PQ634392	PQ650460	PQ650478	N/A	present study
C. longiphialidica	**CBS 112.87**	**OQ910643**	**OQ911002**	N/A	**OQ944655**	**OQ927712**	Zhao et al. (2023)
C. lucifer	**CBS 100008**	**AF210683**	**OQ911003**	**AF358208**	**OQ944656**	**OQ927713**	Schroers (2001)
C. miodochialis	**CBS 997.69**	**NR_137649**	**NG_064076**	**AF358210**	**OQ944658**	**OQ927715**	Schroers (2001)
C. moreaui	CBS:127881	OQ910647	OQ911006	OQ982678	OQ944659	OQ927716	Zhao et al. (2023)
C. motuoensis	**HKAS 133181**	**PQ522506**	**PQ634393**	**PQ650461**	**PQ650479**	N/A	present study
C. motuoensis	HKAS 133182	PQ522507	PQ634394	PQ650462	PQ650480	N/A	present study
C. oblongispora	**CBS 100285**	**AF358248**	**OQ911007**	**AF358169**	**OQ944660**	**OQ927717**	Schroers (2001)
C. obovatispora	CBS:118752	OQ910649	OQ911008	OQ982680	OQ944661	OQ927718	Zhao et al. (2023)

Taxa	Voucher no.	GenBank accession numbers					Reference
		ITS	28S	*tub2*	*tef1*	*rpb2*	
C. oligospora	**HMAS 290895**	**OP205473**	N/A	**OP205322**	N/A	N/A	Zeng and Zhuang (2022)
C. pallens	**PAD S00004**	**MT554899**	N/A	N/A	N/A	N/A	Forin et al. (2020)
C. palmae	**CBS 119.87**	**OQ910650**	**OQ911009**	**OQ982681**	**OQ944662**	**OQ927719**	Zhao et al. (2023)
C. parasporodochialis	**CBS 192.93**	**OQ910651**	**OQ911010**	**OQ982682**	**OQ944663**	**OQ927720**	Zhao et al. (2023)
C. penicillata	**CBS 729.87**	**OQ910654**	**OQ911013**	**OQ982685**	**OQ944666**	**OQ927722**	Zhao et al. (2023)
C. pilosella	CLLG19028	N/A	NG_153902	N/A	N/A	N/A	Lechat et al. (2020)
C. pityrodes	**CBS 102033**	**AF210672**	**OQ911014**	**AF358212**	N/A	**OQ927723**	Schroers (2001)
C. pnagiana	**CLLG19041**	N/A	**NG_153903**	N/A	N/A	N/A	Lechat et al. (2020)
C. pseudochroleuca	**CBS 192.94**	**AF358238**	N/A	**AF358171**	N/A	N/A	Schroers (2001)
C. pseudostriata	CBS 309.96	OQ910673	OQ911032	OQ982704	OQ944685	OQ927741	Zhao et al. (2023)
C. pseudostriatopsis	h116	N/A	N/A	AB237465	N/A	N/A	Hirooka and Kobayashi (2007)
C. ralfsii	CBS 129.87	AF210676	N/A	AF358195	N/A	N/A	Schroers (2001)
C. reniformis	**CBS 695.86**	**OQ910685**	**OQ911044**	**OQ982714**	**OQ944697**	**OQ927753**	Zhao et al. (2023)
C. rhinolophicola	KUMC 21-0438	ON426841	N/A	OR025936	N/A	N/A	Liu et al. (2023)
C. rhinolophicola	**HKAS122257**	**ON426840**	N/A	**OR025937**	N/A	N/A	Liu et al. (2023)
C. rhizophaga	**CBS 202.37**	**AF358225**	**MH867396**	**AF358156**	N/A	N/A	Schroers (2001)
C. rogersoniana	CBS 582.89	AF210691	N/A	AF358189	N/A	N/A	Schroers (2001)
C. rosea	CBS 1221.71	DQ674381	OQ911077	OQ982747	OQ944730	OQ927786	Zhao et al. (2023)
C. samuelsii	CBS 699.97	OQ910812	N/A	AF358190	N/A	N/A	Zhao et al. (2023)
C. setosa	CBS 834.91	AF210670	N/A	AF358211	N/A	N/A	Schroers (2001)
C. solani	CBS 101924	AF358232	OQ911196	AF358180	OQ944847	OQ927902	Schroers (2001)
C. spinulosa	**MFLU 17-0131**	**ON230049**	N/A	**ON238009**	N/A	N/A	Perera et al. (2023)
C. sporodochialis	**CBS 101921**	**AF210685**	N/A	**AF358149**	N/A	N/A	Schroers (2001)
C. squamuligera	**PAD S00020**	**MT554908**	N/A	N/A	N/A	N/A	Forin et al. (2020)
C. squamuligera	PAD S00021	MT554909	N/A	N/A	N/A	N/A	Forin et al. (2020)
C. subquaternata	**CBS 100003**	**MT537603**	N/A	N/A	N/A	N/A	Forin et al. (2020)
C. vacuolata	**CBS 191.93**	**OQ910868**	**OQ911227**	N/A	**OQ944876**	**OQ927931**	Zhao et al. (2023)
C. venezuelae	**CBS 107.87**	**OQ910869**	**OQ911228**	**OQ982884**	**OQ944877**	**OQ927932**	Zhao et al. (2023)
C. vesiculosa	**HMAS 183151**	**NR_119828**	**HM050302**	N/A	N/A	N/A	Luo and Zhuang (2010)
C. viticola	**CAA 944**	**MK156282**	**N/A**	**MK156290**	**MK156286**	N/A	Torcato et al. (2020)
C. viticola	**MFLU 18-2770**	**MT215573**	**MT396164**	**N/A**	**MT212204**	N/A	Perera et al. (2020)
C. wenpingii	**HMAS 172156**	**NR_119651**	**MH874867**	N/A	N/A	N/A	Luo and Zhuang (2007)
C. yadongensis	**HKAS 133183**	**PQ522508**	**PQ634395**	**PQ650463**	**PQ650481**	**PQ538524**	present study
C. yadongensis	HKAS 133184	PQ522509	PQ634396	PQ650464	PQ650482	PQ538525	present study
C. zelandiaenovae	**CBS 100979**	**AF358229**	**OQ911231**	N/A	**OQ944880**	**OQ927935**	Schroers (2001)
C. zelandiaenovae	CBS 232.80	AF210684	N/A	AF358185	N/A	N/A	Schroers (2001)
Mycocitrus coccicola	HD 2016	KU720552	KU720545	N/A	N/A	N/A	Dao et al. (2016)
M. coxeniae	BRIP 49559a	OQ629341	N/A	N/A	N/A	N/A	Zhao et al. (2023)
Sesquicillium aquaticum	**HKAS 125804**	**OP876724**	**OP875077**	N/A	N/A	N/A	Bao et al. (2023)
S. buxi	CBS 696.93	AF210667	KM231721	AF358215	KM231977	KM232416	Schroers (2001)
S. candelabrum	CBS 504.67	AF210668	N/A	N/A	N/A	N/A	Schroers (2001)
S. candelabrum	**YFCC 896**	**MW199067**	N/A	**MW201674**	N/A	N/A	Wang et al. (2023)
S. essexcoheniae	**BRIP 75170a**	**OQ629342**	N/A	N/A	**OQ944511**	**OQ914830**	Zhao et al. (2023)
S. phyllophila	**CBS 921.97**	**NR_137531**	N/A	N/A	N/A	N/A	Schroers (2001)
S. rossmaniae	CBS 210.93	AF358227	N/A	AF358213	N/A	N/A	Vu et al. (2019)
S. saulense	**BRFM 2782**	**MK635054**	N/A	N/A	N/A	N/A	Lechat et al. (2020)
S. sesquicillii	**CBS 180.88**	**AF210666**	**NG_228796**	**AF358214**	**OQ944535**	N/A	Schroers (2001)
S. shanghaiense	**HMAS 351878**	**OL897002**	**OL897044**	N/A	N/A	N/A	Zhang et al. (2023)
S. shanghaiense	GZUIFR 21.916	OL897003	OL897045	N/A	N/A	N/A	Zhang et al. (2023)
Fusarium acutatum	**CBS 402.97**	**NR_111142**	N/A	**MT011051**	N/A	N/A	Luo and Zhuang (2007)
Nectria cinnabarina	CBS 279.48	AF163025	HM484754	HM484802	HM484649	N/A	Hirooka et al. (2011)

The newly generated sequences are in red. The type strains are indicated in bold. The synonymizing are indicated in green. N/A denotes the unavailable data in GenBank.

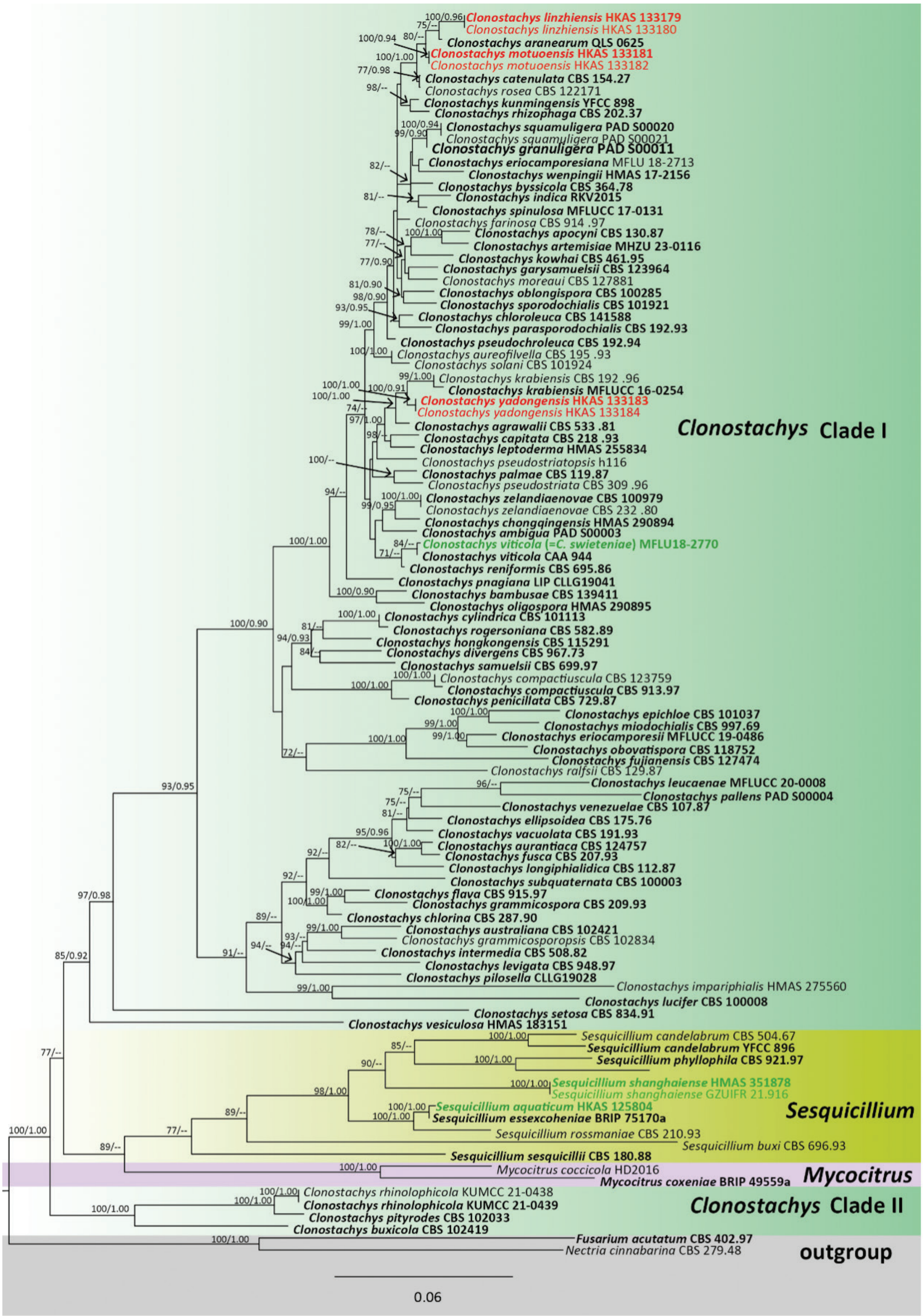

Figure 1. Phylogenetic tree generated from maximum likelihood analysis based on a combined 28S *tef*1, *rpb*2, ITS and *tub*2 sequence dataset. Bootstrap support values for ML equal to or greater than 70% and PP equal to greater than 0.90 are indicated at the nodes as MLB/BYPP. The ex-type strains are in bold, while the new isolates are in red, and the synonymizing taxa are indicated in green.

Taxonomy

Clonostachys

***Clonostachys* Corda, Pracht-Fl. Eur. Schimmelbild: 31 (1839)**
Index Fungorum: IF7701
Facesoffungi Number: FoF02102

Classification. Bionectriaceae, Hypocreales, Sordariomycetes.

Morphological characteristics. Sexual morph: ***Ascomata*** perithecial. ***Perithecia*** superficial, solitary to gregarious, subglobose to globose, papillate or non-papillate, no colour change in 3% KOH or 100% LA. ***Asci*** clavate to subcylindrical, 6–8-spored. ***Ascospores*** ellipsoidal to oblong ellipsoidal, uniseptate, hyaline, smooth-walled, uniseriate or irregular biseriate. **Asexual morph**: Hyphomycetous. ***Conidiophores*** dimorphic or monomorphic, sporodochial, synnematous, hyaline, brown or blackish brown. ***Phialides*** phialidic, cylindrical to flask-shaped. ***Conidia*** aseptate, hyaline, smooth, ovoid to ellipsoid.

Type species. *Clonostachys araucaria* Corda, Pracht-Fl. Eur. Schimmelbild.: 31 (1839)

Notes. *Clonostachys* is the second largest genus in Bionectriaceae, with 130 epithets (Index Fungorum 2025). Several members of *Clonostachys* are ecologically and economically important (Abeywickrama et al. 2023). Some *Clonostachys* spp. are destructive, including parasitic in myxomycetes, nematodes, ticks, molluscs, and leafhoppers (Schroers 2001; Toledo et al. 2006; Perera et al. 2023). *Clonostachys rosea* and *C. catenulata* are reported as destructive to ascomycetes and basidiomycetes (Schroers 2001; Chatterton et al. 2008) and *C. chuyangsinensis* and *C. aranearum* have been reported as spider-pathogenic fungi (Wan et al. 2016; Wang et al. 2023).

Clonostachys rosea has been studied as a potential biological control agent for various plant diseases and pests such as strawberry gray mold (Cota et al. 2008), *Fusarium* head blight of wheat (Xue et al. 2008), and *Pythium tracheiphilum* in Chinese cabbage (Møller et al. 2003). Several closely related species to *Clonostachys rosea*, such as *C. byssicola*, *C. chloroleuca*, *C. rhizophaga*, and *C. solani* also possess biocontrol properties (Mendoza García et al. 2003; Krauss et al. 2013; Sun et al. 2017; Broberg et al. 2021).

***Clonostachys linzhiensis* S.C. He, K.D. Hyde & Q. Zhao, sp. nov.**
Index Fungorum: IF902917
Facesoffungi Number: FoF16789
Fig. 2

Etymology. The species epithet is derived from Linzhi City, where the holotype was collected.

Typification. China • Xizang Autonomous Region, Linzhi City, Motuo County (29°11'N, 95°8'E, 1561 m), on the lower part of the leaves of *Houttuynia cordata*, July 27, 2022, collected by Hong-De Yang, YHD691 (**holotype**: KUN-HKAS 133179); ex-type living culture: KUNCC24-18528). GenBank: ITS: PQ522504, 28S: PQ634391, *tef*1: PQ650477, *tub*2: PQ650459.

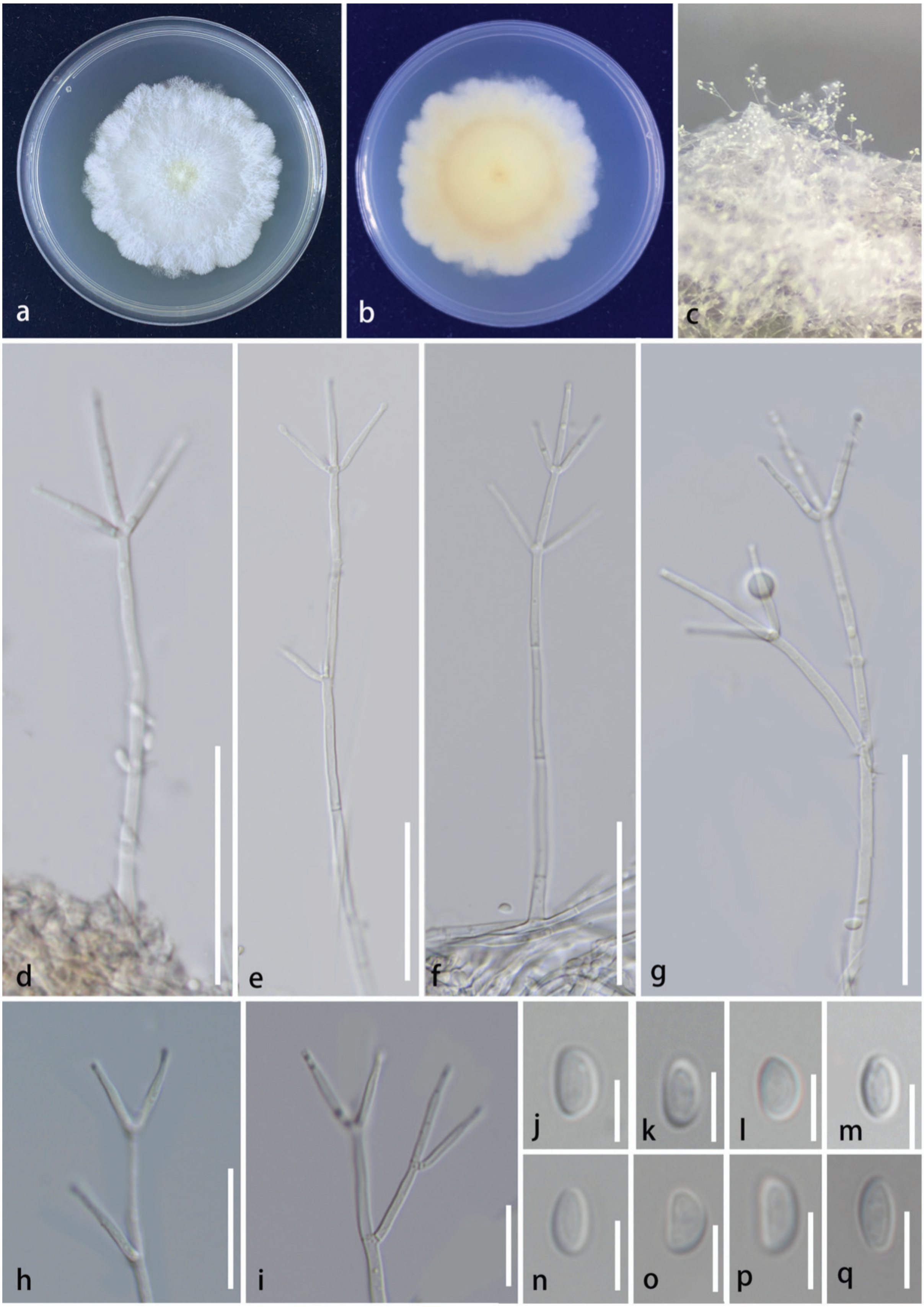

Figure 2. *Clonostachys linzhiensis* (HKAS 133179, Holotype) **a, b** culture on PDA (**a** above **b** below) **c** colonies on WA **d–g** conidiophores **h, i** phialides **j–q** conidia. Scale bars: 50 µm (**d–g**); 50 µm (**h, i**); 5 µm (**j–q**).

Description. Sexual morph: Not observed. **Asexual morph**: Hyphomycetous. ***Colonies*** on the WA, raised, medium sparse, rough, white at apex. ***Conidiophores*** mononematous, erect, simple, verticillium-like, straight or flexuous, branched, smooth-walled, thin-walled, septate, hyaline, produce globose cells at the apex, terminal branches developing into phialides, 110–232 × 2.5–3.9 µm ($\bar{x}$ = 170 × 3.2 µm, n = 20). ***Phialides*** polytretic, terminal on branches, phialides cylindrical but slightly tapering towards the tips, aseptate, hyaline, smooth, thin-walled, terminal developing into conidia, 15.3–23.8 × 1.5–3.3 µm ($\bar{x}$ = 19.8 × 2.2 µm, n = 20). ***Conidia*** amerospores, solitary, acrogenous, simple, doliiform to ellipsoidal, smooth, thin-walled, aseptate, hyaline, 3.9–5.7 × 2.2–3.2 µm ($\bar{x}$ = 4.7 × 2.6 µm, n = 30).

Culture characteristics. Colonies on PDA reaching 5.0–5.5 cm after 20 days of incubation at 25 °C, white above, pale yellow reverse, medium spare, concave in the center, convex around, hairy, lobate, velvety, ciliate, not pigment produced,

Habitat. Leaves of *Houttuynia cordata*.

Additional material examined. China • Xizang Autonomous Region, Linzhi City, Motuo County (29°11'N, 95°8'E, 1561 m), on the lower part of the leaves of *Houttuynia cordata*, July 27, 2022, collected by Hong-De Yang, HSC983 (**isotype**: KUN-HKAS 133180); ex-isotype living culture: KUNCC24-18529). GenBank: ITS: PQ522505, 28S: PQ634392, *tef*1: PQ650478, *tub*2: PQ650460.

Notes. In the phylogenetic analysis, *Clonostachys linzhiensis* shared a close phylogenetic relationship with *C. aranearum* and *C. motuoensis* (Fig. 1). *Clonostachys linzhiensis* shares similar morphology to *C. aranearum* and *C. motuoensis* in having mononematous, erect, verticillium-like conidiophores that are straight or flexuous, smooth-walled, hyaline, phialides are polytretic, terminal, flask-shaped, aseptate, hyaline, smooth and the conidia are amerospores, acrogenous, ellipsoidal, aseptate, hyaline (Wan et al. 2016). However, *Clonostachys linzhiensis* (HKAS 133179 and HKAS 133180) has larger conidiophores (L/W ratio: 53 vs 12 and L/W ratio: 53 vs 35) and longer phialides (L/W ratio: 9 vs 6.7 and L/W ratio: 9 vs 4.7) in comparison to *C. aranearum* and *C. motuoensis*. Furthermore, the ITS and *tub*2 sequence of *Clonostachys linzhiensis* differs from *C. aranearum* which revealed 13/510 (2.5%) and 7/291 (2.4%) base pair differences, respectively. Based on the differences in morphology (larger conidiophores and longer phialides) and phylogeny, along with the guidelines of Maharachchimbukura et al. (2021), we identify our specimen as a new species, *C. linzhiensis*.

Clonostachys motuoensis **S.C. He, K.D. Hyde & Q. Zhao, sp. nov.**

Index Fungorum: IF902918
Facesoffungi Number: FoF16790
Fig. 3

Etymology. The species epithet is derived from the location “Motuo County”, from where the holotype was collected.

Typification. China • Xizang Autonomous Region, Linzhi City, Motuo County (29°11'N, 95°8'E, 1561 m), on the lower part of the leaves of *Houttuynia cordata*, July 27, 2022, collected by Hong-De Yang, YHD669-1 (holotype: KUN-HKAS HKAS 133181); ex-type living culture: KUNCC24-18530). GenBank:ITS: PQ522506, 28S: PQ634393, *tef*1: PQ650479, *tub*2: PQ650461.

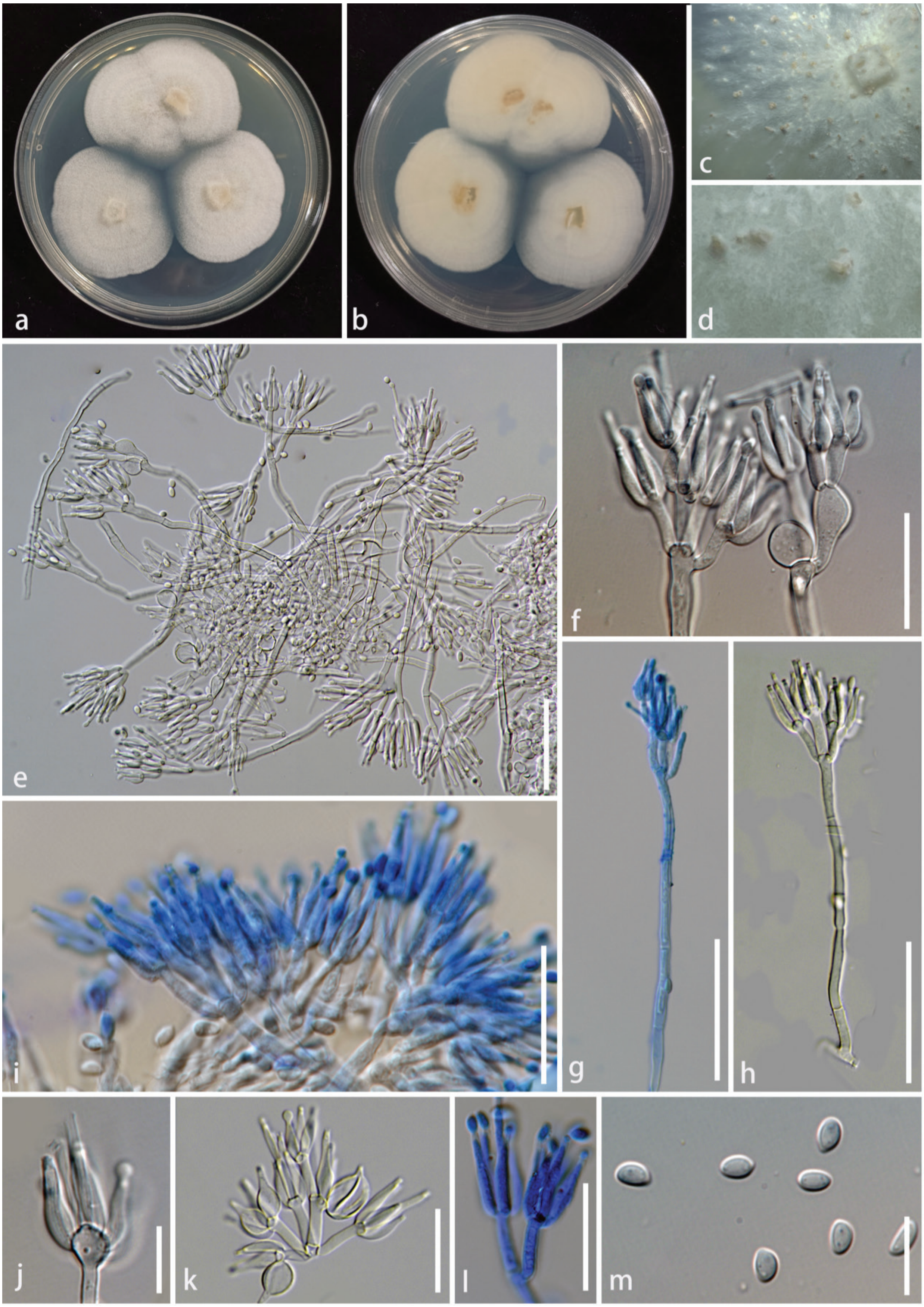

Figure 3. *Clonostachys motuoensis* (HKAS 133181, Holotype) **a, b** culture on PDA (**a** above **b** below) **c, d** colonies on WA **e–h** conidiophores and conidiophores apex **i–l** phialides **m** conidia. Scale bars: 50 µm (**e, g, h**); 25 µm (**f, i, k, l**); 10 µm (**j, m**).

Description. Sexual morph: Not observed. **Asexual morph**: Hyphomycetous. ***Colonies*** on the WA, solitary or gregarious, white to pale yellow, raised, dense, rough. ***Conidiophores*** mononematous, penicillate, straight or flexuous, branched at the apex, smooth, thin-walled, septate, hyaline, conidiophores produce globose cells at the apex, from globose to elongated or continue to differentiate, terminal branches developing into phialides, 94–146 × 2.5–4.7 µm ($\bar{x}$ = 125 × 3.5 µm, n = 20). ***Phialides*** monophialidic, terminal, flask-shaped, aseptate, hyaline, smooth, thin-walled, terminal developing into conidia, 9.1–18.7 × 2.3–3.5 µm ($\bar{x}$ = 13.2 × 2.8 µm, n = 20). ***Conidia*** amerospores, solitary, acrogenous, simple, ellipsoidal to oblong with obtuse ends, smooth, thin-walled, aseptate, hyaline, minutely guttulate, 3.9–5.6 × 2.5–3.3 µm ($\bar{x}$ = 4.6 × 2.9 µm, n = 30).

Culture characteristics. Colonies on PDA reaching 3.5–4 cm after 20 days of incubation at 25 °C, white both above and reverse, medium spare, raised, smooth, fimbriate, velvety, ciliate, not pigment produced.

Habitat. Leaves of *Houttuynia cordata*.

Additional material examined. China • Xizang Autonomous Region, Linzhi City, Motuo County (29°11'N, 95°8'E, 1561 m), on the lower part of the leaves of *Houttuynia cordata*, July 27, 2022, collected by Hong-De Yang, HSC986 (isotype: KUN-HKAS 133182); ex-isotype living culture: KUNCC24-18531). GenBank: ITS: PQ522507, 28S: PQ634394, *tef*1: PQ650480, *tub*2: PQ650462.

Notes. In the phylogenetic analysis, *Clonostachys motuoensis* clustered sister to *C. linzhiensis* and *C. aranearum* (Fig. 1). Morphologically, our specimen (HKAS 133181 and HKAS 133182) has larger conidiophores (L/W ratio: 35 vs 12) and longer phialides (L/W ratio: 4.7 vs 6.7) in comparison to *C. aranearum*. *Clonostachys motuoensis* differs from *C. aranearum* by 6/544 (1%) ITS and 4/294 (1.3%) *tub2* differences in the nucleotides. It is worth noting that *C. aranearum* is parasitic on spiders, while *C. motuoensis* is endophytic on *Houttuynia cordata* leaves. In addition, *C. aranearum* was collected from Qian Ling Shan Park, Guiyang City, Guizhou Province, China, with an altitude of 1100–1369 m, belonging to a plateau subtropical climate (Wan et al. 2016). *Clonostachys motuoensis* was collected from Motuo County, Linzhi City, Xizang Autonomous Region, China, with an altitude of 1561 m, belonging to a tropical rainforest climate. Based on these distinctions and following the guidelines of Maharachchimbukura et al. (2021), we identified our specimen as a new species, *C. motuoensis*.

Clonostachys yadongensis S.C. He, K.D. Hyde & Q. Zhao, sp. nov.

Index Fungorum: IF902919
Facesoffungi Number: FoF16791
Fig. 4

Etymology. The species epithet is derived from Yadong County, where the holotype was collected.

Typification. China • Xizang Autonomous Region, Linzhi City, Yadong County (27°48'N, 88°83'E, 3894 m), on the lower part of the leaves of *Ageratina adenophora* leaves, July 24, 2023, collected by Shu-Cheng He, HSC1025 (holotype: KUN-HKAS 133183); ex-type living culture: KUNCC24-18532). GenBank:ITS: PQ522508, 28S: PQ634395, *tef*1: PQ650481, *tub*2: PQ650463, *rpb2*: PQ538524.

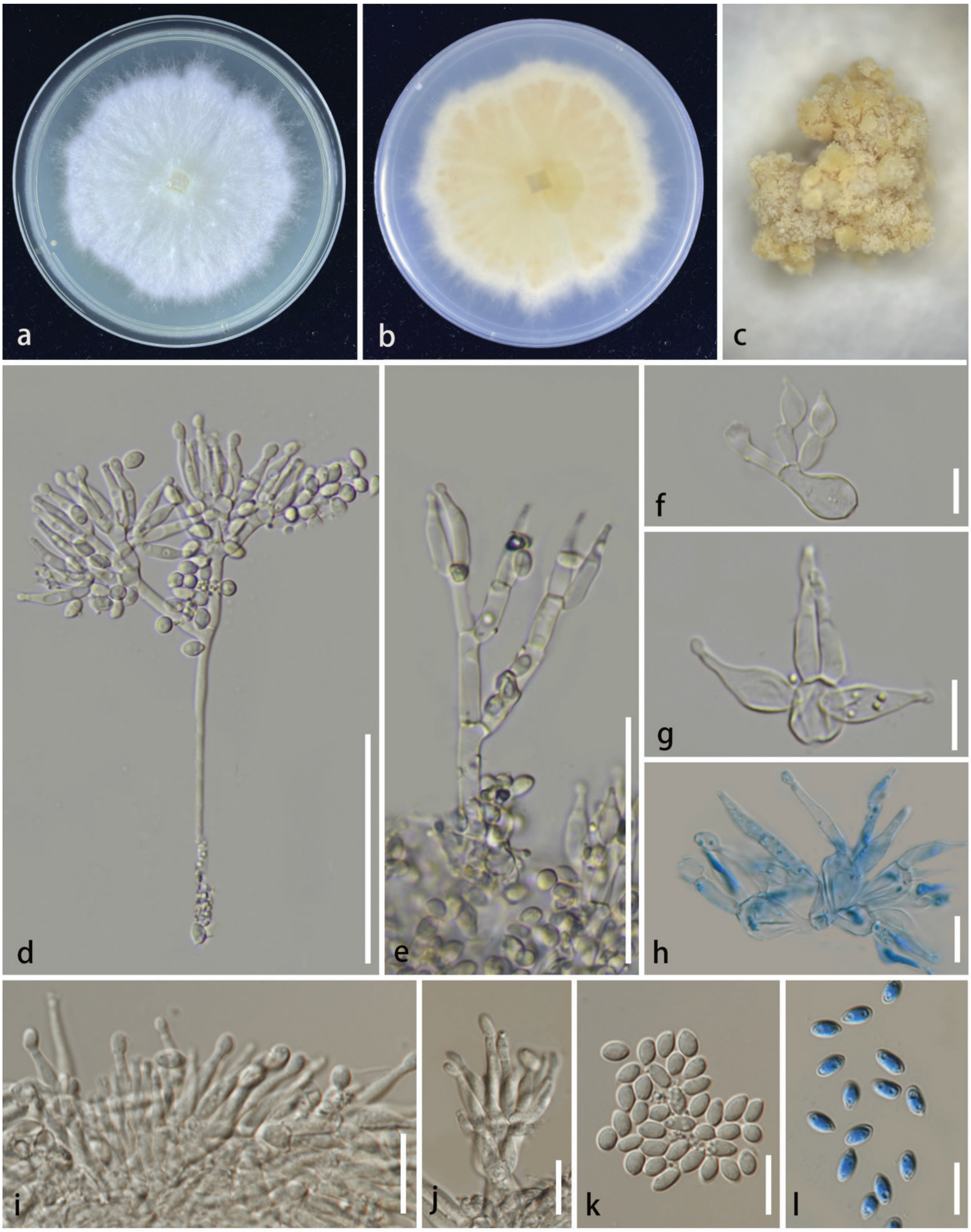

Figure 4. *Clonostachys yadongensis* (HKAS 133183, Holotype) **a, b** culture on PDA (**a** above **b** below); **c** colonies on WA **d–h** conidiophores **f–j** phialides **k, l** conidia. Scale bars: 50 μm (**d–f**); 20 μm (**g–l**).

Description. Sexual morph: Not observed. **Asexual morph:** Hyphomycetous. ***Colonies*** on the WA, solitary or gregarious, white to pale yellow, raised, medium sparse, rough. ***Conidiophores*** mononematous, penicillate, straight or flexuous, branched, smooth-walled, thin-walled, septate, hyaline, produce globose cells at the apex, terminal branches developing into phialides, 80–118 × 2.4–3.4 μm ($\bar{x}$ = 97 × 2.8 μm, n = 20). ***Phialides*** polyblastic, terminal, flask-shaped, aseptate, hyaline, smooth, thin-walled, minutely guttulate, terminal developing into conidia, 9.6–15.6 × 1.7–2.3 μm ($\bar{x}$ = 13.1 × 2 μm, n = 20). ***Conidia*** amerospores, solitary, acrogenous, simple, oval to ellipsoidal, smooth, thin-walled, aseptate, hyaline, minutely guttulate, 3.6–5.4 × 2.6–3.3 μm ($\bar{x}$ = 4.5 × 2.9 μm, n = 30).

Culture characteristics. Colonies on PDA reaching 5.5–6 cm after 20 days of incubation at 25 °C, white above, pale yellow reverse, medium spare, raised, hairy, fimbriate, velvety, ciliate, not pigment produced.

Habitat. Leaves of *Ageratina adenophora*.

Additional material examined. CHINA • Xizang Autonomous Region, Linzhi City, Yadong County (27°48'N, 88°83'E, 3894 m), on the lower part of the leaves of *Ageratina adenophora*, July 24, 2023, collected by Shu-Cheng He, HSC1025A (isotype: KUN-HKAS 133184; ex-isotype living culture: KUNCC24-18533). GenBank:ITS: PQ522509, 28S: PQ634391, *tef*1: PQ650482, *tub*2: PQ650464, *rpb2*: PQ538525.

Notes. In the phylogenetic analysis, *Clonostachys yadongensis* clustered with *C. krabiensis* with 100% MLB and 0.91 BYPP support (Fig. 1). *Clonostachys krabiensis* was introduced by Tibpromma et al. (2018) and is characterized by solitary, superficial, globose to subglobose, orange to brownish orange ascomata, 6–8-spored, cylindrical to clavate asci; fusoid to ellipsoidal, hyaline, with longitudinal striations, granulate ascospores. Its morphology fits well with the generic concept of *Clonostachys* sexual morph (Bao et al. 2023; Perera et al. 2023; Zhao et al. 2023). Our specimen (HKAS 133183) exhibited an asexual morph that is characterized by mononematous, penicillate, erect conidiophores; flask-shaped or cylindrical, aseptate, hyaline phialides; acrogenous, ellipsoidal or oblong with obtuse ends, hyaline conidia. The 28S and ITS sequences of *Clonostachys yadongensis* differ from that of *C. krabiensis* which showed base pair differences, 3/825 (0.35%), 11/513) and (2.1%) respectively. *Clonostachys krabiensis* was reported in Papua New Guinea and Thailand as a saprobe on *Pandanus* sp. and wood litter, while *C. yadongensis* was reported in the Xizang Autonomous Region, China, mainly as an endophyte on *Ageratina adenophora*. *Clonostachys krabiensis* has been reported to have a sexual morph, but *C. yadongensis* has only been observed in its asexual morph. Based on base pair differences and following the guidelines of Maharachchimbukura et al. (2021), we identified our specimen as a new species, *Clonostachys yadongensis*.

Clonostachys viticola **C. Torcato & A. Alves, *Int. J. Syst. Evol. Microbiol*, 6 (2020)**

Index Fungorum: IF835021
Facesoffungi Number: FoF16792

Basionym. *Clonostachys swieteniae* R.H. Perera, E.B.G. Jones & K.D. Hyde, *Mycosphere* 11(1): 2135 (2020)

Description and illustration. Perera et al. 2020 and Torcato et al. 2020.

Notes. In the multigene phylogenetic analyses, *Clonostachys viticola* with *C. swieteniae*, forms a monophyletic clade in *Clonostachys*. The taxa in this clade show low genetic differences. Thus, we recommend treating *C. viticola* and *C. swieteniae* as conspecific. *Clonostachys viticola* was established by Torcato et al. (2020) from the root of *Vitis vinifera* in a terrestrial habitat of Peru (Torcato et al. 2020) and *Clonostachys swieteniae* was established by Perera et al. (2020)

from decaying fruits of *Swietenia mahagoni* in a terrestrial habitat of Thailand (Perera et al. 2020). Morphologically, *C. viticola* with *C. swieteniae* are highly similar, but there are minor differences in phialides (13.1 × 2.1 μm vs 11.4 × 2.6 μm), and conidia (5.6 × 2.9 μm vs 6 × 2.2 μm). Through base pair comparison, the ITS and *tef*1 sequence of *Clonostachys viticola* differs from that of *C. swieteniae* in 0/500 (0%) and 3/406 (0.7%), respectively. The results indicate that different environments have shaped the morphology (Bhunjun et al. 2022; Hyde et al. 2020b; Phukhamsakda et al. 2022). *Clonostachys viticola* was published prior to *C. swieteniae*. Therefore, we propose *C. swieteniae* as a synonym of *C. viticola*.

New combinations of *Sesquicillium*

***Sesquicillium* W. Gams, Acta bot. neerl. 17(6): 455 (1968)**
Index Fungorum: IF9906
Facesoffungi Number: FoF16793

Classification. Bionectriaceae, Hypocreales, Sordariomycetes

Morphological characteristics. Sexual morph: Ascomycetous. ***Perithecia*** solitary, gregarious or loosely aggregated, globose to subglobose, 200–400 μm diam, pale yellow or pale to light orange, not papillate, Perithecial wall either consisting of two or one major wall regions. ***Asci*** clavate, 8-spored, with flat or rounded apex. ***Ascospores*** aseptate or 1-septate, hyaline, spinulose, warted, with short striae, ellipsoidal to fusiform. **Asexual morph.** Hyphomycetous. ***Conidiophores*** macronematous, mononematous, monomorphic or dimorphic, penicillate, verticillate; branches at apex. ***Phialides*** one or two successive intercalary phialides, terminal, terminal whorls consisting of narrowly flask-shaped, hyaline. ***Conidia*** obovoid, ellipsoid, or fusoid, slightly curved or straight, hyaline, aseptate, smooth-walled, thin-walled.

Type species. *Sesquicillium buxi* (J.C. Schmidt ex Link) W. Gams, Acta bot. neerl. 17(6): 455 (1968)

Notes. *Sesquicillium* was established by Gams (1968). Morphologically, *Sesquicillium* shares similar characteristics with *Clonostachys* in that the conidiophores are macronematous, monomorphic or dimorphic, penicillate, verticillate-like, branched, flask-shaped conidiogenous cells (Preedanon et al. 2023; Zhao et al. 2023). Zhao et al. (2023) revealed the close relationship between *Clonostachys* and *Sesquicillium* and reclassified eight species of *Clonostachys* to *Sesquicillium*. The difference between *Sesquicillium* and *Clonostachys* lies in the development of their conidiophores. In *Sesquicillium*, the conidiophore will form a lateral conidia process after bifurcation, leading to the production of conidia. In *Clonostachys*, the conidiophore will not form lateral conidia protrusions after bifurcation. It continues to differentiate into terminal phialides (Gams 1968; Schroers 2001). Based on the research of Chen et al. (2023), and Zhao et al. (2023), we used ITS, 28S, *tef*1, *tub*2, and *rpb*2 to reconstruct a phylogenetic tree to investigate the relationship of *Clonostachys* species. The results show that *Clonostachys aquatica* and *C. shanghaiensis* are far from *Clonostachys* and more closely related to *Sesquicillium*. Therefore, based on morphological and phylogenetic analysis, we propose *C. aquatica* and *C. shanghaiensis* are synonyms of *S. aquaticum* and *S. shanghaiense*.

Sesquicillium aquaticum (D.F. Bao, K.D. Hyde & Z.L. Luo) S.C. He, K.D. Hyde & Jayaward, [as 'aquatica'], comb. nov.
Index Fungorum: IF903022
Facesoffungi Number: FoF16794

Basionym. *Clonostachys aquatica* D.F. Bao, K.D. Hyde & Z.L. Luo, *Fungal Diversity*, (2023).

Holotype. HKAS 125804.

Description and illustration. See Bao et al. 2023.

Notes. *Clonostachys aquatica* was established by Bao et al. (2023) based on ITS and *tub2* sequence data (holotype HKAS 125804). Through the study of Bao et al. (2023), *C. aquatica* clustered as a clade sister to *C. rossmaniae* with strong support (94% MLB, 98% MYPP). Following Bao et al. (2023), we added 28S, *tef*1 and *rpb*2 sequence data, and the results showed that *C. aquatica* clustered with *Sesquicillium essexcoheniae* (100% MLB, 0.97 BYPP), forming a successive sister clade with *S. rossmaniae* (99% MLB,/1.00 BYPP) (Fig. 1). *Clonostachys aquatica* shows a closer relationship with *Sesquicillium* in phylogenetic analysis. Therefore, based on phylogenetic analysis, we propose *C. aquatica* as a synonym of *S. aquaticum*.

Sesquicillium shanghaiense (Zhi Yuan Zhang, Y.F. Han & Z.Q. Liang) S. C. He, K.D. Hyde & Jayaward, [as 'shanghaiensis'], comb. nov.
Index Fungorum: IF903023
Facesoffungi Number: FoF16795

Basionym. *Clonostachys shanghaiensis* Zhi Yuan Zhang, Y.F. Han & Z.Q. Liang, *MycoKeys* 98: 198 (2023).

Holotype. HMAS 351878.

Description and illustration. Zhang et al. (2023).

Notes. *Clonostachys shanghaiensis* was established by Zhang et al. (2023), based on ITS and *tub2* sequence data (HMAS 351878). *Clonostachys shanghaiensis* clustered as a sister clade to *C. rossmaniae* (95% MLB, 0.99 BYPP) (Zhang et al. 2023). In this study, phylogenetic analysis showed that *Clonostachys shanghaiensis* formed a successive sister clade with *S. phyllophila*, *S. saulensis*, and *S. candelabrum* (Fig. 1). It is worth noting that *S. phyllophila*, *S. saulense*, and *S. candelabrum* were renamed by Zhao et al. (2023) as *C. phyllophila* (Schroers 2001), *C. saulensis* (Lechat et al. 2020), *C. candelabrum* (Schroers 2001) and *C. chuyangsinensis* (Wang et al. 2023) based on morphology and phylogenetic analysis. Therefore, based on phylogenetic analysis, we propose *C. shanghaiensis* as a synonym of *S. shanghaiense*.

Discussion

Rossman et al. (2001) studied the asexual species in 15 genera of Bionectriaceae (Hypocreales) using 28S sequence data and showed that Bionectriaceae formed a monophyletic group. Recently, additional DNA gene sequences such as *acl*1, *tub*2, *rpb*1, and *tef*1 have been used to enhance the precision of phylogenetic trees within the *Clonostachys*/*Bionectria* species (Moreira et al. 2016). However, available sequence data for these four protein-encoding gene regions is lacking in GenBank (Moreira et al. 2016). Wang et al. (2023), stated that *tef*1 sequence data showed the highest resolution for distinguishing *Clonostachys* species (*tef*1>*tub*2>ITS) based on the investigation conducted for genetic divergence comparisons of *Clonostachys*. Zhao et al. (2023) investigated the generic delineation with broad taxon sampling with morphology and multi-gene (ITS, 28S, *tef*1, *tub*2, *rpb*2) phylogenetic analysis and found a close relationship to *Sesquicillium*. Further, *Sesquicillium* was resurrected to accommodate the former subgenera *Epiphloea* and *Uniparietina* (Zhao et al. 2023). We constructed a phylogenetic tree (Fig. 1) of *Clonostachys* based on five genes (28S, *tef*1, *rpb*2, ITS, and *tub*2) and show that *Clonostachys*/*Bionectria* form a similar topology with Perera et al. (2023). However, as with other studies, we did not achieve a well-supported clade, as some but not all subgenera are mono- or paraphyletic (Moreira et al. 2016; Bao et al. 2023; Perera et al. 2023; Wang et al. 2023; Zhao et al. 2023). Morphologically, the asexual morphs of *Clonostachys* exhibit similarities with those of *Sesquicillium* (Preedanon et al. 2023), *Penicillium* (Crous et al. 2023), *Verticillium* (Crous et al. 2022), *Gliocladium* (Rehner and Samuels 1994) acremonium-like (Preedanon et al. 2023). They typically feature macronematous, monomorphic penicillate, or dimorphic penicillate conidiophore. Based on recent studies by Bao et al. (2023), Wang et al. (2023), and Zhao et al. (2023), we have clarified the relationships within the *Clonostachys* and proposed that *C. aquatica*, *C. shanghaiensis*, and *C. swieteniae* be considered synonyms of *S. aquaticum*, *S. shanghaiense*, and *C. viticola*, respectively. *Clonostachys aquatica* and *C. shanghaiensis* were positioned in a distantly related clade (Clade II) to *Clonostachys sensu stricto*. *Mycocitrus* and *Sesquicillium*, were positioned between Clade I and II (Fig. 1). Thus, further studies are required for the phylogenetic resolution of *Clonostachys*.

Clonostachys is reported in various plant hosts: Apocynaceae, Arecaceae, Asteraceae, Boraginaceae, Buxaceae, Ericaceae, Fagaceae, Leguminosae, Melampsoraceae, Nelumbonaceae, Pandanaceae, Rosaceae, and Rutaceae (Wang et al. 2023; Jayawardena et al. 2025). Our study reported three new species from Eupatorieae (*C. yadongensis*) and Saururaceae (*C. linzhiensis* and *C. motuoensis*). *Clonostachys* species exhibit a saprobic or endophytic lifestyle, playing crucial roles in nutrient cycling and plant health (Zeng and Zhuang 2022). *Clonostachys* species are significant for their adaptability and potential as biological control agents against plant pathogens (Wang et al. 2023; Zhao et al. 2023).

Acknowledgements

This study is supported by the Second Tibetan Plateau Scientific Expedition and Research (STEP) Program (Grant No. 2019QZKK0503), the Yunnan Revitalization Talent Support Program: Science & Technology Champion Project (202305AB350004), the Major Science and Technology projects and key R&D plans/programs, Yunnan Province (202202AE090001) and the Survey of Wildlife Resources in Key Areas of Tibet (ZL202303601), the grant number E1644111K1, titled “Flexible introduction of high-level expert program, Kunming Institute of Botany, Chinese academy of sciences” for its financial support. Vinodhini Thiyagaraja thanks Yunnan Province “Caiyun Postdoctoral Program” in 2023, Choi Wan Postdoctoral Program in 2023, and National Postdoctoral funding, China. Chitrabhanu S. Bhunjun would like to thank the National Research Council of Thailand (NRCT) grant “Total fungal diversity in a given forest area with implications towards species numbers, chemical diversity, and biotechnology" (grant no. N42A650547). The authors extend their appreciation to the Researchers Supporting Project number (RSP2025R114), King Saud University, Riyadh, Saudi Arabia. Shu-cheng He thanks Mae Fah Luang University for the basic research scholar 2567 grant.

Additional information

Conflict of interest

The authors have declared that no competing interests exist.

Ethical statement

No ethical statement was reported.

Funding

This work was supported by the Chinese Research Fund, grant number E1644111K1, titled "Flexible introduction of the high-level expert program, Kunming Institute of Botany, Chinese Academy of Sciences.

Author contributions

S.-C.H and V.T. conceived and designed the study. H.-D. Y provided two new species. Y.-W.Z make two plates. S.-C.H and Y.-W.Z. generated the DNA sequence data. S.-C.H analyzed the data. S.-C.H. wrote the manuscript draft. V.T., C.S.B., P.C., L.S.D., R.S.J., Q.Z., K.D.H. revised the manuscript. FO provided financial support. All authors have read and agreed to the published version of the manuscript.

Author ORCIDs

Shucheng He https://orcid.org/0009-0008-7364-4727
Vinodhini Thiyagaraja https://orcid.org/0000-0002-8091-4579
Chitrabhanu S. Bhunjun https://orcid.org/0000-0001-8098-3390
Putarak Chomnunti https://orcid.org/0000-0003-2989-1735
Lakmali S. Dissanayake https://orcid.org/0000-0003-2933-3127
Ruvishika S. Jayawardena https://orcid.org/0000-0001-7702-4885
Yun Wei Zhao https://orcid.org/0009-0006-8211-5232
Fatimah Al-Otibi https://orcid.org/0000-0003-3629-5755
Qi Zhao https://orcid.org/0000-0001-8169-0573
Kevin D. Hyde https://orcid.org/0000-0002-2191-0762

Data availability

All of the data that support the findings of this study are available in the main text.

Reference

Abeywickrama PD, Qian N, Jayawardena RS, Li Y, Zhang W, Guo K, Zhang L, Zhang G, Yan J, Li X, Guo Z, Hyde KD, Peng Y, Zhao W (2023) Endophytic fungi in green manure crops; friends or foe? Mycosphere 14(1): 1–106. https://doi.org/10.5943/mycosphere/14/1/1

Abreu LM, Moreira GM, Ferreira D, Rodrigues-Filho E, Pfenning LH (2014) Diversity of *Clonostachys* species assessed by molecular phylogenetics and MALDI-TOF mass spectrometry. Fungal Biology 118(12): 1004–1012. https://doi.org/10.1016/j.funbio.2014.10.001

Bao DF, Hyde KD, Maharachchikumbura SSN, Perera RH, Thiyagaraja V, Hongsanan S, Wanasinghe DN, Shen HW, Tian XG, Yang LQ, Nalumpang S, Luo ZL (2023) Taxonomy, phylogeny and evolution of freshwater Hypocreomycetidae (Sordariomycetes). Fungal Diversity 121(1): 1–94. https://doi.org/10.1007/s13225-023-00521-8

Bhunjun CS, Phillips AJ, Jayawardena RS, Promputtha I, Hyde KD (2021) Importance of molecular data to identify fungal plant pathogens and guidelines for pathogenicity testing based on Koch'S postulates. Pathogens (Basel, Switzerland) 10(9): 1096. https://doi.org/10.3390/pathogens10091096

Bhunjun CS, Niskanen T, Suwannarach N, Wannathes N, Chen Y-J, McKenzie EHC, Maharachchikumbura SSN, Buyck B, Zhao C-L, Fan Y-G, Zhang J-Y, Dissanayake AJ, Marasinghe DS, Jayawardena RS, Kumla J, Padamsee M, Chen Y-Y, Liimatainen K, Ammirati JF, Phukhamsakda C, Liu J-K, Phonrob W, Randrianjohany É, Hongsanan S, Cheewangkoon R, Bundhun D, Khuna S, Yu W-J, Deng L-S, Lu Y-Z, Hyde KD, Lumyong S (2022) The numbers of fungi : Are the most speciose genera truly diverse? Fungal Diversity 114(1): 387–462. https://doi.org/10.1007/s13225-022-00501-4

Broberg M, Dubey M, Iqbal M, Gudmundssson M, Ihrmark K, Schroers HJ, Funck Jensen D, Brandström Durling M, Karlsson M (2021) Comparative genomics highlights the importance of drug efflux transporters during evolution of mycoparasitism in *Clonostachys* subgenus *Bionectria* (Fungi, Ascomycota, Hypocreales). Evolutionary Applications 14(2): 476–497. https://doi.org/10.1111/eva.13134

Carbone I, Kohn LM (1999) A method for designing primer sets for speciation studies in filamentous ascomycetes. Mycologia 91(3): 553–556. https://doi.org/10.1080/00275514.1999.12061051

Chatterton S, Jayaraman J, Punja ZK (2008) Colonization of cucumber plants by the biocontrol fungus *Clonostachys rosea* f. *catenulata*. Biological Control 46(2): 267–278. https://doi.org/10.1016/j.biocontrol.2008.02.007

Chen WH, Han YF, Liang JD, Zou X, Liang ZQ, Jin DC (2016) A new araneogenous fungus of the genus *Clonostachys*. Mycosystema 35: 1061–1069. https://doi.org/10.13346/j.mycosystema.150244

Chen YP, Su PW, Hyde KD, Maharachchikumbura SSN (2023) Phylogenomics and diversification of Sordariomycetes. Mycosphere 14(1): 414–451. https://doi.org/10.5943/mycosphere/14/1/5

Chethana KWT, Manawasinghe IS, Hurdeal VG, Bhunjun CS, Appadoo MA, Gentekaki E, Raspé O, Promputtha I, Hyde KD (2021) What are fungal species and how to delineate them? Fungal Diversity 109(1): 1–25. https://doi.org/10.1007/s13225-021-00483-9

Clewley JP (1995) Macintosh sequence analysis software - DNAStar's LaserGene. Molecular Biotechnology 3(3): 221–224. https://doi.org/10.1007/BF02789332

Corda ACJ (1839) Icones fungorum hucusque cognitorum, vol. 3.

Cota LV, Maffia LA, Mizubuti ESG, Macedo PEF, Antunes RF (2008) Biological control of strawberry gray mold by *Clonostachys rosea* under field conditions. Biological Control 46(3): 515–522. https://doi.org/10.1016/j.biocontrol.2008.04.023

Crous PW, Boers J, Holdom D, Osieck ER, Steinrucken TV, Tan YP, Vitelli JS, Shivas RG, Barrett M, Boxshall AG, Broadbridge J, Larsson E, Lebel T, Pinruan U, Sommai S, Alvarado P, Bonito G, Decock CA, De la Peña-Lastra S, Delgado G, Houbraken J, Maciá-Vicente JG, Raja HA, Rigueiro-Rodríguez A, Rodríguez A, Wingfield MJ, Adams SJ, Akulov A, AL-Hidmi T, Antonín V, Arauzo S, Arenas F, Armada F, Aylward J, Bellanger J-M, Berraf-Tebbal A, Bidaud A, Boccardo F, Cabero J, Calledda F, Corriol G, Crane JL, Dearnaley JDW, Dima B, Dovana F, Eichmeier A, Esteve-Raventós F, Fine M, Ganzert L, García D, Torres-Garcia D, Gené J, Gutiérrez A, Iglesias P, Istel Ł, Jangsantear P, Jansen GM, Jeppson M, Karun NC, Karich A, Khamsuntorn P, Kokkonen K, Kolarík M, Kubátová A, Labuda R, Lagashetti AC, Lifshitz N, Linde C, Loizides M, Luangsa-ard JJ, Lueangjaroenkit P, Mahadevakumar S, Mahamedi AE, Malloch DW, Marincowitz S, Mateos A, Moreau P-A, Miller AN, Molia A, Morte A, Navarro-Ródenas A, Nebesářová J, Nigrone E, Nuthan BR, Oberlies NH, Pepori AL, Rämä T, Rapley D, Reschke K, Robicheau BM, Roets F, Roux J, Saavedra M, Sakolrak B, Santini A, Ševčíková H, Singh PN, Singh SK, Somrithipol S, Spetik M, Sridhar KR, Starink-Willemse M, Taylor VA, van Iperen AL, Vauras J, Walker AK, Wingfield BD, Yarden O, Cooke AW, Manners AG, Pegg KG, Groenewald JZ (2022) Fungal Planet description sheets: 1383–1435. Persoonia 48(1): 261–371. https://doi.org/10.3767/persoonia.2022.48.08

Crous PW, Osieck ER, Shivas RG, Tan YP, Larsson E, Pancorbo F, Balashov S, Baseia IG, Boekhout T, Chandranayaka S, Cowan DA, Cruz RHSF, Czachura P (2023) Fungal Planet description sheets: 1478–1549. Persoonia 50(1): 158–310. https://doi.org/10.3767/persoonia.2023.50.05

Dao HT, Beattie GAC, Rossman AY, Burgess LW, Holford P (2016) Four putative entomopathogenic fungi of armoured scale insects on Citrus in Australia. Mycological Progress 15: 1–14. https://doi.org/10.1007/s11557-016-1188-6

Dong W, Hyde KD, Jeewon R, Liao CF, Zhao HJ, Kularathnage ND, Li H, Yang YH, Pem D, Shu YX, Gafforov Y, Manawasinghe IS, Doilom M (2023) Mycosphere notes 449–468: Saprobic and endophytic fungi in China, Thailand, and Uzbekistan. Mycosphere 14(1): 2208–2262. https://doi.org/10.5943/mycosphere/14/1/26

Forin N, Vizzini A, Nigris S, Ercole E, Voyron S, Girlanda M, Baldan B (2020) Illuminating type collections of nectriaceous fungi in Saccardo's fungarium. Persoonia: Molecular Phylogeny and Evolution of Fungi 45: 221–249. https://doi.org/10.3767/persoonia.2020.45.09

Gams KW (1968) Die systematische Stellung der Schimmelpilze *Fusidium buxi* und *Verticillium candelabrum*. Acta Botanica Neerlandica 17(6): 455–460. https://doi.org/10.1111/j.1438-8677.1968.tb00552.x

Hall T (1999) BioEdit auser-friendly biological sequence alignment editor and analysis program for Windows 95/98/NT. Nucleic Acids Symposium Series 41: 95–98.

He SC, Wei DP, Bhunjun CS, Zhao Q, Jayawardena RS (2023) A new species of *Stephanonectria* (Bionectriaceae) from southwestern China. Asian Journal of Mycology 6(1): 98–106. https://doi.org/10.5943/ajom/6/1/9

He SC, Wei DP, Bhunjun CS, Apurillo CCS, Thiyagaraja V, Jayawardena RS, Zhao YW, Zhao Q (2024a) A new species of *Neotorula* (Pleosporales) from the Southwest, China. Phytotaxa 662(3): 251–261. https://doi.org/10.11646/phytotaxa.662.3.4

He SC, Wei DP, Bhunjun CS, Jayawardena RS, Thiyagaraja V, Zhao Q, Al-Otibi F, Hyde KD (2024b) Morphology and multi-gene phylogeny reveal a new species of family Torulaceae from Yunnan Province, China. Diversity 16(9): 551. https://doi.org/10.3390/d16090551

He SC, Thiyagaraja V, Bhunjun CS, Jayawardena RS, Chomnunti P, Al-Otibi F, Zhao YW, Zhao Q, Hyde KD (2024c) A new *Myxospora* (Hypocreales, Sordariomycetes) species from the Tibetan Plateau, China. New Zealand Journal of Botany: 1–17. https://doi.org/10.1080/0028825X.2024.2438411

Hirooka Y, Kobayashi T (2007) Taxonomic studies of nectrioid fungi in Japan. II: The genus *Bionectria*. Mycoscience 48: 81–89. https://doi.org/10.1007/s10267-006-0331-7

Hirooka Y, Rossman AY, Chaverri P (2011) A morphological and phylogenetic revision of the *Nectria cinnabarina* species complex. Studies in Mycology 68: 35–56. https://doi.org/10.3114/sim.2011.68.02

Hyde KD, Jeewon R, Chen YJ, Bhunjun CS, Calabon MS, Jiang HB, Lin CG, Norphanphoun C, Sysouphanthong P, Pem D, Tibpromma S, Zhang Q, Doilom M, Jayawardena RS, Liu JK, Maharachchikumbura SSN, Phukhamsakda C, Phookamsak R, Al-Sadi AM, Thongklang N, Wang Y, Gafforov Y, Gareth Jones EB, Lumyong S (2020a) The numbers of fungi: Is the descriptive curve flattening? Fungal Diversity 103(1): 219–271. https://doi.org/10.1007/s13225-020-00458-2

Hyde KD, Norphanphoun C, Maharachchikumbura SSN, Bhat DJ, Jones EBG, Bundhun D, Chen YJ, Bao DF, Boonmee S, Calabon MS, Chaiwan N, Chethana KWT, Dai DQ, Dayarathne MC, Devadatha B, Dissanayake AJ, Dissanayake LS, Doilom M, Dong W, Fan XL, Goonasekara ID, Hongsanan S, Huang SK, Jayawardena RS, Jeewon R, Karunarathna A, Konta S, Kumar V, Lin CG, Liu JK, Liu NG, Luangsa-ard J, Lumyong S, Luo ZL, Marasinghe DS, McKenzie EHC, Niego AGT, Niranjan M, Perera RH, Phukhamsakda C, Rathnayaka AR, Samarakoon MC, Samarakoon SMBC, Sarma VV, Senanayake IC, Shang QJ, Stadler M, Tibpromma S, Wanasinghe DN, Wei DP, Wijayawardene NN, Xiao YP, Yang J, Zeng XY, Zhang SN, Xiang MM (2020b) Refined families of Sordariomycetes. Mycosphere 11(1): 305–1059. https://doi.org/10.5943/mycosphere/11/1/7

Hyde KD, Noorabadi MT, Thiyagaraja V, He MQ, Johnston PR, Wijesinghe SN, Armand A, Biketova AY, Chethana KWT, Erdoğdu M, Ge ZW, Groenewald JZ, Hongsanan S, Kušan I, Leontyev DV, Li DW, Lin CG, Liu NG, Matočec N, May TW, McKenzie EHC, Mešić A, Perera RH, Phukhamsakda C, Piątek M, Samarakoon MC, Selcuk F, Senanayake IC, Tanney JB, Tian Q, Vizzini A, Wanasinghe DN, Wannasawang N, Wijayawardene NN, Zhao RL (2024) The 2024 Outline of Fungi and fungus-like taxa. Mycosphere 15(1): 5146–6239. https://doi.org/10.5943/mycosphere/15/1/25

Jayasiri SC, Hyde KD, Ariyawansa HA, Bhat J, Buyck B, Cai L, Dai YC, Abd-Elsalam KA, Ertz D, Hidayat I, Jeewon R, Jones EBG, Bahkali AH, Karunarathna SC, Liu JK, Luangsa-ard JJ, Lumbsch HT, Maharachchikumbura SSN, McKenzie EHC, Moncalvo JM, Ghobad-Nejhad M, Nilsson H, Pang KL, Pereira OL, Phillips AJL, Raspé O, Rollins AW, Romero AI, Etayo J, Selçuk F, Stephenson SL, Suetrong S, Taylor JE, Tsui CKM, Vizzini A, Abdel-Wahab MA, Wen TC, Boonmee S, Dai DQ, Daranagama DA, Dissanayake AJ, Ekanayaka AH, Fryar SC, Hongsanan S, Jayawardena RS, Li WJ, Perera RH, Phookamsak R, de Silva NI, Thambugala KM, Tian Q, Wijayawardene NN, Zhao RL, Zhao Q, Kang JC, Promputtha I (2015) The Faces of Fungi database: Fungal names linked with morphology, phylogeny and human impacts. Fungal Diversity 74(1): 3–18. https://doi.org/10.1007/s13225-015-0351-8

Jayawardena RS, Hyde KD, Aumentado HDR, Abeywickrama PD, Avasti S (2025) One stop shop V: taxonomic update with molecular phylogeny for important phytopathogenic genera: 101–125 (2024). Fungal Diversity 98. https://doi.org/10.1007/s13225-024-00542-x

Katoh K, Rozewicki J, Yamada KD (2018) MAFFT online service: Multiple sequence alignment, interactive sequence choice and visualization. Briefings in Bioinformatics 20(4): 1160–1166. https://doi.org/10.1093/bib/bbx108

Krauss U, ten Hoopen M, Rees R, Stirrup T, Argyle T, George A, Arroyo C, Corrales E, Casanoves F (2013) Mycoparasitism by *Clonostachys byssicola* and *Clonostachys rosea* on *Trichoderma* spp. from cocoa (*Theobroma cacao*) and implication for the design of mixed biocontrol agents. Biological Control 67(3): 317–327. https://doi.org/10.1016/j.biocontrol.2013.09.011

Lechat C, Fournier J, Chaduli D, Favel A, Lechat C, Fournier J, Chaduli D, Lesage-meessen L Clonos- AF, Lechat C, Fournier J, Lesage-meessen L (2020) *Clonostachys saulensis* (Bionectriaceae, Hypocreales), a new species from French Guiana. Ascomycete 11: 65–68. https://doi.org/10.25664/ART-0260

Liu YJ, Whelen S, Hall BD (1999) Phylogenetic relationships among ascomycetes: Evidence from an RNA polymerse II subunit. Molecular Biology and Evolution 16(12): 1799–1808. https://doi.org/10.1093/oxfordjournals.molbev.a026092

Liu XF, Tibpromma S, Hughes AC, Chethana KWT, Wijayawardene NN, Dai DQ, Du TY, Elgorban AM, Stephenson SL, Suwannarach N, Xu JC, Lu L, Xu RF, Maharachchikumbura SSN, Zhao CL, Bhat DJ, Sun YM, Karunarathna SC, Mortimer PE (2023) Culturable mycota on bats in central and southern Yunnan Province, China. Mycosphere 14(1): 497–662. https://doi.org/10.5943/mycosphere/14/1/7

Luo J, Zhuang WY (2007) A new species and two new Chinese records of *Bionectria* (Bionectriaceae, Hypocreales). Mycotaxon 101: 315–323.

Luo J, Zhuang WY (2010) *Bionectria vesiculosa* sp. nov. from Yunnan, China. Mycotaxon 113(1): 243–249. https://doi.org/10.5248/113.243

Maharachchikumbura SSN, Chen Y, Ariyawansa HA, Hyde KD, Haelewaters D, Perera RH, Samarakoon MC, Wanasinghe DN, Bustamante DE, Liu JK, Lawrence DP, Cheewangkoon R, Stadler M (2021) Integrative approaches for species delimitation in Ascomycota. Fungal Diversity 109(1): 155–179. https://doi.org/10.1007/s13225-021-00486-6

Mazen MBH, Moharram AM, Hassan SHA, Abdel-Latif SM, Al-Bedak OA (2022) Contribution to the soil-based Egyptian mycobiota in Hypocreales (Sordariomycetes) from Egypt. Studies in Fungi 7(1): 1–6. https://doi.org/10.48130/SIF-2022-0007

Mendoza García RA, Martijn Ten Hoopen G, Kass DCJ, Sánchez Garita VA, Krauss U (2003) Evaluation of mycoparasites as biocontrol agents of *Rosellinia* root rot in cocoa. Biological Control 27(2): 210–227. https://doi.org/10.1016/S1049-9644(03)00014-8

Møller K, Jensen B, Andersen HP, Stryhn H, Hockenhull J (2003) Biocontrol of Pythium tracheiphilum in Chinese cabbage by *Clonostachys rosea* under field conditions. Biocontrol Science and Technology 13: 171–182. https://doi.org/10.1080/0958315021000073448

Moreira GM, Abreu LM, Carvalho VG, Schroers HJ, Pfenning LH (2016) Multilocus phylogeny of *Clonostachys* subgenus *Bionectria* from Brazil and description of *Clonostachys chloroleuca* sp. nov. Mycological Progress 15(10-11): 1031–1039. https://doi.org/10.1007/s11557-016-1224-6

Perera RH, Hyde KD, Maharachchikumbura SSN, Jones EBG, McKenzie EHC, Stadler M, Lee HB, Samarakoon MC, Ekanayaka AH, Camporesi E, Liu JK (2020) Fungi on wild seeds and fruits. Mycosphere 11(1): 2108–2480. https://doi.org/10.5943/mycosphere/11/1/14

Perera RH, Hyde KD, Jones EBG, Maharachchikumbura SSN, Bundhun D, Camporesi E, Akulov A, Liu JK, Liu ZY (2023) Profile of Bionectriaceae, Calcarisporiaceae, Hypocreaceae, Nectriaceae, Tilachlidiaceae, Ijuhyaceae fam. nov., Stromatonectriaceae fam. nov. and Xanthonectriaceae fam. nov. Fungal Diversity 118(1): 95–271. https://doi.org/10.1007/s13225-022-00512-1

Phukhamsakda C, Nilsson RH, Bhunjun CS, Theiss B, Tennakoon N, Kuo CH (2022) The numbers of fungi: Contributions from traditional taxonomic studies and challenges of metabarcoding. Fungal Diversity 114(1): 327–386. https://doi.org/10.1007/s13225-022-00502-3

Piombo E, Guaschino M, Jensen DF, Karlsson M, Dubey M (2023) Insights into the ecological generalist lifestyle of *Clonostachys* fungi through analysis of their predicted secretomes. Frontiers in Microbiology 14: 1–16. https://doi.org/10.3389/fmicb.2023.1112673

Prasher IB, Chauhan R (2017) *Clonostachys indicus* sp. nov. from India. Kavaka 48: 22–26.

Preedanon S, Suetrong S, Srihom C, Somrithipol S, Kobmoo N, Saengkaewsuk S, Srikitikulchai P, Klaysuban A, Nuankaew S, Chuaseeharonnachai C, Chainuwong B, Muangsong C, Zhang ZF, Cai L, Boonyuen N (2023) Eight novel cave fungi in Thailand's Satun Geopark. Fungal Systematics and Evolution 12(1): 1–30. https://doi.org/10.3114/fuse.2023.12.01

Rathnayaka AR, Tennakoon DS, Jones GEB, Wanasinghe DN, Bhat DJ, Priyashantha AK, Stephenson SL, Tibpromma S, Karunarathna SC (2024) Significance of precise documentation of hosts and geospatial data of fungal collections, with an emphasis on plant-associated fungi. New Zealand Journal of Botany, 1–28. https://doi.org/10.1080/0028825X.2024.2381734

Rehner SA, Samuels GJ (1994) Taxonomy and phylogeny of *Gliocladium* analysed from nuclear large subunit ribosomal DNA sequences. Mycological Research 98(6): 625–634. https://doi.org/10.1016/S0953-7562(09)80409-7

Research MP, Service AR (1997) Two divergent intragenomic rDNA ITS2 types within a monophyletic lineage of the fungus *Fusarium* are nonorthologous. Molecular Phylogenetics and Evolution 7(1): 103–116. https://doi.org/10.1006/mpev.1996.0376

Rossman AY, McKemy JM, Pardo-Schultheiss RA, Schroers H-J (2001) Molecular studies of the Bionectriaceae using large subunit rDNA sequences. Mycologia 93(1): 100–110. https://doi.org/10.1080/00275514.2001.12061283

Rossman AY, Seifert KA, Samuels GJ, Minnis AM, Schroers HJ, Lombard L, Crous PW, Põldmaa K, Cannon PF, Summerbell RC, Geiser DM, Zhuang W, Hirooka Y, Herrera C, Salgado-Salazar C, Chaverri P (2013) Genera in Bionectriaceae, Hypocreaceae, and Nectriaceae (Hypocreales) proposed for acceptance or rejection. IMA Fungus 4(1): 41–51. https://doi.org/10.5598/imafungus.2013.04.01.05

Schroers HJ (2001) A monograph of *Bionectria* (Ascomycota, Hypocreales, Bionectriaceae) and its *Clonostachys* anamorphs. Studies in Mycology 46: 215.

Schroers HJ, Samuels GJ, Seifert KA, Gams W (1999) Classification of the mycoparasite *Gliocladium roseum* in *Clonostachys* as *C. rosea*, its relationship to *Bionectria ochroleuca*, and notes on other gliocladium -like fungi. Mycologia 91(2): 365–385. https://doi.org/10.1080/00275514.1999.12061028

Senanayake IC, Rathnayaka AR, Marasinghe DS, Calabon MS, Gentekaki E, Lee HB, Hurdeal VG, Pem D, Dissanayake LS, Wijesinghe SN, Bundhun D, Nguyen TT, Goonasekara ID, Abeywickrama PD, Bhunjun CS, Jayawardena RS, Wanasinghe DN (2020) Morphological approaches in studying fungi: Collection, examination, isolation, sporulation and preservation. Mycosphere 11(1): 2678–2754. https://doi.org/10.5943/mycosphere/11/1/20

Spegazzini CL (1918) Fungi Costaricenses nonnulli.(Reliquiae Mycologicae Tropicae). Boletín de la Academia Nacional de Ciencias 23: 541–593.

Sun Z, Sun M-H, Zhou M, Li S-D (2017) Transformation of the endochitinase gene Chi67-1 in *Clonostachys rosea* 67-1 increases its biocontrol activity against *Sclerotinia sclerotiorum*. AMB Express 7(1): 1–9. https://doi.org/10.1186/s13568-016-0313-x

Thiyagaraja V, He SC, Luo L, Meng QF, Yang H, Yan YY (2024) Research Profiles – I. The research of Vinodhini Thiyagaraja and her team at Kunming Institute of Botany, CAS, P.R. China. Current Research in Environmental & Applied Mycology (Journal of Fungal Biology) 14(1): 49–62. https://doi.org/10.5943/cream/14/1/2

Tibpromma S, Hyde KD, McKenzie EHC, Bhat DJ, Phillips AJL, Wanasinghe DN, Samarakoon MC, Jayawardena RS, Dissanayake AJ, Tennakoon DS, Doilom M, Phookamsak R, Tang AMC, Xu J, Mortimer PE, Promputtha I, Maharachchikumbura SSN, Khan S, Karunarathna SC (2018) Fungal diversity notes 840–928: Micro-fungi associated with Pandanaceae. Fungal Diversity 93(1): 1–160. https://doi.org/10.1007/s13225-018-0408-6

Toledo AV, Virla E, Humber RA, Paradell SL, Lastra CCL (2006) First record of *Clonostachys rosea* (Ascomycota: Hypocreales) as an entomopathogenic fungus of *Oncometopia tucumana* and *Sonesimia grossa* (Hemiptera: Cicadellidae) in Argentina. Journal of Invertebrate Pathology 92(1): 7–10. https://doi.org/10.1016/j.jip.2005.10.005

Torcato C, Gonçalves MFM, Rodríguez-Gálvez E, Alves A (2020) *Clonostachys viticola* sp. nov., a novel species isolated from vitis vinifera. International Journal of Systematic and Evolutionary Microbiology 70(7): 4321–4328. https://doi.org/10.1099/ijsem.0.004286

Vaidya G, Lohman DJ, Meier R (2011) SequenceMatrix: Concatenation software for the fast assembly of multi-gene datasets with character set and codon information. Cladistics 27(2): 171–180. https://doi.org/10.1111/j.1096-0031.2010.00329.x

Vilgalys R, Hester M (1990) Rapid genetic identification and mapping of enzymatically amplified ribosomal DNA from several *Cryptococcus* species. Journal of Bacteriology 172(8): 4238–4246. https://doi.org/10.1128/jb.172.8.4238-4246.1990

Vu D, Groenewald M, de Vries M, Gehrmann T, Stielow B, Eberhardt U, Al-Hatmi A, Groenewald JZ, Cardinali G, Houbraken J, Boekhout T, Crous PW, Robert V, Verkley GJM (2019) Large-scale generation and analysis of filamentous fungal DNA barcodes boosts coverage for kingdom fungi and reveals thresholds for fungal species and higher taxon delimitation. Studies in Mycology 92: 135–154. https://doi.org/10.1016/j.simyco.2018.05.001

Wan HC, Yan FH, Liang JD, Zou X, Liang ZQ, Jin DC (2016) A new araneogenous fungus of the genus *Clonostachys*. Mycosystema 35: 1061–1069. https://doi.org/10.13346/j.mycosystema.150244

Wang Y, Tang DX, Luo R, Wang YB, Thanarut C, Dao VM, Yu H (2023) Phylogeny and systematics of the genus *Clonostachys*. Frontiers in Microbiology 14: 1–14. https://doi.org/10.3389/fmicb.2023.1117753

White TJ, Bruns T, Lee S, Taylor J (1990) PCR Protocols Amplification and direct sequencing of fungal ribosomal RNA genes for phylogenetics. Academic Press, Inc. 315–322. https://doi.org/10.1016/B978-0-12-372180-8.50042-1

Wijayawardene N, Hyde K, Dai D, Sánchez-García M, Goto B, Saxena R, Erdoğdu M, Selçuk F, Rajeshkumar K, Aptroot A, Błaszkowski J, Boonyuen N, da Silva G, de Souza F, Dong W, Ertz D, Haelewaters D, Jones E, Karunarathna S, Kirk P, Kukwa M, Kumla J, Leontyev D, Lumbsch H, Maharachchikumbura S, Marguno F, Martínez-Rodríguez P, Mešić A, Monteiro J, Oehl F, Pawłowska J, Pem D, Pfliegler W, Phillips A, Pošta A, He M, Li J, Raza M, Sruthi O, Suetrong S, Suwannarach N, Tedersoo L, Thiyagaraja V, Tibpromma S, Tkalčec Z, Tokarev Y, Wanasinghe D, Wijesundara D, Wimalaseana S, Madrid H, Zhang G, Gao Y, Sánchez-Castro I, Tang L, Stadler M, Yurkov A, Thines M (2022) Outline of Fungi and fungus-like taxa – 2021. Mycosphere 13(1): 53–453. https://doi.org/10.5943/mycosphere/13/1/2

Xue A, Chen Y, Voldeng H, Savard M, Tian X (2008) Biological control of fusarium head blight of wheat with *Clonostachys rosea* strain acm941. Cereal Research Communications 36(Supplement 6): 695–699. https://doi.org/10.1556/CRC.36.2008.Suppl.B.62

Zeng Z, Zhuang WY (2022) Three new species of *Clonostachys* (Hypocreales, Ascomycota) from China. Journal of Fungi (Basel, Switzerland) 8(10): 1–11. https://doi.org/10.3390/jof8101027

Zeng XY, Tan TJ, Tian FH, Wang Y, Wen TC (2023) – OFPT: A one-stop software for fungal phylogeny. Mycosphere 14(1): 1730–1741. https://doi.org/10.5943/mycosphere/14/1/20

Zhang ZY, Li X, Chen WH, Liang JD, Han YF (2023) Culturable fungi from urban soils in China II, with the description of 18 novel species in Ascomycota (Dothideomycetes, Eurotiomycetes, Leotiomycetes and Sordariomycetes). MycoKeys 98: 167–220. https://doi.org/10.3897/mycokeys.98.102816

Zhao L, Groenewald JZ, Hernández-Restrepo M, Schroers H-J, Crous PW (2023) Revising *Clonostachys* and allied genera in Bionectriaceae. Studies in Mycology 105(1): 204–265. https://doi.org/10.3114/sim.2023.105.03

MycoKeys 115: 67–85 (2025)
DOI: 10.3897/mycokeys.115.143994

Research Article

Three new species of *Dicephalospora* (Leotiomycetes, Helotiales) from Northern Thailand and Southwestern China

Le Luo[1,2,3,4], Kandawatte Wedaralalage Thilini Chethana[2,3], Qi Zhao[1], Vinodhini Thiyagaraja[1], Kitiphong Khongphinitbunjong[3], Fatimah Al-Otibi[5], Kevin D. Hyde[1,2,5]

1 *State Key Laboratory of Phytochemistry and Natural Medicines, Kunming Institute of Botany, Chinese Academy of Sciences, Kunming 650201, Yunnan, China*
2 *Center of Excellence in Fungal Research, Mae Fah Luang University, Chiang Rai 57100, Thailand*
3 *School of Science, Mae Fah Luang University, Chiang Rai 57100, Thailand*
4 *Guiyang Institute of Humanities and Technology, Guiyang 550025, China*
5 *Department of Botany and Microbiology, College of Science, King Saud University, P.O. Box 22452, Riyadh 11495, Saudi Arabia*
Corresponding authors: Kandawatte Wedaralalage Thilini Chethana (kandawatte.thi@mfu.ac.th); Kevin D. Hyde (kdhyde3@gmail.com)

Abstract

Dicephalospora is a discomycetous genus belonging to the family Helotiaceae (Helotiales). The genus currently comprises 19 species. Among them, 17 species have been reported from Asia, of which 14 were reported from China. During a survey of Leotiomycetes, we collected six specimens of *Dicephalospora* species from southwest China and northern Thailand. The samples were examined based on the phylogenetic analyses of LSU and ITS sequence data, along with morphological characterization, and our results demarcate three new *Dicephalospora* species, viz., *D. tengyueica*, *D. maetaengica* and *D. menghaica*. *Dicephalospora tengyueica* **sp. nov.** formed a distinct clade closely related to *D. rufocornea*, *D. irregularis* and *D. sagerae*, whereas *D. maetaengica* **sp. nov.** clustered closer to *D. menghaica* **sp. nov.** with 100% ML and 1.00 BIPP statistical support. All three species have similar apothecia sizes but differ in their coloration. *Dicephalospora tengyueica* has aseptate ascospores, while *D. menghaica* and *D. maetaengica* have 7-septate ascospores. The paraphyses in *D. menghaica* are branched, while they are unbranched in the other two species. An updated key to the known species of *Dicephalospora* is also provided.

Key words: 3 new species, Helotiaceae, morphology, phylogeny, taxonomy

This article is part of:
Exploring the Hidden Fungal Diversity: Biodiversity, Taxonomy, and Phylogeny of Saprobic Fungi
Edited by Samantha C. Karunarathna, Danushka Sandaruwan Tennakoon, Ajay Kumar Gautam

Academic editor:
Danushka Sandaruwan Tennakoon
Received: 9 December 2024
Accepted: 6 February 2025
Published: 11 March 2025

Citation: Luo L, Chethana KWT, Zhao Q, Thiyagaraja V, Khongphinitbunjong K, Al-Otibi F, Hyde KD (2025) Three new species of *Dicephalospora* (Leotiomycetes, Helotiales) from Northern Thailand and Southwestern China. MycoKeys 115: 67–85. https://doi.org/10.3897/mycokeys.115.143994

Introduction

Dicephalospora belongs to Helotiaceae (Helotiales) and was described by Spooner in 1987, with *D. calochroa* (Syd. and P. Syd.) Spooner as the type species (Spooner 1987; Hyde et al. 2024). The taxonomy of the Helotiales has undergone multiple revisions, driven largely by advances in molecular phylogenetics (Ekanayaka et al. 2019; Johnston et al. 2019). Two gene regions, ITS and LSU, have been primarily used in the phylogenetic analyses of Helotiales, further supporting the inclusion of *Dicephalospora* within Helotiaceae (Han et al. 2014; Zhao et al. 2016; Ekanayaka et al. 2019). Helotiaceae is the most heterogeneous family in Helotiales and is characterized by parallel hyphae, angular to isodiametric cells, interwoven hyphae, and margins and flanks that may be covered with hairs or completely absent (Groves 1968; Korf 1973; Wijayawardene et al. 2022). The taxonomy of Helotiales, including Helotiaceae, has been widely researched and debated. Notably, a multi-gene phylogenetic analysis incorporating up to 15 genes across 279 specimens has provided a more resolved, refined classification framework for Leotiomycetes, including members of Helotiaceae (Johnston et al. 2019). After multiple revisions, a total of 26 genera are now accepted within the family, many of which are saprobic on plant material (Ekanayaka et al. 2019; Wijayawardene et al. 2022).

Morphologically, *Dicephalospora* species are distinct due to their erumpent or superficial, stipitate apothecia, which can vary in color from yellow and orange to red and blackish. The ectal excipulum comprises "*textura prismatica*" cells with refractive walls, while the medullary excipulum consists of cells of "*textura intricata*". The asci are filiform and show variable reactions in Melzer's reagent (J+ or J-). The paraphyses are straight or slightly curved at the apex, and the ascospores are hyaline, sub-ellipsoid to fusoid, guttulate, and often have a mucilaginous cap at the poles (Hosoya et al. 1999; Zhuang et al. 2016). The taxa are predominantly distributed in Asia (Phutthacharoen et al. 2022), with 17 of 19 listed species reported from this region (Luo et al. 2024). Exceptionally, *D. chrysotricha* is reported from New Zealand (Zheng and Zhuang 2019), *D. sagerae* is reported from Australia, and *D. calochroa* shows extended distribution and is reported in China and Papua New Guinea (Spooner 1987). So far, 14 species (viz., *D. albolutea*, *D. aurantiaca*, *D. calochroa*, *D. contracta*, *D. damingshanica*, *D. dentata*, *D. huangshanica*, *D. phaeoparaphysis*, *D. pinglongshanica*, *D. rufocornea*, *D. sessilis*, *D. shennongjiana*, *D. xishuangbannaensis* and *D. yunnanica*) have been reported from China (Phutthacharoen et al. 2022; Luo et al. 2024).

Hosoya et al. (1999) discovered dicephalosterol from the culture of *D. rufocornea*, which has a potential application for prostatic hypertrophy. However, the applications of *Dicephalospora* species are poorly explored due to the difficulty in obtaining pure cultures and their slow growth on artificial media, as well as their minimal biomass in nature (Zheng and Zhuang 2019).

Dicephalospora represents a morphologically distinct and phylogenetically significant genus within Helotiaceae. While challenges remain in cultivating these fungi and exploring their biochemical potential, ongoing molecular studies continue to advance our understanding of their taxonomy, ecology, and potential applications. During the investigation of Leotiomycetes, six collections of *Dicephalospora* were obtained from southwest China and northern Thailand. Morphological and phylogenetic analyses based on LSU and ITS data were performed to confirm their taxonomic placement, which revealed three new *Dicephalospora* species based on a polyphasic approach, along with an updated dichotomous key for the genus.

Material and methods

Collection and morphological examinations

Six specimens were collected from southwest China and northern Thailand, primarily in highly humid, natural broadleaf forests and protected areas with minimal human interference. The fruiting bodies were found on the surface of decaying wood and were photographed in the field before placing them in plastic containers for transport to the laboratory. The samples were dehydrated using a dehydrator set to a temperature between 25–30 °C. Further, the samples were examined using morphological and phylogenetic analyses. For detailed morphological examination, dried specimens were observed under a stereomicroscope (C-PSN, Nikon, Japan) with images captured using a digital camera (Canon EOS 70D, Japan) attached to the microscope. Free-hand sections of the dried specimens were mounted in water to observe microscopic characteristics such as apothecia, exciple, paraphyses, asci, and ascospores using a Nikon compound microscope (Nikon, Japan) with a DS-Ri2 camera. Sections were also treated with Melzer's reagent for the iodine test (Tochihara and Hosoya 2022). Measurements of the microstructures were taken using the Tarosoft (R) Image Frame Work program v.0.97 (Tarosoft, Thailand). These measurements are presented in the format (a–) b–c(–d), where 'a' represents the minimum value, 'd' the maximum value, and 'b–c' the 90% confidence interval. The specimens were deposited in the Cryptogamic Herbarium of the Kunming Institute of Botany, Chinese Academy of Sciences (KUN-HKAS), and the Mae Fah Luang University Herbarium (Herb. MFLU). The Facesoffungi and the Index Fungorum numbers were obtained following the procedures outlined by Jayasiri et al. (2015) and Index Fungorum (2025), respectively. The morphological description and the phylogenetic tree of the new species were submitted to the Greater Mekong Subregion webpage (Chaiwan et al. 2021). Images used for figures were processed with Adobe Photoshop CS6 Extended version 13.0 × 64 (Adobe Systems, USA).

DNA extraction, PCR amplifications and sequencing

Genomic DNA was extracted from the dried apothecia using a TSP101 DNA extraction kit (TSINGKE, China). Following the latest studies (Phutthacharoen et al. 2022; Luo et al. 2024), LSU and ITS regions were subjected to PCR amplification, using the primers LR0R/LR5 (Vilgalys and Hester 1990) and ITS1/ITS4 (White et al. 1990; Gardes and Bruns 1993), respectively. The total volume of PCR amplifications was 25 μL, including 12.5 μL of 2X PCR G013 Taq MasterMix with Dye (Applied Biological Materials, Canada), 1 μL of each primer (10 μM), 2 μL of genomic DNA, and 8.5 μL of sterilized, distilled water. Amplifications were conducted under the following conditions: pre-denaturation at 95 °C for 5 minutes, followed by 35 cycles of denaturation at 95 °C for 20 seconds, annealing at 55 °C for 10 seconds, elongation at 72 °C for 20 seconds and final elongation at 72 °C for 7 minutes. Gel electrophoresis with 1% TAE and TSJ003 GoldView nucleic acid dye (TSINGKE, China) was used to test the obtained PCR products. Finally, the PCR products were sequenced by Tsingke Biotechnology Co., Ltd., Kunming, China. Newly produced sequences were deposited in the GenBank and the accession numbers were given in Table 1.

Phylogenetic analyses

Newly generated DNA sequences were assembled using BioEdit v.7.2.5 (Hall 1999) to obtain consensus sequences. The concatenated sequences were used to search for the close relatives in the NCBI (Johnson et al. 2008). The closely related sequences were downloaded from GenBank following the recent papers (Phutthacharoen et al. 2022; Luo et al. 2024) (Table 1). *Pleuroascus nicholsonii*

(CBS 345.73) and *Connersia rilstonii* (CBS 537.74) were selected as outgroup taxa. The phylogenetic analysis was conducted based on the datasets, including reference DNA sequences and newly generated DNA sequences using OFPT (Zeng et al. 2023) with the following protocol. Datasets of each gene region were first independently aligned with the 'auto' strategy (based on data size) by MAFFT (Katoh and Standley 2013) and trimmed with the 'gappyout' option (based on gaps' distribution) by TrimAl (Capella-Gutiérrez et al. 2009). The best-fit nucleotide substitution models for each dataset were then selected based on the Bayesian information criterion (BIC) from twenty-two common DNA substitution models with rate heterogeneity by ModelFinder (Kalyaanamoorthy et al. 2017). All datasets were concatenated with partition information for the subsequent phylogenetic analyses. Maximum likelihood with 1000 replicates was performed using ultrafast bootstrap approximation (Hoang et al. 2018) with SH-like approximate likelihood ratio test (SH-aLRT) (Guindon et al. 2010) by IQ-TREE (Nguyen et al. 2015). The consensus tree was summarized based on the extended majority rule. Bayesian inference was performed with two parallel Metropolis-coupled (one 'cold' chain and three heated chains) Markov chain Monte Carlo runs by MrBayes (Ronquist et al. 2012), with trees sampling every 100th generations. The consensus tree was summarized after discarding the first 25% of samples when the average standard deviation of split frequencies fell below 0.01. The resulting trees were visualized in FigTree v1.4.3 (http://tree.bio.ed.ac.uk/software/figtree/). The polyphasic approach recommended by Chethana et al. (2021) was followed to establish the new species.

Results

Phylogenetic analysis

The data matrix consisted of LSU and ITS sequences, representing 62 taxa distributed across 17 genera of Helotiaceae with 1192 characters after trimming, including gaps (ITS: 404 bp and LSU: 788 bp). The matrix had 390 distinct alignment patterns, with 28.73% undetermined characters or gaps. Estimated parameters for the tree are as follows: total tree length (sum of branch lengths): 1.4788; sum of internal branch lengths: 0.9205 (62.2453% of tree length); gamma distribution shape parameter $\alpha = 0.7196$. The best IQ-Tree with a final likelihood value of -7128.2117 is presented in Fig. 1. The tree topology inferred from ML analysis is similar to that of BI analysis. Index Fungorum (2025) listed 19 species epithets for *Dicephalospora*, and 15 of them are included in our phylogenetic analyses (Fig. 1), and four species (*D. calochroa*, *D. damingshanica*, *D. pinglongshanica* and *D. phaeoparaphysis*) are excluded due to a lack of molecular data. The phylogenetic result showed that *Dicephalospora* species clustered together and concurred with the previous studies (Zheng and Zhuang 2019; Phutthacharoen et al. 2022; Luo et al. 2024). *Dicephalospora* species formed a monophyletic clade separated from an assemblage of *Endoscypha* and *Hymenotorrendiella* taxa by 93% maximum likelihood bootstrap support (MLBS) and 1.00 Bayesian inference posterior probability (BIPP) support. The new species *D. tengyueica* formed a distinct clade closely related to *D. rufocornea*, *D. irregularis*, and *D. sagerae*, with 93% MLBS and 0.99 BIPP support (Fig. 1). The two new species, *D. maetaengica* and *D. menghaica*, were closely related, supported by 100% MLBS and 1.00 BIPP, and together formed a sister clade to *D. albolutea*, with 98% MLBS and 1.00 BIPP support (Fig. 1).

Table 1. The taxa included in the phylogenetic analysis along with their corresponding GenBank accession numbers. Newly identified taxa are in bold. Names with (^{T}) indicate type specimens and '-' denotes unavailable data in the GenBank.

Species	Strain	GenBank Accession No.		Reference
		ITS	LSU	
Amylocarpus encephaloides	CBS 129.60	MH857920	MH869464	Vu et al. (2019)
Amylocarpus encephaloides	017cN	KM272369	KM272361	Rämä et al. (2014)
Bryoscyphus dicrani	M141	EU940183	EU940107	Stenroos et al. (2010)
Connersia rilstonii	CBS 537.74	KJ755499	AF096189	Suh and Blackwell (1999)
Crocicreas amenti	F-147481	FJ005093	FJ005124	Peláez et al. (2011)
Crocicreas cacaliae	F-148706	FJ005107	FJ005126	Peláez et al. (2011)
Crocicreas cyathoideum	MFLU 18-0698	MK584943	MK591970	Ekanayaka et al. (2019)
Crocicreas tomentosum	MFLU 17-0082	MK584988	MK592008	Ekanayaka et al. (2019)
Cudoniella clavus	AFTOL-ID 166	DQ491502	DQ470944	Spatafora et al. (2006)
Cyathicula microspora	M267	EU940165	EU940088	Baral et al. (2009)
Dicephalospora albolutea	HMAS 279693	MK425601	–	Zheng and Zhuang (2019)
Dicephalospora aurantiaca	MFLU 16-0591a	MK584962	MK591988	Ekanayaka et al. (2019)
Dicephalospora chiangraiensis	MFLU 21-0019	MZ241818	MZ241827	Phutthacharoen et al. (2022)
Dicephalospora chiangraiensis	MFLU 21-0018$^{(T)}$	MZ241817	MZ241826	Phutthacharoen et al. (2022)
Dicephalospora chrysotricha	PDD:91762	KF727411	–	Unpublished
Dicephalospora chrysotricha	PDD:58197	KF727409	–	Unpublished
Dicephalospora chrysotricha	PDD:93932	MH578487	–	Unpublished
Dicephalospora chrysotricha	PDD:81537	KF727410	OQ466391	Unpublished
Dicephalospora dentata	3093	KP204263	–	Liu et al. (2016)
Dicephalospora huangshanica	MFLU 18-1828	MK584979	MK591979	Ekanayaka et al. (2019)
Dicephalospora huangshanica	KUS-F52405	JN033408	JN086711	Han et al. (2014)
Dicephalospora inthanonensis	MFLU 22-0050$^{(T)}$	ON606312	ON604634	Phutthacharoen et al. (2022)
Dicephalospora inthanonensis	MFLU 22-0053	ON606313	ON604635	Phutthacharoen et al. (2022)
Dicephalospora irregularis	MFLU 22-0054$^{(T)}$	ON511117	ON514038	Phutthacharoen et al. (2022)
Dicephalospora maetaengica	**MFLU24-0330$^{(T)}$**	**PQ481904**	**PQ481910**	This study
Dicephalospora maetaengica	**MFLU24-0331**	**PQ481905**	**PQ481911**	This study
Dicephalospora menghaica	**HMAS 135692$^{(T)}$**	**PQ481908**	**PQ481914**	This study
Dicephalospora menghaica	**HMAS 135690**	**PQ481909**	**PQ481915**	This study
Dicephalospora rufocornea	MFLU 16-1860	MK584989	MK592011	Ekanayaka et al. (2019)
Dicephalospora rufocornea	MFLU 19-2083	MZ241816	MZ241825	Phutthacharoen et al. (2022)
Dicephalospora rufocornea	TNS:F:36242	LC136911	–	Unpublished
Dicephalospora rufocornea	TNS:F:40155	LC136918	–	Unpublished
Dicephalospora rufocornea	MFLU 16-1858	MK584991	–	Ekanayaka et al. (2019)
Dicephalospora rufocornea	FCATAS5710	PP622049	–	Unpublished
Dicephalospora sagerae	BRIP 72428d	NR_182617	–	Tan and Shivas (2022)
Dicephalospora sessilis	MFLU 18-1823$^{(T)}$	NR_163779	NG_068621	Ekanayaka et al. (2019)
Dicephalospora shennongjiana	HMAS 279698	MK425606	–	Zheng and Zhuang (2019)
Dicephalospora xishuangbannaensis	HMAS 131157	OR948047	–	Luo et al. (2024)
Dicephalospora xishuangbannaensis	HMAS 131164$^{(T)}$	OR948048	–	Luo et al. (2024)
***Dicephalospora* tengyueica**	**HMAS 135691$^{(T)}$**	**PQ481906**	**PQ481912**	This study
***Dicephalospora* tengyueica**	**HMAS 135694**	**PQ481907**	**PQ481913**	This study
Dicephalospora yunnanica	HMAS 279701	MK425609	–	Zheng and Zhuang (2019)
Dicephalospora yunnanica	HMAS 279700	MK425608	–	Zheng and Zhuang (2019)
Dicephalospora yunnanica	HMAS 61850	DQ986486	–	Zheng and Zhuang (2019)
Endoscypha perforans	PDD:102231	KF727424	MK039717	Unpublished
Glarea lozoyensis	ATCC 20868$^{(T)}$	NR_137138	–	Bills et al. (1999)

Species	Strain	GenBank Accession No.		Reference
		ITS	LSU	
Glarea sp.	C2B	KX610435	–	Yokoya et al. (2017)
Gloeotinia granigena	CBS 417.50	–	MH868212	Vu et al. (2019)
Hymenoscyphus fructigenus	CBS 186.47	MH856211	MH867741	Vu et al. (2019)
Hymenoscyphus occultus	KUS-F52847	KP068064	–	Gross and Han (2015)
Hymenoscyphus pseudoalbidus	Hokk_14	KJ511191	–	Gross et al. (2014)
Hymenotorrendiella eucalypti	PDD:70105	MH578483	–	Unpublished
Hymenotorrendiella eucalypti	CPC 11050$^{(T)}$	DQ195788	DQ195800	Zhao (2014)
Lanzia berggrenii	ICMP:19614	KC164645	KC164640	Johnston and Park (2013)
Ombrophila violacea	WZ0024	AY789366	AY789365	Wang et al. (2005)
Phaeohelotium epiphyllum	TNS: F-40042	AB926061	AB926130	Zhao (2014)
Pirottaea palmicola	PDD:60282	KM677208	–	Unpublished
Pirottaea palmicola	PDD:65971	KM677206	–	Unpublished
Pleuroascus nicholsonii	CBS 345.73	KJ755519	AF096196	Zhao (2014)
Roesleria subterranea	CBS 339.96	EF060308	EF608074	Kirchmair et al. (2008)
Roesleria subterranea	CBS 407.51	MH856922	–	Vu et al. (2019)

Taxonomy

Dicephalospora tengyueica **L. Luo & K.D. Hyde, sp. nov.**
Index Fungorum: IF902889
Facesoffungi Number: FoF16773
Fig. 2

Etymology. The epithet "*tengyueica*" refers to the collection site, Tengyue street, where the holotype specimen was collected.

Holotype. HKAS135691.

Description. ***Saprobic*** on dead twigs. **Sexual morph**: ***Apothecia*** 1.2–3.2 mm diam., when dry arising solitary or gregarious in a small group, scattered on wood, centrally stipitate, superficial, orange when fresh, become light brown when dry. ***Stipe*** 0.9–2.3 mm height at the base, yellow when fresh, and light yellow to white when dry. ***Receptacle*** orange and discoid. ***Margins*** slightly rough, orange to dark orange. ***Disc*** slightly convex and orange. ***Ectal excipulum*** 30–66 µm ($\bar{x}$ = 46 µm, n = 20), multi-layered, and thin-walled, with hyaline cells of ***textura globulosa***. ***Medullary excipulum*** 21–48 µm ($\bar{x}$ = 33 µm, n = 30), composed of thin-walled, hyaline, gelatinized cells of ***textura globulosa*** to ***porrecta***, small cells condensed. ***Hymenium*** 84–171 µm ($\bar{x}$ = 131 µm, n = 60), hyaline to yellowish, inner mixed with asci and paraphyses. ***Paraphyses*** 1.1–3.2 µm wide ($\bar{x}$ = 1.9 µm, n = 30), at the terminal cell, filiform, numerous, lengths exceeding the asci, unbranched, aseptate, apical cells swollen and globose, filled with oil droplets. ***Asci*** (85–)90–118(–125) × 5.9–12.5 µm ($\bar{x}$ = 102 × 9.5 µm, n = 50), eight-spored, unitunicate, cylindrical, and clavate, J- in Melzer's reagent, tapered long stipitate base. ***Ascospores*** (17–)19–32(–35) × 2–3.5 µm ($\bar{x}$ = 27.4 × 2.9 µm, n = 60), uniseriate to biseriate, fusiform, aseptate, both ends are filled with oil droplets of different sizes, some narrowed ends capped with a small and gelatinous collar. **Asexual morph**: Not observed.

Material examined. CHINA • Yunnan Province, Tengchong City, Tengyue Street, altitude 1749 m, on the decayed unidentified twigs, 19 August 2022, Le Luo, ly289 (HKAS 135691, holotype); • *ibid*., ly290 (HKAS 135694, paratype).

Notes. Our specimens of *D. tengyueica* (HKAS 135691 and HKAS 135694) formed a distinct clade (93% MLBS and 0.99 BIPP), closely related to *D. rufocornea*,

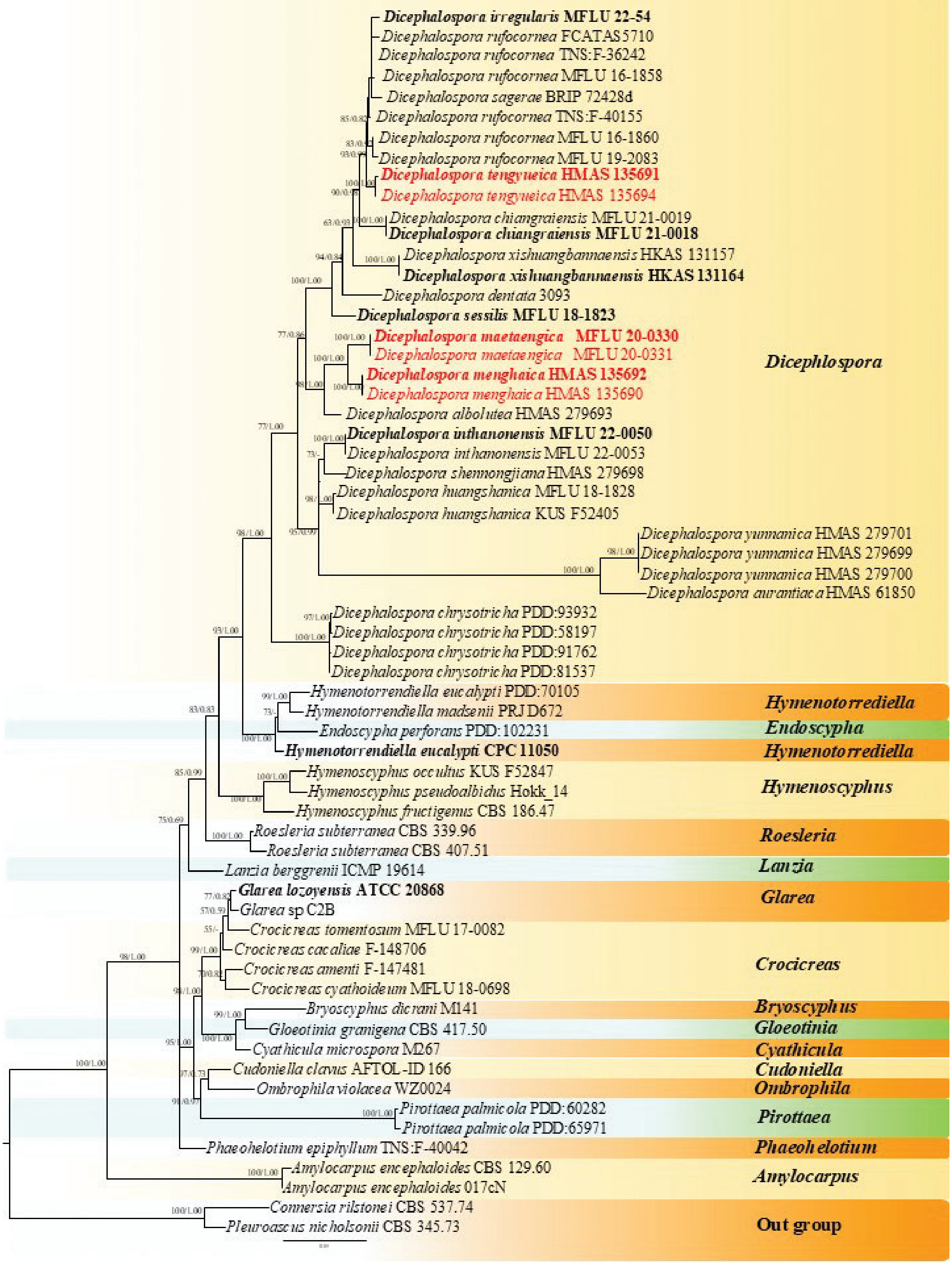

Figure 1. The IQ-Tree phylogram based on the combined LSU and ITS dataset. The MLBS ≥ 70% and BIPP ≥ 0.90 are shown at the nodes as MLBS/BIPP. The MLBS < 70% and BPP < 0.90 are expressed as a hyphen ("-"). Type strains are in bold. Names in red indicate isolates from the current study.

D. irregularis and *D. sagerae* (Fig. 1). However, the new species exhibit distinct morphological features in having orange to light brown apothecia, light yellow stipe, tapered long stipitate base, aseptate ascospores, and aseptate paraphyses. *Dicephalospora rufocornea* has red or reddish-orange apothecia, red stipe, and sessile base with septate paraphyses (Ekanayaka et al. 2019), whereas *D. irregularis*

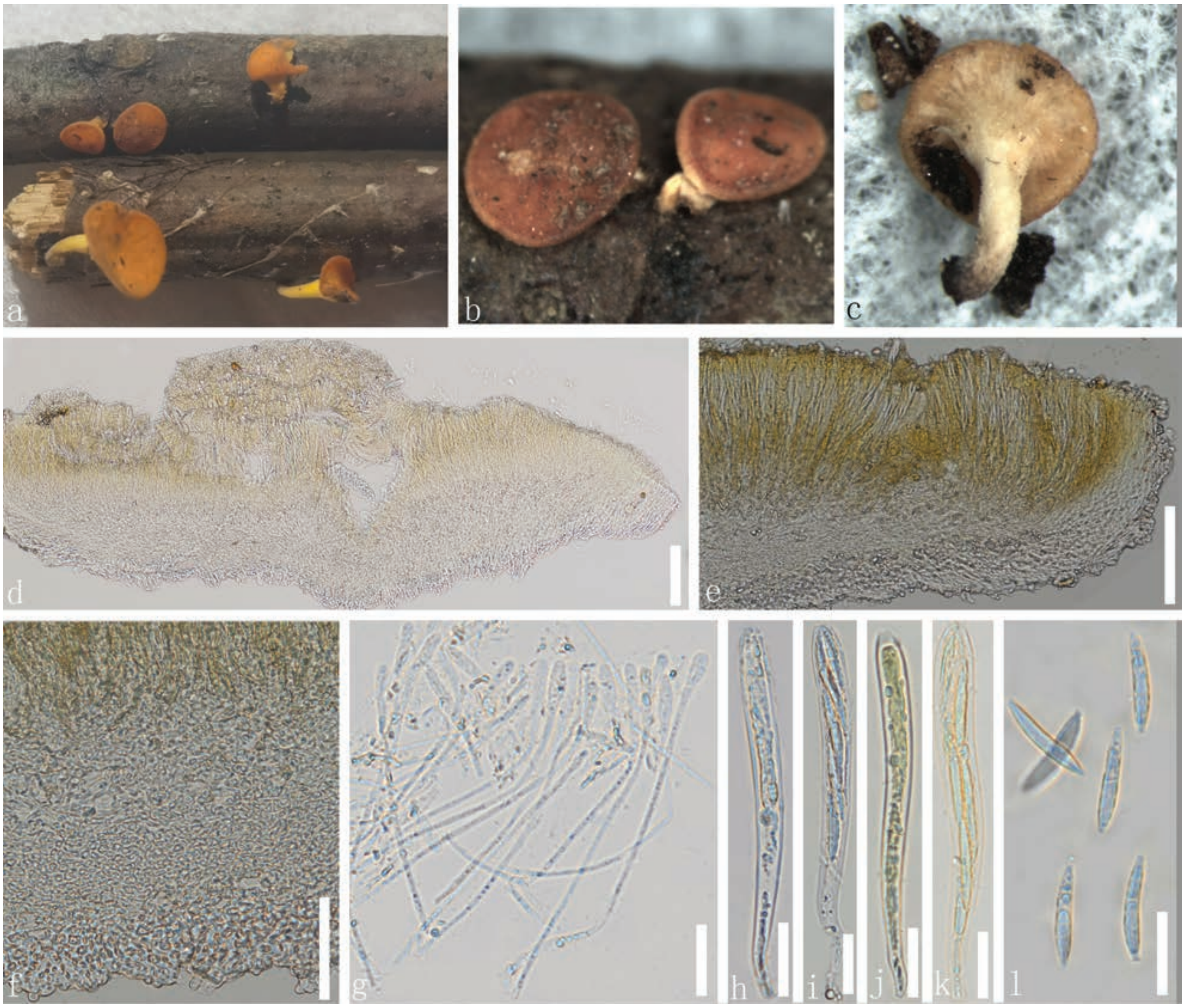

Figure 2. *Dicephalospora tengyueica* (HKAS 135691, holotype) **a** fresh apothecia growing on dead wood **b**, **c** dried apothecia **d**, **e** vertical sections of an apothecia **f** excipulum **g** paraphyses **h–k** asci (**j–k** asci in Meltzer's reagent) **l** ascospores. Scale bars: 5 mm (**a**); 2 mm (**b, c**); 100 µm (**d, e**); 50 µm (**f**); 20 µm (**g–l**).

has sessile apothecia, asci arising from simple septa without basal protuberance, aseptate to septate ascospores that are wider than *D. tengyueica* (5.5–7.5 µm vs. 2–3.5 µm) (Phutthacharoen et al. 2022). The detailed morphological description is not available for *D. sagerae* (Tan & Shivas, 2022) but it differs from *D. tengyueica* in the ITS base pair comparison, which revealed 8.5% differences. Therefore, *D. tengyueica* is introduced here as a new species.

Dicephalospora maetaengica **L. Luo & K.D. Hyde, sp. nov.**
Index Fungorum: IF902890
Facesoffungi Number: FoF16774
Fig. 3

Etymology. The epithet "*maetaengica*" refers to the collection site, MaeTaeng District, where the holotype specimen was collected.

Holotype. MFLU 24-0330.

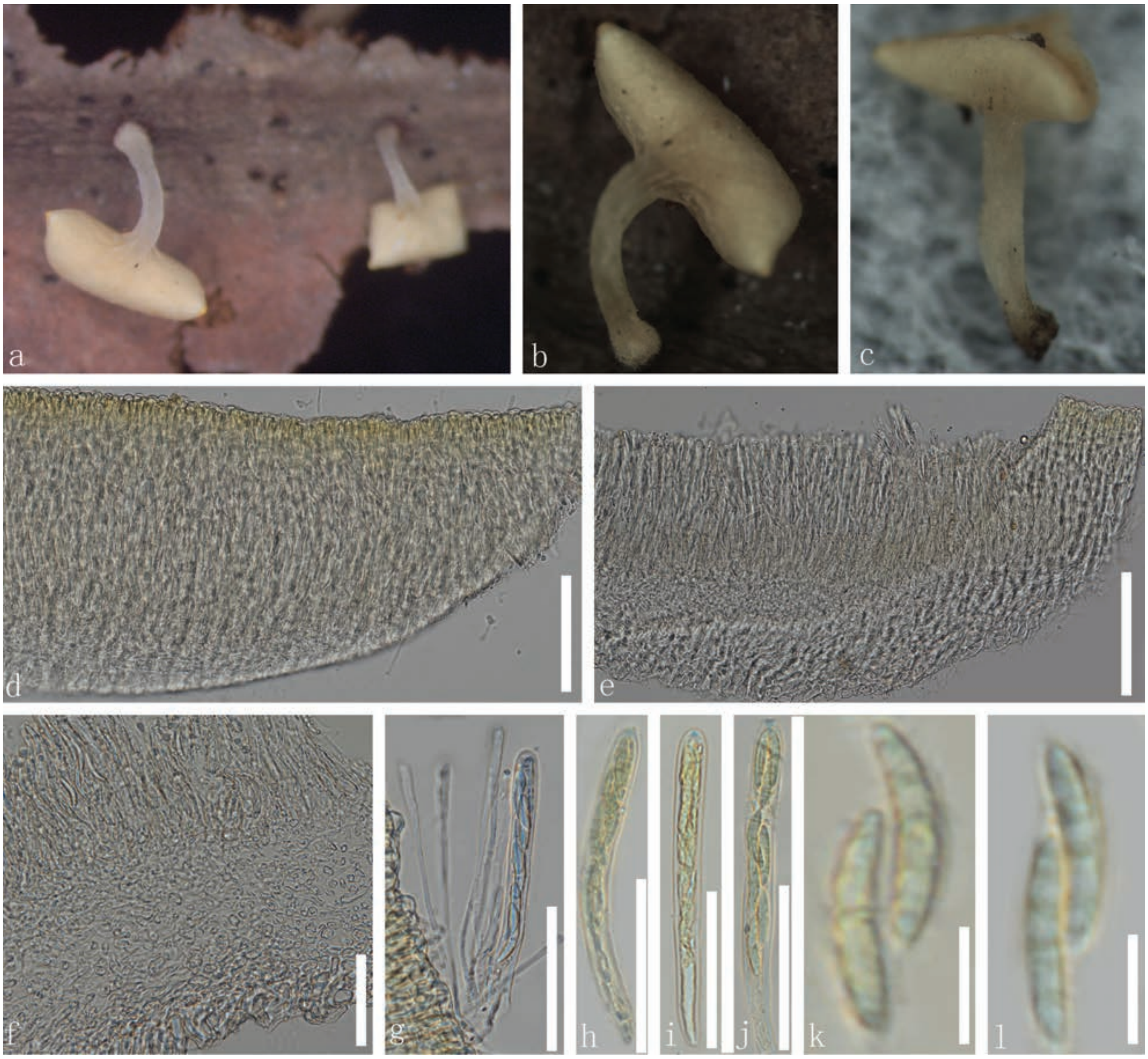

Figure 3. *Dicephalospora maetaengica* (MFLU 24-0330, holotype) **a** fresh apothecia growing on a dead wood **b**, **c** dried apothecia **d**, **e** vertical sections of the apothecia **f** excipulum **g** paraphyses and part of asci **h–j** asci (**i–j** asci in Meltzer's reagent) **k–l** ascospores. Scale bars: 2 mm (**a–c**); 100 µm (**d, e**); 50 µm (**f–j**); 10 µm (**k, l**).

Description. ***Saprobic*** on dead leaves. **Sexual morph**: ***Apothecia*** 1.5–3.3 mm diam., when dry arising solitary, uniseriate on the stem of the leaves, centrally long stipitate, superficial, yellow when fresh and dry. ***Stipe*** 1.2–2.5 mm height, slightly hyaline to light yellow at the base. ***Receptacle*** yellow and cupulate. ***Margins*** smooth, yellow to pale yellow. ***Disc*** slightly sunken and yellow. ***Ectal excipulum*** 23–44 µm ($\bar{x}$ = 33 µm, n = 60), multi-layered, thin-walled, hyaline to light yellow or pale green cells of ***textura globulosa***, slightly larger cells condensed. ***Medullary excipulum*** 28–61 µm ($\bar{x}$ = 45 µm, n = 60), composed of thin-walled, hyaline to yellowish, gelatinized cells of ***textura porrecta*** to ***globulosa***, small cells condensed. ***Hymenium*** 99–146 µm ($\bar{x}$ = 123 µm, n = 60), hyaline to yellow, inner mixed with asci and paraphyses. ***Paraphyses*** 1.1–2.1 µm wide ($\bar{x}$ = 1.6 µm, n = 60), filiform, numerous, lengths exceeding the asci, unbranched, aseptate, slightly swollen, small, globose at the apex. ***Asci*** (75–)81–111(–118) × 5.6–10.7 µm ($\bar{x}$ = 99 ×

8.5 µm, n = 50), eight-spored, unitunicate, cylindrical, clavate, amyloid (J+) having a rounded apex in Melzer's reagent, tapered long stipitate base. ***Ascospores*** (12.5–)14.5–21.8(–22.5) × 2.4–4.2 µm (x̅ = 18.2 × 3.3 µm, n = 60), uniseriate to biseriate, fusiform, guttulate, 0–1–septate. **Asexual morph**: Not observed.

Material examined. THAILAND • Chiang Mai Province, MaeTaeng District, Pha Deng Village, Mushroom Research Center (MRC), altitude 863 m, on the decayed unidentified leaf, 18 August 2023, Le Luo, RB1 (MFLU 24-0330, holotype); • *ibid*., RB101 (MFLU 24-0331, paratype).

Notes. *Dicephalospora maetaengica* formed a clade closer to *D. menghaica* with 100% MLBS and 1.00 BIPP support (Fig. 1). These two species grouped as a sister clade and together formed a closely related clade to *D. albolutea* with 98% MLBS and 1.00 BIPP (Fig. 1) bootstrap support. *Dicephalospora maetaengica* differs from *D. menghaica* by having larger (1.5–3.3 mm vs. 1–1.6 mm), yellow apothecia, long stipe (1.2–2.5 mm vs. 0.6–1 mm), slightly hyaline to light yellow at the base of stipe, 0–1–septate ascospores with paraphyses that are unbranched and aseptate, while *D. menghaica* has smaller apothecia, shorter stipe and slightly hyaline to light yellow at the base with branched paraphyses. *Dicephalospora albolutea* differs from *D. maetaengica* in having yellowish-white apothecia, longer asci (140–156 × 9.5–10.5 µm vs. 81–111 × 5.6–10.7 µm) and ascospores (26–31 × 3.8–5 µm vs. 14.5–21.8 × 2.4–4.2 µm) with aseptate paraphyses and ascospores (Zheng and Zhuang 2019). Therefore, *D. maetaengica* is introduced here as a new species.

Dicephalospora menghaica L. Luo & K.D. Hyde, sp. nov.

Index Fungorum: IF902891
Facesoffungi Number: FoF16775
Fig. 4

Etymology. The epithet "*menghaica*" refers to the collection site, Menghai County, where the holotype specimen was collected.

Holotype. HKAS135692.

Description. ***Saprobic*** on a dead leaf. **Sexual morph**: ***Apothecia*** 1–1.6 mm diam. when dry, arising solitary, uniseriate on petiole of leaves. Stipe 0.6–1 mm height and light brown to brown at the base. ***Receptacle*** orange and cupulate. ***Margins*** smooth and yellow when fresh. ***Disc*** slightly sunken and light yellow. ***Ectal excipulum*** 21–37 µm (x̅ = 28 µm, n = 60), multi-layered, thin-walled, with hyaline to light yellow cells of ***textura porrecta***. ***Medullary excipulum*** 24–50 µm (x̅ = 41 µm, n = 60), composed of thin-walled, hyaline to yellowish, gelatinized cells of ***textura intricata*** to ***globulosa***, small cells condensed. ***Hymenium*** 83–166 µm (x̅ = 122 µm, n = 60), hyaline to yellowish and inner mixed with asci and paraphyses. ***Paraphyses*** 0.8–2.1 µm wide (x̅ = 1.2 µm, n = 60), at the terminal cell, filiform, numerous, and have lengths exceeding the asci, smooth, branched, aseptate, slightly swollen, small, and globose at the apex. ***Asci*** (79–)82–125(130–) × 6.5–11.6 µm (x̅ = 101 × 9.4 µm, n = 50), 8-spored, unitunicate, cylindrical, and clavate, with the amyloid (J+) having a rounded apex, tapered, long stipitate base. ***Ascospores*** (16–)18–24(26–) × 2–3.7 µm (x̅ = 22 × 2.9 µm, n = 60), uniseriate to biseriate, fusoid-clavate with rounded ends, 7-septate, narrowed ends capped with pigments. **Asexual morph**: Not observed.

Figure 4. *Dicephalospora menghaica* (HKAS 135692, holotype) **a** fresh apothecia growing on a dead wood **b, c** dried apothecia **d** a vertical section of the apothecium **e, f** excipulum **g** paraphyses **h** paraphyses and part of asci **i–m** asci (**j–m** asci in Meltzer's reagent) **n**–**q** ascospores. Scale bars: 3 mm (**a**); 1 mm (**b, c**); 100 μm (**d**); 50 μm (**e–m**); 20 μm (**n–q**).

Material examined. China • Yunnan Province, Xishuangbanna City, Menghai County, altitude 1595 m, on the decayed unidentified leaves, 8 September 2022, Le Luo, ly958 (HKAS 135692, holotype); • *ibid*., ly972 (HKAS 135690, paratype).

Notes. *Dicephalospora menghaica* clustered with *D. maetaengica* by 100% MLBS and 1.00 BIPP support (Fig. 1), and clustered sister to *D. albolutea* with 98% MLBS and 1.00 BIPP support (Fig. 1). *Dicephalospora menghaica* differs from *D. albolutea* by having smaller (1–1.6 mm vs. 1–2.5 mm), light brown apothecia, slightly hyaline to light yellow at the base with branched, aseptate paraphyses, shorter asci (82–125 × 6.5–11.6 μm vs. 140–156 × 9.5–10.5 μm) and smaller ascospores (18–24 × 2–3.7 μm vs. 26–31 × 3.8–5 μm), whereas *D. albolutea* has cream to yellowish-white apothecia, with unbranched, septate paraphyses (Zheng and Zhuang 2019). *Dicephalospora menghaica* also differs morphologically from *D. maetaengica* as discussed previously under the notes of *D. maetaengica*. Therefore, based on the morphological and phylogenetic analysis, *D. menghaica* is introduced here as a new species.

Discussion

The members of Leotiomycetes are characterized by a diverse array of species with various ecological roles, including plant pathogens, endophytes, and saprobes (O’Brien et al. 2005; Sieber 2007; Baral 2016). They occur in aquatic to terrestrial ecosystems and play significant roles in decomposition and nutrient cycling (Quandt and Haelewaters 2021). In China, the diversity of Leotiomycetes is substantial due to the varied climates and ecosystems (Li et al. 2022; Su et al. 2023; Luo et al. 2024; Guo et al. 2024; Zhang et al. 2024). Ongoing research continues to uncover new species and understand their roles in ecosystem functioning, highlighting the importance of preserving fungal diversity for ecological health and agricultural sustainability (Li et al. 2022; Su et al. 2023; Luo et al. 2024).

The identification of *Dicephalospora* species has traditionally relied on morphological features, such as the color of the apothecia, anatomical structures, and the characteristics of asci and ascospores (Zheng and Zhuang 2019; Phutthacharoen et al. 2022; Luo et al. 2024). However, morphology-based identification became challenging due to the morphological variability observed even within the same species collected from the same geographical locations (Phutthacharoen et al. 2022). Morphological variation within a single fungal species can be influenced by genetic diversity, environmental conditions, transposable elements, and symbiotic relationships (Taylor et al. 2017; Senanayake et al. 2020). Similarly, apothecia and ascospores showed morphological diversity in *Dicephalospora rufocornea* isolates reported from the same province in Thailand (Phutthacharoen et al. 2022). This variability underscores the difficulty of relying solely on morphological characteristics for species identification and emphasizes the importance of integrating morphological data with molecular phylogenetics for accurate identification and classification. In this study, we updated the dichotomous key for the identification of *Dicephalospora* species.

DNA sequence data, particularly ITS and LSU gene sequences, play a crucial role in the delineation of fungal species (Hibbett et al. 2016; Jeewon and Hyde 2016). Our phylogenetic analyses based on these sequences provide robust support for the differentiation of the new species within *Dicephalospora*. The two new species, *D. menghaica* and *D. maetaengica*, are characterized by apothecial characters, with paraphyses that are either unbranched or branched. The phylogenetic relationships among *Dicephalospora* species in our study concurred with those reported by Phutthacharoen et al. (2022), who identified one main cluster and another subclade comprising *D. chrysotricha* isolates closer to the *Hymenoscyphus* clade. This discrepancy highlights the need for further research and more extensive sampling to clarify these relationships.

This study expands our understanding of *Dicephalospora*, particularly through the discovery and description of three new species from Xishuangbanna, Yunnan Province, China, and northern Thailand. *Dicephalospora* species are primarily saprobic, decomposing organic matter such as rotten wood, twigs, and leaf petioles. This saprobic activity plays a crucial role in nutrient cycling within their ecosystems. The tropical monsoon climate of Xishuangbanna, with its high humidity, provides a unique habitat for fungi, exemplified by the discovery of these species on wet decaying wood (Luo et al. 2024).

This finding contrasts with previous observations that *Dicephalospora* were typically found in highly humid and cold areas, suggesting a broader ecological range and adaptability to various climatic conditions (Phutthacharoen et al. 2022). This study expands the *Dicephalospora* species up to 22 species, of which 16 were reported from China, four from Thailand (*D. chiangraiensis*, *D. irregularis*, *D. inthanonensis*, *D. maetaengica*), one from New Zealand (*D. chrysotricha*), and one from Australia (*D. sagerae*) (Spooner 1987; Zhuang et al. 2016; Zheng and Zhuang 2019; Phutthacharoen et al. 2022; Luo et al. 2024). China appears to harbor a high diversity of *Dicephalospora* species that are yet to be discovered.

This study contributes to the taxonomy and phylogeny of *Dicephalospora* by describing new species and clarifying their relationships within the Helotiaceae. In addition, a dichotomous key to the species in *Dicephalospora* is presented. Future studies should aim to include a wider range of genera and utilize additional genetic markers to further resolve the phylogenetic position of *Dicephalospora* and related taxa.

A dichotomous key to the species of *Dicephalospora*

1	Receptacle surface with hairs	***D. chrysotricha***
–	Receptacle surface without hairs	**2**
2	Sessile apothecia	**3**
–	Stipitate apothecia	**5**
3	Asci J^+	***D. calochroa***
–	Asci J^-	**4**
4	Disc concave with unbranched paraphyses	***D. sessilis***
–	Disc slightly convex with branched paraphyses	***D. irregularis***
5	Margin dentate	***D. dentata***
–	Margin not dentate	**6**
6	Disc cream to yellowish, white apothecia	***D. albolutea***
–	Disc and apothecia concolorous	**7**
7	Paraphyses with dark pigment contents	***D. phaeoparaphysis***
–	Paraphyses without dark pigment contents	**8**
8	Asci J^-	**9**
–	Asci J^+	**11**
9	Stipe base dark	***D. pinglongshanica***
–	Stipe base not dark	**10**
10	Apothecia orange when fresh, light brown when dry	***D. tengyueica***
–	Apothecia yellow to orange when fresh and dry	***D. xishuangbannaensis***
11	Ascospore cap mucilaginous	**12**
–	Ascospore cap non-mucilaginous	**13**
12	Ascospore lemon-shaped, 9–12.7 μm wide	***D. damingshanica***
–	Ascospore fusoid	***D. rufocornea***
13	Ascospores constricted in the middle	***D. contracta***
–	Ascospores not constricted in the middle	**14**
14	Ascospores elliptical-subfusoid	***D. shennongjiana***
–	Ascospores fusoid	**15**
15	Disc convex	***D. inthanonensis***
–	Disc flat	**16**

16 Paraphyses septate **17**
– Paraphyses aseptate **18**
17 Ascospores multiseriate, ectal excipulum globose at the tips .... ***D. huangshanica***
– Ascospores biseriate, 16.5–25.3 × 3.3–3.5 µm .... ***D. yunnanica***
18 Paraphyses branched .... ***D. menghaica***
– Paraphyses unbranched **19**
19 Ascospore aseptate .... ***D. aurantiaca***
– Ascospore septate **20**
20 Stipe and apothecia concolorous .... ***D. maetaengica***
– Stipe and apothecia not concolorous .... ***D. chiangraiensis***

Acknowledgements

Le luo thanks Dr Shaun Pennycook for his valuable assistance with the Latin binomial nomenclature.

Additional information

Conflict of interest

The authors have declared that no competing interests exist.

Ethical statement

No ethical statement was reported.

Funding

This work was supported by the Second Tibetan Plateau Scientific Expedition and Research (STEP) Program (Grant No. 2019QZKK0503). This work also was supported by the Chinese Research Fund (project no E1644111K1) entitled “Flexible introduction of high-level expert program, Kunming Institute of Botany, Chinese Academy of Sciences”. The authors extend their appreciation to the Researchers Supporting Project number (RSP2025R114), King Saud University, Riyadh, Saudi Arabia.

Author contributions

Supervision: KWTC, KK. Writing - original draft: LL, FAO. Writing - review and editing: VT, QZ, KDH.

Author ORCIDs

Le Luo https://orcid.org/0009-0006-7213-0498
Kandawatte Wedaralalage Thilini Chethana https://orcid.org/0000-0002-5816-9269
Qi Zhao https://orcid.org/0000-0001-8169-0573
Vinodhini Thiyagaraja https://orcid.org/0000-0002-8091-4579
Kitiphong Khongphinitbunjong https://orcid.org/0000-0002-4548-2790
Fatimah Al-Otibi https://orcid.org/0000-0003-3629-5755
Kevin D. Hyde https://orcid.org/0000-0002-2191-0762

Data availability

All of the data that support the findings of this study are available in the main text.

References

Baral HO (2016) Inoperculate discomycetes. In: Jaklitsch W, Baral HO, Lücking R, Lumbsch HT, Frey W (Eds) Syllabus of plant families: A. Engler's syllabus der Pflanzenfamilien part 1/2. Borntraeger, Stuttgart, 157–205.

Baral HO, De Sloover J, Huhtinen S, Laukka T, Stenroos S (2009) An emendation of the genus *Hyaloscypha* to include *Fuscoscypha* (Hyaloscyphaceae, Helotiales, Ascomycotina). Karstenia 49(1): 1–17. https://doi.org/10.29203/ka.2009.430

Bills GF, Platas G, Peláez F, Masurekar P (1999) Reclassification of a pneumocandin-producing anamorph, *Glarea lozoyensis* gen. et. sp. nov., previously identified as *Zalerion arboricola*. Mycological Research 103(2): 179–192. https://doi.org/10.1017/S095375629800687X

Capella-Gutiérrez S, Silla-Martínez JM, Gabaldón T (2009) trimAl: A tool for automated alignment trimming in large-scale phylogenetic analyses. Bioinformatics (Oxford, England) 25(15): 1972–1973. https://doi.org/10.1093/bioinformatics/btp348

Chaiwan N, Gomdola D, Wang S, Monkai J, Tibpromma S, Doilom M, Wanasinghe D, Mortimer P, Lumyong S, Hyde KD (2021) An online database providing updated information of microfungi in the Greater Mekong Subregion. Mycosphere 12(1): 1513–1526. https://doi.org/10.5943/mycosphere/12/1/19

Chethana KWT, Manawasinghe S, Hurdeal VG, Bhunjun CS, Appadoo MA, Gentekaki E, Raspé O, Promputtha I, Hyde KD (2021) What are fungal species and how to delineate them? Fungal Diversity 109(1): 1–25. https://doi.org/10.1007/s13225-021-00483-9

Ekanayaka AH, Hyde KD, Gentekaki EG, McKenzie EHC, Zhao Q, Bulgakov TS, Camporesi E (2019) Preliminary classification of Leotiomycetes. Mycosphere 10(1): 310–489. https://doi.org/10.5943/mycosphere/10/1/7

Gardes M, Bruns TD (1993) ITS primers with enhanced specificity for basidiomycetes-application to the identification of mycorrhizae and rusts. Molecular Ecology 2(2): 113–118. https://doi.org/10.1111/j.1365-294X.1993.tb00005.x

Groves JW (1968) Two new species of *Ascocalyx*. Canadian Journal of Botany 46(10): 1273–1278 https://doi.org/10.1139/b68-169

Gross A, Han JG (2015) *Hymenoscyphus fraxineus* and two new *Hymenoscyphus* species identified in Korea. Mycological Progress 14(4): 1–13. https://doi.org/10.1007/s11557-015-1035-1

Gross A, Hosoya T, Queloz V (2014) Population structure of the invasive forest pathogen *Hymenoscyphus pseudoalbidus*. Molecular Ecology 23(12): 2943–2960. https://doi.org/10.1111/mec.12792

Guindon S, Dufayard JF, Lefort V, Anisimova M, Hordijk W, Gascuel O (2010) New algorithms and methods to estimate maximum-likelihood phylogenies: Assessing the performance of PhyML 3.0. Systematic Biology 59(3): 307–321. https://doi.org/10.1093/sysbio/syq010

Guo MJ, Zhuo L, Wang SJ, Sui XN, Zhou H, Cai SR, Luo JT, Lei RH, Shen XY, Piepenbring M, Hou CL (2024) Hyperdiverse Rhytismatales on twigs of *Rhododendron* spp. Mycosphere 15(1): 764–880. https://doi.org/10.5943/mycosphere/15/1/6

Hall T (1999) BioEdit: A user-friendly biological sequence alignment editor and analysis program for Windows 95/98/NT. Nucleic Acids Symposium Series 41: 95–98.

Han JG, Hosoya T, Sung GH, Shin HD (2014) Phylogenetic reassessment of Hyaloscyphaceae *sensu lato* (Helotiales, Leotiomycetes) based on multi-gene analyses. Fungal Biology 118(2): 150–167. https://doi.org/10.1016/j.funbio.2013.11.004

Hibbett D, Abarenkov K, Kõljalg U, Öpik M, Chai B, Cole J, Wang Q, Crous P, Robert V, Helgason T, Herr JR, Kirk P, Lueschow S, Donnell KO, Nilsson RH, Oono R, Schoch C, Smyth C, Walker DM, Porras-Alfaro A, Taylor JW, Geiser DM (2016) Sequence-based classification and identification of Fungi. Mycologia 108: 1049–1068.

Hoang DT, Chernomor O, Von Haeseler A, Minh BQ, Vinh LS (2018) UFBoot2: Improving the ultrafast bootstrap approximation. Molecular Biology and Evolution 35(2): 518–522. https://doi.org/10.1093/molbev/msx281

Hosoya T, Hamano K, Sugano M, Ogura Y, Hatano E, Hamada T (1999) Discovery of dicephalosterol, a new testosterone 5α-reductase inhibitor, and some new mycological aspects of its producer, *Dicephalospora rufocornea* (Sclerotiniaceae, Discomycetes). Mycoscience 40(6): 525–529. https://doi.org/10.1007/BF02461030

Hyde KD, Noorabadi MT, Thiyagaraja V, He MQ et al. (2024) The 2024 Outline of Fungi and fungus-like taxa. Mycosphere 15(1): 5146–6239. https://doi.org/10.5943/mycosphere/15/1/25

Index Fungorum (2025) Index Fungorum. http://www.indexfungorum.org/names/Names.asp [Accessed on: 2025-2-11]

Jayasiri SC, Hyde KD, Ariyawansa HA, Bhat J, Buyck B, Cai L, Dai YC, Abd-Elsalam KA, Ertz D, Hidayat I, Jeewon R, Jones EBG, Bahkali AH, Karunarathna SC, Liu JK, Luangsa-ard JJ, Lumbsch HT, Maharachchikumbura SSN, McKenzie EHC, Moncalvo J-M, Ghobad-Nejhad M, Nilsson H, Pang K-L, Pereira OL, Phillips AJL, Raspé O, Rollins AW, Romero AI, Etayo J, Selçuk F, Stephenson SL, Suetrong S, Taylor JE, Tsui CKM, Vizzini A, Abdel-Wahab MA, Wen TC, Boonmee S, Dai DQ, Daranagama DA, Dissanayake AJ, Ekanayaka AH, Fryar SC, Hongsanan S, Jayawardena RS, Li WJ, Perera RH, Phookamsak R, de Silva NI, Thambugala KM, Tian Q, Wijayawardene NN, Zhao RL, Zhao Q, Kang JC, Promputtha I (2015) The Faces of Fungi database: Fungal names linked with morphology, phylogeny and human impacts. Fungal Diversity 74(1): 3–18. https://doi.org/10.1007/s13225-015-0351-8

Jeewon R, Hyde KD (2016) Establishing species boundaries and new taxa among fungi: Recommendations to resolve taxonomic ambiguities. Mycosphere 7(11): 1669–1677. https://doi.org/10.5943/mycosphere/7/11/4

Johnson M, Zaretskaya I, Raytselis Y, Merezhuk Y, McGinnis S, Madden TL (2008) NCBI BLAST: A better web interface. Nucleic Acids Research 36(Web Server): W5–W9. https://doi.org/10.1093/nar/gkn201

Johnston PR, Park D (2013) The phylogenetic position of *Lanzia berggrenii* and its sister species. Junwu Xuebao 32: 366–385.

Johnston PR, Quijada L, Smith CA, Baral H-O, Hosoya T, Baschien C, Pärtel K, Zhuang WY, Haelewaters D, Park D, Carl S, López-Giráldez F, Wang Z, Townsend JP (2019) A multigene phylogeny toward a new phylogenetic classification of Leotiomycetes. IMA Fungus 10(1): 1–22. https://doi.org/10.1186/s43008-019-0002-x

Kalyaanamoorthy S, Minh BQ, Wong TK, Von Haeseler A, Jermiin LS (2017) ModelFinder: Fast model selection for accurate phylogenetic estimates. Nature Methods 14(6): 587–589. https://doi.org/10.1038/nmeth.4285

Katoh K, Standley DM (2013) MAFFT multiple sequence alignment software version 7: Improvements in performance and usability. Molecular Biology and Evolution 30(4): 772–780. https://doi.org/10.1093/molbev/mst010

Kirchmair M, Neuhauser S, Buzina W, Huber L (2008) The taxonomic position of *Roesleria subterranea*. Mycological Research 112(10): 1210–1219. https://doi.org/10.1016/j.mycres.2008.04.009

Korf RP (1973) Discomycetes and tuberales. The fungi, 249–319.

Li CJY, Chethana KWT, Lu ZY, Zhao Q (2022) Two novel species of Lachnaceae (Helotiales, Leotiomycetes) from southwestern China. Current Research in Environmental & Applied Mycology (Journal of Fungal Biology) 12: 333–345. https://doi.org/10.5943/cream/12/1/20

Li CJY, Chethana KWT, Eungwanichayapant PD, Zhou DQ, Zhao Q (2024a) Additional four species of *Tatraea* (Leotiomycetes, Helotiales) in Yunnan Province, China. MycoKeys 102: 127–154. https://doi.org/10.3897/mycokeys.102.112565

Li CJY, Chethana KWT, Eungwanichayapant PD, Luo L, Yang ZL, Dong WJ, Guo YY, Liu CH, Alotibi F, Hyde KD, Zhao Q (2024b) *Longistipes* gen. nov. and four novel species of Hyphodiscaceae along with six new collections of Leotiomycetes in Yunnan Province, China. Mycosphere 15(1): 4744–4787. https://doi.org/10.5943/mycosphere/15/1/20

Liu XX, Zhuang WY, Zeng ZQ, Zhao P (2016) Newly discovered sclerotiniaceous fungi from China. Nova Hedwigia 102(3–4): 347–357. https://doi.org/10.1127/nova_hedwigia/2015/0310

Luo L, Wei D, Zhao Q, Chethana KWT (2024) Unveiling the diversity: A novel species of *Dicephalospora* (Helotiaceae, Helotiales) discovered in China. Phytotaxa 652(1): 59–68. https://doi.org/10.11646/phytotaxa.652.1.5

Luo L, Chethana KWT, Zhao Q, Thiyagaraja V, Al-Otibi F, Hyde KD (2025) Unveiling fungal diversity: a novel species of *Proliferodiscus* (Lachnaceae, Helotiales) discovered in China. Phytotaxa 682(3): 227–239. https://doi.org/10.11646/phytotaxa.682.3.3

Nguyen L-T, Schmidt HA, Von Haeseler A, Minh BQ (2015) IQ-TREE: A fast and effective stochastic algorithm for estimating maximum-likelihood phylogenies. Molecular Biology and Evolution 32(1): 268–274. https://doi.org/10.1093/molbev/msu300

O’Brien HE, Parrent JL, Jackson JA, Moncalvo JM, Vilgalys R (2005) Fungal community analysis by large-scale sequencing of environmental samples. Applied and Environmental Microbiology 71(9): 5544–5550. https://doi.org/10.1128/AEM.71.9.5544-5550.2005

Peláez F, Collado J, Platas G, Overy DP, Martín J, Vicente F, González del Val A, Basilio A, De la Cruz M, Tormo JR, Fillola A, Arenal F, Villareal M, Rubio V, Baral HO, Galán R, Bills GF (2011) Phylogeny and intercontinental distribution of the pneumocandin-producing anamorphic fungus *Glarea lozoyensis*. Mycology 2(1): 1–17. https://doi.org/10.1080/21501203.2010.544334

Phutthacharoen K, Chethana KWT, Lestari AS, Stadler M, Hyde KD (2022) Three new species of *Dicephalospora* (Helotiaceae, Helotiales) from Thailand. Diversity 14(8): 645. https://doi.org/10.3390/d14080645

Quandt CA, Haelewaters D (2021). Phylogenetic advances in Leotiomycetes, an understudied clade of taxonomically and ecologically diverse fungi. Encyclopedia of Mycology 1: 284–294. https://doi.org/10.1016/B978-0-12-819990-9.00052-4

Rämä T, Mathiassen GH, Kauserud H (2014) Marine fungi new to Norway, with an outlook to the overall diversity. Agarica : Mykologisk Tidsskrift 35: 35–47.

Ronquist F, Teslenko M, Van Der Mark P, Ayres DL, Darling A, Höhna S, Larget B, Liu L, Suchard MA, Huelsenbeck JP (2012) MrBayes 3.2: Efficient Bayesian phylogenetic inference and model choice across a large model space. Systematic Biology 61(3): 539–542. https://doi.org/10.1093/sysbio/sys029

Senanayake IC, Rathnayaka AR, Marasinghe DS, Calabon MS, Gentekaki E, Lee HB, Hurdeal VG, Pem D, Dissanayake LS, Wijesinghe SN, Bundhun D, Nguyen TT, Goonasekara ID, Abeywickrama PD, Bhunjun CS, Jayawardena RS, Wanasinghe DN, Jeewon R, Bhat DJ, Xiang MM (2020) Morphological approaches in studying fungi: collection, examination, isolation, sporulation and preservation. Mycosphere 11(1): 2678–2754. https://doi.org/10.5943/mycosphere/11/1/20

Sieber TN (2007) Endophytic fungi in forest trees: Are they mutualists? Fungal Biology Reviews 21(2–3): 75–89. https://doi.org/10.1016/j.fbr.2007.05.004

Spatafora JW, Sung G-H, Johnson D, Hesse C, O'Rourke B, Serdani M, Spotts R, Lutzoni F, Hofstetter V, Miadlikowska J, Reeb V, Gueidan C, Fraker E, Lumbsch T, Lücking R, Schmitt I, Hosaka K, Aptroot A, Roux C, Miller AN, Geiser DM, Hafellner J, Hestmark G, Arnold AE, Büdel B, Rauhut A, Hewitt D, Untereiner WA, Cole MS, Scheidegger C, Schultz M, Sipman H, Schoch CL (2006) A five-gene phylogeny of Pezizomycotina. Mycologia 98(6): 1018–1028. https://doi.org/10.1080/15572536.2006.11832630

Spooner BM (1987) Helotiales. of Australasia: Geoglossaceae, Orbiliaceae, Sclerotiniaceae, Hyaloscyphaceae. Bibliotheca Mycologica 116: 470–474.

Stenroos S, Laukka T, Huhtinen S, Döbbeler P, Myllys L, Syrjänen K, Hyvönen J (2010) Multiple origins of symbioses between ascomycetes and bryophytes suggested by a five-gene phylogeny. Cladistics 26(3): 281–300. https://doi.org/10.1111/j.1096-0031.2009.00284.x

Su HL, Chethana KWT, Li L, Li W, Zhao Q (2022) *Diplocarpa constans* sp. nov., a new species of Cordieritidaceae from Yunnan, China. Phytotaxa 561(1): 75–84. https://doi.org/10.11646/phytotaxa.561.1.7

Su HL, Chethana KWT, Zeng M, Zhao Q (2023) Two new species of *Erioscyphella* (Lachnaceae) from southwestern. Current Research in Environmental & Applied Mycology 13(1): 16–33. https://doi.org/10.5943/cream/13/1/2 [Journal of Fungal Biology]

Suh SO, Blackwell M (1999) Molecular phylogeny of the cleistothecial fungi placed in Cephalothecaceae and Pseudeurotiaceae. Mycologia 91(5): 836–848. https://doi.org/10.1080/00275514.1999.12061089

Tan YP, Shivas R (2022) Index of Australian Fungi no. 1. Zenodo, 1–18. https://doi.org/10.5281/zenodo.7250859

Taylor JW, Branco S, Gao C, Hann-Soden C, Montoya L, Sylvain I, Gladieux P (2017) Sources of fungal genetic variation and associating it with phenotypic diversity. The Fungal Kingdom, 635–655. https://doi.org/10.1128/microbiolspec.FUNK-0057-2016

Tochihara Y, Hosoya T (2022) Examination of the generic concept and species boundaries of the genus *Erioscyphella* (Lachnaceae, Helotiales, Ascomycota) with the proposal of new species and new combinations based on the Japanese materials. MycoKeys 87: 1–52. https://doi.org/10.3897/mycokeys.87.73082

Vilgalys R, Hester M (1990) Rapid genetic identification and mapping of enzymatically amplified ribosomal DNA from several *Cryptococcus* species. Journal of Bacteriology 172(8): 4238–4246. https://doi.org/10.1128/jb.172.8.4238-4246.1990

Vu D, Groenewald M, De Vries M, Gehrmann T, Stielow B, Eberhardt U, Al-Hatmi A, Groenewald JZ, Cardinali G, Houbraken J, Boekhout T, Crous PW, Robert V, Verkley GJM (2019) Large-scale generation and analysis of filamentous fungal DNA barcodes boosts coverage for kingdom fungi and reveals thresholds for fungal species and higher taxon delimitation. Studies in Mycology 92(1): 135–154. https://doi.org/10.1016/j.simyco.2018.05.001

Wang Z, Binder M, Hibbett D (2005) Life history and systematics of the aquatic discomycete *Mitrula* (Helotiales, Ascomycota) based on cultural, morphological, and molecular studies. American Journal of Botany 92(9): 1565–1574. https://doi.org/10.3732/ajb.92.9.1565

Wijayawardene NN, Hyde KD, Dai DQ, Sánchez-García M, Goto BT, Saxena RK, Erdoğdu M, Selçuk F, Rajeshkumar KC, Aptroot A, Błaszkowski J, Boonyuen N, da Silva GA, de Souza FA, Dong W, Ertz D, Haelewaters D, Jones EBG, Karunarathna SC, Kirk PM, Kukwa M, Kumla J, Leontyev DV, Lumbsch HT, Maharachchikumbura SSN, Marguno F, Martínez-Rodríguez P, Mešić A, Monteiro JS, Oehl F, Pawłowska J, Pem D, Pfliegler WP, Phillips AJL, Pošta A, He MQ, Li JX, Raza M, Sruthi OP, Suetrong S, Suwannarach N, Tedersoo L, Thiyagaraja V, Tibpromma S, Tkalčec Z, Tokarev YS, Wanasinghe DN, Wijesundara DSA, Wimalaseana SDMK, Madrid H, Zhang GQ, Gao Y, Sánchez-Castro I, Tang LZ, Stadler M, Yurkov A, Thines M (2022) Outline of Fungi and fungus-like taxa–2021. Mycosphere 13: 53–453. https://doi.org/10.5943/mycosphere/13/1/2

White TJ, Bruns T, Lee S, Taylor J (1990) Amplification and direct sequencing of fungal ribosomal RNA genes for phylogenetics. PCR protocols: a guide to methods and applications. 18: 315–322. https://doi.org/10.1016/B978-0-12-372180-8.50042-1

Yokoya K, Postel S, Fang R, Sarasan V (2017) Endophytic fungal diversity of *Fragaria vesca*, a crop wild relative of strawberry, along environmental gradients within a small geographical area. PeerJ 5: e2860. https://doi.org/10.7717/peerj.2860

Zeng XY, Tan TJ, Tian FH, Wang Y, Wen TC (2023) OFPT: A one-stop software for fungal phylogeny. Mycosphere 14(1): 1730–1741. https://doi.org/10.5943/mycosphere/14/1/20

Zhang ZY, Pan H, Tao G, Li X, Han YF, Feng Y, Tong SQ, Ding CY (2024) Culturable mycobiota from Guizhou Wildlife Park in China. Mycosphere 15(1): 654–763. https://doi.org/10.5943/mycosphere/15/1/5

Zhao YJ (2014) Taxonomic study of *Lambertella* (Rutstroemiaceae, Helotiales) and allied substratal stroma forming fungi from Japan. University of Tsukuba, Tsukuba, Japan.

Zhao YJ, Hosaka K, Hosoya T (2016) Taxonomic re-evaluation of the genus *Lambertella* (Rutstroemiaceae, Helotiales) and allied stroma-forming fungi. Mycological Progress 15(12): 1215–1228. https://doi.org/10.1007/s11557-016-1225-5

Zheng HD, Zhuang WY (2019) Three new species of *Dicephalospora* from China as revealed by morphological and molecular evidence. MycoKeys 55: 87–99. https://doi.org/10.3897/mycokeys.55.33859

Zhuang WY, Zeng ZQ, Liu XX (2016) Taxonomic revision of the genus *Dicephalospora* (Helotiales) in China. Mycosystema 35: 791–801. https://doi.org/10.13346/j.mycosystema.160047

MycoKeys

MycoKeys 115: 87–135 (2025)
DOI: 10.3897/mycokeys.115.142433

Research Article

Molecular phylogeny and morphology reveal four new species in Hymenochaetales and one new species in Cantharellales from Southwestern China

Jianling Zhang[1*], Zirui Gu[1*], Chunqin Zhou[2], Hongmin Zhou[1,3]

1 *College of Forestry, Southwest Forestry University, Kunming 650224, China*
2 *Yunnan Wumeng Mountains National Nature Reserve, Zhaotong 657000, China*
3 *The Key Laboratory of Forest Resources Conservation and Utilization in the South-west Mountains of China Ministry of Education, Key Laboratory of National Forestry and Grassland Administration on Biodiversity Conservation in Southwest China, Yunnan Provincial Key Laboratory for Conservation and Utilization of In-forest Re-source, Southwest Forestry University, Kunming 650224, China*
Corresponding author: Hongmin Zhou (zhouhongmin@swfu.edu.cn)

Abstract

Wood-decaying fungi represent a vital group of higher fungi that drive the cycling of matter and energy in forest ecosystems, and they have been the focus of thorough investigation. In this study, five new species, *viz*. *Botryobasidium daweishanense*, *Inonotus subglobisporum*, *Kneiffiella bubalina*, *Xylodon granulanoides*, and *X*. *granulans* from China, are described and illustrated based on the morphological characteristics and molecular phylogenetic analyses, in which the sequences of ITS+nLSU genes were used for the phylogenetic analyses by maximum likelihood and Bayesian inference methods. The phylogeny revealed that the *Botryobasidium daweishanense* groups with three taxa, *viz*., *B*. *intertextum*, *B*. *leptocystidiatum*, and *B*. *subcoronatum*. *Inonotus subglobisporum* is closely related to *I*. *radiatus*. *Kneiffiella bubalina* clustered sister to *K*. *subalutacea*. *Xylodon granulanoides* and *X*. *granulans* have a close relationship with *X*. *bambusinus*, *X*. *fissuratus*, *X*. *subclavatus*, *X*. *montanus*, and *X*. *wenshanensis*. Additionally, *Xylodon granulanoides* and *X*. *granulans* clustered together. *Botryobasidium daweishanense* is characterized by an araneose hymenial surface, fusiform, and cyanophilous basidiospores (6.1–7.3 × 3.3–3.9 µm). *Inonotus subglobisporum* is characterized by perennial basidiomata with lateral stipes, polygon pores measuring 4–6 per mm, and subglobose, cyanophilous basidiospores (3.6–4.3 × 2.8–3.5 µm). *Kneiffiella bubalina* is characterized by cream basidiomata and cylindrical to slightly allantoid basidiospores (8.0–8.9 × 1.8–2.3 µm). *Xylodon granulanoides* is characterized by grandinioid hymenial surfaces, various cystidia, and broadly ellipsoid, thick-walled basidiospores (4.7–5.3 × 3.6–4.1 µm). *Xylodon granulans* is characterized by grandinioid hymenial surfaces, capitate and clavate cystidia, and broadly ellipsoid basidiospores (3.8–4.2 × 2.9–3.3 µm). Phylogenetic analysis based on internal transcribed spacer (ITS) and nuclear large subunit RNA (nLSU) shows that the four species are members of Hymenochaetales, and one belongs to Cantharellales. All five new species are compared with morphologically and phylogenetically closely related species. The present study contributes to understanding the species diversity, taxonomy, and phylogeny of macrofungi in Southwestern China.

Key words: Biodiversity, Cantharellales, Hymenochaetales, new taxa, wood-inhabiting fungi

This article is part of:
Exploring the Hidden Fungal Diversity: Biodiversity, Taxonomy, and Phylogeny of Saprobic Fungi
Edited by Samantha C. Karunarathna, Danushka Sandaruwan Tennakoon, Ajay Kumar Gautam

Academic editor:
Samantha C. Karunarathna
Received: 22 November 2024
Accepted: 12 February 2025
Published: 12 March 2025

Citation: Zhang J, Gu Z, Zhou C, Zhou H (2025) Molecular phylogeny and morphology reveal four new species in Hymenochaetales and one new species in Cantharellales from Southwestern China. MycoKeys 115: 87–135. https://doi.org/10.3897/mycokeys.115.142433

---

[*] These authors contributed equally to this work and share the first authorship.

Introduction

Wood-inhabiting fungi thrive on various types of wood, including vigorous wood, dead wood, and fallen branches. They play a crucial role in degrading the lignin, cellulose, or hemicellulose present in wood, making them an important group of higher fungi (M'Barek et al. 2020; Runnel et al. 2021; Dong et al. 2023, 2024a). These fungi are the cornerstones of matter cycles and energy flows in forest ecosystems and play a vital ecological role in the regulation of carbon storage (Phookamsak et al. 2019; Ponce et al. 2023). A robust understanding of wood-fungi diversity is required to explain their rise to forest dominance; however, the classification of some taxa remains unknown.

The genus *Botryobasidium* Donk belongs to the family Botryobasidiaceae Jülich (Cantharellales, Basidiomycota) and is typified by *Botryobasidium subcoronatum* (Höhn. & Litsch.) Donk. Species of the corticioid *Botryobasidium* are saprobic fungi that cause white rot in forested areas (Langer et al. 2000b; Bondartseva and Zmitrovich 2023). They are commonly found on a range of hosts or substrates, from litter and fallen trunks to the stems of living trees, including macrophanerophytes (Langer et al. 2000a, 2000b; Hjortstam et al. 2005; Zhou et al. 2024a). Fungi in this genus have resupinate, smooth to grandinioid basidiomata; branched right-angled hyphae with or without clamp connections; short, cylindrical or subcylindrical to suburniform basidia with 2–8 sterigmata generally arranged in clusters; and narrow to globose, smooth to tuberculate or laciniate, and inamyloid basidiospores (Langer et al. 2000a; Bernicchia et al. 2010). According to the Index Fungorum (www.indexfungorum.org; accessed on 26 January 2025), the genus *Botryobasidium* has 116 specific registered names, with 101 species accepted worldwide (Dong et al. 2024b; Liu et al. 2024; Zhou et al. 2024a; Zhou et al. 2024b). Based on ITS data analysis, we demonstrated that the genus *Botryobasidium* formed a well-supported monophyletic group, as previously demonstrated by its micromorphological and ultrastructural characteristics (Langer and Langer 1998; Moncalvo et al. 2006; Zhou et al. 2024b).

Frey et al. (1977) established the order Hymenochaetales Oberw., using Hymenochaetaceae Donk as the type family (He et al. 2024). Hymenochaetales is a large order of Agaricomycetes with 14 families, 83 genera, and 1205 species, including wood-inhabiting and ectomycorrhizal fungi. These fungi have different kinds of basidiomata, such as polyporoid, stereoid, corticioid, hydnoid, coralloid, and agaricoid (Hibbett et al. 2014; He et al. 2024). Hymenochaetaceae includes species with brownish basidiomata and generative hyphae without clamp connections. This family includes six genera, namely, *Coltricia* Gray, *Cyclomyces* Kunze ex Fr., *Hydnochaete* Bres., *Hymenochaete* Lév., *Inonotus* P. Karst, and *Phellinus* Quél, laying the foundational framework for the classification of Hymenochaetaceae (Hibbett et al. 2014; Wijayawardene et al. 2022; He et al. 2024). However, the phylogeny of *Hymenochaete* is not well understood, and researchers have investigated the phylogenetic relationships of these genera (Wagner and Fischer 2002). Phylogenetic analyses of *Hymenochaete* and its allied genera have been performed, and the results have been verified by mycologists (Larsson et al. 2006; Dai 2010). Furthermore, a series of studies indicated that certain species have a high degree of host specificity (Dai 2010; Purahong et al. 2018; Wang et al. 2021, 2022; Wu et al. 2022; Zhao et al. 2023a; Zhou et al. 2023). The diversity of *Hymenochaete* fungi and the number of species recorded in China have also been extensively studied (Korotkin et al. 2018; Wu et al. 2022; Zhao et al. 2023a, 2024).

Inonotus, one of the largest genera within the Hymenochaetaceae family, is typified by *Inonotus hispidus* (Bull.) P. Karst; it is primarily found as parasites or saprophytes on various types of wood (Wagner and Fischer 2002; Zhou et al. 2015). Fungi of this genus have annual to perennial, resupinate, effused reflexed or pileate, yellowish to brown, hispid, velutinate to rough or glabrous pilei; a brown pore surface; homogeneous, brown, corky context basidiomata; a monomitic hyphal system; and generative hyphae with simple septa. Hymenial setae may be present or absent; hyphoid setae are found in some species and are ellipsoid, hyaline to brownish, thick-walled basidiospores. Previous phylogenetic analyses indicated that *Inonotus sensu lato* had polyphyletic origins, and four more narrowly defined genera, namely *Inocutis* Fiasson & Niemelä, *Inonotopsis* Parmasto, *Mensularia* Lázaro Ibiza, and *Onnia* P. Karst., were segregated from *Inonotus* (Wagner and Fischer 2002; Dai 2010). Meanwhile, two new genera were proposed (Zhou et al. 2016): *Sanghuangporus* Sheng H. Wu, L.W. Zhou & Y.C. Dai, and *Tropicoporus* L.W. Zhou, Y.C. Dai & Sheng H. Wu. *Inonotus* is a well-known species commonly used in traditional medicine to treat various ailments (Delgersaikhan et al. 2024; Yu et al. 2024). The genus produces white rot and exhibits a worldwide distribution (Wagner and Fischer 2002; Dai 2010), with 289 specific registered names and 128 species accepted worldwide (www.indexfungorum.org; accessed on 26 January 2025) (Wagner and Fischer 2002; Dai 2010; Zhou et al. 2016; Wu et al. 2022).

The genus *Kneiffiella* P. Karst belongs to the family Chaetoporellaceae Jülich (Hymenochaetales, Basidiomycota) and is typified by *Kneiffiella barba-jovis* (Bull.) P. Karst. Fungi of this genus prefer dark microhabitats that slowly dry on tree trunks, leading to particularly severe wood decay, such as on hollow areas and undersides (Běťák et al. 2021). They have resupinate, smooth to grandinioid, coralloid, or irpicoid basidiomata; a white to brown or ochraceous hymenial surface; a monomitic to pseudodimitic hyphal system; generative hyphae with clamp connections; tubular and clavate cystidia; cylindrical to utriform, or barrel-like, basidia with four sterigmata; and cylindrical to ellipsoid or allantoid, inamyloid, and acyanophilous basidiospores (Wang et al. 2021). According to the Index Fungorum (www.indexfungorum.org; accessed on 26 January 2025), the genus *Kneiffiella* has 84 specific registered names, with 40 species accepted worldwide (Běťák et al. 2021; Wang et al. 2021; Viner et al. 2024).

The genus *Xylodon* (Pers.) Gray belongs to the family Schizoporaceae Jülich (Hymenochaetales, Basidiomycota) and is typified by *Xylodon quercinus* (Pers.) Gray (Bernicchia and Gorjón 2010). *Xylodon* is a large genus of corticioid fungi with a cosmopolitan distribution (Guan et al. 2023; Yurchenko et al. 2024; Zhang et al. 2024a). Species of *Xylodon* inhabit dead wood of various sizes, ranging from twigs of several millimeters in diameter to large fallen trunks, and they cause white rot (Greslebin and Rajchenberg 2000; Kotiranta and Saarenoksa 2000; Girometta et al. 2020; Guan et al. 2023). In some cases, basidiomata of *Xylodon* species appear on the living parts of trees (Yurchenko 2008) and non-woody plant remains, such as fern rachises

(Kotiranta and Saarenoksa 2000), herb stems, fallen leaves (Viner et al. 2018), and dead polypore basidiomata (Viner et al. 2023). Fungi in this genus have resupinate or effuse, smooth basidiomata; a tuberculate, grandinioid, odontioid, coralloid, irpicoid, or poroid hymenial surface; a monomitic or dimitic hyphal system that is generative with clamp connections; different types of cystidia; utriform or suburniform basidia; and cylindrical to ellipsoid to globose basidiospores (Gray 1821; Bernicchia and Gorjón 2010; Zhang et al. 2024a). According to the Index Fungorum (www.indexfungorum.org; accessed on 26 January 2025), the genus *Xylodon* has 241 specific registered names, with 157 species accepted worldwide. Remarkably, new species have been described in this genus at an accelerated pace owing to advances in morphological taxonomy and molecular phylogeny (Luo et al. 2022; Qu et al. 2022; Guan et al. 2023; Yurchenko et al. 2024; Zhang et al. 2024a).

In addition, host specificity is essential for determining the taxonomy and phylogeny of Hymenochaetales, with various types identified in a series of studies, including angiosperms, gymnosperms, both angiosperms and gymnosperms, and bryophytes (Dai 2010; Zhao et al. 2024). Most species in Hymenochaetales are polyporous and corticioid fungi, whereas certain species, such as *Blasiphalia* Redhead, *Contumyces* Redhead, and *Rickenella* Raithelh, basidiomata in those taxa are agarics. Beyond morphological diversity, various trophic modes, including saprotrophs, parasites, and symbiotes (with both trees and moss), also exist within Hymenochaetales (Wang and Zhou 2024). Many new Hymenochaetales taxa have recently been described due to research on the diversity of wood-inhabiting fungi in Yunnan Province (Chen and Zhao 2020; Luo et al. 2021; Qu et al. 2022; Guan et al. 2023; Yuan and Zhao 2024; Zhang et al. 2024a). These studies provide an important foundation for further exploration of species diversity and taxonomic status within Hymenochaetales.

This study collected five new species of wood-inhabiting fungi from Yunnan Province, China. To clarify the taxonomic placement of these species, morphological and phylogenetic analyses based on the ITS and nLSU sequences were conducted to identify them as new species of *Botryobasidium*, *Inonotus*, *Kneiffiella*, and *Xylodon*. This study provides full descriptions, color photographs, detailed comparisons with closely related taxa, and phylogenetic placements of the five new species. New data have been added to the biodiversity research on the genera *Botryobasidium*, *Inonotus*, *Kneiffiella*, and *Xylodon*, further affirming the rich biodiversity of southwestern China.

Materials and methods

Sample collection and herbarium specimen preparation

The fresh basidiomata were collected on the fallen angiosperm branches from Yunnan Province, China, and collection information was recorded (Rathnayaka et al. 2024). The samples were photographed *in situ*, and fresh macroscopic details were recorded. Photographs were taken by a Nikon D7100 camera. All the photos were focus-stacked using Helicon Focus software. Macroscopic details were recorded, and the fruit bodies were transported to a field station where they were dried in an electric food dryer at 45 °C (Hu et al. 2022). Once dried, the specimens were sealed in an envelope and zip-lock plastic bags and labeled (Zhang et al. 2024b). The dried specimens were deposited in the herbarium of the Southwest Forestry University (SWFC), Kunming, Yunnan Province, China.

Morphological studies

The macro-morphology was based on the fresh specimens, while the micro-morphology was studied based on dried specimens. The color terms in the description followed Anonymous (1969) and Petersen (1996). Micro-morphology was studied at magnifications of 1000 ×, using a Nikon Eclipse 80i microscope with phase contrast illumination. Melzer's reagent (IKI), Cotton Blue (CB), and 5% potassium hydroxide (KOH) were used. Drawings were made with the aid of a drawing tube. In the text, further abbreviations were used: IKI– = non-dextrinoid and non-amyloid, IKI+ = amyloid, CB– = acyanophilous, CB+ = cyanophilous, L = mean basidiospore length (arithmetic average of all basidiospores), W = mean basidiospore width (arithmetic average of all basidiospores), Q = variation in the L/W ratios, n = the number of basidiospores measured.

DNA Extraction, polymerase chain reaction, and sequencing genomic

The CTAB rapid plant genome extraction kit-DN14 (Aidlab Biotechnologies Co., Ltd., Beijing) was used to obtain DNA from dried specimens. PCR was performed according to the manufacturer's instructions with some modifications (Yang et al. 2023). The nuclear ribosomal ITS region was amplified with the primers ITS5 and ITS4 (White et al. 1990). The nuclear ribosomal nLSU gene was amplified with the primers LR0R and LR7 (Vilgalys and Hester 1990; Rehner and Samuels 1994). The PCR procedure for ITS was as follows: initial denaturation at 95 °C for 3 min, followed by 35 cycles at 94 °C for 40 s, 54 °C for 45 s, and 72 °C for 1 min; and a final extension at 72 °C for 10 min. The PCR procedure for nLSU was as follows: initial denaturation at 94 °C for 1 min, followed by 35 cycles at 94 °C for 30 s, 50 °C for 1 min, and 72 °C for 1.5 min; and a final extension at 72 °C for 10 min (Zhou et al. 2024c). All newly generated sequences were submitted to GenBank and are listed in Table 1.

Phylogenetic analyses

Sequences generated for this study were aligned with additional sequences downloaded from GenBank. Sequences were aligned using MAFFT v.7 (https://mafft.cbrc.jp/alignment/server/), adjusting the direction of nucleotide sequences according to the first sequence (accurate enough for most cases), and selecting the G-INS-i iterative refinement method (Katoh et al. 2019). Alignments were manually adjusted to maximize alignment and minimize gaps with BioEdit v.7.0.9 (Hall 1999). A dataset of concatenated ITS and nLSU sequences was used to determine the phylogenetic position of the new species. Maximum likelihood (ML) analysis was performed using the CIPRES Science Gateway based on the dataset using the RA×ML-HPC BlackBox tool, with setting RA×ML halt bootstrapping automatically and 0.25 for maximum hours and obtaining the best tree using ML search (Miller et al. 2010). Other parameters in ML analysis used default

Table 1. Names, sample numbers, locations, references, and corresponding GenBank accession numbers of the taxa used in this study. [New species are shown in bold; * is shown as type material, holotype; — indicates sequence unavailability].

Species	Sample No.	GenBank No.		Country	References
		ITS	nLSU		
Alloclavaria purpurea	H6047663	MF319055	MF318905	Finland	Cho et al. 2024
Alloclavaria purpurea	M. Korhonen 10305	MF319044	MF318895	Finland	Cho et al. 2024
Antrodia subserpens	Dai 13233	KP715309	KT968830	China	Chen and Cui 2015
Atheloderma mirabile	TAA 169235	DQ873592	DQ873592	Estonia	Larsson et al. 2006
Basidioradulum radula	LWZ 20201017-62	ON063684	ON063884	China	Wang et al. 2023
Blasiphalia pseudogrisella	P. Hoijer 4118	MF319047	MF318898	Finland	Cho et al. 2024
Blasiphalia pseudogrisella	P. Hoijer 4393	MF319048	MF318899	Estonia	Cho et al. 2024
Botryobasidium acanthosporum	Yuan18083*	PP229512	PP218361	China	Zhou et al. 2024c
Botryobasidium acanthosporum	Yuan16326	PP229497	—	China	Zhou et al. 2024c
Botryobasidium asperulum	RAS552	OR471090	OR470959	USA	Swenie et al. 2023
Botryobasidium asperulum	FP102150	OR471075	OR47094	USA	Swenie et al. 2023
Botryobasidium aureum	GEL 2910	AJ389783	—	Germany	Langer et al. 2000b
Botryobasidium bambusinum	CLZhao29916	PQ539057	PQ539060	China	Dong et al. 2024b
Botryobasidium bambusinum	CLZhao29936*	PQ539058	PQ539061	China	Dong et al. 2024b
Botryobasidium botryosum	KHL11081	AY463387	AY586638	Sweden	Larsson et al. 2004
Botryobasidium botryosum	AFTOL-ID 604	DQ267124	—	USA	Zhou et al. 2024c
Botryobasidium candicans	UC2022891	KP814227	—	USA	Vu et al. 2018
Botryobasidium candicans	UC2022944	KP814546	—	USA	Vu et al. 2018
Botryobasidium candicans	UC2022893	KP814200	—	USA	Vu et al. 2018
Botryobasidium coniferarum	LWZ20171016-15	OR557262	—	China	Dong et al. 2024b
Botryobasidium coniferarum	LWZ20210928-3*	OR557259	—	China	Dong et al. 2024b
Botryobasidium conspersum	AFTOL-ID 1766	DQ911612	DQ521414	USA	Cao et al. 2021
Botryobasidium daweishanense	CLZhao40061	PQ373983	—	China	Present study
Botryobasidium daweishanense	**CLZhao40061**	**PQ373983**	—	**China**	**Present study**
Botryobasidium daweishanense	**CLZhao40062***	**PQ373984**	**PQ373977**	**China**	**Present study**
Botryobasidium gossypirubiginosum	CLZhao 26052*	OR668924	OR708665	China	Zhou et al. 2024b
Botryobasidium incanum	CLZhao 26697*	OR668923	OR708664	China	Zhou et al. 2024b
Botryobasidium indicum	NFCCI4480	NR171230	—	India	Zhou et al. 2024b
Botryobasidium indicum	AMH:10054	MK391496	—	India	Zhou et al. 2024b
Botryobasidium indicum	hr5326	OP806032	—	China	Zhou et al. 2024b
Botryobasidium indicum	CLZhao21791	ON406471	—	China	Zhou et al. 2024b
Botryobasidium indicum	AMH:10054	MK391496	MK391493	India	Zhou et al. 2024b
Botryobasidium intertextum	UC2022959	KP814540	—	North American	Zhou et al. 2024b
Botryobasidium laeve	RAS762	OR471128	—	USA	Swenie et al. 2023
Botryobasidium leptocystidiatum	Yuan17548	PP209211	—	China	Zhou et al. 2024c
Botryobasidium leptocystidiatum	Yuan17708*	PP209197	—	China	Zhou et al. 2024c
Botryobasidium robustius	CBS:945.69	MH859491	MH871272	Czech Republic	Fukami et al. 2010
Botryobasidium simile	RAS793	OR471146	—	USA	Swenie et al. 2023
Botryobasidium simile	RAS794	OR471147	—	USA	Swenie et al. 2023
Botryobasidium simile	GEL2348	KP171641	DQ898730	Canada	Cao et al. 2021
Botryobasidium subcoronatum	RAS620 SV1	OR471110	—	USA	Swenie et al. 2023
Botryobasidium subcoronatum	RAS789	OR471144	—	USA	Swenie et al. 2023
Botryobasidium subcoronatum	FP101015	OR471077	—	USA	Swenie et al. 2023
Botryobasidium subcoronatum	FP151108	OR471078	—	USA	Swenie et al. 2023
Botryobasidium subcoronatum	AFTOL-ID 614	DQ200924	AY647212	USA	Cao et al. 2021
Botryobasidium subovalibasidium	Yuan18179*	PP209196	—	China	Zhou et al. 2024c
Botryobasidium subovalibasidium	Yuan16439	PP209199	—	China	Zhou et al. 2024c
Botryobasidium tubulicystidium	DK14139	OL436769	—	USA	Zhou et al. 2024b
Botryobasidium yunnanense	CLZhao24877*	OR668925	—	China	Zhou et al. 2024b
Bridgeoporus sinensis	Cui 10013	KY131832	KY131891	China	Cho et al. 2024
Bryoclavula phycophila	TNS F-79667	NR169921	LC508118	Japan	Masumoto and Degawa 2020

Species	Sample No.	GenBank No.		Country	References
		ITS	nLSU		
Bryoclavula phycophila	S-287-FB3	LC544109	LC544110	Japan	Masumoto and Degawa 2020
Bryopistillaria sagittiformis	IO.14.164	MT232349	MT232303	Sweden	Olariaga et al. 2020
Burgella lutea	Etayo 27623	KC336076	KC336075	Bolivia	Diederich et al. 2014
Burgoa verzuoliana	CBS 131.38	NR145334	NG058614	Japan	Cao et al. 2021
Cantharellopsis prescotii	H6059300	MF319051	MF318903	Finland	Cho et al. 2024
Cantharellus albidolutescens	BB 08.070*	KF981365	KF294646	Madagascar	Cao et al. 2021
Cantharellus alborufescens	AH44223	KR677493	KR677531	Spain	Olariaga et al. 2015
Cantharellus alborufescens	BB 12.075	KX907209	KX929161	Switzerland	Olariaga et al. 2017
Cantharellus ambohitantelyensis	BB 08.336*	KF981366	KF294656	Madagascar	Cao et al. 2021
Cantharellus amethysteus	BB 07.284	JN944020	KF294639	Slovakia	Olariaga et al. 2017
Cantharellus amethysteus	AH44796*	KR677512	KR677550	Spain	Olariaga et al. 2015
Cantharellus anzutake	TNS-F-61925*	LC085359	LC085415	Japan	Cao et al. 2021
Cantharellus californicus	OSC 122878 *	KX828768	KX828795	USA	Olariaga et al. 2017
Cantharellus cascadensis	OSC 75908	AY041181	AY041160	USA	Olariaga et al. 2015
Cantharellus chicagoensis	PRL8916	KP639201	KP639218	USA	Leacock et al. 2016
Cantharellus chicagoensis	PRL8332	KP639200	KP639214	USA	Leacock et al. 2016
Cantharellus cibarius	BIO-Fungi 10986*	KR677501	KR677539	Sweden	Olariaga et al. 2015
Cantharellus cyphelloides	TNS:F-61721*	NR154853	NG059027	Japan	Suhara and Kurogi 2015
Cantharellus decolorans	469/BB 08.278	NR154788	KF294654	Madagascar	Olariaga et al. 2017
Cantharellus ferruginascens	BIO-Fungi 11700	KR677486	KR677524	Spain	Olariaga et al. 2015
Cantharellus hygrophorus	BB 08.196*	KF981368	KF294650	Madagascar	Cao et al. 2021
Cantharellus lewisii	BB 07.003*	JN944021	JN940597	USA	Olariaga et al. 2015
Cantharellus pallens	BB 09.409	KX929162	KX907215	Italy	Olariaga et al. 2017
Cantharellus romagnesianus	AH44218	KX828784	KX828807	Spain	Olariaga et al. 2017
Cantharellus roseocanus	DAOM220723	KX828787	KX828810	Canada	Olariaga et al. 2017
Cantharellus sebosus	BB 08.234*	NR154789	KF294652	Madagascar	Cao et al. 2021
Cantharellus sebosus	BB 08.162	KF981371	KF294649	Madagascar	Cao et al. 2021
Cantharellus subalbidus	OSC 75937	AY041179	AY041149	USA	Dunham et al 2003
Cantharellus subincarnatus	BB 06.096	KF981372	KF294602	Madagascar	Cao et al. 2021
Cantharellus subminor	Yuan 13917*	MW980545	MW979522	China	Cao et al. 2021
Cantharellus subminor	Yuan 13925	MW980546	MW979523	China	Cao et al. 2021
Cantharellus subminor	Yuan 13926	MW980547	MW979524	China	Cao et al. 2021
Cantharellus tabernensis	BB 07.064	JN944012	JN940608	USA	Olariaga et al. 2015
Cantharellus tabernensis	BB 07.040	JN944013	JN940609	USA	Olariaga et al. 2015
Cantharellus tenuithrix	BB 07.125*	JN944017	JN940600	USA	Olariaga et al. 2017
Cantharellus vaginatus	HKAS55730*	HQ416692	HM594681	China	Cao et al. 2021
Cantharellus yunnanensis	Yuan 14539	MW980541	MW979514	China	Cao et al. 2021
Cantharellus yunnanensis	Yuan 14636	MW980542	MW979515	China	Cao et al. 2021
Ceratobasidium globisporum	CBS 569.83	DQ278942	MH873365	Australia	Cao et al. 2021
Ceratobasidium sp.	CAG6	AF354083	AF354083	USA	Gonzalez et al. 2001
Ceratorhiza hydrophila	E14504F	MT381956	MT381951	Ecuador	Adaku et al. 2020
Cerioporus squamosus	Cui 10595	KU189778	KU189809	China	Zhou et al. 2016
Clavulina cerebriformis	MCA4022*	NR121504	JN228222	Guyana	Cao et al. 2021
Clavulina cf. cristata	MES426	JN228225	JN228225	China	Cho et al. 2024
Clavulina cinereoglebosa	TH8561	JN228218	JN228232	Guyana	Cho et al. 2024
Clavulina cristata	JKU8	JN228227	JN228227	USA	Cho et al. 2024
Clavulina sp.	MB03-034	DQ202266	AY745694	USA	Cao et al. 2021
Coltricia abieticola	Cui 10321	KX364785	—	China	Unpublished
Coniferiporia qilianensis	Yuan 6424	NR_158318	NG_060411	China	Wu et al. 2022
Coniferiporia weirii	FP-134599-SP	MT420695	MT416461	China	Cho et al. 2024
Contumyces rosellus	MGW1462	MF319059	MF318912	USA	Cho et al. 2024
Cotylidia fbrae	FM639	NR_176148	NG_088193	China	Cho et al. 2024
Cotylidia sp.	AFTOL-700	AY854079	AY629317	USA	Cho et al. 2024
Craterellus atratoides	TH8473	JQ915103	JQ915129	Guyana	Wilson et al. 2012
Craterellus atratoides	TH9232*	JQ915111	NG042660	Guyana	Wilson et al. 2012

Species	Sample No.	GenBank No.		Country	References
		ITS	nLSU		
Craterellus atratus	MCA1070	JQ915092	JQ915118	Guyana	Wilson et al. 2012
Craterellus atratus	MCA990	JQ915100	JQ915126	Guyana	Wilson et al. 2012
Craterellus atrobrunneolus	Yuan 13878	MN902353	MN894058	China	Wilson et al. 2012
Craterellus badiogriseus	Yuan 14776*	MW980548	MW979532	China	Cao et al. 2021
Craterellus badiogriseus	Yuan 14779	MW980549	MW979533	China	Cao et al. 2021
Craterellus cinereofimbriatus	TH8999	JQ915104	JQ915130	Guyana	Wilson et al. 2012
Craterellus cinereofimbriatus	TH9075*	JQ915105	JQ915131	Guyana	Wilson et al. 2012
Craterellus croceialbus	Yuan 14623*	MW980572	MW979529	China	Cao et al. 2021
Craterellus croceialbus	Yuan 14647	MW980573	MW979530	China	Cao et al. 2021
Craterellus excelsus	TH7515	JQ915101	JQ915127	Guyana	Wilson et al. 2012
Craterellus excelsus	TH8235*	JQ915102	JQ915128	Guyana	Wilson et al. 2012
Craterellus fallax	AFTOL-ID 286	DQ205680	AY700188	USA	Cao et al. 2021
Craterellus indicus	PUN 3884*	NR119831	NG060387	India	Kumari et al. 2012
Craterellus luteus	GDGM48105*	MG727896	MG701171	China	Zhong et al. 2018
Craterellus luteus	GDGM46432	MG727897	MG727898	China	Zhong et al. 2018
Craterellus macrosporus	Yuan 14782	MW980574	MW979531	China	Cao et al. 2021
Craterellus olivaceoluteus	MCA3186	JQ915098	JQ915124	Guyana	Wilson et al. 2012
Craterellus olivaceoluteus	TH9205*	JQ915109	JQ915135	Guyana	Wilson et al. 2012
Craterellus parvogriseus	CAL 1533*	MF421099	MF421098	India	Cao et al. 2021
Craterellus Pleurotoides	MCA3124	JQ915097	JQ915123	Guyana	Wilson et al. 2012
Craterellus pleurotoides	TH9220	JQ915110	JQ915136	Guyana	Wilson et al. 2012
Craterellus strigosus	MCA1750	JQ915094	JQ915120	Guyana	Wilson et al. 2012
Craterellus strigosus	TH9204*	JQ915108	JQ915134	Guyana	Wilson et al. 2012
Cylindrosporus flavidus	Dai 13213	KP875564	KP875561	China	Wu et al. 2022
Dacrymyces australis	CBS:196.63	MH858261	MH869866	USA	Cao et al. 2021
Fasciodontia brasiliensis	MSK-F 7245a*	MK575201	MK598734	Brazil	Yurchenko et al. 2020a
Fasciodontia bugellensis	KAS-FD 10705a	MK575203	MK598735	France	Yurchenko et al. 2020a
Fasciodontia yunnanensis	CLZhao 6280	MK811275	MZ146327	China	Luo and Zhao 2021
Fibrodontia gossypina	AFTOL-ID 599	DQ249274	—	USA	Unpublished
Flaviporellus splitgerberi	JV 1908/6	MZ484525	MZ437386	French Guiana	Wu et al. 2022
Fomitiporella inermis	JV 0509/57K	KX181305	KX181346	USA	Ji et al. 2018
Fomitiporella subinermis	Dai 15114	KX181308	KX181344	China	Ji et al. 2018
Fomitiporella vietnamensis	Dai 18377*	NR_158436	NG_060441	Vietnam	Ji et al. 2018
Fomitiporia langloisii	MUCL 46375	EF429242	EF429225	USA	Decock et al. 2007
Fomitopsis pinicola	AFTOL 770	AY854083	AY684164	USA	Unpublisheded
Fulvifomes indicus	Yuan 5932	KC879261	JX866777	China	Wu et al. 2022
Fuscoporia ferruginosa	JV0408/28	KX961103	KY189103	China	Chen and Yuan 2017
Globulicium hiemale	Hjm 19007	DQ873595	DQ873595	Sweden	Larsson et al. 2006
Gyroflexus brevibasidiatus	IO.14.230	MT232351	MT232305	Sweden	Olariaga et al. 2020
Hastodontia halonata	HHB-17058	MK575207	MK598738	Mexico	Yurchenko et al. 2020a
Heterobasidion annosum	06129/6	KJ583211	KJ583225	China	Chen et al. 2014
Hirschioporus abietinus	Cui 2667	OQ449096	OQ449033	China	Cho et al. 2024
Hirschioporus abietinus	Dai 23760	OQ449039	OQ449034	China	Cho et al. 2024
Hirschioporus acontextus	Dai 19097	OQ449140	OQ449199	China	Cho et al. 2024
Hirschioporus acontextus	Dai 23793*	OQ449141	OQ449200	China	Cho et al. 2024
Hirschioporus beijingensis	Dai 18907	OQ449142	OQ449201	China	Cho et al. 2024
Hirschioporus beijingensis	Dai 23704*	OQ449143	OQ449202	China	Cho et al. 2024
Hirschioporus chinensis	Dai 20264	OQ449101	OQ449204	China	Cho et al. 2024
Hirschioporus chinensis	Dai 23048	OQ437349	OQ438002	China	Cho et al. 2024
Hirschioporus fuscoviolaceus	Dai 20988	OQ437357	OQ438006	Belarus	Cho et al. 2024
Hirschioporus fuscoviolaceus	Cui 10439	OQ437361	OQ438010	China	Cho et al. 2024
Hirschioporus fuscoviolaceus	KUC20131001-03	KJ668436	KJ668288	South Korea	Jang et al. 2015
Hirschioporus pubescens	Dai 17064*	OQ437377	OQ438019	China	Cho et al. 2024
Hirschioporus pubescens	Dai 23710	OQ512026	OQ449059	China	Cho et al. 2024
Hirschioporus tianschanicus	Dai 19067*	OQ448960	OQ449067	China	Cho et al. 2024

Species	Sample No.	GenBank No.		Country	References
		ITS	nLSU		
Hirschioporus tianschanicus	Dai 19064	OQ437386	OQ449066	China	Cho et al. 2024
Holtermanniella Wattica	CBS 9496*	NR138371	NG058307	Antarctica	Cao et al. 2021
Hydnoporia olivacea	Dai 12789	KT828678	KT828679	USA	Yang et al. 2016
Hydnoporia tabacina	LWZ 20210924-26a	ON063651	ON063851	China	Wang et al. 2023
Hydnum albomagnum	AFTOL-ID 471	DQ218305	AY700199	USA	Cao et al. 2021
Hydnum albomagnum	Wei 10194	MW980550	MW979536	China	Cao et al. 2021
Hydnum albomagnum	Wei 10247	MW980551	MW979537	China	Cao et al. 2021
Hydnum Berkeleyanum	CAL 1656*	NR158533	NG070500	India	Cao et al. 2021
Hydnum Berkeleyanum	HKAS77834	KU612525	KU612667	China	Cao et al. 2021
Hydnum berkeleyanum	Wei 10375	MW980552	MW979538	China	Cao et al. 2021
Hydnum brevispinum	Wei 10214*	MW980578	MW979559	China	Cao et al. 2021
Hydnum cremeoalbum	HKAS92345	KU612619	KU612676	China	Cao et al. 2021
Hydnum ellipsosporum	FD3281	KX086215	KX086217	Switzer	Cao et al. 2021
Hydnum flabellatum	Yuan 14708*	MW980575	MW979556	China	Cao et al. 2021
Hydnum flavidocanum	Yuan 13903a*	MW980559	MW979545	China	Cao et al. 2021
Hydnum flavidocanum	Yuan 13900a	MW980560	MW979546	China	Cao et al. 2021
Hydnum jussii	Yuan 14008	MW980553	MW979539	China	Cao et al. 2021
Hydnum jussii	Yuan 14009	MW980554	MW979540	China	Cao et al. 2021
Hydnum longibasidium	Wei 10383*	MW980556	MW979541	China	Cao et al. 2021
Hydnum longibasidium	Wei 10367	MW980555	MW979542	China	Cao et al. 2021
Hydnum magnorufescens	voucher 161209	KU612549	KU612669	China	Cao et al. 2021
Hydnum minum	N.K.Zeng2819	KY407533	KY407528	China	An et al. 2017
Hydnum minum	Wei 10252	MW980557	MW979543	China	Cao et al. 2021
Hydnum minum	Wei 10260	MW980558	MW979544	China	Cao et al. 2021
Hydnum Pallidocroceum	Yuan 14023*	MW980568	MW979554	China	Cao et al. 2021
Hydnum pallidocroceum	Yuan 14017	MW980569	MW979555	China	Cao et al. 2021
Hydnum pallidomarginatum	Yuan 13928a*	MW980566	MW979552	China	Cao et al. 2021
Hydnum pallidomarginatum	Yuan 13940a	MW980567	MW979553	China	Cao et al. 2021
Hydnum repandum	H 6003710*	KX388650	—	Finland	Dong et al. 2024b
Hydnum sphaericum	Wei 10243*	MW980563	MW979549	China	Cao et al. 2021
Hydnum subolympicum	F1188765	KU612599	KU612653	USA	Cao et al. 2021
Hydnum Subrufescens	F1188749	KU612535	KU612663	USA	Cao et al. 2021
Hydnum tangerinum	Wei 10245*	MW980580	MW979561	China	Cao et al. 2021
Hydnum tenuistipitum	Wei 10410*	MW980576	MW979557	China	Cao et al. 2021
Hydnum ventricosum	Yuan 14536*	MW980561	MW979547	China	Cao et al. 2021
Hymenochaete rubiginosa	He 1049	JQ716407	JQ279667	China	He and Li 2012
Hyphodontia abieticola	GEL2924	DQ340332	—	Germany	Unpublished
Hyphodontia abieticola	KHL 12498	DQ873601	—	Sweden	Unpublished
Hyphodontia alutaria	GEL3183	DQ340318	—	Germany	Zhang et al. 2024a
Hyphodontia alutaria	KHL 11889	DQ873603	—	Sweden	Unpublished
Hyphodontia alutaria	KHL 11978	EU118631	—	Norway	Unpublished
Hyphodontia argut	Wu 0806-44	JN571548	—	China	Unpublished
Hyphodontia arguta	KHL11938	EU118632	—	Sweden	Larsson 2007
Hyphodontia borbonica	FR-0219441*	KR349240	—	France	Unpublished
Hyphodontia borbonica	FR-0219444	KR349241	—	France	Unpublished
Hyphodontia curvispora	1591a	DQ873615	—	Finland	Unpublished
Hyphodontia hastata	GEL2143	DQ340323	—	Germany	Unpublished
Hyphodontia hastata	GEL3124	DQ340311	—	Germany	Unpublished
Hyphodontia mongolica	Cui 13240	KY290985	—	China	Unpublished
Hyphodontia mongolica	Cui 13239*	KY290984	—	China	Unpublished
Hyphodontia pachyspora	LWZ20180905-6	MT319425	—	China	Wang et al. 2021
Hyphodontia pachyspora	LWZ 20170908-5*	MT319426	MT319160	China	Wang et al. 2021
Hyphodontia pallidula	KAS-GEL2097	DQ340317	—	Germany	Zhang et al. 2024a
Hyphodontia sp.	LWZ20180511-2	MT319418	—	China	Wang et al. 2021
Hyphodontia sp.	LWZ20170814-15	MT319417	—	China	Wang et al. 2021

Species	Sample No.	GenBank No.		Country	References
		ITS	nLSU		
Hyphodontia subdetritica	TU114869	OP620786	–	France	Viner et al. 2023
Hyphodontia subdetritica	FR-0261087	KY081794	–	France	Unpublished
Hyphodontia subdetritica	FR-0261085	KY081793	–	France	Unpublished
Hyphodontia tropica	ICMP 13835	AF145586	–	China	Viner et al. 2023
Hyphodontia tropica	ICMP 13837	AF145587	–	China	Unpublished
Hyphodontia wongiae	LWZ20180417-16	MT319416	–	China	Wang et al. 2021
Hyphodontia wongiae	LWZ20180417-8	MT319415	–	China	Wang et al. 2021
Hyphodontia wongiae	LWZ20180414-16*	MT319414	–	China	Wang et al. 2021
Hyphodontia zhixiangii	LWZ 20170818-13	MT319420	MT319151	China	Wang et al. 2021
Hyphodontia zhixiangii	LWZ20180903-5	MT319423	–	China	Luo et al. 2022
Hyphodontia zhixiangii	LWZ20170820-31	MT319422	–	China	Wang et al. 2021
Hyphodontia zhixiangii	LWZ20170820-27	MT319421	–	China	Wang et al. 2021
Hyphodontia zhixiangii	LWZ20180903-9	MT319424	–	China	Wang et al. 2021
Hyphodontia zhixiangii	LWZ 20160909-8	KY440397	–	China	Wang et al. 2021
Hyphodontia zhixiangii	LWZ 20160909-4*	KY440396	–	China	Wang et al. 2021
Hyphodontia zhixiangii	LWZ 20160909-9	KY440398	–	China	Wang et al. 2021
Hyphodontia zhixiangii	LWZ20180904-12	MT319419	–	China	Wang et al. 2021
Inonotopsis subiculosa	Dai 14799	KU598212	KU598217	China	Unpublished
Inonotus andersonii	SFCC 50025	AY558599	AY558599	South Korea	Unpublished
Inonotus andersonii	JV 1209/66	KF446594	–	China	Unpublished
Inonotus andersonii	CS-65-92-14-B	OQ539568	–	Indiana	Unpublished
Inonotus boninensis	Dai 18868	MZ484601	–	Australia	Wu et al. 2022
Inonotus costaricensis	JV 1511/171J	MZ484602	–	USA	Wu et al. 2022
Inonotus cuticularis	JV 0609/22	MN318442	MN318442	Czech Republic	Wu et al. 2022
Inonotus dentiporus	MUCL 4227	MZ484608	–	Brazil	Wu et al. 2022
Inonotus griseus	LWZ 20130810-20*	KM434333	–	China	Zhou and Wang 2015
Inonotus henanensis	Dai 13157*	KP030783	KX832918	China	Zhou and Wang 2015
Inonotus henanensis	Dai 12220	MZ484603	–	China	Wu et al. 2022
Inonotus henanensis	Dai 13157	KX674581	–	China	Wu et al. 2022
Inonotus hispidus	Cui 11932	MZ484604	–	China	Wu et al. 2022
Inonotus hispidus	S45	EU282482	–	Spain	Wu et al. 2022
Inonotus krawtzewii	JV 8709/35	KF446598	–	China	Wu et al. 2022
Inonotus krawtzewii	PRM 607951	KF446600	–	China	Wu et al. 2022
Inonotus latemarginatus	Dai 9758*	KP030784	–	China	Zhou and Wang 2015
Inonotus micantissimus	URM90186	MG576057	–	Brazil	Wu et al. 2022
Inonotus nidus-pici	JV01076	MN318440	–	Czech Republic	Wu et al. 2022
Inonotus niveomarginatus	Dai 12318*	KC456245	–	China	Yu et al. 2013
Inonotus obliquus	JV 0408/36	KF446605	–	China	Wu et al. 2022
Inonotus obliquus	Dai 10715	MZ484606	–	Finland	Wu et al. 2022
Inonotus plorans	Yang 52	MZ484607	–	China	Wu et al. 2022
Inonotus portoricensis	JV 1504/121	MN318447	MN318447	Costa Rica	Unpublished
Inonotus pseudoglomeratus	JV1707/15J	MN318437	–	Costa Rica	Wu et al. 2022
Inonotus quercustris	193	AY072026	–	Argentina	Gottlieb et al. 2002
Inonotus radiatus	SAT-10-240-02	MT955156	MT955156	USA	Unpublished
Inonotus radiatus	HBAU15722	MW862276	–	China	Unpublished
Inonotus radiatus	HMAS 292289	OR237100	–	China	Unpublished
Inonotus radiatus	HMAS 281802	OR236984	–	China	Unpublished
Inonotus radiatus	MQ18R132-QFB30648	MN992228	–	Canada	Unpublished
Inonotus radiatus	DM1160	MT644872	–	Denmark	Unpublished
Inonotus radiatus	Cui 10321	KX364785	–	China	Unpublished
Inonotus rickii	Dai 12996	KC479128	–	China	Wu et al. 2022
Inonotus rickii	JV 1612/21J	MZ484609	–	China	Wu et al. 2022
Inonotus setulosocroceus	STE-U7801	KP279294	–	South Korea	Wu et al. 2022
Inonotus subglobisporum	**CLZhao 8331**	**PQ373985**	**–**	**China**	**Present study**
Inonotus subglobisporum	**CLZhao 8387**	**PQ373986**	**PQ373978**	**China**	**Present study**

Species	Sample No.	GenBank No.		Country	References
		ITS	nLSU		
Inonotus subglobisporum	**CLZhao 8433**	**PQ373987**	**PQ373979**	**China**	**Present study**
Inonotus subglobisporum	**CLZhao 8453**	**PQ373988**	**–**	**China**	**Present study**
Inonotus subglobisporum	**CLZhao 8500**	**PQ373989**	**PQ373980**	**China**	**Present study**
Inonotus subglobisporum	**CLZhao 8678**	**PQ373990**	**–**	**China**	**Present study**
Inonotus subglobisporum	**CLZhao 8737**	**PQ373991**	**–**	**China**	**Present study**
Inonotus subglobisporum	**CLZhao 8765***	**PQ373992**	**–**	**China**	**Present study**
Inonotus subglobisporum	**CLZhao 8789**	**PQ373993**	**–**	**China**	**Present study**
Inonotus subradiatus	Dai 20201*	MZ484610	–	China	Wu et al. 2022
Inonotus tenuicontextus	Yuan 5526*	NR_119969	–	China	Zhou and Qin 2011
Inonotus ulmicola	H 6012614	KF446606	–	China	Wu et al. 2022
Inonotus ungulatus	Dai 18864	MZ484611	–	Australia	Wu et al. 2022
Inonotus vieinamensis	Dai 18310	MZ484613	–	Viet Nam	Wu et al. 2022
Inonotus vieinamensis	Dai 18288*	MZ484612	–	Viet Nam	Zhou and Qin 2011
Inonotus vitis	OC 1*	MN108118	MN113944	USA	Brown et al .2019
Kneiffiella barba-jovis	KHL 11730	DQ873609	DQ873610	Sweden	Unpublished
Kneiffiella subglobosa	LWZ 20180416-6	MT319413	MT319145	China	Wang et al. 2021
Kneiffiella abdita	Miettinen 22165	ON188809	ON188809	Finland	Viner et al. 2024
Kneiffiella abieticola	KHL 12498 (GB)	DQ873601	–	Sweden	Larsson et al. 2006
Kneiffiella alienata	CBS 127219	MH864327	–	USA	Vu et al. 2018
Kneiffiella altaica	PRM 956491	OM971678	–	Czech Republic	Langer et al. 2022
Kneiffiella altaica	PRM 956489	OM971676	–	Czech Republic	Langer et al. 2022
Kneiffiella altaica	PRM 956490	OM971677	–	Czech Republic	Langer et al. 2022
Kneiffiella altaica	PRM 953309	OM971675	–	Czech Republic	Langer et al. 2022
Kneiffiella alutacea	KAS-GEL 2284	DQ340340	–	Germany	Yurchenko et al. 2020a
Kneiffiella alutacea	Miettinen 21701	ON188808	ON188808	Finland	Viner et al. 2024
Kneiffiella barba-jovis	KHL 11730	DQ873609	–	Sweden	Larsson et al. 2006
Kneiffiella bubalina	**CLZhao 15708***	**PQ373994**	**–**	**China**	**Present study**
Kneiffiella cineracea	KAS-GEL 4958	DQ340336	–	Germany	Yurchenko et al. 2020a
Kneiffiella curvispora	PRM 954540	MW345630	–	Slovakia	Běťák et al. 2021
Kneiffiella curvispora	Pennanen 4040	OP620787	OP620787	Finland	Viner et al. 2024
Kneiffiella decorticans	SP 415980	KY081795	–	Argentina	Riebesehl and Langer 2017
Kneiffiella efibulata	GB-0151167,	KY081796	–	Sweden	Riebesehl and Langer 2017
Kneiffiella eucalypticola	LWZ20180515-9	MT319411	–	Australia	Luo et al. 2022
Kneiffiella eucalypticola	LWZ 20180509-11*	MT319410	MT319142	China	Wang et al. 2021
Kneiffiella floccosa	UC 2022902	KP814441	–	USA	Rosenthal et al. 2017
Kneiffiella microspora	Miettinen 11418	OP620788	OP620788	Indonesia	Viner et al. 2024
Kneiffiella palmae	FR 7	KP689185	–	China	Wang et al. 2016
Kneiffiella palmae	KAS-GEL 3456	DQ340333	–	China	Yurchenko et al. 2020a
Kneiffiella pilaecystidiata	MSK-F 4723	MK575208	–	Belarus	Yurchenko et al. 2020a
Kneiffiella pilaecystidiata	Helo 1517	OP620789	OP620789	Finland	Viner et al. 2024
Kneiffiella pseudoabdita	LWZ 20210624-6b*	OQ540894	–	China	Liu et al. 2024
Kneiffiella pseudoalutacea	LWZ 20210625-5b*	OQ540895	–	China	Liu et al. 2024
Kneiffiella stereicola	Blackwell 2141*	KY081797	–	USA	Riebesehl and Langer 2017
Kneiffiella subaltaica	HHB-20039*	OM971679	–	USA	Langer et al. 2022
Kneiffiella subalutacea	KAS-GEL 2196	DQ340341	–	Norway	Yurchenko et al. 2020a
Kneiffiella subalutacea	KAS-GEL2196	DQ340341	–	Norway	Yurchenko et al. 2020a
Kneiffiella subefibulata	Dai 10803	KT989971	–	China	Chen et al. 2016
Kneiffiella subglobosa	Wu 890805-2	KY081798	–	Taiwan	Riebesehl and Langer 2017
Lawrynomyces capitatus	KHL 8464	DQ677491	DQ677491	Sweden	Cho et al. 2024
Leifia brevispora	LWZ 20170820-48	MK343470	MK343474	China	Liu et al. 2019
Leucophellinus hobsonii	Cui 6468	KT203288	KT203309	China	Cho et al. 2024
Leucophellinus irpicoides	Yuan 2690	KT203289	KT203310	China	Cho et al. 2024
Lyomyces allantosporus	FR 0249548*	KY800397	KY795963	Reunion	Yurchenko et al. 2017
Lyomyces bambusinus	CLZhao 4831*	MN945968	MW264919	China	Chen and Zhao 2020
Lyomyces fimbriatus	Wu 911204-4	MK575210	MK598740	China	Yurchenko et al. 2020a

Species	Sample No.	GenBank No.		Country	References
		ITS	nLSU		
Lyomyces mascarensis	KASGEL 4833*	KY800399	KY795964	Reunion	Yurchenko et al. 2020a
Lyomyces niveus	CLZhao 6431	MZ262541	MZ262526	China	Unpublished
Lyomyces niveus	CLZhao 6442	MZ262542	MZ262527	China	Unpublished
Lyomyces ochraceoalbus	CLZhao 4385	MZ262535	MZ262521	China	Unpublished
Lyomyces ochraceoalbus	CLZhao 4725	MZ262536	MZ262522	China	Unpublished
Lyomyces orientalis	LWZ 20170909-7	MT319436	MT319170	China	Luo et al. 2022
Lyomyces sambuci	KASJR 7	KY800402	KY795966	Germany	Yurchenko et al. 2017
Meganotus everhartii	JV 0108/30	MZ484529	MZ437388	USA	Unpublished
Minimedusa obcoronata	CBS 120605	GQ303278	GQ303309	Thailand	Cheewangkoon et al. 2009
Minimedusa polyspora	CBS 113.16*	MH854646	MH866167	USA	Cao et al. 2021
Multiclavula corynoides	Lutzoni 930804-2	U66440	U66440	USA	Cao et al. 2021
Multiclavula Mucida	TUB 011734	EU909345	EU909345	Germany	Cao et al. 2021
Multiclavula petricola	356 ex*	LC516464	LC516465	Japan	Cao et al. 2021
Multiclavula Vernalis	Lutzoni 930806-1	U66439	U66439	USA	Cao et al. 2021
Muscinupta laevis	V. Haikonen 19745	MF319066	MF318921	Finland	Cho et al. 2024
Neoburgoa freyi	LF1256*	KX423756	KX423756	Switzerland	Lawrey et al. 2016
Neoburgoa freyi	JL596-16	KX423754	KX423755	Switzerland	Lawrey et al. 2016
Neomensularia duplicata	LWZ 20150529-4	KX078217	KX078221	China	Wu et al. 2016
Neophellinus uncisetus	MUCL 47061	GU461972	GU462000	Argentina	Amalfi et al. 2010
Nigrohirschioporus durus	Dai 20642	OL470321	OL462835	China	Cho et al. 2024
Nigrohirschioporus durus	He 20120724-11	OQ448973	OQ449076	China	Cho et al. 2024
Nigrohirschioporus griseofuscus	B3942	OQ448975	OQ438022	Brazil	Cho et al. 2024
Nigrohirschioporus griseofuscus	JV 1909/ 6	OQ437343	OQ438024	French Guiana	Cho et al. 2024
Nigrohirschioporus sector	AS 2707	OQ437344	OQ438025	Brazil	Cho et al. 2024
Nigrohirschioporus trimiticus	B696*	OQ453308	OQ453535	Brazil	Cho et al. 2024
Nothophellinus andinopatagonicus	JV 1911/20	MZ484532	MZ437391	Chile	Wu et al. 2022
Oliveonia subfibrillosa	TH 2018074	MT235650	MT235618	Finland	Cao et al. 2021
Oliveonia subfibrillosa	TH 2018179	MT235649	MT235617	Finland	Cao et al. 2021
Oliveonia subfibrillosa	VS 9048	MT235647	MT235615	Russia	Cao et al. 2021
Oliveonia subfibrillosa	VS 9053	MT235645	MT235614	Russia	Cao et al. 2021
Onnia tomentosa	Dai 22935	OL473604	OL473617	China	Cho et al. 2024
Onnia tomentosa	Niemela 9079	MF319075	MF318931	Finland	Wu et al. 2022
Pachynotus punctatus	Dai 17803*	MZ484535	MZ437394	Singapore	Wu et al. 2022
Pallidohirschioporus biformis	Dai 12746	OQ453311	OQ453538	USA	Cho et al. 2024
Pallidohirschioporus biformis	Dai 19466	OQ453223	OQ453548	China	Cho et al. 2024
Pallidohirschioporus brastagii	Dai 22919	OQ453371	OQ453297	China	Cho et al. 2024
Pallidohirschioporus polycystidiatus	Dai 19100	OQ453378	OQ453301	China	Cho et al. 2024
Pallidohirschioporus versicolor	Dai 19331	OQ453386	OQ474951	China	Cho et al. 2024
Peniophorella aspersa	CLZhao 17063	OM985730	OM985771	China	Cho et al. 2024
Peniophorella aspersa	F24809*	NR_172775	NG_073750	China	Yurchenko et al. 2020b
Peniophorella crystallifera	F23666*	NR_171802	NG_073751	China	Yurchenko et al. 2020b
Peniophorella crystallifera	LWZ 20210626-4a	ON063685	ON063885	China	Wang et al. 2023
Peniophorella fissurata	CLZhao 9421*	NR177497	NG154027	China	Guan et al. 2020
Peniophorella odontiiformis	CLZhao 9862	MT247004	OM985779	China	Cho et al. 2024
Peniophorella odontiiformis	SFC20150108-37	OQ996168	OQ996199	South Korea	Cho et al. 2024
Peniophorella pallida	CLZhao 3017	OM985738	OM985780	China	Cho et al. 2024
Peniophorella praetermissa	AFTOL-ID 518	AY854081	AY700185	USA	Cho et al. 2024
Peniophorella praetermissa	LWZ 20180903-14	ON063686	ON063886	China	Wang et al. 2023
Peniophorella pubera	LWZ 20210624-16b	ON063687	ON063887	China	Wang et al. 2023
Peniophorella reticulata	F22559*	NR172776	NG073752	China	Yurchenko et al. 2020b
Peniophorella rude	F30649	MN062105	MN062153	China	Yurchenko et al. 2020b
Peniophorella rude	LWZ 20171026-7	ON063688	ON063888	China	Wang et al. 2023
Peniophorella subpraetermissa	LWZ 20190816-3b	ON063689	ON063889	China	Wang et al. 2023
Perennihirschioporus variabilis	B856	OQ474942	OQ474957	Brazil	Cho et al. 2024
Perenninotus shoreicola	Dai 13614	KJ575522	KT749416	Thailand	Wu et al. 2022

Species	Sample No.	GenBank No.		Country	References
		ITS	nLSU		
Phellinidium ferrugineofuscum	Cui 10042	KC782527	KC782529	China	Wu et al. 2022
Phellinopsis conchata	L-7601	KU139188	KU139257	USA	Brazee 2015
phylloporia gabonensis	MUCL 55571	NR_154331	NG_059641	Gabon	Unpublished
phylloporia nodostipitata	FLOR 51173*	KJ639055	KJ631412	Brazil	Wu et al. 2022
phylloporia perangusta	Dai 18139	MH151169	MG738803	China	Wu et al. 2022
Porodaedalea pini	No-6170-T	JX110037	JX110081	Porrugal	Brazee and Lindner 2013
Pseudoinonotus dryadeus	JV 1907/7	MZ484540	MZ437400	Czechia	Wu et al. 2022
Pyrrhoderma adamantinum	Dai 13832	MF860790	MF860736	China	Wu et al. 2022
Resinicium austroasianum	LWZ 20180417-5*	NR173962	NG088188	China	Yu et al. 2021
Resinicium austroasianum	LWZ 20191208-11	ON063691	ON063891	China	Wang et al. 2023
Resinicium bicolor	AFTOL-810	DQ218310	AF393061	USA	Cho et al. 2024
Resinicium lateastrocystidium	LWZ 20180414-15*	NR173963	MW414455	China	Yu et al. 2021
Resinicium lateastrocystidium	LWZ 20180416-10	MW414510	MW414456	China	Yu et al. 2021
Resinicium monticola	FP-150360*	NR_111226	DQ863697	Jamaica	Cho et al. 2024
Resinicium mutabile	FP-102989*	NR_119612	DQ863699	Puerto Rico	Cho et al. 2024
Resinicium rimulosum	KUC20131022-12	KJ668464	KJ668315	South Korea	Jang et al. 2016
Rhizoctonia solani	BRS17	MK481078	MN078809	India	Cao et al. 2021
Rickenella fibula	HBK013	MF319081	MF318941	USA	Cho et al. 2024
Rickenella fibula	SFC20230704-06	OR758634	OR758646	South Korea	Cho et al. 2024
Rickenella fibula	RAS051	MF319094	MF318972	USA	Cho et al. 2024
Rickenella fibula	HBK016	MF319084	MF318944	USA	Cho et al. 2024
Rickenella fibula	HBK014	MF319082	MF318942	USA	Cho et al. 2024
Rickenella indica	SFC20140626-39	OQ996172	OQ996203	South Korea	Cho et al. 2024
Rickenella mellea	CBS 579.87	MH862106	MH873795	France	Vu et al. 2018
Rickenella mellea	CBS 581.87	MH862107	MH873796	France	Vu et al. 2018
Rickenella minuta	MES1950	MF319097	MF318964	Argentina	Cho et al. 2024
Rickenella minuta	MES1892	MF318966	MF288881	Argentina	Cho et al. 2024
Rickenella minuta	MES1965	MF319105	MF318963	Argentina	Cho et al. 2024
Rickenella umbelliformis	SFC20150701-65*	OQ996173	OQ996204	South Korea	Cho et al. 2024
Rickenella umbelliformis	SFC20160713-77	OQ996175	OQ996205	South Korea	Cho et al. 2024
Rickenella umbelliformis	SFC20180704-81	OQ996176	OQ996206	South Korea	Cho et al. 2024
Rigidoporus corticola	KUC20130718-79	KJ668502	KJ668354	South Korea	Jang et al. 2016
Rigidoporus corticola	LWZ 20190819-3b	ON063673	ON063872	China	Wang et al. 2023
Rigidoporus corticola	SFC20230816-48	OR758635	OR758647	South Korea	Cho et al. 2024
Rigidoporus cuneatus	Cui 10855	OQ930254	OQ924530	South Korea	Cho et al. 2024
Rigidoporus cuneatus	Dai 7339	KT203294	KT203315	China	Cho et al. 2024
Rigidoporus ginkgonis	Cui 5555	KT203295	KT203316	China	Cho et al. 2024
Rigidoporus ginkgonis	SFC20230630-23	OR758636	OR758648	South Korea	Cho et al. 2024
Rigidoporus juniperinus	YG 1070	MK433641	MK433643	Uzbekistan	Cho et al. 2024
Rigidoporus juniperinus	Dai 17100	OQ930261	OQ924537	Uzbekistan	Cho et al. 2024
Rogersiomyces malaysianus	LE-BIN 3507-10	KT779285	KU820986	Vietnam	Cao et al. 2021
Sanghuangporus weigelae	LWZ 20210623-2a	ON063671	ON063870	China	Wang et al. 2023
Sanghuangporus zonatus	Dai 10841	OP962417	KP030775	China	Wu et al. 2022
Schizocorticium lenis	LWZ 20180921-7*	MW414521	MW414467	China	Yu et al. 2021
Schizocorticium magnosporum	Wu 1510-34*	MK405351	MK405337	China	Wang and Zhou 2024
Schizocorticium mediosporum	Chen 2456*	MK405359	MK405345	China	Wang and Zhou 2024
Schizocorticium parvosporum	GC 1508-127*	MK405361	MK405347	China	Wang and Zhou 2024
Sidera minutipora	Cui 16720	MN621349	MN621348	Australia	Wang and Zhou 2024
Sidera minutissima	Dai 19529	MN621352	MN621350	Sri Lanka	Du et al. 2020
Sidera parallela	Dai 22038	MW477793	MW474964	China	Cho et al. 2024
Sidera srilankensis	Dai 19654*	NR_172780	NG_075310	Sri Lanka	Cho et al. 2024
Sidera tenuis	Dai 18697*	NR_171833	NG_075283	Singapore	Cho et al. 2024
Sidera tibetica	SFC20230317-17	OQ996177	OQ996207	South Korea	Cho et al. 2024
Sidera tibetica	Dai 23648*	NR_177641	OM974245	China	Liu et al. 2022
Sidera vesiculosa	BJFC 025377*	NR164588	NG066418	Singapore	Cho et al. 2024

Species	Sample No.	GenBank No.		Country	References
		ITS	nLSU		
Sidera vulgaris	Dai 21057	MW198484	MW192009	Singapore	Liu et al. 2021
Sistotrema confluens	FCUG298	DQ267125	AY647214	USA	Cao et al. 2021
Sistotrema confluens	PV174	AY463466	AY586712	Czechia	Larsson et al. 2004
Sistotrema subconfluens	Dai 12577	JX076812	JX076810	China	Zhou and Qin 2013
Sistotremella perpusilla	CBS 126048	MH864061	MH875516	USA	Cao et al. 2021
Skvortzovia dabieshanensis	LWZ 20201012-22*	NR_173964	NG_088189	China	Yu et al. 2021
Skvortzovia dabieshanensis	LWZ 20210918-15b	ON063694	ON063894	China	Yu et al. 2021
Skvortzovia pinicola	LWZ 20210623-18b	ON063695	ON063895	China	Wang et al. 2023
Skvortzovia qilianensis	LWZ 20180904-16*	NR173965	NG088190	China	Yu et al. 2021
Skvortzovia qilianensis	LWZ 20180904–20	MW414520	MW414466	China	Yu et al. 2021
Skvortzovia yunnanensis	CLZhao 16084	MW472754	MW473473	China	Dong et al. 2021
Trichaptum byssogenum	Dai 15555	OQ449085	OQ449026	China	Cho et al. 2024
Trichaptum perrottetii	JV 1908/ 45	OQ449092	OQ449031	French Guiana	Cho et al. 2024
Trichosporon insectorum	CBS 10422*	KF036603	KY109953	Panama	Cao et al. 2021
Tubulicrinis accedens	MICH:352299	OL756001	OL742444	USA	Cho et al. 2024
Tubulicrinis calothrix	LWZ 20210919-1b	ON063704	ON063904	China	Wang et al. 2023
Tubulicrinis glebulosus	LWZ 20180903-13	ON063705	ON063905	China	Wang et al. 2023
Tubulicrinis subulatus	LWZ 20190914-7	ON063706	ON063906	China	Wang et al. 2023
Tubulicrinis xantha	CLZhao 2869	MT153875	MT153882	China	He et al. 2020
Tulasnella asymmetrica	AFTOL-ID 1678	DQ520101	DQ520101	Germany	Cao et al. 2021
Tulasnella irregularis	CBS 574.83	NR160166	NG057720	Australia	Cao et al. 2021
Tulasnella pruinosa	DAOM 17641	DQ457642	AF518662	USA	Cao et al. 2021
Tulasnella violea	AFTOL-ID 1879	DQ520097	DQ520097	Germany	Cao et al. 2021
Xylodon acuminatus	Larsson 16029	ON197552	–	Brazil	Viner et al. 2023
Xylodon acystidiatus	LWZ 20180514-9*	MT319474	MT319211	Australia	Luo et al. 2022
Xylodon afromontanus	H 7006811*	OQ645463	–	Rwanda	Yurchenko et al. 2024
Xylodon angustisporus	Ryvarden 50691b*	OK273831	–	Cameroon	Viner et al. 2021
Xylodon apacheriensis	Wu 0910-58	KX857797	KX857822	China	Chen et al. 2017
Xylodon apacheriensis	Canfield 180	KY081800	–	USA	Wang et al. 2021
Xylodon asiaticus	CLZhao 2282	OM959481	OM967416	China	Zhang et al. 2024a
Xylodon asiaticus	CLZhao 10368*	OM959479	OM967417	China	Zhang et al. 2024a
Xylodon asiaticus	CLZhao 10430	OM959480	OM967418	China	Zhang et al. 2024a
Xylodon asiaticus	CLZhao 2282	OM959481	OM967416	China	Zhang et al. 2024a
Xylodon asperus	Spirin 11923	OK273838	–	Russia	Viner et al. 2021
Xylodon astrocystidiatus	TNM F24764	NR154054	–	China	Yurchenko and Wu 2014
Xylodon astrocystidiatus	Wu 9211-71*	JN129972	JN129973	China	Yurchenko and Wu 2014
Xylodon attenuatus	Spirin 8775*	MH324476	–	America	Wang et al. 2021
Xylodon australis	LWZ 20180509-8	MT319503	–	China	Wang et al. 2021
Xylodon bambusinus	CLZhao 11310*	MW394660	–	China	Ma and Zhao 2021
Xylodon bambusinus	CLZhao 9174	MW394657	MW394650	China	Ma and Zhao 2021
Xylodon bambusinus	CLZhao 9174	MW394657	MW394650	China	Ma and Zhao 2021
Xylodon borealis	JS 26064	AY463429	–	Norway	Larsson et al. 2004
Xylodon brevisetus	JS 17863	AY463428	–	Norway	Larsson et al. 2004
Xylodon crystalliger	LWZ 20170816-33	MT319521	MT319269	China	Luo et al. 2022
Xylodon crystalliger	KUN 2312*	NR166242	–	China	Viner et al. 2018
Xylodon cymosus	Miettinen 19606*	ON197554	–	USA	Viner et al. 2023
Xylodon cystidiatus	FR 0249200	MH880195	MH884896	France	Riebesehl et al. 2019
Xylodon damansaraensis	LWZ 20180417-23	MT319499	–	Malaysia	Wang et al. 2021
Xylodon daweishanense	CLZhao 18357	OP730715	–	China	Guan et al. 2023
Xylodon daweishanense	CLZhao 18492	OP730719	–	China	Guan et al. 2023
Xylodon detriticus	Zíbarová 30.10.17	MH320793	–	Czech Republic	Wang et al. 2021
Xylodon dissiliens	Ryvarden 44817*	OK273856	–	Uganda	Viner et al. 2021
Xylodon echinatus	OM 18237	OQ645464	–	Indonesia	Yurchenko et al. 2024
Xylodon exilis	TUB-FO42565*	MH880198	MH884898	China	Riebesehl et al. 2019
Xylodon filicinus	MSKF 12869*	MH880199	NG067836	China	Riebesehl et al. 2019

Species	Sample No.	GenBank No.		Country	References
		ITS	nLSU		
Xylodon fissuratus	CLZhao 9407*	OP730714	–	China	Guan et al. 2023
Xylodon flaviporus	FR-0249797	MH880201	MH884901	Reunion	Riebesehl et al. 2019
Xylodon flocculosus	CLZhao 18342*	MW980776	–	China	Qu and Zhao 2022
Xylodon follis	FR-0249814*	MH880204	MH884902	Reunion	Riebesehl et al. 2019
Xylodon gloeocystidiifer	BLS M-5232*	OQ645467	–	Ecuador	Yurchenko et al. 2024
Xylodon gloeocystidiifer	EYu 190720-11	OR240822	–	Ecuador	Unpublished
Xylodon gossypinus	CLZhao 4465	MZ663803	MZ663812	China	Luo et al. 2021
Xylodon gossypinus	CLZhao 8375*	MZ663804	–	China	Luo et al. 2021
Xylodon gossypinus	CLZhao 4465	MZ663803	MZ663812	China	Luo et al. 2021
Xylodon grandineus	CLZhao 6425	OM338090	–	China	Luo et al. 2022
Xylodon granulanoides	**CLZhao 17253***	**PQ373995**	**PQ373981**	**China**	**Present study**
Xylodon granulans	**CLZhao 17804**	**PQ373996**	**–**	**China**	**Present study**
Xylodon granulans	**CLZhao 17866***	**PQ373997**	**PQ373982**	**China**	**Present study**
Xylodon hastifer	K(M) 172400*	NR166558	–	America	Riebesehl and Langer 2017
Xylodon heterocystidiatus	LWZ20180921-19	MT319676	MT319266	Australia	Zhang et al 2024a
Xylodon heterocystidiatus	Wei 17-314	MT731753	MT731754	China	Zhang et al. 2024a
Xylodon hjortstamii	Gorjon 3187	ON188816	–	Chile	Yuan and Zhao 2024
Xylodon hyphodontinus	KAS-GEL9222	MH880205	–	Kenya	Riebesehl et al. 2019
Xylodon jacobaeus	MA-Fungi 91340*	MH430073	–	Spain	Wang et al. 2021
Xylodon kunmingensis	TUB-FO 42565	MH880198	–	China	Wang et al. 2021
Xylodon laceratus	CLZhao 9892*	OL619258	OL619266	China	Qu et al. 2022
Xylodon lagenicystidiatus	LWZ 20180513-16*	MT319634	MT319368	Australia	Luo et al. 2022
Xylodon lanatus	CFMR FP-101864-A*	OQ645474	–	USA	Yurchenko et al. 2024
Xylodon lenis	Wu 890714-3	KY081802	–	China	Riebesehl et al. 2019
Xylodon macrosporus	CLZhao 10226*	MZ663809	MZ663817	China	Luo et al. 2021
Xylodon magallanesii	MA: Fungi:90397*	MT158729	–	Chile	Fernandez-Lopez et al. 2020
Xylodon mantiqueirensis	MV 529	OQ645478	–	Brazil	Yurchenko et al. 2024
Xylodon mollissimus	LWZ 20160318-3*	KY007517	MT319347	China	Luo et al. 2022
Xylodon montanus	CLZhao 8179*	OL619260	OL619268	China	Qu et al. 2022
Xylodon muchuanensis	LWZ 20200819-3a	OQ540903	–	China	Unpublished
Xylodon muchuanensis	LWZ 20200819-2b*	OQ540902	–	China	Unpublished
Xylodon neotropicus	MV 580	OQ645479	–	Brazil	Yurchenko et al. 2024
Xylodon nesporii	LWZ 20180921-35	MT319655	MT319238	China	Luo et al. 2022
Xylodon niemelaei	LWZ 20150707-13	MT319630	MT319365	China	Luo et al. 2022
Xylodon nongravis	GC 1412-22*	KX857801	KX857818	China	Chen et al. 2017
Xylodon nothofagi	ICMP 13842	AF145583	–	China	Wang et al. 2021
Xylodon ovisporus	LWZ 20170815-31	MT319666	MT319346	China	Luo et al. 2022
Xylodon papillosus	CBS 114.71	MH860026	–	Netherlands	Vu et al. 2018
Xylodon paradoxus	Dai 14983	MT319519	MT319267	China	Luo et al. 2022
Xylodon patagonicus	ICMP 13832	AF145581	–	Argentina	Wang et al. 2021
Xylodon pruinosus	Spirin 2877	MH332700	–	Estonia	Wang et al. 2021
Xylodon pruniaceus	Ryvarden 11251	OK273828	–	Malawi	Viner et al. 2021
Xylodon pseudolanatus	FP 150922*	MH880220	NG067837	Belize	Riebesehl et al. 2019
Xylodon pseudotropicus	Dai 16167	MT319509	MT319255	China	Luo et al. 2022
Xylodon pseudotropicus	Dai 10768*	KF917543	–	China	Wang et al. 2021
Xylodon pseudotropicus	Dai 16167	MT319509	MT319255	China	Luo et al. 2022
Xylodon puerensis	CLZhao 8142*	OP730720	–	China	Guan et al. 2023
Xylodon punctus	CLZhao 17691*	OM338092	–	China	Luo et al. 2022
Xylodon punctus	CLZhao 17908	OM338093	–	China	Luo et al. 2022
Xylodon quercinus	Otto Miettinen 15050,1	KT361632	–	Finland	Ariyawansa et al. 2015
Xylodon quercinus	Spirin 12030	OK273841	–	Russia	Viner et al. 2021
Xylodon quercinus	Otto Miettinen 15050,1	KT361632	–	Finland	Ariyawansa et al. 2015
Xylodon quercinus	KHL 11076	KT361633	AY586678	Sweden	Larsson et al. 2004
Xylodon quercinus	KHL 11076	KT361633	AY586678	Sweden	Larsson et al. 2004
Xylodon raduloides	FCUG 2433	AF145570	–	Russia	Wang et al. 2021

Species	Sample No.	GenBank No.		Country	References
		ITS	nLSU		
Xylodon ramicida	Spirin 7664*	NR138013	–	America	Yuan and Zhao 2024
Xylodon reticulatus	Wu 1109-178	KX857805	–	China	Wang et al. 2021
Xylodon reticulatus	GC 1512-1	KX857808	–	China	Wang et al. 2021
Xylodon rhizomorphus	Dai 12367*	NR154067	–	China	Wang et al. 2021
Xylodon rhododendricola	LWZ 20180513-9	MT319621	MT319357	Australia	Luo et al. 2022
Xylodon rimosissimus	Ryberg 021031	DQ873627	DQ873628	Sweden	Larsson et al. 2006
Xylodon serpentiformis	LWZ 20170816-15	MT319673	MT319218	China	Luo et al. 2022
Xylodon sinensis	CLZhao 9197	MZ663810	MZ663818	China	Luo et al. 2021
Xylodon sinensis	CLZhao 11120*	OK560885	–	China	Luo et al. 2021
Xylodon spathulatus	LWZ 20180804-10	MT319646	MT319354	China	Luo et al. 2022
Xylodon subclavatus	FO 42167	MH880232	–	China	Wang et al. 2021
Xylodon subflaviporus	Wu 0809-76	KX857803	KX857815	China	Chen et al. 2017
Xylodon subflaviporus	TNM F29958*	NR184880	–	China	Chen et al. 2017
Xylodon subpunctus	CLZhao 6165	PP537958	–	China	Unpublished
Xylodon subpunctus	CLZhao 31242*	PP537957	–	China	Unpublished
Xylodon subserpentiformis	LWZ 20180512-16	MT319486	MT319226	Australia	Luo et al. 2022
Xylodon subtilissimus	Spirin 12228	ON188818	–	Russia	Yuan and Zhao 2024
Xylodon subtropicus	LWZ 20180510-24	MT319541	MT319308	China	Luo et al. 2022
Xylodon taiwanianus	CBS 125875	MH864080	MH875537	New Zealand	Vu et al. 2018
Xylodon tropicus	CLZhao 3351*	OL619261	OL619269	China	Qu et al. 2022
Xylodon ussuriensis	KUN 1989*	NR166241	–	America	Yuan and Zhao 2024
Xylodon verecundus	KHL 12261	DQ873642	DQ873643	Sweden	Larsson et al. 2006
Xylodon victoriensis	LWZ 20180510-29	MT319487	MT319228	Australia	Luo et al. 2022
Xylodon wenshanensis	CLZhao 15729*	OM338097	–	China	Luo et al. 2022
Xylodon wenshanensis	CLZhao 10790	OM338095	–	China	Luo et al. 2022
Xylodon wenshanensis	CLZhao 15782	OM338098	–	China	Luo et al. 2022
Xylodon wenshanensis	CLZhao 15718	OM338096	–	China	Luo et al. 2022
Xylodon xinpingensis	CLZhao 11224	MW394662	MW394654	China	Ma and Zhao 2021
Xylodon xinpingensis	CLZhao 9174*	MW394657	–	China	Ma and Zhao 2021
Xylodon yarraensis	LWZ 20180510-5	MT319639	MT319378	Australia	Luo et al. 2022
Xylodon yunnanensis	LWZ 20180922-47	MT319660	–	China	Wang et al. 2021

settings, and statistical support values were obtained using nonparametric bootstrapping with 1,000 replicates. Bayesian inference (BI) analysis based on the dataset was performed using MrBayes v.3.2.6 (Ronquist and Huelsenbeck 2003). The best substitution model for the dataset was selected by ModelFinder using a Bayesian information criterion, and the model was used for Bayesian analysis (Kalyaanamoorthy et al. 2017). Four Markov chains were run from random starting trees. Trees were sampled every 1.00th generation. The first 25% of sampled trees were discarded as burn-in, whereas other trees were used to construct a 50% majority consensus tree and for calculating Bayesian posterior probabilities (BPPs).

The branches of the consensus tree that received bootstrap support for ML were greater than or equal to 70%, and Bayesian posterior probabilities were greater than or equal to 0.95, respectively.

Results

BI analysis yielded a similar topology to MP and ML analysis; thus, the MP tree is provided (Figs 1–6). Branches that received bootstrap support for ML (ML-BS) and BI (BPP) greater than or equal to 70% (MP-BS and ML-BS) and 0.95 (BPP) were considered as significantly supported, respectively.

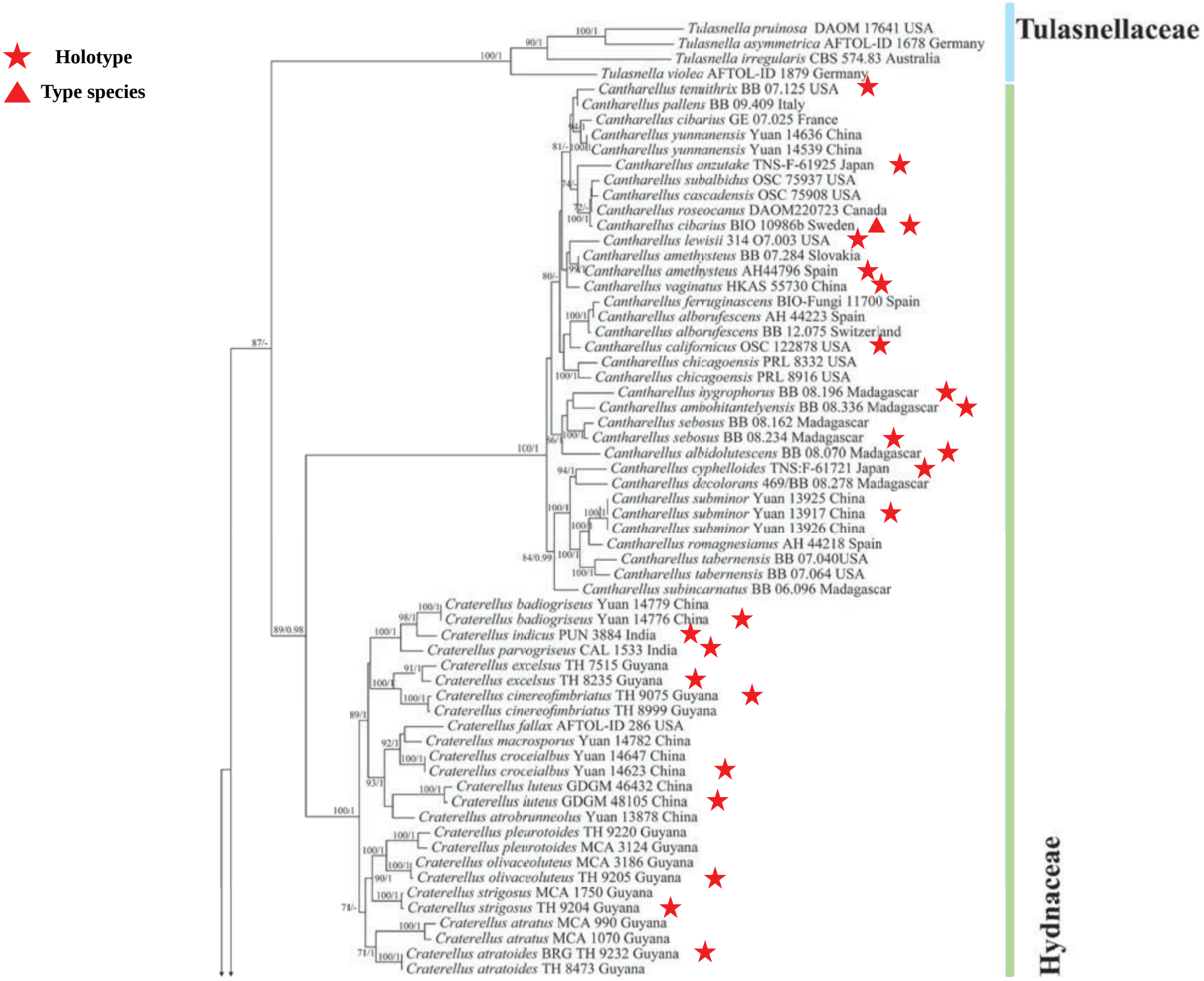

Figure 1. Phylogeny of species in Cantharellales generated by maximum likelihood based on ITS+nLSU sequence data. Branches are labeled with maximum likelihood bootstrap ≥ 70% and Bayesian posterior probabilities ≥ 0.95, respectively.

The phylogeny of Cantharellales

The ITS and nLSU dataset contained sequences from 135 fungal specimens representing 97 Cantharellales taxa. The average SD of split frequencies in BI analyses is 0.013339 (BI), and the effective sample size (ESS) for Bayesian analysis across the two runs is double the average ESS (avg ESS) = 725. The phylogenetic tree (Fig. 1) reveals that the Cantharellales new species were grouped into the genus *Botryobasidium* (Botryobasidiaceae).

The phylogeny of *Botryobasidium*

The ITS dataset contained sequences from 39 fungal specimens representing 22 *Botryobasidium* taxa. The average SD of split frequencies in BI analyses is 0.006652 (BI), and the effective sample size (ESS) for Bayesian analysis across the two runs is double the average ESS (avg ESS) = 1700.5. The phylogenetic tree (Fig. 2) reveals that the new species groups with three taxa, *Botryobasidium intertextum* (Schwein.) Jülich & Stalper, *B. leptocystidiatum* L.J. Zhou & H.S. Yuan, and *B. subcoronatum*.

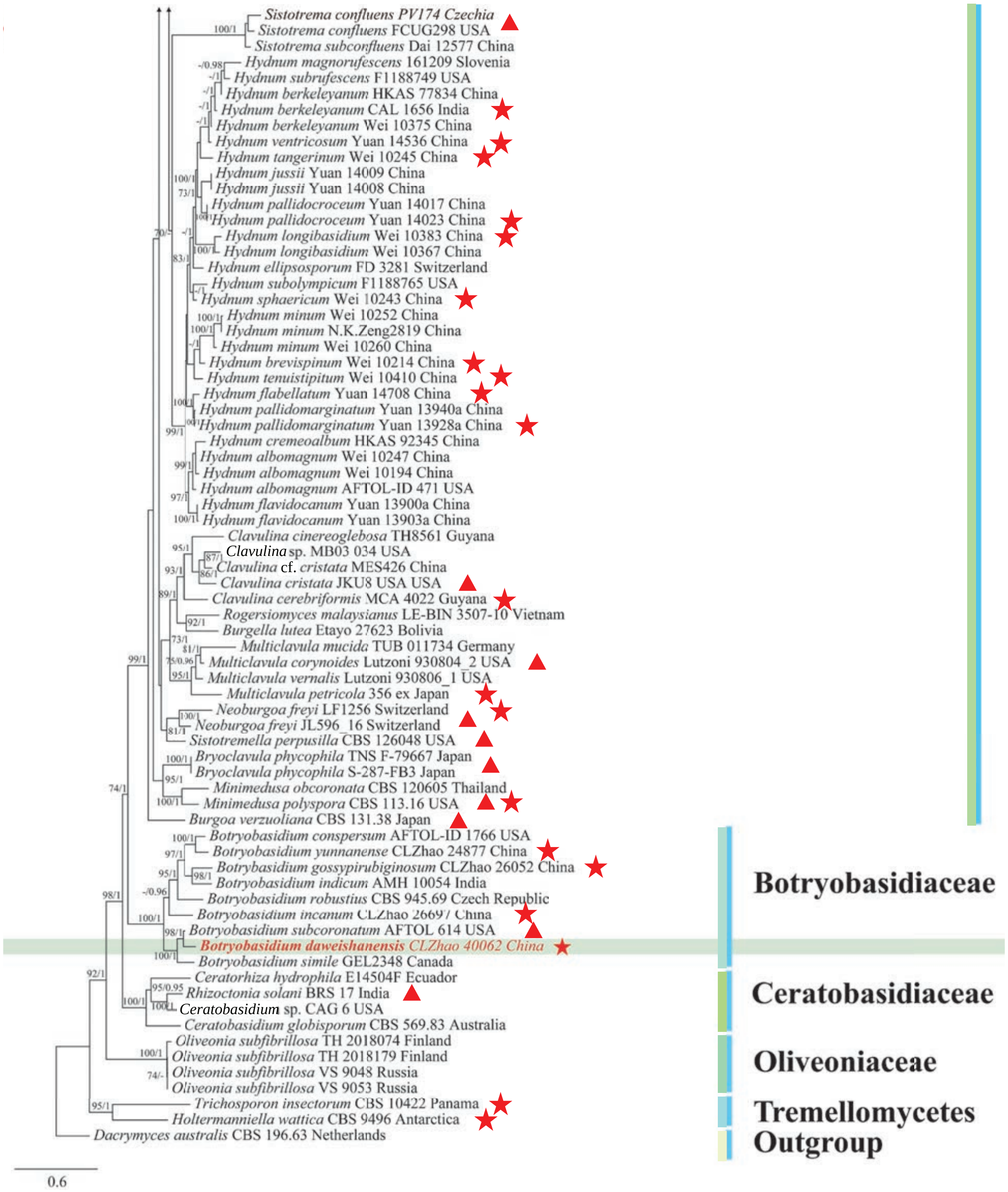

Figure 1. Continued.

The phylogeny of Hymenochaetales

The ITS dataset contained sequences from 239 fungal specimens representing 196 Hymenochaetales taxa. The average SD of split frequencies in BI analyses is 0.013469 (BI), and the effective sample size (ESS) for Bayesian analysis across the two runs is double the average ESS (avg ESS) = 671.5. The phylogenetic tree (Fig. 3) reveals the four new Hymenochaetales species grouped into Hymenochaetaceae, Hyphodontiaceae, and Schizoporaceae.

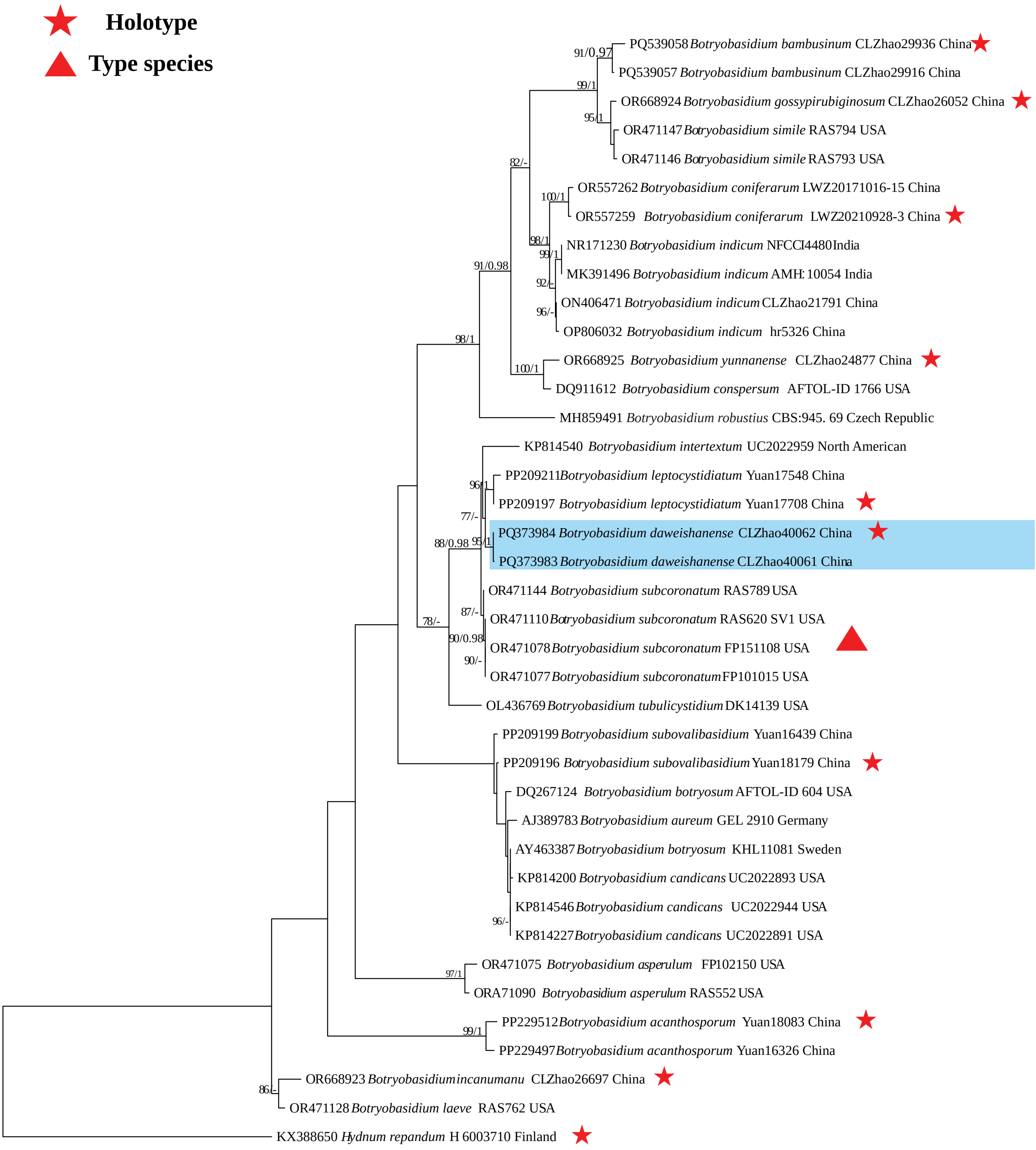

Figure 2. Phylogeny of species in *Botryobasidium* generated by maximum likelihood based on ITS sequence data. Branches are labeled with maximum likelihood bootstrap ≥ 70% and Bayesian posterior probabilities ≥ 0.95, respectively.

The phylogeny of *Inonotus*

The ITS dataset contained sequences from 49 fungal specimens representing 26 *Inonotus* taxa. The average SD of split frequencies in BI analyses is 0.004227 (BI), and the effective sample size (ESS) for Bayesian analysis across the two runs is double the average ESS (avg ESS) = 2018.5. The phylogenetic tree (Fig. 4) reveals that the new species is closely related to *Inonotus radiatus* (Sowerby) P. Karst.

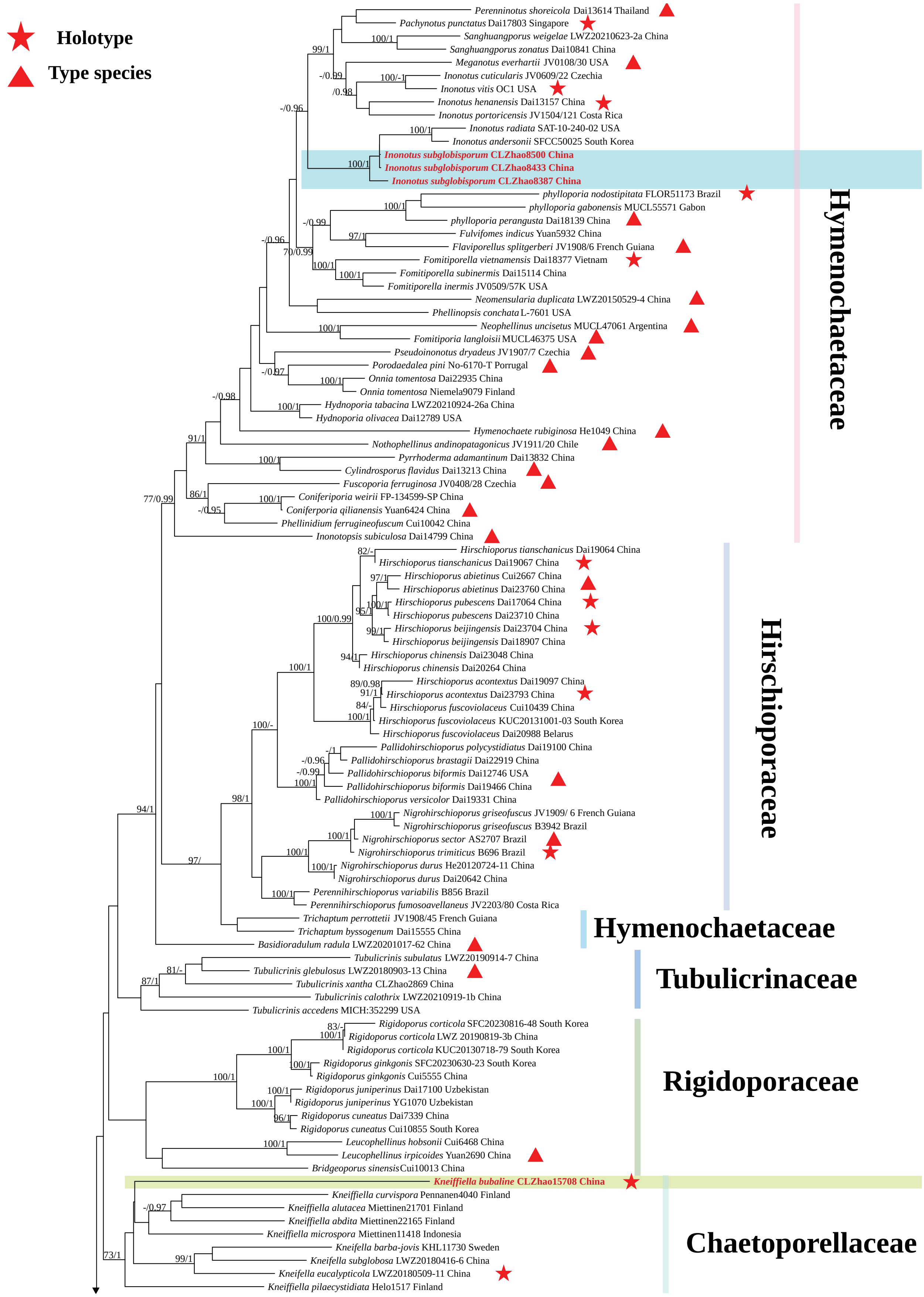

Figure 3. Phylogeny of species in Hymenochaetales generated by maximum likelihood based on ITS+nLSU sequence data. Branches are labeled with maximum likelihood bootstrap ≥ 70% and Bayesian posterior probabilities ≥ 0.95, respectively.

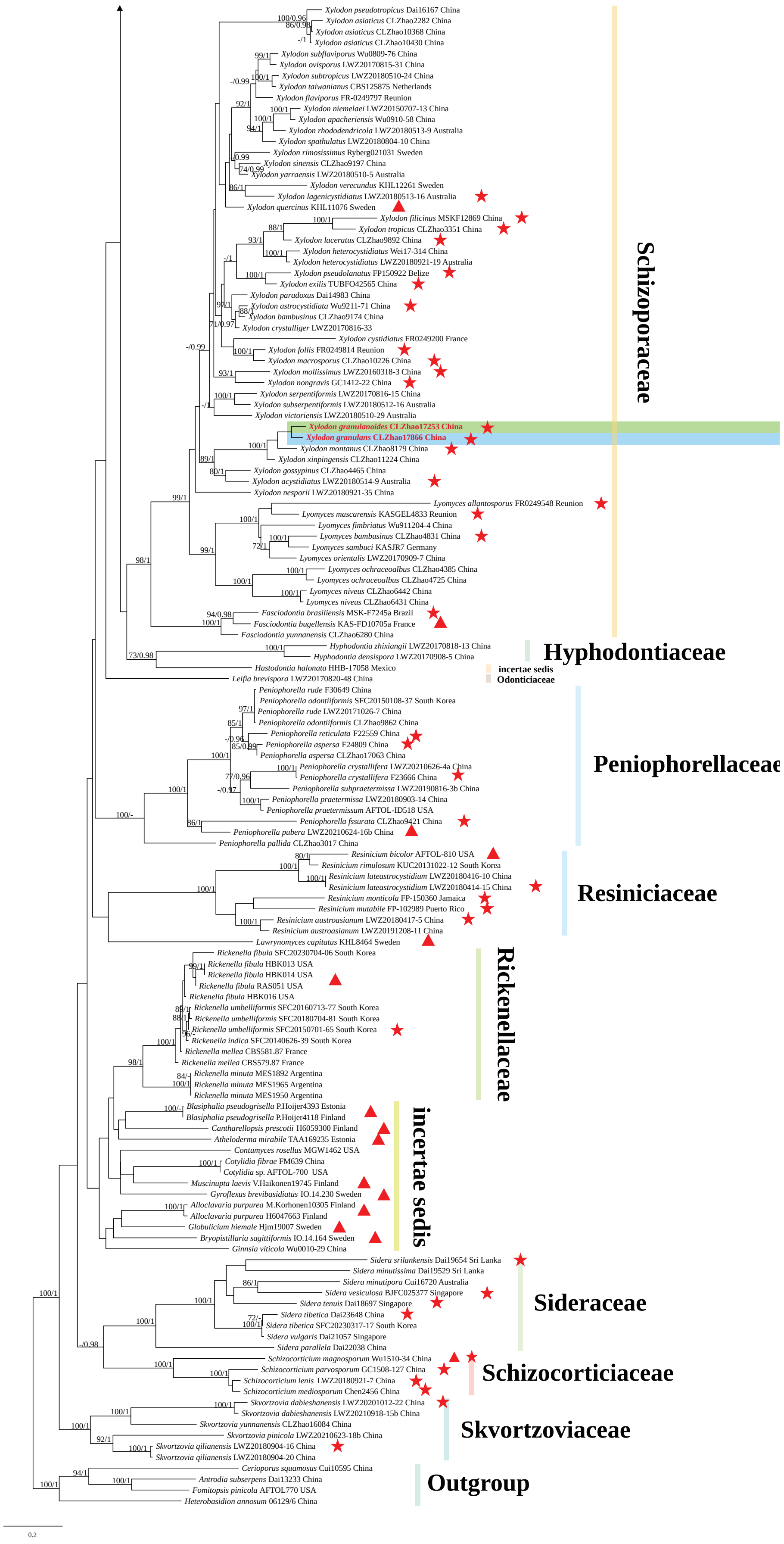

Figure 3. Continued.

Figure 4. Phylogeny of species in *Inonotus* generated by maximum likelihood based on ITS sequence data. Branches are labeled with maximum likelihood bootstrap ≥ 70% and Bayesian posterior probabilities ≥ 0.95, respectively.

The phylogeny of *Kneiffiella*

The ITS dataset contained sequences from 26 fungal specimens representing 21 *Kneiffiella* taxa. The average SD of split frequencies in BI analyses is 0.007515 (BI), and the effective sample size (ESS) for Bayesian analysis across the two runs is double the average ESS (avg ESS) = 4107.5. The phylogenetic tree (Fig. 5) reveals that the new species is closely related to *Kneiffiella subalutacea* (P. Karst.) Jülich & Stalpers.

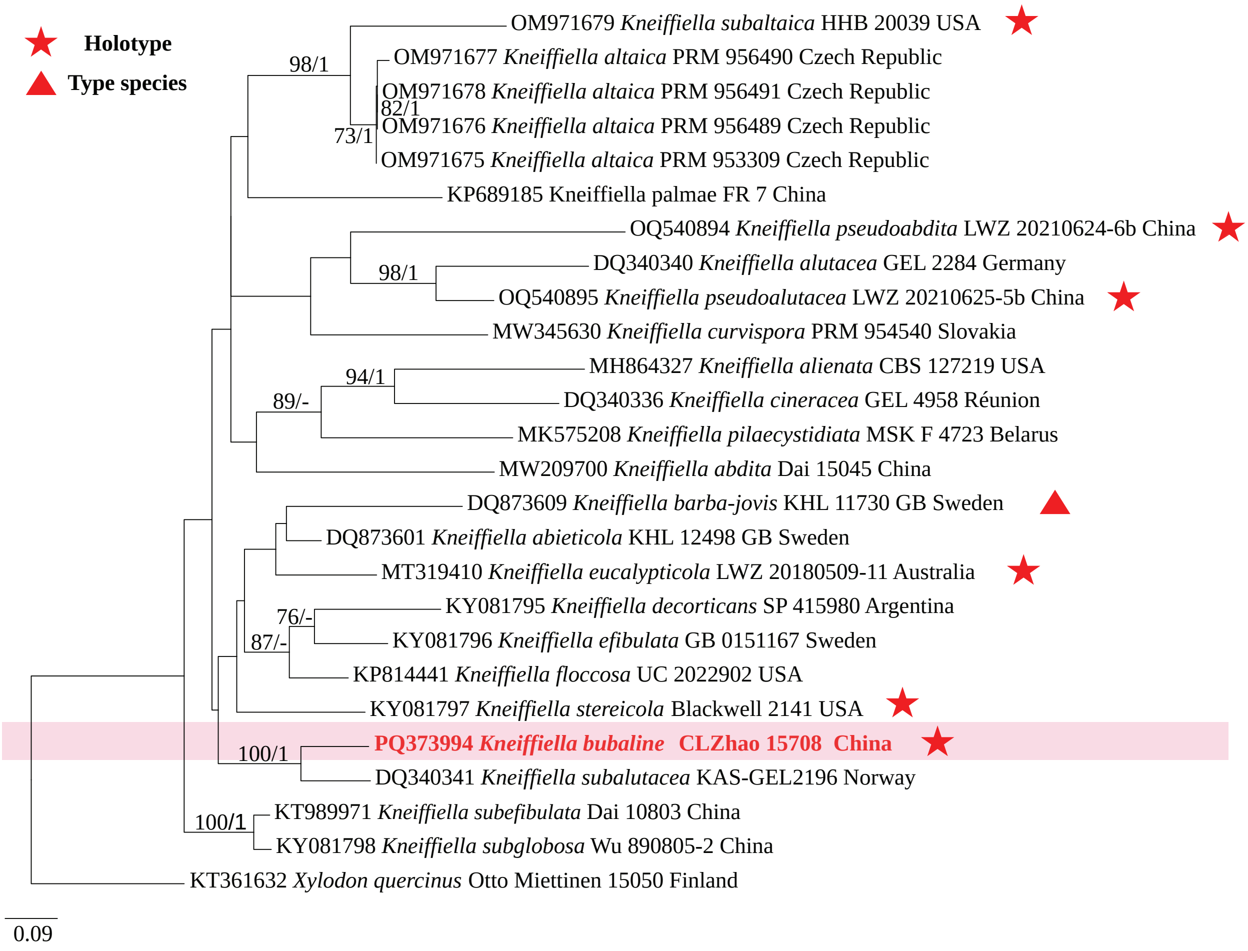

Figure 5. Phylogeny of species in *Kneiffiella* generated by maximum likelihood based on ITS sequence data. Branches are labeled with maximum likelihood bootstrap ≥ 70% and Bayesian posterior probabilities ≥ 0.95, respectively.

The phylogeny of *Xylodon*

The ITS dataset contained sequences from 149 fungal specimens representing 94 *Xylodon* taxa, 15 *Hyphodontia* J. Erikss taxa, five *Lyomyces* P. Karst taxa, and four *Kneiffiella* taxa. The average SD of split frequencies in BI analyses is 0.020943 (BI), and the effective sample size (ESS) for Bayesian analysis across the two runs is double the average ESS (avg ESS) = 1031.5. The phylogenetic tree (Fig. 6) reveals that the new species has a close relationship with *Xylodon bambusinus* C.L. Zhao & X. Ma, *X. fissuratus* C.L. Zhao, *X. subclavatus* (Yurchenko, H.X. Xiong and Sheng H. Wu) Riebesehl, Yurch. & Langer, *X. montanus* C.L. Zhao and *X. wenshanensis* K.Y. Luo & C.L. Zhao. Additionally, *Xylodon granulanoides* and *X. granulans* clustered together.

Taxonomy

Botryobasidium daweishanense **J.L. Zhang, H.M. Zhou & C.L. Zhao, sp. nov.**
MycoBank No: 856337
Figs 7, 8

Diagnosis. *Botryobasidium daweishanense* differs from *B. subcoronatum* by its araneose hymenial surface, smaller basidia, fusiform, cyanophilous, and wider basidiospores.

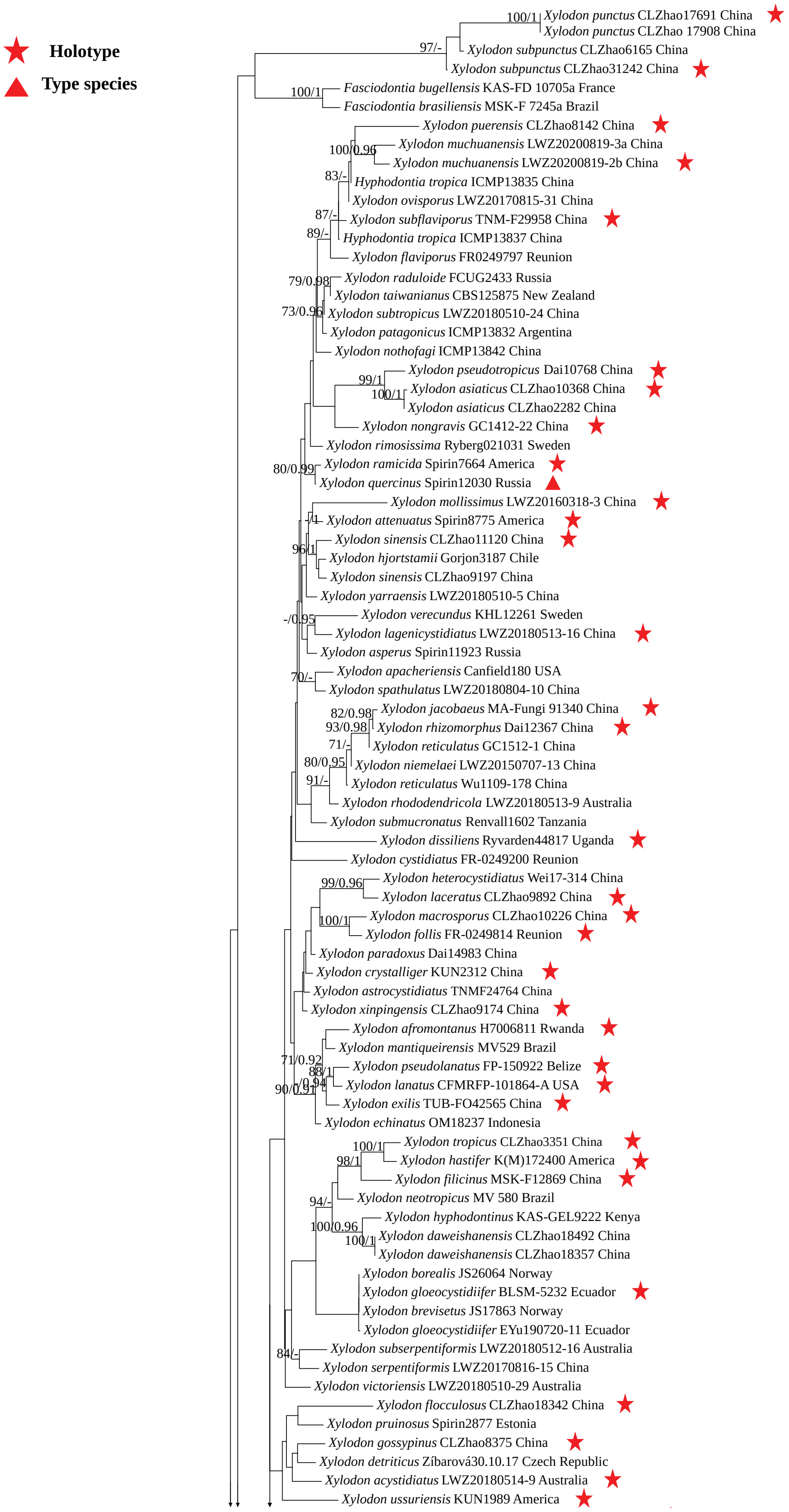

Figure 6. Phylogeny of species in *Xylodon* generated by maximum likelihood based on ITS sequence data. Branches are labeled with maximum likelihood bootstrap ≥ 70% and Bayesian posterior probabilities ≥ 0.95, respectively.

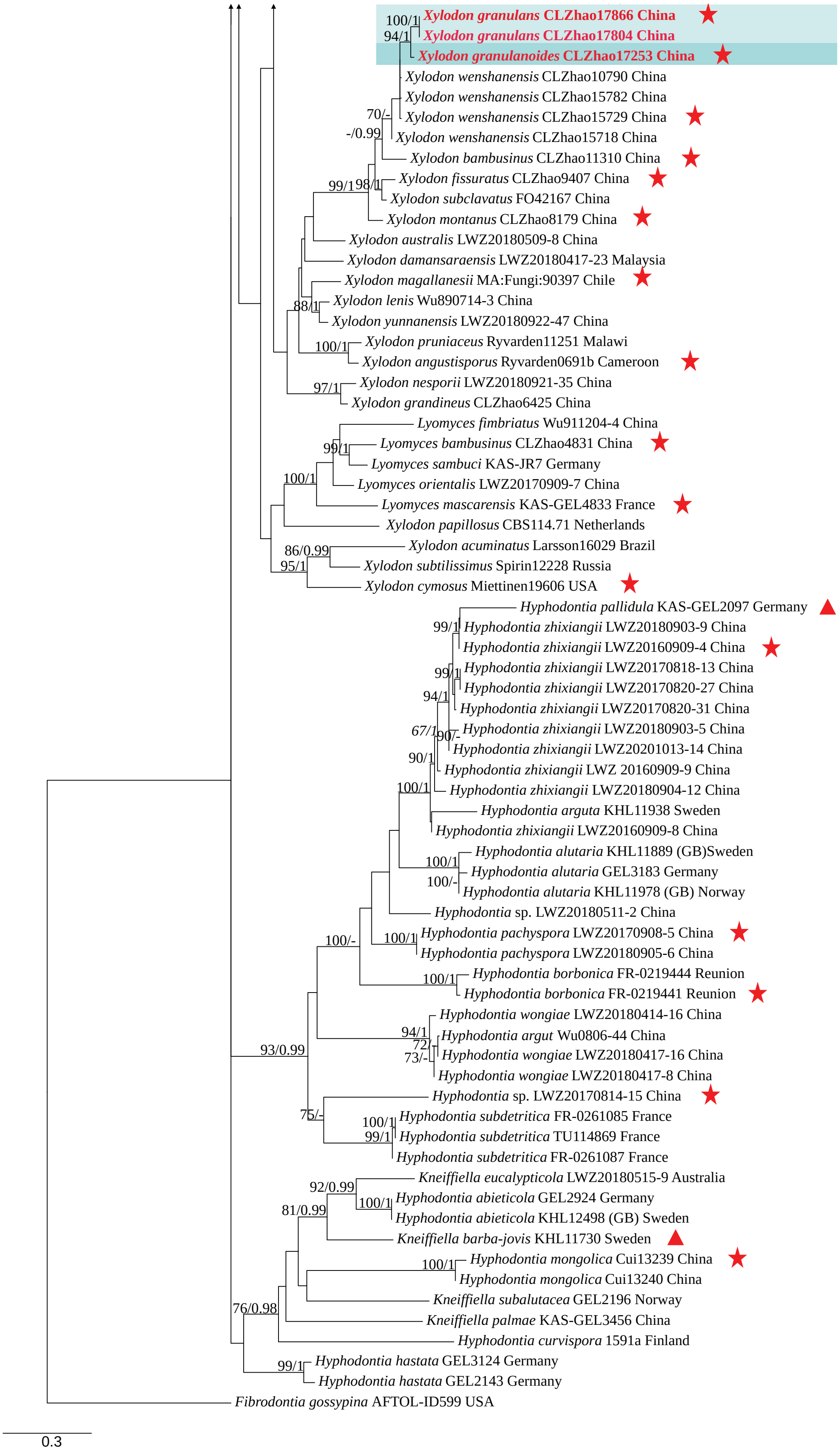

Figure 6. Continued.

Holotype. China • Yunnan Province, Honghe, Pingbian County, Daweishan National Nature Reserve, 28°42'N, 114°11'E, evel. 1356 m asl., on fallen angiosperm branch, 1 August 2019, CLZhao 40062 (SWFC).

Etymology. *Daweishanense* (Lat.) refers to the type location "Daweishan National Nature Reserve," China.

Description. ***Basidiomata*.** Annual, resupinate, coriaceous, without odor or taste when fresh, up to 1.6 cm long, 1.5 cm wide, and 100 µm thick. Hymenial surface araneose, cream when fresh, straw-yellow to yellowish when dry. Sterile margin thin, indistinct, slightly yellowish, up to 0.5 mm.

***Hyphal system*.** Monomitic; generative hyphae with clamp connections, hyaline, thin to slightly thick-walled, frequently branched, interwoven, 5.0–8.0 µm in diam, IKI–, CB+; tissues unchanged in KOH.

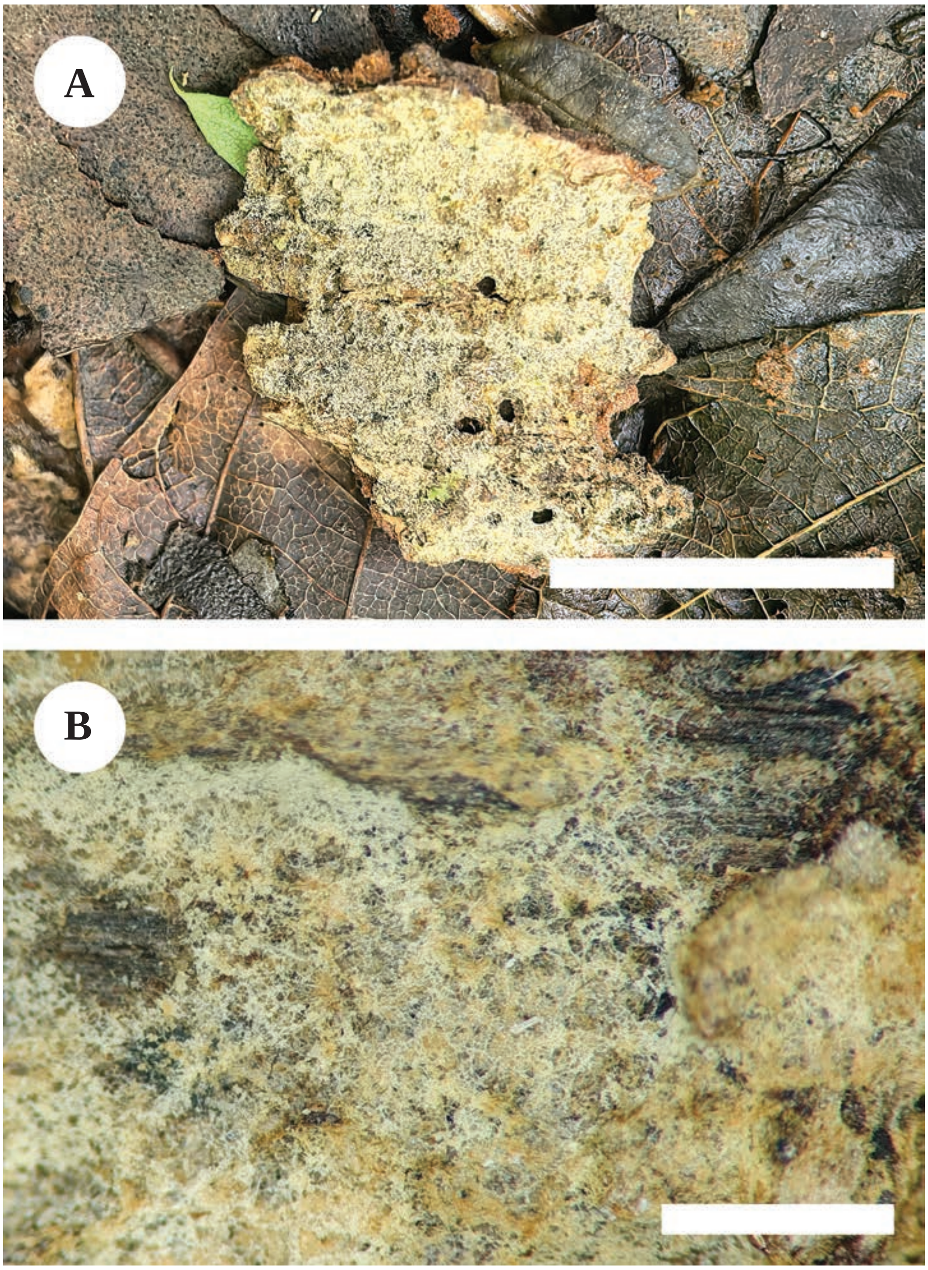

Figure 7. Basidiomata of *Botryobasidium daweishanense* (holotype, CLZhao 40062) **A** the front of the basidiomata **B** characteristic hymenophore. Scale bars: 1 cm (**A**); 1 mm (**B**).

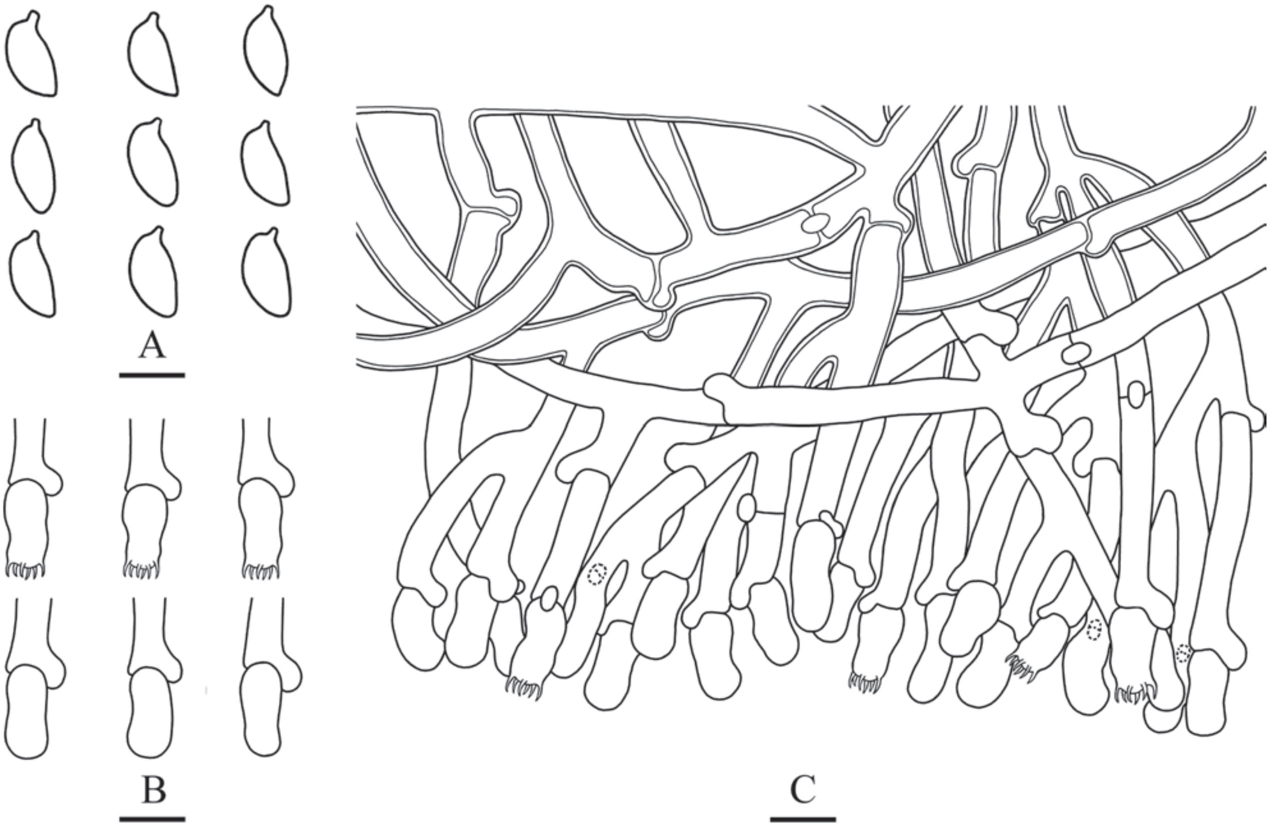

Figure 8. Microscopic structures of *Botryobasidium daweishanense* (holotype, CLZhao 40062) **A** basidiospores **B** basidia and basidioles **C** a section of hymenium. Scale bars: 5 µm (**A**); 10 µm (**B, C**); 10 × 100 oil.

***Hymenium*.** Cystidia and cystidoles absent. Basidia barred, slightly sinuous, with six short sterigmata and a basal clamp connection, 11.5–18.0 × 5.0–8.0 µm; basidioles dominant, in shape similar to basidia, but slightly smaller. ***Basidiospores*.** Fusiform, hyaline, thin-walled, smooth, IKI–, CB+, (6.0–)6.1–7.3 × (3.1–)3.3–3.9(–4.1) µm, L = 6.65 µm, W = 3.64 µm, Q = 1.81–1.85 (n = 60/2).

Additional specimens examined. China • Yunnan Province, Honghe, Pingbian County, Daweishan National Nature Reserve, 28°42'N, 114°11'E, evel. 1356 m asl., on fallen angiosperm branch, 1 August 2019, CLZhao 40061 (SWFC).

Inonotus subglobisporum **J.L. Zhang, H.M. Zhou & C.L. Zhao, sp. nov.**

MycoBank No: 856340
Figs 9, 10

Diagnosis. *Inonotus subglobisporum* differs from *I. radiata* by its perennial basidiomata, laterally stipitate, polygon pores, tapered, dark brown, thick-walled setae, and subglobose, thick-walled, hyaline basidiospores.

Holotype. China • Yunnan Province, Puer, Jingdong County, Ailaoshan National Nature Reserve, 23°42'N, 101°52'E, evel. 2450 m asl., on fallen angiosperm trunk, 25 August 2018, CLZhao 8765 (SWFC).

Etymology. *Subglobisporum* (Lat.) refers to the subglobose basidiospores.

Description. *Basidiomata*. Perennial, laterally stipitate, solitary, without odor or taste when fresh. Pilei fan-shaped, cortical to cork, extend up to 1.3 cm long, 2.2 cm wide, and 6 mm thick in diam at the base. Pileal surface honey-yellow

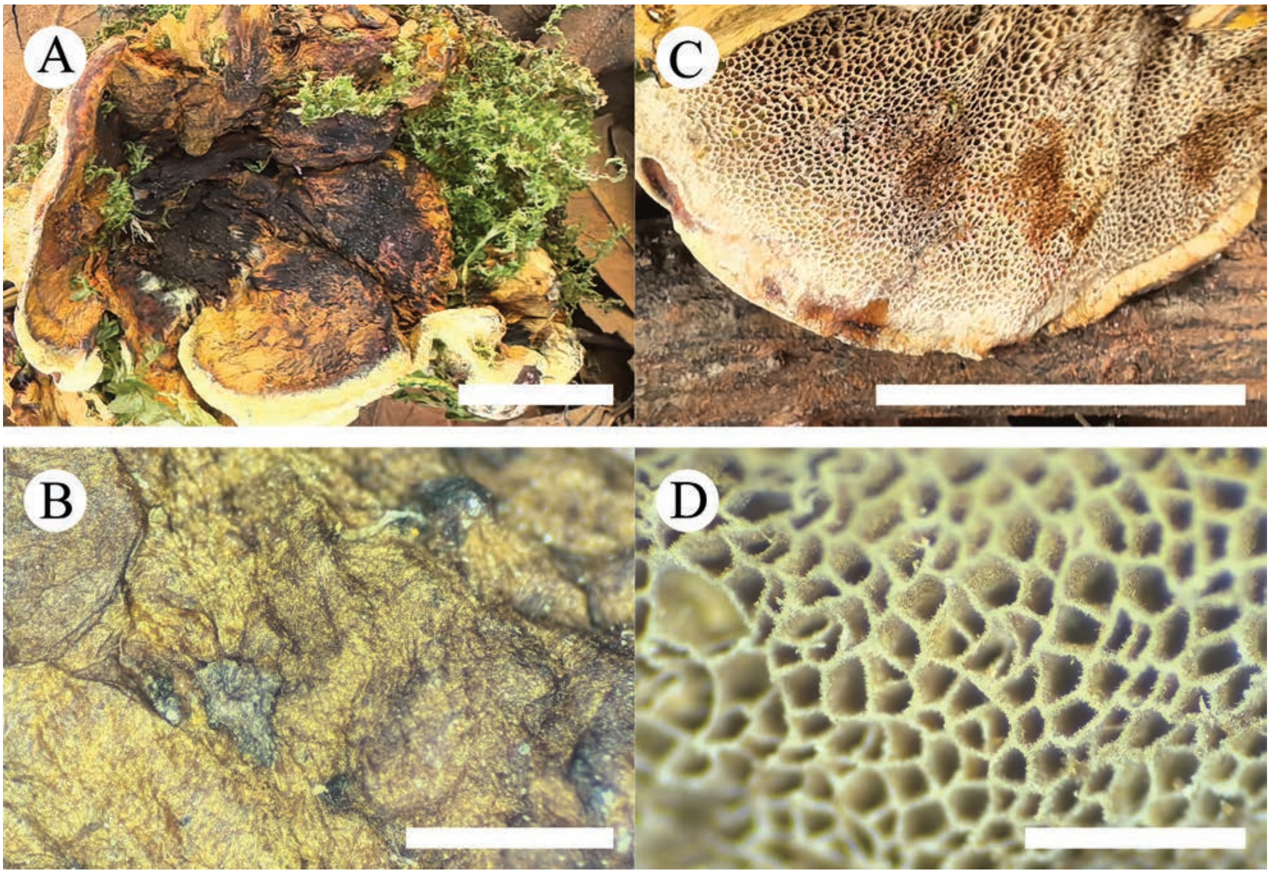

Figure 9. Basidiomata of *Inonotus subglobisporum* (holotype, CLZhao 8765) **A, B** the front of the basidiomata **C, D** characteristic hymenophore. Scale bars: 1 cm (**A, C**); 1 mm (**B, D**).

to fuscous when fresh, vinaceous brown to fuscous when dry. Pore surface cream, when fresh, becomes cream to fawn when dry; pores polygonal, 4–6 per mm. Context cinnamon-buff when dry, cork, up to 5 mm thick. Tubes cream to fawn when dry, cork, up to 1 mm long. Stipe with the same color as pores, up to 23 mm long and 15 mm in diameter when dry.

***Hyphal structure*.** Monomitic; generative hyphae, simple-septate, slightly thick-walled, frequently branched, interwoven. Generative hyphae in the tube frequent, brownish, slightly thick-walled, easily collapsing, 2.5–5.0 μm in diam. Generative hyphae in the context frequent, brown, slightly thick-walled, 3.0–7.0 μm in diam, IKI–, CB–; tissues brownish in KOH. ***Context*.** Setae numerous, tapered, dark brown, thick-walled, strongly encrusted in the surface, and almost entirely buried, 12.0–69.5 × 4.0–11.0 μm, cystidoles absent. Basidia clavate, with four short sterigmata and a basal simple-septate, 5.5–13.0 × 2.5–6.5 μm; basidioles in shape similar to basidia, but slightly smaller. ***Basidiospores*.** Subglobose, hyaline, thick-walled, smooth, IKI–, CB+, (3.5–)3.6–4.3(–4.4) × (2.6–)2.8–3.5(–3.6) μm, L = 3.99 μm, W = 3.20 μm, Q = 1.22–1.27 (n = 120/4).

Other specimens examined. CHINA • Yunnan Province, Puer, Jingdong County, Ailaoshan National Nature Reserve, 23°42'N, 101°52'E, evel. 2450 m asl., on fallen angiosperm trunk, 23 August 2018, CLZhao 8331; CLZhao 8387; CLZhao 8433; CLZhao 8543; 24 August 2018, CLZhao 8500; 25 August 2018, CLZhao 8678; CLZhao 8737; CLZhao 8789 (SWFC).

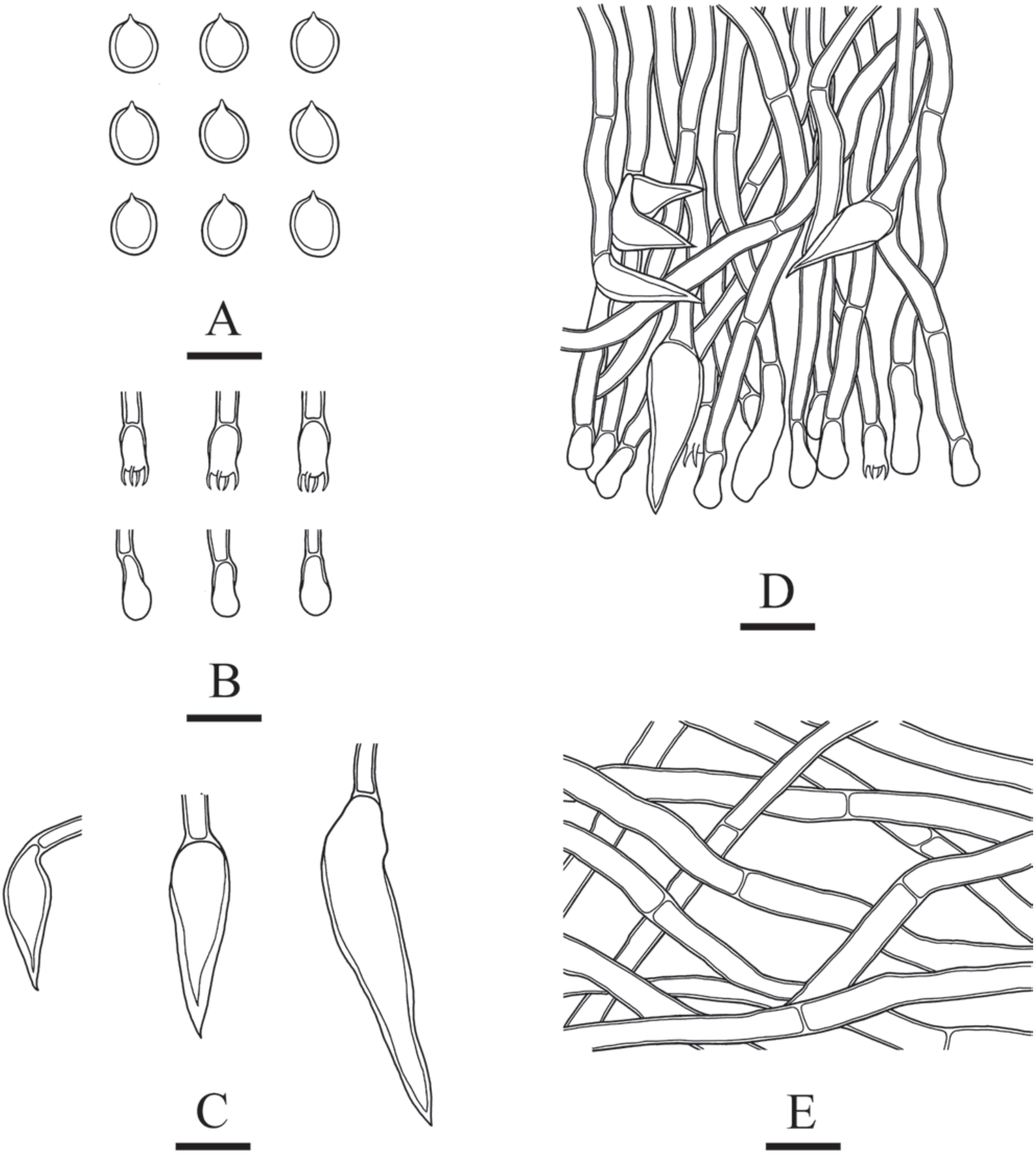

Figure 10. Microscopic structures of *Inonotus subglobisporum* (holotype, CLZhao 8765) **A** basidiospores **B** basidia and basidioles **C** setae **D** hymenium and hyphae from trama **E** hyphae from context. Scale bars: 5 µm (**A**); 10 µm (**B–E**); 10 × 100 oil.

Kneiffiella bubalina **J.L. Zhang, H.M. Zhou & C.L. Zhao, sp. nov.**

MycoBank No: 856342
Figs 11, 12

Diagnosis. *Kneiffiella bubalina* differs from *K. subalutacea* by its cream basidiomata and cylindrical to slightly allantoid basidiospores.

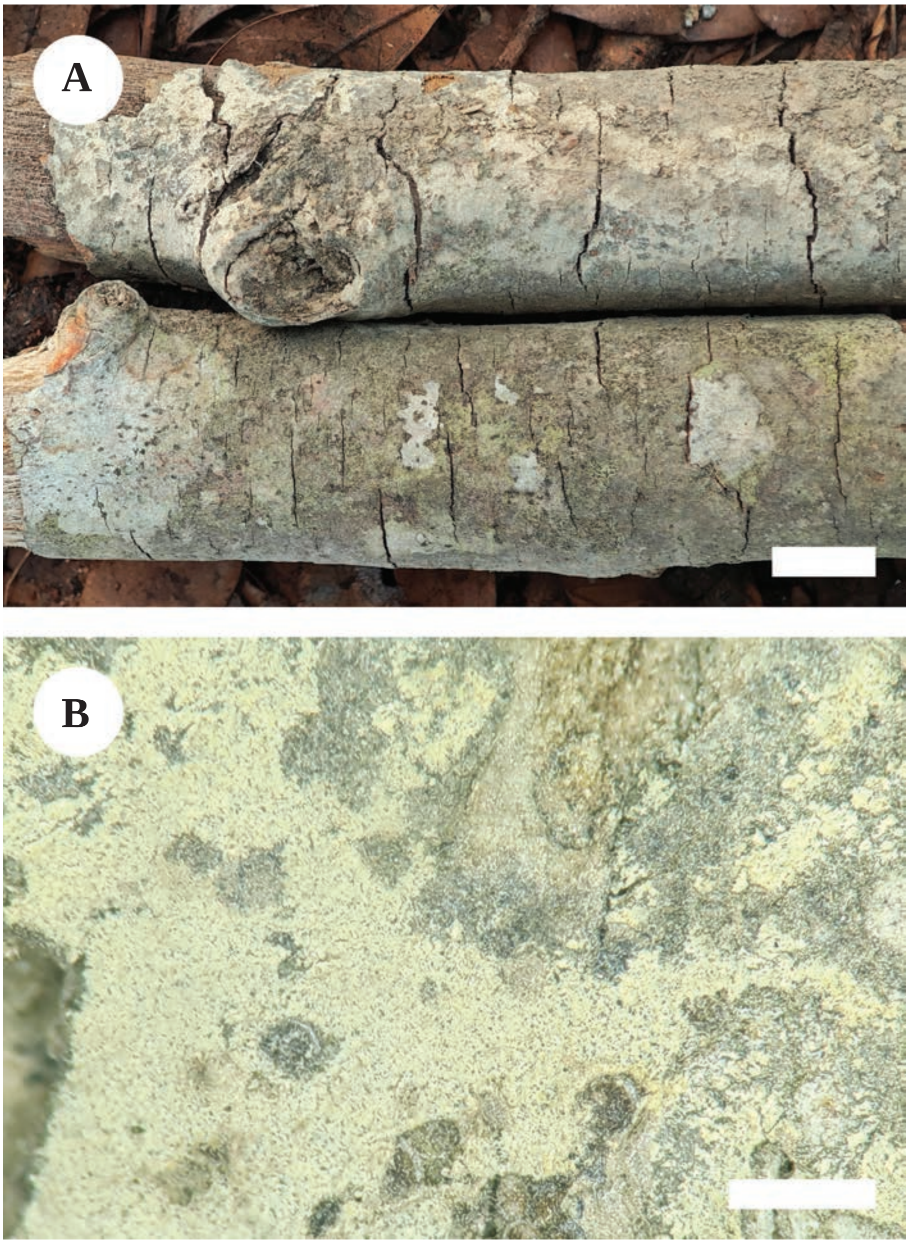

Figure 11. Basidiomata of *Kneiffiella bubalina* (holotype, CLZhao 15708) **A** the front of the basidiomata **B** characteristic hymenophore. Scale bars: 1 cm (**A**); 1 mm (**B**).

Holotype. China • Yunnan Province, Wenshan, Xichou County, Jiguanshan Forestry Park, 23°53'N, 104°82'E, evel. 1730 m asl., on fallen angiosperm branch, 22 July 2019, CLZhao 15708 (SWFC).

Etymology. *Bubalina* (Lat.) refers to its buff-colored hymenial surface.

Description. ***Basidiomata*.** Annual, resupinate, smooth, membranous, without odor or taste when fresh, up to 1.6 cm long, 1.1 cm wide, and 0.1–0.2 mm thick. Hymenial surface araneose, white to cream when fresh, buff when dry. Sterile margin thin, indistinct, slightly buff, up to 1 mm.

***Hyphal system*.** Monomitic; generative hyphae with clamp connections, slightly thick-walled, frequently branched, interwoven, IKI–, CB–, 2.5–3.5 µm in diam; tissues unchanged in KOH.

***Hymenium*.** Cystidia numerous, tubular, rising from subiculum with a basal clamp connection, hyaline, thick-walled except in the apical part, smooth,

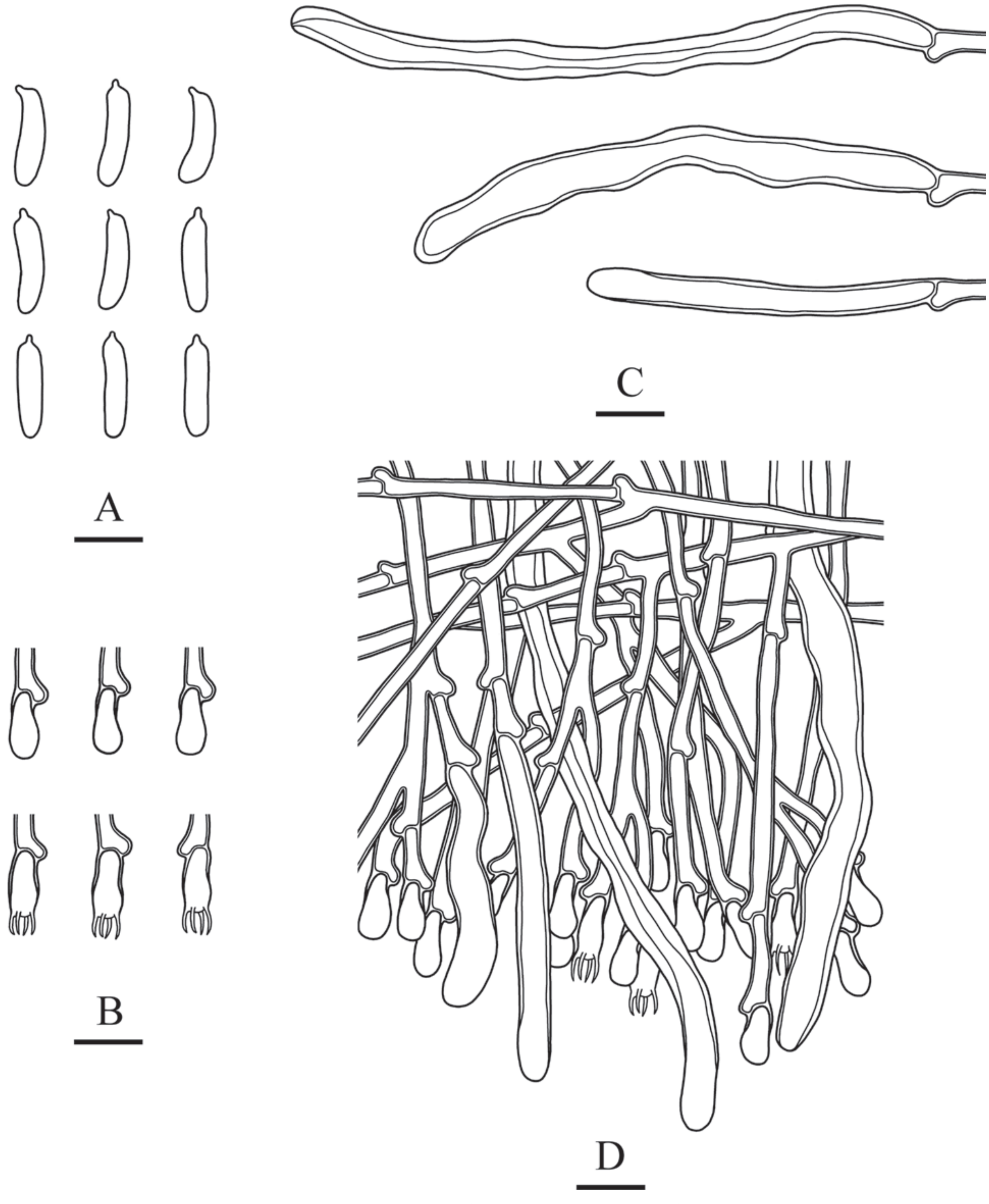

Figure 12. Microscopic structures of *Kneiffiella bubalina* (holotype, CLZhao 15708) **A** basidiospores **B** basidia and basidioles **C** cystidia **D** a section of hymenium. Scale bars: 5 µm (**A**); 10 µm (**B–D**); 10 × 100 oil.

103.5–162.5 × 6.0–8.0 µm; cystidioles absent. Basidia club-shaped, slight constriction in the middle part, with four sterigmata and a basal clamp connection, 10.0–14.0 × 4.5–5.0 µm; basidioles dominant, in shape similar to basidia, but slightly smaller. ***Basidiospores*.** Cylindrical to slightly allantoid, slightly narrower in apical part, hyaline, thin-walled, smooth, IKI–, CB–, 8.0–8.9(–9.1) × (1.7–)1.8–2.3(–2.6) µm, L = 8.41 µm, W = 2.03 µm, Q = 4.15 (n = 30/1).

Xylodon granulanoides J.L. Zhang, H.M. Zhou & C.L. Zhao, sp. nov.
MycoBank No: 856343
Figs 13, 14

Diagnosis. *Xylodon granulanoides* differs from *X*. *granulans*. by its varied cystidia and broadly ellipsoid, thick-walled basidiospores measuring 4.7–5.3 × 3.6–4.1 µm.

Holotype. China • Yunnan Province, Wenshan, Pingbian County, Wenshan National Nature Reserve, 23°22'N, 103°93'E, evel. 1753 m asl., on fallen angiosperm branch, 28 July 2019, CLZhao 17253 (SWFC).

Etymology. *Granulanoides* (Lat.) refers to the new species' resemblance to *Xylodon granulans*.

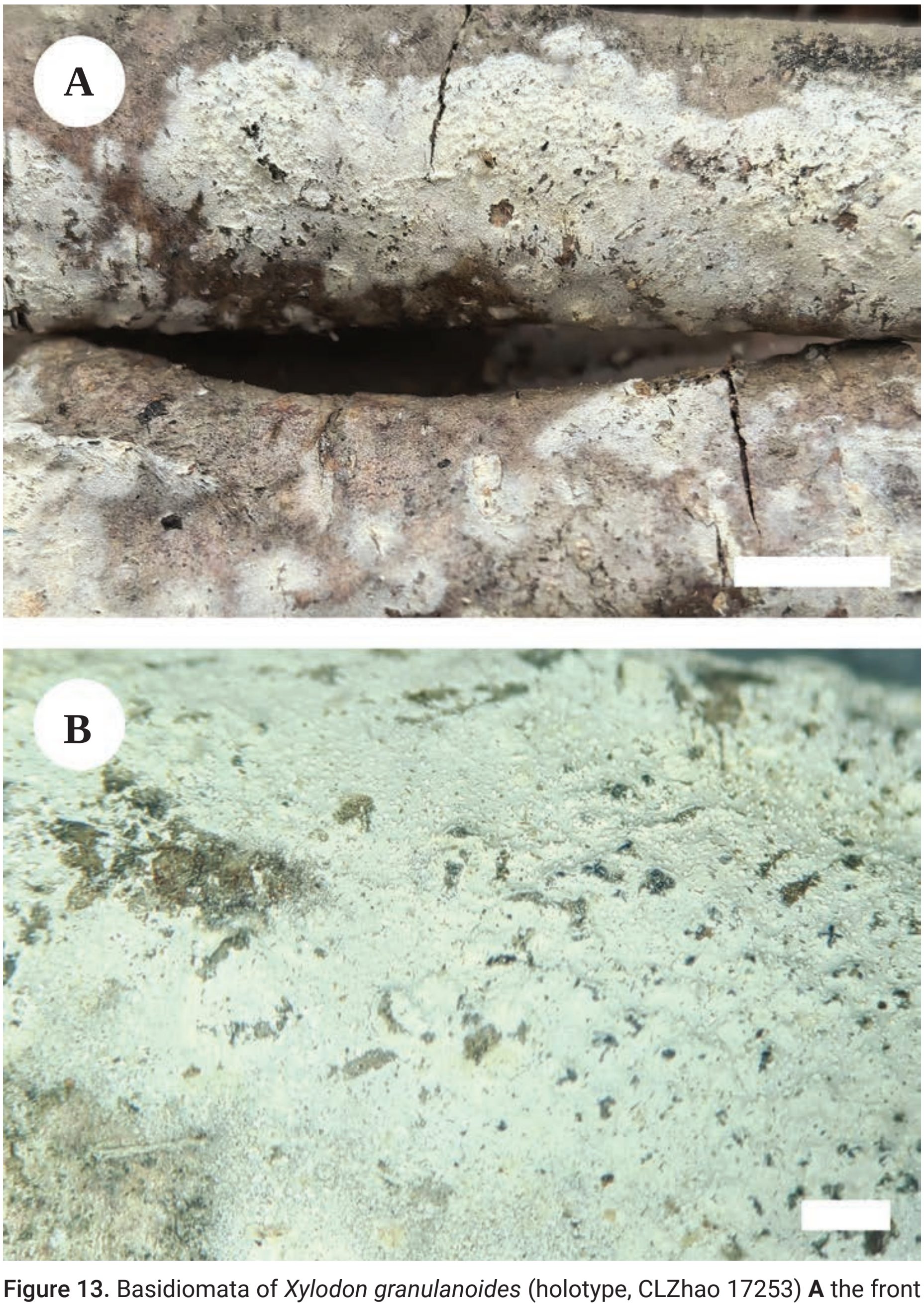

Figure 13. Basidiomata of *Xylodon granulanoides* (holotype, CLZhao 17253) **A** the front of the basidiomata **B** characteristic hymenophore. Scale bars: 1 cm (**A**); 1 mm (**B**).

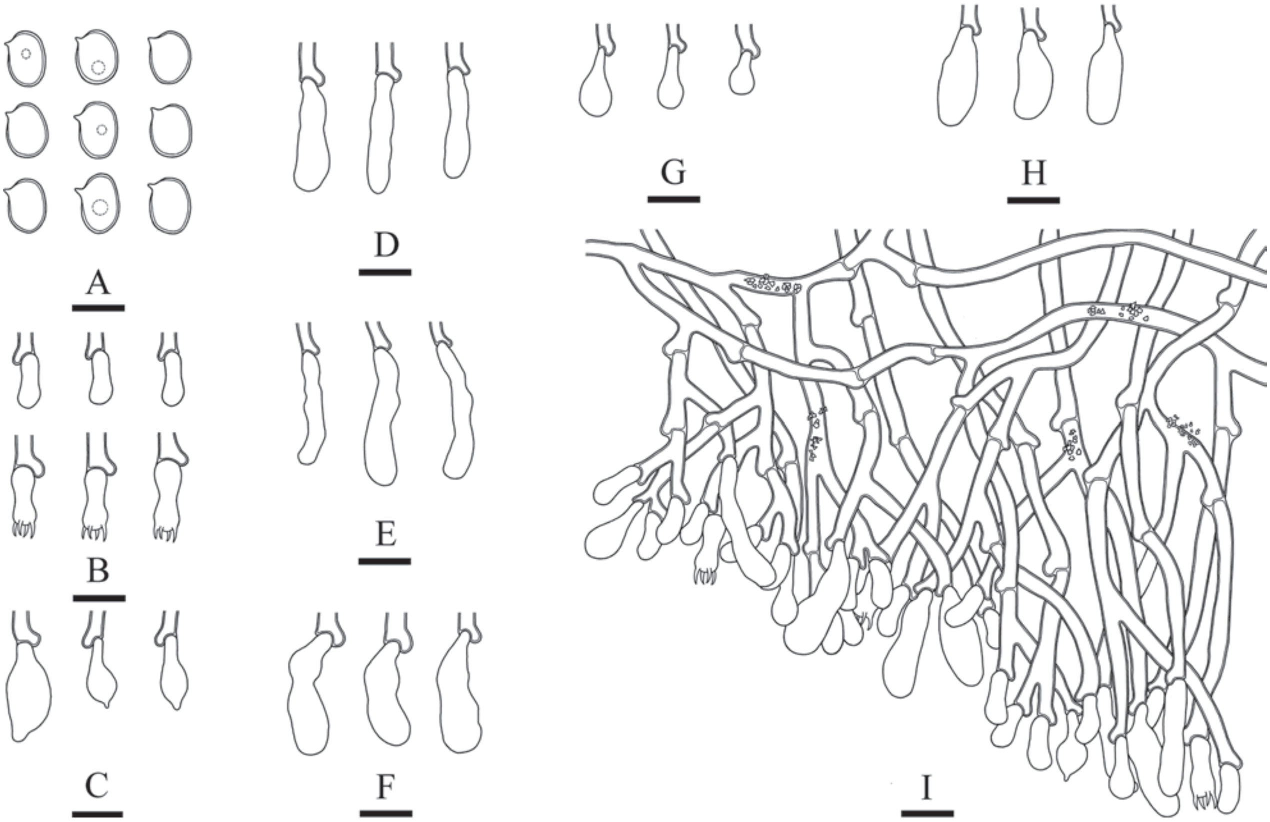

Figure 14. Microscopic structures of *Xylodon granulanoides* (holotype, CLZhao 17253) **A** basidiospores **B** basidia and basidioles **C** cystidioles **D–H** cystidia **I** a section of hymenium. Scale bars: 5 µm (**A**); 10 µm (**B–I**); 10 × 100 oil.

Description. ***Basidiomata*.** Annual, resupinate, adnate, membranous, without odor or taste when fresh, brittle when dry, up to 5.3 cm long, 2.5 cm wide, and 0.1 mm thick. Hymenial surfaces grandinioid, white to cream when fresh, cream to slightly buff upon drying. Sterile margin thin, indistinct, slightly cream, up to 1 mm.

***Hyphal system*.** Monomitic; generative hyphae with clamp connections slightly encrusted with crystals amongst generative hyphae, hyaline, slightly thick-walled, frequently branched, interwoven, 2.5–3.5 µm in diam, IKI–, CB–; tissues unchanged in KOH.

***Hymenium*.** Cystidia numerous, subclavate to cylindrical, or slightly subcapitate, hyaline, thin-walled, 9.5–29.0 × 4.0–9.5 µm; cystidioles are present, subcapitate, hyaline, thin-walled, 13.5–21.0 × 5.0–9.0 µm. Basidia subcylindrical to clavate, hyaline, thin-walled, with four sterigmata and a basal clamp connection, 11.0–16.0 × 4.0–5.5 µm; basidioles dominant, in shape similar to basidia, but slightly smaller. ***Basidiospores*.** Broadly ellipsoid, part has a large drop of oil, hyaline, slightly thick-walled, smooth, IKI–, CB–, (4.6–)4.7–5.3(–5.3) × (3.4–)3.6–4.1(–4.2) µm, L = 4.92 µm, W = 3.90 µm, Q = 1.26 (n = 30/1).

Xylodon granulans **J.L. Zhang, H.M. Zhou & C.L. Zhao, sp. nov.**

MycoBank No: 856344
Figs 15, 16

Diagnosis. *Xylodon granulans* differs from *X. wenshanensis* by its broadly ellipsoid, thin-walled basidiospores measuring 3.8–4.2 × 2.9–3.3 µm.

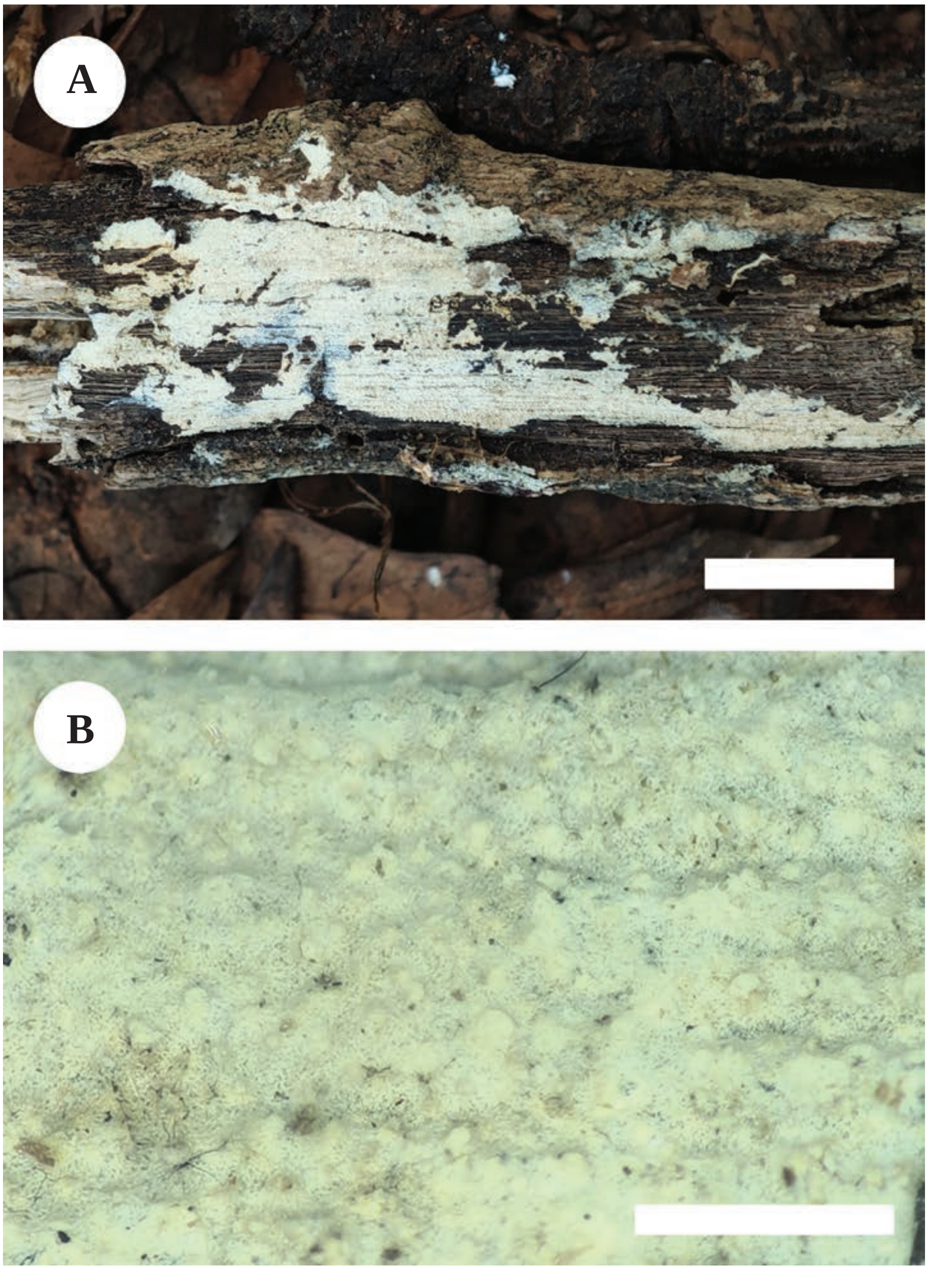

Figure 15. Basidiomata of *Xylodon granulans* (holotype, CLZhao 17866) **A** the front of the basidiomata **B** characteristic hymenophore. Scale bars: 1 cm (**A**); 1 mm (**B**).

Holotype. China • Yunnan Province, Honghe, Pingbian County, Daweishan National Nature Reserve, 28°42'N, 114°11'E, evel. 1356 m asl. on fallen angiosperm branch, 1 August 2019, CLZhao 17866 (SWFC).

Etymology. *Granulans* (Lat.) refers to the granulated hymenial surface.

Description. ***Basidiomata*.** Basidiomata annual, resupinate, adnate, membranous, without odor or taste when fresh, up to 2.4 cm long, 1.3 cm wide, and 50–70 µm thick. Hymenial surface grandinioid, cream when fresh, white to slightly cream when dry. Sterile margin thin, indistinct, slightly cream, up to 1 mm.

***Hyphal system*.** Monomitic; generative hyphae with clamp connections slightly encrusted with crystals amongst generative hyphae, hyaline, slightly

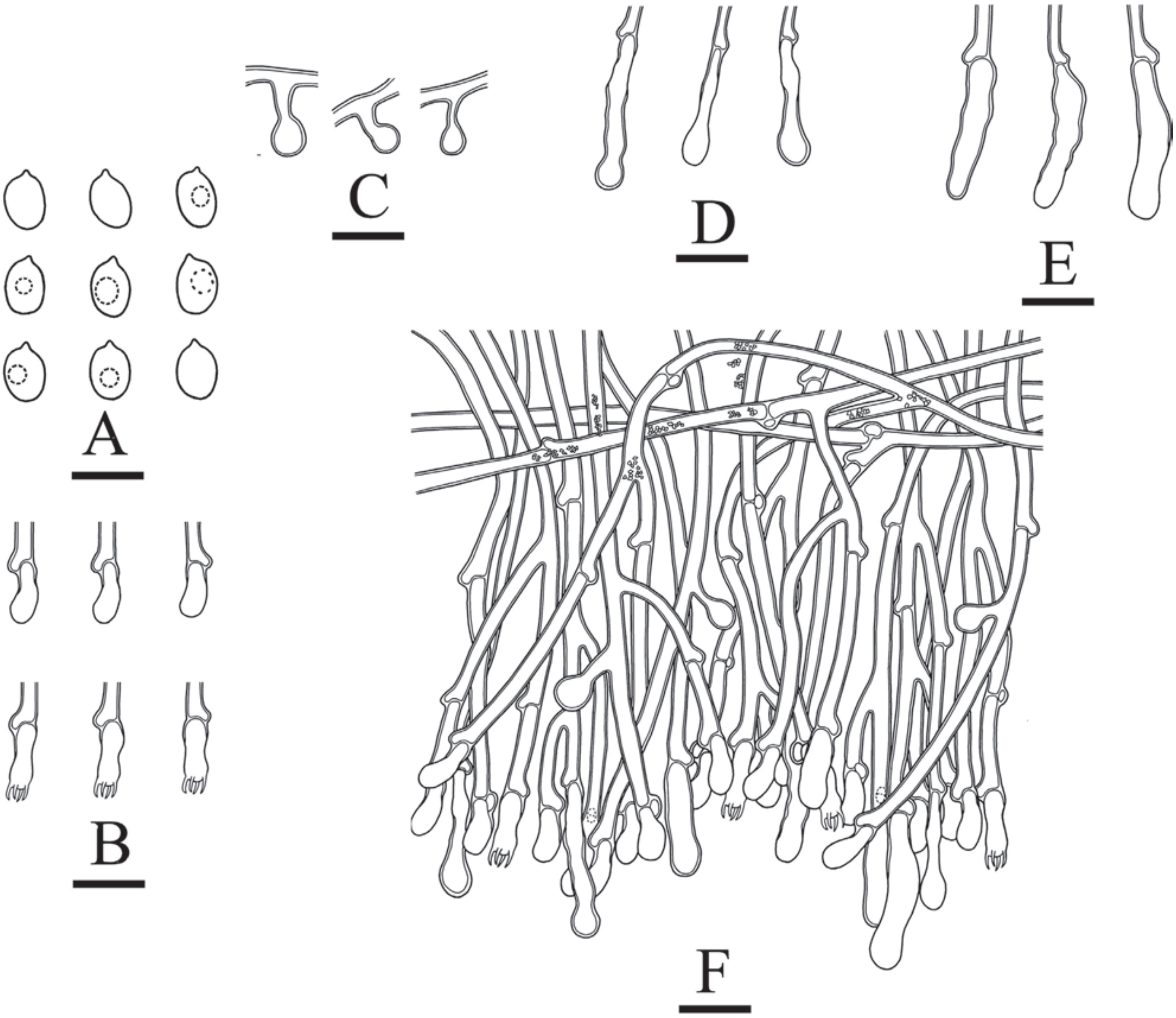

Figure 16. Microscopic structures of *Xylodon granulans* (holotype, CLZhao 17866) **A** basidiospores **B** basidia and basidioles **C–E** cystidia **F** a section of hymenium. Scale bars: 5 µm (**A**); 10 µm (**B–F**); 10 × 100 oil.

thick-walled, frequently branched, interwoven, 2.0–2.5 µm in diam, IKI–, CB–; tissues unchanged in KOH.

***Hymenium*.** Cystidia of two types: (1) Capitate cystidia in hymenium and subiculum, hyaline, slightly thick-walled, smooth, slightly constricted at the neck, with a globose head, 4.5–23.5 × 3.0–4.5 µm; (2) Clavate cystidia, slightly sinuous, hyaline, slightly thick-walled, smooth, 13.0–24.0 × 4.0–5.0 µm. Basidia clavate, slightly sinuous, with four sterigmata and a basal clamp connection, 9.0–12.0 × 3.5–4.5 µm; basidioles dominant, in shape similar to basidia, but slightly smaller. ***Basidiospores*.** Broadly ellipsoid, some of them with an oily drop, hyaline, thin-walled, smooth, IKI–, CB–, (3.7–)3.8–4.2(–4.3) × (2.8–)2.9–3.3(–3.4) µm, L = 4.03 µm, W = 3.12 µm, Q = 1.29–1.29 (n = 60/2).

Other specimen examined. China • Yunnan Province, Honghe, Pingbian County, Daweishan National Nature Reserve, 28°42'N, 114°11'E, evel. 1356 m asl., on fallen angiosperm branch, 1 August 2019, CLZhao 17804 (SWFC).

Discussion

Numerous wood-inhabiting fungal taxa have recently been identified over the last few years (Cui et al. 2019; Guan et al. 2023; Zhao et al. 2023b; Luo et al. 2024; Zhou et al. 2024b). The most recent taxonomic framework recognizes 14 families within Hymenochaetales (Wang et al. 2023; He et al. 2024; Wang and Zhou 2024). To further investigate the wood inhabiting fungal diversity, collections representing five new species *viz*. *Inonotus subglobisporum*, *Kneiffiella bubalina*, *Xylodon granulanoides*, *X*. *granulans* (Hymenochaetales), and *Botryobasidium daweishanense* (Cantharellales) from Yunnan Province were collected and are introduced based on a combination of morphological features and molecular evidence.

Botryobasidium daweishanense is characterized by an araneose hymenial surface, generative hyphae with clamp connections, subcylindrical basidia (11.5–18.0 × 5.0–8.0 μm), and fusiform, cyanophilous basidiospores (6.1–7.3 × 3.3–3.9 μm). In several previous studies, molecular data have confirmed phylogenetic relationships showing that the genus *Botryobasidium* is nested within the cantharelloid clade and grouped with related genera such as *Cantharellus* Lam., *Clavulina* J. Schröt, *Craterellus* Pers, and *Hydnum* L. (Moncalvo et al. 2006; Bernicchia and Gorjón 2010). Macromorphologically, species of *Botryobasidium* are often mistaken for certain genera, such as *Ceratobasidium* D.P. Rogers, *Sistotrema* Fr., and *Tulasnella* J. Schröt (Donk 1956; Oberwinkler 1982). However, *Botryobasidium* is distinguished from these genera by the absence of epibasidia, sturdy and long sterigmata, and oily inclusions (Kotiranta and Saarenoksa 2005; Gorjón and Hallenberg 2008; Oberwinkler et al. 2017; Zhou et al. 2024c). The phylogram created based on inferences from the ITS+nLSU data in the present study aligns with previous research. According to the phylogram (Fig. 1), the new species of *Botryobasidium daweishanense* was grouped into the genus *Botryobasidium* (Botryobasidiaceae). Phylogenetic analysis of the ITS system (Fig. 2) revealed that the new species *Botryobasidium daweishanense* is grouped with three taxa: *B*. *intertextum*, *B*. *leptocystidiatum*, and *B*. *subcoronatum*. However, morphologically, *Botryobasidium intertextum* differs macroscopically from *B*. *daweishanense* in being initially thin, hypochnoid, and white and later displaying pellicular and yellowish hymenial surfaces. In contrast, the hymenial surface of *B*. *daweishanense* is araneose and exhibits a straw-yellow to cream color when dry. In addition, at the micro level, *Botryobasidium intertextum* is distinguishable from *B*. *daweishanense* by its larger basidiospores (7.0–9.5 × 1.8–2.81 μm) and basidia (15–21 × 5–6.5 μm; Kotiranta and Saarenoksa 1990). *Botryobasidium leptocystidiatum* and *B*. *daweishanense* both display an arachnoid hymenial surface macroscopically; however, *B*. *daweishanense* appears cream-colored when fresh and straw-yellow to yellowish when dry, whereas *B*. *leptocystidiatum* is grayish-white to smoky gray when fresh and grayish-white to ivory when dry. Additionally, microscopically, *B*. *leptocystidiatum* features tubular cystidia, 6–7 sterigmata, and smaller basidia (10.5–15 × 7–8 μm) and longer basidiospores (6.5–7.8 × 2.9–3.7 μm) than *B*. *daweishanense* (Zhou et al. 2024c). *Botryobasidium subcoronatum* is distinguished from *B*. *daweishanense* by the former being thin, floccose to hypochnoid, and whitish at first, followed by having a yellowish to ochraceous hymenial surface. On a microscopic level, the species *Botryobasidium subcoronatum* has relatively larger basidia (20–25 × 7–9 μm) and narrower basidiospores (6–7.5 × 2.5–3 μm; Eriksson and Ryvarden 1973).

Inonotus subglobisporum is characterized by perennial, laterally stipitate basidiomata; tapered, dark brown, thick-walled setae (12.0–69.5 × 4.0–11.0 μm); and subglobose, cyanophilous basidiospores (3.6–4.3 × 2.8–3.5 μm). In the phylogenetic tree of Wu et al. (2022), species of *Inonotus* formed a monophyletic clade; however, *Inonotus* may still be a polyphyletic genus because most species within the genus have not been phylogenetically analysed. Wagner and Fischer also regarded *Inonotus* as a polyphyletic group (Wagner and Fischer 2002; Lin et al. 2023). In the present study, the phylogenetic analysis of the ITS system (Fig. 4) was consistent with previous reports and revealed that the species *Inonotus subglobisporum* was a sister to *I. radiatus*. However, morphologically, the species *Inonotus radiatus* differs from *I. subglobisporum* in terms of its annual basidiomata, which are typically in imbricate clusters; hooked setae; and ellipsoid, hyaline to pale yellowish basidiospores (3.8–5 × 2.6–3.5 μm; Dai 2010).

Kneiffiella bubalina is characterized by cream-colored basidiomata, slightly thick-walled generative hyphae, and cylindrical to slightly allantoid basidiospores (8.0–8.9 × 1.8–2.3 μm). Riebesehl and Langer (2017) showed the monophyly of *Kneiffiella* species by inferring ITS sequences using Bayesian analysis. Wang et al. (2021) classified *Kneiffiella* as belonging to the family Chaetoporellaceae (Riebesehl and Langer 2017; Wang et al. 2021; Langer et al. 2022). Based on a phylogenetic analysis of the ITS + nLSU system (Fig. 3), we determined that the genus *Kneiffiella* is nested in the Chaetoporellaceae clade. Phylogenetic analysis of the ITS system (Fig. 5) revealed that the new species, *Kneiffiella bubalina*, is a sister to *K. subalutacea*. Morphologically, *Kneiffiella subalutacea* resembles *K. bubalina* because of its smooth hymenial surface, tubular, obtuse apical part, and thick-walled cystidia. However, *Kneiffiella subalutacea* can be distinguished from *K. bubalina* by its yellowish basidiomata and allantoid, smooth, thin-walled basidiospores (6–8 × 1.5–2.0 μm; Eriksson and Ryvarden 1976).

Xylodon granulanoides is characterized by grandinioid hymenial surfaces, varied cystidia, and broadly ellipsoid, thick-walled basidiospores (4.7–5.3 × 3.6–4.1 μm). *Xylodon granulans* is characterized by grandinioid hymenial surfaces, capitate cystidia and clavate cystidia, and broadly ellipsoid, thin-walled basidiospores (3.8–4.2 × 2.9–3.3 μm). In several previous phylogenetic studies based on multiple loci in the family Schizoporaceae, three genera, *Fasciodontia* Yurchenko & Riebesehl, *Lyomyces*, and *Xylodon*, were located in this family (Wang et al. 2021; Yuan and Zhao 2024). The present study's phylogram inferred from the ITS+nLSU data (Fig. 3) shows that two new species, *Xylodon granulanoides* and *X. granulans*, are grouped within the family Schizoporaceae. Based on the ITS topology (Fig. 6), these two new species are closely clustered with five other species: *Xylodon bambusinus*, *X. fissuratus*, *X. montanus*, *X. subclavatus*, and *X. wenshanensis*; meanwhile, the taxon *X. granulans* is a sister to *X. granulanoides*. However, morphologically, *Xylodon granulans* differs from *X. granulanoides* in that *X. granulans* lacks cystidioles and exists as broadly ellipsoid, thin-walled basidiospores (3.8–4.2 × 2.9–3.3 μm). *Xylodon bambusinus* differs from *X. granulans* and *X. granulanoides* in its ceraceous basidiomata, fusiform cystidia and capitate cystidia, and broad, ellipsoid, thin-walled basidiospores (4–5.5 × 3–4 μm; Ma and Zhao 2021). *Xylodon fissuratus* and *X. montanus* differ from *X. granulans* and *X. granulanoides* in that *X. fissuratus* and *X. montanus* have only one cystidia. In contrast, *X. fissuratus* has capitate cystidia, a thin-walled hyphal structure, and ellipsoid, thin-walled basidiospores (4.0–5.0 × 3.0–4.0 μm; Guan et al.

2023). *Xylodon montanus* has a smooth hymenial surface, moniliform cystidia, and ellipsoid to broad ellipsoid basidiospores (3.9–5.3 × 3.2–4.3 μm; Qu et al. 2022). *Xylodon subclavatus* can be distinguished from *X*. *granulans* and *X*. *granulanoides* by its cracked, aculei wart-like to conical, blunt to acute hymenial surface, and four types of cystidia: subclavate, hyphoid, capitate to sucapitate, and moniliform (Yurchenko et al. 2013). *Xylodon wenshanensis* can be distinguished from *X*. *granulans* and *X*. *granulanoides* by its capitate cystidia, clavate cystidia, and ellipsoid, thin-walled basidiospores (3–5 × 2–3.5 μm; Luo et al. 2022).

The families Chaetoporellaceae, Hymenochaetaceae, and Schizoporaceae represent a well-studied group within Hymenochaetales (Luo and Zhao 2021; Langer et al. 2022; Cho et al. 2024; Freire and Soares 2024; Viner et al. 2024); however, the diversity of species in China remains poorly understood, particularly in the southwestern region. Additionally, the genus *Botryobasidium* has rarely been reported in recent years, particularly in southwestern China. Therefore, the species diversity of Cantharellales and Hymenochaetales in China, particularly in the subtropical and tropical regions, has not been sufficiently studied. This study contributes to our understanding of fungal diversity in these areas and underscores the urgent need for further fieldwork and molecular analyses to identify new taxa. Our findings confirm that fungal diversity is abundant in southwestern China.

Additional information

Conflict of interest

The authors have declared that no competing interests exist.

Ethical statement

No ethical statement was reported.

Funding

The research was supported by the National Natural Science Foundation of China (Project No. 3246006), the Scientific Research Fund of Yunnan Provincial Department of Education (2024J0668), and the Forestry Innovation Programs of Southwest Forestry University (Project No: LXXK-2023M07).

Author contributions

Conceptualization, HZ and JZ; methodology, HZ and JZ; software, HZ, JZ, and ZG; validation, HZ and JZ; formal analysis, HZ and JZ; investigation, HZ, CZ, and JZ; resources, HZ; writing—original draft preparation, HZ, JZ, and ZG; writing—review and editing, HZ and JZ; visualization, HZ and JZ; supervision, HZ and JZ; project administration, HZ; funding acquisition, HZ. All authors have read and agreed to the published version of the manuscript.

Author ORCIDs

Jianling Zhang https://orcid.org/0009-0005-3268-7665
Zirui Gu https://orcid.org/0000-0003-1476-9040
Chunqin Zhou https://orcid.org/0009-0004-8117-1537
Hongmin Zhou https://orcid.org/0000-0002-0724-5815

Data availability

All of the data that support the findings of this study are available in the main text.

References

Adaku N, Park HB, Spakowicz DJ, Tiwari MK, Strobel SA, Crawford JM, Rogers FA (2020) A DNA repair inhibitor isolated from an Ecuadorian fungal endophyte exhibits synthetic lethality in PTEN-deficient glioblastoma. Journal of Natural Products 83(6): 1899–1908. https://doi.org/10.1021/acs.jnatprod.0c00012

Amalfi M, Yombiyeni P, Decock C (2010) *Fomitiporia* in sub-Saharan Africa: Morphology and multigene phylogenetic analysis support three new species from the Guineo-Congolian rainforest. Mycologia 102(6): 1303–1317. https://doi.org/10.3852/09-083

An DY, Liang ZQ, Jiang S, Su MS, Zeng NK (2017) *Cantharellus hainanensis* a new species with a smooth hymenophore from tropical China. Mycoscience 58(6): 438–444. https://doi.org/10.1016/j.myc.2017.06.004

Anonymous (1969) Flora of British Fungi. Colour Identification Chart. Her Majesty's Stationery Office, London.

Ariyawansa HA, Hyde KD, Jayasiri SC, Buyck B, Kandawatte TC, Dai DQ, Dai YC, Daranagama DA, Jayawardena RS, Lücking R, Nejhad MG, Niskanen T, Thambugala KM, Voigt K, Zhao RL, Li GJ, Doilom M, Boonmee S, Yang ZL, Cai Q, Cui YY, Bahkali AH, Chen J, Cui BK, Chen JJ, Dayarathne MC, Dissanayake AJ, Ekanayaka AH, Hashimoto A, Hongsanan S, Gareth Jones EB, Larsson E, Li WJ, Li QR, Liu JK, Luo ZL, Maharachchikumbura SSN, Mapook A, McKenzie EHC, Norphanphoun C, Konta S, Pang KL, Perera RH, Phookamsak R, Phukhamsakda C, Pinruan U, Randrianjohany E, Singtripop C, Tanaka K, Tian CM, Tibpromma S, Abdel-Wahab MA, Wanasinghe DN, Wijayawardene NN, Zhang JF, Zhang H, Abdel-Aziz FA, Wedin M, Westberg M, Ammirati JF, Bulgakov T, Lima DX, Callaghan TM, Callac P, Chang CH, Coca LF, Dal-Forno M, Flad V, Fliegerová K, Greiner K, Griffith GW, Ho HM, Valerie H, Jeewon R, Kang JC, Wen TC, Kirk PM, Kytövuori I, Lawrey J, Xing J, Li H, Liu ZY, Liu XZ, Liimatainen K, Lumbsch T, Matsumura M, Moncada B, Nuankaew S, Parnmen S, Santiago A, Sommai S, Song Y, Souza CAF, Souza-Motta CM, Su HY, Suetrong S, Wang Y, Wei SF, Wen TC, Yuan HS, Zhou LW, Réblová M, Fournier J, Erio C, Luangsa-Ard JJ, Tasanathai K, Khonsanit A, Thanakitpipattana D, Somrithipol S, Diederich P, Millanes AM, Common R, Stadler M, Yan J, Li XH, Lee HW, Nguyen TTT, Lee HB, Battistin E, Marsico O, Vizzini A, Vila J, Ercole E, Eberhardt U, Simonini G, Wen HA, Chen XH (2015) Fungal diversity notes 111–252—Taxonomic and phylogenetic contributions to fungal taxa. Fungal Diversity 75(1): 27–274. https://doi.org/10.1007/s13225-015-0346-5

Bernicchia A, Gorjón SP (2010) Fungi Europaei 12: Corticiaceae s.l.; Edizioni Candusso Publishers, Salamanca, Spain, 1–1007.

Bernicchia A, Langer GJ, Gorjón SP (2010) *Botryobasidium sassofratinoense* sp. nov. (Cantharellales, Basidiomycota) from Italy. Mycotaxon 111(1): 403–409. https://doi.org/10.5248/111.403

Běťák J, Holec J, Beran M, Riebesehl J (2021) Ecology and distribution of *Kneiffiella curvispora* (Hymenochaetales, Basidiomycota) in Central Europe and its phylogenetic placement. Nova Hedwigia 113(1–2): 161–189. https://doi.org/10.1127/nova_hedwigia/2021/0635

Bondartseva MA, Zmitrovich IV (2023) Order Cantharellales: Taxonomic and ecological diversification. Biology Bulletin Reviews 13(S1): S1–S16. https://doi.org/10.1134/S2079086423070046

Brazee NJ (2015) Phylogenetic relationships among species of *Phellinus* sensu stricto, cause of white trunk rot of hardwoods, from Northern North America. Forests 6(11): 4191–4211. https://doi.org/10.3390/f6114191

Brazee NJ, Lindner DL (2013) Unravelling the *Phellinus pini* s.l. complex in North America: A multilocus phylogeny and differentiation analysis of *Porodaedalea*. Forest Pathology 43(2): 132–143. https://doi.org/10.1111/efp.12008

Cao T, Hu YP, Yu JR, Wei TZ, Yuan HS (2021) A phylogenetic overview of the Hydnaceae (Cantharellales, Basidiomycota) with new taxa from China. Studies in Mycology 99(1): 100–121. https://doi.org/10.1016/j.simyco.2021.100121

Cheewangkoon R, Groenewald JZ, Summerell B, Hyde KD, To-Anun C, Crous PW (2009) Myrtaceae, a cache of fungal biodiversity. Persoonia 23(1): 55–85. https://doi.org/10.3767/003158509X474752

Chen YY, Cui BK (2015) Phylogenetic analysis and taxonomy of the *Antrodia heteromorpha* complex in China. Mycoscience 57(1): 1–10. https://doi.org/10.1016/j.myc.2015.07.003

Chen Q, Yuan Y (2017) A new species of *Fuscoporia* (Hymenochaetales, Basidiomycota) from Southern China. Mycosphere 8(6): 1238–1245. https://doi.org/10.5943/mycosphere/8/6/9

Chen JZ, Zhao CL (2020) Morphological and molecular identification of four new resupinate species of *Lyomyces* (Hymenochaetales) from Southern China. MycoKeys 65: 101–118. https://doi.org/10.3897/mycokeys.65.48660

Chen JJ, Shen LL, Cui BK (2014) *Amylosporus succulentus* sp. nov. (Russulales, Basidiomycota) evidenced by morphological characters and phylogenetic analysis. Cryptogamie. Mycologie 35(3): 271–282. https://doi.org/10.7872/crym.v35.iss3.2014.271

Chen JJ, Zhou LW, Ji XH, Zhao CL (2016) *Hyphodontia dimitica* and *H. subefibulata* spp. nov. (Schizoporaceae, Hymenochaetales) from Southern China based on morphological and molecular characters. Phytotaxa 269(1): 1–13. https://doi.org/10.11646/phytotaxa.269.1.1

Chen CC, Wu SH, Chen CY (2017) Three new species of *Hyphodontia* s.l. (Basidiomycota) with poroid or raduloid hymenophore. Mycological Progress 16(5): 553–564. https://doi.org/10.1007/s11557-017-1286-0

Cho Y, Kim D, Lim YW (2024) Phylogenetic assessment of understudied families in Hymenochaetales (Basidiomycota, Fungi)-reporting uncovered species and reflecting the recent taxonomic updates in the republic of Korea. Journal of Microbiology 62(6): 429–447. https://doi.org/10.1007/s12275-024-00120-5

Cui BK, Li HJ, Ji X, Zhou JL, Song J, Si J, Yang ZL, Dai YC (2019) Species diversity, taxonomy and phylogeny of Polyporaceae (Basidiomycota) in China. Fungal Diversity 97(1): 137–392. https://doi.org/10.1007/s13225-019-00427-4

Dai YC (2010) Hymenochaetaceae (Basidiomycota) in China. Fungal Diversity 45(1): 131–343. https://doi.org/10.1007/s13225-010-0066-9

Decock C, Figueroa SA, Robledo G, Castillo G (2007) *Fomitiporia punctata* (Basidiomycota, Hymenochaetales) and its presumed taxonomic synonyms in America: Taxonomy and phylogeny of some species from tropical/subtropical areas. Mycologia 99(5): 733–752. https://doi.org/10.1080/15572536.2007.11832537

Delgersaikhan N, Odkhuu E, Khaltar P, Samdan E, Dugarsuren U, Dalkhsuren S, Dorjkhuu A, Aldartsogt D, Amgalanbaatar A (2024) Antidiabetic activity of *Inonotus obliquus* water extract in alloxan-induced diabetic mice. Journal of Complementary & Integrative Medicine 21(4): 472–480. https://doi.org/10.1515/jcim-2024-0316

Diederich P, Lawrey J, Capdet M, Pereira S, Romero AI, Etayo J, Flakus A, Sikaroodi M, Ertz D (2014) New lichen-associated bulbil forming species of Cantharellales (Basidiomycetes). Lichenologist (London, England) 46(3): 333–347. https://doi.org/10.1017/S0024282913000583

Dong JH, He X, Zhao CL (2021) *Skvortzovia yunnanensis* sp. nov. a new species of corticioid fungus from Southern China. Kew Bulletin 76(2): 549–555. https://doi.org/10.1007/s12225-021-09959-y

Dong JH, Gu JY, Zhao CL (2023) Diversity of wood-decaying fungi in Wenshan Area, Yunnan Province, China. Mycosystema 42(3): 638–662. https://doi.org/10.13346/j.mycosystema.220205

Dong JH, Li Q, Yuan Q, Luo YX, Zhang XC, Dai YF, Zhou Q, Liu XF, Deng YL, Zhou HM, Zhao CL, Akmal M (2024a) Species diversity, taxonomy, molecular systematics and divergence time of wood-inhabiting fungi in Yunnan-Guizhou Plateau, Asia. Mycosphere 15(1): 1110–1293. https://doi.org/10.5943/mycosphere/15/1/10

Dong JH, Wang XY, He SY, Zhang JL, Yin HJ, Zhang SH, Zhao CL (2024b) *Botryobasidium bambusinum* (Botryobasidiaceae, Cantharellales): A new species from Yunnan, Southwest China, based on morphology and phylogeny. New Zealand Journal of Botany 1–18. https://doi.org/10.1080/0028825X.2024.2438181

Donk MA (1956) Notes on resupinate Hymenomycetes-II. The tulasnelloid fungi. Reinwardtia 3(3): 363–379.

Du R, Wu F, Gate GM, Dai YC, Tian XM (2020) Taxonomy and phylogeny of *Sidera* (Hymenochaetales, Basidiomycota): Four new species and keys to species of the genus. MycoKeys 68: 115–135. https://doi.org/10.3897/mycokeys.68.53561

Dunham SM, O'dell T, Molina R (2003) Analysis of nrDNA sequences and microsatellite allele frequencies reveals a cryptic chanterelle species *Cantharellus cascadensis* sp. nov. from the American Pacific Northwest. Mycological Research 107(10): 1163–1177. https://doi.org/10.1017/S0953756203008475

Eriksson J, Ryvarden L (1973) The Corticiaceae of North Europe, 2. Fungiflora Publishers, Norway.

Eriksson J, Ryvarden L (1976) The Corticiaceae of North Europe, 4. Fungiflora Publishers, Norway.

Fernandez-Lopez J, Telleria MT, Duenas M, Laguna-Castro M, Schliep K, Martín MP (2020) Linking morphological and molecular sources to disentangle the case of *Xylodon australis*. Scientific Reports 10(1): 2045–2322. https://doi.org/10.1038/s41598-020-78399-8

Freire RBM, Soares AM (2024) Taxonomic study of Hymenochaetaceae species (Agaricomycetes, Basidiomycota) in the municipalities of Tomé-Açu and Bujaru, Pará, Brazil. Anais da Academia Brasileira de Ciências 96(suppl 1): e20230338. https://doi.org/10.1590/0001-3765202420230338

Frey W, Hurka K, Oberwinkler F (1977) Beiträge zur Biologie der niederen Pflanzen. Systematik, Stammesgeschichte, ökologie. Gustav Fischer Verlag, Stuttgart/New York.

Fukami T, Dickie IA, Wilkie P, Paulus BC, Park D, Roberts A, Buchanan PK, Allen RB (2010) Assembly history dictates ecosystem functioning: Evidence from wood decomposer communities. Ecology Letters 13(6): 675–684. https://doi.org/10.1111/j.1461-0248.2010.01465.x

Girometta CE, Bernicchia A, Baiguera RM, Bracco F, Buratti S, Cartabia M, Picco AM, Savino E (2020) An Italian research culture collection of wood decay fungi. Diversity 12(2): 58. https://doi.org/10.3390/d12020058

Gonzalez D, Carling DE, Kuninaga S, Vilgalys R, Cubeta MA (2001) Ribosomal DNA systematics of *Ceratobasidium* and *Thanatephorus* with *Rhizoctonia* anamorphs. Mycologia 93(6): 1138–1150. https://doi.org/10.1080/00275514.2001.12063247

Gorjón SP, Hallenberg N (2008) New records of *Sistotrema* species (Basidiomycota) from the Iberian Peninsula. Sydowia 60(2): 205–212.

Gottlieb AM, Wright JE, Moncalvo JM (2002) *Inonotus* s. l. in Argentina-morphology, cultural characters and molecular analyses. Mycological Progress 1(3): 299–313. https://doi.org/10.1007/s11557-006-0028-5

Gray SF (1821) A natural arrangement of British plants. Nabu Press, London, UK, 649 pp.

Greslebin A, Rajchenberg M (2000) The genus *Hyphodontia* in the Patagonian Andes Forest of Argentina. Mycologia 92(6): 1155–1165. https://doi.org/10.1080/00275514.2000.12061263

Guan QX, Zhao TJ, Zhao CL (2020) Morphological characters and phylogenetic analyses reveal two new species of *Peniophorella* from Southern China. Mycological Progress 19(4): 397–404. https://doi.org/10.1007/s11557-020-01568-6

Guan QX, Huang J, Huang J, Zhao CL (2023) Five new species of Schizoporaceae (Basidiomycota, Hymenochaetales) from East Asia. MycoKeys 96: 25–56. https://doi.org/10.3897/mycokeys.96.99327

Hall TA (1999) Bioedit: A user-friendly biological sequence alignment editor and analysis program for windows 95/98/NT. Nucleic Acids Symposium Series 41: 95–98. https://doi.org/10.1021/bk-1999-0734.ch008

He SH, Li HJ (2012) *Pseudochaete latesetosa* and *P. subrigidula* spp. nov. (Hymenochaetales, Basidiomycota) from China based on morphological and molecular characters. Mycological Progress 12(2): 331–339. https://doi.org/10.1007/s11557-012-0838-6

He X, Shi ZJ, Zhao CL (2020) Morphological and molecular identification of two new species of *Tubulicrinis* (Hymenochaetaceae, Hymenochaetales) from Southern China. Mycoscience 61(4): 184–189. https://doi.org/10.1016/j.myc.2020.03.008

He MQ, Cao B, Liu F, Boekhout T, Denchev TT, Schoutteten N, Denchev CM, Kemler M, Gorjón SP, Begerow D, Valenzuela R, Davoodian N, Niskanen T, Vizzini A, Redhead SA, Ramírez CV, Papp V, Dudka VA, Dutta AK, García SR, Liu XZ, Kijpornyongpan T, Savchenko A, Tedersoo L, Theelen B, Trierveiler PL, Wu F, Zamora JC, Zeng XY, Zhou LW, Liu SL, Ghobad NM, Giachini AJ, Li GJ, Kakishima M, Olariaga I, Haelewaters D, Sulistyo B, Sugiyama J, Svantesson S, Yurkov A, Alvarado P, Antonín V, da Silva AF, Druzhinina I, Gibertoni TB, Guzmán DL, Justo A, Karunarathna SC, Galappaththi MCA, Toome HM, Hosoya T, Liimatainen K, Márquez R, Mešić A, Moncalvo JM, Nagy LG, Varga T, Orihara T, Raymundo T, Salcedo I, Silva FAGS, Tkalčec Z, Wartchow F, Zhao CL, Bau T, Cabarroi HM, Cortés PA, Decock C, Lange RD, Weiss M, Menolli JN, Nilsson RH, Fan YG, Verbeken A, Gaforov Y, Meiras OA, Mendes ARL, Zeng NK, Wu Q, Hyde KD, Kirk PM, Zhao RL (2024) Phylogenomics, divergence times and notes of orders in Basidiomycota. Fungal Diversity 126(3): 127–406. https://doi.org/10.1007/s13225-024-00535-w

Hibbett DS, Bauer R, Binder M, Giachini AJ, Hosaka K, Justo A, Larsson E, Larsson KH, Lawrey JD, Miettinen O, Nagy LG, Nilsson RH, Weiss M, Thorn RG (2014) 14 Agaricomycetes. In: McLaughlin D, Spatafora J (Eds) Systematics and evolution. The Mycota (A comprehensive treatise on fungi as experimental systems for basic and applied research), vol 7A. Springer, Berlin, 373–429. https://doi.org/10.1007/978-3-642-55318-9_14

Hjortstam K, Ryvarden L, Iturriaga T (2005) Studies in corticioid fungi from Venezuela II (Basidiomycotina, Aphyllophorales). Synopsis Fungorum 20: 42–78.

Hu YW, Karunarathna SC, Li HL, Galappaththi MA, Zhao CL, Kakumyan P, Mortimer PE (2022) The impact of drying temperature on basidiospore size. Diversity 14(4): 239. https://doi.org/10.3390/d14040239

Jang Y, Jang S, Min M, Hong JH, Lee H, Lee AH, Lim YW, Kim JJ (2015) Comparison of the diversity of Basidiomycetes from dead wood of the *Manchurian fir* (*Abies holophylla*) as evaluated by fruiting body collection, mycelial isolation, and 454 Sequencing. Microbial Ecology 70(3): 634–645. https://doi.org/10.1007/s00248-015-0616-5

Jang Y, Jang S, Lee J, Lee H, Lim YW, Kim C, Kim JJ (2016) Diversity of wood inhabiting polyporoid and corticioid fungi in Odaesan National Park, South Korea. Mycobiology 44(4): 217–236. https://doi.org/10.5941/MYCO.2016.44.4.217

Ji HX, Vlasak J, Tian MX, Dai CY (2018) Three new species of *Fomitiporella* (Hymenochaetales, Basidiomycota) based on the evidence from morphology and DNA sequence data. MycoKeys 30(30): 73–89. https://doi.org/10.3897/mycokeys.30.23109

Kalyaanamoorthy S, Minh BQ, Wong TKF, Haeseler A, Jermiin LS (2017) ModelFinder: Fast model selection for accurate phylogenetic estimates. Nature Methods 14(6): 587–589. https://doi.org/10.1038/nmeth.4285

Katoh K, Rozewicki J, Yamada KD (2019) MAFFT online service: Multiple sequence alignment, interactive sequence choice and visualization. Briefings in Bioinformatics 20(4): 1160–1166. https://doi.org/10.1093/bib/bbx108

Korotkin HB, Swenie RA, Miettinen O, Budke JM, Chen KH, Lutzoni F, Smith ME, Matheny PB (2018) Stable isotope analyses reveal previously unknown trophic mode diversity in the Hymenochaetales. American Journal of Botany 105(11): 1869–1887. https://doi.org/10.1002/ajb2.1183

Kotiranta H, Saarenoksa R (1990) Reports of Finnish corticolous Aphyllophorales (Basidiomycetes). Karstenia 30(2): 43–69. https://doi.org/10.29203/ka.1990.280

Kotiranta H, Saarenoksa R (2000) Three new species of *Hyphodontia* (Corticiaceae). Annales Botanici Fennici 37(4): 255–278.

Kotiranta H, Saarenoksa R (2005) *Ceratobasidium* and *Oliveonia* (Basidiomycota, Aphyllophorales) in Finland. Annales Botanici Fennici 42(4): 237–245. https://doi.org/10.3732/ajb.92.1.179

Kumari D, Upadhyay RC, Reddy MS (2012) *Craterellus indicus* sp. nov., a new species associated with *Cedrus deodara* from the Western Himalayas, India. Mycological Progress 11(3): 769–774. https://doi.org/10.1007/s11557-011-0788-4

Langer G, Langer E (1998) *Haplotrichum parmastii* sp. nov. collected in Costa Rica. Folia Cryptogamica Estonica 33: 63–69.

Langer G, Langer E, Chen CJ (2000a) *Botryobasidium musaisporum* sp. nov. collected in Taiwan. Mycological Research 104(4): 510–512. https://doi.org/10.1017/S0953756299002336

Langer G, Langer E, Oberwinkler F, Chen J (2000b) Speciation of *Botryobasidium subcoronatum* (Basidiomycota) collected in Taiwan: Morphology, mating tests, and molecular data. Mycoscience 41(3): 201–210. https://doi.org/10.1007/BF02489672

Langer EJ, Běťák J, Holec J, Klug A, Riebesehl J (2022) *Kneiffiella altaica* and *Kneiffiella subaltaica* sp. nov. – a rare species found in European old-growth forests and a closely related new species from North America. Nova Hedwigia 115(1–2): 205–225. https://doi.org/10.1127/nova_hedwigia/2022/0709

Larsson KH (2007) Re-thinking the classification of corticioid fungi. Mycological Research 111(9): 1040–1063. https://doi.org/10.1016/j.mycres.2007.08.001

Larsson KH, Larsson E, Koljalg U (2004) High phylogenetic diversity among corticioid homobasidiomycetes. Mycological Research 108(9): 983–1002. https://doi.org/10.1017/S0953756204000851

Larsson KH, Parmasto E, Fischer M, Langer E, Nakasone KK, Redhead SA (2006) Hymenochaetales: A molecular phylogeny for the hymenochaetoid clade. Mycologia 98(6): 926–936. https://doi.org/10.1080/15572536.2006.11832622

Lawrey JD, Zimmermann E, Sikaroodi M, Diederich P (2016) Phylogenetic diversity of bulbil-forming lichenicolous fungi in Cantharellales including a new genus and species. The Bryologist 119(4): 341–349. https://doi.org/10.1639/0007-2745-119.4.341

Leacock PR, Riddell J, Wilson AW, Zhang R, Ning C, Mueller GM (2016) *Cantharellus chicagoensis* sp. nov. is supported by molecular and morphological analysis as a new *yellow chanterelle* in midwestern United States. Mycologia 108(4): 765–772. https://doi.org/10.3852/15-230

Lin YC, Chen CY, Chen CC, Wu SH (2023) *Inonotus chrysomarginatus*, a newly recorded species in Taiwan, and a list of Taiwan's known *Inonotus* species as well as segregated species from the genus. Fungi Science 38(1): 1–12.

Liu SL, Gafforov Y, Zhang XY, Wang HL, Wang XW, Zhou LW (2019) Reinstatement of the corticioid genus *Leifia* (Hymenochaetales, Basidiomycota) with a new species *L. brevispora* from Hubei, Central China. MycoKeys 51: 85–96. https://doi.org/10.3897/mycokeys.51.33262

Liu ZB, Zhou M, Yuan Y, Dai YC (2021) Global diversity and taxonomy of *Sidera* (Hymenochaetales, Basidiomycota): Four new species and keys to species of the genus. Journal of Fungi 7(4): 251. https://doi.org/10.3390/jof7040251

Liu ZB, Zhou M, Wu F, Yu J (2022) Two New Species of *Sidera* (Hymenochaetales, Basidiomycota) from Southwest China. Journal of Fungi 8(4): 385. https://doi.org/10.3390/jof8040385

Liu SL, Wang XW, Li GJ, Deng CY, Rossi W, Leonardi M, Liimatainen K, Kekki T, Niskanen T, Smith ME, Ammirati J, Bojantchev D, Abdel-Wahab MA, Zhang M, Tian E, Lu Y-Z, Zhang J-Y, Ma J, Dutta AK, Acharya K, Du T-Y, Xu J, Kim JS, Lim YW, Gerlach A, Zeng N-K, Han Y-X, Razaghi P, Raza M, Cai L, Calabon MS, Jones EBG, Saha R, Kumar TKA, Krishnapriya K, Thomas A, Kaliyaperumal M, Kezo K, Gunaseelan S, Singh SK, Singh PN, Lagashetti AC, Pawar KS, Jiang S, Zhang C, Zhang H, Qing Y, Bau T, Peng X-C, Wen T-C, Ramirez NA, Niveiro N, Li M-X, Yang ZL, Wu G, Tarafder E, Tennakoon DS, Kuo C-H, da Silva TM, Souza-Motta CM, Bezerra JDP, He G, Ji X-H, Suwannarach N, Kumla J, Lumyong S, Wannathes N, Rana S, Hyde KD, Zhou L-W (2024) Fungal diversity notes 1717–1817: Taxonomic and phylogenetic contributions on family, genera and species of fungal taxa. Fungal Diversity 124(6): 1–216. https://doi.org/10.1007/s13225-023-00529-0

Luo KY, Zhao CL (2021) *Fasciodontia yunnanensis* (Schizoporaceae, Hymenochaetales), a new species from Southern China. Annales Botanici Fennici 58(4–6): 259–266. https://doi.org/10.5735/085.058.0411

Luo KY, Qu MH, Zhao CL (2021) Additions to the knowledge of corticioid *Xylodon* (Schizoporaceae, Hymenochaetales): Introducing three new *Xylodon* species from Southern China. Diversity 13(11): 581. https://doi.org/10.3390/d13110581

Luo KY, Chen ZY, Zhao CL (2022) Phylogenetic and taxonomic analyses of three new wood-inhabiting fungi of *Xylodon* (Basidiomycota) in a forest ecological system. Journal of Fungi 8(4): 405. https://doi.org/10.3390/jof8040405

Luo KY, Su JQ, Zhao CL (2024) Morphological and molecular identification for four new wood inhabiting species of *Trechispora* (Basidiomycota) from China. MycoKeys 105: 155–178. https://doi.org/10.3897/mycokeys.105.120438

M'Barek HN, Arif S, Taidi B, Hajjaj H (2020) Consolidated bioethanol production from olive mill waste: Wood-decay fungi from central Morocco as promising decomposition and fermentation biocatalysts. Biotechnology Reports 28: 1–10. https://doi.org/10.1016/j.btre.2020.e00541

Ma X, Zhao CL (2021) *Xylodon bambusinus* and *X. xinpingensis* spp. nov. (Hymenochaetales) from Southern China. Phytotaxa 511(3): 231–247. https://doi.org/10.11646/phytotaxa.511.3.3

Masumoto H, Degawa Y (2020) *Bryoclavula phycophila* gen. et sp. nov. belonging to a novel lichenised lineage in Cantharellales (Basidiomycota). Mycological Progress 19(7): 705–714. https://doi.org/10.1007/s11557-020-01588-2

Miller MA, Pfeiffer W, Schwartz T (2010) Creating the CIPRES science gateway for inference of large phylogenetic trees. Proceedings of the Gateway Computing Environments Workshop, New Orleans, 8 pp. https://doi.org/10.1109/GCE.2010.5676129

Moncalvo JM, Nilsson RH, Koster B, Dunham SM, Bernauer T, Matheny PB, Porter TM, Margaritescu S, Weiss M, Garnica S, Danell E, Langer GJ, Langer EJ, Larsson E, Larsson KH, Vilgalys R (2006) The cantharelloid clade: Dealing with incongruent gene trees and phylogenetic reconstruction methods. Mycologia 98(6): 937–948. https://doi.org/10.1080/15572536.2006.11832623

Oberwinkler F (1982) The Significance of the Morphology of the Basidium in the Phylogeny of Basidiomycetes. In: Wells K, Wells EK (Eds) Basidium and Basidiocarp. Springer Series in Microbiology. Springer, New York, NY, 9–35. https://doi.org/10.1007/978-1-4612-5677-9_2

Oberwinkler F, Cruz D, Suárez JP (2017) Biogeography and ecology of Tulasnellaceae. Biogeography of Mycorrhizal Symbiosis 230: 237–271. https://doi.org/10.1007/978-3-319-56363-3_12

Olariaga I, Buyck B, Esteve-Raventós F, Valerie H, Manjón JL, Moreno G, Salcedo I (2015) Assessing the taxonomic identity of white and orange specimens of *Cantharellus*: Occasional colour variants or independent species? Cryptogamie. Mycologie 36(4): 1–14. https://doi.org/10.7872/crym/v36.iss3.2015.287

Olariaga I, Moreno G, Manjon JL, Salcedo I, Hofstetter V, Rodriguez D, Buyck B (2017) *Cantharellus* (Cantharellales, Basidiomycota) revisited in Europe through a multigene phylogeny. Fungal Diversity 83(1): 263–292. https://doi.org/10.1007/s13225-016-0376-7

Olariaga I, Huhtinen S, Laessoe T, Petersen JH, Hansen K (2020) Phylogenetic origins and family classification of typhuloid fungi, with emphasis on *Ceratellopsis*, *Macrotyphula* and *Typhula* (Basidiomycota). Studies in Mycology 96(11): 155–184. https://doi.org/10.1016/j.simyco.2020.05.003

Petersen JH (1996) Farvekort. The Danish Mycological Society's colour-chart. Foreningen til Svampekundskabens Fremme, Greve, 6 pp.

Phookamsak R, Hyde K, Jeewon R, Bhat DJ, Jones EBG, Maharachchikumbura S, Raspé O, Karunarathna SC, Wanasinghe DN, Hongsanan S, Doilom M, Tennakoon DA, Machado AR, Firmino AL, Ghosh A, Karunarathna A, Mesic A, Dutta AK, Karbowy-Thongbai B, Devadatha B, Norphanphoun C, Senwanna C, Deping W, Pem D, Ackah FK, Wang GN, Jiang HB, Madrid H, Lee HB, Goonasekara ID, Manawasinghe I, Kušan I, Cano J, Gené J, Li JF, Das K, Acharya K, Raj KNA, Latha KPD, Kandawatte TC, He MQ, Dueñas M, Jadan M, Martín MP, Samarakoon MC, Samarakoon M, Raza M, Park MS, Telleria MT, Chaiwan N, Matočec N, Silva NI, Pereira OL (2019) Fungal diversity notes 929–1035: Taxonomic and phylogenetic contributions on genera and species of fungi. Fungal Diversity 95(1): 1–273. https://doi.org/10.1007/s13225-019-00421-w

Ponce Á, Salerni E, D'Aguanno MN, Perini C (2023) Wood-decay fungi fructifying in Mediterranean deciduous oak forests: A community composition, richness and productivity study. Forests 14(7): 1326. https://doi.org/10.3390/f14071326

Purahong W, Wubet T, Krüger D, Buscot F (2018) Molecular evidence strongly supports dead wood-inhabiting fungi exhibiting unexpected tree species preferences in temperate forests. The ISME Journal 12(1): 289–295. https://doi.org/10.1038/ismej.2017.177

Qu MH, Zhao CL (2022) *Xylodon flocculosus* sp. nov. from Yunnan, China. Mycotaxon 137(2): 189–201. https://doi.org/10.5248/137.189

Qu MH, Wang DQ, Zhao CL (2022) A phylogenetic and taxonomic study on *Xylodon* (Hymenochaetales): Focusing on three new *Xylodon* species from Southern China. Journal of Fungi 8(1): 35. https://doi.org/10.3390/jof8010035

Rathnayaka AR, Tennakoon DS, Jones GE, Wanasinghe DN, Bhat DJ, Priyashantha AH, Stephenson SL, Tibpromma S, Karunarathna SC (2024) Significance of precise documentation of hosts and geospatial data of fungal collections, with an emphasis on plant-associated fungi. New Zealand Journal of Botany, 1–28. https://doi.org/10.1080/0028825X.2024.2381734

Rehner SA, Samuels GJ (1994) Taxonomy and phylogeny of *Gliocladium* analysed from nuclear large subunit ribosomal DNA sequences. Mycological Research 98(6): 625–634. https://doi.org/10.1016/S0953-7562(09)80409-7

Riebesehl J, Langer E (2017) *Hyphodontia* s.l. (Hymenochaetales, Basidiomycota): 35 new combinations and new keys to currently all 120 species. Mycological Progress 16(6): 637–666. https://doi.org/10.1007/s11557-017-1299-8

Riebesehl J, Yurchenko E, Nakasone KK, Langer E (2019) Phylogenetic and morphological studies in *Xylodon* (Hymenochaetales, Basidiomycota) with the addition of four new species. MycoKeys 47: 97–137. https://doi.org/10.3897/mycokeys.47.31130

Ronquist F, Huelsenbeck JP (2003) MrBayes 3: Bayesian phylogenetic inference under mixed models. Bioinformatics 19(12): 1572–1574. https://doi.org/10.1093/bioinformatics/btg180

Rosenthal L, Larsson KH, Branco S, Chung JA, Glassman SI, Liao HL, Peay K, Smith DP, Talbot JM, Taylor JW, Vellinga E, Vilgalys R, Bruns TD (2017). Survey of corticioid fungi in North American pinaceous forests reveals hyperdiversity, underpopulated sequence databases, and species that are potentially ectomycorrhizal. Mycologia 109(1): 115–127. https://doi.org/10.1080/00275514.2017.1281677

Runnel K, Miettinen O, Lõhmus A (2021) Polypore fungi as a flagship group to indicate changes in biodiversity–a test case from Estonia. IMA Fungus 12(1): 1–31. https://doi.org/10.1186/s43008-020-00050-y

Suhara H, Kurogi S (2015) *Cantharellus cyphelloides* (Cantharellales), a new and unusual species from a Japanese evergreen broad-leaved forest. Mycological Progress 14(8): 55. https://doi.org/10.1007/s11557-015-1079-2

Swenie RA, Looney B, Ke YH, Rojas JA, Cubeta MA, Langer GJ, Vilgalys R, Matheny PB (2023) PacBio high-throughput multi-locus sequencing reveals high genetic diversity in mushroom-forming fungi. Molecular Ecology Resources 24(15): e13885. https://doi.org/10.1111/1755-0998.13885

Vilgalys R, Hester M (1990) Rapid genetic identification and mapping of enzymatically amplified ribosomal DNA from several *Cryptococcus* species. Journal of Bacteriology 172(8): 4238–4246. https://doi.org/10.1128/jb.172.8.4238-4246.1990

Viner I, Spirin V, Zíbarová L, Larsson KH (2018) Additions to the taxonomy of *Lagarobasidium* and *Xylodon* (Hymenochaetales, Basidiomycota). MycoKeys 41: 65–90. https://doi.org/10.3897/mycokeys.41.28987

Viner I, Bortnikov F, Ryvarden L, Miettinen O (2021) On six African species of *Lyomyces* and *Xylodon.* Fungal Systematics and Evolution 8: 163–178. https://doi.org/10.3114/fuse.2021.08.13

Viner I, Spirin V, Larsson KH, Miettinen O (2023) Systematic placement of *Lagarobasidium cymosum* and description of two new species. Mycologia 115(1): 122–134. https://doi.org/10.1080/00275514.2022.2146978

Viner I, Larsson KH, Spirin V, Langer EJ, Miettinen O (2024) Revision of *Kneiffiella* with segregation of *Egonia* gen. nov. (Hymenochaetales, Agaricomycetes): How similar morphology can hide taxonomic diversity in the molecular era. Persoonia 53: 1–28. https://doi.org/10.3767/persoonia.2024.53.01

Vu D, Groenewald M, de Vries M, Gehrmann T, Stielow B, Eberhardt U, Al-Hatmi AMS, Groenewald JZ, Cardinali G, Houbraken J, Boekhout T, Crous PW, Robert V, Verkley GJM (2018) Large-scale generation and analysis of filamentous fungal DNA barcodes boosts coverage for kingdom fungi and reveals thresholds for fungal species and higher taxon delimitation. Studies in Mycology 92(1): 135–154. https://doi.org/10.1016/j.simyco.2018.05.001

Wagner T, Fischer M (2002) Proceedings towards a natural classification of the worldwide taxa *Phellinus* s.l. and *Inonotus* s.l., and phylogenetic relationships of allied genera. Mycologia 94(6): 998–1016. https://doi.org/10.1080/15572536.2003.11833156

Wang XW, Zhou LW (2024) Umbellaceae fam. nov. (Hymenochaetales, Basidiomycota) for *Umbellus sinensis* gen. et sp. nov. and three new combinations. Journal of Fungi 10(1): 22. https://doi.org/10.3390/jof10010022

Wang XW, May TW, Liu SL, Zhou LW (2021) Towards a Natural Classification of *Hyphodontia* sensu lato and the trait evolution of basidiocarps within Hymenochaetales (Basidiomycota). Journal of Fungi 7(6): 478. https://doi.org/10.3390/jof7060478

Wang XW, Jiang JH, Liu SL, Gafforov Y, Zhou LW (2022) Species diversification of the coniferous pathogenic fungal genus *Coniferiporia* (Hymenochaetales, Basidiomycota) in association with its biogeography and host plants. Phytopathology 112(2): 404–413. https://doi.org/10.1094/PHYTO-05-21-0181-R

Wang XW, Liu SL, Zhou LW (2023) An updated taxonomic framework of Hymenochaetales (Agaricomycetes, Basidiomycota). Mycosphere 14(1): 452–496. https://doi.org/10.5943/mycosphere/14/1/6

Wang Y, Lai Z, Li XX, Yan RM, Zhang ZB, Yang HL, Zhu D (2016) Isolation, diversity and acetylcholinesterase inhibitory activity of the culturable endophytic fungi harboured in Huperzia serrata from Jinggang Mountain, China. World Journal of Microbiology and Biotechnology 32(2): 20. https://doi.org/110.1007/s11274-015-1966-3

White TJ, Bruns T, Lee S, Taylor J (1990) Amplification and direct sequencing of fungal ribosomal RNA genes for phylogenetics. In: MA, Gefand DH, Sninsky JJ, White MJT (Eds) PCR Protocols: a guide to methods and applications. Academic Press, San Diego, 315–322. https://doi.org/10.1016/B978-0-12-372180-8.50042-1

Wijayawardene NN, Hyde KD, Dai DQ, Sánchez-García M, Goto B, Saxena RK, Erdoğdu M, Selçuk F, Rajeshkumar KC, Aptroot A, Błaszkowski J, Boonyuen N, da Silva GA, de Souza FA, Dong W, Ertz D, Haelewaters D, Jones EBG, Karunarathna SC, Kirk PM, Kukwa M, Kumla J, Leontyev DV, Lumbsch HT, Maharachchikumbura SSN, Marguno F, Martínez-Rodríguez P, Mešić A, Monteiro JS, Oehl F, Pawłowska J, Pem D, Pfliegler WP, Phillips AJL, Pošta A, He MQ, Li JX, Raza M, Sruthi OP, Suetrong S, Suwannarach N, Tedersoo L, Thiyagaraja V, Tibpromma S, Tkalčec Z, Tokarev YS, Wanasinghe DN, Wijesundara DSA, Wimalaseana SDMK, Madrid H, Zhang GQ, Gao Y, Sánchez-Castro I, Tang LZ, Stadler M, Yurkov A, Thines M (2022) Outline of Fungi and fungus-like taxa–2021. Mycosphere 13(1): 53–453. https://doi.org/10.5943/mycosphere/13/1/2

Wilson AW, Aime MC, Dierks J, Mueller GM, Henkel TW (2012) Cantharellaceae of Guyana I: New species, combinations and distribution records of *Craterellus* and a synopsis of known taxa. Mycologia 104(6): 1466–1477. https://doi.org/10.3852/11-412

Wu F, Zhou LW, Dai YC (2016) *Neomensularia duplicata* gen. et sp. nov. (Hymenochaetales, Basidiomycota) and two new combinations. Mycologia 108(5): 891–898. https://doi.org/10.3852/16-020

Wu F, Zhou LW, Josef V, Dai YC (2022) Global diversity and systematics of Hymenochaetaceae with poroid hymenophore. Fungal Diversity 113(1): 1–192. https://doi.org/10.1007/s13225-021-00496-4

Yang J, Dai LD, He SH (2016) *Hymenochaetopsis* nom. nov. proposed to replace *Pseudochaete* (Hymenochaetales, Basidiomycota) with descriptions of *H. laricicola* sp. nov and *H. gigasetosa* new to China. Mycological Progress 15(2): 13. https://doi.org/10.1007/s11557-015-1153-9

Yang Y, Jiang Q, Li Q, Yang J, Cha L, Cheng L, Yang S, Zhao C, Zhou H (2023) Molecular systematics and taxonomic analyses of three new wood-inhabiting fungi of *Hyphoderma* (Hyphodermataceae, Basidiomycota). Journal of Fungi 9(11): 1044. https://doi.org/10.3390/jof9111044

Yu HY, Zhao CL, Dai YC (2013) *Inonotus niveomarginatus* and *I. tenuissimus* spp. nov. (Hymenochaetales), resupinate species from tropical China. Mycotaxon 124(1): 61–68. https://doi.org/10.5248/124.61

Yu J, Wang XW, Liu SL, Shen S, Zhou LW (2021) Taxonomy and phylogeny of *Resinicium* sensu lato from Asia-Pacific revealing a new genus and five new species (Hymenochaetales, Basidiomycota). IMA Fungus 12(1): 19. https://doi.org/10.1186/s43008-021-00071-1

Yu SC, Lai ZX, Xue HM, Zhu JH, Yue GH, Wang JW, Jin LH (2024) *Inonotus obliquus* aqueous extract inhibits intestinal inflammation and insulin metabolism defects in *Drosophila*. Toxicology Mechanisms and Methods 34(9): 1–52. https://doi.org/10.1080/15376516.2024.2402865

Yuan Q, Zhao CL (2024) Morphology and multigene phylogeny revealed four new species of *Xylodon* (Schizoporaceae, Basidiomycota) from Southern China. MycoKeys 107: 161–187. https://doi.org/10.3897/mycokeys.107.128223

Yurchenko E (2008) Corticioid fungi (Basidiomycota) on living wooden plants in Belarus: Species inventory and host colonization strategies. Botanica Lithuanica 14(3): 177–189.

Yurchenko E, Wu SH (2014) Three new species of *Hyphodontia* with peg-like hyphal aggregations. Mycological Progress 13(3): 533–545. https://doi.org/10.1007/s11557-013-0935-1

Yurchenko E, Xiong HX, Wu SH (2013) Four new species of *Hyphodontia* (*Xylodon* s.s. Hjortstam & Ryvarden, Basidiomycota) from Taiwan. Nova Hedwigia 96(3): 545–558. https://doi.org/10.1127/0029-5035/2013/0092

Yurchenko E, Riebesehl J, Langer EJ (2017) Clarification of *Lyomyces sambuci* complex with the descriptions of four new species. Mycological Progress 16(9): 865–876. https://doi.org/10.1007/s11557-017-1321-1

Yurchenko E, Riebesehl J, Langer EJ (2020a) *Fasciodontia* gen. nov. (Hymenochaetales, Basidi omycota) and the taxonomic status of *Deviodontia*. Mycological Progress 19(2): 171–184. https://doi.org/10.1007/s11557-019-01554-7

Yurchenko E, Wu SH, Maekaw N (2020b) Three new species of *Peniophorella* (Basidiomycota) from East Asia. Nova Hedwigia 111(3): 473–495. https://doi.org/10.1127/nova_hedwigia/2020/0598

Yurchenko E, Riebesehl J, Viner I, Motato-Vásquez V, Miettinen O (2024) *Xylodon lanatus* complex and other additions to *Xylodon*. Mycological Progress 23(1): 9. https://doi.org/10.1007/s11557-024-01947-3

Zhang XC, Li YC, Wang YY, Xu Z, Zhao CL, Zhou HM (2024a) *Xylodon asiaticus* (Hymenochaetales, Basidiomycota), a new species of corticioid fungus from Southern China. Phytotaxa 634(1): 1–15. https://doi.org/10.11646/phytotaxa.634.1.1

Zhang XJ, Shi FL, Yang K, Zhao CL (2024b) The diversity and taxonomy of *Tomentella* (Thelephoraceae, Thelephorales) with descriptions of four new species from Southwestern China. MycoKeys 109: 1–29. https://doi.org/10.3897/mycokeys.109.132941

Zhao CL, Qu MH, Huang RX, Karunarathna SC (2023b) Multi-gene phylogeny and taxonomy of the wood-rotting fungal genus *Phlebia* sensu lato (Polyporales, Basidiomycota). Journal of Fungi 9(3): 201–241. https://doi.org/10.3390/jof9030320

Zhao H, Dai YC, Wu F, Liu XY, Maurice S, Krutovsky KV, Pavlov IN, Lindner DL, Martin FM, Yuan Y (2023a) Insights into the ecological diversification of the Hymenochaetales based on comparative genomics and phylogenomics with an emphasis on *Coltricia*. Genome Biology and Evolution 15(8): 136. https://doi.org/10.1093/gbe/evad136

Zhao H, Wu F, Maurice S, Pavlov I, Krutovsky K, Liu HG, Yuan Y, Dai YC (2024) Large-scale phylogenomic insights into the evolution of the Hymenochaetales. Mycology, 1–18. https://doi.org/10.1080/21501203.2024.2391527

Zhong XR, Li TH, Jiang ZD, Deng WQ, Huang H (2018) A new yellow species of *Craterellus* (Cantharellales, Hydnaceae) from China. Phytotaxa 360(1): 35. https://doi.org/10.11646/phytotaxa.360.1.3

Zhou LW, Qin WM (2011) *Inonotus* sp. nov. (Hymenochaetaceae) from Guizhou, Southwest China with a preliminary discussion on the phylogeny of its kin. Mycological Progress 11(3): 791–798. https://doi.org/10.1007/s11557-011-0792-8

Zhou LW, Qin WM (2013) *Sistotrema subconfluens* sp. nov. (Cantharellales, Basidiomycota) from Changbaishan Nature Reserve, northeastern China. Mycoscience 54(3): 178–182. https://doi.org/10.1016/j.myc.2012.08.005

Zhou LW, Wang XY (2015) *Inonotus griseus* sp. nov. from eastern China. Mycotaxon 130(3): 661–669. https://doi.org/10.5248/130.661

Zhou LW, Vlasák J, Decock C, Assefa A, Stenlid J, Abate D, Wu SH, Dai YC (2015) Global diversity and taxonomy of the *Inonotus* linteus complex (Hymenochaetales, Basidiomycota): *Sanghuangporus* gen. nov., *Tropicoporus excentrodendri* and *T. guanacastensis* gen. et spp. nov., and 17 new combinations. Fungal Diversity 77(1): 335–347. https://doi.org/10.1007/s13225-015-0335-8

Zhou JL, Zhu L, Chen H, Cui BK (2016) Taxonomy and Phylogeny of *Polyporus* Group *Melanopus* (Polyporales, Basidiomycota) from China. PLoS ONE 11(8): e0159495. https://doi.org/10.1371/journal.pone.0159495

Zhou M, Dai YC, Vlasák J, Liu HG, Yuan Y (2023) Revision and updated systematics of *Trihaptum* s.l. (Hymenochaetales, Basidiomycota). Mycosphere 14(1): 815–917. https://doi.org/10.5943/mycosphere/14/1/11

Zhou HM, Zhang XC, Li JT, Wu F, Zhao CL (2024a) Morphological characteristics and phylogenetic analyses revealed four new wood-inhabiting fungi (Agaricomycetes, Basidiomycota) in Xizang Autonomous Region, China. MycoKeys 106: 201–224. https://doi.org/10.3897/mycokeys.106.125831

Zhou Q, Jiang QQ, Yang X, Yang JW, Zhao CL, Zhao J (2024b) Phylogenetic and Taxonomic analyses of five new wood-inhabiting fungi of *Botryobasidium*, *Coltricia* and *Coltriciella* (Basidiomycota) from China. Journal of Fungi 10(3): 205. https://doi.org/10.3390/jof10030205

Zhou LJ, Li XL, Yuan HS (2024c) Three new wood inhabiting fungi of *Botryobasidium* (Cantharellales, Basidiomycota) from subtropical forests of Southwestern China. MycoKeys 109: 337–354. https://doi.org/10.3897/mycokeys.109.133325

MycoKeys 115: 137–153 (2025)
DOI: 10.3897/mycokeys.115.145774

Research Article

Morphological and multi-locus phylogenetic analyses reveal three new branched species of *Clavaria* (Clavariaceae, Agaricales) from China

Jun Yan[1,2], Li Xiong[2], Li-Xun Yang[3], Zheng-Mi He[1], Ping Zhang[1], Ke Liao[2]

1 *College of Life Science, Hunan Normal University, Changsha 410081, China*
2 *Hunan Provincial Demonstration Center of Forestry Seeding Breeding, Changsha 410329, China*
3 *Bureau of Forestry, Tongdao Dong Autonomous County, Huaihua 418500, China*
Corresponding authors: Ping Zhang (zhangping0000@163.net); Ke Liao (hncslk@126.com)

Abstract

Based on morphological and molecular evidence, 12 specimens have been identified as belonging to three previously unrecognized species of *Clavaria*, which are here described as *C. divergens*, *C. orientalis*, and *C. tongdaoensis*. *Clavaria divergens* is characterized by its branched, white basidiomata. *Clavaria orientalis* and *C. tongdaoensis* are very similar to *C. zollingeri* in the field. However, *C. orientalis* is distinguished by its more robust branches, while *C. tongdaoensis* differs by its varied or paler color of basidiomata. A concatenated sequence dataset (ITS-nrLSU-*RPB*2) was used for multi-locus phylogenetic analysis. The phylogenetic tree of *Clavaria* showed that the three branched species each formed a distinct lineage with strong support. A key to the known branched species of *Clavaria* in China is provided.

Key words: Clavariaceae, morphology, phylogeny, taxonomy

Academic editor: Bao-Kai Cui
Received: 2 January 2025
Accepted: 24 February 2025
Published: 12 March 2025

Citation: Yan J, Xiong L, Yang L-X, He Z-M, Zhang P, Liao K (2025) Morphological and multi-locus phylogenetic analyses reveal three new branched species of *Clavaria* (Clavariaceae, Agaricales) from China. MycoKeys 115: 137–153. https://doi.org/10.3897/mycokeys.115.145774

Introduction

Vaillant (1727) described three clavarioid species and first used the term “Clavaria” to name them. Subsequently, Linnaeus (1753) formally established the genus *Clavaria* Vaill. ex L. in *Species Plantarum* and described five species with branched basidiomata. However, as an increasing number of species with branches were discovered, infrageneric groups of *Clavaria* species with branched basidiomata, such as *Clavaria* α *Ramaria* Pers., *Clavaria* trib. Botryoideae Fr., and *Clavaria* trib. Ramariae Fr., were proposed (Persoon 1801; Fries 1821). With further research, species of *Clavaria* with branches have been sequentially segregated as separate genera, such as *Artomyces* Jülich, *Clavulina* J. Schröt., *Clavulinopsis* Overeem, *Ramaria* Fr. ex Bonord., and *Ramariopsis* (Donk) Corner (Corner 1950). At present, species of *Clavaria* with authentically branched fruit bodies are not common, with only seven species recognized before the present study (Léveillé 1846; Corner 1967; Lazo 1972; Furtado et al. 2016; Yan et al. 2020).

Among the seven branching species, *Clavaria griseolilacina* P. Zhang and *Clavaria sinensis* P. Zhang are native to China and were described in 2020 (Yan et al. 2020). Their type specimens have been compared with the new species identified in the current study. In addition, *Clavaria diverticulata* A.N.M. Furtado & M.A. Neves and *Clavaria martinii* Corner are recorded only in the Americas, and their basidiomata are yellow (Corner 1967; Furtado et al. 2016). Therefore, the white or slightly yellowish pink *Clavaria pumanquensis* Lazo and the cosmopolitan *Clavaria zollingeri* Lév. (Corner 1950; Lazo 1972) are more directly relevant for careful differentiation from the three new species in this study.

In China, purple branching *Clavaria* species have often been identified as *C. zollingeri* in the past. However, a comparison of specimens collected during the past 20 years has revealed a clear morphological difference between species distributed in northern and southern China. In the present study, only specimens collected in Jilin Province (northern China) have larger basidiomata and longer branches and conform with *C. zollingeri*; specimens collected in Hubei and Hunan provinces (southern China) belong to species new to science based on morphological and molecular evidence. An additional new species, *C. divergens*, has a white, stably branched basidiomata, which is a very rare character combination in *Clavaria*.

Materials and methods

Morphological examination

Twelve specimens of the three new species were collected by the authors in Hunan or Hubei provinces between 2003 and 2022. Habitat photographs of basidiomata were taken in the field, and macromorphological data were recorded from fresh specimens. The color of the basidiomata was described with reference to color codes (Kornerup and Wanscher 1978) and color names (Ridgway 1912). Specimens were deposited in the Mycological Herbarium of Hunan Normal University (MHHNU), Changsha, China, after drying. Micromorphological features were recorded from microscopic observations. The handling of dried vouchers followed the procedures of Yan et al. (2023). The abbreviation [*n*/*m*/*p*] indicates that *n* basidiospores were measured from *m* basidiomata of *p* specimens. Dimensions of basidiospores are presented in the form (a–)b–c(–d), where a and d represent extreme values, and the range b–c comprises 90% of the measured values. All measurement data were analyzed with SPSS 14.0 (SPSS, Inc.). Q is the “length/width ratio” of a basidiospore in lateral view, and Q indicates the average Q of all basidiospores ± sample standard deviation.

DNA extraction, PCR amplification, and sequencing

Total genomic DNA was extracted from dried vouchers using the modified cetyltrimethylammonium bromide method introduced by Doyle and Doyle (1987) or the Ezup Column Fungi Genomic DNA Purification Kit (Sangon Biotech, Shanghai, China). The primer pairs ITS4/ITS5 (White et al. 1990) and LR0R/LR5 (Vilgalys and Hester 1990) were used to amplify the internal transcribed spacer (ITS) region and the nuclear ribosomal large subunit (nrLSU) region, respectively. The primers f*RPB*2-5F, f*RPB*2-6F, and f*RPB*2-7.1R (Liu et al. 1999; Matheny et al. 2007) were used to amplify the RNA polymerase II second largest subunit (*RPB*2) region. The PCR reaction volume and thermal-cycling conditions followed those of Yan et al. (2022) and He et al. (2023). The PCR products were examined and sequenced by Sangon Biotech. Sequences generated in this study were deposited in GenBank.

Alignment and phylogenetic analyses

The dataset used for phylogenetic analyses included the newly generated sequences and sequences downloaded from GenBank. Detailed information on the sequences is listed in Table 1.

The ITS, nrLSU, and *RPB*2 sequences were respectively aligned using MAFFT v7.471 (Katoh and Standley 2016) and manually edited in BIOEDIT v7.2.5 (Hall 1999) where necessary. The combined matrix of ITS, nrLSU, and *RPB*2 sequences was assembled with SEQUENCEMATRIX 1.7.8 (Vaidya et al. 2011). The concatenated sequence dataset was analyzed using maximum likelihood (ML) and Bayesian inference approaches with RAXML v8.0.20 (Stamatakis 2006) and MRBAYES v3.2.7 (Ronquist and Huelsenbeck 2003), respectively. The ML analysis was conducted using the GTR+Gamma evolutionary model with 1000 bootstrap replicates. The Bayesian inference analysis ran for 1,000,000 generations using the GTR+I+G optimal evolutionary model selected with MRMODELTEST v2.4 (Nylander 2004). The phylogenetic trees were visualized using FigTree v1.4.2 (Rambaut 2012) and further refined using Adobe Photoshop CS6 and Illustrator CS5 (Adobe Systems, Inc., San Jose, CA, USA).

Results

Phylogenetic analyses

The data matrix consisted of 210 sequences (90 ITS, 88 nrLSU, and 32 *RPB*2) from 97 samples, among which 33 (12 ITS, 12 nrLSU, and 9 *RPB*2) were newly generated in the present study. The aligned concatenated ITS–nrLSU–*RPB*2 dataset, comprising a total of 2450 nucleotide positions, was used for the BI and ML analyses. The ML analysis yielded a tree topology with branch lengths and support values represented in Fig. 1, and the BI analysis yielded an almost identical phylogenetic construction (not shown). Bayesian posterior probabilities > 0.95 and bootstrap values > 50% are shown at the nodes in Fig. 1.

The ML and Bayesian analyses showed that two accessions of *Mucronella* Fr. (as the outgroup) and 54 species of *Clavaria* formed independent lineages, named Clade 1 to Clade 54 in turn. Eight main clades were resolved among the 54 species of *Clavaria*, which is similar to previous studies (Kautmanová et al. 2012; Birkebak et al. 2016). Clades 1 to 11 formed a well-supported (ML 100%/BI 1) clade (*Clavaria fumosa* clade); the *Clavaria pullei* clade (ML 100%/BI 1) included *Clavaria atroumbrina*, *Clavaria lametina*, and *Clavaria pullei*; *Clavaria* sensu stricto (ML 100%/BI 1) included the species *Clavaria aspersa*, *Clavaria fragilis* (the type for the genus), and *Clavaria rosea*; *Clavaria atrofusca* and *Clavaria griseobrunnea* formed the *Clavaria atrofusca* clade (ML 91%); and *Clavaria greletii* and *Clavaria neonignta* formed the *Clavaria greletii* clade (ML 100%/BI 1). The remaining species were resolved in three main clades; these species are united in possessing a loop-like clamp at the base of the basidium. Our three new species each formed a distinct monophyletic lineage with strong support (ML 100%/BI 1).

Table 1. Voucher information and GenBank accession of taxa used in this study.

Identification	Specimen No.	GenBank No. (ITS)	GenBank No. (28S)	GenBank No. (RPB2)	Location
Clavaria alboglobospora	JAC15834	OR567635	OR567767	–	New Zealand
C. amonenoides	Lueck4	KP965768	KP965786	–	Germany
C. amonenoides	MHHNU10306	ON228386	ON231688	ON246172	China
C. amonenoides	MHHNU10522	ON228387	ON231689	ON246173	China
C. appendiculata	AMB 18348	MN022549	MN018833	–	Italy
C. apulica	AMB 150	MT853065	MT853066	–	Italy
C. argillacea	K(M)126733	KC759438	JQ415931	–	United Kingdom
C. argillacea	BRACR 16025	KC759439	JQ415930	–	Slovakia
C. aspersa	MHHNU32157	ON228390	ON231692	ON246176	China
C. aspersa	MHHNU32397	ON228391	ON231693	ON246177	China
C. asterospora	BIO-Fungi 12390	KC759440	–	–	Spain
C. atrofusca	BRACR 13264	HQ606080	HQ606081	–	Norway
C. atroumbrina	K(M)143730	–	JN315789	–	United Kingdom
C. calabrica	ZT Myc 58697	MF972889	MF972885	–	Italy
C. californica	AMB 18558	MT055940	–	–	Italy
C. californica	TENN026785	HQ179660	–	–	USA
C. citrinorubra	TENN040464	HQ179661	HQ877686	–	Australia
C. crosslandii	BIO-Fungi 12762	KC759441	–	–	Spain
C. cupreicolor	TENN043696	KP257109	KP257187	–	New Zealand
C. divergens	**MHHNU8277**	**PQ819508**	**PQ814267**	–	**China**
C. divergens	**MHHNU9857**	**PQ819509**	**PQ814268**	**PO806984**	**China**
C. divergens	**MHHNU10164**	**PQ819510**	**PQ814269**	**PO806985**	**China**
C. divergens	**MHHNU10165**	**PQ819511**	**PQ814270**	**PO806986**	**China**
C. echino-olivacea	TENN043686	KP257110	KP257188	–	New Zealand
C. flavipes	BRACR 15121	KC759450	KC759472	–	Slovakia
C. flavipes	TENN063740	KP257119	EF535267	–	United Kingdom
C. flavostellifera	BIO-Fungi 10433	KC759461	JX069828	–	Slovakia
C. flavostellifera	BRACR 16695	KC759462	JX069827	–	Slovakia
C. fragilis	MHHNU10527	ON228394	ON231696	ON246179	China
C. fragilis	MHHNU32418	ON228395	ON231697	ON246180	China
C. fragilis	TENN033244	KP257121	KP257195	–	USA
C. fumosa	MR00170	JN214482	HQ877696	–	USA
C. fumosa	TENN060724	KP257126	KP257199	–	Russia
C. fuscata	JMB08181001	KP257128	HQ877691	KP257253	USA
C. gibbsiae	PDD 111979	OR567704	OR567794	–	New Zealand
C. globospora	TENN045945	KP257130	KP257201	–	USA
C. greletii	ERRO 2014102101	MF503244	–	–	Spain
C. greletii	C(F) s/n	–	JN416778	–	Denmark
C. griseobrunnea	BIO-Fungi 12566	KY091644	–	–	Spain
C. griseolilacina	MHHNU9722	MT028142	ON231725	ON246185	China
C. griseolilacina	MHHNU10149	MT028141	ON231726	ON246186	China
C. hupingshanensis	MHHNU7362	ON228396	ON231698	ON246181	China
C. incarnata	AMB 18345	MK908007	MK898930	–	Italy
C. incarnata	BIO-Fungi 12560	KC759452	–	–	Spain
C. incarnata	MA53113	KC759453	JQ415948	–	Spain
C. lametina	AMB 18933	OQ595227	OQ595225	OQ594954	Italy
C. cf. *macounii*	PK1536	KP257131	KP257202	KP257254	Canada
C. megaspinosa	JAC14897	OR567613	OR567751	–	New Zealand
C. megaspinosa	JAC16538	OR567650	OR567778	–	New Zealand
C. messapica f. *alborosea*	AMB 18346	MN017594	MN017499	–	Italy
C. messapica	AMB 12800	–	KM486538	–	Italy
C. messapica	IHI-20Cla01	MW786738	MW786737	–	Germany

Identification	Specimen No.	GenBank No. (ITS)	GenBank No. (28S)	GenBank No. (RPB2)	Location
C. musculospinosa	PDD 82582	OR567692	OR567786	–	New Zealand
C. neonigrita	Ceska06112010	JN214481	JN214484	–	Canada
C. orientalis	**MHHNU6801**	**PQ819512**	**PQ814271**	–	**China**
C. orientalis	**MHHNU7352**	**PQ819513**	**PQ814272**	**PO806987**	**China**
C. orientalis	**MHHNU7586**	**PQ819514**	**PQ814273**	**PO806988**	**China**
C. orientalis	**MHHNU7767**	**PQ819515**	**PQ814274**	–	**China**
C. orientalis	**MHHNU32116**	**PQ819516**	**PQ814275**	**PO806989**	**China**
C. parvispora	BRACR 13266	–	MH727523	–	Norway
C. parvispora	BRACR 21309	–	MH727524	–	Slovakia
C. pisana	AMB 18620	MW355011	MW355012	–	Italy
C. pseudoincarnata	AMB 17377	MN017595	MN017500	–	Italy
C. pseudoincarnata	AMB 17379	MN017596	MN017501	–	Italy
C. pullei	MONI 2018122801	MW549781	MW549780	–	Spain
C. pullei	SAV F3139	KP257132	KP257203	KP257255	Czech Republic
C. redoleoalii	JAC14916	OR567617	OR567755	–	New Zealand
C. redoleoalii	JAC14917	OR567642	OR567772	–	New Zealand
C. rosea	TENN063100	KP257133	KP257205	KP257256	USA
C. rosea	TENN065117	KP257134	KP257206	KP257257	USA
C. roseoviolacea	JAC14915	OR567616	OR567754	–	New Zealand
C. roseoviolacea	JAC15786	OR567632	OR567764	–	New Zealand
C. rubicundula	JLH MyCoPortal 6603126	MK578690	–	–	USA
C. cf. *rubicundula*	JMB10061005	–	HQ877690	–	USA
C. salentina	AMB 010297	MF972892	MF972888	–	Italy
C. sinensis	MHHNU8198	MT028140	ON231727	ON246187	China
C. sphagnicola	BRACR 13593	KC759455	KC759471	–	Norway
C. sphagnicola	BRNM 747282	KC759456	KC759470	–	Czech Republic
C. stegasauroides	JAC14852	OR567586	OR567742	–	New Zealand
C. stegasauroides	PBM3373	–	HQ877698	KP257261	Australia
C. stellifera	IHI-19Cla01	OK239673	OK239677	–	Germany
C. straminea	BRACR 12807	KC759449	JQ415944	–	Slovakia
C. subviolacea	JAC14150	OR567566	OR567726	–	New Zealand
C. tenuipes	ARAN-Fungi 11295	MW248489	MW248513	–	Spain
C. tongdaoensis	**MHHNU11091**	**PQ819517**	**PQ814276**	**PO806990**	**China**
C. tongdaoensis	**MHHNU11093**	**PQ819518**	**PQ814277**	**PO806991**	**China**
C. tongdaoensis	**MHHNU11094**	**PQ819519**	**PQ814278**	**PO806992**	**China**
C. tyrrhenica	ZT Myc 58698	MF972890	MF972886	–	Italy
C. ypsilonidia	PDD 46673	NR174884	NG079629	–	New Zealand
C. ypsilonidia	TENN042411	KP257140	KP257210	KP257262	New Zealand
C. zollingeri	MHHNU10528	ON228397	ON231699	ON246182	China
C. zollingeri	MHHNU10548	ON228398	ON231700	ON246183	China
C. zollingeri	MHHNU10550	ON228399	ON231701	ON246184	China
C. zollingeri	TENN064095	KP257141	HQ877700	KP257263	USA
C. zollingeri	TENN58652	AY854071	AY639882	AY480940	–
Mucronella flava	IO.16.84	MT232354	MT232307	–	Sweden
Mucronella sp	PDD 95742	HQ533013	–	–	New Zealand

The new species *Clavaria divergens* formed a distinct lineage (Clade 12) sister to the *Clavaria fumosa* clade, to which *Clavaria crosslandii* (Clade 17) and *Clavaria salentina* (Clade 16) were also phylogenetically close. The other two new species, *Clavaria orientalis* and *Clavaria tongdaoensis*, formed genetically distinct lineages (Clade 2 and Clade 3) that were phylogenetically closest to *Clavaria zollingeri* within the *Clavaria fumosa* clade.

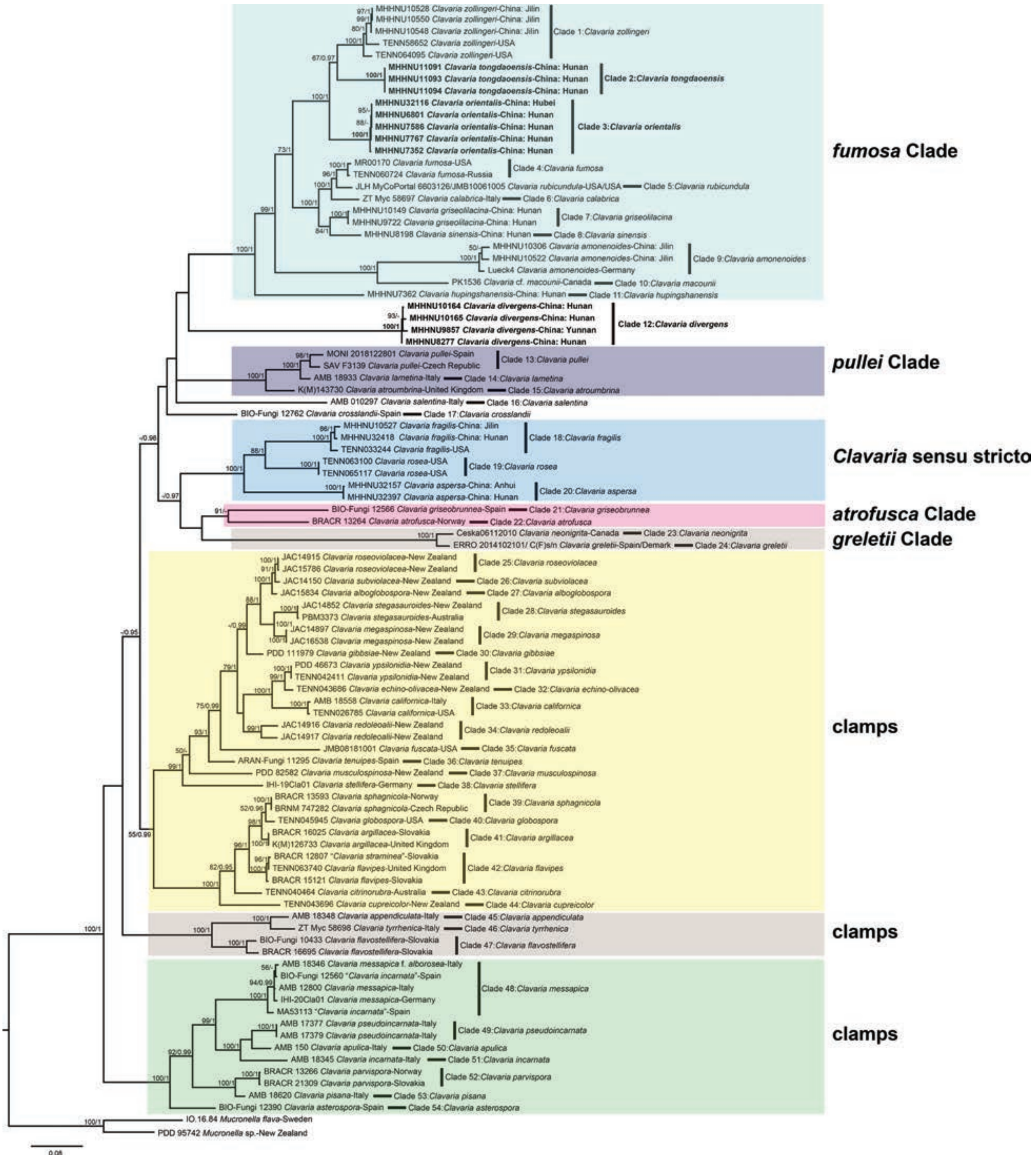

Figure 1. Phylogenetic relationships of *Clavaria* species inferred from ITS, nrLSU, and *RPB*2 sequences under the maximum likelihood optimality criterion. Bayesian posterior probabilities over 0.95 and bootstrap values over 50% are reported at nodes (BI/MP); the sign "–" means under the reported level. Our new species are shown in boldface text.

Taxonomy

***Clavaria divergens* P. Zhang & Ju. Yan, sp. nov.**
MycoBank No: 857600
Figs 2, 3

Etymology. *divergens* (Latin) refers to the basidioma with dichotomous to irregularly divergent branches.

Figure 2. Basidiomata of *Clavaria divergens* **a** MHHNU9857 **b** MHHNU10165. Scale bars: 2 cm.

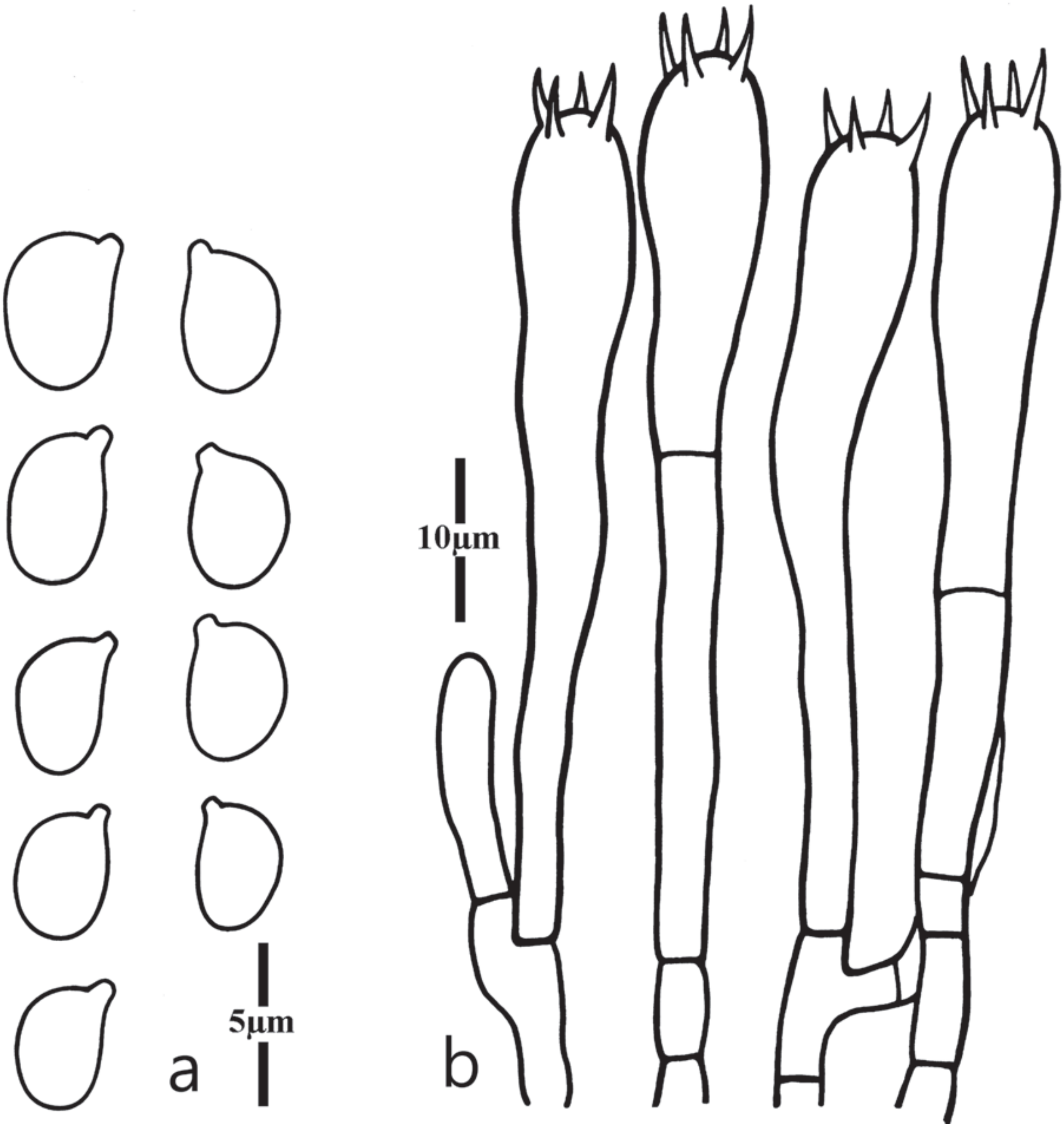

Figure 3. Microscopic features of *Clavaria divergens* (MHHNU9857) **a** basidiospores **b** basidia.

Holotype. China • Yunnan Province: Malipo County, Donggan Town, alt. 1580 m, 23°21'41.98"N, 105°09'44.17" E, 6 August 2018, P. Zhang (MHHNU9857).

Diagnosis. This species differs from other species within *Clavaria* subg. *Syncoryne* in its white branched basidiomata and 4-spored basidia.

Description. Basidiomata (Fig. 2a, b) branched, brittle, scattered, or gregarious clusters; clusters 10–50 mm high, 10–30 mm broad; branches terete, 1–3 mm wide, 2–4 times, dichotomous, or irregularly divergent in the ultimate rank; branch tips subacuminate, often antler-like or claw-like. Fertile part coralloid, smooth, slightly curved, occasionally with a longitudinal depression in center, white [A1; White]. Apex white, becoming yellowish or tawny with age. Sterile part distinct, white, smooth, without tomentum and mycelial patch. Flesh concolorous with surface of basidiomata.

Basidiospores (Fig. 3a) [100/6/4] (4.0)4.2–5.0 × (2.4)2.7–3.8(4.0) μm [Q = (1.25)1.26–1.56(1.60), Q = 1.39 ± 0.10], mostly ellipsoid, sometimes also broadly ellipsoid, smooth, hyaline, nonamyloid, thin-walled; hilar appendix small (<1.0 μm in length). Basidia (Fig. 3b) 48–65 × 6.5–9.0 μm, clavate, 4-spored, hyaline, thin-walled or slightly thick-walled, sometimes with secondarily septated; sterigmata up to 5.2 μm long. Incrustations or crystals absent. Hyphae of the context parallel, thin-walled, hyaline, cylindrical to inflated, secondarily septated. Clamp connections absent in all parts of basidiomata.

Habitat, ecology, and distribution. Scattered or gregarious in humus layers of soil under mixed coniferous–broadleaved forests or broadleaved forests. Basidiomata produced in summer, usually throughout the months of July to August; known from subtropical zones of Central and Southwestern China.

Additional specimens examined. China • Hunan Province: Yongshun County, Xiaoxi National Nature Reserve, alt. 1068 m, 28°47'45.84"N, 110°12'13.89"E, 28 August 2014, P. Zhang (MHHNU8277); • Guzhang County, Gaofeng Town, alt. 573 m, 28°40'45.42"N, 110°08'28.56"E, 23 July 2020, Ju. Yan (MHHNU10164, MHHNU10165).

Clavaria orientalis **P. Zhang & Ju. Yan, sp. nov.**

MycoBank No: 857601
Figs 4, 5

Etymology. *orientalis* (Latin), meaning eastern, refers to the occurrence of the species in East Asia.

Holotype. China • Hunan Province: Shimen County, Hupingshan Nature Reserve, alt. 1828 m, 30°02'58.50"N, 110°31'24.90"E, 11 September 2012, P. Zhang (MHHNU7767).

Diagnosis. Differs from *Clavaria zollingeri* in its stout branches, lesser degree of branching, and shorter basidia.

Description. Basidiomata (Fig. 4a, b) branched, brittle, gregarious to caespitose clusters; clusters 50–80 mm high, 10–30 mm broad; branches terete, 1–3 mm wide, 1–4 times, dichotomous; branch tips obtuse, broadly rounded, or narrowly rounded. Fertile part coralloid, smooth, obviously curved or slightly twisted, deep amethyst [15A4-7, 15B4-6, 16A4-6; Amparo Purple, Lobelia Violet, Vinaceous Purple] to lilac [14A2-3, 15A2-3; Pale Vinaceous Purple, Pale Lobelia Violet], and changing to pale greyish purple [16A2, 17A2; Lavender Gray, Pale Payne's Gray,

Figure 4. Basidiomata of *Clavaria orientalis* **a** MHHNU7767 **b** MHHNU32116. Scale bars: 2 cm.

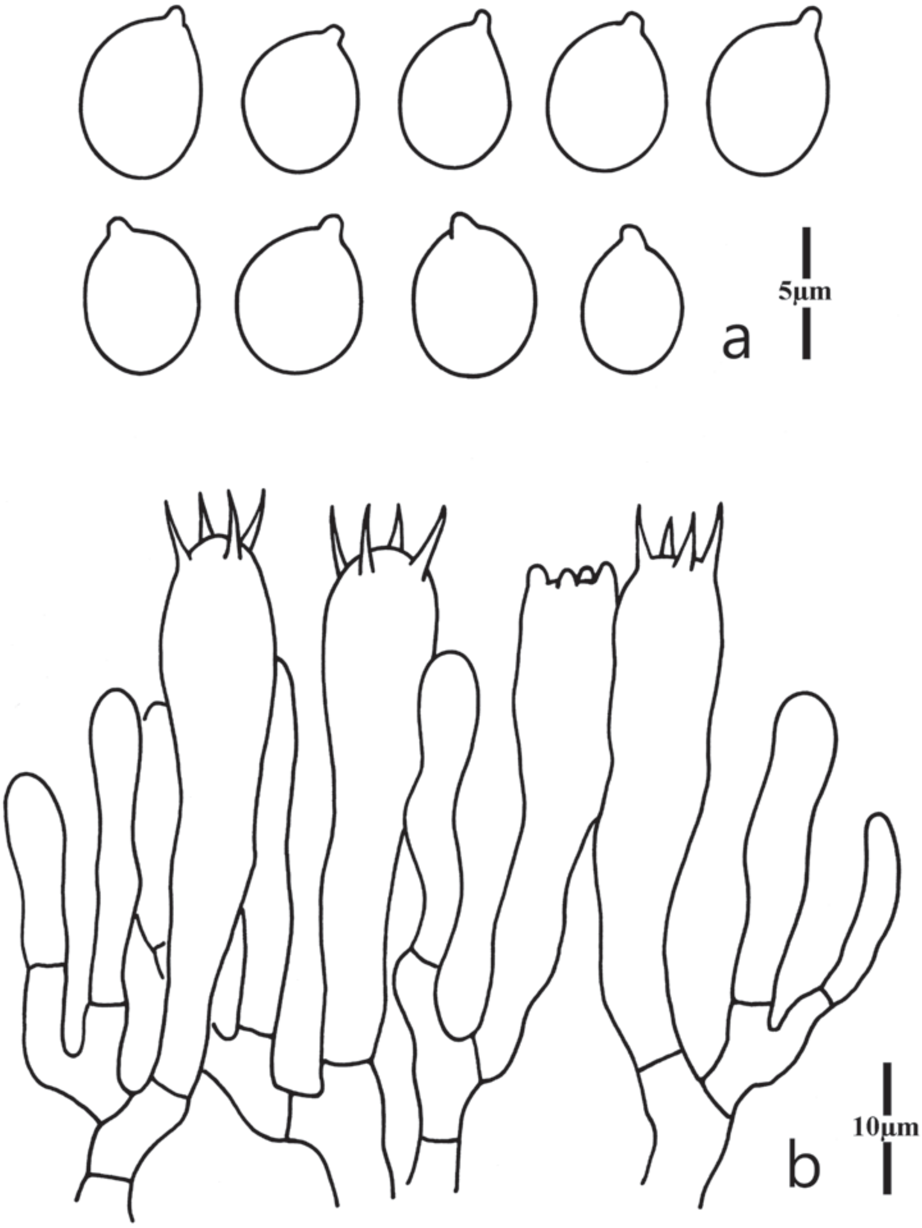

Figure 5. Microscopic features of *Clavaria orientalis* (MHHNU7767) **a** basidiospores **b** basidia.

Pale Verbena Violet] with age. Apex concolorous with lower part, becoming yellowish or tawny with age. Stipe distinct, sterile, smooth, often terete, semi-translucent, hygrophanous, and darker than the fertile part, sometimes flattened and pallid. Flesh concolorous or slightly paler than surface of basidiomata.

Basidiospores (Fig. 5a) [100/5/5] (4.8)5.0–6.0 × 4.0–5.0(5.5) µm [Q = (1.09)1.13–1.38(1.43), Q = 1.21 ± 0.11], mostly broadly ellipsoid, sometimes ellipsoid or subglobose, smooth, hyaline, nonamyloid, thin-walled; hilar appendage present (<2.0 µm in length). Basidia (Fig. 5b) 34–48 × 5.0–8.0 µm, clavate, 4-spored, hyaline, thin-walled; sterigmata below 5.0 µm long. Incrustations or crystals absent. Hyphae of the context parallel, thin-walled, hyaline, cylindrical to inflated, secondarily septated. Clamp connections absent in all parts of basidiomata.

Habitat, ecology, and distribution. Gregarious to caespitose in humus layers of soil under broadleaved forests, coniferous forests, or mixed coniferous–broadleaved forests. Basidiomata produced in summer or autumn, usually throughout the months of July to September; known from subtropical zones of southern China.

Additional specimens examined. China • Hunan Province: Sangzhi County, Badagongshan National Nature Reserve, alt. 1500 m, 29°46'58.17"N, 110°4'51.68"E, 22 July 2003, P. Zhang (MHHNU6801); • Shimen County, Hupingshan Nature Reserve, alt. 1828 m, 30°02'58.50"N, 110°31'24.90"E, 31 August 2010, P. Zhang (MHHNU7352); • 26 September 2011, P. Zhang (MHHNU7586). • Hubei Province: Hefeng County, Mulinzi National Nature Reserve, alt. 1413 m, 30°03'32.17"N, 110°12'34.35"E, 1 August 2020, Z.H. Chen (MHHNU32116).

Clavaria tongdaoensis P. Zhang & Ju. Yan, sp. nov.

MycoBank No: 857602
Figs 6, 7

Etymology. *tongdaoensis* (Latin) refers to the type locality in Tongdao County, Hunan Province, China.

Holotype. China • Hunan Province: Tongdao County, Fengshuwan Forest Park, alt. 400 m, 26°09'45.66"N, 109°46'31.52"E, 6 July 2022, P. Zhang and Li-Xun Yang (MHHNU11094).

Diagnosis. Distinguished from *Clavaria orientalis* and *Clavaria zollingeri* by its smaller basidiomata and basidiospores.

Description. Basidiomata (Fig. 6a, b) branched, brittle, gregarious to caespitose clusters; clusters 25–45 mm high, 30–40 mm broad; branches terete, 2–3 mm wide, 1–3 times, dichotomous; branch tips narrowly rounded or awl-shaped. Fertile part coralloid, smooth, often curved or slightly twisted, pale purple to pale purplish pink [13A2-3, 14A2-3; Pale Lavender Violet, Pale Lobelia Violet, Pale Purplish Vinaceous], turning white with age. Apex concolorous with lower part, becoming yellowish or tawny with age. Stipe distinct, sterile, smooth, terete, semi-translucent, hygrophanous, slightly darker color than the fertile part. Flesh concolorous with surface of basidiomata.

Basidiospores (Fig. 7a) [100/5/3] 3.5–5.0 × 3.0–4.2(4.5) µm [Q = (1.05)1.06–1.33, Q = 1.16 ± 0.08], broadly ellipsoid, sometimes subglobose, smooth, hyaline, nonamyloid, thin-walled; hilar appendage present. Basidia (Fig. 7b)

Figure 6. Basidiomata of *Clavaria tongdaoensis* **a** MHHNU11093 **b** MHHNU11094. Scale bars: 2 cm.

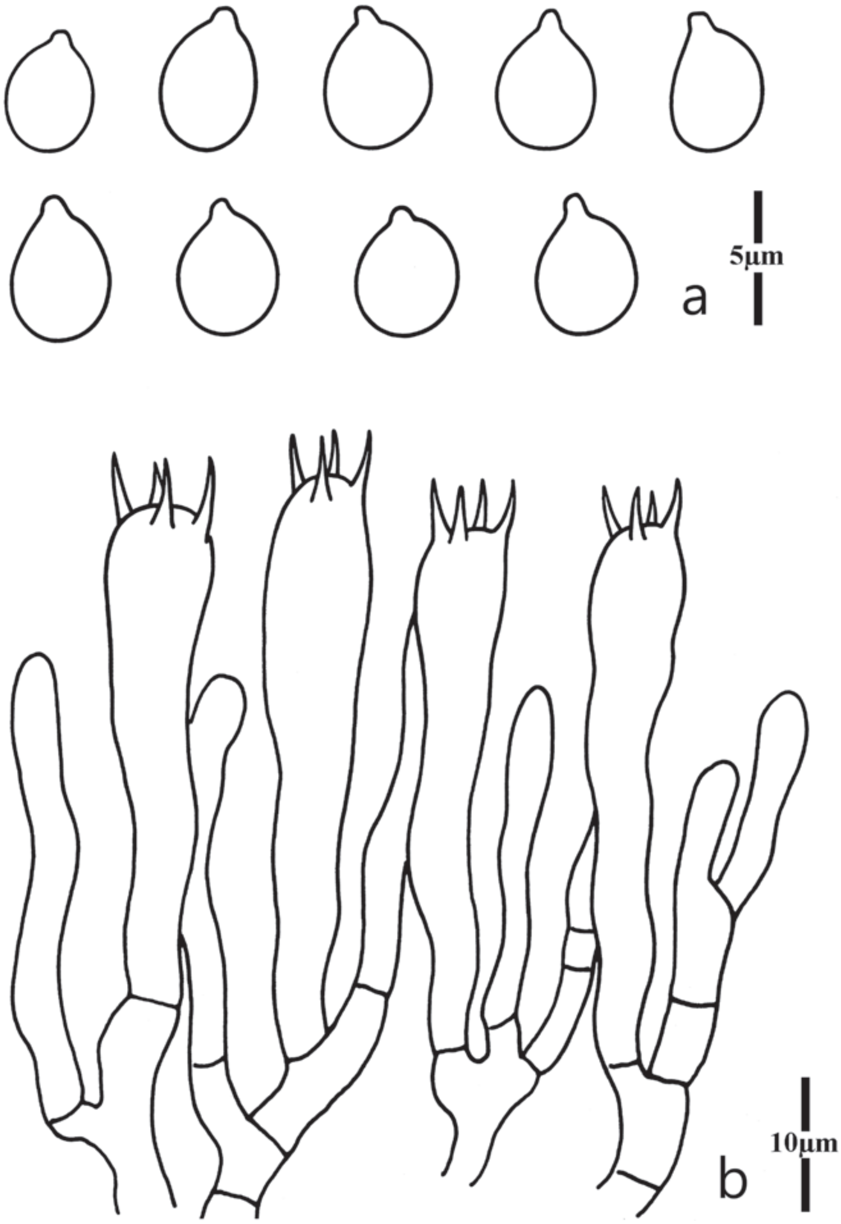

Figure 7. Microscopic features of *Clavaria tongdaoensis* (MHHNU11094) **a** basidiospores **b** basidia.

26–43 × 6.5–8.0 µm, clavate, 4-spored, hyaline, thin-walled; sterigmata below 5.0 µm long. Incrustations or crystals absent. Hyphae of the context parallel, thin-walled, hyaline, cylindrical to inflated, secondarily septated. Clamp connections absent in all parts of basidiomata.

Habitat, ecology, and distribution. Gregarious to caespitose in humus layers of soil under broadleaved forests. Basidiomata produced in summer; known only from the type locality, China.

Additional specimens examined. CHINA • Hunan Province: Tongdao County, Fengshuwan Forest Park, alt. 400 m, 26°09'45.66"N, 109°46'31.52"E, 6 July 2022, P. Zhang and Li-Xun Yang (MHHNU11091, MHHNU11093).

Discussion

In this study, three new species of *Clavaria* within subg. *Syncoryne* were identified from specimens collected in China. The three species have in common the absence of a loop-like clamp connection at the base of the basidia and obvious branching of the basidiomata. Before the present study, only seven species within *Clavaria* were known to stably produce branched basidiomata, namely, *C. diverticulata* A.N.M. Furtado & M.A. Neves (Furtado et al. 2016), *C. griseolilacina* P. Zhang (Yan et al. 2020), *C. hupingshanensis* P. Zhang & Ju. Yan (Yan et al. 2022), *C. martinii* Corner (Corner 1967), *C. pumanquensis* Lazo (Lazo 1972), *C. sinensis* P. Zhang (Yan et al. 2020), and *C. zollingeri* Lév. (Léveillé 1846). Among these seven branched species, *C. zollingeri* is of greatest relevance in the present study.

We initially mistook *C. orientalis* and *C. tongdaoensis* to be *C. zollingeri* based on the purple color of their basidiomata until we collected material of *C. zollingeri* (MHHNU10528, Fig. 8) in Jilin Province (northern China) that matched a previous description of that species. A comparison of the specimens revealed the differences among the three species. More specifically, Corner noted that, for *C. zollingeri*, the basidioma is 15–75 mm high, the spores are 4.0–7.0 × 3.0–5.0 µm, the basidia are 50–60 × 7–10 µm, and the sterigmata are 4–7 µm (Corner 1950). Franchi and Marchetii (2021) noted that the basidiomata of *C. zollingeri* are up to 80 mm high and the basidia are 50–60 × 8–10 µm. In contrast, *C. orientalis* discovered in southern China has shorter basidia (34–48 × 5.0–8.0 µm) and shorter sterigmata (< 5.0 µm long) than those of *C. zollingeri*. An additional species collected from southern China, *C. tongdaoensis*, has shorter basidia (26–43 × 6.5–8.0 µm), smaller spores (3.5–5.0 × 3.0–4.2(4.5) µm), and shorter sterigmata than *C. zollingeri*. In addition, the branches of *C. orientalis* often are not as profuse as the branches of *C. zollingeri*, and, compared with *C. zollingeri*, the basidiomata of *C. tongdaoensis* are smaller (25–45 mm high). *Clavaria divergens* is quite unique within *Clavaria*. Based on the color of the basidiomata, *C. divergens* is similar to *C. fragilis* or *C. gibbsiae*, but *C. fragilis* and *C. gibbsiae* always have a simple basidiomata, occasionally once-furcate. Compared with the branched *Clavaria* species mentioned above, *C. divergens* is distinctive with its white basidiomata and subacuminate branch tips.

In the phylogeny for *Clavaria*, 54 species are supported based on molecular data, which is much higher than previous records or predictions. For example, 28 species of *Clavaria* were recognized in Ainsworth and Bisby's "Dictionary of the Fungi", 10th edn. (Kirk et al. 2008), and Olariaga et al. (2015) estimated that the genus comprises 30–35 species. Two of the new species, *C. orientalis* and *C. tongdaoensis*, together with *C. zollingeri*, formed a clade with strong support

Figure 8. Basidiomata of *Clavaria zollingeri* (MHHNU10528). Scale bars: 2 cm.

(ML 100%/BI 1), a relationship consistent with the morphological similarity of the three species. In the phylogenetic analysis, sequence data for five specimens of *C. zollingeri* were included, two of which were collected in the United States and the other three were collected from Jilin Province, China. This finding supports the contention that *C. zollingeri* in North America and populations in northern China are conspecific. In contrast, eight specimens collected from southern China were genetically distinct from *C. zollingeri* and showed morphological differences and thus were identified as new species, named here *C. orientalis* and *C. tongdaoensis*. Moreover, *C. divergens* was indicated to be genetically very distinct in the phylogenetic tree. Although the phylogeny indicated that *C. divergens* has a close relationship with the *Clavaria fumosa* clade and represented a sister lineage to that clade, the node was not statistically supported. Nevertheless, the phylogenetic analysis supported its genetic distinctness and monophyly as an independent lineage and verified its identity as a previously unrecognized species. However, its phylogenetic relationships with other species of *Clavaria* require further research.

In summary, most species of *Clavaria* are unbranched, but three branching species are described in this article. Among them, *C. orientalis* and *C. tongdaoensis* are distinguished from *C. zollingeri*, which is considered to be distributed only in northern China. *Clavaria divergens* is the first species discovered in China with stable white branches. The records of these three species enrich the species diversity of the genus *Clavaria* and increase the number of species with branched basidiomata in the genus.

Key to branched species of *Clavaria* in China

1 Basidiomata white to pink ... **2**
– Basidiomata purple ... **3**
2 Basidiomata 10–50 mm tall, white ... ***C. divergens***
– Basidiomata 35–70 mm tall, rose-white to seashell-pink ... ***C. hupingshanensis***
3 Basidiomata sparsely branched ... ***C. griseolilacina***
– Basidiomata profusely branched ... **4**
4 Fruiting body usually lighter colored ... **5**
– Fruiting body color usually darker colored ... **6**
5 Basidiomata 30–70 mm tall, basidiospores 5.0–6.0 × 3.5–4.5 μm ... ***C. sinensis***
– Basidiomata 25–45 mm tall, basidiospores 3.5–5.0 × 3.0–4.2 μm ... ***C. tongdaoensis***
6 Basidiomata branching stout, 1–4 times, distribution in southern China ... ***C. orientalis***
– Basidiomata branching slim, 3–5 times, distribution in northern China ... ***C. zollingeri***

Acknowledgements

The authors are very grateful to Drs. Ke-Rui Huang and PhD students Peng-Tao Deng for their help with our image processing and writing. We thank Prof. Zuo-Hong Chen for providing specimens. We thank Robert McKenzie, PhD, from Liwen Bianji (Edanz) (www.liwenbianji.cn) for editing a draft of this manuscript.

Additional information

Conflict of interest

The authors have declared that no competing interests exist.

Ethical statement

No ethical statement was reported.

Funding

This study was financially supported by the National Natural Science Foundation of China (Grant No. 31670015, 31750001, and 32400010) and the Natural Science Foundation of Hunan Province of China (Grant No. 2024JJ6308).

Author contributions

Conceptualization: Ping Zhang and Ke Liao; methodology: Jun Yan and Li Xiong; performing the experiment: Jun Yan and Li Xiong; resources: Ping Zhang, Ke Liao, Li-Xun Yang, and Jun Yan; writing—original draft preparation: Jun Yan; writing—review and editing: Ping Zhang; supervision: Ping Zhang; project administration: Ping Zhang and Ke Liao; funding acquisition: Ping Zhang and Zheng-Mi He. All authors have read and agreed to the published version of the manuscript.

Author ORCIDs

Jun Yan https://orcid.org/0000-0002-2832-8046
Li Xiong https://orcid.org/0009-0007-3568-7737
Li-Xun Yang https://orcid.org/0009-0003-3086-4424
Zheng-Mi He https://orcid.org/0000-0001-8754-3427
Ping Zhang https://orcid.org/0000-0002-8751-704X

Data availability

All of the data that support the findings of this study are available in the main text or Supplementary Information.

References

Birkebak JM, Adamčík S, Looney BP, Matheny PB (2016) Multilocus phylogenetic reconstruction of the Clavariaceae (Agaricales) reveals polyphyly of agaricoid members. Mycologia 108(5): 860–868. https://doi.org/10.3852/15-370

Corner EJH (1950) A monograph of Clavaria and allied genera. Oxford University press, London, 740 pp.

Corner EJH (1967) Notes on *Clavaira*. Transactions of the British Mycological Society 50(1): 33–44. https://doi.org/10.1016/S0007-1536(67)80061-5

Doyle JJ, Doyle JL (1987) A rapid DNA isolation procedure for small quantities of fresh leaf tissue. Phytochemical Bulletin 19: 11–15.

Franchi P, Marchetti M (2021) I Funghi Clavarioidi in Italia. Vol. 1. A. M. B., Vicenza, Italy, 664 pp.

Fries E (1821) Systema mycologicum: sistens fungorum ordines, genera et species, huc usque cognitas. Confederatio Europaea Mycologiae Mediterraneensis AE, Berlin, 520 pp. https://doi.org/10.5962/bhl.title.5378

Furtado ANM, Daniëls PP, Neves MA (2016) New species and new records of Clavariaceae (Agaricales) from Brazil. Phytotaxa 253(1): 1–26. https://doi.org/10.11646/phytotaxa.253.1.1

Hall TA (1999) BioEdit: A user-friendly biological sequence alignment editor and analysis program for windows 95/98/NT. Nucleic Acids Symposium Series 41: 95–98. https://doi.org/10.1021/bk-1999-0734.ch008

He ZM, Chen ZH, Bau T, Wang GS, Yang ZL (2023) Systematic arrangement within the family Clitocybaceae (Tricholomatineae, Agaricales): Phylogenetic and phylogenomic evidence, morphological data and muscarine-producing innovation. Fungal Diversity 123(1): 1–47. https://doi.org/10.1007/s13225-023-00527-2

Katoh K, Standley DM (2016) A simple method to control over-alignment in the MAFFT multiple sequence alignment program. Bioinformatics 32(13): 1933–1942. https://doi.org/10.1093/bioinformatics/btw108

Kautmanová I, Tomšovský M, Dueñas M, Martín, MP (2012) European species of Clavaria (Agaricales, Agaricomycetes) with dark basidiomata – a morphological and molecular study. Persoonia – Molecular Phylogeny and Evolution of Fungi 29: 133–145. https://doi.org/10.3767/003158512X661543

Kirk PM, Cannon PF, Minter DW Stalpers (2008) Ainsworth & Bisby's Dictionary of the Fungi, 10th edn. CAB International Press, Wallingford, 783 pp. https://doi.org/10.1079/9780851998268.0000

Kornerup A, Wanscher JH (1978) Methuen handbook of colour, 3rd edn. Methuen, London, 252 pp.

Lazo W (1972) Some Clavariaceae from Chile. Mycologia 64(1–6): 73–80. https://doi.org/10.1080/00275514.1972.12019236

Léveillé JH (1846) Descriptions des champignons de l'herbier du Muséum de Paris. Ann Sci Nat Bot, ser 3, 5: 111–167.

Linnaeus C (1753) Species Plantarum. Impensis Laurentii Salvii, Stockholm, 1200 pp.

Liu YJ, Whelen S, Hall BDI (1999) Phylogenetic relationships among ascomycetes: Evidence from an RNA polymerse II subunit. Molecular Biology and Evolution 16(12): 1799–1808. https://doi.org/10.1093/oxfordjournals.molbev.a026092

Matheny PB, Wang Z, Binder M, Curtis JM, Hibbett DS (2007) Contributions of rpb2 and tef1 to the phylogeny of mushrooms and allies (Basidiomycota, Fungi). Molecular Phylogenetics and Evolution 43(2): 430–451. https://doi.org/10.1016/j.ympev.2006.08.024

Nylander JAA (2004) MrModeltest v2. Program distributed by the author. Evolutionary Biology Centre, Uppsala University.

Olariaga I, Salcedo I, Daniëls PP, Spooner B, Kautmanová I (2015) Taxonomy and phylogeny of yellow *Clavaria* species with clamped basidia—*Clavaria flavostellifera* sp. nov. and the typification of *C. argillacea*, *C. flavipes* and *C. sphagnicola*. Mycologia 107(1): 104–122. https://doi.org/10.3852/13-315

Persoon CH (1801) Synopsis methodica fungorum: sistens enumerationem omnium huc usque detectarum specierum, cum brevibvs descriptionibus nec non synonymis et observationibus selectis. Dieterich, 706 pp. https://doi.org/10.5962/bhl.title.166151

Rambaut A (2012) FigTree v1. 4. University of Edinburgh, Edinburgh, UK. http://tree.bio.ed.ac.uk/software/figtree

Ridgway R (1912) Color standards and color nomenclature. Published by the author, Washington. https://doi.org/10.5962/bhl.title.144788

Ronquist F, Huelsenbeck JP (2003) MrBayes 3: Bayesian phylogenetic inference under mixed models. Bioinformatics 19(12): 1572–1574. https://doi.org/10.1093/bioinformatics/btg180

Stamatakis A (2006) RAxML-VI-HPC: Maximum likelihoodbased phylogenetic analyses with thousands of taxa and mixed models. Bioinformatics 22(21): 2688–2690. https://doi.org/10.1093/bioinformatics/btl446

Vaidya G, Lohman DJ, Meier R (2011) Sequencematrix: Concatenation software for the fast assembly of multi-gene datasets with character set and codon information. Cladistics 27(2): 171–180. https://doi.org/10.1111/j.1096-0031.2010.00329.x

Vaillant S (1727) Botanicon Parisiense, ou Dénombrement par Ordre Alphabétique des Plantes, qui se Trouvent dans les Environs de Paris. J. & H. Verbeek, Leiden, Amsterdam, 205 pp. https://doi.org/10.5962/bhl.title.738

Vilgalys R, Hester M (1990) Rapid genetic identification and mapping of enzymatically amplified ribosomal DNA from several Cryptococcus species. Journal of Bacteriology 172: 4238–4246. https://doi.org/10.1128/jb.172.8.4238-4246.1990

White TJ, Bruns T, Lee S, Taylor J (1990) Amplification and direct sequencing of fungal ribosomal RNA genes for phylogenies. PCR protocols, a guide to methods and applications 18: 315–322. https://doi.org/10.1016/B978-0-12-372180-8.50042-1

Yan J, Wang XY, Wang XH, Chen ZH, Zhang P (2020) Two new species of *Clavaria* (Agaricales, Basidiomycota) from Central China. Phytotaxa 477(1): 71–80. https://doi.org/10.11646/phytotaxa.477.1.5

Yan J, Li GW, Liu WH, Chen ZH, Zhang P (2022) Updated taxonomy of Chinese *Clavaria* subg. *Syncoryne* (Clavariaceae, Agaricales): Description of two new species and one newly recorded species. Mycological Progress 21(8): 67. https://doi.org/10.1007/s11557-022-01815-y

Yan J, Wen J, Li GW, Wu SW, Zhang P (2023) Taxonomy and Phylogenetic Relationships of *Clavulinopsis* (Clavariaceae, Agaricales): Description of Six New Species and One Newly Recorded Species from China. Journal of Fungi 9(6): 656. https://doi.org/10.3390/jof9060656

Supplementary material 1

ITS sequence dataset

Author: Jun Yan

Data type: fas

Explanation note: The ITS sequences were respectively aligned using MAFFT v7.471, and manually edited in BIOEDIT v7.2.5 where necessary.

Link: https://doi.org/10.3897/mycokeys.115.145774.suppl1

Supplementary material 2

LSU sequence dataset

Author: Jun Yan

Data type: fas

Explanation note: The LSU sequences were respectively aligned using MAFFT v7.471, and manually edited in BIOEDIT v7.2.5 where necessary.

Link: https://doi.org/10.3897/mycokeys.115.145774.suppl2

Supplementary material 3

RPB2 sequence dataset

Author: Jun Yan

Data type: fas

Explanation note: The *RPB2* sequences were respectively aligned using MAFFT v7.471, and manually edited in BIOEDIT v7.2.5 where necessary.

Link: https://doi.org/10.3897/mycokeys.115.145774.suppl3

MycoKeys

MycoKeys 115: 155–185 (2025)
DOI: 10.3897/mycokeys.115.145330

Research Article

Unveiling Sordariomycetes taxa associated with woody litter in Northern Thailand

Chayanard Phukhamsakda[1], Kevin D. Hyde[1,2,3], Milan C. Samarakoon[4], Johnny Louangphan[1,2], Kedsara Navasit[1], Fatimah Al-Otibi[3], Chitrabhanu S. Bhunjun[1,5]

1 Center of Excellence in Fungal Research, Mae Fah Luang University, Chiang Rai 57100, Thailand
2 CAS Key Laboratory for Plant Diversity and Biogeography of East Asia, Kunming Institute of Botany, Chinese Academy of Science, Kunming, Yunnan 650201, China
3 Department of Botany and Microbiology, College of Science, King Saud University, P.O. Box 22452, Riyadh 11495, Saudi Arabia
4 Department of Entomology and Plant Pathology, Faculty of Agriculture, Chiang Mai University, Chiang Mai 50200, Thailand
5 School of Science, Mae Fah Luang University, Chiang Rai 57100, Thailand
Corresponding author: Chitrabhanu S. Bhunjun (chitrabhanu.bhu@mfu.ac.th)

This article is part of:
Exploring the Hidden Fungal Diversity: Biodiversity, Taxonomy, and Phylogeny of Saprobic Fungi
Edited by Samantha C. Karunarathna, Danushka Sandaruwan Tennakoon, Ajay Kumar Gautam

Academic editor:
Danushka Sandaruwan Tennakoon
Received: 25 December 2024
Accepted: 12 February 2025
Published: 17 March 2025

Citation: Phukhamsakda C, Hyde KD, Samarakoon MC, Louangphan J, Navasit K, Al-Otibi F, Bhunjun CS (2025) Unveiling Sordariomycetes taxa associated with woody litter in Northern Thailand. MycoKeys 115: 155–185. https://doi.org/10.3897/mycokeys.115.145330

Abstract

Sordariomycetes species are abundant in woody litter samples. In this study, we introduce two novel species, *Diaporthe thailandica* (Diaporthaceae) and *Occultitheca chiangraiensis* (Xylariaceae), from woody litter materials. We also describe a new host record of *D. tulliensis* and a new geographical record for *D. melonis*. All collections were identified based on morphology and phylogenetic analyses of combined datasets. The morphologies of the taxa fit the generic concepts of *Diaporthe* and *Occultitheca*, respectively. *Diaporthe thailandica* formed a sister clade with *D. raonikayaporum* but differs from *D. raonikayaporum* in the sizes of conidiomata, conidiogenous cells, and beta conidia. *Diaporthe thailandica* also differs from *D. raonikayaporum* by the absence of gamma conidia. *Occultitheca chiangraiensis* differs from the sister taxon *O. rosae* in having smaller ascomata and a thicker mucilaginous sheath. We also provide a synopsis of *Occultitheca* species with details on their morphology, host, and country. These findings provide valuable insights into the diversity and ecological roles of Sordariomycetes, emphasising the need for continued exploration of fungal biodiversity in various environments.

Key words: 2 new records, 2 new taxa, anthostomella-like taxa, phylogeny, saprobes, taxonomy

Introduction

Plant litter plays an important role in shaping ecological processes and supporting biodiversity, which represents a major source of organic carbon and nutrient cycling (Zhang et al. 2023). As natural decomposers, fungi hold a significant role in the breakdown of woody litter by degrading complex organic compounds efficiently (Dashtban et al. 2010; Hyde et al. 2019; Mapook et al. 2022). Although woody litter harbours various groups of fungi, comprehensive studies are limited (Hyde et al. 2020a; Phukhamsakda et al. 2022; Wanasinghe and Mortimer 2022; Xu et al. 2022; Madagammana et al. 2023).

Diaporthe (Diaporthaceae, Diaporthales, Sordariomycetes, Ascomycota) was established by Fuckel (1867) with *D. alnea* as the type species. *Diaporthe* is an important plant pathogen that also comprises endophytes and saprobes on a wide range of hosts (Dissanayake et al. 2017; Hyde et al. 2020b; Phukhamsakda et al. 2020; Bhunjun et al. 2022). As pathogens, *Diaporthe* cause diebacks, cankers, leaf spots, blights, melanoses, stem-end rots, and gummosis on economically and ecologically important plants (Gomes et al. 2013; Manawasinghe et al. 2021; Bhunjun et al. 2024a). The sexual morph of *Diaporthe* is characterised by immersed ascomata, erumpent pseudostroma with elongated perithecial necks, and unitunicate asci that produce hyaline ascospores (Udayanga et al. 2011; Hongsanan et al. 2023). The asexual morph has ostiolate conidiomata, cylindrical phialides, and aseptate and hyaline conidia (alpha, beta, and gamma) (Udayanga et al. 2011; Gomes et al. 2013). Molecular approaches are essential for accurate identification due to overlapping morphological characters among distinct species (Bhunjun et al. 2022; Norphanphoun et al. 2022). The taxonomy of *Diaporthe* species has been the subject of several studies (Gomes et al. 2013; Udayanga et al. 2014; Gao et al. 2017; Sun et al. 2021; Norphanphoun et al. 2022). The genus has recently been revised, and 31 species were synonymised based on multi-gene phylogeny, GCPSR (Genealogical Concordance Phylogenetic Species Recognition), as well as coalescence-based analyses of ITS, *tef1*, *tub2*, *cal*, and *his3* sequences (Dissanayake et al. 2024). Pereira and Phillips (2024) further reduced 53 species to synonymy and introduced a new species, *D. pygmaeae*, based on several molecular approaches.

Occultitheca (Xylariaceae, Xylariales) is characterised by immersed ascomata, short pedicellate asci with J+ apical ring, brown ascospores with hyaline dwarf cells, and a straight germ slit (Rogers and Ju 2003; Samarakoon et al. 2022). The genus is notable for having the uppermost ascospore distant from the ascus apex (Rogers and Ju 2003; Samarakoon et al. 2022). The second species, *O. rosae*, was described almost two decades later from a dead branch of *Rosa* species in Guizhou, China (Samarakoon et al. 2022). Tian et al. (2024) introduced *O. ananasi* from dead pineapple leaves from Chiang Rai, Thailand, based on morphological and molecular analyses.

Chiang Rai and Chiang Mai are located in the northern part of Thailand and are considered biodiversity hotspots (Hyde et al. 2018). During the study of woody litter microfungi in northern Thailand, two novel species and two new records were discovered based on morphology and multigene phylogeny. This underscores a critical gap in our understanding of fungal biodiversity and its ecological significance in the area, thus highlighting the need for further research (Hyde et al. 2024).

Materials and methods

Fungal collection, isolation, and observation

Woody litter samples were collected from forest areas in Chiang Mai and Chiang Rai Provinces, Thailand. The area is covered with a canopy of tall trees, such as dipterocarp species and *Bambusa* species. The specimens were maintained in paper bags for transport to the laboratory. The fungal structures were observed using a Leica EZ4 stereomicroscope (Leica Microsystems (SEA) Pte Ltd, Singapore). and photographed using a Nikon ECLIPSE Ni compound microscope (Nikon, Japan) equipped with a Nikon DS-Ri2 camera. Tarosoft (R) Image Frame Work version 3.9.3.74 was used for measurements, and Adobe Photoshop CS6 software was used for the photo plates.

Single spore isolation was conducted to obtain pure culture on potato dextrose agar (PDA) as described in Senanayake et al. (2020). The culture plates were incubated at room temperature (25 ± 5 °C) for 4 weeks. Herbarium materials were deposited in the Mae Fah Luang University Fungarium (MFLU), and ex-type living cultures were deposited in the Mae Fah Luang University Culture Collection (MFLUCC) in Chiang Rai, Thailand. Index Fungorum (Index Fungorum 2024) and Facesoffungi numbers (FoF) (Jayasiri et al. 2015) were obtained. The data of the novel species will also be uploaded to the Fungalpedia website (Hyde et al. 2023).

DNA extraction, amplification, and sequencing

Fresh mycelium was scraped from a 4-week-old culture on PDA, and DNA was extracted using the E.Z.N.A. Forensic DNA Kit (BIO-TEK) according to the manufacturer's instructions. The polymerase chain reaction (PCR) was used to amplify the ITS region (ITS5/ITS4) (White et al. 1990), *cal* (CAL228F/CAL737R) (Carbone and Kohn 1999), *his3* (CYLH3F/H3-1b) (Glass and Donaldson 1995), LSU (LR0R/LR5) (Vilgalys and Hester 1990), *rpb2* (fRPB25f/fRPB2-7cR) (Liu et al. 1999), *tef1* (EF-728F/EF-986R) (Carbone and Kohn 1999), and *tub2* (T1/T22 and BT2a/BT2b) genes (Glass and Donaldson 1995; O'Donnell and Cigelnik 1997). The PCR conditions for each primer were set up following Samarakoon et al. (2022) and Dissanayake et al. (2024). A PCR reaction was carried out in a 25 µL reaction volume containing 12.5 µL of 2 × PCR MasterMix, 9.5 µL of double-distilled water, 1 µL of 20 µmol for each forward and reverse primer, and 1 µL of 30 ng of DNA template. The PCR products were visualised on 1% agarose gels with 6 µl of 4S green dye per 100 mL. Successful PCR products were purified and sequenced by Biogenomed Co., Ltd., South Korea. The newly generated sequences were deposited in GenBank (Tables 1, 2).

Alignments and phylogenetic analyses

Consensus sequences were assembled using Geneious Prime 2025 (Biomatters Ltd., Auckland, New Zealand) and were used for BLASTn search against the NCBI nucleotide non-redundant database (Sayers et al. 2022). For *Diaporthe*, sequences were downloaded from GenBank (Table 1) following the classification in Dissanayake et al. (2024). For Xylariales, related sequences were downloaded from GenBank (Table 2) based on recent publications (Samarakoon et al. 2022; Sugita et al. 2022; Voglmayr et al. 2022). The sequences were aligned using MAFFT version 7 (Katoh et al. 2019) with minimal adjustment of any ambiguous nucleotides using AliView version 1.26 (Larsson 2014). The alignments were concatenated using SequenceMatrix version 1.8 (Vaidya et al. 2011).

Table 1. GenBank accession numbers of the taxa used in the phylogenetic analyses of *Diaporthe* section *sojae*.

Species	Strain	ITS	*tef1*	*tub2*	*cal*	*his3*
Diaporthe acaciarum	CBS 138862^{T}	KP004460	N/A	KP004509	N/A	KP004504
D. amaranthophila	MAFF 246900^{T}	LC459575	LC459577	LC459579	LC459583	LC459581
D. amaranthophila	MAFF 246901	LC459576	LC459578	LC459580	LC459584	LC459582
D. ambigua	CBS 114015^{T}	MH862953	KC343736	KC343978	KC343252	KC343494
D. ambigua	CBS 117167	KC343011	KC343737	KC343979	KC343253	KC343495
D. angelicae	CBS 111592^{T}	KC343027	KC343753	KC343995	KC343269	KC343511
D. angelicae	CBS 100871	KC343025	KC343751	KC343993	KC343267	KC343509
D. arctii	CBS 139280^{T}	KJ590736	KJ590776	KJ610891	KJ612133	KJ659218
D. arezzoensis	MFLU 19-2880^{T}	MT185503	MT454019	MT454055	N/A	N/A
D. batatas	CBS 122.21^{T}	KC343040	KC343766	KC344008	KC343282	KC343524
D. beilharziae	BRIP 54792^{T}	JX862529	JX862535	KF170921	N/A	N/A
D. biguttulata	CFCC 52584^{T}	MH121519	MH121561	MH121598	MH121437	MH121477
D. biguttulata	CFCC 52585	MH121520	MH121562	MH121599	MH121438	MH121478
D. brasiliensis	CBS 133183^{T}	KC343042	KC343768	KC344010	KC343284	KC343526
D. brasiliensis	LGMF926	KC343043	KC343769	KC344011	KC343285	KC343527
D. breyniae	CBS 148910^{T}	ON400846	ON409188	ON409186	ON409189	ON409187
D. caatingaensis	URM7485^{T}	KY085927	KY115604	KY115601	KY115598	KY115605
D. caatingaensis	URM7484	KY085928	N/A	KY115602	KY115599	KY115606
D. caryae	CFCC 52563^{T}	MH121498	MH121540	MH121580	MH121422	MH121458
D. caryae	CFCC 52564	MH121499	MH121541	MH121581	MH121423	MH121459
D. chimonanthi	SCHM 3614^{T}	AY622993	N/A	N/A	N/A	N/A
D. chimonanthi	SCHM 3603	AY620820	N/A	N/A	N/A	N/A
D. cichorii	MFLUCC 17-1023^{T}	KY964220	KY964176	KY964104	KY964133	N/A
D. cinnamomi	CFCC 52569^{T}	MH121504	MH121546	MH121586	N/A	MH121464
D. cinnamomi	CFCC 52570	MH121505	MH121547	MH121587	N/A	MH121465
D. citriasiana	ZJUD30^{T}	JQ954645	JQ954663	KC357459	KC357491	N/A
D. citriasiana	ZJUD81	KJ490616	KJ490495	KJ490437	N/A	KJ490558
D. convolvuli	CBS 124654^{T}	KC343054	KC343780	KC344022	KC343296	KC343538
D. convolvuli	FAU649	KJ590721	KJ590765	N/A	KJ612130	KJ659210
D. coracoralinae	URM 8912^{T}	PP192078	PP430449	PP402241	PP408214	PP421133
D. coracoralinae	FCCUFG 39	PP192079	N/A	PP402242	PP408215	PP421134
D. cucurbitae	DAOM 42078^{T}	KM453210	KM453211	KP118848	N/A	KM453212
D. cucurbitae	CBS 136.25	KC343031	KC343757	KC343999	KC343273	KC343515
D. cuppatea	CBS 117499^{T}	KC343057	KC343783	KC344025	KC343299	KC343541
D. cyatheae	YMJ-1364^{T}	JX570889	KC465406	KC465403	KC465410	N/A
D. discoidispora	ZJUD89^{T}	KJ490624	KJ490503	KJ490445	N/A	KJ490566
D. discoidispora	GZCC 22-0065	OP056659	OP150498	OP150576	OP150655	OP150730
D. eleutharrhenae	01^{T*}	OK017069	OK017070	OK017071	N/A	N/A
D. eleutharrhenae	02*	OK648457	OK648458	OK648459	N/A	N/A
D. fici-septicae	NCYUCC 19-0108^{T}	MW114349	MW192212	MW148269	N/A	N/A
D. fici-septicae	MFLU 20-20178	MW114348	MW192211	MW148268	N/A	N/A
D. foliorum	CMRP 1321^{T}	MT576688	MT584310	MT584327	MT584341	MT584338
D. foliorum	CMRP 1330	MT576671	MT584309	MT584328	MT584342	MT584340
D. ganjae	CBS 180.91^{T}	KC343112	KC343838	KC344080	KC343354	KC343596
D. ganjae	PSCG489	MK626955	MK654897	MK691287	MK691202	MK726204
D. goulteri	BRIP 55657a^{T}	KJ197290	KJ197252	KJ197270	N/A	N/A
D. gulyae	BRIP 54025^{T}	JF431299	JN645803	N/A	N/A	N/A
D. gulyae	BRIP 53158	JF431284	JN645799	N/A	N/A	N/A
D. guttulata	CGMCC3.20100^{T}	MT385950	MT424685	MT424705	MW022470	MW022491
D. guttulata	GZCC 19-0371	MT797178	MT793021	MT793032	MW022471	MW022492
D. helianthi	CBS 592.81^{T}	KC343115	KC343841	KC344083	KC343357	KC343599

Species	Strain	ITS	*tef1*	*tub2*	*cal*	*his3*
D. helianthi	CBS 344.94	KC343114	KC343840	KC344082	KC343356	KC343598
D. hordei	CBS 481.92^{T}	KC343120	KC343846	KC344088	KC343362	KC343604
D. infecunda	CBS 133812^{T}	KC343126	KC343852	KC344094	KC343368	KC343610
D. infertilis	CBS 230.52^{T}	KC343052	KC343778	KC344020	KC343294	KC343536
D. infertilis	CPC 20322	KC343053	KC343779	KC344021	KC343295	KC343537
D. juglandigena	GUCC 422.16^{T}	OP581229	OP688534	OP688559	N/A	N/A
D. juglandigena	GUCC 422.161	OP581230	OP688535	OP688560	N/A	N/A
D. kyushuensis	STE-U2675^{T}	AF230749	N/A	N/A	N/A	N/A
D. kyushuensis	ch-D-1	AB302250	N/A	N/A	N/A	N/A
D. leucospermi	CBS 111980^{T}	N/A	KY435632	KY435673	KY435663	KY435653
D. leucospermi	CAA763	MK792291	MK828064	MK837915	MK883823	MK871433
D. longicolla	FAU599^{T}	KJ590728	KJ590767	KJ610883	KJ612124	KJ659188
D. longicolla	CBS 100.87	KC343196	KC343922	KC344164	KC343438	KC343680
D. longispora	CBS 194.36^{T}	KC343135	KC343861	KC344103	KC343377	KC343619
D. lusitanicae	CBS 123213^{T}	KC343137	KC343863	KC344105	KC343379	KC343621
D. lusitanicae	CBS 123212	KC343136	KC343862	KC344104	KC343378	KC343620
D. machilii	SAUCC194.111^{T}	MT822639	MT855951	MT855836	MT855718	MT855606
D. mayteni	CBS 133185^{T}	KC343139	KC343865	KC344107	KC343381	KC343623
D. megalospora	CBS 143.27^{T}	KC343140	KC343866	KC344108	KC343382	KC343624
D. melonis	CBS 507.78^{T}	KC343142	KC343868	KC344110	KC343384	KC343626
D. melonis	FAU640	KJ590702	KJ590741	KJ610858	KJ612099	KJ659184
D. melonis	ZHKUCC 20-0014	MT355684	MT409338	MT409292	MT409314	N/A
D. melonis	**MFLUCC 24-0522**	**OR936658**	**PQ774278**	**PQ774285**	**N/A**	**PQ774293**
D. melonis	**MFLUCC 23–0300**	**PQ777476**	**PQ774277**	**PQ774284**	**PQ774290**	**N/A**
D. middletonii	BRIP 54884e^{T}	KJ197286	KJ197248	KJ197266	N/A	N/A
D. middletonii	BRIP 57329	KJ197285	KJ197247	KJ197265	N/A	N/A
D. minusculata	CGMCC3.20098^{T}	MT385957	MT424692	MT424712	MW022475	MW022499
D. minusculata	GZCC 19-0345	MT797184	MT793027	MT793038	MW022476	MW022500
D. monetii	MF Ha18-048^{T}	MW008493	MW008515	MW008504	MZ671938	MZ671964
D. monetii	MF Ha18-049	MW008494	MW008516	MW008505	MZ671939	MZ671965
D. morindendophytica	ZHKUCC 22-0069^{T}	ON322897	ON315053	ON315087	N/A	ON315027
D. morindendophytica	ZHKUCC 22-0070	ON322898	ON315054	ON315088	N/A	ON315028
D. myracrodruonis	URM 7972^{T}	MK205289	MK213408	MK205291	MK205290	N/A
D. neoarctii	CBS 109490^{T}	KC343145	KC343871	KC344113	KC343387	KC343629
D. novem	CBS 127270^{T}	KC343156	KC343882	KC344124	KC343398	KC343640
D. novem	CBS 127271	KC343157	KC343883	KC344125	KC343399	KC343641
D. novem	PL42	JQ697843	JQ697856	N/A	N/A	N/A
D. orixae	KUNCC 21-10714^{T}	OK283041	N/A	N/A	OK484485	OK484486
D. orixae	GZCC 21-1085	OL889852	OL944724	OL944726	N/A	N/A
D. ovalispora	CGMCC3.17256^{T}	KJ490628	KJ490507	KJ490449	N/A	KJ490570
D. oxe	CBS 133186^{T}	KC343164	KC343890	KC344132	KC343406	KC343648
D. oxe	CBS 133187	KC343165	KC343891	KC344133	KC343407	KC343649
D. pachirae	CDA 728^{T}	MG559537	MG559539	MG559541	MG559535	N/A
D. pachirae	CDA 730	MG559538	MG559540	MG559542	MG559536	N/A
D. paranensis	CBS 133184^{T}	KC343171	KC343897	KC344139	KC343413	KC343655
D. paranensis	LMICRO417	KY461115	KY461116	N/A	N/A	N/A
D. passiflorae	CBS 132527^{T}	JX069860	N/A	N/A	N/A	KY435654
D. passiflorae	CAA953	MN190308	MT309430	MT309456	MT309447	MT309439
D. pedratalhadensis	URM 8304^{T}	PP192073	PP430438	PP402232	N/A	PP421129
D. pedratalhadensis	FCCUFG 49	PP192075	N/A	N/A	PP408217	PP421131
D. phaseolorum	AR4203^{T}	KJ590738	KJ590739	KJ610893	KJ612135	KJ659220
D. pseudobauhiniae	MFLUCC 17-1669^{T}	MF190119	MF377598	N/A	N/A	N/A
D. pseudobauhiniae	MFLUCC 17-1670	MF190118	MF377599	N/A	N/A	N/A
D. quercicola	CSUFTCC104^{T}	ON076567	ON081659	N/A	ON081670	ON081667

Species	Strain	ITS	*tef1*	*tub2*	*cal*	*his3*
D. quercicola	CSUFTCC105	ON076568	ON081660	N/A	ON081671	ON081668
D. racemosae	CBS 143770^{T}	MG600223	MG600225	MG600227	MG600219	MG600221
D. raonikayaporum	CBS 133182^{T}	KC343188	KC343914	KC344156	KC343430	KC343672
D. raonikayaporum	MFLUCC 14-1133	KU712448	KU749368	KU743987	KU749355	N/A
D. raonikayaporum	MFLUCC 14-1136	KU712449	KU749369	KU743988	KU749356	N/A
D. rosae	MFLUCC 17-2658^{T}	MG828894	N/A	MG843878	MG829273	N/A
D. rosae	MFLUCC 17-2574	MG906793	MG968954	MG968952	N/A	N/A
D. rosiphthora	COAD 2914^{T}	N/A	QOI91674	N/A	QOI91672	N/A
D. sackstonii	BRIP 54669b^{T}	KJ197287	KJ197249	KJ197267	N/A	N/A
D. schini	CBS 133181^{T}	KC343191	KC343917	KC344159	KC343433	KC343675
D. schini	LGMF 910	KC343192	KC343918	KC344160	KC343434	KC343676
D. schoeni	MFLU 15-1279^{T}	KY964226	KY964182	KY964109	KY964139	N/A
D. schoeni	MFLU 15-2609	KY964229	KY964185	KY964112	KY964141	N/A
D. sclerotioides	CBS 296.67^{T}	MH858974	KC343919	KC344161	KC343435	KC343677
D. sclerotioides	CBS 710.76	KC343194	KC343920	KC344162	KC343436	KC343678
D. serafiniae	BRIP 55665a^{T}	KJ197274	KJ197236	KJ197254	N/A	N/A
D. serafiniae	BRIP 54136	KJ197273	KJ197235	KJ197253	N/A	N/A
D. siamensis	MFLUCC 10-0573a^{T}	JQ619879	JX275393	JX275429	JX197423	N/A
D. siamensis	MFLUCC 12-0300	KT459417	KT459451	KT459435	KT459467	N/A
D. sojae	FAU635^{T}	KJ590719	KJ590762	KJ610875	KJ612116	KJ659208
D. sojae	CBS 116019	KC343175	KC343901	KC344143	KC343417	KC343659
D. stewartii	CBS 193.36	MH867279	GQ250324	JX275421	JX197415	N/A
D. stewartii	MN1	KX668416	KX852355	N/A	N/A	N/A
D. submersa	CGMCC3.24297^{T}	OP056717	OP150556	OP150633	OP150710	OP150786
D. submersa	GZCC 22-0007	OP056718	OP150557	OP150634	OP150711	OP150787
D. subordinaria	CBS 464.90^{T}	KC343214	KC343940	KC344182	KC343456	KC343698
D. subordinaria	CBS 101711	KC343213	KC343939	KC344181	KC343455	KC343697
D. tarchonanthi	CBS 146073^{T}	MT223794	N/A	MT223733	N/A	MT223759
D. tecomae	CBS 100547^{T}	KC343215	KC343941	KC344183	KC343457	KC343699
D. tectoendophytica	MFLUCC 13-0471^{T}	KU712439	KU749367	KU743986	KU749354	N/A
D. tectonendophytica	LC8115	KY491550	KY491560	KY491570	N/A	N/A
D. terebinthifolii	CBS 133180^{T}	KC343216	KC343942	KC344184	KC343458	KC343700
D. terebinthifolii	LGMF907	KC343217	KC343943	KC344185	KC343459	KC343701
D. thailandica	**MFLUCC 24-0523^{T}**	**OR946374**	**PQ774276**	**PQ774283**	**N/A**	**PQ774292**
D. thailandica	**MFLUCC 23–0299**	**PQ777475**	**PQ774275**	**PQ774282**	**PQ774289**	**N/A**
D. thunbergiicola	MFLUCC 12-0033^{T}	KP715097	KP715098	N/A	N/A	N/A
D. tulliensis	BRIP 62248a^{T}	KR936130	KR936133	KR936132	N/A	N/A
D. tulliensis	JZB320128	MK335814	MK523573	MK500152	MK500240	N/A
D. tulliensis	MFLUCC 14-1139	KU712438	KU749366	KU743985	KU749353	N/A
D. tulliensis	**MFLUCC 24-0524**	**PQ777478**	**PQ774280**	**PQ774287**	**N/A**	**PQ774294**
D. tulliensis	**MFLUCC 23–0301**	**PQ777477**	**PQ774279**	**PQ774286**	**PQ774291**	**N/A**
D. ueckerae	FAU656^{T}	KJ590726	KJ590747	KJ610881	KJ612122	KJ659215
D. ueckerae	BRIP 54736j	KJ197282	KJ197244	KJ197262	N/A	N/A
D. unshiuensis	ZJUD50^{T}	KJ490585	KJ490464	KJ490406	N/A	KJ490527
D. unshiuensis	PSCG339	MK626928	MK654879	MK691300	MK691181	MK726188
D. vangoghii	MF Ha18-045^{T}	MW008491	MW008513	MW008502	MZ671936	MZ671962
D. vangoghii	MF Ha18-046	MW008492	MW008514	MW008503	MZ671937	MZ671963
D. vargemgrandensis	URM 8784^{T}	PP192069	PP430456	PP421092	PP421068	PP421135
D. vexans	CBS 127.14	KC343229	KC343955	KC344197	KC343471	KC343713
D. vexans	FAU597	KJ590734	KJ590774	KJ610889	KJ612131	KJ659216
D. vochysiae	LGMF1583^{T}	MG976391	MK007526	MK007527	MK007528	MK033323
D. yunnanensis	CGMCC3.18289^{T}	KX986796	KX999188	KX999228	KX999290	KX999267
D. yunnanensis	LC8107	KY491542	KY491552	KY491562	KY491572	N/A

The newly generated sequences are in bold. Type and reference collections are denoted with "^{T}" while missing data are shown as "N/A". * The species name is invalid but included for taxon sampling.

Table 2. GenBank accession numbers of the taxa used in the phylogenetic analyses of Xylariales.

Species	Strain	ITS	LSU	*rpb2*	*tub2*
Albicollum vincensii	CBS 147286^{T}	ON869297	ON869297	ON808475	ON808519
Amphirosellinia nigrospora	HAST 91092308^{T}	GU322457	N/A	GQ848340	GQ495951
Anthostomella helicofissa	MFLUCC 14-0173^{T}	MW240653	MW240583	KP340534	KP406617
Anthostomella lamiacearum	MFLU18-0101^{T}	MW240669	MW240599	MW658648	N/A
Anthostomelloides brabeji	CBS 110128	EU552098	EU552098	N/A	N/A
Anthostomelloides krabiensis	MFLUCC 15-0678^{T}	KX305927	KX305928	KX305929	N/A
Anthostomelloides leucospermi	CBS 110126^{T}	EU552100	EU552100	N/A	N/A
Barrmaelia macrospora	CBS 142768^{T}	KC774566	KC774566	MF488995	MF489014
Biscogniauxia nummularia	MUCL 51395^{T}	KY610382	KY610427	KY624236	KX271241
Chaetomium elatum	CBS 374.66	KC109758	KC109758	KF001820	KC109776
Circinotrichum circinatum	CBS 148326	ON400743	ON400796	ON399328	N/A
Circinotrichum maculiforme	CBS 140016^{T}	KR611874	KR611895	ON399338	N/A
Clypeosphaeria mamillana	CBS 140735^{T}	KT949897	KT949897	MF489001	MH704637
Clypeosphaeria mamillana	WU 33599	KT949898	KT949898	N/A	N/A
Clypeosphaeria oleae	CPC 36779	MN562130	MN567637	N/A	N/A
Coniocessia maxima	CBS 593.74^{T}	GU553332	MH878275	N/A	N/A
Coniocessia nodulisporioides	CBS 281.77^{T}	MH861061	MH872831	N/A	N/A
Dematophora bunodes	CBS 124028	MN984619	MN984625	N/A	MN987245
Didymobotryum rigidum	JCM 8837^{T}	LC228650	LC228707	N/A	N/A
Digitodochium amoenum	CBS 147285^{T}	ON869303	ON869303	ON808481	ON808525
Digitodochium rhodoleucum	NBRC 32296	LC146732	LC146732	N/A	N/A
Emarcea castanopsidicola	CBS 117105	AY603496	MK762717	MK791285	MK776962
Emarcea eucalyptigena	CBS 139908	KR476733	MK762718	MK791286	MK776963
Entalbostroma erumpens	ICMP 21152^{T}	KX258206	N/A	KX258204	KX258205
Entoleuca mammata	JDR 100	GU300072	N/A	GQ844782	GQ470230
Entosordaria perfidiosa	CBS 142773^{T}	MF488993	MF488993	MF489003	MF489021
Fasciatispora arengae	MFLUCC 15-0326a^{T}	MK120275	MK120300	MK890794	MK890793
Fasciatispora cocoes	MFLUCC 18-1445^{T}	MN482680	MN482675	MN481517	MN505154
Graphostroma platystomum	CBS 270.87^{T}	JX658535	DQ836906	KY624296	HG934108
Gyrothrix verticillata	CBS 148806	ON400759	ON400813	ON399318	N/A
Halorosellinia krabiensis	MFLU 17-2596^{T}	MN047119	MN017883	N/A	MN431493
Hansfordia pruni	CBS 194.56^{T}	MK442585	MH869122	KU684307	N/A
Hansfordia pulvinata	CBS 144422	MK442587	MK442527	N/A	N/A
Helicogermslita clypeata	MFLU 18-0852^{T}	MW240666	MW240596	MW658647	MW775614
Hypocopra rostrata	NRRL 66178	KM067909	KM067909	N/A	N/A
Hypocopra zeae	MFLU 18-0809^{T}	MW240671	MW240601	MW658650	MW775616
Hypocreodendron sanguineum	J.D.R.169^{T}	GU322433	N/A	GQ844819	GQ487710
Hypomontagnella monticulosa	MFLUCC 18-0362	MN337231	MN336235.2	MN366246	MN509783
Muscodor thailandicus	MFLUCC 17-2669	MK762707	MK762714	MK791283	MK776960
Muscodor ziziphi	MFLUCC 17-2662	MK762705	MK762712	MK791281	MK776958
Jackrogersella multiformis	CBS 119016^{T}	KC477234	KY610473	KY624290	KX271262
Kretzschmaria deusta	CBS 163.93	KC477237	KY610458	KY624227	KX271251
Kretzschmariella culmorum	JDR 88	KX430043	N/A	KX430045	KX430046
Linosporopsis ischnotheca	CBS 145761^{T}	MN818952	MN818952	MN820708	MN820715
Magnostiolata mucida	MFLU 19-2133^{T}	MW240673	MW240603	MW658652	MW775618
Melanographium phoenicis	MFLUCC 18-1481^{T}	MN482677	MN482678	N/A	N/A
Melanographium smilacis	MFLU 21-0075^{T}	MZ538514	MZ538548	N/A	N/A
Nemania serpens	HAST 235	GU292820	N/A	GQ844773	GQ470223
Neoanthostomella fici	MFLU 19-2765^{T}	MW114390	MW114445	MW177711	N/A
Neoxylaria juruensis	HAST 92042501	GU322439	N/A	GQ844825	GQ495932
Nigropunctata bambusicola	MFLU 19-2145^{T}	MW240664	MW240594	MW658646	N/A
Nigropunctata nigrocircularis	MFLU 19-2130^{T}	MW240661	MW240591	N/A	MW775612
Occultitheca ananasi	MFLU 23-0251^{T}	OR438426	OR438886	N/A	N/A
Occultitheca ananasi	MFLUCC 23-0120	OR438427	OR438887	OR634962	OR538094

Species	Strain	ITS	LSU	*rpb2*	*tub2*
Occultitheca chiangraiensis	**MFLU 24-0414^{T}**	**PQ777479**	**PQ778042**	**PQ774295**	**PQ774288**
Occultitheca rosae	HKAS 102393^{T}	MW240672	MW240602	MW658651	MW775617
Podosordaria mexicana	WSP 176	GU324762	N/A	GQ853039	GQ844840
Poronia punctata	CBS 656.78^{T}	KT281904	KY610496	KY624278	KX271281
Pseudoanthostomella pini-nigrae	MFLUCC 16-0478^{T}	KX533453	KX533454	KX789492	N/A
Pseudoceratocladium polysetosum	FMR 10750^{T}	KY853430	KY853490	ON399348	N/A
Rosellinia chiangmaiensis	MFLUCC 15-0015^{T}	KU246226	KU246227	N/A	N/A
Rosellinia lamprostoma	HAST 89112602	EF026118	N/A	GQ844778	EF025604
Sarcoxylon compunctum	CBS 359.61	KT281903	KT281898	KY624230	KX271255
Sordaria fimicola	CBS 723.96	MH862606	MH874231	DQ368647	N/A
Spiririma gaudefroyi	CBS 147284^{T}	ON869320	ON869320	ON808497	ON808541
Spirodecospora melnikii	MAFF 247746^{T}	LC731937	LC731946	LC731955	N/A
Spirodecospora paulospiralis	MAFF 247749^{T}	LC731940	LC731949	LC731957	N/A
Stromatoneurospora phoenix	BCC 82040	MT703666	MT735133	MT742605	MT700438
Vamsapriya indica	MFLUCC 12-0544	KM462839	KM462840	KM462841	KM462838
Xenoanthostomella chromolaenae	MFLUCC 17-1484^{T}	MN638863	MN638848	MN648729	N/A
Xenoanthostomella cycadis	CBS 137969^{T}	KJ869121	KJ869178	ON399350	N/A
Xylaria acuminatilongissima	HAST 95060506^{T}	EU178738	N/A	GQ853028	GQ502711
Xylaria arbuscula	CBS 126415	KY610394	KY610463	KY624287	KX271257
Xylaria botuliformis	HAST 89091627	MN089652	N/A	MN095399	MN095400
Xylaria brunneovinosa	HAST 720^{T}	EU179862	N/A	GQ853023	GQ502706
Xylaria ellisii	DAOM 628556^{T}	MN218820	MN218817	MN216186	N/A
Xylaria eucalypti	CPC 36723	MN562127	MN567634	N/A	N/A
Xylaria hypoxylon	CBS 122620^{T}	AM993141	KM186301	KM186302	KM186300

The newly generated sequences are in bold. Type and reference collections are denoted with “^{T},” while missing data are shown as “N/A”.

Maximum likelihood analyses (ML), including 1000 bootstrap pseudoreplicates, were performed at the CIPRES web portal (Miller et al. 2017) using RAxML version 8.2.12 (Stamatakis 2014). The general time reversible (GTR) model with a discrete gamma distribution plus invariant site (GTR + I + G) was used as the nucleotide substitution model. The best model for each gene was determined in JModelTest version 2.1.10 (Darriba et al. 2012) for the Bayesian analysis. The Bayesian inference posterior probabilities (BPP) distribution (Zhaxybayeva and Gogarten 2002) was estimated by Markov Chain Monte Carlo sampling (MCMC) in MrBayes version 3.2.2 on XSEDE (Ronquist et al. 2012) with four runs of MCMC for 1,000,000 generations, sampling trees every 100th generation. The first 25% of trees were excluded as burn-in, and the remaining trees were used to calculate posterior probabilities (BPP). The trees were visualised using FigTree version 1.4.4 (Rambaut 2012) and edited using Adobe Illustrator® CS6 (Adobe Systems, USA).

Genealogical concordance phylogenetic species recognition analysis

The closely related strains were further analysed using the genetic distances by performing a pairwise homoplasy index test (Φw) (Taylor et al. 2000; Bruen et al. 2006). A pairwise homoplasy index (PHI) test was performed in SplitsTree (CE 6.0.0) using Kimura’s two-parameter (K2P) models for low genetic distance datasets (Huson and Bryant 2024). LogDet transformation was applied for the average of nucleotide frequencies and splits decomposition graph options (Gu and Li 1996a, b; Taylor et al. 2000; Bruen et al. 2006; Huson and Bryant 2006; Gioan and Paul 2012; Nishimaki and Sato 2019). The standard deviation of split frequencies PHI test result (Φw) < 0.05 indicates significant recombination within the dataset.

Results

Phylogenetic analyses of section *sojae*

The phylogeny represents taxa from section *sojae* based on the concatenated dataset of ITS, *tef1*, *tub2*, *cal*, and *his3* sequences. The combined sequence alignment comprised 159 taxa with 3279 characters, including gaps (ITS: 1–587, *tef1*: 588–1131, *tub2*: 1132–2067, *cal*: 2068–2682, *his3*: 2683–3279). The ML and BI analyses showed similar topologies (Fig. 1). The best scoring ML tree had a final likelihood value of -47785.673. The matrix had 1463 constant sites, 1408 parsimony informative sites, and 2202 distinct site patterns. Estimated base frequencies were as follows: A = 0.213, C = 0.325, G = 0.239, T = 0.224, substitution rates: AC = 1.16629, AG = 3.42597, AT = 1.16629, CG = 1.00000, CT = 4.44139, GT = 1.000, gamma distribution shape parameter = 0.954, and tree length = 7.506.

Sordariomycetes O.E. Erikss. & Winka
Diaporthales Nannf.
Diaporthaceae Höhn. ex Wehm.

***Diaporthe melonis* Beraha & M.J. O'Brien, Phytopath. Z. 94(3): 205 (1979)**
Index Fungorum: IF312933
Facesoffungi Number: FoF17285
Fig. 2

Description. ***Saprobic*** on dead unidentified branch. ***Sexual morph*****:** not observed. ***Asexual morph*****:** ***Conidiomata*** 148–374 × 128–338 µm high ($\bar{x}$ = 250 × 225 µm, n = 15), pycnidial, mostly scattered, immersed, slightly erumpent through the host surface, discoid or subglobose, with a solitary undivided locule. ***Conidiophores*** reduced to conidiogenous cells. ***Alpha conidiogenous cells*** 5.7–25 × 1.1–2.5 µm ($\bar{x}$ = 15.6 × 1.7 µm, n = 50), hyaline, rarely branched, mostly aseptate, densely aggregated, cylindrical, straight to slightly curved and smooth. ***Alpha conidia*** 5–7.3 × 1.9–2.7 µm ($\bar{x}$ = 6.3 × 2.3 µm, n = 40), unicellular, fusiform to ellipsoidal, apex and base rounded, hyaline, smooth, bi-guttulate. ***Beta conidiogenous cells*** 6.2–16 × 1.6–2.6 µm ($\bar{x}$ = 9.4 × 2.1 µm, n = 40), phialidic, subcylindrical, tapering towards the apex, hyaline. ***Beta conidia*** 19–27 × 1–2 µm ($\bar{x}$ = 23 × 1.5 µm, n = 40), filiform, aseptate, hyaline, smooth-walled, straight from base, and curve at apex. ***Gamma conidia*** not observed.

Culture characteristics. Colonies on PDA, reaching 20 mm diam., after 3 weeks at 25 °C, initially white, turning beige after 7–10 days, flat, felty with a thick texture at the centre and marginal area, lacking aerial mycelium; reverse, glossy grey, radiating outwardly.

Material examined. Thailand, Chiang Rai Province, Muang District, on a dead unidentified dicot branch, 16 January 2023, J. Louangphan, CR1-02 (MFLU 23–0474); living culture MFLUCC 24–0522 = MFLUCC 23–0300.

Hosts. *Annona squamosa* (Annonaceae), *Berberis aristata* (Berberidaceae), *Carapa guianensis* (Meliaceae), *Citrus grandis* cv. *Tomentosa* (Rutaceae), *Cucumis melo* (Cucurbitaceae), *Glottidium* sp. (Fabaceae), *Glycine max*, *G. soja* (Fabaceae), unidentified branch (Dong et al. 2021a, b; Hongsanan et al. 2023; This study).

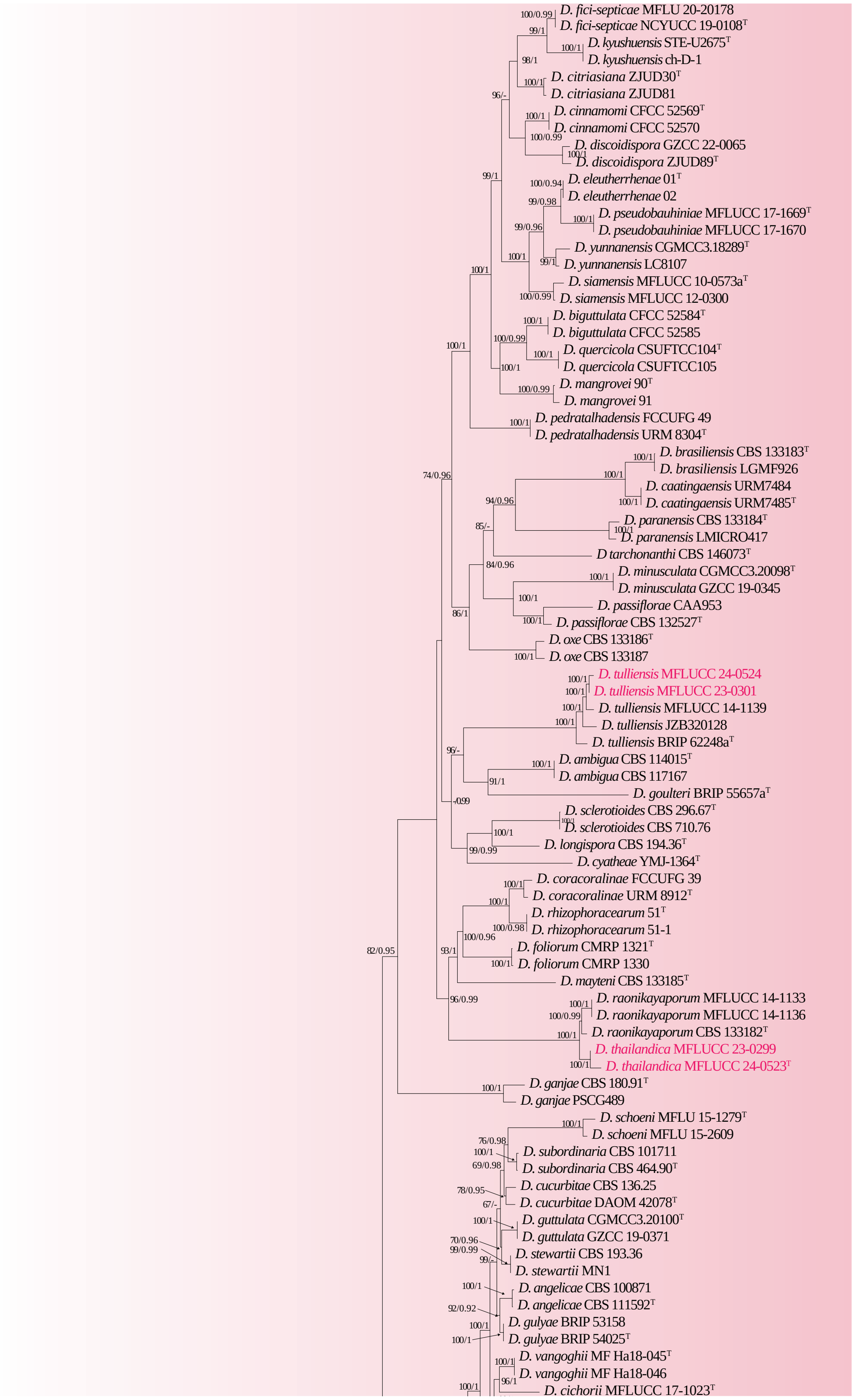

Figure 1. Phylogram of the *Diaporthe sojae* species complex generated from a maximum likelihood analysis based on the combined ITS, *tef1*, *tub2*, *cal,* and *his3* sequence data. *Diaporthella corylina* (CBS 121124) was used as the outgroup. Bootstrap support values ≥ 60% ML/≥0.90 BPP are given at the nodes. The newly generated taxa are indicated in red. The holotype/ex-type strains are denoted with ^{T}.

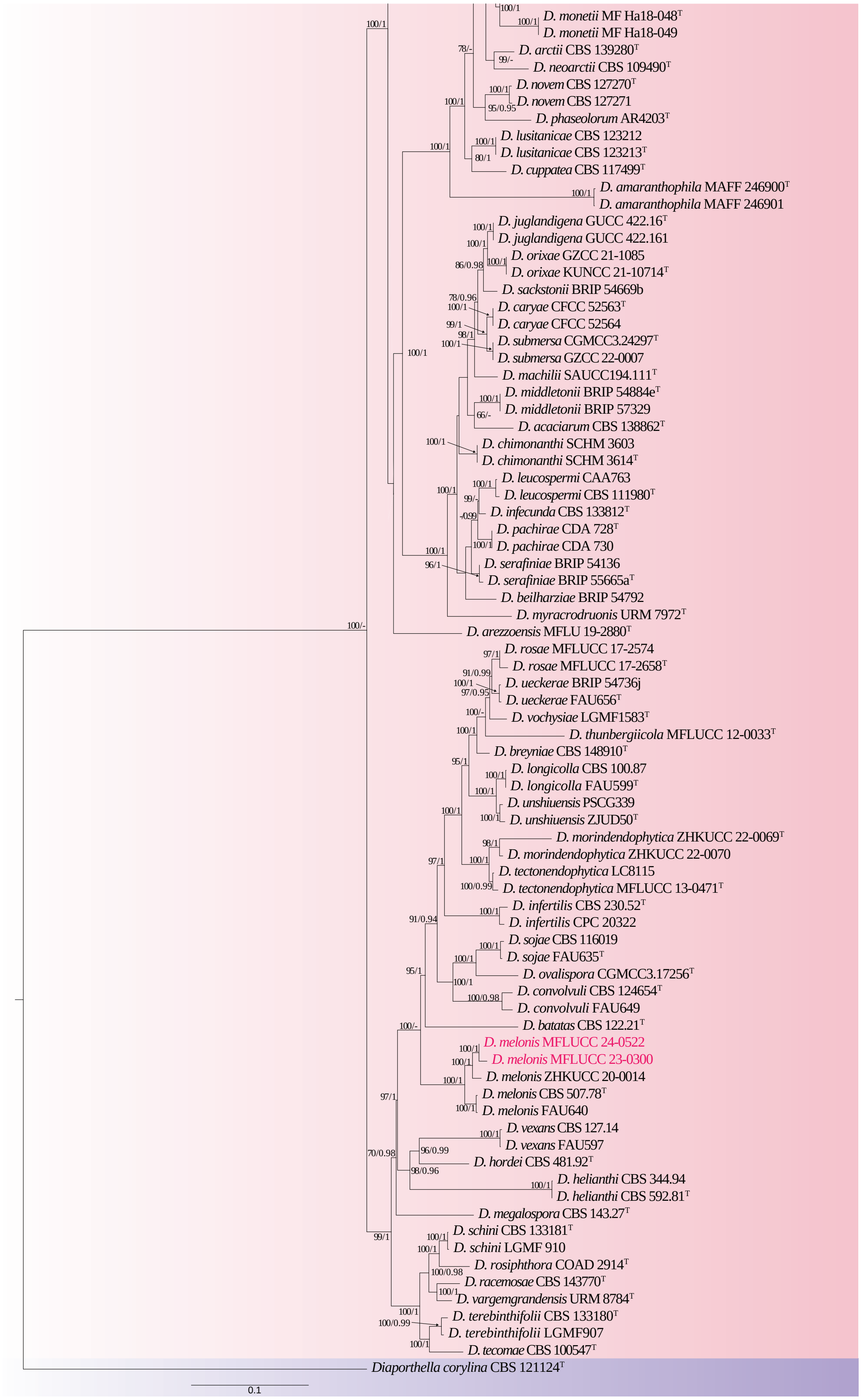

Figure 1. Continued.

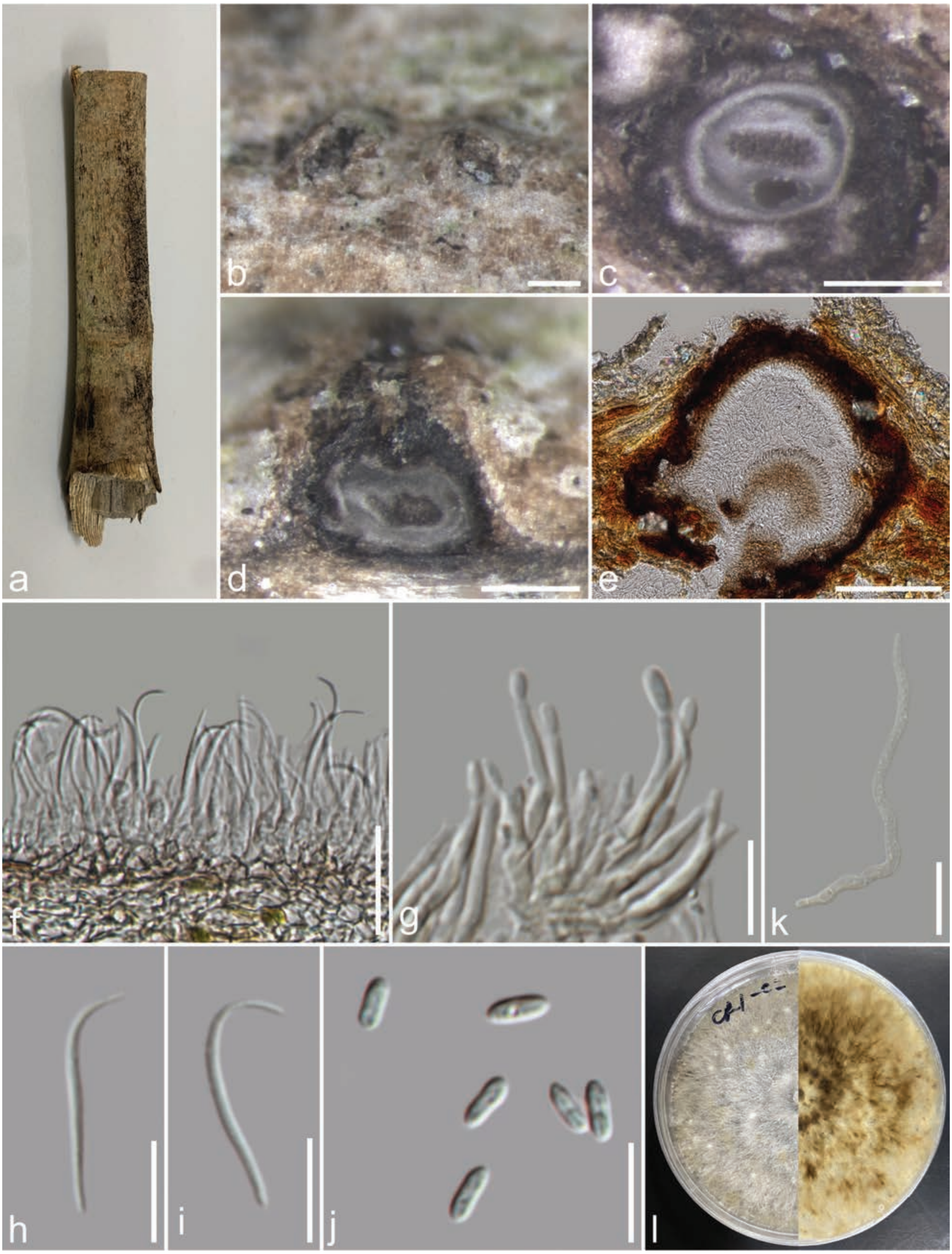

Figure 2. *Diaporthe melonis* (MFLU 23–0474) **a** host substrate **b** conidiomata on substrate **c** transverse section of conidioma **d, e** vertical section through conidiomata **f, g** conidiophores and conidiogenous cells **h, i** beta conidia **j** alpha conidia **k** a germinated conidium **l** front and reverse view of the colony on PDA. Scale bars: 200 µm (**b–d**); 100 µm (**e**); 20 µm (**f, k**); 10 µm (**g, h–j**).

Distribution. China, Myanmar, India, Indonesia, Japan, Thailand, the United States (Dong et al. 2021a, b; Hongsanan et al. 2023; this study).

Notes. Our isolates (MFLUCC 23–0300 and MFLUCC 24–0522) clustered with *D. melonis* isolates (CBS 507.78, FAU640, and ZHKUCC 20-0014) with 100% ML/1.00 BPP support (Fig. 1). Our isolate has a similar morphology to *D. melonis* but differs in having smaller conidiomata (148–374 µm vs. 100–500 µm diam.) and smaller alpha conidia (6.3 × 2.3 µm vs. 8.3 × 2.6 µm) (Beraha and O'Brien 1979). Our isolate has a beige culture compared to the brown culture of *D. melonis* (Beraha and O'Brien 1979). Our isolate also differs from *D. melonis* (*D. guangdongensis* ZHKUCC 20-0014) in the size of conidiomata (128–338 × 148–374 µm *vs.* 130–515 × 100–390 µm), alpha conidia (5–7.3 × 1.9–2.7 µm vs. 6–8 × 2–4 µm), and beta conidia (19–27 × 1–2 µm vs. 14–35 × 1–2 µm) (Dong et al. 2021a, b). Therefore, we report our isolate as a new geographical record of *D. melonis* from Thailand.

Diaporthe thailandica **Louangphan, Phukhams., K.D. Hyde & Bhunjun, sp. nov.**

Index Fungorum: IF903043
Facesoffungi Number: FoF17286
Figs 3, 4

Etymology. The name refers to the country where the holotype was collected.

Holotype. MFLU 23–0473.

Description. ***Saprobic*** on decaying dicot, visible as black necks immerging through the host surface. ***Sexual morph*****:** ***Ascomata*** 328–495 × 303–371 µm ($\bar{x}$ = 400 × 343 µm, n = 10), immersed in the host epidermis, globose to sub-globose, solitary or occur in clusters, black, ostiolate, papillate. ***Ostiole neck*** 220 × 86 µm, long, filled with periphysate. ***Peridium*** 20–50 µm wide, composed of several layers of cells of *textura angularis*, outer layers dark brown and inner layers hyaline to brown, thin-walled. ***Paraphyses*** 3.2–6.6 µm (n = 20), thin-walled, 2–4-septate, hyaline, wide at base, tapering towards the apex. ***Asci*** 45–58.9 × 8.6–12.7 µm ($\bar{x}$ = 51.5 × 10.5 µm, n = 40), unitunicate, 8-spored, clavate to subclavate, straight to slightly curved, sessile, with a J-, apical ring. ***Ascospores*** 11–15.5 × 3.9–5.6 µm ($\bar{x}$ = 13.5 × 4.7 µm, n = 40) L/W = 2.8, overlapping uniseriate to biseriate, 1-septate, constricted at the septum, ellipsoidal, smooth-walled, 2–4-guttulate, straight, hyaline, without appendages or a mucilaginous sheath. ***Asexual morph*** on PDA: ***Conidiomata*** 500–700 × 300–600 µm ($\bar{x}$ = 580 × 480 µm, n = 10), pycnidial, scattered or aggregated, globose or variable in shape, ostiolate with prominent neck, dark brown to black, pycnidal wall brown, consisting of thick-walled cells of *textura angularis*, conidial mass globose, initially hyaline to yellowish, becoming white to cream, conidial droplets exuding from central ostioles. ***Conidiophores*** 10–29.5 × 1.3–2.5 µm ($\bar{x}$ = 16.9 × 1.9 µm, n = 40), ampulliform to subcylindrical, filiform, branched to unbranched, 1–3-septate, hyaline, smooth, straight or slightly curved, wider at base, tapering towards the apex. ***Conidiogenous cells*** 2.1–8.1 × 1–2.3 µm ($\bar{x}$ = 4.2 × 1.5 µm, n = 40), subcylindrical, filiform, straight to curved, tapering towards the apex, collarette not flared, hyaline. ***Alpha conidia*** 5.3–8.8 × 2.3–3.5 µm ($\bar{x}$ = 7.3 × 2.9 µm, n = 40), ellipsoid, apex bluntly rounded, base obtuse to subtruncate, smooth, hyaline, bi- to multi-guttulate. ***Beta conidia*** 8.5–18.5 × 1.2–2 µm ($\bar{x}$ = 13.3 × 1.7 µm, n = 40), filiform, flexible to slightly curved, hyaline, base subtruncate, and aseptate. ***Gamma conidia*** not observed.

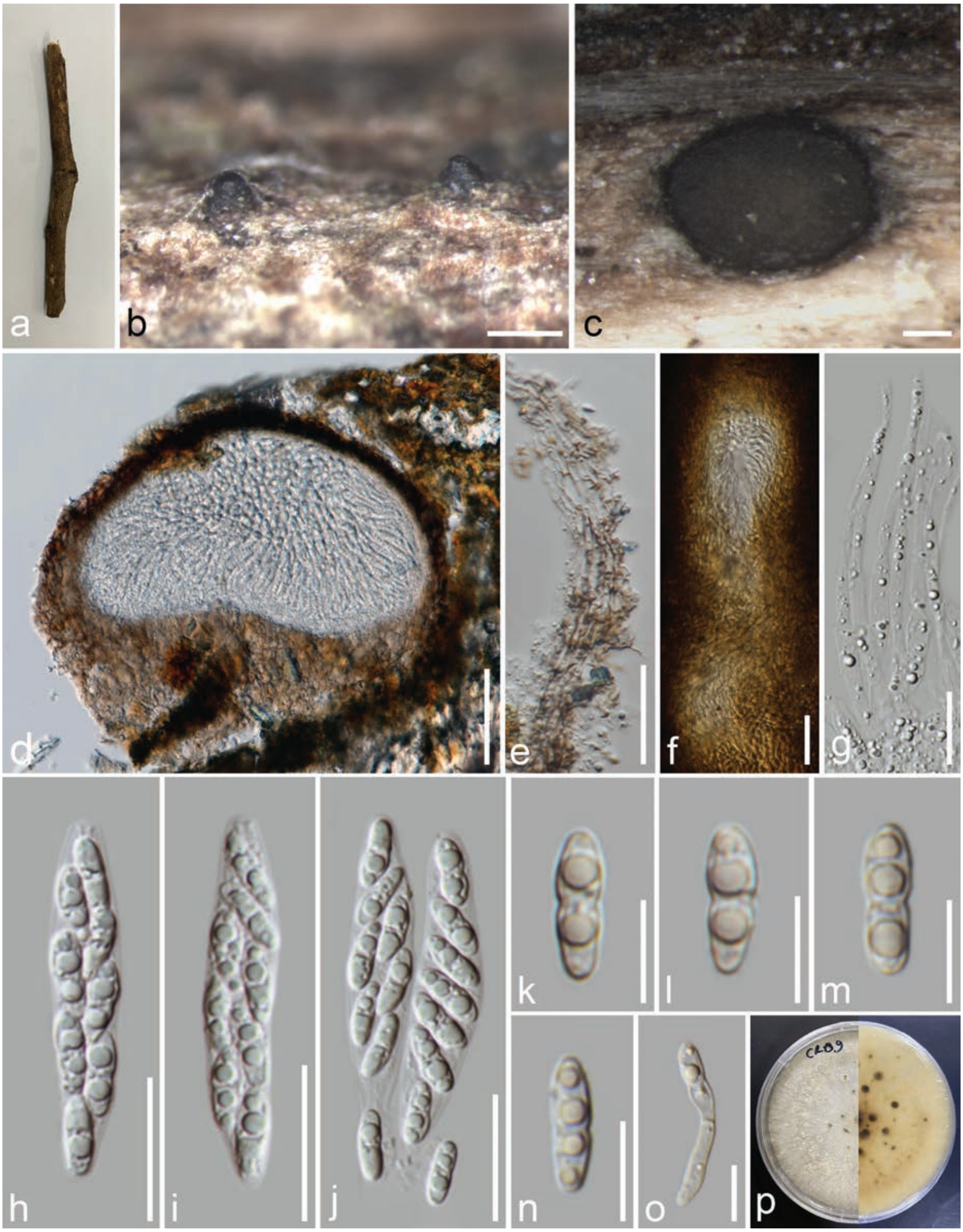

Figure 3. *Diaporthe thailandica* (MFLU 23–0473, holotype) **a** host substrate **b, c** ascomata on host substrate **d** vertical section through ascoma **e** peridium **f** ostiole **g** hamathecium **h–j** asci **k–n** ascospores **o** a germinated ascospore **p** front and reverse view of the colony on PDA. Scale bars: 200 µm (**b**); 100 µm (**c, d**); 20 µm (**e–j**); 10 µm (**k–o**).

Culture characteristics. Colonies on PDA, reaching 40 mm diam., after 2 weeks at 25 °C, initially white, turning pale brown after 7–10 days, radiating to the edge, margin undulate, medium dense, flat or umbonate; reverse, cream, radiating white outwardly with grey patches.

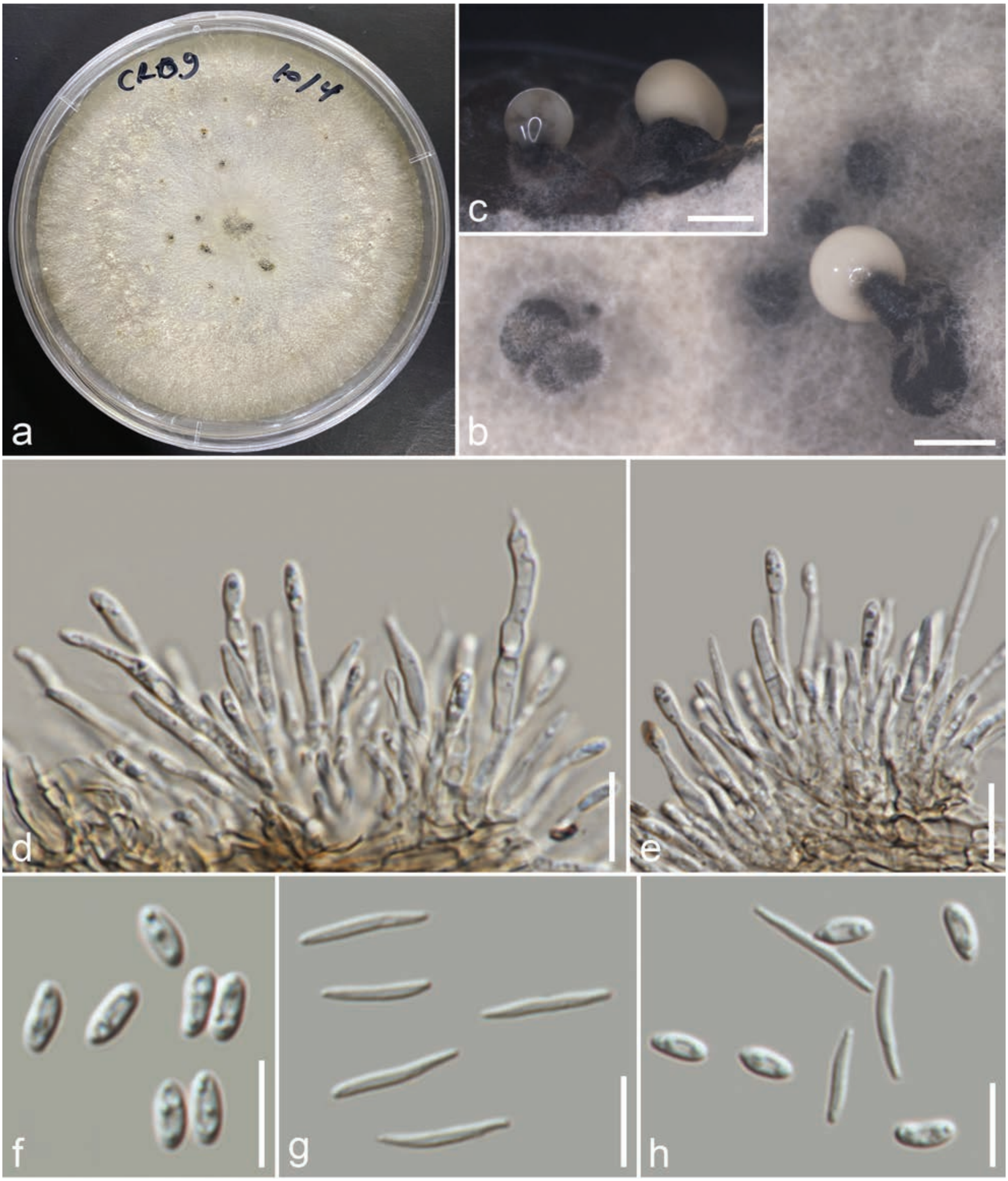

Figure 4. *Diaporthe thailandica* (Asexual morph, MFLUCC 24–0523) **a** culture on pda **b, c** conidiomata sporulating on pda **d, e** conidiogenous cells giving rise to conidia **f** alpha conidia **g** beta conidia **h** alpha and beta conidia. Scale bars: 500 µm **(b, c)**; 10 µm **(d–h)**.

Material examined. Thailand, Chiang Rai Province, Muang District, on a dead unidentified dicot, 16 January 2023, J. Louangphan, CR1-09 (MFLU 23–0473, ***holotype***); ex-type MFLUCC 24–0523 = MFLUCC 23–0299.

Host. Unidentified branch (this study).

Distribution. Thailand (this study).

Notes. *Diaporthe thailandica* (MFLUCC 23-0299 and MFLUCC 24–0523) formed a sister clade with isolates of *D. raonikayaporum* (CBS 133182, MFLUCC 14–1133, and MFLUCC 14–1136) with 100% ML/1.00 BPP support (Fig. 1). *Diaporthe thailandica* differs from *D. raonikayaporum* in its conidiomata (500–700 × 300–600 µm *vs.* 110–200 × 50–130 µm), conidiophores (10–29.5 × 1.3–2.5 µm vs. 16–26 × 2–3 µm), conidiogenous cells (2.1–8.1 × 1–2.3 µm *vs.* 5–10 × 2–3 µm), and beta conidia (8.5–18.5 *vs.* 7–13 µm) (Gomes et al. 2013). *Diaporthe thailandica* differs from *D. raonikayaporum* (=*D. neoraonikayaporum* MFLUCC 14–1133) in its conidiomata (500–700 × 300–600 µm vs. 690–1190 × 805–1285 µm), conidiophores (10–29.5 µm *vs.* 15–23 µm), alpha conidia (5.3–8.8 × 2.3–3.5 µm *vs.* 4–6 × 2–3 µm), and beta conidia (8.5–18.5 µm *vs.* 13–21 µm) (Doilom et al. 2017). Gamma conidia was observed in *D. raonikayaporum* (= *D. neoraonikayaporum*) but not in *D. thailandica* (Doilom et al. 2017). *Diaporthe thailandica* further differs from *D. raonikayaporum*, which has only been reported as an asexual morph (Gomes et al. 2013; Doilom et al. 2017). Our strain differs significantly (> 2.5%) compared to the sequence data of *D. raonikayaporum* (Table 3). However, our isolate does not have *cal* sequence data, while *his3* sequence data is not available for *D. raonikayaporum* (MFLUCC 14–1133 and MFLUCC 14–1136). A pairwise homoplasy index showed Φw = 1.0 when a genealogical correlation model was applied between *Diaporthe thailandica* and *D. raonikayaporum* (Fig. 5). Thus, *Diaporthe thailandica* is reported as a new species based on morphology and molecular evidence.

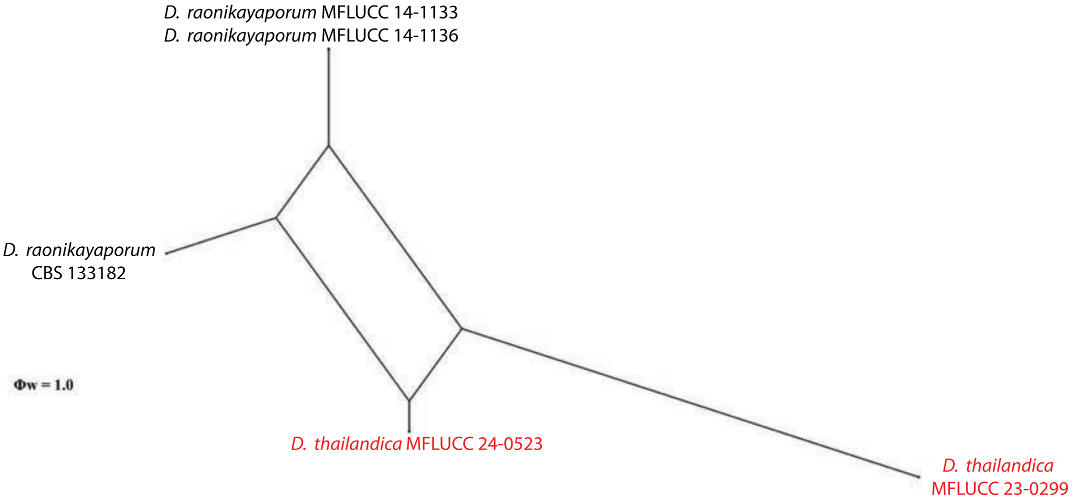

Figure 5. The splits graph from the pairwise homoplasy index (PHI) test generated from the combined ITS, *tef1*, *tub2*, *cal*, and *his3* sequence data of *Diaporthe thailandica* (indicated in red) and closely related taxa using both LogDet transformation and splits decomposition. PHI test results (Φw) < 0.05 indicate significant recombination within the dataset.

Table 3. Pairwise comparison of the sequences of *Diaporthe thailandica* and *D. raonikayaporum* isolates (excluding gaps).

Sequences	*D. raonikayaporum* (CBS 133182)	*D. raonikayaporum* (MFLUCC 14-1133)	*D. raonikayaporum* (MFLUCC 14-1136)
ITS	3.4% (18/529)	2.6% (14/529)	3.0% (16/529)
tef1	6.5% (21/323)	7.4% (24/323)	8.4% (27/323)
tub2	4.3% (18/415)	6.5% (27/415)	7.7% (32/415)
cal	–	–	–
his3	3.7% (17/450)	–	–

– Data not available.

Diaporthe tulliensis **R.G. Shivas, Vawdrey & Y.P. Tan, Persoonia 35: 301 (2015)**
Index Fungorum: IF812896
Facesoffungi Number: FoF16300
Fig. 6

Description. ***Saprobic*** on decaying *Bambusa*. ***Sexual morph*****:** Undetermined. ***Asexual morph*****:** ***Conidiomata*** 91–148 × 311–974 µm ($\bar{x}$ = 120 × 583 µm, n = 20), pycnidial, scattered or aggregated, embedded in host surface, slightly erumpent through

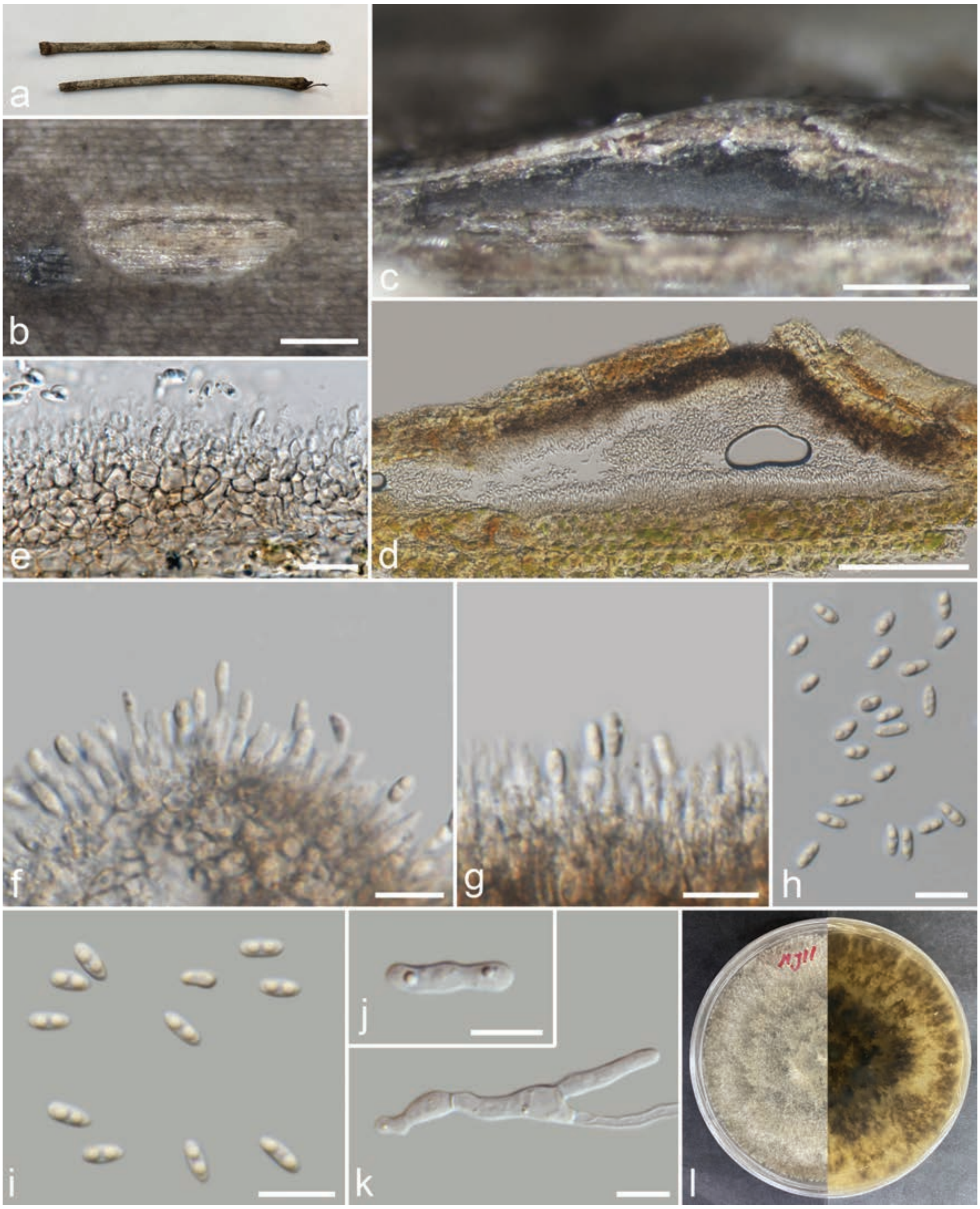

Figure 6. *Diaporthe tulliensis* (MFLU 23–0475) **a, b** conidiomata on host **c** longitudinal section through conidioma **d, e** transverse section of conidioma **f, g** conidiogenous cells giving rise to conidia **h, i** alpha conidia **j, k** germinated conidia **l** front and reverse view of the colony on PDA. Scale bars: 200 µm (**b–d**); 20 µm (**e**); 10 µm (**f–k**).

host surface, 1–3-locular conidioma, nearly flat, elongated, discoid, or variable in shape, black, consisting of hyaline, thin-walled cells of *textura angularis*, outer layer thick walled. ***Conidiophores*** reduced to conidiogenous cells. ***Conidiogenous cells*** 4–16 × 1.2–2.6 µm ($\bar{x}$ = 7.5 × 1.8 µm, n = 40), cylindrical, unbranched, aseptate, smooth, straight or slightly curved, tapering towards the apex, wider at base, hyaline. ***Alpha conidia*** 4.1–7.8 × 1.7–3.1 µm ($\bar{x}$ = 5.8 × 2.5 µm, n = 40), apex bluntly rounded, 1–2-guttulate, mostly bi-guttulate, oval or oblong to ellipsoid, hyaline, smooth, base obtuse to subtruncate. ***Beta*** and ***Gamma conidia*** not observed.

Culture characteristics. Colonies on PDA, reaching 40 mm diam., after 2 weeks at 25 °C, initially white, turning olivaceous grey after 7–10 days, darker at the centre and marginal area, lacking aerial mycelium; reverse, olivaceous grey bordered by dark margins.

Material examined. Thailand, Chiang Mai Province, Mae Taeng District, on dead terrestrial stem of *Bambusa* (Poaceae), 19 November 2022, J. Louangphan, MJ11 (MFLU 23–0475); living culture, MFLUCC 24–0524 = MFLUCC 23–0301.

Hosts. *Actinidia* spp. (Actinidiaceae), *Alangium kurzii* (Cornaceae), *Bambusa* sp. (Poaceae), *Bougainvillea glabra* (Nyctaginaceae), *Celtis formosana* (Ulmaceae), *Morinda officinalis* (Rutaceae), *Tectona grandis* (Lamiaceae), *Theobroma cacao* (Malvaceae), Soil, *Vitis vinifera* (Vitaceae) (Chang et al. 2005; Crous et al. 2015; Bai et al. 2017; Doilom et al. 2017; Yang et al. 2018; Manawasinghe et al. 2019; Tennakoon et al. 2021; Luo et al. 2022; this study).

Distribution. Australia, China, Korea, Thailand (Chang et al. 2005; Crous et al. 2015; Bai et al. 2017; Doilom et al. 2017; Yang et al. 2018; Manawasinghe et al. 2019; Tennakoon et al. 2021; Luo et al. 2022; this study).

Notes. In the phylogenetic analysis, our isolates (MFLUCC 23–0301 and MFLUCC 24–0524) clustered with *D. tulliensis* isolates (MFLUCC 14–1139, JZB320128, and BRIP 62248a) with 100% ML/1.00 BPP support (Fig. 1). Our isolate has a similar morphology to *D. tulliensis* isolates but differs from *D. tulliensis* in the size of conidiomata (up to 500 µm (= *D. celtidis* and *D. tulliensis*) *vs.* up to 510 µm (= *D. hubeiensis*) *vs.* 135–330 µm (= *D. alangii*) *vs.* 50–380 µm (= *D. morindae*) *vs.* 725–820 µm diam. (= *D. tectonae*)) (Crous et al. 2015; Doilom et al. 2017; Yang et al. 2018; Manawasinghe et al. 2019; Luo et al. 2022). Our isolate also differs due to the absence of beta conidia, which has been reported in some *D. tulliensis* isolates (Chang et al. 2005; Crous et al. 2015; Doilom et al. 2017; Manawasinghe et al. 2019). Therefore, we report our isolate as a new host record of *D. tulliensis*.

Phylogenetic analyses of Xylariales

The phylogeny represents selected taxa in Xylariales based on the concatenated dataset of ITS, LSU, *rpb2*, and *tub2* sequences. The combined sequence alignment comprised 78 strains with 3624 characters, including gaps (ITS: 1–578, LSU: 579–1432, *rpb2*: 1433–2573, *tub2*: 2574–3624). The ML and BI analyses of single and multi-gene showed similar topologies. The best scoring ML tree with a final likelihood value of -54607.950 (Fig. 7). The matrix had 1992 constant sites, 1349 parsimony informative sites, and 2026 distinct site patterns. Estimated base frequencies were as follows: A = 0.2405, C = 0.2618, G = 0.2637, T = 0.2337, substitution rates: AC = 1.4137, AG = 3.9195, AT = 1.4543, CG = 1.1208, CT = 7.4615, GT = 1.000, gamma distribution shape parameter = 0.759631, and tree length = 7.506.

Xylariales Nannf.
Xylariaceae Tul. & C. Tul.
***Occultitheca* J.D. Rogers & Y.M. Ju**

***Occultitheca chiangraiensis* Louangphan, Phukhams., K.D. Hyde & Bhunjun, sp. nov.**
Index Fungorum: IF903235
Facesoffungi Number: FoF17287
Fig. 8

Etymology. The name refers to the province where the holotype was collected.

Holotype. MFLU 24–0414.

Description. ***Saprobic*** on early decaying branch. ***Sexual morph*: *Ascomata*** 220–342 × 228–395 µm (x̄ = 290 × 324 µm, n = 15), immersed, solitary, scattered, globose to subglobose, erumpent through host surface, visible as black dot of ostiole, surrounded by a whitish halo. ***Clypeus*** carbonaceous, rudimentary, thick-walled, the ostiolar opening surrounded with black cells. ***Ostioles*** centric, ostiolar canal periphysate. ***Peridium*** 17–30 µm (x̄ = 23 µm, n = 20) wide, tightly attached to the host tissue, with two cell layers, outer layer thick-walled, comprising yellowish brown cells of *textura angularis*, inner layer thin, composed of hyaline cells of *textura angularis*. ***Paraphyses*** 3.7–7.6 µm (x̄ = 5.4 µm, n = 25) wide, wider at the base, longer than the asci, filamentous, septate, constricted at the septa, embedded in gelatinous matrix. ***Asci*** 112–158 × 8.5–13.7 µm (x̄ = 131 × 11 µm, n = 25), 8-spored, unitunicate, cylindrical, short pedicellate, apically rounded, with 3.9–5.6 × 2.5–3.7 µm (x̄ = 5 × 3 µm, n = 18), rectangular to slightly obconic, apical ring, J+ in Melzer's reagent. ***Ascospores*** 14.5–17.6 × 6–7.4 µm (x̄ = 16.3 × 6.7 µm, n = 30), L/W 2.4, oblong to ellipsoidal, uniseriate, brown, inequilaterally unicellular, apical cell 13–15.5 µm (x̄ = 14.5 µm, n = 30) long, usually with large guttules, brown cell with a mucilaginous sheath covering most of the spore length when mature, with a small, hyaline, rounded, basal cell, 1.3–2.3 µm (x̄ = 1.8 µm, n = 30), lack of germ slit. ***Asexual morph*:** Undetermined.

Culture characteristics. Colonies on PDA, reaching 40 mm diam., after 21 days at 25 °C, circular, entire edge, smooth surface, flat, slightly woolly, smooth margin, above ash white from the centre to white at the edge with concentric rings of woolly; from below: light brown at the centre, white at the margin, with ash white mycelium.

Material examined. Thailand, Chiang Rai, Mae Fah Luang District, Mae Salong Nok, on a dead unidentified dicot branch, 16 January 2023, J. Louangphan, CR1–19 (MFLU 24–0414, holotype); ex-type MFLUCC 25–0158.

Host. Unidentified branch (this study).

Distribution. Thailand (this study).

Notes. Based on multi-gene phylogenetic analyses of ITS, LSU, *rpb2*, and *tub2* sequences, *Occultitheca chiangraiensis* (MFLU 24–0414) clustered with *O. rosae* (HKAS 102393) and *Clypeosphaeria oleae* (CPC 36779) with 100% ML and 1.00 BPP support (Fig. 7). *Clypeosphaeria oleae* was reported only from the asexual morph (Crous et al. 2019); thus, we could not compare the morphology between the species as we could not obtain the asexual morph of our strain, and therefore the link between them cannot be confirmed. Furthermore, *C. oleae* lacks *rpb2* and *tub2* data, which is important to confirm its

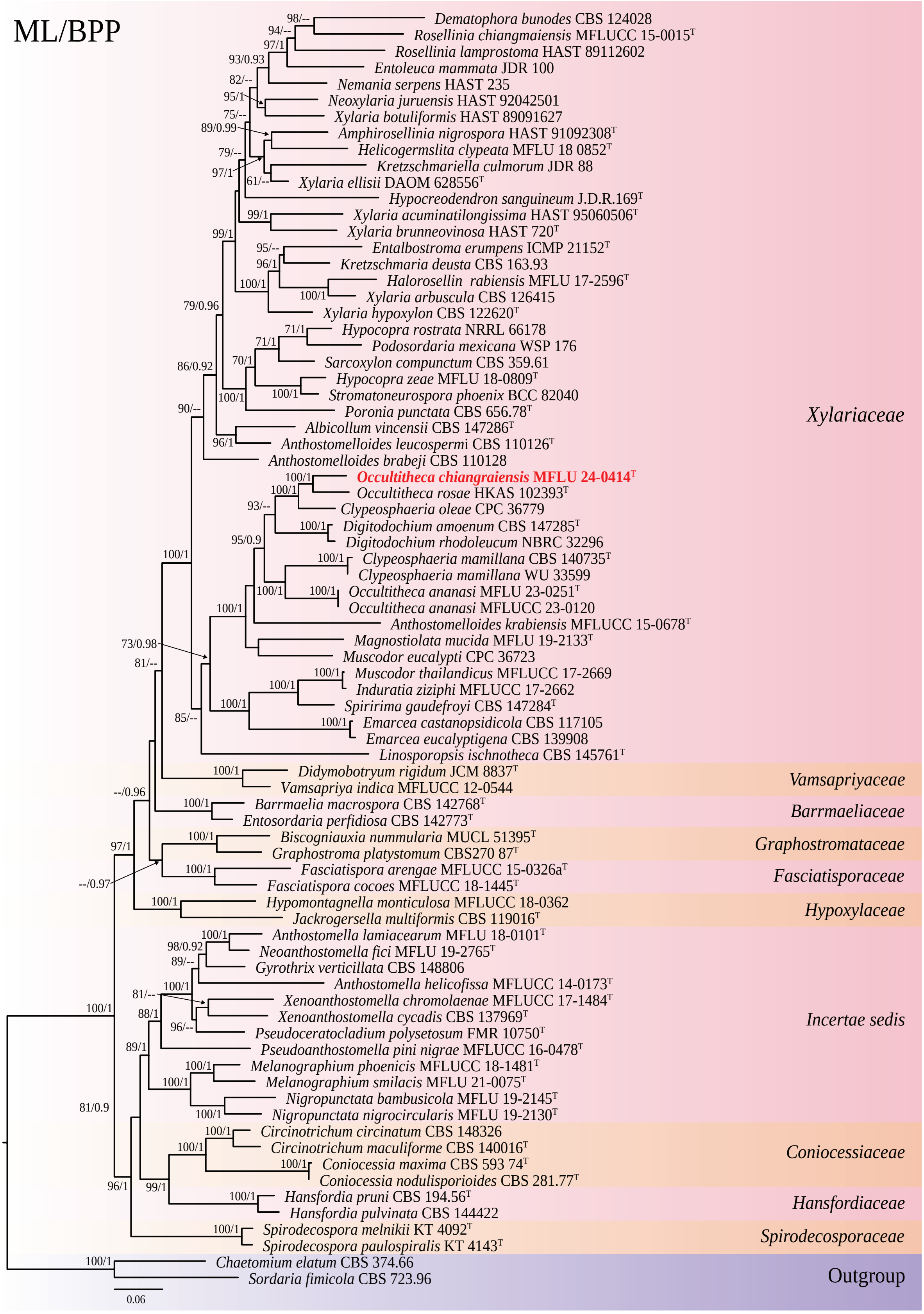

Figure 7. Phylogram generated from maximum likelihood analyses based on combined ITS-LSU-*rpb2*-*tub2* datasets. The tree is rooted with *Chaetomium elatum* (CBS 374.66) and *Sordaria fimicola* (CBS 723.96) as the outgroup taxa. Bootstrap support values ≥ 60% ML/≥0.90 BPP are given at the nodes. The newly generated taxa are indicated in red. The holotype/ex-type strains are denoted with ^{T}.

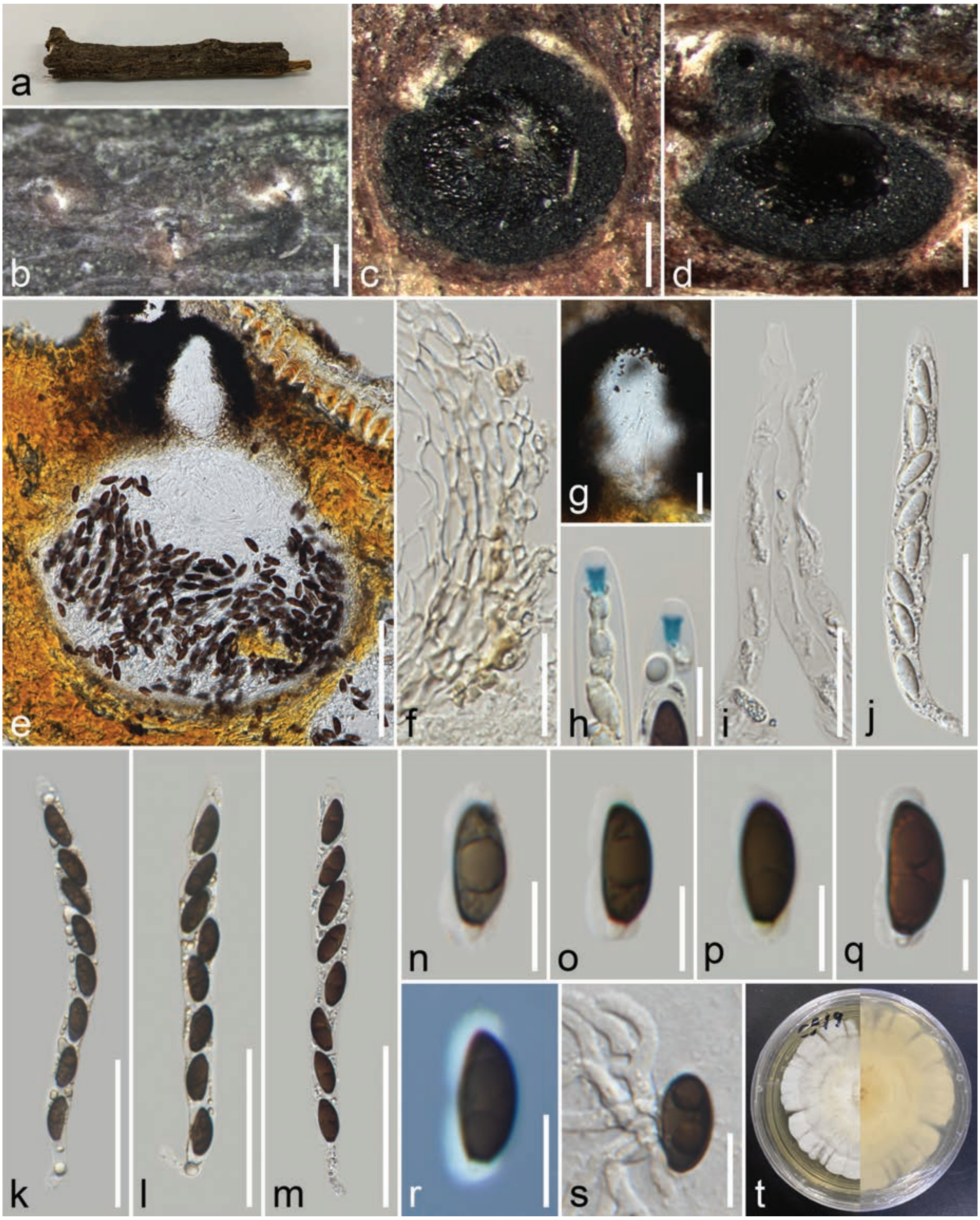

Figure 8. *Occultitheca chiangraiensis* (MFLU 24–0414, holotype) **a** host substrate **b** ascomata in host surface **c, d** horizontal and vertical section of ascoma **e** section through ascoma **f** peridium **g** ostiole **h** apical ring stained with melzer's reagent **i** paraphyses **j–m** immature and mature asci **n–r** ascospores (**r** ascospores show mucilaginous sheath in indian ink) **s** a germinated spore **t** front and reverse view of the colony on PDA. Scale bars: 200 µm (**b**); 100 µm (**c–e**); 20 µm (**f, g, i**); 10 µm (**h, n–s**); 50 µm (**j–m**).

phylogenetic placement. Morphologically, *Occultitheca chiangraiensis* fits the generic concept of *Occultitheca* in having immersed ascomata, short pedicellate asci with a J+, apical ring, a long distance between the ascus apex and the uppermost ascospore, and hyaline basal cells attached to brown ascospores

Table 4. Synopsis of *Occultitheca* species.

Species	***O. costaricensis***	***O. rosae***	***O. ananasi***	***O. chiangraiensis***
Host	Unidentified decaying wood	*Rosa* sp.	*Ananas comosus*	Unidentified decaying wood
Country	Costa Rica	China	Thailand	Thailand
Ascomata (μm)	400–600	360–385 × 350–420	190–230 × 160–260	220–342 × 228–395
Peridium (μm)	–	18–25	15–20	17–30
Paraphyses (μm)	–	3–6.5	3–5	3.7–7.6
Asci (μm)	185–190 × 10–10.5	90–140 × 11–13	70–90 × 5–10	112–158 × 8.5–13.7
Apical ring (μm)	6 × 3	3.5–4.5 × 2.8–3.2	–	3.9–5.6 × 2.5–3.7
Ascospores (μm)	14.5–23.5 × 7–10.5	16.5–20 × 6.5–8 L/W 2.6	10–12.5 × 3.5–4.5 L/W 2.9	14.5–17.6 × 6–7.4 L/W 2.4
Basal cell (μm)	1.5–4.5	1.5–2.2	–	1.3–2.3
Spore sheath	No	Thin	Thin	One side thick
Germ slit	Straight	Straight	Straight	No
References	Rogers and Ju (2003)	Samarakoon et al. (2022)	Tian et al. (2024)	This study

– Data not available.

(Rogers and Ju 2003; Samarakoon et al. 2022). Our isolate was compared to *Occultitheca* species as detailed in Table 4. *Occultitheca chiangraiensis* differs from *O. rosae* by having smaller ascomata ($\bar{x}$ = 290 × 324 μm vs. 370 × 385 μm), a lack of a germ slit, and possesses a thicker mucilaginous sheath compared to *O. rosae* (Samarakoon et al. 2022). Our strain differs from *O. ananasi*, which has uniseriate, olive-greenish ascospores becoming 2-seriate in the middle and thin mucilaginous sheath (Tian et al. 2024). *Occultitheca chiangraiensis* was also compared to the type species *O. costaricensis* as it lacks molecular data. *Occultitheca chiangraiensis* differs by having 1–2 individual ascomata and ascospores with a mucilaginous sheath, while *O. costaricensis* has 2–12 ascomata in a cluster and ascospores without a sheath (Rogers and Ju 2003). Additionally, some *Anthostomella* species have similar characteristics in terms of ascoma, asci, and ascospores with draft cells and lack germ slits, such as *A. clypeata* and *A. clypeoides*, but differ in a short space of the top ascospore and the ascus apex and shape of the sheath compared to *Occultitheca* species (Lu and Hyde 2000; Rogers and Ju 2003). Our strain differs by 6% in the ITS region (30/482, 4 gaps), 2% in LSU (14/745, 4 gaps), 15% in *rpb2* (117/798, no gap), 16% in *tub2* (120/754, 22 gap), and 3% in *tef1* (31/915, 1 gap) sequences compared to *O. rosae* (HKAS 102393). Thus, *Occultitheca chiangraiensis* is reported as a new species based on morphology and phylogenetic evidence.

Discussion

In this study, two novel species, *Diaporthe thailandica* and *Occultitheca chiangraiensis*, along with a new host record of *D. tulliensis* and a new geographical record of *D. melonis*, are introduced based on morphology and molecular data. This study expands the known diversity of these taxa and highlights the importance of saprobic microfungi in ecological systems.

Diaporthe is a species-rich genus with a diverse host range and global distribution (Dissanayake et al. 2017; Phukhamsakda et al. 2020; Hongsanan et al. 2023; Bhunjun et al. 2024b). The species have overlapping morphological traits. There are more than 1200 epithets under *Diaporthe* in Index Fungorum (2024); thus, the boundaries of the species/species complexes within the genus have been revised by several studies. *Diaporthe* was recently restructured into seven sections and 15 species complexes based on molecular analyses. Several *Diaporthe* species have been synonymised under *D. tulliensis* (*D. alangii*, *D. celtidis*, *D. glabrae*, *D. hubeiensis*, *D. morindae*, and *D. tectonae*), and these taxa formed a clade in our trees (including in the backbone tree with 226 taxa; data not shown), similar to Dissanayake et al. (2024). *Diaporthe melonis* (= *D. guangdongensis*) also formed a clade in our trees (including in the backbone tree; data not shown), similar to Dissanayake et al. (2024). The implementation of the markers (ITS, *tef-1*, and *tub*) proved to be phylogenetically informative in this study, resulting in a similar topology as previous studies based on five-marker combinations. The GCPSR analysis was also used to support the novelty of the *Diaporthe* species in this study. Therefore, molecular data and morphological evidence are needed for accurate species identification, thus reinforcing the importance of integrative approaches.

Morphologically, *Occultitheca* is considered an inconspicuous xylarialean and treated as anthostomella-like taxa in terms of having immersed, clypeate ascomata, asci with a J+, apical ring, ascospores with a large brown cell, and a basal hyaline dwarf cell (Daranagama et al. 2018; Samarakoon et al. 2022). Anthostomella-like taxa have now been split into five genera as suspected by Daranagama et al. (2015). These include *Anthocanalis*, *Astrocystis*, *Brunneiperidium*, *Lunatiannulus*, and *Pyriformiascoma*, and they differ in terms of ascomata and asexual morph characters. *Occultitheca* has a distinctive ostiole surrounded by a whitish halo and apiosporous ascospores with a small hyaline dwarf cell at one end and a dark brown, larger cell. There are only three species in *Occultitheca*, and all of them were found as saprobes as sexual morphs from terrestrial ecosystems. *Occultitheca* has a limited distribution and a narrow range of hosts, as only one species was found in Costa Rica (Rogers and Ju 2003), one in China, and one in Thailand (Samarakoon et al. 2022; Tian et al. 2024). Here, we provide a new addition to *Occultitheca* from unidentified decaying wood in Chiang Rai, Thailand. *Occultitheca chiangraiensis* was reported only as a sexual morph due to failure to obtain the asexual morphs from cultures. Thus, the link between the sexual and asexual morphs of this genus remains unknown. Due to the uncertainty of asexual and sexual morphologies and the low number of collections, *Occultitheca* has been placed under Xylariales genera *incertae sedis* (Samarakoon et al. 2022; Tian et al. 2024) and has also been considered to be part of Xylariaceae based on phylogenetic analyses (Voglmayr et al. 2022; this study). Expanding the sample collection will improve the representativeness of the genus.

This study provides a vital contribution to our understanding of Sordariomycetes diversity. Introducing new taxa is significant as they contribute to the broader understanding of fungal evolution, taxonomy, and ecology. It also contributes to the growing knowledge about the diversity of fungi associated with woody litter. It emphasises the necessity for continued exploration of fungal biodiversity across various habitats. As global ecosystems undergo rapid changes due to climate shifts and habitat destruction, understanding these dynamics will be crucial for conservation efforts and ecosystem management. Therefore, this study encourages further exploration in understudied substrates and regions, which could unveil additional species and enrich our comprehension of fungal ecology and taxonomy.

Acknowledgements

Chayanard Phukhamsakda would like to thank the Basic Research Fund (Fundamental Fund) supported by the National Science, Research, and Innovation Fund under Grant No. 672A16008 for financial support. The authors thank Dr. Shaun Pennycook from Manaaki Whenua, Landcare Research, New Zealand. Chitrabhanu S. Bhunjun would like to thank Thailand Science Research and Innovation (TSRI) and the National Science Research and Innovation Fund (NSRF) (Fundamental Fund: Grant no. 662A16047) entitled "Biodiversity, ecology, and applications of plant litter-inhabiting fungi for waste degradation." Kevin David Hyde would like to thank the National Research Council of Thailand (NRCT) grant "Total fungal diversity in a given forest area with implications towards species numbers, chemical diversity, and biotechnology" (grant no. N42A650547). The authors extend their appreciation to the Researchers Supporting Project number (RSP2025R114), King Saud University, Riyadh, Saudi Arabia.

Additional information

Conflict of interest

The authors have declared that no competing interests exist.

Ethical statement

No ethical statement was reported.

Funding

This work was funded by the Basic Research Fund (Fundamental Fund) supported by the National Science, Research, and Innovation Fund under Grant No. 672A16008, Thailand Science Research and Innovation (TSRI) and the National Science Research and Innovation Fund (NSRF) (Fundamental Fund: Grant no. 662A16047) entitled "Biodiversity, ecology, and applications of plant litter-inhabiting fungi for waste degradation".

Author contributions

The authors confirm contributions to the paper as follows: Fungal specimen collection and isolation, fungal specimen deposition, and manuscript writing: Chayanard Phukhamsakda, Johnny Louangphan, Kedsara Navasit, Chitrabhanu S. Bhunjun; fungal identification and contributed to the revision of the manuscript: Chayanard Phukhamsakda, Kevin D. Hyde, Milan C. Samarakoon, Fatimah O. Alotibi, Chitrabhanu S. Bhunjun. All authors have read and agreed to the published version of the manuscript. All authors reviewed the results and approved the final version of the manuscript.

Author ORCIDs

Chayanard Phukhamsakda https://orcid.org/0000-0002-1033-937X
Kevin D. Hyde https://orcid.org/0000-0002-2191-0762
Milan C. Samarakoon https://orcid.org/0000-0002-4815-125X
Johnny Louangphan https://orcid.org/0000-0003-3845-6145
Kedsara Navasit https://orcid.org/0009-0004-8167-0600
Fatimah Al-Otibi https://orcid.org/0000-0003-3629-5755

Data availability

All of the data that support the findings of this study are available in the main text.

References

Bai Q, Wang GP, Hong N, Guo YS, Fu M (2017) First report of *Diaporthe tulliensis* and *Diaporthe actinidiae* causing kiwifruit stem canker in Hubei and Anhui provinces, China. Plant Disease 101(3): 508–509. https://doi.org/10.1094/PDIS-10-16-1445-PDN

Beraha L, O'Brien MJ (1979) *Diaporthe melonis* sp. nov., a new soft rot of market cantaloupes. Phytopathologische Zeitschrift 94(3): 1. https://doi.org/10.1111/j.1439-0434.1979.tb01551.x

Bhunjun CS, Niskanen T, Suwannarach N, Wannathes N, Chen YJ, McKenzie EHC, Maharachchikumbura SSN, Buyck B, Zhao CL, Fan YG, Zhang JY, Dissanayake AJ, Marasinghe DS, Jayawardena RS, Kumla J, Padamsee M, Chen YY, Liimatainen K, Ammirati JF, Lumyong S, Phukhamsakda C, Liu JK, Phonrob W, Randrianjohany É, Hongsanan S, Cheewangkoon R, Bundhun D, Khuna S, Yu WJ, Deng LS, Lu YZ, Hyde KD (2022) The numbers of fungi: Are the most speciose genera truly diverse? Fungal Diversity 114(1): 387–462. https://doi.org/10.1007/s13225-022-00501-4

Bhunjun CS, Chen YJ, Phukhamsakda C, Boekhout T, Groenewald JZ, McKenzie EHC, Francisco EC, Frisvad JC, Groenewald M, Hurdeal VG, Luangsa-ard J, Perrone G, Visagie CM, Bai FY, Błaszkowski J, Braun U, de Souza FA, de Queiroz MB, Dutta AK, Gonkhom D, Goto BT, Guarnaccia V, Hagen F, Houbraken J, Lachance MA, Li JJ, Luo KY, Magurno F, Mongkolsamrit S, Robert V, Roy N, Tibpromma S, Wanasinghe DN, Wang DQ, Wei DP, Zhao CL, Aiphuk W, Ajayi-Oyetunde O, Arantes TD, Araujo JC, Begerow D, Bakhshi M, Barbosa RN, Behrens FH, Bensch K, Bezerra JDP, Bilański P, Bradley CA, Bubner B, Burgess TI, Buyck B, Čadež N, Cai L, Calaça FJS, Campbell LJ, Chaverri P, Chen YY, Chethana KWT, Coetzee B, Costa MM, Chen Q, Custódio FA, Dai YC, Damm U, de Azevedo Santiago ALCM, De Miccolis Angelini RM, Dijksterhuis J, Dissanayake AJ, Doilom M, Dong W, Alvarez-Duarte E, Fischer M, Gajanayake AJ, Gené J, Gomdola D, Gomes AAM, Hausner G, He MQ, Hou L, Iturrieta-González I, Jami F, Jankowiak R, Jayawardena RS, Kandemir H, Kiss L, Kobmoo N, Kowalski T, Landi L, Lin CG, Liu JK, Liu XB, Loizides M, Luangharn T, Maharachchikumbura SSN, Makhathini Mkhwanazi GJ, Manawasinghe IS, Marin-Felix Y, McTaggart AR, Moreau PA, Morozova OV, Mostert L, Osiewacz HD, Pem D, Phookamsak R, Pollastro S, Pordel A, Poyntner C, Phillips AJL, Phonemany M, Promputtha I, Rathnayaka AR, Rodrigues AM, Romanazzi G, Rothmann L, Salgado-Salazar C, Sandoval-Denis M, Saupe SJ, Scholler M, Scott P, Shivas RG, Silar P, Souza-Motta CM, Silva-Filho AGS, Spies CFJ, Stchigel AM, Sterflinger K, Summerbell RC, Svetasheva TY, Takamatsu S, Theelen B, Theodoro RC, Thines M, Thongklang N, Torres R, Turchetti B, van den Brule T, Wang XW, Wartchow F, Welti S, Wijesinghe SN, Wu F, Xu R, Yang ZL, Yilmaz N, Yurkov A, Zhao L, Zhao RL, Zhou N, Hyde KD, Crous PW (2024a) What are the 100 most cited fungal genera? Studies in Mycology 108(1): 1–412. https://doi.org/10.3114/sim.2024.108.01

Bhunjun CS, Phukhamsakda C, Hyde KD, McKenzie EHC, Saxena RK, Li Q (2024b) Do all fungi have ancestors with endophytic lifestyles? Fungal Diversity 125(1): 73–98. https://doi.org/10.1007/s13225-023-00516-5

Bruen TC, Philippe H, Bryant D (2006) A simple and robust statistical test for detecting the presence of recombination. Genetics 172(4): 2665–2681. https://doi.org/10.1534/genetics.105.048975

Carbone I, Kohn LM (1999) A method for designing primer sets for speciation studies in filamentous ascomycetes. Mycologia 91(3): 553–556. https://doi.org/10.1080/00275514.1999.12061051

Chang C, Yinghui C, Meimei X, Zide J, Peikun C (2005) New species of *Phomopsis* on woody plants in Fujian Province. Junwu Xuebao 24(1): 6–11.

Crous PW, Wingfield MJ, Le Roux JJ, Richardson DM, Strasberg D, Shivas RG, Alvarado P, Edwards J, Moreno G, Sharma R, Sonawane MS, Tan YP, Altés A, Barasubiye T, Barnes CM, Blanchette RA, Boertmann D, Bogo A, Carlavilla JR, Cheewangkoon R, Daniel R, de Beer ZW, de Jesús Yáñez-Morales M, Duong TA, Fernández-Vicente J, Geering ADW, Guest DI, Held BW, Heykoop M, Hubka V, Ismail AM, Kajale SC, Khemmuk W, Kolařík M, Kurli R, Lebeuf R, Lévesque CA, Lombard L, Magista D, Manjón JL, Marincowitz S, Mohedano JM, Nováková A, Oberlies NH, Otto EC, Paguigan ND, Pascoe IG (2015) Fungal Planet description sheets: 371–399. Persoonia 35(1): 264–327. https://doi.org/10.3767/003158515X690269

Crous PW, Wingfield MJ, Lombard L, Roets F, Swart WJ, Alvarado P, Carnegie AJ, Moreno G, Luangsaard J, Thangavel R, Alexandrova AV, Baseia IG, Bellanger JM, Bessette AE, Bessette AR, De la Peña-Lastra S, García D, Gené J, Pham THG, Heykoop M, Malysheva E, Malysheva V, Martín MP, Morozova OV, Noisripoom W, Overton BE, Rea AE, Sewall BJ, Smith ME, Smyth CW, Tasanathai K, Visagie CM, Adamčík S, Alves A, Andrade JP, Aninat MJ, Araújo RVB, Bordallo JJ, Boufleur T, Baroncelli R, Barreto RW, Bolin J, Cabero J, Caboň M, Cafà G, Caffot MLH, Cai L, Carlavilla JR, Chávez R, de Castro RRL, Delgat L, Deschuyteneer D, Dios MM, Domínguez LS, Evans HC, Eyssartier G, Ferreira BW, Figueiredo CN, Liu F, Fournier J, Galli-Terasawa LV, Gil-Durán C, Glienke C, Gonçalves MFM, Gryta H, Guarro J, Himaman W, Hywel-Jones N, Iturrieta-González I, Ivanushkina NE, Jargeat P, Khalid AN, Khan J, Kiran M, Kiss L, Kochkina GA, Kolařík M, Kubátová A, Lodge DJ, Loizides M, Luque D, Manjón JL, Marbach PAS, Massola NS Jr, Mata M, Miller AN, Mongkolsamrit S, Moreau PA, Morte A, Mujic A, Navarro-Ródenas A, Németh MZ, Nóbrega TF, Nováková A, Olariaga I, Ozerskaya SM, Palma MA, Petters-Vandresen DAL, Piontelli E, Popov ES, Rodríguez A, Requejo Ó, Rodrigues ACM, Rong IH, Roux J, Seifert KA, Silva BDB, Sklenář F, Smith JA, Sousa JO, Souza HG, De Souza JT, Švec K, Tanchaud P, Tanney JB, Terasawa F, Thanakitpipattana D, Torres-Garcia D, Vaca I, Vaghefi N, van Iperen AL, Vasilenko OV, Verbeken A, Yilmaz N, Zamora JC, Zapata M, Jurjević Ž, Groenewald JZ (2019) Fungal Planet description sheets: 951-1041. Persoonia 43(1): 223–425. https://doi.org/10.3767/persoonia.2019.43.06

Daranagama DA, Camporesi E, Tian Q, Liu X, Chamyuang S, Stadler M, Hyde KD (2015) *Anthostomella* is polyphyletic comprising several genera in Xylariaceae. Fungal Diversity 73(1): 203–238. https://doi.org/10.1007/s13225-015-0329-6

Daranagama DA, Hyde KD, Sir EB, Thambugala KM, Tian Q, Samarakoon MC, McKenzie EH, Jayasiri SC, Tibpromma S, Bhat JD, Liu X, Stadler M (2018) Towards a natural classification and backbone tree for Graphostromataceae, Hypoxylaceae, Lopadostomataceae and Xylariaceae. Fungal Diversity 88(1): 1–165. https://doi.org/10.1007/s13225-017-0388-y

Darriba D, Taboada GL, Doallo R, Posada D (2012) jModelTest 2: More models, new heuristics and high-performance computing. Nature Methods 9(8): 772. https://doi.org/10.1038/nmeth.2109

Dashtban M, Schraft H, Syed TA, Qin W (2010) Fungal biodegradation and enzymatic modification of lignin. International Journal of Biochemistry and Molecular Biology 1(1): 36–50. https://pmc.ncbi.nlm.nih.gov/articles/PMC3180040/

Dissanayake AJ, Phillips AJL, Hyde KD, Yan JY, Li XH (2017) The current status of species in *Diaporthe*. Mycosphere 8(5): 1106–1156. https://doi.org/10.5943/mycosphere/8/5/5

Dissanayake AJ, Zhu JT, Chen YY, Maharachchikumbura SS, Hyde KD, Liu JK (2024) A re-evaluation of *Diaporthe*: Refining the boundaries of species and species complexes. Fungal Diversity 126(1): 1–25. https://doi.org/10.1007/s13225-024-00538-7

Doilom M, Dissanayake AJ, Wanasinghe DN, Boonmee S, Liu JK, Bhat DJ, Taylor JE, Bahkali AH, McKenzie EH, Hyde KD (2017) Microfungi on *Tectona grandis* (teak) in Northern Thailand. Fungal Diversity 82(1): 107–182. https://doi.org/10.1007/s13225-016-0368-7

Dong H, Mu TC, Zhang ZX, Zhang XG, Xia JW (2021a) Molecular phylogenetic analysis reveals two new species of *Diaporthe* from Yunnan Province, southwestern China. Junwu Xuebao 40(3): 436–446.

Dong Z, Manawasinghe IS, Huang Y, Shu Y, Phillips AJ, Dissanayake AJ, Hyde KD, Xiang M, Luo M (2021b) Endophytic *Diaporthe* associated with *Citrus grandis* cv. *Tomentosa* in China. Frontiers in Microbiology 11: 609387. https://doi.org/10.3389/fmicb.2020.609387

Fuckel L (1867) Fungi rhenani cent. 18 (1), no 1702–1764. Hedwigia 6: 174–175.

Gao Y, Liu F, Duan W, Crous PW, Cai L (2017) *Diaporthe* is paraphyletic. IMA Fungus 8(1): 153–187. https://doi.org/10.5598/imafungus.2017.08.01.11

Gioan E, Paul C (2012) Split decomposition and graph-labelled trees: Characterizations and fully dynamic algorithms for totally decomposable graphs. Discrete Applied Mathematics 160(6): 708–733. https://doi.org/10.1016/j.dam.2011.05.007

Glass NL, Donaldson GC (1995) Development of primer sets designed for use with the PCR to amplify conserved genes from filamentous ascomycetes. Applied and Environmental Microbiology 61(4): 1323–1330. https://doi.org/10.1128/aem.61.4.1323-1330.1995

Gomes RR, Glienke C, Videira SIR, Lombard L, Groenewald JZ, Crous PW (2013) *Diaporthe*: A genus of endophytic, saprobic and plant pathogenic fungi. Persoonia 31(1): 1–41. https://doi.org/10.3767/003158513X666844

Gu X, Li WH (1996a) A general additive distance with time-reversibility and rate variation among nucleotide sites. Proceedings of the National Academy of Sciences of the United States of America 93(10): 4671–4676. https://doi.org/10.1073/pnas.93.10.4671

Gu X, Li WH (1996b) Bias-corrected paralinear and LogDet distances and tests of molecular clocks and phylogenies under nonstationary nucleotide frequencies. Molecular Biology and Evolution 13(10): 1375–1383. https://doi.org/10.1093/oxfordjournals.molbev.a025584

Hongsanan S, Norphanphoun C, Senanayake IC, Jayawardena RS, Manawasinghe IS, Abeywickrama PD, Khuna S, Suwannarach N, Senwanna C, Monkai J, Hyde KD, Gentekaki E, Bhunjun CS (2023) Annotated notes on *Diaporthe* species. Mycosphere 14(1): 918–1189. https://doi.org/10.5943/mycosphere/14/1/12

Huson DH, Bryant D (2006) Application of phylogenetic networks in evolutionary studies. Molecular Biology and Evolution 23(2): 254–267. https://doi.org/10.1093/molbev/msj030

Huson DH, Bryant D (2024) The SplitsTree App: Interactive analysis and visualization using phylogenetic trees and networks. Nature Methods 21(10): 1773–1774. https://doi.org/10.1038/s41592-024-02406-3

Hyde KD, Norphanphoun C, Chen J, Dissanayake AJ, Doilom M, Hongsanan S, Jayawardena RS, Jeewon R, Perera RH, Thongbai B, Wanasinghe DN, Wisitrassameewong K, Tibpromma S, Stadler M (2018) Thailand's amazing diversity: Up to 96% of fungi in northern Thailand may be novel. Fungal Diversity 93(1): 215–239. https://doi.org/10.1007/s13225-018-0415-7

Hyde KD, Xu JC, Rapior S, Jeewon R, Lumyong S, Niego AGT, Abeywickrama PD, Aluthmuhandiram JVS, Brahamanage RS, Brooks S, Chaiyasen A, Chethana KWT, Chomnunti P, Chepkirui C, Chuankid B, de Silva NI, Doilom M, Faulds C, Gentekaki E, Gopalan V, Kakumyan P, Harishchandra D, Hemachandran H, Hongsanan S, Karunarathna A, Karunarathna SC, Khan S, Kumla J, Jayawardena RS, Liu JK, Liu N, Luangharn T, Macabeo APG, Marasinghe DS, Meeks D, Mortimer PE, Mueller P, Nadir S, Nataraja KN, Nontachaiyapoom S, O'Brien M, Penkhrue W, Phukhamsakda C, Ramanan US, Rathnayaka AR, Sadaba RB, Sandargo B, Samarakoon BC, Tennakoon DS, Siva R, Sriprom W, Suryanarayanan TS, Sujarit K, Suwannarach N, Suwunwong T, Thongbai B, Thongklang N, Wei DP, Wijesinghe SN, Winiski J, Yan J, Yasanthika E, Stadler M (2019) The amazing potential of fungi: 50 ways we can exploit fungi industrially. Fungal Diversity 97(1): 1–36. https://doi.org/10.1007/s13225-019-00430-9

Hyde KD, Jeewon R, Chen YJ, Bhunjun CS, Calabon MS, Jiang HB, Lin CG, Norphanphoun C, Sysouphanthong P, Pem D, Tibpromma S, Zhang Q, Doilom M, Jayawardena RS, Liu JK, Maharachchikumbura SSN, Phukhamsakda C, Phookamsak R, Al-Sadi AM, Thongklang N, Wang Y, Gafforov Y, Jones EBG, Lumyong S (2020a) The numbers of fungi: Is the descriptive curve flattening? Fungal Diversity 103(1): 219–271. https://doi.org/10.1007/s13225-020-00458-2

Hyde KD, Norphanphoun C, Maharachchikumbura SSN, Bhat DJ, Jones EBG, Bundhun D, Chen YJ, Bao DF, Boonmee S, Calabon MS, Chaiwan N, Chethana KWT, Dai DQ, Dayarathne MC, Devadatha B, Dissanayake AJ, Dissanayake LS, Doilom M, Dong W, Fan XL, Goonasekara ID, Hongsanan S, Huang SK, Jayawardena RS, Jeewon R, Karunarathna A, Konta S, Kumar V, Lin CG, Liu JK, Liu NG, Luangsa-ard J, Lumyong S, Luo ZL, Marasinghe DS, McKenzie EHC, Niego AGT, Niranjan M, Perera RH, Phukhamsakda C, Rathnayaka AR, Samarakoon MC, Samarakoon SMBC, Sarma VV, Senanayake IC, Shang QJ, Stadler M, Tibpromma S, Wanasinghe DN, Wei DP, Wijayawardene NN, Xiao YP, Yang J, Zeng XY, Zhang SN, Xiang MM (2020b) Refined families of Sordariomycetes. Mycosphere 11(1): 305–1059. https://doi.org/10.5943/mycosphere/11/1/7

Hyde KD, Amuhenage TB, Apurillo CCS, Asghari R, Aumentado HD, Bahkali AH, Bera I, Bhunjun CS, Calabon MS, Chandrasiri S, Chethana KWT, Doilom M, Dong W, Fallahi M, Gajanayake AJ, Gomdola D, Gunarathne A, Hongsanan S, Huanraluek N, Jayawardena RS, Kapov SA, Khyaju S, Le L, Li CJY, Li QR, Li YX, Lin CG, Linn MM, Liu JK, Liu NG, Luangharn T, Madagammana AD, Manawasinghe IS, Marasinghe DS, McKenzie EHC, Meakala N, Meng QF, Mukhopadhyay S, Norphanphoun C, Pem D, Phukhamsakda C, Sarma VV, Selcuk F, Senanayake IC, Shah S, Shu YX, Silva HVS, Su HL, Tavakol M, Thakshila SAD, Thiyagaraja V, Thongklang N, Tian Q, Tibpromma S, Tun ZL, Ulukapi M, Wang Y, Wannasawang N, Wijayawardene NN, Wimalasena SDMK, Xiao Y, Xiong YR, Yasanthika WAE, Li Q, Dai DQ (2023) Fungalpedia, an illustrated compendium of the fungi and fungus-like taxa. Mycosphere 14(1): 1835–1959. https://doi.org/10.5943/mycosphere/14/1/22

Hyde KD, Saleh A, Aumentado HD, Boekhout T, Bera I, Khyaju S, Bhunjun CS, Chethana KW, Phukhamsakda C, Doilom M, Thiyagaraja V, Mortimer PE, Maharachchikumbura SSN, Hongsanan S, Jayawardena RS, Dong W, Jeewon R, Al-Otibi F, Wijesinghe SN, Wanasinghe DN (2024) Fungal numbers: Global needs for a realistic assessment. Fungal Diversity 7: 1–35. https://doi.org/10.1007/s13225-023-00532-5

Index Fungorum (2024) Index Fungorum. http://www.indexfungorum.org/names/Names.asp [Accessed on: 2024-12-03]

Jayasiri SC, Hyde KD, Ariyawansa HA, Bhat DJ, Buyck B, Cai L, Dai YC, Abd-Elsalam KA, Ertz D, Hidayat I, Jeewon R, Jones EBG, Bahkali AH, Karunarathna SC, Liu JK, Luangsa-ard JJ, Lumbsch HT, Maharachchikumbura SSN, McKenzie EHC, Moncalvo JM, Ghobad-Nejhad M, Nilsson H, Pang KL, Pereira OL, Phillips AJL, Raspé O, Rollins AW, Romero AI, Etayo J, Selçuk F, Stephenson SL, Suetrong S, Taylor JE, Tsui CKM, Vizzini A, Abdel-Wahab MA, Wen TC, Boonmee S, Dai DQ, Daranagama DA, Dissanayake AJ, Ekanayaka AH, Fryar SC, Hongsanan S, Jayawardena RS, Li WJ, Perera RH, Phookamsak R, Silva NI, Thambugala KM, Tian Q, Wijayawardene NN, Zhao RL, Zhao Q, Kang JC, Promputtha I (2015) The Faces of Fungi database: Fungal names linked with morphology, phylogeny and human impacts. Fungal Diversity 74(1): 3–18. https://doi.org/10.1007/s13225-015-0351-8

Katoh K, Rozewicki J, Yamada KD (2019) MAFFT online service: Multiple sequence alignment, interactive sequence choice and visualization. Briefings in Bioinformatics 20(4): 1160–1166. https://doi.org/10.1093/bib/bbx108

Larsson A (2014) AliView: A fast and lightweight alignment viewer and editor for large datasets. Bioinformatics 30(22): 3276–3278. https://doi.org/10.1093/bioinformatics/btu531

Liu YJ, Whelen S, Hall BD (1999) Phylogenetic relationships among ascomycetes: Evidence from an RNA polymerse II subunit. Molecular Biology and Evolution 16(12): 1799–1808. https://doi.org/10.1093/oxfordjournals.molbev.a026092

Lu B, Hyde KD (2000) A world monograph of *Anthostomella*. HKU Fungal Diversity Press, Fungal Diversity Research Series.

Luo M, Guo W, Zhao M, Manawasinghe IS, Guarnaccia V, Liu J, Hyde KD, Dong Z, You C (2022) Endophytic *Diaporthe* associated with *Morinda officinalis* in China. Journal of Fungi 8(8): 806. https://doi.org/10.3390/jof8080806

Madagammana AD, Samarakoon MC, Phukhamsakda C, Bhunjun CS, Huanraluek N, Liu JK, Hyde KD (2023) Unveiling the holomorph and novel host records of *Shearia formosa* (Longiostiolaceae, Pleosporales) in China. New Zealand Journal of Botany 62(2-3): 123–137. https://doi.org/10.1080/0028825X.2023.2267775

Manawasinghe IS, Dissanayake AJ, Li X, Liu M, Wanasinghe DN, Xu J, Zhao W, Zhang W, Zhou Y, Hyde KD, Brooks S, Yan J (2019) High genetic diversity and species complexity of *Diaporthe* associated with grapevine dieback in China. Frontiers in Microbiology 10: 1936. https://doi.org/10.3389/fmicb.2019.01936

Manawasinghe IS, Jayawardena RS, Li HL, Zhou YY, Zhang W, Phillips AJL, Wanasinghe DN, Dissanayake AJ, Li XH, Li YH, Hyde KD, Yan JY (2021) Microfungi associated with *Camellia sinensis*: A case study of leaf and shoot necrosis on tea in Fujian, China. Mycosphere 12(1): 430–518. https://doi.org/10.5943/mycosphere/12/1/6

Mapook A, Hyde KD, Hassan K, Kemkuignou BM, Čmoková A, Surup F, Kuhnert E, Paomephan P, Cheng T, de Hoog S, Song Y, Jayawardena RS, Al-Hatmi A, Mahmoudi T, Ponts N, Studt L, Richard-Forget F, Chethana KWT, Harishchandra DL, Mortimer PE, Li H, Lumyong S, Aiduang W, Kumla J, Suwannarach N, Bhunjun CS, Yu FM, Zhao Q, Schaefer D, Stadler M (2022) Ten decadal advances in fungal biology leading towards human well-being. Fungal Diversity 116(1): 547–614. https://doi.org/10.1007/s13225-022-00510-3

Miller MA, Pfeiffer W, Schwartz T (2017) Creating the CIPRES Science Gateway for inference of large phylogenetic trees. 2010 gateway computing environments workshop (GCE), 1–8. https://doi.org/10.1109/GCE.2010.5676129

Nishimaki T, Sato K (2019) An extension of the Kimura two-parameter model to the natural evolutionary process. Journal of Molecular Evolution 87(1): 60–67. https://doi.org/10.1007/s00239-018-9885-1

Norphanphoun C, Gentekaki E, Hongsanan S, Jayawardena R, Senanayake IC, Manawasinghe IS, Abeywickrama PD, Bhunjun CS, Hyde KD (2022) *Diaporthe*: Formalizing the species-group concept. Mycosphere 13(1): 752–819. https://doi.org/10.5943/mycosphere/13/1/9

O’Donnell K, Cigelnik E (1997) Two divergent intragenomic rDNA ITS2 types within a monophyletic lineage of the fungus *Fusarium* are nonorthologous. Molecular Phylogenetics and Evolution 7(1): 103–116. https://doi.org/10.1006/mpev.1996.0376

Pereira DS, Phillips AJL (2024) *Diaporthe* species on palms – integrative taxonomic approach for species boundaries delimitation in the genus *Diaporthe*, with the description of *D. pygmaeae* sp. nov. Studies in Mycology 109(1): 487–594. https://doi.org/10.3114/sim.2024.109.08

Phukhamsakda C, McKenzie EHC, Phillips AJL, Gareth Jones EB, Jayarama Bhat D, Stadler M, Bhunjun CS, Wanasinghe DN, Thongbai B, Camporesi E, Ertz D, Jayawardena RS, Perera RH, Ekanayake AH, Tibpromma S, Doilom M, Xu J, Hyde KD (2020) Microfungi associated with *Clematis* (Ranunculaceae) with an integrated approach to delimiting species boundaries. Fungal Diversity 102(1): 1–203. https://doi.org/10.1007/s13225-020-00448-4

Phukhamsakda C, Nilsson RH, Bhunjun CS, de Farias ARG, Sun YR, Wijesinghe SN, Raza M, Bao D-F, Lu L, Tibpromma S, Dong W, Tennakoon DS, Tian X-G, Xiong Y-R, Karunarathna SC, Cai L, Luo Z-L, Wang Y, Manawasinghe IS, Camporesi E, Kirk PM, Promputtha I, Kuo C-H, Su H-Y, Doilom M, Li Y, Fu Y-P, Hyde KD (2022) The numbers of fungi: Contributions from traditional taxonomic studies and challenges of metabarcoding. Fungal Diversity 114(1): 327–386. https://doi.org/10.1007/s13225-022-00502-3

Rambaut A (2012) FigTree version 1.4.4. Institute of Evolutionary Biology, University of Edinburgh, Edinburgh. http://tree.bio.ed.ac.uk/software/figtree/

Rogers JD, Ju YM (2003) *Occultitheca costaricensis* gen. et sp. nov. and *Apiocamarops pulvinata* sp. nov. from Costa Rica. Sydowia 55(2): 359–364.

Ronquist F, Teslenko M, van der Mark P, Ayres DL, Darling A, Höhna S, Larget B, Liu L, Suchard MA, Huelsenbeck JP (2012) MrBayes 3.2: Efficient Bayesian phylogenetic inference and model choice across a large model space. Systematic Biology 61(3): 539–542. https://doi.org/10.1093/sysbio/sys029

Samarakoon MC, Hyde KD, Maharachchikumbura SSN, Stadler M, Gareth Jones EB, Promputtha I, Suwannarach N, Camporesi E, Bulgakov TS, Liu JK (2022) Taxonomy, phylogeny, molecular dating and ancestral state reconstruction of Xylariomycetidae (Sordariomycetes). Fungal Diversity 112(1): 1–88. https://doi.org/10.1007/s13225-021-00495-5

Sayers EW, Bolton EE, Brister JR, Canese K, Chan J, Comeau DC, Connor R, Funk K, Kelly C, Kim S, Madej T, Marchler-Bauer A, Lanczycki C, Lathrop S, Lu Z, Thibaud-Nissen F, Murphy T, Phan L, Skripchenko Y, Tse T, Wang J, Williams R, Trawick BW, Pruitt KD, Sherry ST (2022) Database resources of the national center for biotechnology information. Nucleic Acids Research 50(D1): D20–D26. https://doi.org/10.1093/nar/gkab1112

Senanayake IC, Rathnayaka AR, Marasinghe DS, Calabon MS, Gentekaki E, Lee HB, Hurdeal VG, Pem D, Dissanayake LS, Wijesinghe SN, Bundhun D, Nguyen TT, Goonasekara ID, Abeywickrama PD, Bhunjun CS, Jayawardena RS, Wanasinghe DN, Jeewon R, Bhat DJ, Xiang MM (2020) Morphological approaches in studying fungi: Collection, examination, isolation, sporulation and preservation. Mycosphere 11(1): 2678–2754. https://doi.org/10.5943/mycosphere/11/1/20

Stamatakis A (2014) RAxML version 8: A tool for phylogenetic analysis and post-analysis of large phylogenies. Bioinformatics 30(9): 1312–1313. https://doi.org/10.1093/bioinformatics/btu033

Sugita R, Hirayama K, Shirouzu T, Tanaka K (2022) Spirodecosporaceae fam. nov. (Xylariales, Sordariomycetes) and two new species of *Spirodecospora*. Fungal Systematics and Evolution 10(1): 217–229. https://doi.org/10.3114/fuse.2022.10.09

Sun W, Huang S, Xia J, Zhang X, Li Z (2021) Morphological and molecular identification of *Diaporthe* species in south-western China, with description of eight new species. MycoKeys 77: 65–95. https://doi.org/10.3897/mycokeys.77.59852

Taylor JW, Jacobson DJ, Kroken S, Kasuga T, Geiser DM, Hibbett DS, Fisher MC (2000) Phylogenetic species recognition and species concepts in fungi. Fungal Genetics and Biology 31(1): 21–32. https://doi.org/10.1006/fgbi.2000.1228

Tennakoon DS, Kuo CH, Maharachchikumbura SS, Thambugala KM, Gentekaki E, Phillips AJ, Bhat DJ, Wanasinghe DN, de Silva NI, Promputtha I, Hyde KD (2021) Taxonomic and phylogenetic contributions to *Celtis formosana*, *Ficus ampelas*, *F. septica*, *Macaranga tanarius* and *Morus australis* leaf litter inhabiting microfungi. Fungal Diversity 108(1): 1–215. https://doi.org/10.1007/s13225-021-00474-w

Tian XG, Bao DF, Karunarathna SC, Jayawardena RS, Hyde KD, Bhat DJ, Luo ZL, Elgorban AM, Hongsanan S, Rajeshkumar KC, Maharachchikumbura SSN, Suwannarach N, Dawoud TM, Lu YZ, Han JJ, Xiao YP, Du TY, Lu L, Xu RF, Dai DQ, Liu XF, Liu C, Tibpromma S (2024) Taxonomy and phylogeny of ascomycetes associated with selected economically important monocotyledons in China and Thailand. Mycosphere 15(1): 1–274. https://doi.org/10.5943/mycosphere/15/1/1

Udayanga D, Liu X, McKenzie EH, Chukeatirote E, Bahkali AH, Hyde KD (2011) The genus *Phomopsis*: Biology, applications, species concepts and names of common phytopathogens. Fungal Diversity 50(1): 189–225. https://doi.org/10.1007/s13225-011-0126-9

Udayanga D, Castlebury LA, Rossman AY, Chukeatirote E, Hyde KD (2014) Insights into the genus *Diaporthe*: Phylogenetic species delimitation in the *D. eres* species complex. Fungal Diversity 67(1): 203–229. https://doi.org/10.1007/s13225-014-0297-2

Vaidya G, Lohman DJ, Meier R (2011) SequenceMatrix: Concatenation software for the fast assembly of multi-gene datasets with character set and codon information. Cladistics 27(2): 171–180. https://doi.org/10.1111/j.1096-0031.2010.00329.x

Vilgalys R, Hester M (1990) Rapid genetic identification and mapping of enzymatically amplified ribosomal DNA from several *Cryptococcus* species. Journal of Bacteriology 172(8): 4238–4246. https://doi.org/10.1128/jb.172.8.4238-4246.1990

Voglmayr H, Tello S, Jaklitsch WM, Friebes G, Baral HO, Fournier J (2022) About spirals and pores: Xylariaceae with remarkable germ loci. Persoonia 49(1): 58–98. https://doi.org/10.3767/persoonia.2022.49.02

Wanasinghe DN, Mortimer PE (2022) Taxonomic and phylogenetic insights into novel Ascomycota from forest woody litter. Biology (Basel) 11(6): 889. https://doi.org/10.3390/biology11060889

White TJ, Bruns T, Lee S, Taylor J (1990) Amplification and direct sequencing of fungal ribosomal RNA Genes for phylogenetics. PCR Protocols: A Guide to Methods and Applications. Academic Press, San Diego, 315–322. https://doi.org/10.1016/B978-0-12-372180-8.50042-1

Xu R, Su W, Tian S, Bhunjun CS, Tibpromma S, Hyde KD, Li Y, Phukhamsakda C (2022) Synopsis of Leptosphaeriaceae and introduction of three new taxa and one new record from China. Journal of Fungi 8(5): 416. https://doi.org/10.3390/jof8050416

Yang Q, Fan XL, Guarnaccia V, Tian CM (2018) High diversity of *Diaporthe* species associated with dieback diseases in China, with twelve new species described. MycoKeys 39: 97–149. https://doi.org/10.3897/mycokeys.39.26914

Zhang WP, Fornara D, Yang H, Yu RP, Callaway RM, Li L (2023) Plant litter strengthens positive biodiversity–ecosystem functioning relationships over time. Trends in Ecology & Evolution 38(5): 473–484. https://doi.org/10.1016/j.tree.2022.12.008

Zhaxybayeva O, Gogarten JP (2002) Bootstrap, Bayesian probability and maximum likelihood mapping: Exploring new tools for comparative genome analyses. BMC Genomics 3(1): 1–5. https://doi.org/10.1186/1471-2164-3-4

MycoKeys 115: 187–208 (2025)
DOI: 10.3897/mycokeys.115.140683

Research Article

Morphology and phylogeny of two new species within Cordycipitaceae (Hypocreales) from China

Yingling Lu[1,2*], Songyu Li[1,2*], Zuoheng Liu[1,2], Jing Zhao[1,2], Zhiyong Yu[3], Zongli Liang[3], Hailong He[3], Jianhong Li[3], Yun Huang[3], Xinming Li[3], Hong Yu[1,2]

1 Yunnan Herbal Laboratory, College of Ecology and Environmental Sciences, Yunnan University, Kunming, Yunnan 650504, China
2 The International Joint Research Center for Sustainable Utilization of Cordyceps Bioresources in China and Southeast Asia, Yunnan University, Kunming 650091, China
3 Yunnan Jinping Fenshuiling National Nature Reserve, Honghe, Yunnan 661500, China
Corresponding author: Hong Yu (hongyu@ynu.edu.cn, herbfish@163.com)

Abstract

Simplicillium and *Leptobacillium*, sister genera in the family Cordycipitaceae, exhibit a broad range of hosts or substrates. The identification of two novel species, from *Simplicillium* and *Leptobacillium*, was achieved by analysing morphological characteristics and phylogenetic data obtained from six molecular markers (ITS, nrSSU, nrLSU, *tef-1α*, *rpb1* and *rpb2*). The two recently documented species are *S. puwenense* and *L. longiphialidum*. Morphologically, *S. puwenense* possessed slender solitary rod-shaped or columnar phialides with elliptical oval or cylindrical conidia forming small spherical heads at the apex of phialides. On the other hand, *L. longiphialidum* had solitary columnar phialides with elliptic or subspherical apical conidia while other conidia were narrow columnar or fusiform in shape. Phylogenetic analysis revealed that *S. puwenense* formed an independent branch as a sister species to *S. formicae*, whereas *L. longiphialidum* clustered with *L. marksiae* exhibiting stable topological structure. The Bayesian inference posterior probability and the maximum likelihood bootstrap-ratio provided robust statistical evidence, indicating the presence of two novel species within the genera of *Simplicillium* and *Leptobacillium*. The present study contributes to the discovery of species diversity in *Simplicillium* and *Leptobacillium*, while also providing a taxonomic foundation for their rational development and sustainable utilisation.

Key words: *Leptobacillium*, morphology, new taxa, phylogenetic analysis, *Simplicillium*, taxonomy

Academic editor: Marc Stadler
Received: 31 October 2024
Accepted: 25 February 2025
Published: 17 March 2025

Citation: Lu Y, Li S, Liu Z, Zhao J, Yu Z, Liang Z, He H, Li J, Huang Y, Li X, Yu H (2025) Morphology and phylogeny of two new species within Cordycipitaceae (Hypocreales) from China. MycoKeys 115: 187–208. https://doi.org/10.3897/mycokeys.115.140683

Introduction

As was well known, many species in the family Cordycipitaceae Kreisel ex G.H. Sung, Hywel-Jones & Spatafora were entomogenous (Mongkolsamrit et al. 2018; Wang et al. 2020). Amongst them, the genera *Simplicillium* W. Gams & Zare and *Leptobacillium* Zare & W. Gams were sister genera (Zare and Gams 2001, 2016).

In 2001, Zare and Gams established the genus *Simplicillium*, which included *S. lanosoniveum* (J.F.H. Beyma) Zare & W. Gams (type species), *S. lamellicola*

---

[*] These authors contributed equally to this work.

(F.E.V. Sm.) Zare & W. Gams, *S. obclavatum* (W. Gams) Zare & W. Gams and *S. wallacei* H.C. Evans. The key distinguishing characteristic of the *Simplicillium* genus was the solitary presence of phialides, with conidia typically adhering to the apex of phialides in chains that resemble spherical, sticky or tile-like structures, ultimately forming octahedral crystals (Zare and Gams 2001). The solitary phialides enabled the distinction between the genus *Simplicillium* and its closely-related genus *Lecanicillium* W. Gams & Zare (Chen et al. 2021). Species belonging to the *Simplicillium* genus exhibited ecological diversity, including their presence in various environments, such as soil, endophytic fungi of plants, rocks and decaying wood (Liu and Cai 2012; Nonaka et al. 2013; Zhang et al. 2017; Crous et al. 2018, 2021). *S. chinense* F. Liu & L. Cai was the first *Simplicillium* species discovered in China (Liu and Cai 2012).

In 2016, the genus *Leptobacillium* was established by Zare and Gams during the revision of the former *Verticillium* Nees section *Albo-erecta*. The name of the genus referred to its characteristic narrow microconidia, with the model species being *L. leptobactrum* (W. Gams) Zare & W. Gams (Zare and Gams 2016). The genus *Leptobacillium* comprised species that exhibited two distinct types of conidia. Individual cells aggregated to form chains, with nearly spherical or elliptical conidia located at the apex of long chains, while narrow cylindrical (rod-shaped) to fusiform conidia were found elsewhere within the chain (Zare and Gams 2016; Leplat et al. 2022). Zare and Gams (2016) initially described *L. leptobactrum*, a species consisting of two varieties, namely *L. leptobactrum* var. *leptobactrum* (W. Gams) Zare & W. Gams and *L. leptobactrum* var. *calidius* Zare & W. Gams, which were distinguished by their optimal growth temperatures. The species of *Leptobacillium* exhibited a wide range of host and substrate diversity, having been isolated from various sources including Lepidoptera insects, fungi, plants, fresh water, murals and rocks (Liu and Cai 2012; Zare and Gams 2016; Gomes et al. 2018; Crous et al. 2018; Sun et al. 2019; Okane et al. 2020). The nematophagous properties of *Leptobacillium* species have been extensively studied (Regaieg et al. 2011; Leplat et al. 2022).

Phylogenetic studies of species in the genera *Simplicillium* and *Leptobacillium* have focused on the nuclear ribosomal internal transcribed spacer region (ITS) and the nuclear ribosomal large subunit (nrLSU). Currently, several other DNA loci are frequently used to study species in the Cordycipitaceae family (Kepler et al. 2017; Wang et al. 2020; Leplat et al. 2022). Based on a phylogenetic analysis, *S. wallacei* was transplanted into the genus *Lecanicillium* and later Zhang et al. placed *L. wallacei* in the genus *Gamszarea* Z.F. Zhang & L. Cai (Zare and Gams 2001, 2008; Zhang et al. 2021). Phylogenetic analysis, based on five locus data, showed that *S. coffeanum* A.A.M. Gomes & O.L. Pereira, *S. chinensis* F. Liu & L. Cai and *S. filiforme* R.M.F. Silva, R.J.V. Oliveira, Souza-Motta, J.L. Bezerra & G.A. Silva were transferred to the genus *Leptobacillium* (Zare and Gams 2008; Okane et al. 2020; Chen et al. 2021).

Based on a comparative analysis of morphological characteristics and a multigene molecular phylogeny, we characterised in this study two newly-identified species from China, namely *S. puwenense* Hong Yu bis, Y.L. Lu & J. Zhao, sp. nov., from the genus of *Simplicillium* and *L. longiphialidum* Hong Yu bis, Y.L. Lu & J. Zhao, sp. nov., from the genus of *Leptobacillium*, respectively. This investigation has contributed to the expansion of the species diversity within the genera of *Simplicillium* and *Leptobacillium*, providing a solid taxonomic foundation to facilitate the rational development and sustainable use of these valuable resources.

Material and method

Material collection and isolation

The specimens of a dead spider infected with fungi were collected in China. One specimen was collected from Puwen Town, Jinghong City, Xishuangbanna Dai Autonomous Prefecture, Yunnan Province, China and the Xilong Mountains in Jinping County, Honghe Hani and Yi Autonomous Prefecture, Yunnan Province, China. Another was collected from Limushan National Forest Park, Limushan Town, Qiongzhong City, Hainan Province, China and 511 Township Road, Boluo County, Huizhou City, Guangdong Province, China. The specimens were photographed, assigned numbers and their collection details including habitat, elevation, latitude and longitude were documented. Subsequently, they were placed in freezing tubes within a vehicle-mounted refrigerator set at 4 °C for transportation back to the laboratory. Upon arrival at the laboratory, the specimens underwent initial observation and measurement using an Optec SZ660 stereo dissecting microscope. A select number of fungal conidia were then carefully picked with an inoculation needle and inoculated into PDA solid medium containing 0.05 g tetracycline and 0.1 g streptomycin using the plate streak method (Wang et al. 2020). The pure culture was incubated at a temperature of 25 °C, while the purified strain was transferred to a bevelled test tube containing PDA medium and stored at 4 °C (Wang et al. 2020). The specimens were deposited in the Yunnan Herbal Herbarium (YHH), while the strains were conserved in the Yunnan Fungal Culture Collection (YFCC).

Morphological observations

The pure cultures were transferred to PDA solid medium and incubated at 25 °C for 14 days. Colony diameters were measured, colony characteristics were recorded and photographs of the front and back of the colonies were captured using a Canon camera (Tokyo, Japan). To observe the microscopic morphology of the colonies, filter paper was cut to fit a petri dish and placed inside. A U-shaped glass shelf, a slide and two coverlids that had been sterilised at 121 °C for 30 minutes and then dried were prepared. A layer of PDA medium with a thickness of 1 mm and size of approximately 5 mm was applied onto the slide. A small amount of mycelia was selected from each culture and transferred to the centre of the medium. It was covered with a coverslip, sterile water was added to moisten the medium and sealed in an incubator at 25 °C for cultivation. The microstructure was observed, measured and photographed using fluorescence microscopes CX40 (Tokyo, Japan) and BX53 (Tokyo, Japan).

DNA extraction, polymerase chain reaction (PCR) and sequencing

The total genomic DNA of fungi was extracted using the CTAB method described by Liu et al. (2001). The ITS region was amplified using primer pairs ITS4 and ITS5 (White et al. 1990). The nuclear ribosomal small subunit (nrSSU) and nrLSU were amplified using primer pairs nrSSU-CoF with nrSSU-CoR and LR5 with LR0R, respectively (Vilgalys and Hester 1990; Rehner and Samuels 1994; Wang et al. 2015b). The translation elongation factor 1α (*tef-1α*) was amplified using primer pairs EF1α-EF and EF1α-ER (Bischoff et al. 2006; Sung et al.

2007). Finally, the largest subunit of RNA polymerase II (*rpb1*) and the second largest subunit of RNA polymerase II (*rpb2*) were amplified using primer pairs RPB1-5'F with RPB1-5'R and RPB2-5'F with RPB2-5'R, respectively, as described by Bischoff et al. (2006) and Sung et al. (2007).

The final volume of all PCR reactions was 25 μl, consisting of 17.25 μl of sterile deionised water, 2.5 μl of PCR10 Buffer (2 mmol/l Mg^{2+}) from Transgen Biotech in Beijing, China, 2 μl of dNTP (2.5 mmol/l), 1 μl each of forward and reverse primers, 0.25 μl of Taq DNA polymerase from Transgen Biotech in Beijing, China and 1 μl of DNA template. The polymerase chain reaction (PCR) for the five genes and ITS was conducted using a BIO-RAD T100TM thermal cycler manufactured by BIO-RAD Laboratories in Hercules, CA, United States (Bischoff et al. 2006; Wang et al. 2015a). The PCR products were analysed through electrophoresis on a 1.0% agarose gel and subsequently stored at -20 °C until they were dispatched in dry ice to BGI Co., Ltd, Shenzhen, China for sequencing.

Phylogenetic analyses

After aligning the six-gene sequences of related species obtained from GenBank with those of the present study using the Clustal W programme in MEGA v.5.0 software, we concatenated the six-gene datasets (ITS, nrSSU, nrLSU, *tef-1α*, *rpb1* and *rpb2*) into a combined matrix comprising all six genes. To both single gene and six-gene datasets, we respectively employed the ModelFinder programme in PhyloSuite v.1.2.2 software to determine the optimal model for the maximum likelihood analysis, based on Corrected AIC (AICc) and IQ-TREE model selection methods. The remaining parameters were set to their default values. Subsequently, we utilised the IQ-TREE programme with 5,000 bootstrap replicates to construct a maximum likelihood tree while selecting appropriate optimal model parameters.

The ModelFinder programme in PhyloSuite v.1.2.2 software was utilised to determine the optimal model for the Bayesian inference using Corrected AIC (AICc) and the MrBayes model, while keeping default settings for other parameters. Subsequently, the MrBayes programme was employed to select appropriate optimal model parameters and run for 2,000,000 generations to construct the BI tree. The constructed phylogenetic trees were visualised in FigTree v.1.4.2 to figure the maximum likelihood method of bootstrap proportion (BP) and the Bayesian inference posterior probability (BPP) and then formatted for editing with Adobe Illustrator CS6.

Results

Phylogenetic analyses

Phylogenetic analysis of single gene molecular fragments

Using single gene fragments of ITS, nrSSU, nrLSU, *tef-1α* and *rpb1* were used to construct *Simplicillium* and *Leptobacillium* phylogenetic trees, respectively. *Beauveria bassiana* ARSEF 1564 and *B. brongniartii* ARSEF 617 were employed as outgroups (Table 1). Among them, the ITS matrix had 64 sequences, 711 bp of bases, including 783 columns, 381 distinct patterns, 218 parsimony-informative,

Table 1. Relevant species information and GeneBank accession numbers for phylogenetic research in this study.

Species	Strain	ITS	nrSSU	nrLSU	*tef-1α*	*rpb1*	*rpb2*	Reference
Beauveria bassiana	ARSEF 1564	HQ880761	-	AF373871	HQ880974	HQ880833	HQ880905	Rehner et al. (2011)
Beauveria brongniartii	ARSEF 617	HQ880782	AB027335	-	HQ880991	HQ880854	HQ880926	Rehner et al. (2011)
Leptobacillium cavernicola	LRMH C212	OM622523	OM628842	OM628781	OM654332	OM677781	OM654321	Leplat et al. (2022)
Leptobacillium cavernicola	LRMH C216	OM622524	OM628843	OM628782	OM654333	OM677782	OM654322	Leplat et al. (2022)
Leptobacillium chinense	CGMCC 3.14969	JQ410323	-	JQ410321	-	-	-	Okane et al. (2020)
Leptobacillium chinense	CGMCC 3.14970	JQ410324	-	JQ410322	-	-	-	Okane et al. (2020)
Leptobacillium coffeanum	COAD 2057	MF066034	-	MF066032	-	-	-	Okane et al. (2020)
Leptobacillium coffeanum	COAD 2061	MF066035	-	MF066033	-	-	-	Okane et al. (2020)
Leptobacillium filiforme	URM 7918	-	-	MH979399	-	-	-	Okane et al. (2020)
Leptobacillium latisporum	TBRC 16288	OP856540	OP850838	OP856529	-	-	-	Preedanon et al. (2023)
Leptobacillium leptobactrum	ZJ14B02	PP385689	-	PP381743	-	-	-	Unpublished
Leptobacillium leptobactrum	AH17C05	PP384754	-	PP380808	-	-	-	Unpublished
Leptobacillium leptobactrum var. *calidius*	CBS 703.86	EF641866	EF641850	KU382226	-	-	-	Zare and Gams (2016)
Leptobacillium leptobactrum var. *leptobactrum*	CBS 771.69	EF641868	EF641852	KU382224	-	-	-	Zare and Gams (2016)
Leptobacillium longiphialidum	**YFCC 23039272^{T}**	**PQ509282**	**PQ508806**	**PQ508808**	**PQ560997**	**PQ567240**	-	**This study**
Leptobacillium longiphialidum	**YFCC 24079491**	**PQ509281**	**PQ508805**	**PQ508807**	**PQ560996**	**PQ567239**	-	**This study**
L. marksiae	BRIP 70307a	PQ061114	-	PQ047739	-	-	-	Tan and Bishop-Hurley (direct submission)
Leptobacillium muralicola	CGMCC 3.19014	MH379983	-	MH379997	-	-	-	Sun et al. (2019)
Leptobacillium muralicola	CGMCC 3.19015	MH379985	-	MH379999	-	-	-	Sun et al. (2019)
Leptobacillium symbioticum	NBRC 113865	LC485673	-	LC506046	-	-	-	Okane et al. (2020)
Leptobacillium symbioticum	OPTF00168	LC485675	-	LC506047	-	-	-	Okane et al. (2020)
Simplicillium album	LC12442	-	-	-	MK336068	-	-	Zhang et al. (2021)
Simplicillium aogashimaense	JCM 18167	AB604002	-	LC496874	LC496904	-	-	Nonaka et al. (2013)
Simplicillium aogashimaense	JCM 18168	AB604004	-	LC496875	-	-	-	Nonaka et al. (2013)
Simplicillium araneae	DY101811	OM743774	-	OM743792	OM818465	-	-	Chen et al. (2022)
Simplicillium araneae	DY101812	OM743840	-	OM743846	OM818466	-	-	Chen et al. (2022)
Simplicillium calcicola	LC5586	KU746706	-	KU746752	KX855252	-	-	Zhang et al. (2017)
Simplicillium calcicola	LC5371	KU746705	-	KU746751	KX855251	-	-	Zhang et al. (2017)
Simplicillium cicadellidae	GY11012	MN006244	-	-	MN022264	MN022272	-	Chen et al. (2019)
Simplicillium cicadellidae	GY11011	MN006243	-	-	MN022263	MN022271	-	Chen et al. (2019)
Simplicillium coccinellidae	DY101791	MT453861	MT453863	-	MT471341	-	-	Chen et al. (2021)
Simplicillium coleopterorum	SD05381	OM743920	-	OM743925	OM818467	-	-	Chen et al. (2022)
Simplicillium coleopterorum	SD05382	OM744109	-	OM744170	OM818468	-	-	Chen et al. (2022)
Simplicillium cylindrosporum	JCM 18169	AB603989	-	LC496876	LC496906	-	-	Nonaka et al. (2013)
Simplicillium cylindrosporum	JCM 18170	AB603994	-	LC496877	LC496907	-	-	Nonaka et al. (2013)
Simplicillium formicae	DY09641	OR121054	-	OR121057	OR126571	-	-	Unpublished
Simplicillium formicae	DY09642	OR121055	-	OR121056	OR126572	-	-	Unpublished
Simplicillium guizhouense	DY10051	OM743225	-	OM743226	OM818453	-	-	Chen et al. (2022)
Simplicillium guizhouense	DY10052	OM743241	-	OM743252	OM818454	-	-	Chen et al. (2022)
Simplicillium humicola	LC 12494	-	-	-	MK336072	-	-	Zhang et al. (2021)
Simplicillium humicola	CGMCC 3.19573	NR_172845	-	MK329041	MK336071	-	-	Unpublished
Simplicillium hymenopterorum	DY101692	MT453851	-	-	MT471338	-	-	Unpublished
Simplicillium hymenopterorum	DY101691	MT453848	MT453849	-	MT471337	MT471344	-	Unpublished
Simplicillium lamellicola	JC-1	MT807906	MT807908	MT807907	-	-	-	Unpublished

Species	Strain	ITS	nrSSU	nrLSU	*tef-1α*	*rpb1*	*rpb2*	Reference
Simplicillium lamellicola	CBS 116.25	AJ292393	-	-	DQ522356	DQ522404	DQ522462	Nonaka et al. (2013)
Simplicillium lanosoniveum	CBS 704.86	AJ292396	-	-	DQ522358	DQ522406	DQ522464	Nonaka et al. (2013)
Simplicillium larvatum	DY101731	OM743438	-	OM743441	OM818462	OM818460	-	Chen et al. (2022)
Simplicillium lepidopterorum	GY29132	MN006245	-	-	MN022266	MN022274	-	Chen et al. (2019)
Simplicillium lepidopterorum	GY29131	MN006246	-	-	MN022265	MN022273	-	Chen et al. (2019)
Simplicillium minatense	JCM 18176	AB603992	LC496893	LC496878	LC496908	-	-	Nonaka et al. (2013)
Simplicillium minatense	JCM 18178	AB603993	LC496894	LC496879	LC496909	-	-	Nonaka et al. (2013)
Simplicillium neolepidopterorum	DY101752	MT453857	-	-	MT471340	-	-	Chen et al. (2021)
Simplicillium neolepidopterorum	DY101751	MT453854	MT453856	-	MT471339	-	-	Chen et al. (2021)
Simplicillium obclavatum	CBS 311.74	AJ292394	-	AF339517	EF468798	-	-	Nonaka et al. (2013)
Simplicillium obclavatum	SUF81	-	-	MK788174	-	-	-	Unpublished
Simplicillium pechmerlense	CBS 147188	MW031272	-	MW031268	MW033224	MW033222	-	Leplat et al. (2021)
Simplicillium puwenense	**YFCC 23129490^{T}**	**PQ508796**	**PQ508799**	**PQ508802**	**PQ537122**	**PQ560994**	-	**This study**
Simplicillium puwenense	**YFCC 23089322**	**PQ508797**	**PQ508800**	**PQ508803**	**PQ537123**	-	-	**This study**
Simplicillium puwenense	**YFCC 23069492**	**PQ508798**	**PQ508801**	**PQ508804**	**PQ537124**	**PQ560995**	-	**This study**
Simplicillium scarabaeoidea	DY101392	MT453845	-	-	MT471336	-	-	Chen et al. (2021)
Simplicillium scarabaeoidea	DY101391	MT453842	MT453843	-	MT471335	MT471343	-	Chen et al. (2021)
Simplicillium sinense	AFMCCC 16a	OQ332403	-	-	OQ352167	-	-	Yan et al. (2023)
Simplicillium sinense	AFMCCC 16b	OQ332404	-	-	OQ352168	-	-	Yan et al. (2023)
Simplicillium spumae	JCM 39054	LC496871	-	LC496887	LC496917	-	-	Kondo et al. (2020)
Simplicillium spumae	JCM 39050	LC496869	LC496898	LC496883	LC496913	-	-	Kondo et al. (2020)
Simplicillium subtropicum	JCM 18180	AB603990	-	LC496880	LC496910	-	-	Nonaka et al. (2013)
Simplicillium subtropicum	JCM 18181	AB603995	-	LC496881	LC496911	-	-	Nonaka et al. (2013)
Simplicillium sympodiophorum	JCM 18184	AB604003	-	LC496882	LC496912	-	-	Nonaka et al. (2013)
Simplicillium yunnanense	YFCC 7134	-	MN576729	MN576785	MN576955	MN576845	-	Wang et al. (2020)
Simplicillium yunnanense	YFCC 7133	-	MN576728	MN576784	MN576954	MN576844	-	Wang et al. (2020)

64 singleton sites, 500 constant sites. The Best-fit model of the ML tree constructed by the ITS matrix was TIM2+F+I+G4 and the BI tree was GTR+F+I+G4 (Fig. 1). The nrSSU matrix consisted of 21 sequences, 1,122 bp of bases, 2,333 columns, 163 distinct patterns, 30 parsimony-informative, 48 singleton sites and 2,255 constant sites. The Best-fit model for building the nrSSU ML tree was TIM3e+I and the BI tree was SYM+I (Fig. 2). The nrLSU had 52 sequences with 1,126 columns, 325 distinct patterns, 91 parsimony-informative, 340 singleton sites, 695 constant sites and 1,019 bp bases. Based on ML and BI, the Best-fit models used to construct the nrLSU phylogenetic framework were K2P+R5, GTR+F+G4, respectively (Fig. 3). The *tef-1α* matrix consists of 52 sequences, 1,090 columns, 431 distinct patterns, 289 parsimony-informative, 82 singleton sites, 719 constant sites and 1,154 bp bases. The Best-fit model of the ML tree constructed by the *tef-1α* matrix was TIM3+F+R8 and the BI tree was GTR+F+I+G4 (Fig. 4). The *rpb1* matrix consisted of 20 sequences, 803 bp bases, 2,971 columns, 390 distinct patterns, 294 parsimony-informative, 113 singleton sites and 2,564 constant sites. Based on ML and BI, the Best-fit models used to construct the *rpb1* phylogenetic framework were TIM2e+I+G4, SYM+I+G4, respectively (Fig. 5). The tree shapes constructed, based on ML and BI, were

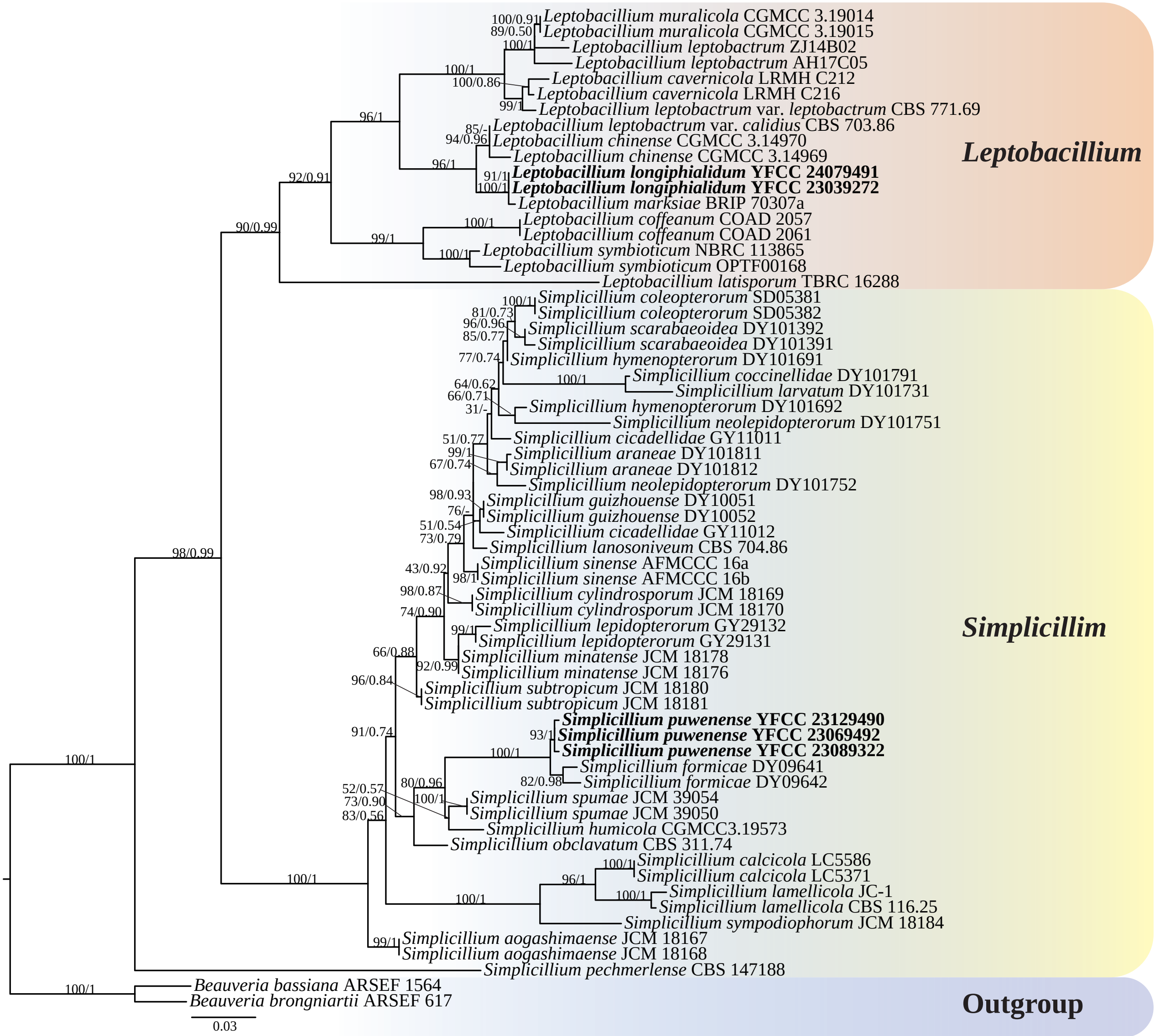

Figure 1. The phylogenetic tree of *Simplicillium* and *Leptobacillium* was inferred from ITS sequence, based on the Bayesian inference and the maximum likelihood analyses. Each value at a node indicates a bootstrap proportion (the left) and Bayesian posterior probability (the right). The scale bar 0.03 indicates the number of expected mutations per site. The species in bold black font of the *Simplicillium* and *Leptobacillium* were from this study. *B. bassiana* ARSEF 1564 and *B. brongniartii* ARSEF 617 were designated as outgroups.

basically the same and the topological structure adopted in this study was a phylogenetic tree constructed by the maximum likelihood method (Figs 1–5).

Based on the phylogenetic framework constructed by single gene fragments, it was found that the resulting topologies were roughly similar and there was no obvious conflict between different gene fragments. The species *S. puwenense* and *L. longiphialidum* collected and described in this study were located in roughly the same position in each phylogenetic tree, forming monophyletic, with high support rate and stable topological structure. In the topology constructed, based on ITS, nrLSU and *tef-1α* matrices, *S. puwenense* and *S. formicae* D.P. Wei & K.D. Hyde were closely related. In phylogenetic trees constructed by ITS and nrLSU matrices, *L. longiphialidum* and *L. marksiae* Tan, Bishop-Hurley & Marney came together.

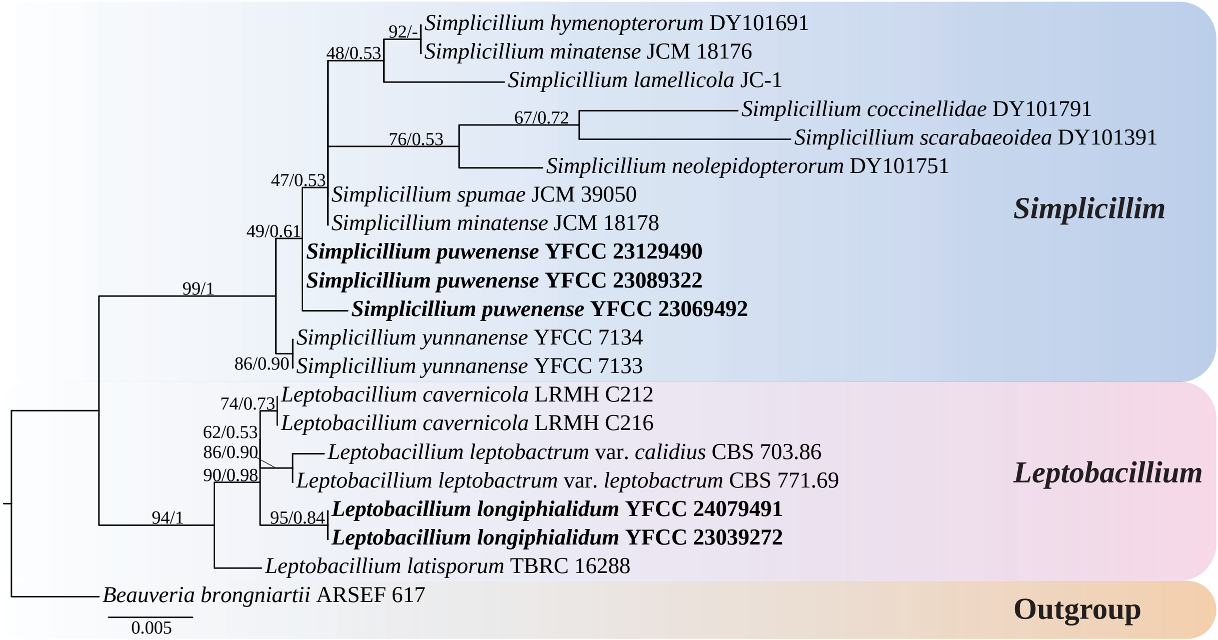

Figure 2. The phylogenetic tree of *Simplicillium* and *Leptobacillium* was inferred from nrSSU sequence, based on the Bayesian inference and the maximum likelihood analyses. Each value at a node indicates a bootstrap proportion (the left) and Bayesian posterior probability (the right). The scale bar 0.005 indicates the number of expected mutations per site. The species in bold black font of the *Simplicillium* and *Leptobacillium* were from this study. *B. brongniartii* ARSEF 617 was designated as outgroup.

Phylogenetic tree reconstructed from multi-gene combined dataset

The phylogenetic framework for the genera *Simplicillium* and *Leptobacillium*, comprising 70 taxonomic units, was constructed, based on a six-gene dataset utilising the maximum likelihood method and Bayesian inference. *B. bassiana* ARSEF 1564 and *B. brongniartii* ARSEF 617 were employed as outgroups (Table 1). The joint matrix comprised 14,494 columns, 1,873 distinct patterns, 1,190 parsimony-informative, 770 singleton sites and 12,534 constant sites. The most appropriate model for the ML analysis amongst the 286 models simulated by ModelFinder was TIM2+F+R10, which achieved an IQ-TREE best score of -32893.153 and a Total tree length of 2.122. The parameters of the TIM2+F+R10 model used to analyse the dataset were estimated, based on the following nucleotide frequencies: A = 0.243, C = 0.262, G = 0.261, T = 0.233, A–C = 1.15866, A–G = 2.32357, A–T = 1.15866, C–G = 1.00000, C–T = 5.27826 and G–T = 1.00000. The GTR+F+I+G4 model was determined as the most suitable model for the BI analysis using ModelFinder amongst the 24 simulated models. It achieved an IQ-TREE best score of -33090.992 and a total tree length of 1.634. The phylogenetic trees constructed using the maximum likelihood (ML) and the Bayesian inference (BI) methods exhibited a high degree of similarity, as depicted in Fig. 6.

The phylogenetic tree of the six-gene joint dataset revealed that the majority of species were grouped in distinct branches with robust support, indicating a stable topology (Fig. 6). The strains YFCC 23129490, YFCC 23069492 and YFCC 23089322, collected and described in this study, formed a well-supported single branch. *S. puwenense* and *S. formicae* were identified as sister species, constituting an independent clade with BP and BPP values of 100% and 1, respectively, while maintaining topological stability. YFCC 24079491 and

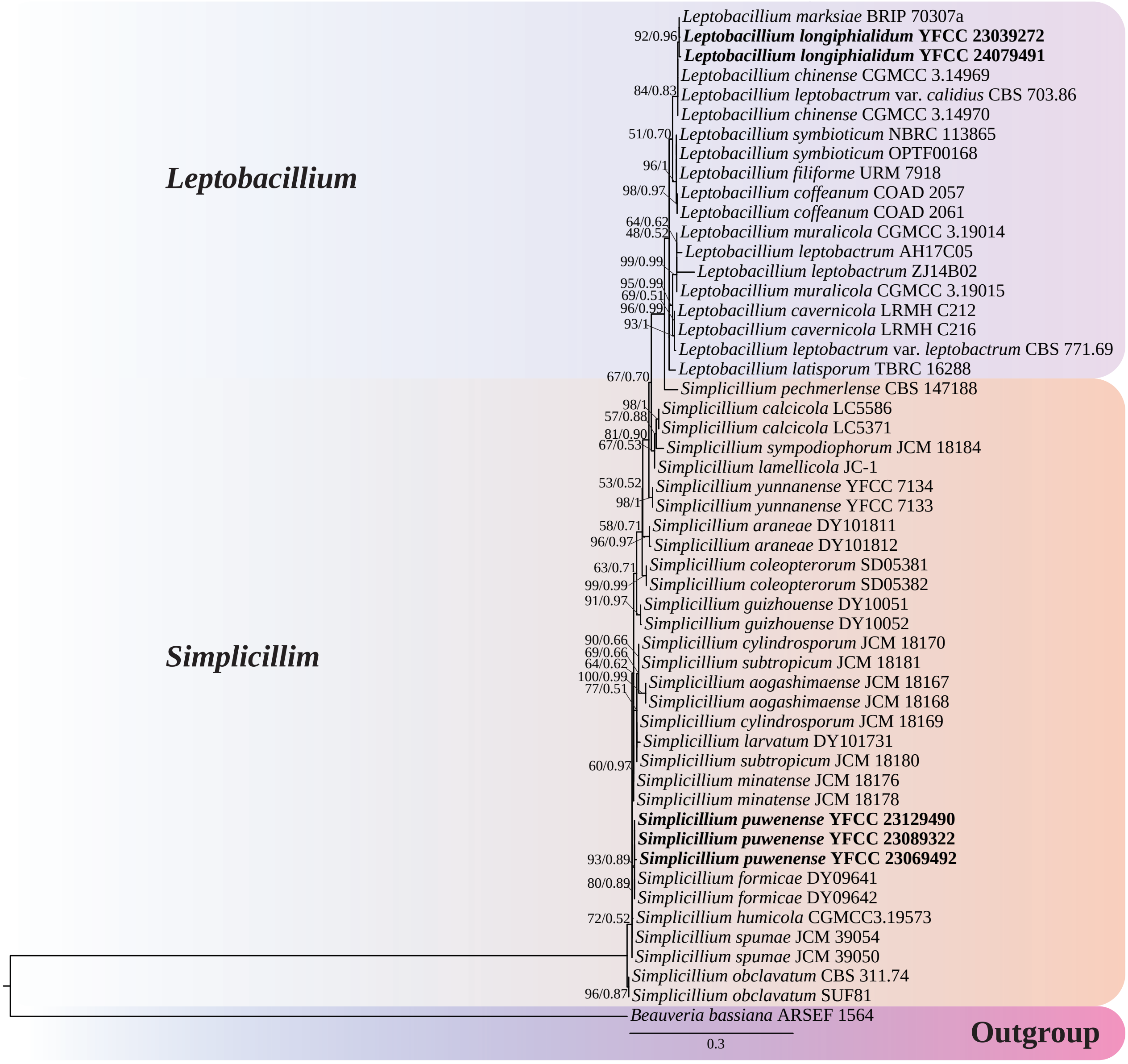

Figure 3. The phylogenetic tree of *Simplicillium* and *Leptobacillium* was inferred from nrLSU sequence, based on the Bayesian inference and the maximum likelihood analyses. Each value at a node indicates a bootstrap proportion (the left) and Bayesian posterior probability (the right). The scale bar 0.3 indicates the number of expected mutations per site. The species in bold black font of the *Simplicillium* and *Leptobacillium* were from this study. *B. bassiana* ARSEF 1564 was designated as outgroup.

YFCC 23039272 clustered together (BP = 100%, BPP = 1). *L. longiphialidum* and *L. marksiae* clustered into a clade, with BP and BPP of 97% and 1, respectively, forming sister species and receiving high support.

Taxonomy

Simplicillium puwenense **Hong Yu bis, Y.L. Lu & Jing Zhao, sp. nov.**
MycoBank No: 856314
Fig. 7

Etymology. Named after the location Puwen Town where the pattern material was collected.

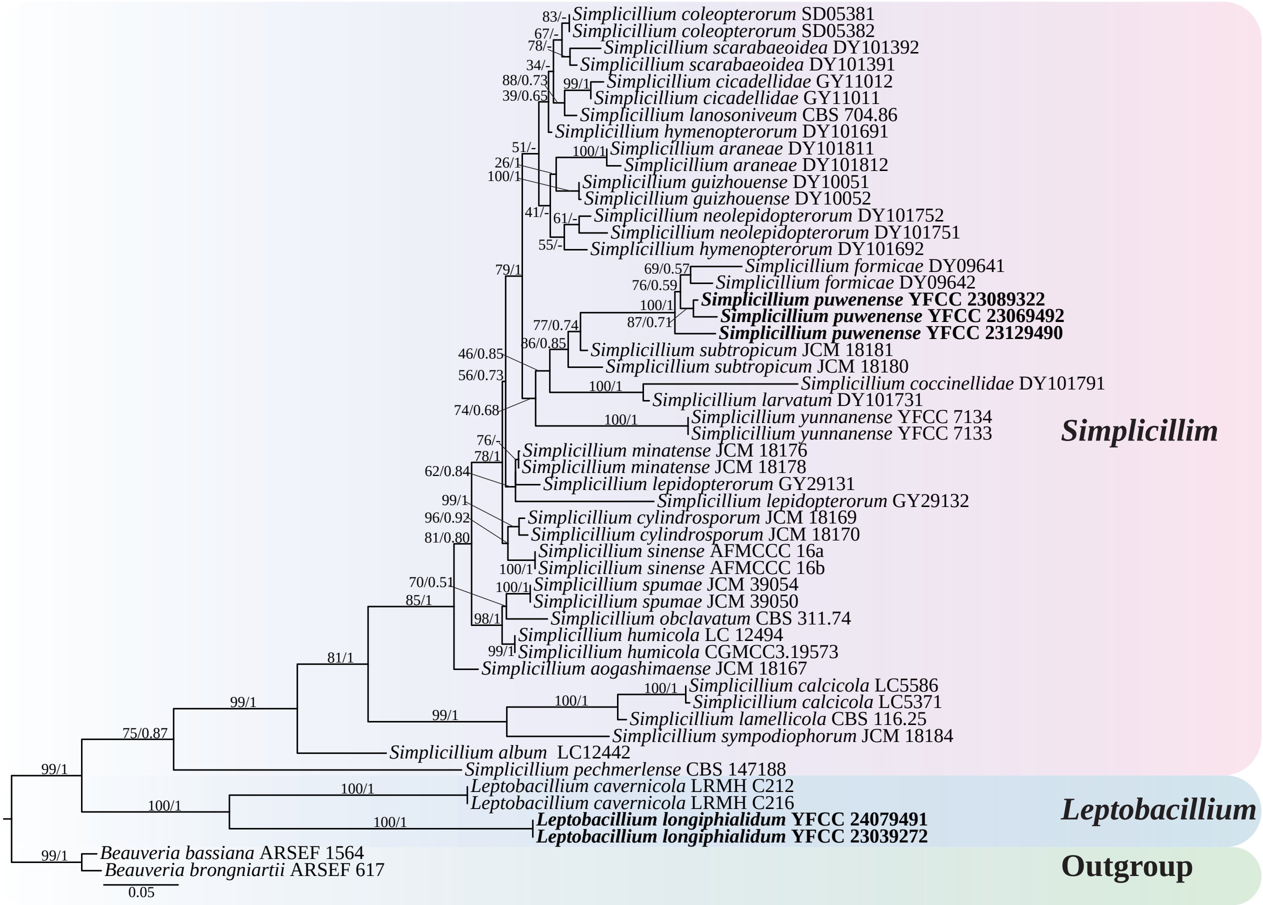

Figure 4. The phylogenetic tree of *Simplicillium* and *Leptobacillium* was inferred from *tef-1α* sequence, based on the Bayesian inference and the maximum likelihood analyses. Each value at a node indicates a bootstrap proportion (the left) and Bayesian posterior probability (the right). The scale bar 0.05 indicates the number of expected mutations per site. The species in bold black font of the *Simplicillium* and *Leptobacillium* were from this study. *B. bassiana* ARSEF 1564 and *B. brongniartii* ARSEF 617 were designated as outgroups.

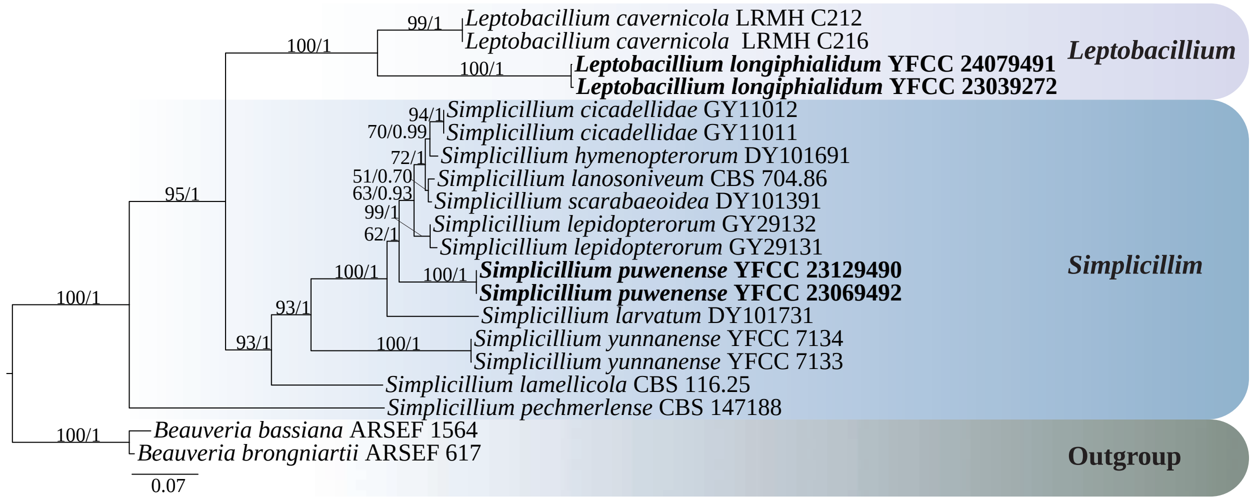

Figure 5. The phylogenetic tree of *Simplicillium* and *Leptobacillium* was inferred from *rpb1* sequence, based on the Bayesian inference and the maximum likelihood analyses. Each value at a node indicates a bootstrap proportion (the left) and Bayesian posterior probability (the right). The scale bar 0.07 indicates the number of expected mutations per site. The species in bold black font of the *Simplicillium* and *Leptobacillium* were from this study. *B. bassiana* ARSEF 1564 and *B. brongniartii* ARSEF 617 were designated as outgroups.

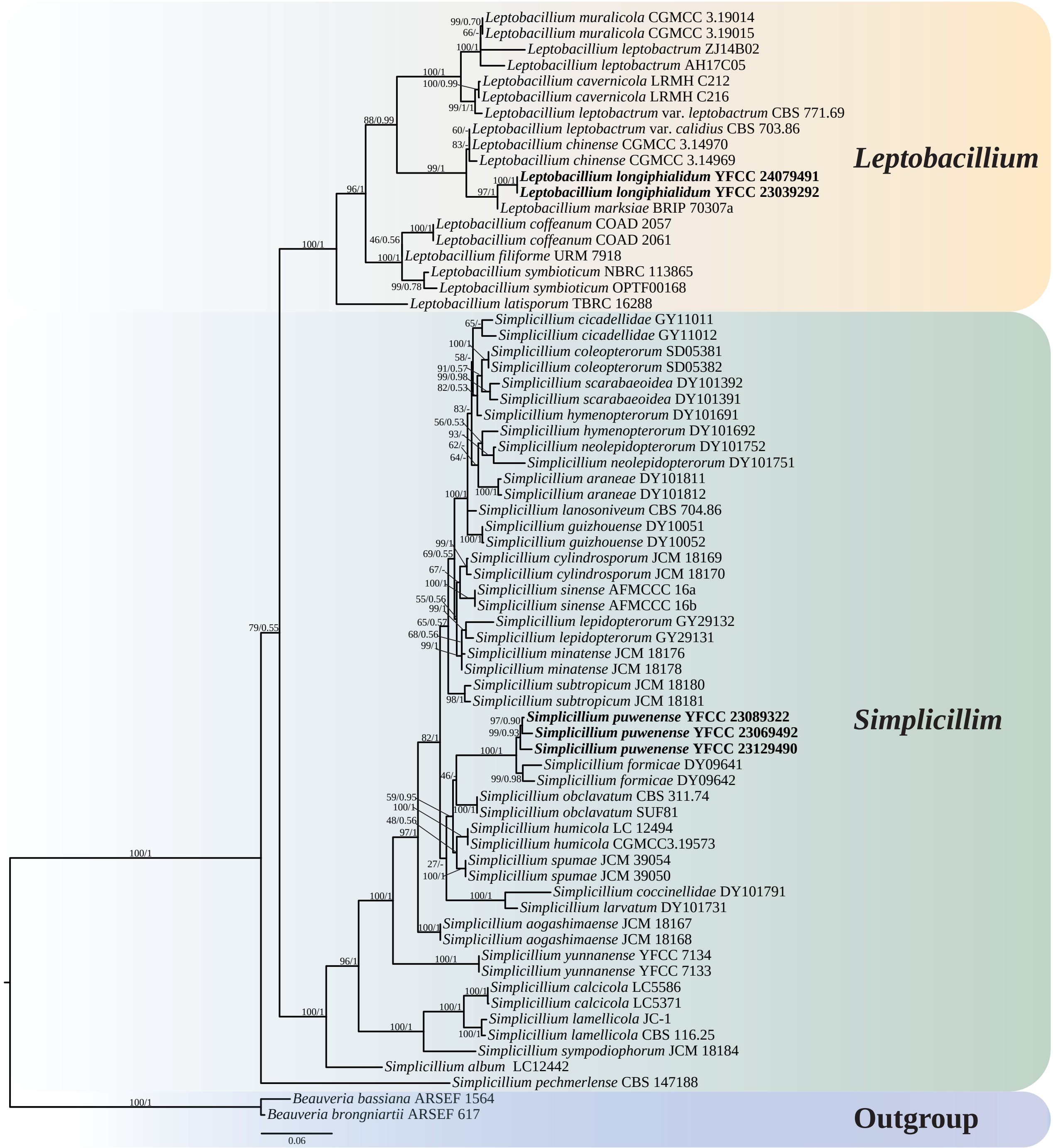

Figure 6. The phylogenetic tree of *Simplicillium* and *Leptobacillium* was inferred from six-gene dataset (ITS, nrSSU, nrLSU, *tef-1α*, *rpb1*, *rpb2*), based on the Bayesian inference and the maximum likelihood analyses. Each value at a node indicates a bootstrap proportion (the left) and Bayesian posterior probability (the right). The scale bar 0.06 indicates the number of expected mutations per site. The species in bold black font of the *Simplicillium* and *Leptobacillium* were from this study. *B. bassiana* ARSEF 1564 and *B. brongniartii* ARSEF 617 were designated as outgroups.

Holotype. China • Yunnan Province, Xishuangbanna Dai autonomous prefecture, Jinghong City, Puwen Town. Specimens were collected from an evergreen broad-leaved forest, alt. 1,062 m, 100°58'60"E, 22°31'20"N, 13 December 2023, Hong Yu (***holotype***: YHH SP2312001, ***ex-type living culture***: YFCC 23129490).

Description. ***Sexual morph.*** Not found.

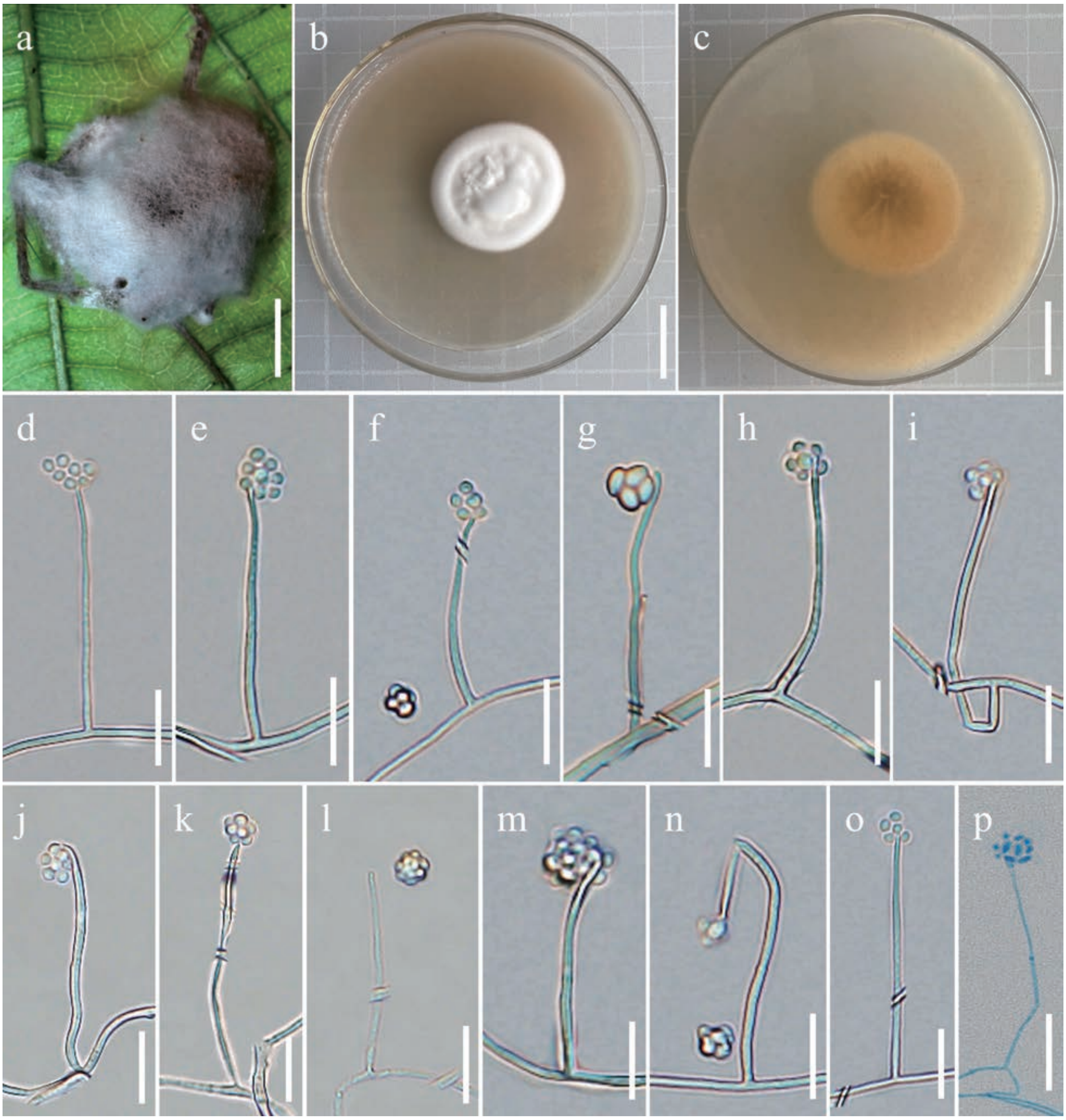

Figure 7. Morphology of *Simplicillium puwenense* **a** wild material **b** colonies obverse in PDA at 25 °C **c** colonies reverse on PDA at 25 °C **d–p** phialides bearing conidia. Scale bars: 3 mm (**a**); 3 cm (**b, c**); 10 µm (**d–f**); 8 µm (**g**); 10 µm (**h, i**); 12 µm (**j**); 10 µm (**k, l**); 8 µm (**m**); 10 µm (**n, o**); 15 µm (**p**).

Asexual morph. Colonies on PDA medium moderate growth,diameter of 32–35 mm at 25 °C for 14 days, convex in middle surface, white fluffy to cotton like, dense, octahedral crystals absent, reverse brown to light brown with radial emission grooves. Hyphae septate, branched, transparent, with a diameter of 0.67–1.76 µm and smooth-walled. Cultures readily produced phialides and conidia after 14 days on PDA medium at room temperature. Phialides arising were slender, solitary, rod-shaped or columnar, measuring 3.37–52.57 µm in length and 0.5–1.6 µm in width. Conidia, transparent, single celled, smooth-walled, elliptical or oval or cylindrical, 1.19–2.41 × 0.88–1.6 µm. The conidia aggregated into a spherical shape at the top of the phialides, with a size of approximately 3.59–6.59 × 2.6–6.7 µm.

Host. Spider.

Distribution. China, Yunnan Province.

Additional material examined. China • Yunnan Province, Honghe Hani and Yi autonomous prefecture, the Xilong Mountains. Specimens were collected from an evergreen broad-leaved forest, alt. 1,715 m, 102°32'48"E, 22°45'20"N, 1 June 2023, Jing Zhao (paratype: YHH SP2306001, ex-paratype living culture: YFCC 23069492); • Puwen Town,collected from an evergreen broad-leaved forest, alt. 1,019 m, 100°58'42"E, 22°31'10"N, 4 August 2023, Hong Yu (Specimen number: YHH SP2308001, Strain number: YFCC 23089322).

Remarks. Phylogenetically, three samples of *S. puwenense* were grouped together on a single branch, forming a monophyletic clade. It was identified as the sister species to *S. formicae*, supported by robust statistical evidence from both the Bayesian inference (BPP = 1) and the maximum likelihood analysis (BP = 100%). Both *S. puwenense* and *S. formicae* exhibited a stable topological structure with BP and BPP values of 100%. Morphologically, the surface of *S. puwenense* appeared centrally convex and exhibited a white, fluffy or cotton-like texture with densely arranged radial emission grooves ranging from reverse brown to light brown. Additionally, the conidia were observed to aggregate into spherical clusters at the apex of phialides (Table 2).

Table 2. Morphological comparisons of asexual morphs in the genus *Simplicillium*.

Species	Colony on PDA	Phialides (μm)	Conidia (μm)	Octahedral crystals	References
S. album	White, with a yellowish discharge, reverse beige to thick yellow, fluted	2–3 whorls or Solitary, 13.0–40.0 × 1.5–3.0 μm	Two conidia: macroconidia sickle-shaped or fusiform, 8.0–11.0 (−13.0) × 2.0–3.5 μm; Microconidia oval or oblong, 3.0–4.0 × 1.5–2.0 μm	Present	Zhang et al. (2021)
S. aogashimaense	White, reverse yellow white	Solitary, a few 2–3 whorls, slender and long (19–) 23–53 × 1.2–2.0 μm	Cylindrical, 4.2–6.5 × 1.2–2.0 (−2.3), conidia aggregate into spherical small heads at the top of bottle stem	Present	Nonaka et al. (2013)
S. araneae	White fluff, reverse yellow to brown	Solitary, slender, tapering from base to top, 32.9–47.1 × 1.2–2.4 μm	Subspherical, spherical, or elliptical, 1.8–2.9 × 1.2–1.8 μm	Absent	Chen et al. (2022)
S. calcicola	White or yellow, reverse light yellow to yellow	2–3 whorled or solitary, 14.0–38.0 × 1.0–2.0 μm	Two conidia: macroconidial fusiform, 4.5–8.0 × 1.0–2.0 μm; microconidia oval or globose or spherical, 2.0–3.5 × 1–1.5 μm	Absent	Zhang et al. (2017)
S. cicadellidae	White, reverse yellow	Solitary, 12.9–18.3 × 0.8–1.1 μm	Ellipsoid, 1.8–2.8 × 1.4–1.8 μm	Absent	Chen et al. (2019)
S. coccinellidae	White fluff, reverse yellow to light brown	Solitary, 4.9–62.1 × 1.0–1.5 μm	Subspherical or cylindrical or elliptical, 2.0–3.4 × 1.6–2.0 μm	Absent	Chen et al. (2021)
S. coleopterorum	White fluff, reverse light brown to brown	Solitary, 34.5–64.1 × 0.7–1.2 μm	Spherical or subspherical or elliptical, 2.1–3.3 × 1.5–1.9 μm	Absent	Chen et al. (2022)
S. cylindrosporum	White, reverse blond	2–3 whorled or solitary, 17–32 × 1.2–2.0 (−2.5) μm	Spherical or cylindrical, 3.0–4.5(−5.0) × 1.0–2.0 μm	Present	Nonaka et al. (2013)
S. formicidae	White, reverse light brown to brown, brown secretions	Solitary, 51–70.1 × 0.7–0.9 μm	Conidia aggregate into spherical slimy heads, mostly filamentous or fusiform, 3.9–7.9 × 0.8–1.3 μm	Absent	Chen et al. (2019)
S. guizhouense	White, reverse yellow to light yellow	Solitary, 1.1–52.2 × 1.0–1.8 μm	Oval or spherical, 2.4–2.9 × 1.6–1.8 μm	Absent	Chen et al. (2022)
S. humicola	White, light-yellow secretions, reverse light yellow to brown	2–3 whorled or solitary, 20.0–35.0 (−47.0) × 1.5–3.0 μm	Oblong or oval, 3.0–5.0 × 1.5–3.0 μm	Present	Zhang et al. (2021)
S. hymenopterorum	White, reserve light yellow	Mainly solitary, rarely whorls, 19.3–46.2 × 1.1–2.3 μm	Cylindrical to subellipsoidal, 2.1–2.8 × 1.3–1.9 μm, forming a subspherical small head at the top of the stem	Absent	Chen et al. (2021)
S. lamellicola	White, reserve light yellow	15–50 × 0.7–1.0 μm	Two conidia: macroconidia fusiform, 4.5–9.0 × 0.8–1.0 μm; microconidia ovoid to ellipsoid, 2.0–3.0 × 0.7–1.2 μm	Present	Zare and Gams (2001)

Species	Colony on PDA	Phialides (μm)	Conidia (μm)	Octahedral crystals	References
S. lanosoniveum	White or cream, reverse brownish cream to light yellow	Solitary, 20.0–40.0 × 1.1–2.0 μm	Spherical or ellipsoidal, 2.0–4.5 × 1.0–3.0 μm, forming a spherical or ellipsoidal tip at the top of the phialides,		Wei et al. (2019)
S. lepidopterorum	White, reserve light yellow	Solitary, 15.3–26.2 × 0.7–1.4 μm	Spindle-shaped or oval, 1.6– 2.4 × 1.4–1.7 μm, forming a slimy spherical head at the top of the phialides	Absent	Chen et al. (2019)
S. minatense	White, no secretion, reverse brown	Mainly solitary, rarely in whorls of 2–3, 11.0–31.0 (−47.0) × 1.0–1.7 μm	Spherical, 2.0–3.5 × 1.8–2.5 (−2.8) μm, forming a subglobose or ellipsoidal tip at the top of the phialides	Present	Nonaka et al. (2013)
S. neolepidopterorum	White, reverse yellow to light yellow	Solitary, 34.1–44.3 × 1.0–1.7 μm Solitary, 34.1–44.3 × 1.0–1.7 μm	Solitary, ellipsoidal to cylindrical, occasionally in short imbricate chains, 2.5–3.8 × 1.5–2.1 μm	Absent	Chen et al. (2021)
S. niveum	White	2–5 whorled, 10–20.5 (25.0) × 1–2 μm	Top growth, elongated or elliptical in shape, 3.0–4.5 (−6) × 1–2 μm		Crous et al. (2021)
S. pechmerlense	White, reverse light yellow to orange	Solitary, 16.0–31.0 × 0.9–1.2 μm	Two conidia: macroconidia fusiform, 5.0–8.0 × 1–1.6 μm; microconidia subglobular or elliptic, 1.8–3.0 × 0.9–1.5 μm, forming a slimy spherical head at the top of the phialides,	Absent	Leplat et al. (2021)
S. puwenense	**White fluffy to cotton like, convex in middle surface, reverse brown to light brown with radial emission grooves**	**Slender, solitary, rod-shaped or columnar, measuring 3.37–52.57 μm in length and 0.5–1.6 μm in width**	**Elliptical or oval or cylindrical, 1.19–2.41 × 0.88–1.6 μm. forming a spherical shape at the top of the phialides, 3.59–6.59 × 2.6–6.7 μm in size**	**Absent**	**This study**
S. scarabaeoidea	White, reverse light yellow	Solitary, 18.5–63.4 × 1.1–1.4 μm	Ellipsoidal, 1.9–2.9 × 1.4–2.0 μm	Absent	Chen et al. (2021)
S. subtropicum	White, reverse brownish orange to brown	(15.0–) 20–42 (−50.0) × 1.0–2.3 μm; Solitary, rarely in whorls of 2–3, (15.0–) 20.0–42.0 (−50.0) × 1.0–2.3 μm	Subglobose or ellipsoid, 2.3–4.0 (−4.5) × 1.5–3.3 μm, forming a spherical tip at the top of the phialides, 2.3–4.0 (−4.5) × 1.5–3.3 μm in size	Present	Nonaka et al. (2013)
S. sympodiophorum	White, reverse yellow white	2–4 whorled or solitary, 20.0–34 (−47.0) × 0.5–1.3 μm	Oval to ellipsoidal, 2.2–3.5 × 1.0–2.0 μm	Present	Nonaka et al. (2013)
S. yunnanense	White to light yellow, grayish orange to brown on back	Solitary, 5.8–16.9 × 1.1–1.5 μm	Cylindrical, 2.5–3.4 × 0.7–1.1 μm, conidia usually form chains at the top of the phialides	-	Wang et al. (2020)

Leptobacillium longiphialidum **Hong Yu bis, Y.L. Lu & Jing Zhao, sp. nov.**
MycoBank No: 856313
Fig. 8

Etymology. Referring to its longer phialides than those of the close relationship species in this genus.

Holotype. CHINA • Hainan Province, Qiongzhong City, Limushan Town, Limushan National Forest Park. Specimens were collected from an evergreen broad-leaved forest, alt. 589.9 m, 109°44'28"E, 19°10'41"N, 8 March 2023, Jing Zhao (***holotype*****:** YHH LL2303001, ***ex-type living culture*****:** YFCC 23039272).

Description. ***Sexual morph*****.** Not found.

Asexual morph**.** The colony was incubated at 25 °C on PDA medium for 14 days, the growth rate was slow, the diameter was 25–27 mm, the middle was fluffy to cotton, dense, convex and radial wrinkles, white and reverse brown to light yellow on the back. Mycelium branches, smooth walls, septate, transparent, with a diameter of approximately 0.97 × 1.72 μm. Cultures readily produced phialides and conidia after 10 days on PDA medium at room temperature. Phialides solitary, columnar, tapering from base to apex, 24.01–205.77 μm long, 1.00–2.24 μm wide. Conidia 2.88–4.54 × 1.18–1.95 μm, transparent, single celled in chains, smooth walls, narrow columnar or spindle-shaped, with apical conidia elliptical or nearly spherical in shape.

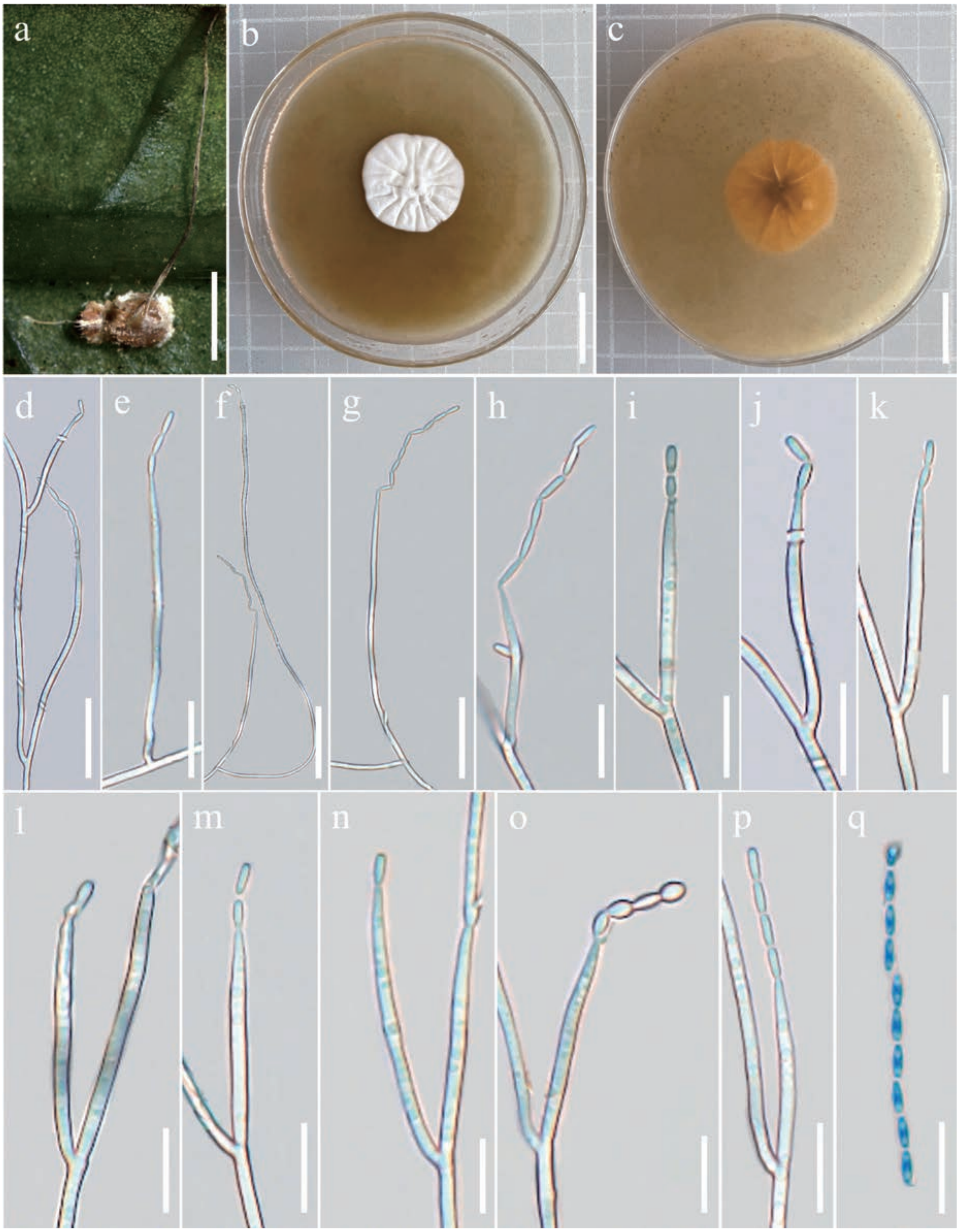

Figure 8. Morphology of *Leptobacillium longiphialidum* **a** wild material **b** colonies obverse in PDA at 25 °C **c** colonies reverse on PDA at 25 °C **d–p** phialides bearing conidia **q** conida. Scale bars: 2 mm (**a**); 2 cm (**b, c**); 20 μm (**d**); 12 μm (**e**); 30 μm (**f**); 20 μm (**g**); 10 μm (**h–k**); 9 μm (**l**); 10 μm (**m**); 7 μm (**n**); 8 μm (**o**); 10 μm (**p, q**).

Host. Spider.

Distribution. China, Hainan Province, Guangdong Province.

Additional material examined. China • Guangdong Province, Huizhou City, Boluo County, 511 Township Road. Specimens were collected from an evergreen

Table 3. Morphological comparisons of asexual morphs in the genus *Leptobacillium*.

Species	Colony on PDA	Phialides (μm)	Conidia (μm)	References
L. cavernicola	White, reverse usually dark brown	Mainly solitary, slender, tapering toward tip, 5.1–27.2 × 1.2–1.7 μm	Forming long, slender chains, narrowly cylindrical to slightly fusiform, some were slightly lemon-shaped, first-formed conidium were usually shorter, obovoid to pyriform with a rounded distal end, 3.1–6.9 × 0.9–1.5 μm	Leplat et al. (2022)
L. chinense	White, reverse cream to light yellow	Solitary, (6.0–) 15–30 (–68.0) × 1.5 μm	Ellipsoidal or oval or cylindrical, 3.5–5.0 × 1.0–1.5 μm, the conidia aggregate into chains, with the apex conidia subspherical or obovoid, 1.5–2.5 × 1.5–2.0 μm	Liu and Cai (2012)
L. coffeanum	White, reverse cream	Solitary, few 2–3 whorls, 11.0–44.0 (–70.0) × 1.0–2.4 μm	Two conidia, macroconidia spindle-shaped, 5.3–8.8 × 1.0–1.6 μm; microconidia oval to fusiform, 2.2–3.8 × 0.8–1.5 μm	Gomes et al. (2018)
L. filiforme	White, reverse light yellow	Solitary, 9.0–18.0 × 1.0 μm	Fusiform to filamentous, chained, sometimes forming zigzag chains, 7.2–12.5 × 1.0 μm	Crous et al. (2018)
L. latisporum	White, reverse greyish orange to orange white	13.2–40.8 × 2.9–4.8 μm	Shuttle shaped to narrow cylindrical, with single cells forming long chains, 3.9–6.3 × 1.9–3.9 μm	Preedanon et al. (2023)
L. longiphialidum	**White, reverse brown to light yellow**	**Solitary, 24.01–205.77 × 1.00–2.24 μm**	**Narrow columnar or spindle shaped, 2.88–4.54 × 1.18–1.95 μm, single celled in chains, with apical conidia elliptical or nearly spherical in shape**	**This study**
L. leptobactrum var. *calidius*	White to cream, reverse Light yellow to brown	Solitary, few 1–2 whorls, 18.4–60.0 × 0.7–2.0 μm	Narrow cylindrical (rod-shaped) to slightly fusiform, 3.0–5.7 × 0.7–1.7 μm	Zare and Gams (2016)
L. leptobactrum var. *leptobactrum*	White to cream, reverse Light yellow to yellowish brown	15.8–31.7 × 0.7–1.5 μm Solitary, few 2–3 whorls, 15.8–31.7 × 0.7–1.5 μm	Narrow rod-shaped or narrow cylindrical (rod-shaped), 3.0–6.1 × 0.8–2.1 μm	Zare and Gams (2016)
L. leptobactrum	White, gray white to pinkish white, reverse orange to orange brown, gray white, light yellow, milky white to dark yellow	Solitary, few 1–2 branches, 20.0–45.0 μm long, Base width 1–2 μm, top width 0.5–0.7 μm	Narrow cylindrical (rod-shaped) to slightly fusiform, 4.5–8.0 × 0.8–1.5 (–2.0) μm	Zare and Gams (2016)
L. muralicola	White, gray white to green white, reverse light yellow, milky white to dark yellow, orange to orange brown, ochraceous	Solitary, few 1–2 branches, 20.0–45.0 μm long, Base width 1.0–2.0 μm, top width 0.5–0.7 μm	Narrow cylindrical (rod-shaped) to slightly fusiform, 4.5–6.0 × 1.0–2.0 μm	Sun et al. (2019)
L. symbioticum	White, reverse orange yellow to orange-brown	Solitary, few 2–3 whorls, 7.1–30.6 × 1.6–3.5 μm	Slightly fusiform to narrowly cylindrical, 4.0–6.9 × 0.7–1.6 μm	Okane et al. (2020)

broad-leaved forest, alt. 29.4 m, 114°24'5"E, 23°14'32"N, 23 July 2024, Hong Yu and Y.L. Lu (paratype: YHH LL2407001, ex-paratype living culture: YFCC 24079491.

Remarks. The key characteristic of *L. longiphialidum* was its independent, columnar shape and the presence of narrow or fusiform spores. Phylogenetic analyses showed that *L. longiphialidum* belonged to the *Leptobacillium* clade and was closest to *L. marksiae*. However, the host and collection sites of *L. longiphialidum* were spiders and China, respectively and the host and collection sites of *L. marksiae* were an unidentified dead insect and Queensland, Australia, respectively. *L. longiphialidum* and *L. marksiae* were distinguished by genetic distance. (Table 3).

Discussion

The genera of *Simplicillium* and *Leptobacillium* were found to be the most closely related within the family of Cordycipitaceae. They exhibited a wide distribution and were commonly observed on various substrates or hosts, including air, seawater, rocks, leaves, soil, insects, fungi, freshwater environments, murals, rocks and caves (Liu and Cai 2012; Zare and Gams 2016; Crous et al. 2018; Gomes et al. 2018; Sun et al. 2019; Wei et al. 2019; Kondo et al. 2020; Okane et al. 2020; Wang et al. 2020;

Leplat et al. 2021). Chen et al. (2019) first reported insect-associated species of *Simplicillium* while later reporting an additional eight arthropod-related species of the genus *Simplicillium* (Chen et al. 2021, 2022). Furthermore, Leplat et. al (2022) isolated *L. cavernicola* Leplat from caves as a representative species of the genus *Leptobacillium* whereas *L. muralicola* Z. Sun, Qin Y. Ge, Zhi B. Zhu & Xing Z. Liu was isolated from mural paintings in a Koguryo tomb in China (Sun et al. 2019).

The macroscopic and microscopic morphology of most species in the genera of *Simplicillium* and *Leptobacillium* are quite similar and it is difficult to distinguish specific species, based on only morphological features. Thus, it is often necessary to combine morphological and molecular data for species identification. The utilisation of ITS and nrLSU by Liu and Cai (2012) yielded more accurate outcomes in the identification of *Simplicillium* species. To date, multi-site phylogenies incorporating the combined analysis of ribosomal DNA and functional protein-coding genes have been extensively employed in fungal phylogeny research, yielding numerous significant findings (Sung et al. 2007; Luangsa-ard et al. 2017; Mongkolsamrit et al. 2020; Wang et al. 2020). The results showed that the molecular phylogenies of *Simplicillium* and *Lecanicillium*, based on ITS fragment, nrLSU fragment and six-gene combined dataset, were more stable in topology. This was consistent with the results of previous studies. In this study, two novel species, *S. puwenense* and *L. longiphialidum*, were identified and characterised through meticulous morphological examination and rigorous phylogenetic analysis.

Through morphological observation, it was found that phialides of species in the genus of *Simplicillium* were solitary and could be distinguished from those of the genus of *Lecanicillium* (Chen et al. 2021). It was observed that a prominent characteristic of species within the *Simplicillium* genus was the solitary nature of phialides, wherein conidia typically adhered to the apex of phialides in chains exhibiting spherical, sticky, or tile-like properties, ultimately resulting in the formation of octahedral crystals (Zare and Gams 2001). The primary distinguishing feature of *Leptobacillium* species lay in the presence of two conidia; single cells arranged in clusters with near-spherical or elliptical conidia at the apex and other narrow columnar (rod) to fusiform-shaped conidia (Zare and Gams 2016; Leplat et al. 2022). The phialides of *S. puwenense* collected in this study were slender, solitary, rod-shaped or columnar; the conidia were transparent, single-celled with smooth walls and had an oval or cylindrical shape. They formed aggregates into a spherical structure at the apex of the phialides. These characteristics aligned closely with the primary identification features described for *Simplicillium* species by Zare and Gams (2001). The phialides of *L. longiphialidum* appeared as solitary and columnar structures. Two types of conidia were observed, i.e. one type consisted of single cells clustered together in chains, while the other type was oval or nearly spherical and located at the apex. Additionally, there was another type of narrow columnar or spindle-shaped conidium present, which was consistent with previous studies on *Leptobacillium* species (Zare and Gams 2016; Leplat et al. 2022).

In phylogenetic trees, most species of the genera *Simplicillium* and *Leptobacillium* were clustered in their separate clades and were well supported and topologically stable. However, the phylogenetic framework showed that two samples of *L. leptobactrum*, ZJ14B02 and AH17C05, did not form a monophyletic clade. The ITS sequence and nrLSU sequence of strain ZJ14B02 contained 547 bp and 909 bp, respectively. The ITS and nrLSU sequences of strain AH17C05 contained 557 bp and 929 bp, respectively. It was found that the head and tail bases of ITS sequence of samples ZJ14B02 and AH17C05 were different from those of nrLSU sequences. It was speculated that the two samples of *L. leptobactrum* did not form a monophyletic clade, which might be caused by the poor processing of the fore-tail primer sequence. Zare and Gams (2016) initially described *L. leptobactrum*, composed of *L. leptobactrum* var. *leptobactrum* and *L. leptobactrum* var. *calidius*, which were distinguished by their optimal growth temperature. The optimum temperature for growth of *L. leptobactrum* var. *leptobactrum* was 18–21 °C, no growth at 30 °C (Zare and Gams 2016). The optimum temperature for growth of *L. leptobactrum* var. *calidius* was 24–27 °C, reduced growth at 30 °C, no growth at 33 °C (Zare and Gams 2016). Phylogenetic studies had placed two strains in unexpected clades, namely *L. leptobactrum* var. *leptobactrum* and *L. leptobactrum* var. *calidius*. In the phylogenetic framework constructed by nrSSU, *L. leptobactrum* var. *leptobactrum* and *L. leptobactrum* var. *calidius* clustered into a clade. The findings of phylogenetic frameworks, based on ITS, nrLSU and six-gene datasets, revealed that *L. leptobactrum* var. *calidius* and *L. chinense* formed a cluster, while *L. leptobactrum* var. *leptobactrum* and *L. cavernicola* also clustered together. This was consistent with the findings of Leplat et al. (2022).

S. pechmerlense J. Leplat constituted an independent clade that exhibited slight differences compared to the previously studied phylogenetic framework (Leplat et al. 2021). However, it was the same as the phylogenetic framework reconstructed by Chen et al. (2022). Additionally, Leplat et al. (2021) found that the underside of the colony of *S. pechmerlense* was light yellow to orange, the phialides was solitary and there were two kinds of conidium, the macroconidia was spindle, 5.0–8.0 × 1.0–1.6 μm. The microconidia were subspherical or elliptic, 1.8–3.0 × 0.9–1.5 μm, forming slimy globular heads at the top of the phialides. *S. pechmerlense* phialides solitary and conidia attached to the top of the phialides with slimy heads fit the main identification characteristics of *Simplicillium* (Zare and Gams 2001). *S. pechmerlense* was morphologically similar to *S. calcicola* Z.F. Zhang, F. Liu & L. Cai and *S. album* Z.F. Zhang & L. Cai (Leplat et al. 2021). The phialides of *S. calcicola* and *S. album* were 2–3-whorled or solitary (Zhang et al. 2017, 2021), while *S. pechmerlense* were solitary. The solitary phialides could distinguish *S. pechmerlense* from *S. calcicola* and *S. album*. Species of *Simplicillium* have frequently been identified using ITS and nrLSU sequences (Liu and Cai 2012). Phylogenetic analyses, based on single gene fragments revealed an unstable systematic position for *S. pechmerlense*. However, the morphological characteristics of *S. pechmerlense* align with the primary identification features of *Simplicillium*. Consequently, it was determined that *S. pechmerlense* should be retained within the genus *Simplicillium*. The inclusion of supplementary materials, such as morphological data, would be essential for further verification since only one strain of polygenic sequence data was available for *L. leptobactrum* var. *leptobactrum* and *L. leptobactrum* var. *calidius*.

Acknowledgements

Many thanks to Peng Ronghua of Guangdong Small Worm Biotechnology Co., Ltd. for his help in this study. At the same time, we also thank the two reviewers and editors for their critiques and suggestions which greatly improved our manuscript.

Additional information

Conflict of interest

The authors have declared that no competing interests exist.

Ethical statement

No ethical statement was reported.

Funding

This work was supported by the National Natural Science Foundation of China (32200013) and supported by the Research and Innovation Fund for Graduate Students of Yunnan University (KC-23235594).

Author contributions

Yingling Lu: Responsible for investigation, article conception, writing and editing, and species identification; Songyu Li: Responsible for investigation, article conception, writing and editing, morphological analysis and phylogenetic analysis; Zuoheng Liu: Collecting the information of specimens and GenBank entry number required for research; Jing Zhao: Responsible for picture editing and processing; Zhiyong Yu, Zongli Liang, Hailong He, Jianhong Li, Yun Huang, Xinming Li: Responsible for investigation; Hong Yu: Responsible for investigation, conceptualisation, writing – review and editing and supervision.

Author ORCIDs

Yingling Lu https://orcid.org/0009-0008-8119-1975
Songyu Li https://orcid.org/0009-0007-9589-0892
Zuoheng Liu https://orcid.org/0000-0003-4118-3694
Jing Zhao https://orcid.org/0000-0001-7871-2209
Zhiyong Yu https://orcid.org/0000-0001-8276-5901
Zongli Liang https://orcid.org/0009-0006-5553-8811
Hailong He https://orcid.org/0009-0000-7862-0865
Jianhong Li https://orcid.org/0009-0001-1234-7816
Yun Huang https://orcid.org/0009-0007-3429-1490
Xinming Li https://orcid.org/0009-0001-7198-281X
Hong Yu https://orcid.org/0000-0002-2149-5714

Data availability

All of the data that support the findings of this study are available in the main text.

References

Bischoff JF, Rehner SA, Humber RA (2006) *Metarhizium frigidum* sp. nov.: A cryptic species of *M. anisopliae* and a member of the *M. flavoviride* Complex. Mycologia 98(5): 737–745. https://doi.org/10.1080/15572536.2006.11832645

Chen WH, Liu C, Han YF, Liang JD, Tian WY, Liang ZQ (2019) Three novel insect-associated species of *Simplicillium* (Cordycipitaceae, Hypocreales) from Southwest China. MycoKeys 58: 83–102. https://doi.org/10.3897/mycokeys.58.37176

Chen WH, Han YF, Liang JD, Liang ZQ (2021) Taxonomic and phylogenetic characterizations reveal four new species of *Simplicillium* (Cordycipitaceae, Hypocreales) from Guizhou, China. Scientific Reports 11(1): 15300. https://doi.org/10.1038/s41598-021-94893-z

Chen W, Liang J, Ren X, Zhao J, Han Y, Liang Z (2022) Multigene phylogeny, phylogenetic network, and morphological characterizations reveal four new arthropod-associated *Simplicillium* species and their evolutional relationship. Frontiers in Microbiology 13: 950773. https://doi.org/10.3389/fmicb.2022.950773

Crous P, Luangsa-Ard J, Wingfield M, Carnegie A, Hernández-Restrepo M, Lombard L, Roux J, Barreto R, Baseia I, Cano Lira J, Martín MP, Morozova OV, Stchigel AM, Summerell BA, Brandrud TE, Dima B, García D, Giraldo A, Guarro J, Gusmão LFP, Khamsuntorn P, Noordeloos ME, Nuankaew S, Pinruan U, Rodríguez-Andrade E, Souza-Motta CM, Thangavel R, van Iperen AL, Abreu VP, Accioly T, Alves JL, Andrade JP, Bahram M, Baral H-O, Barbier E, Barnes CW, Bendiksen E, Bernard E, Bezerra JDP, Bezerra JL, Bizio E, Blair JE, Bulyonkova TM, Cabral TS, Caiafa MV, Cantillo T, Colmán AA, Conceição LB, Cruz S, Cunha AOB, Darveaux BA, da Silva AL, da Silva GA, da Silva GM, da Silva RMF, de Oliveira RJV, Oliveira RL, De Souza JT, Dueñas M, Evans HC, Epifani F, Felipe MTC, Fernández-López J, Ferreira BW, Figueiredo CN, Filippova NV, Flores JA, Gené J, Ghorbani G, Gibertoni TB, Glushakova AM, Healy R, Huhndorf SM, Iturrieta-González I, Javan-Nikkhah M, Juciano RF, Jurjević Ž, Kachalkin AV, Keochanpheng K, Krisai-Greilhuber I, Li Y-C, Lima AA, Machado AR, Madrid H, Magalhães OMC, Marbach PAS, Melanda GCS, Miller AN, Mongkolsamrit S, Nascimento RP, Oliveira TGL, Ordoñez ME, Orzes R, Palma MA, Pearce CJ, Pereira OL, Perrone G, Peterson SW, Pham THG, Piontelli E, Pordel A, Quijada L, Raja HA, Rosas de Paz E, Ryvarden L, Saitta A, Salcedo SS, Sandoval-Denis M, Santos TAB, Seifert KA, Silva BDB, Smith ME, Soares AM, Sommai S, Sousa JO, Suetrong S, Susca A, Tedersoo L, Telleria MT, Thanakitpipattana D, Valenzuela-Lopez N, Visagie CM, Zapata M, Groenewald JZ (2018) Fungal Planet description sheets: 785–867. Persoonia 41(1): 238–417. https://doi.org/10.3767/persoonia.2018.41.12

Crous PW, Cowan DA, Maggs-Kölling G, Yilmaz N, Thangavel R, Wingfield MJ, Noordeloos ME, Dima B, Brandrud TE, Jansen GM, Morozova OV, Vila J, Shivas RG, Tan YP, Bishop-Hurley S, Lacey E, Marney TS, Larsson E, Le Floch G, Lombard L, Nodet P, Hubka V, Alvarado P, Berraf-Tebbal A, Reyes JD, Delgado G, Eichmeier A, Jordal JB, Kachalkin AV, Kubátová A, Maciá-Vicente JG, Malysheva EF, Papp V, Rajeshkumar KC, Sharma A, Spetik M, Szabóová D, Tomashevskaya MA, Abad JA, Abad ZG, Alexandrova AV, Anand G, Arenas F, Ashtekar N, Balashov S, Bañares Á, Baroncelli R, Bera I, Biketova AY, Blomquist CL, Boekhout T, Boertmann D, Bulyonkova TM, Burgess TI, Carnegie AJ, Cobo-Diaz JF, Corriol G, Cunnington JH, da Cruz MO, Damm U, Davoodian N, de A Santiago ALCM, Dearnaley J, de Freitas LWS, Dhileepan K, Dimitrov R, Di Piazza S, Fatima S, Fuljer F, Galera H, Ghosh A, Giraldo A, Glushakova AM, Gorczak M, Gouliamova DE, Gramaje D, Groenewald M, Gunsch CK, Gutiérrez A, Holdom D, Houbraken J, Ismailov AB, Istel Ł, Iturriaga T, Jeppson M, Jurjević Ž, Kalinina LB, Kapitonov VI, Kautmanová I, Khalid AN, Kiran M, Kiss L, Kovács Á, Kurose D, Kušan I, Lad S, Læssøe T, Lee HB, Luangsa-Ard JJ, Lynch M, Mahamedi AE, Malysheva VF, Mateos A, Matočec N, Mešić A, Miller AN, Mongkolsamrit S, Moreno G, Morte A, Mostowfizadeh-Ghalamfarsa R, Naseer A, Navarro-Ródenas A, Nguyen TTT, Noisripoom W, Ntandu JE, Nuytinck J, Ostrý V, Pankratov TA, Pawłowska J, Pecenka J, Pham THG, Polhorský A, Pošta A, Raudabaugh DB, Reschke K, Rodríguez A, Romero M, Rooney-Latham S, Roux J, Sandoval-Denis M, Smith MT, Steinrucken TV, Svetasheva TY, Tkalčec Z, van der Linde EJ, V D Vegte M, Vauras J, Verbeken A, Visagie CM, Vitelli JS, Volobuev SV, Weill A, Wrzosek M, Zmitrovich IV, Zvyagina EA, Groenewald JZ (2021) Fungal Planet description sheets: 1182–1283. Persoonia 46: 313–528. https://doi.org/10.3767/persoonia.2021.46.11

Gomes AA, Pinho DB, Cardeal Z, Menezes HC, De Queiroz MV, Pereira OL (2018) *Simplicillium coffeanum*, a new endophytic species from Brazilian coffee plants, emitting antimicrobial volatiles. Phytotaxa 333(2): 188–198. https://doi.org/10.11646/phytotaxa.333.2.2

Kepler RM, Luangsa-Ard JJ, Hywel-Jones NL, Quandt CA, Sung GH, Rehner SA, Aime MC, Henkel TW, Sanjuan T, Zare R, Chen M, Li Z, Rossman AY, Spatafora JW, Shrestha B (2017) A phylogenetically-based nomenclature for Cordycipitaceae (Hypocreales). IMA Fungus 8(2): 335–353. https://doi.org/10.5598/imafungus.2017.08.02.08

Kondo N, Iwasaki H, Tokiwa T, Mura S, Nonaka K (2020) *Simplicillium spumae* (Cordycipitaceae, Hypocreales), a new hyphomycetes from aquarium foam in japan. Mycoscience 61(3): 116–121. https://doi.org/10.1016/j.myc.2020.02.002

Leplat J, Francois A, Bousta F (2021) *Simplicillium pechmerlensis*, a new fungal species isolated from the air of the Pech-Merle show cave. Phytotaxa 521(2): 80–94. https://doi.org/10.11646/phytotaxa.521.2.2

Leplat J, Francois A, Bousta F (2022) *Leptobacillium cavernicola*, a newly discovered fungal species isolated from several Paleolithic-decorated caves in France. Phytotaxa 571(2): 186–196. https://doi.org/10.11646/phytotaxa.571.2.5

Liu F, Cai L (2012) Morphological and molecular characterization of a novel species of *Simplicillium* from China. Cryptogamie Mycologie 33(2): 137–144. https://doi.org/10.7872/crym.v33.iss2.2012.137

Liu ZY, Liang ZQ, Whalley AJS, Yao YJ, Liu AY (2001) *Cordyceps brittlebankisoides*, a new pathogen of grubs and its anamorph, *Metarhizium anisopliae* var. *majus*. Journal of Invertebrate Pathology 78(3): 178–182. https://doi.org/10.1006/jipa.2001.5039

Luangsa-ard JJ, Mongkolsamrit S, Thanakitpipattana D, Khonsanit A, Tasanathai K, Noisripoom W, Humber RA (2017) Clavicipitaceous entomopathogens: new species in *Metarhizium* and a new genus *Nigelia*. Mycological Progress 16(4): 369–391. https://doi.org/10.1007/s11557-017-1277-1

Mongkolsamrit S, Noisripoom W, Thanakitpipattana D, Wutikhun T, Spatafora JW, Luangsa-Ard J (2018) Disentangling cryptic species with *Isaria*-like morphs in Cordycipitaceae. Mycologia 110(1): 230–257. https://doi.org/10.1080/00275514.2018.1446651

Mongkolsamrit S, Khonsanit A, Thanakitpipattana D, Tasanathai K, Noisripoom W, Lamlertthon S, Himaman W, Houbraken J, Samson RA, Luangsa-ard J (2020) Revisiting *Metarhizium* and the description of new species from Thailand. Studies in Mycology 95(1): 171–251. https://doi.org/10.1016/j.simyco.2020.04.001

Nonaka K, Kaifuchi S, Ōmura S, Masuma R (2013) Five new *Simplicillium* species (Cordycipitaceae) from soils in Tokyo, Japan. Mycoscience 54(1): 42–53. https://doi.org/10.1016/j.myc.2012.07.002

Okane I, Nonaka K, Kurihara Y, Abe JP, Yamaoka Y (2020) A new species of *Leptobacillium*, *L. symbioticum*, isolated from mites and sori of soybean rust. Mycoscience 61(4): 165–171. https://doi.org/10.1016/j.myc.2020.04.006

Preedanon S, Suetrong S, Srihom C, Somrithipol S, Kobmoo N, Saengkaewsuk S, Srikitikulchai P, Klaysuban A, Nuankaew S, Chuaseeharonnachai C, Chainuwong B, Muangsong C, Zhang ZF, Cai L, Boonyuen N (2023) Eight novel cave fungi in Thailand's Satun Geopark. Fungal Systematics and Evolution 12(1): 1–30. https://doi.org/10.3114/fuse.2023.12.01

Regaieg H, Ciancio A, Raouani NH, Rosso L (2011) Detection and biocontrol potential of *Verticillium leptobactrum* parasitizing *Meloidogyne* spp. World Journal of Microbiology and Biotechnology 27(7): 1615–1623. https://doi.org/10.1007/s11274-010-0615-0

Rehner SA, Samuels GJ (1994) Taxonomy and phylogeny of Glio cladium analysed from nuclear large subunit ribosomal DNA sequences. Mycological Research 98(6): 625–634. https://doi.org/10.1016/S0953-7562(09)80409-7

Rehner SA, Minnis AM, Sung GH, Luangsa-ard JJ, Devotto L, Humber RA (2011) Phylogeny and systematics of the anamorphic, entomopathogenic genus *Beauveria*. Mycologia 103(5): 1055–1073. https://doi.org/10.3852/10-302

Sun JZ, Ge QY, Zhu ZB, Zhang XL, Liu XZ (2019) Three dominating hypocrealean fungi of the 'white mold spots' on acrylic varnish coatings of the murals in a Koguryo tomb in China. Phytotaxa 397(3): 225–236. https://doi.org/10.11646/phytotaxa.397.3.2

Sung GH, Hywel-Jones NL, Sung JM (2007) Phylogenetic classification of Cordyceps and the clavicipitaceous fungi. Studies in Mycology 57: 5–59. https://doi.org/10.3114/sim.2007.57.01

Vilgalys R, Hester M (1990) Rapid genetic identification and mapping of enzymatically amplified ribosomal DNA from several *Cryptococcus* species. Journal of Bacteriology 172(8): 4238–4246. https://doi.org/10.1128/jb.172.8.4238-4246.1990

Wang YB, Yu H, Dai YD, Chen ZH, Zeng WB, Yuan F, Liang ZQ (2015a) *Polycephalomyces yunnanensis* (Hypocreales), a new species of *Polycephalomyces* parasitizing *Ophiocordyceps* nutans and stink bugs (hemipteran adults). Phytotaxa 208: 034–044.

Wang YB, Yu H, Dai YD, Wu CK, Zeng WB, Yuan F, Liang ZQ (2015b) Polycephalomyces agaricus, a new hyperparasite of *Ophiocordyceps* sp. infecting melolonthid larvae in southwestern China. Mycological Progress 14(9): 70. https://doi.org/10.1007/s11557-015-1090-7

Wang YB, Wang Y, Fan Q, Duan DE, Zhang GD, Dai RQ, Dai YD, Zeng WB, Chen ZH, Li DD, Tang DX, Xu ZH, Sun T, Nguyen T, Tran N, Dao V, Zhang CM, Huang LD, Liu YJ, Zhang XM, Yang DR, Sanjuan T, Liu XZ, Yang ZL, Yu H (2020) Multigene phylogeny of the family Cordycipitaceae (Hypocreales): New taxa and the new systematic position of the Chinese cordycipitoid fungus *Paecilomyces hepiali*. Fungal Diversity 103: 1–46. https://doi.org/10.1007/s13225-020-00457-3

Wei DP, Wanasinghe DN, Hyde KD, Mortimer PE, Xu J, Xiao YP, Bhunjun CS, To-Anun C (2019) The genus *Simplicillium*. MycoKeys 60: 69–92. https://doi.org/10.3897/mycokeys.60.38040

White TJ, Bruns TD, Lee SB, Taylor JW (1990) Amplification and direct sequencing of fungal ribosomal RNA genes for phylogenet ics. In: Innis MA, Gelfand DH, Sninsky JJ, White TJ (Eds) PCR protocols: a guide to methods and applications. Academic, New York, 315–322. https://doi.org/10.0000/PMID1793

Yan QH, Ni QR, Gu WJ, Liu HW, Yuan XY, Sun JZ (2023) *Simplicillium sinense* sp. nov., a novel potential pathogen of tinea faciei. Frontiers in Microbiology 14: 1156027. https://doi.org/10.3389/fmicb.2023.1156027

Zare R, Gams W (2001) A revision of *Verticillium* section *Prostrata*. IV. The genera *Lecanicillium* and *Simplicillium* gen. nov. Nova Hedwigia 73(1–2): 1–50. https://doi.org/10.1127/nova.hedwigia/73/2001/1

Zare R, Gams W (2008) A revision of the *Verticillium fungicola* species complex and its affinity with the genus *Lecanicillium*. Mycological Research 112(7): 811–824. https://doi.org/10.1016/j.mycres.2008.01.019

Zare R, Gams W (2016) More white verticillium-like anamorphs with erect conidiophores. Mycological Progress 15(10–11): 993–1030. https://doi.org/10.1007/s11557-016-1214-8

Zhang ZF, Liu F, Zhou X, Liu XZ, Liu SJ, Cai L (2017) Culturable mycobiota from Karst caves in China, with descriptions of 20 new species. Persoonia 39(1): 1–31. https://doi.org/10.3767/persoonia.2017.39.01

Zhang ZF, Zhou SY, Eurwilaichitr L, Ingsriswang S, Raza M, Chen Q, Zhao P, Liu F, Cai L (2021) Culturable mycobiota from Karst caves in China II, with descriptions of 33 new species. Fungal Diversity 106(1): 29–136. https://doi.org/10.1007/s13225-020-00453-7

MycoKeys 115: 209–220 (2025)
DOI: 10.3897/mycokeys.115.144718

Research Article

Phylogeny of the European *Collema* species (Peltigerales, Lecanoromycetes)

Alica Košuthová[1], Fredrik Jonsson[2], Ulrika Nordin[2], Mats Wedin[1]

1 *Department of Botany, Swedish Museum of Natural History, P.O. Box 50007, SE-104 05 Stockholm, Sweden*
2 *Alsens-Ede 227, SE-835 96 Trångsviken, Sweden*
Corresponding author: Alica Košuthová (kosuthova.alica@gmail.com)

Abstract

The phylogenetic relationships and morphological diversity within European *Collema* s. str. species were investigated. A total of 104 new sequences (four molecular markers; mtSSU, b-tub, MCM7, and RPB2 genes) from 28 specimens were generated, and analysed and used for multi-locus phylogenetic analyses. Our results suggest that *Collema* is only monophyletic if *Collema glebulentum* is considered part of *Leptogium s. str*. where it originally was described. This is supported by its paraplectenchymatous thallus. Degelius´ informal *Collema* “*Flaccidum*”- and “*Nigrescens*”-groups are not natural, as the “*Flaccidum*”-group is nested within the “*Nigrescens*”-group. Based on our findings, seven currently accepted *Collema* occur in Europe: *C. flaccidum*, *C. subflaccidum*, *C. curtisporum*, *C. furfuraceum*, *C. nigrescens*, *C. ryssoleum*, and *C. subnigrescens*. *Collema furfuraceum* is further non-monophyletic, suggesting a need for taxonomic revision.

Key words: Ascomycota, Collemataceae, cyanolichens, integrative taxonomy, systematics

Academic editor: Thorsten Lumbsch
Received: 17 December 2024
Accepted: 19 January 2025
Published: 18 March 2025

Citation: Košuthová A, Jonsson F, Nordin U, Wedin M (2025) Phylogeny of the European *Collema* species (Peltigerales, Lecanoromycetes). MycoKeys 115: 209–220. https://doi.org/10.3897/mycokeys.115.144718

Introduction

The generic delimitation of Collemataceae s. str. was for a long time unnatural, relying primarily on a single trait: the presence of a cellular cortex in *Leptogium* or its absence in *Collema* (Degelius 1954, 1974; Jørgensen 2007). Degelius (1954) had, however, already questioned whether *Collema* and *Leptogium* represented natural, monophyletic groupings. Subsequent molecular studies (Wiklund and Wedin 2003; Miadlikowska and Lutzoni 2004; Miadlikowska et al. 2014) supported this, revealing that the gelatinous genera with simple spores, traditionally assigned to Collemataceae, actually belonged to other families (Wedin et al. 2009; Otálora et al. 2010; Ekman et al. 2014; Weerakoon et al. 2018). It was not until the comprehensive analysis by Otálora et al. (2013a, 2013b) that a revised generic classification of Collemataceae s. str. was proposed. Their work confirmed the non-monophyletic nature of *Collema* and *Leptogium*, proposing the recognition of ten distinct monophyletic groups as separate genera. This revision retained the names *Collema* and *Leptogium* in restricted senses and reintroduced six older generic names (*Blennothallia*, *Enchylium*, *Lathagrium*, *Pseudoleptogium*, *Rostania*, and *Scytinium*), while also establishing two new genera, *Callome* and *Paracollema*.

The European species of *Collema* in the sense of Otálora et al. (2013b), the focus of the present study, correspond to Degelius' "*Flaccidum*" and "*Nigrescens*"-groups (Degelius 1954). These groups are relatively small, with three species currently recognized in the "*Flaccidum*"-group and five in the "*Nigrescens*"-group. The two groups are closely related, sharing several characteristics, including their occurrence in sheltered, humid environments, and the two groups contain both corticolous and saxicolous species. Species within these groups are large in size, typically measuring about 2.0–8.0 cm in diameter, though some individuals may reach up to 15 cm. Their thalli are thin to moderately thin (50–150 μm), lacking both a paraplectenchymatous medulla, and a true cortex. The lobes are generally broad and rounded, measuring approximately 5.0–12.0 mm in diameter. The spores of both groups are ranging from 25–35 × 6–7 μm to 40–90 × 3–6 μm, and are narrowly ellipsoid to fusiform with transverse septation. Spores in the "*Nigrescens*"-group show greater polymorphism than those in the "*Flaccidum*"-group. A distinguishing feature between the two groups is that species in the "*Flaccidum*"-group lack pustules and ridges, whereas those are present in species of the "*Nigrescens*"-group. Both groups are distributed across Europe, with their distribution range and selected morphological features summarized in Table 1. Degelius (1954, 1974) accepted three European species in the "*Flaccidum*"-group: *Collema flaccidum* (Ach.) Ach., *C. glebulentum* (Cromb.) Degel., and *C. subflaccidum* Degel. previously known as *C. subfurvum* (Müll. Arg.) Degel. The five European species in the "*Nigrescens*"-groups include *C. curtisporum* Degel., *C. furfuraceum* (Arn.) DR. em. Degel., *C. nigrescens* (Huds.) DC., *C. ryssoleum* (Tuck.) Schneid., and *C. subnigrescens* Degel.

Otálora et al. (2013a, 2013b) included only four species (*C. curtisporum*, *C. flaccidum*, *C. furfuraceum* and *C. nigrescens*) of the European *Collema* s. str. in their phylogenies, with Miadlikowska et al. (2014) also including *C. subnigrescens*. As a result, the taxonomic positions of five out of eight species within this group have been tested using molecular methods, while the remaining three species have not yet been examined. As there is a substantial variation in shape and size of the thallus, lobes, apothecia, ascospores, and isidia among them, and as several former *Collema* species have been shown to belong elsewhere, the delimitation of the genus needs investigation. Here, we will test the current delimitation of *Collema* in Europe and propose a phylogenetic hypothesis of known species. Finally, we will note and comment on any indication of species non-monophyly in this genus.

Material and methods

Specimen selection and morphological observations

We sampled 28 specimens, representing species of the European "*Flaccidum*" *and* "*Nigrescens*"-groups from Scandinavia and including some extra-Scandinavian material for comparison. The collections resulting from our own recent fieldwork are deposited in the herbarium S, with additional material studied from GZU, hb. Malíček, TBS, UPS and S. Collections and the sequences used are summarized in Table 2. Herbarium acronyms follow Thiers (2018).

Table 1. Characteristic morphological features of European *Collema* species summarised according to Degelius (1954, 1974). Characters unique for the species in the "*Flaccidum*" and "*Nigrescens*" -groups are in bold.

Group	Species	Morphology													
	(*Collema*)	**Pustules/ ridges**	**Thallus (cm)**	**Thallus thickness (µm)**	**Thallus colour**	**Lobes (cm)**	**Isidia**	**Isidia width (mm)**	**Isidia length (mm)**	**Apothecium (mm)**	**Apothecium disc**	**Spore measurements (µm)**	**Spore shape**	**Spore septas**	**Habitat**	**Distribution**
Flaccidum	*flaccidum*	N	to 6	70–170	olive-green-blackish	0.5–1.5(3)	**squamiform** (juv. globular)	0.2–0.5	min. 0.2–0.5	rare, to 1.5	pale red to dark red, sometimes pruinose	(20)26–34(45) × 6–6.5(8.5)	fusiform with acute ends	4 to 6	saxi- and corti-colous	wide, suboceanic
	glebulentum	N	(1)3–6	(50)65–135(200)	light to dark olive-green-blackish	to 1	teretiform, coralloid, **capitate**	0.1	1.5	N	N	N	N	N	**saxicolous**	**arctic-alpine**
	subflaccidum	N	to 6	80–130	olive-green-blackish	0.5–1.5(3)	**globular,** old teretiform & coralloid	0.05–0.1	min. 0.3	rare, to 1.5	pale red to dark red, epruinose	42–60(65) × (3)4.5–6.5(10.5)	broadly to narrowly fusiform, acicular	(4)6–8	corti- and saxi-colous	**oceanic**
Nigrescens	*curtisporum*	Y	to 3(4)	65–106	dark olive-green-blackish	0.5–1	N	N	N	0.5–1.5	pale-red-dark red-brown-blackish, epruinose	**(18)26–34(40) × 3–4.5**	bacillar, straight or **curved, obtuse ends**	4(5–6)	corticolous	**boreal**
	furfuraceum	Y	3–6(10)	(50)60–105	dark olive-green-blackish	0.5–1	**teretiform, coralloid, branched** (juv. globular)	**0.05–0.15**(0.2)	**0.3**	very rare, 0.5–1.5	pale-red-dark red-brown-blackish, epruinose	40–80 × 3–6(8.5)	bacillar-narrowly fusiform with acute end, one end thicker and usually curved	5 to 6	corticolous	wide, suboceanic
	nigrescens	Y	to 10	**(60)90–150**	dark olive-green, brownish-blackish	0.5–1	**globular**	**0.2**	**0.2**	often, 0.6–1	pale-red-dark red-brown-blackish, epruinose	**50–90(112) × 3–4.5**	**acicular to bacillar**	**(5)6–13**	corticolous	wide, suboceanic
	ryssoleum	Y	to 22	50–85	dark olive-green-blackish	0.5–1.5	N	N	N	0.6–1(1.5)	dark red-blackish, epruinose	**(22)26–40(47) × (4.5)5–8.5(10.5)**	ellipsoid or fusiform, **broader in middle,** with acute ends	4 to 6	**saxicolous**	**temperate - mediterranean zone**
	subnigrescens	Y	5–10(20)	60–100	dark olive-green-blackish	0.5–1.5	N	N	N	often, 1–1.5(2)	pale-red-dark red-brown-blackish, epruinose	(34)40–75 × 6–6.5(7)	narrowly fusiform with acute end, one end thicker and usually curved	5 to 6	corticolous	wide, suboceanic

Table 2. Sequences utilized in this study. Newly produced sequences in bold with herbarium vouchers of the specimens given, remaining sequences downloaded from GenBank. For specimens of *Collema glebulentum*, origin of both, state and provinces are given.

Specimen	DNA-voucher	Year	Locality & Herbarium voucher	mtSSU	BT	MCM7	RPB2 5-7	RPB2 7-11
Leptogium byssinum			Norway: *Westberg* (S)	KT240180		KT240183		
Leptogium terrenum			Portugal: *van den Boom 41781* (hb. van den Boom)	KT240181		KT240184		
Collema glebulentum	AL561	2015	Sweden, Pite Lappmark (Arjeplog): *Westberg 15-254* (S-F277955)	**PQ932211**	**PV021123**		**PV021148**	
Collema glebulentum	AL560	1988	Sweden, Åsele Lappmark (Vilhelmina): *Thor 7711* (S-L49768)	**PQ932210**				
Collema glebulentum	AL674	2018	Sweden, Värmland (Säffle-Lurö): *Košuthová et al. 401* (S-F492346)	**PQ932212**	**PV021124**		**PV021149**	
Collema glebulentum	AL366	2017	Sweden, Närke (Örebro): *Berglund* (S-F492347)	**PQ932209**	**PV021122**			
Leptogium azureum			Chile: *Cornejo 26507* (MA)	JX992939	KC119021	JX993002		
Leptogium denticulatum		2010	Argentina: *Wedin 8690* (S-F332474)	JX992947	KC119025	JX993012	**PV021147**	
Collema subconveniens		2010	New Zealand: *Wedin 9225* (S-F335747)	JX992937	KC119019	JX992996	**PV021150**	
Collema leptaleum			Argentina: *Wedin 8822* (S)	JX992928	KC119038	JX992986		
Collema flaccidum	AL540	2016	Sweden: *Westberg et al. 244* (UPS-L872188)	**PQ932216**	**PV021129**	**PV021173**	**PV021154**	
Collema flaccidum	AL496	2017	Sweden: *Odelvik 17-523* (S-F317108)	**PQ932215**	**PV021128**	**PV021172**	**PV021153**	**PV021189**
Collema flaccidum	AL531_AL494	2018	Slovakia: *Košuthová et al. 601* (S-F492348)	**PQ932217**	**PV021130**	**PV021174**	**PV021155**	**PV021190**
Collema subflaccidum	AL649	2016	Russia: *Malíček et al. 10619* (S-F492349 & dupl. herb. Malíček)	**PQ932214**	**PV021132**		**PV021152**	
Collema subflaccidum	AL495	2018	Norway: *Aptroot 76306* (S-F492350)	**PQ932213**	**PV021131**		**PV021151**	**PV021188**
Collema nigrescens	AL511	2018	Spain: *Westberg* (UPS-L934034)	**PQ932220**	**PV021127**		**PV021158**	
Collema nigrescens	AL493	2018	Slovakia: *Košuthová et al. 600* (S-F492351)	**PQ932219**	**PV021126**		**PV021157**	
Collema nigrescens	AL603	2018	Sweden : *Košuthová & Arvidsson 571* (S-F492352)	**PQ932218**	**PV021125**	**PV021175**	**PV021156**	
Collema curtisporum	AL411	2017	Sweden: *Jonsson & U.Nordin FU6546* (S-F492353)	**PQ932221**	**PV021133**		**PV021159**	**PV021191**
Collema curtisporum	AL568	1994	Sweden: *Hermansson 4603* (UPS-L111603)	**PQ932222**		**PV021176**	**PV021160**	
Collema furfuraceum	AL668_AL721	2002	Sweden: *Jonsson 2254* (S-F492354)	**PQ932223**		**PV021177**	**PV021161**	**PV021192**
Collema furfuraceum	AL640_AL720	1998	Sweden: *Bergsten* (S-F492355)	**PQ932224**		**PV021178**	**PV021162**	**PV021193**
Collema ryssoleum	AL518	2001	Italy: *Trietach* (TSB-35166)	**PQ932231**	**PV021135**	**PV021184**	**PV021168**	**PV021196**
Collema ryssoleum	AL534_AL513	1974	Spain: *Tibell 5610* (UPS-L933969)	**PQ932232**	**PV021136**			
Collema ryssoleum	AL566	1994	Madeira: *Nordin 3524* (UPS-L178905)	**PQ932233**	**PV021134**			
Collema subnigrescens	AL407	2017	Sweden: *Jonsson & U.Nordin FU6531* (S-F492356)	**PQ932227**	**PV021140**	**PV021180**	**PV021165**	
Collema subnigrescens	AL500	2006	Greece: *Spribille 19637* (GZU66-201)	**PQ932226**	**PV021141**		**PV021164**	
Collema subnigrescens	AL570	2004	Estonia: *Odelvik 0485* (S-F57732)	**PQ932228**	**PV021142**	**PV021181**	**PV021166**	**PV021195**
Collema subnigrescens	AL344	2017	Sweden: *Berglund* (S-F492357)	**PQ932225**	**PV021139**	**PV021179**	**PV021163**	**PV021194**
Collema furfuraceum	AL644	2018	Scotland: *Malíček 12545* (herb. Malíček)	**PQ932230**	**PV021143**	**PV021183**		
Collema furfuraceum	AL666	2012	Italy: *Jonsson A2* (S-F492358)	**PQ932229**		**PV021182**	**PV021167**	
Collema furfuraceum	AL712	2022	Sweden: *Westberg* (UPS-L1049804)	**PQ932235**	**PV021138**	**PV021186**	**PV021170**	
Collema furfuraceum	AL536	2018	Spain: *Westberg* (UPS-L934040)	**PQ932234**	**PV021137**	**PV021185**	**PV021169**	**PV021197**
Collema furfuraceum	AL665	2012	France: *Jonsson A3* (S-F492359)	**PQ932236**	**PV021144**	**PV021187**	**PV021171**	
Paracollema italicum3			Croatia: *Nordin 2763* (UPS)	JX992926		JX992985		
Paracollema italicum1			Croatia: *Nordin 2708* (UPS)	JX992925	KC119015	JX992984		
Callome multipartita1			Norway: *Haugan 7015* (O)	GQ259019				
Callome multipartita2	AL419	2009	Austria: *Hafellner 74818* (GZU-18–2009)	MK445271	MK451935		**PV021146**	
Enchylium bachmanianum	MWE111	1985	Sweden: *Nordin 1521* (UPS-L133627)	JX992914	MK451936	JX992974	**PV021145**	

Anatomical features were studied using a light microscope on thin sections cut with a razor blade or squash preparations mounted in water. Measurements of mature spores were taken outside of the asci under × 1000 magnification using oil immersion with a precision of 0.5 µm, or from calibrated digital photographs using NIS-Elements (Nikon, Japan) with a precision of 0.1 µm. Spore measurements are presented in the format: (minimum value observed–) range including 80% of the observed values (–maximum value observed), with the mean of all observed values in the center and italicized (Table 1). Full lists of specimens examined in this study with DNA voucher codes and GenBank Accession numbers for newly generated sequences are given in Table 2.

DNA extraction, amplification and sequencing

Two apothecia with surrounding thalline parts, or a thallus fragment in the case of sterile samples, were selected for extraction. We extracted total DNA using the Plant DNA Mini Kit (Qiagen, Hilden, Germany) following the manufacturer's instructions except in order to increase the concentration of DNA, we used half the amount of Elution buffer in the last step. We amplified one mitochondrial ribosomal and three nuclear protein-coding genes. Approximately 0.8 kb of the small subunit of the mitochondrial rDNA (mtSSU) was amplified using the primers mrSSU1 and mrSSU3R (Zoller et al. 1999). Approximately 0.6 kb of Beta-tubulin (b-tub) was amplified and sequenced using the primers Bt3-LM5 and Bt10-LM3 (Myllys et al. 2001) and BetaCollF and BetaCollR (Otálora et al. 2013a). The PCR primers were used in the following combinations: Bt3-LM5 and Bt10-LM3, BetaCollF and BetaCollR, Bt3-LM5 and BetaCollR, BetaCollF and Bt10-LM3 (the best working combination), BetaCollF and BetaColl-intR, and BetaColl-intF2 and Bt10LM3. About 0.6 kb of mini–chromosome maintenance complex component 7 DNA replication licensing factor (MCM7) was amplified and sequenced using the primers Mcm7-709for and Mcm7-1348rev (Schmitt et al. 2009). The locus RNA polymerase II protein coding gene (RPB2, ~2 kb) was amplified as two parts: ~ 1 kb for RPB2 5–7 and ~ 1 kb for RPB2 7–11. Amplification was performed using the primers fRPB2-5F, fRPB2-7cF, fRPB2-7cR and fRPB2-11aR (Liu et al. 1999), which were also used as sequencing primers. PCR amplifications were performed using Illustra™ Hot Start PCR beads, according to manufacturer's instructions. PCR reactions were performed using the same settings as in previous studies (Košuthová et al. 2016, 2019; Otálora et al. 2013a).

Sequence editing, alignment and phylogenetic analyses

The generated sequences were assembled and edited using Geneious version R8 (http://www.geneious.com, Kearse et al. 2012). All edited sequences underwent initial identity verification through BLAST searches (Zhang et al. 2000). The alignment of these sequences was performed using the MUSCLE algorithm (Edgar 2004) in AliView 1.09 (Larsson 2014). An intron in the b-tub was excluded. Indels in the mtSSU were not deleted, allowing smaller gap positions within the final block. The five genetic regions defined above were analysed separately using Maximum Likelihood (ML). As no significant incongruence was detected, the alignments were concatenated. The final alignment has been deposited in TREEBASE (http://www.treebase.org) with accession number (http://purl.org/phylo/treebase/phylows/study/TB:S31975). After concatenation, we inferred phylogenetic relationships using ML with the same settings used as in the individual gene analyses utilizing RAxML. Likelihood and ML bootstrapping were executed through RAxML 8 (Stamatakis 2014) implementing a general time reversible (GTR) model of nucleotide substitution with gamma distributed rate heterogeneity (GTRGAMMA). One thousand bootstrap (BS) replicates were completed using the non-parametric BS algorithm of RAxML–HPC v.8 on XSEDE using the CIPRES Web Portal (Miller et al. 2010).

For the final concatenated dataset, we included 131 nucleotide sequences of mtSSU, b-tub, MCM7, and the two parts of RPB2 (5–7 and 7–11). This dataset encompassed 4140 nucleotide positions (843 bp for mtSSU, 708 bp for b-tub, 597 bp for MCM7, and 1074 bp for RPB2 5–7 and 918 bp for RPB2 7–11) with 39 terminals. It incorporates representatives from selected genera within the Collemataceae, in conjunction with additional data sourced from GenBank (utilized in Otálora et al 2013a, 2013b; Košuthová et al. 2019), with *Enchylium bachmanianum* as the outgroup. None of the sequences of the *"Nigrescens*" and "*Flaccidum*"-groups previously used in phylogenetic analyses and uploaded to GenBank (Otálora et al. 2010, 2013a, 2013b; Miadlikowska et al. 2014), were included in this study due to concerns about specimen misidentification. Sequences used in this study are summarized in Fig. 1, Table 2.

Results and discussion

Dataset and phylogenetic analyses

We generated 104 new sequences (Table 2), comprising 28 mtSSU, 23 b-tub, 16 MCM7, 27 RPB2. Our analyses resulted in a topology (Fig. 1) very similar to the findings of Otálora et al. (2013a, 2013b).

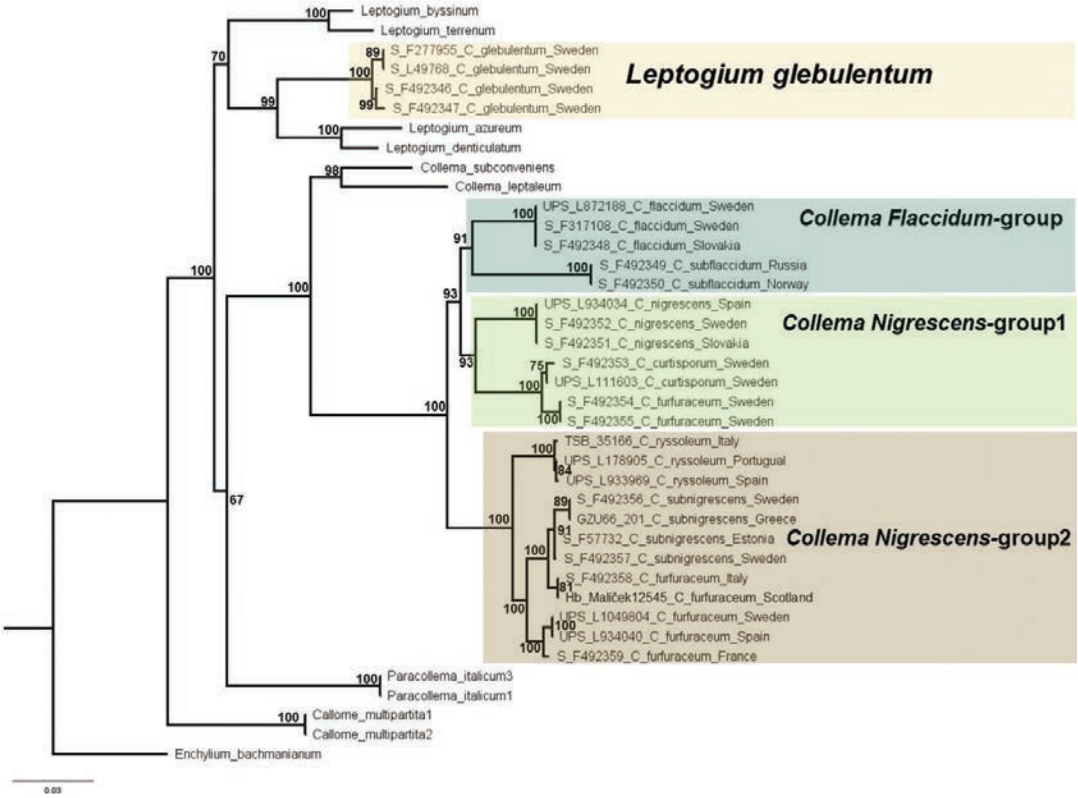

Figure 1. The most likely tree from RAxML analysis based on 4140 aligned characters of mtSSU, b-tub, MCM7 and RPB2 5–7 and 7–11 from 39 specimens. Support values (Likelihood BS) given when BS ≥ 60%. The scale bars indicate 0.03 substitution.

Our phylogenetic analysis reveals that European *Collema* should be treated as including *C. curtisporum*, *C. flaccidum*, *C. furfuraceum*, *C. nigrescens*, *C. ryssoleum*, *C. subflaccidum* and *C. subnigrescens*, but excluding *C. glebulentum* as this species clearly groups within *Leptogium* together with *Leptogium azureum*, the conserved type species of *Leptogium* (Fig. 1). The groups within *Collema* as informally circumscribed by Degelius (1954), are not supported by our phylogeny. The "*Flaccidum*"-group, consisting of *C. flaccidum* and *C. subflaccidum*, is nested within the "*Nigrescens*" -group. This indicates that these two informal groups are not useful for a phylogenetically based classification (Fig. 1). *Collema furfuraceum* is further non-monophyletic, suggesting the need for further taxonomic revision.

Morphological analyses

Degelius (1954) differentiated his informal groups in European *Collema* based on morphological characteristics, noting that species within the "*Flaccidum*"-group are all isidiate but not pustulate (Table 1, Fig. 2A–F). Isidia in *Collema flaccidum* are typically numerous and squamiform (flattened) when fully developed, rounded, and about 0.2–0.5 mm broad or larger. Larger isidia are often crenate or lobulate, with occasional teretiform isidia mixed in (Fig. 2B). In contrast, *C. subflaccidum* has smaller, globular isidia approximately 0.05–0.1 mm in diameter that become slightly teretiform as they mature, reaching at least 0.3 mm in length, with simple or slightly branched forms (Fig. 2C, D). *Collema glebulentum* (Fig. 2E, F) has, sometimes together with a primitive pseudocortex, a distinct typical pseudocortex, often developed on the lower surface, especially on smaller lobes. When a typical pseudocortex is present, it is composed of several cell layers where the cells can be quite large, reaching up to 15 µm in diameter (Fig. 3A). Parts of the thallus may have an entirely paraplectenchymatous structure. This characteristic, noted by Degelius (1954), actually supports the original classification of *C. glebulentum* in *Leptogium* (Fig. 3B). In areas where the thallus is not entirely paraplectenchymatous, its structure resembles that of other species in the "*Flaccidum*" and "*Nigrescens*"-groups. The entire thallus in species from these groups is composed of hyphae that are either loosely or compactly interwoven, or arranged distinctly perpendicular to the upper and lower cortices throughout the thallus (Fig. 3C).

Species within the "*Nigrescens*"-group are characterized by their pustulate and ridged thalli (Fig. 2G–P) and can be divided into non-isidiate species and those that produce isidia. Among the non-isidiate species, *Collema ryssoleum* (Fig. 2G, H) is distinct due to its spore morphology. The spores are short, measuring up to 40 µm in length, similar to those in *C. curtisporum*. However, unlike others in the group, *C. ryssoleum* spores are relatively wide (up to 8.5 µm) with acute ends (Table 1). Additionally, this species exhibits a unique Mediterranean distribution in the temperate zone and is adapted to a saxicolous habitat (Fig. 3D). *Collema subnigrescens* is characterized by an up to 20 cm large thallus (Fig. 2I) and by its narrowly fusiform to irregularly clavate spores with twisted, acute ends (5-celled, occasionally up to 12 cells; Fig. 3E). It closely resembles *C. curtisporum*, which, however, has a smaller, up to 4 cm wide thallus (Fig. 2J) and shorter, mostly 3-celled bacillariform spores with obtuse ends and a typical "curved-acute shape" (Fig. 3F). Spores in *C. nigrescens* differ from the other species in being acicular to bacillariform, longer and thinner than those in *C. subnigrescens* (usually around 60 µm long and less than 5 µm wide), 6–13 celled (Fig. 3G).

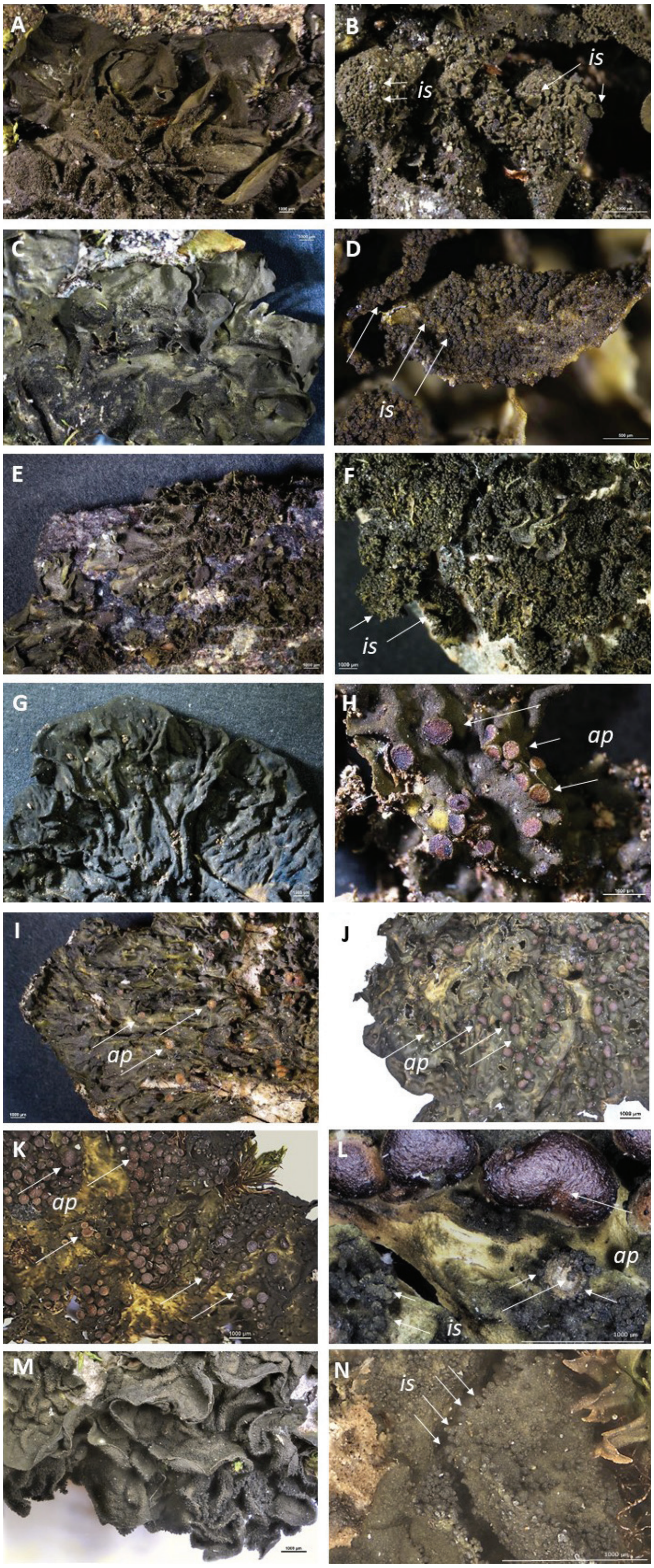

Figure 2. Thallus habitus and isidia of **A** *Collema flaccidum* (UPS-L872188) **B** *C. flaccidum* (UPS-L872188) **C** *C. subflaccidum* (S-F492349) **D** *C. subflaccidum* (S-F492350) **E** *Leptogium glebulentum* (S-L49768) **F** *L. glebulentum* – dwarf form (S-L49768) **G** *C. ryssoleum* (UPS-L933969) **H** *C. ryssoleum* (UPS-L933969) **I** *C. subnigrescens* (S-F57732) **J** *C. curtisporum* (UPS-L111603) **K** *C. nigrescens* (UPS-L934034) **L** *C. nigrescens* (UPS-L934034) **M** *C. furfuraceum* (UPS-L934040) **N** *C. furfuraceum* (UPS-L934040). ***is*** = isidia, ***ap*** = apothecium. Scale bar: **A–C**, **E–N**: 1 mm, **D**: 0.5 mm.

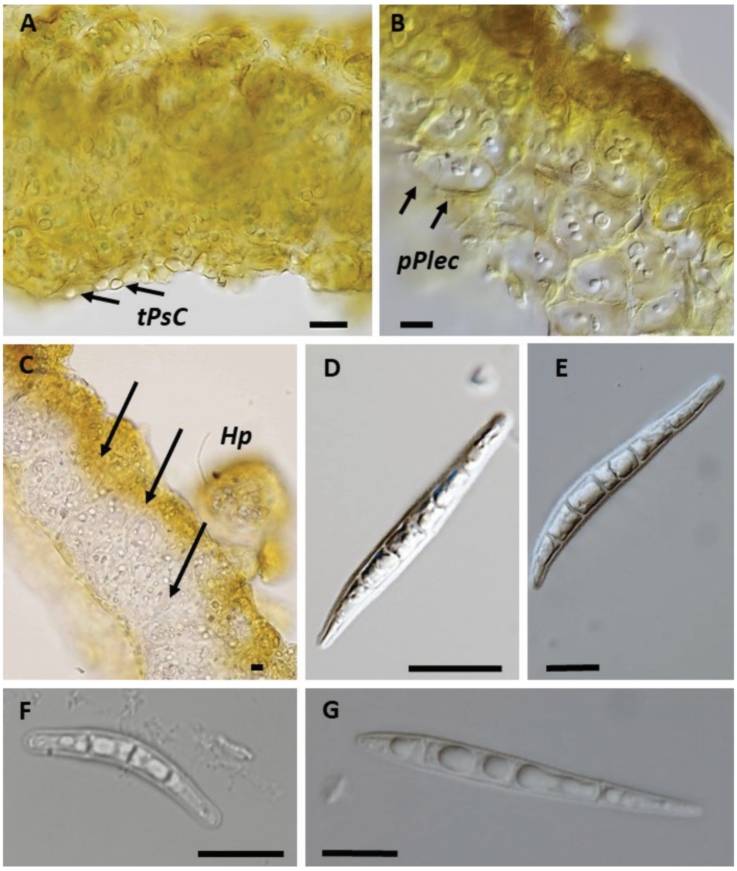

Figure 3. Thalli transversal cross-sections in water **A–C**, ascospores **D–G** **A** thallus with typical pseudocortex (*Leptogium glebulentum* S-L49768) **B** thallus paraplectenchymateous throughout (*Leptogium glebulentum* S-L49768), **C** thallus with hyphae which are perpendicular to the surface (*C. furfuraceum* S-F492354) **D** spore of *C. ryssoleum* (UPS-L178905) **E** spore of *C. subnigrescens* (GZU66-201) **F** spore of *C. curtisporum* (UPS-L111603) **G** *C. nigrescens* (S-F492352), ***tPsC*** = typical pseudocortex, ***Hp*** = hyphae, ***pPlect*** = paraplechtenchyma. Scale bar: 10 µm.

Among the isidiate species, *Collema nigrescens* is notable for its globular isidia (ca 0.2 mm in diameter; Fig. 2K, L), whereas *C. furfuraceum* has thinner, teretiform isidia (ca 0.05–0.15 mm wide) that become coralloid and reach up to 0.3 mm in length (Fig. 2M, N). Degelius (1974) later included *Collema luzonense* Räs. from the Philippines as a variety of *C. furfuraceum* and the var. *luzorense*, was distinguished by its euparaplectenchymatous excipulum proprium and frequent presence of white-pruinose apothecia. Another distinguishing feature of var. *luzorense* is its thicker lobes, reaching up to 300 µm, compared to 100 µm in var. furfuraceum. The var. *luzorense* has not been reported from Europe and the thallus thickness of the samples (which were all sterile) in our study suggests that they belong in var. *furfuraceum*.

Given the results of our phylogenetic analysis, it is crucial to study *C. furfuraceum* further. This study is under way, whereby we also plan to investigate the potential role of isidia as a distinguishing feature for species identification.

Conclusion

This study provides new insights into the phylogenetic relationships and morphological diversity among the European *Collema* species. Our results show that *C. glebulentum* belong in *Leptogium s. str.*, which is supported by its paraplectenchymatous thallus structure. Phylogenetic analysis reveals that Degelius´ (1954) *Collema* “*Flaccidum*” and “*Nigrescens*”-groups are not supported by the actual phylogenetic relationships. The study indicates that there are still substantial taxonomic issues worth studying and clarifying within European *Collema* s. str. We will present the results of such a study in a forthcoming publication.

Acknowledgements

We gratefully acknowledge Lars Arvidsson, Barbara Klein, Martin Westberg, Martin and Maroš Dinga for their kind help during fieldwork. We are grateful to Björn Owe-Larsson for organizing an excursion to the Swedish island Lurö. We further thank Andre Aptroot, Toni Berglund, Johannes Bergsten, Robin Isaksson, Göran Odelvik and Jirka Malíček, for providing samples. Länsstyrelsen of Uppsala län provided a collecting permit for Fiby urskog Nature Reserve. The staff of the herbaria BG, GZU, TSB, S and UPS kindly provided loans. We are grateful to the Department of Bioinformatics and Genetics of the Swedish Museum of Natural History, in particular Bodil Cronholm, for her skillful lab assistance.

Additional information

Conflict of interest

The authors have declared that no competing interests exist.

Ethical statement

No ethical statement was reported.

Funding

We received generous funding from the Swedish Taxonomy Initiative (Svenska Artprojektet) administered by the Swedish Species Information Center (ArtDatabanken; grants 2016-207 4.3 and SLU.dha.2019.4.3-48), and the Stenholms donationsfond (GBT 2018-00002-26).

Author contributions

Conceptualization: MW, AK. Data curation: AK. Formal analysis: AK. Funding acquisition: AK, MW. Investigation: UN, FJ. Methodology: AK. Validation: FJ, UN, MW. Visualization: UN. Writing - original draft: AK. Writing - review and editing: UN, FJ, MW.

Author ORCIDs

Alica Košuthová https://orcid.org/0000-0001-5991-7444
Mats Wedin https://orcid.org/0000-0002-8295-5198

Data availability

All of the data that support the findings of this study are available in the main text.

References

Degelius G (1954) The lichen genus *Collema* in Europe. Symbolae Botanicae Upsalienses 13: 1–499.

Degelius G (1974) The lichen genus *Collema* with special reference to the extra-European species. Symbolae Botanicae Upsalienses 20: 1–215.

Edgar RC (2004) MUSCLE: Multiple sequence alignment with high accuracy and high throughput. Nucleic Acids Research 32(5): 1792–1797. https://doi.org/10.1093/nar/gkh340

Ekman S, Wedin M, Lindblom L, Jørgensen PM (2014) Extended phylogeny and a revised generic classification of the Pannariaceae (Peltigerales, Ascomycota). Lichenologist 46(5): 627–656. https://doi.org/10.1017/S002428291400019X

Jørgensen PM (2007) Collemataceae. Nordic Lichen Flora 3: 14–45.

Kearse M, Moir R, Wilson A, Stones-Havas S, Cheung M, Sturrock S, Buxton S, Cooper A, Markowitz S, Duran C, Thierer T, Ashton B, Meintjes P, Drummond A (2012) Geneious Basic: An integrated and extendable desktop software platform for the organization and analysis of sequence data. Bioinformatics 28(12): 1647–1649. https://doi.org/10.1093/bioinformatics/bts199

Košuthová A, Fernández-Brime S, Westberg M, Wedin M (2016) *Collolechia* revisited, and a re-assessment of ascus characteristics in Placynthiaceae (Peltigerales, Ascomycota). Lichenologist 48(1): 3–12. https://doi.org/10.1017/S0024282915000432

Košuthová A, Westberg M, Otálora MAG, Wedin M (2019) *Rostania* revised: Testing generic delimitations in Collemataceae (Peltigerales, Lecanoromycetes). MycoKeys 47: 17–33. https://doi.org/10.3897/mycokeys.47.32227

Larsson A (2014) AliView: A fast and lightweight alignment viewer and editor for large datasets. Bioinformatics 30(22): 3276–3278. https://doi.org/10.1093/bioinformatics/btu531

Liu YJ, Whelen S, Hall BD (1999) Phylogenetic relationships among ascomycetes: Evidence from an RNA polymerse II subunit. Molecular Biology and Evolution 16(12): 1799–1808. https://doi.org/10.1093/oxfordjournals.molbev.a026092

Miadlikowska J, Lutzoni F (2004) Phylogenetic classification of peltigeralean fungi (Peltigerales, Ascomycota) based on ribosomal RNA small and large subunits. American Journal of Botany 91(3): 449–464. https://doi.org/10.3732/ajb.91.3.449

Miadlikowska J, Kauff F, Högnabba F, Oliver JC, Molnár K, Fraker E, Gaya E, Hafellner J, Hofstetter V, Gueidan C, Otálora MAG, Hodkinson B, Kukwa M, Lücking R, Björk C, Sipman HJM, Burgaz AR, Thell A, Passo A, Myllys L, Goward T, Fernández-Brime S, Hestmark G, Lendemer J, Lumbsch HT, Schmull M, Schoch CL, Sérusiaux E, Maddison DR, Arnold AE, Lutzoni F, Stenroos S (2014) A multigene phylogenetic synthesis for the class Lecanoromycetes (Ascomycota): 1307 fungi representing 1139 infrageneric taxa, 312 genera and 66 families. Molecular Phylogenetics and Evolution 79: 132–168. https://doi.org/10.1016/j.ympev.2014.04.003

Miller MA, Pfeiffer W, Schwartz T (2010) Creating the CIPRES Science Gateway for inference of large phylogenetic trees. Proceedings of the Gateway Computing Environments Workshop (GCE). New Orleans, LA, 1–8. https://doi.org/10.1109/GCE.2010.5676129

Myllys L, Lohtander K, Tehler A (2001) β-Tubulin, ITS and group I intron sequences challenge the species pair concept in *Physcia aipolia* and *P. caesia*. Mycologia 93(2): 335–343. https://doi.org/10.1080/00275514.2001.12063165

Otálora MAG, Aragón G, Molina MC, Martínez I, Lutzoni F (2010) Disentangling the *Collema-Leptogium* complex through a molecular phylogenetic study of the Collemataceae (Peltigerales, lichen-forming Ascomycota). Mycologia 102(2): 279–290. https://doi.org/10.3852/09-114

Otálora MAG, Aragón G, Martínez I, Wedin M (2013a) Cardinal characters on a slippery slope-a re-evaluation of phylogeny, character evolution, and evolutionary rates in the jelly lichens (Collemataceae s. str.). Molecular Phylogenetics and Evolution 68(2): 185–198. https://doi.org/10.1016/j.ympev.2013.04.004

Otálora MAG, Jørgensen PM, Wedin M (2013b) A revised classification of the jelly lichens, Collemataceae. Fungal Diversity 64[2014]: 275–293. https://doi.org/10.1007/s13225-013-0266-1

Schmitt I, Crespo A, Divarak PK, Fankhauser JD, Herman-Sackett E, Kalb K, Nelsen MP, Nelsen NA, Rivas-Plata E, Shimp AD, Widhelm T, Lumbsh HT (2009) New primers for promising single-copy genes in fungal phylogenetics and systematics. Persoonia 23(1): 35–40. https://doi.org/10.3767/003158509X470602

Stamatakis A (2014) RAxML version 8: A tool for phylogenetic analysis and post-analysis of large phylogenies. Bioinformatics 30(9): 1312–1313. https://doi.org/10.1093/bioinformatics/btu033

Thiers B (2018) [Continuously updated] Index Herbariorum: A Global Directory of Public Herbaria and Associated Staff. New York Botanical Garden's Virtual Herbarium. http:// sweetgum.nybg.org/science/ih/

Wedin M, Wiklund E, Jørgensen PM, Ekman S (2009) Slippery when wet: Phylogeny and character evolution in the gelatinous cyanobacterial lichens (Peltigerales, Ascomycetes). Molecular Phylogenetics and Evolution 53(3): 862–871. https://doi.org/10.1016/j.ympev.2009.08.013

Weerakoon G, Aptroot A, Wedin M, Ekman E (2018) *Leightoniella zeylanensis* belongs to the Pannariaceae. Nordic Journal of Botany 36(7): 1–6. https://doi.org/10.1111/njb.01880

Wiklund E, Wedin M (2003) The phylogenetic relationships of the cyanobacterial lichens in the Lecanorales suborder Peltigerineae. Cladistics 19(5): 419–431. https://doi.org/10.1111/j.1096-0031.2003.tb00312.x

Zhang Z, Schwartz S, Wagner L, Miller W (2000) A greedy algorithm for aligning DNA sequences. Journal of Computational Biology 7(1–2): 203–214. https://doi.org/10.1089/10665270050081478

Zoller S, Scheidegger C, Sperisen C (1999) PCR primers for the amplification of mitochondrial small subunit ribosomal DNA of lichen-forming ascomycetes. Lichenologist 31(5): 511–516. https://doi.org/10.1006/lich.1999.0220

MycoKeys 115: 221–240 (2025)
DOI: 10.3897/mycokeys.115.136469

Research Article

Two new pestalotioid fungi from tropical fruits in Iran

Amirreza Amirmijani[1*], Adel Pordel[2*], Kowsar Dehghani[1], Mohammad Javad Pourmoghaddam[3], Hossein Masigol[4], Hans-Peter Grossart[4,5]

1 Department of Plant Protection, Faculty of Agriculture, University of Jiroft, Jiroft, Iran
2 Plant Protection Research Department, Baluchestan Agricultural and Natural Resources Research and Education Center, AREEO, Iranshahr, Iran
3 Department of Plant Protection, Faculty of Agricultural Sciences, University of Guilan, Rasht, Iran
4 Department of Plankton and Microbial Ecology, Leibniz Institute of Freshwater Ecology and Inland Fisheries (IGB), Alte Fischerhuette 2, 16775 Stechlin, Germany
5 Institute of Biochemistry and Biology, Potsdam University, Maulbeerallee 2, 14469 Potsdam, Germany
Corresponding author: Amirreza Amirmijani (ar.amirmijani@ujiroft.ac.ir)

Abstract

In a survey of tropical plant diseases in southern and southeastern Iran, samples of diseased *Mangifera indica* and *Psidium guava* leaves with necrotic symptoms were collected between 2021 and 2022. Six representative isolates of *Neopestalotiopsis* and *Robillarda* (three isolates for each) were studied using morphological characteristics as well as multi-locus phylogenetic analysis based on (i) the internal transcribed spacer (ITS) region of the nuclear rDNA, (ii) part of the translation elongation factor 1-alpha (*tef1*), and (iii) the β-tubulin (*tub2*). After morphological investigation, our phylogenetic analysis revealed that the *Neopestalotiopsis* and *Robillarda* isolates under study differed from all previously described species within these genera. Based on our polyphasic approach, two new species, including *Neopestalotiopsis guava* **sp. nov.** from necrotic *Mangifera indica* and *Robillarda khodaparastii* **sp. nov.** from *Psidium guava* are described and illustrated from Iran.

Key words: Fungal diversity, *Mangifera indica*, Pestalotioid fungi, *Psidium guava*, Tropical fruits, two new species

Academic editor: Ning Jiang
Received: 5 September 2024
Accepted: 19 November 2024
Published: 20 March 2025

Citation: Amirmijani A, Pordel A, Dehghani K, Pourmoghaddam MJ, Masigol H, Grossart H-P (2025) Two new pestalotioid fungi from tropical fruits in Iran. MycoKeys 115: 221–240. https://doi.org/10.3897/mycokeys.115.136469

Introduction

Tropical fruits provide essential nutrition and serve as a source of income for farmers engaged in export production. The major cultivation areas for tropical fruits are predominantly in developing countries, particularly in Asia and Latin America (FAO 2020). Global trade in tropical fruits has expanded to unprecedented levels in recent years, reaching an aggregate export volume of nearly 9 million tons in 2023. Strong demand from key importing countries has driven significant investments in productivity improvements and expansion of cultivation areas in supplying countries, notably for avocados (FAO 2024). Iran is a major producer of fruits, including tropical fruits, due to favorable meteorological conditions, diverse climates, and significant temperature differences between the northern and southern regions (Saboki et al. 2012). Regarding tropical fruit production, the Provinces of Hormozgan and Sistan and Baluchistan, located in

---

* These authors contributed equally to this work.

the south and southeast of Iran, are considered the most suitable regions due to their proximity to the equator, the Oman Sea, and the Indian Ocean (Saboki et al. 2012, 2014).

Pestalotioid fungi are diverse and exhibit various lifestyles, including plant pathogens, endophytes, and saprophytes (Crous et al. 2015a; Sun et al. 2023). Despite uncertainties regarding the generic divisions among pestalotioid fungi, the classification system based on the number of conidia cells in different genera is still in use (Shu et al. 2020). The genus *Pestalotia* was initially described by De Notaris in 1841 (Jiang et al. 2022). Subsequently, based on the number of conidia cells, *Pestalotia* was divided into four distinct genera: *Truncatella* (4 cells), *Pestalotiopsis* (5 cells), *Pestalotia* (6 cells), and *Monochaetia* (5 cells) (Sutton 1980). Phylogenetic analyses have validated Sutton's classification based on morphological characteristics; however, species previously classified under *Pestalotia* have been reassigned to the genus *Seiridium* (Marin-Felix et al. 2019). Additionally, the genus *Pestalotiopsis* has been further categorized into *Pestalotiopsis* sensu stricto, *Neopestalotiopsis*, and *Pseudopestalotiopsis* (Maharachchikumbura et al. 2016). *Neopestalotiopsis* is distinct from *Pestalotiopsis*, characterized by the presence of versicolourous median cells (Jiang et al. 2022).

The genus *Robillarda* was introduced by Saccardo in 1880 to accommodate the type species *R. sessile* (Saccardo 1880). *Robillarda* is a pestalotioid fungus within the family Sporocadaceae, and characterized by conidia with appendage-bearing (Liu et al. 2019). Although the genus includes 41 morphological species, sequence data are available for only some of them (Liu et al. 2019; https://www.indexfungorum.org/names/Names.asp/, accessed 31 Aug 2024).

In the present study, leaf spots on *Mangifera* and *Psidium* were observed in Sistan and Baluchestan Province, Iran. Based on modern taxonomic approaches, we identified two new species of *Neopestalotiopsis* and *Robillarda* from Iran. Detailed morphological descriptions, illustrations, and phylogenetic information are provided here.

Materials and methods

Sampling and fungal isolation

During a survey conducted on tropical and subtropical fruit trees in the summer of 2021, a total of seventy-five samples were collected from mango (*M. indica*) plants displaying symptoms of leaf spot disease. The leaf samples were specifically gathered from various districts in the Provinces of Hormozgan (Siaho district) and Sistan and Baluchestan (Nikshahr, Ghasreghand, Rask, and Konarak districts), which are located in the southern and southeast regions of Iran, respectively. The infected samples were transported to the laboratory and stored in a refrigerator under dry conditions at a temperature of 4 °C. To begin the isolation process, the infected tissues were cut into 7–8 mm pieces, surface–disinfected with a 2% sodium hypochlorite solution for 3 min, rinsed twice with sterile distilled water, dehydrated, and subsequently placed on 2% water-agar (2% WA) in Petri dishes. These Petri dishes were maintained at 25 °C under alternating near-UV light and dark conditions (12 h light/12 h dark) for 7 days. After 48 h, conidia were observed growing on the leaf pieces and transferred to 2% WA using the single-spore method. Hyphal tips emerging from individual conidia were further transferred to a potato dextrose agar (PDA) medium to establish pure cultures (Refaei et al. 2011).

Morphological characterization

Mycelia plugs were extracted from the purified colony and placed on PDA to assess the colony's overall characteristics. Subsequently, the plugs were incubated at 25 °C under alternating near-UV light and dark conditions. After 7–10 d, the color of the colony and the conidial mass were documented. To further analyze the morphological features of the conidiomata and conidia, more than 200 conidiophores and conidia were examined using slide mounts prepared with lactophenol and lactophenol cotton blue. Morphometrical analyses were also conducted on 200 conidiophores and conidia. For this purpose, a BH2 Olympus light microscope (Japan) equipped with a Microbin 12MP USB2.0 camera was utilized. The holotype and ex-type specimens have been deposited in the Herbarium of the Mycology Laboratory at the University of Jiroft, Jiroft, Iran (UJFCC).

DNA extraction, PCR, and sequencing

DNA was extracted from seven-day-old fungal mycelium using the protocol described by Zhong and Steffenson (2001). The entire internal transcribed spacer (ITS1-5.8S-ITS2) regions of the rDNA, the partial translation elongation factor 1-alpha (*tef1*) gene and b-tubulin (*tub2*) gene were amplified using the primer pairs ITS1 (5"-TCCGTAGGTGAACCTGCGG-3") and ITS4 (5"-TCCTCCGCTTATTGATATGC-3") (White et al. 1990), EF1-728F (5"-CATCGAGAAGTTCGAGAAGG-3") and EF2 (5"-GGARGTACCAGTSATCATGTT-3") (Carbone and Kohn 1999; O'Donnell et al. 1998), as well as Bt2a (5"-GGTAACCAAATCGGTGCTGCTTTC-3") and Bt2b (5"-ACCCTCAGTGTAGTGACCCTTGGC-3") (Glass and Donaldson 1995). PCR amplifications were carried out in a final volume of 25 µL. The PCR mixtures contained 10 µL of master mix (CinnaGen, Iran), which included 10 × PCR buffer, $MgCl_2$, dNTPs, Taq DNA Polymerase, 11 µL of double-distilled water, 1 µL of each forward and reverse primers (10 pmol), and 2 µL of template DNA. The PCR amplifications were done using a thermocycler with the following thermal conditions for ITS: initial denaturation at 94 °C for 3 min, followed by 35 cycles of denaturation step at 94 °C for 30 s, annealing at 55 °C for 30 s, and extension at 72 °C for 30 s, and terminated with a final extension step at 72 °C for 10 min; for *tef1*: initial denaturation at 94 °C for 8 min, and then followed by 35 cycles each with denaturation at 94 °C for 15 sec, annealing at 55 °C for 20 sec and the extension at 72 °C for 1 min, and a final extension at 72 °C for 5 min; for *tub2*: initial denaturation at 94 °C for 3 min, and then followed by 35 cycles each with denaturation at 95 °C for 30 s, annealing at 53 °C for 30 s and the extension at 72 °C for 45 s, and a final extension at 72 °C for 90 s. All amplicons were sent to the Codon Genetic Group (Tehran, Iran) for sequencing.

Phylogenetic analyses

To identify closely related taxa, BLASTn searches were done separately for the three loci. Type and reference sequences of related taxa were retrieved from the National Center for Biotechnology Information (**NCBI**), if available, based on recent publications on the genera *Neopestalotiopsis* (Maharachchikumbura et al. 2012, 2014a, 2014b; Fiorenza et al. 2022; Razaghi et al. 2024) and *Robillarda* (Crous et al. 2015a; Liu et al. 2019). All alignments were produced using the server versions of MAFFT v. 7.490 (http://mafft.cbrc.jp/alignment/server/; Katoh et al. 2019) and were manually checked and refined with MEGA Ver. 7 (Kumar et al. 2016). Following the results of BLASTn searches for generated sequences of the three loci (ITS, *tef1*, *tub2*), a phylogenetic analysis was performed for *Neopestalotiopsis* species including 91 isolates. Similarly, a phylogenetic placement was conducted for *Robillarda*, including 11 isolates. *Pestalotiopsis colombiensis* and *P. diversiseta* were selected as the outgroup taxa for both trees (Table 1). After excluding ambiguously aligned and gappy regions, the resulting combined data matrix contained 1363 alignment positions across all three loci (494 from ITS, 471 from *tef1*, and 398 from *tub2*) for *Neopestalotiopsis* and 1306 alignment positions (518 from ITS, 443 from *tef1*, and 345 from *tub2*) for *Robillarda*.

Maximum Likelihood (ML) analyses were performed using RAxML (Stamatakis 2006) as implemented in raxmlGUI 1.3 (Silvestro and Michalak 2012) with the ML + rapid bootstrap setting and the GTRGAMMA substitution model. A total of 1000 bootstrap replicates were conducted.

Maximum Parsimony (MP) analyses were performed with PAUP v. 4.0a169 (Swofford 2002). All molecular characters were treated as unordered and given equal weight, with gaps treated as missing data. The COLLAPSE command was set to MINBRLEN. MP analysis of the combined multilocus matrix was done using 1000 replicates of heuristic search with random addition of sequences, followed by TBR branch swapping (MULTREES option in effect, steepest descent option not in effect). Bootstrap analyses with 1000 replicates were performed similarly, with 10 rounds of random sequence addition and subsequent branch swapping during each bootstrap replicate. Bootstrap values ≤ 70% are considered low, those between 70% and 90% intermediate, and those ≥ 90% high.

Results

Molecular phylogeny

In *Neopestalotiopsis*, of the 1363 characters included in the phylogenetic analyses (ITS-*tef1*-*tub2*), 255 were parsimony-informative (48 in ITS, 120 in *tef1*, and 87 in *tub2*). The phylogram of the best ML tree (lnL = −6,428.7652) obtained using RAxML is shown in Fig. 1. The MP analysis revealed 896 trees with a length of 805 (not shown) that had a similar topology to the ML tree (CI = 0.62, RI = 0.71, and RC = 0.37).

The isolates of *Neopestalotiopsis* from this study form a clade with a well-supported ML and MP BS (80/70%). Table 2 shows the base pair differences among other taxa that might be mistaken for the new species.

In *Robillarda*, of the 1306 characters included in the phylogenetic analyses (ITS-*tef1*-*tub2*), 238 were parsimony-informative (48 in ITS, 144 in *tef1*, and 46 in *tub2*). The phylogram of the best ML tree (lnL = −3,732.5074) obtained using RAxML is presented in Fig. 2. The MP analysis revealed a single tree with a length of 417 (not shown) that exhibited a similar topology to the ML tree (CI = 0.91, RI = 0.91, and RC = 0.08).

Table 1. Isolation and accession numbers of sequences used in the phylogenetic analyses. Isolates/sequences in bold were isolated/sequenced in present study. N/A: not available. [1] T indicates ex-type material.

Species	Strain[1]	Origin	GenBank accession numbers			References
			ITS	*tef1*	*tub2*	
Neopestalotiopsis acrostichi	MFLUCC 17-1754^{T}	Thailand	MK764272	MK764316	MK764338	Norphanphoun et al. (2019)
Neopestalotiopsis alpapicalis	MFLUCC 17-2544^{T}	Thailand	MK357772	MK463547	MK463545	Kumar et al. (2019)
Neopestalotiopsis aotearoa	CBS 367.54^{T}	New Zealand	KM199369	KM199526	KM199454	Maharachchikumbura et al. (2012)
Neopestalotiopsis asiatica	MFLUCC 12-0286^{T}	China	JX398983	JX399049	JX399018	Maharachchikumbura et al. (2012)
Neopestalotiopsis australis	CBS 114159^{T}	Australia	KM199348	KM199537	KM199432	Maharachchikumbura et al.(2014b)
Neopestalotiopsis brachiate	MFLUCC 17-1555^{T}	Thailand	MK764274	MK764318	MK764340	Norphanphoun et al. (2019)
Neopestalotiopsis brasiliensis	COAD 2166^{T}	Brazil	MG686469	MG692402	MG692400	Bezerra et al. (2018)
Neopestalotiopsis cavernicola	KUMCC 20-0269^{T}	China	MW545802	MW550735	MW557596	Liu et al. (2021)
Neopestalotiopsis celtidis	CGMCC 3.23513^{T}	China	OR247900	OR361449	OR381049	Razaghi et al. (2024)
Neopestalotiopsis chrysea	MFLUCC 12-0261^{T}	China	JX398985	JX399051	JX399020	Maharachchikumbura et al. (2012)
Neopestalotiopsis clavispora	MFLUCC 12-0281^{T}	China	JX398979	JX399045	JX399014	Maharachchikumbura et al. (2012)
Neopestalotiopsis coffeae-arabicae	HGUP4019^{T}	China	KF412649	KF412646	KF412643	Song et al. (2013)
Neopestalotiopsis concentrica	CFCC 55162^{T}	China	OK560707	OM622433	OM117698	Peng et al. (2022)
Neopestalotiopsis cubana	CBS 600.96^{T}	Cuba	KM199347	KM199521	KM199438	Maharachchikumbura et al.(2014b)
Neopestalotiopsis dendrobii	MFLUCC 14-0106^{T}	Thailand	MK993571	MK975829	MK975835	Ma et al. (2019)
Neopestalotiopsis dolichoconidiophora	CGMCC 3.23490^{T}	China	OR247911	OR361421	OR381021	Razaghi et al. (2024)
Neopestalotiopsis egyptiaca	CBS 140162^{T}	Egypt	KP943747	KP943748	KP943746	Crous et al. (2015b)
Neopestalotiopsis elaeagni	HGUP10002 ^{T}	China	MW930716	MZ203452	MZ683391	He et al. (2022)
Neopestalotiopsis elaeidis	MFLUCC 15-0735^{T}	Thailand	ON650690	ON734012	N/A	Konta et al. (2023)
Neopestalotiopsis ellipsospora	MFLUCC 12-0283^{T}	China	JX398980	JX399047	JX399016	Maharachchikumbura et al. (2012)
Neopestalotiopsis eucalypticola	CBS 264.37^{T}	N/A	KM199376	KM199551	KM199431	Maharachchikumbura et al.(2014b)
Neopestalotiopsis eucalyptorum	CBS 147684^{T}	Portugal	MW794108	MW805397	MW802841	Diogo et al. (2021)
Neopestalotiopsis foedans	CGMCC 3.9123^{T}	China	JX398987	JX399053	JX399022	Maharachchikumbura et al. (2012)
Neopestalotiopsis formicarum	CBS 362.72^{T}	Ghana	KM199358	KM199517	KM199455	Maharachchikumbura et al.(2014b)
Neopestalotiopsis fragariae	ZHKUCC 22- 0113^{T}	China	ON553410	ON569076	ON569075	Prematunga et al. (2022)
Neopestalotiopsis guajavae	FMBCC 11.1	Pakistan	MF783085	MH460868	MH460871	Ul Haq et al. (2021)
Neopestalotiopsis guangxiensis	CGMCC 3.23505^{T}	China	OR247881	OR361440	OR381040	Razaghi et al. (2024)
Neopestalotiopsis guava	**UJFCC2084^{T}**	**Iran**	**PP038121**	**PP053741**	**PP053735**	**This study**
Neopestalotiopsis guava	**UJFCC2085**	**Iran**	**PP038120**	**PP053740**	**PP053734**	**This study**
Neopestalotiopsis guava	**UJFCC2086**	**Iran**	**PP038122**	**PP053742**	**PP053736**	**This study**
Neopestalotiopsis haikouensis	SAUCC212271^{T}	China	OK087294	OK104877	OK104870	Hsu et al. (2024)
Neopestalotiopsis hispanica	CBS 147686^{T}	Portugal	MW794107	MW805399	MW802840	Diogo et al. (2021)
Neopestalotiopsis honoluluana	CBS 114495^{T}	USA	KM199364	KM199548	KM199457	Maharachchikumbura et al.(2014b)
Neopestalotiopsis hydeana	MFLUCC 20-0132^{T}	Thailand	MW266069	MW251129	MW251119	Huanlauek et al. (2021)
Neopestalotiopsis iberica	CBS 147688^{T}	Portugal	MW794111	MW805402	MW802844	Diogo et al. (2021)
Neopestalotiopsis iranensis	CBS 137768^{T}	Iran	KM074048	KM074051	KM074057	Ayoubi and Soleimani (2016a)
Neopestalotiopsis javaensis	CBS 257.31^{T}	Indonesia	KM199357	KM199543	KM199437	Maharachchikumbura et al.(2014b)
Neopestalotiopsis keteleeriae	MFLUCC 13-0915^{T}	China	KJ023087	KJ023089	KJ023088	Song et al. (2014)
Neopestalotiopsis longiappendiculata	CBS 147690^{T}	Portugal	MW794112	MW805404	MW802845	Diogo et al. (2021)
Neopestalotiopsis macadamiae	BRIP 63737c^{T}	Australia	KX186604	KX186627	KX186654	Akinsanmi et al. (2017)
Neopestalotiopsis maddoxii	BRIP 72266a^{T}	Australia	MZ303782	MZ344167	MZ312675	Prasannath et al. (2021)
Neopestalotiopsis megabetaspora	CGMCC 3.23474^{T}	China	OR247875	OR361410	OR381010	Razaghi et al. (2024)
Neopestalotiopsis mesopotamica	CBS 336.86^{T}	Turkey	KM199362	KM199555	KM199441	Maharachchikumbura et al.(2014b)
Neopestalotiopsis mianyangensis	CGMCC 3.23554^{T}	China	OP546681	OP723490	OP672161	Li et al. (2022)
Neopestalotiopsis musae	MFLUCC 15-0776^{T}	Thailand	NR156311	KX789685	KX789686	Norphanphoun et al. (2019)
Neopestalotiopsis natalensis	CBS 138.41^{T}	South Africa	NR_156288	KM199552	KM199466	Maharachchikumbura et al. (2014a)
Neopestalotiopsis nebuloides	BRIP 66617^{T}	Australia	MK966338	MK977633	MK977632	Crous et al. (2020)
Neopestalotiopsis paeonia-suffruticosa	CGMCC 3.23555^{T}	China	OP082292	OP204794	OP235980	Li et al. (2022)
Neopestalotiopsis pernambucana	URM 7148-01^{T}	Brazil	KJ792466	KU306739	N/A	Silvério et al. (2016)
Neopestalotiopsis perukae	FMBCC 11.3^{T}	Pakistan	MH209077	MH523647	MH460876	Ul Haq et al. (2021)

Species	**Strain**[1]	**Origin**	**GenBank accession numbers**			**References**
			ITS	***tef1***	***tub2***	
Neopestalotiopsis petila	MFLUCC 17-1738^{T}	Thailand	MK764276	MK764320	MK764342	Norphanphoun et al. (2019)
Neopestalotiopsis phangngaensis	MFLUCC 18-0119^{T}	Thailand	MH388354	MH388390	MH412721	Tibpromma et al. (2018)
Neopestalotiopsis photiniae	MFLUCC 22-0129^{T}	China	OP498008	OP753368	OP752131	Sun et al. (2023)
Neopestalotiopsis phyllostachydis	CGMCC 3.23491^{T}	China	OR247891	OR361423	OR381023	Razaghi et al. (2024)
Neopestalotiopsis piceana	CBS 394.48^{T}	UK	KM199368	KM199527	KM199453	Maharachchikumbura et al.(2014b)
Neopestalotiopsis psidii	FMBCC 11.2^{T}	Pakistan	MF783082	MH460874	MH477870	Ul Haq et al. (2021)
Neopestalotiopsis rhizophorae	MFLUCC 17-1551^{T}	Thailand	MK764277	MK764321	MK764343	Norphanphoun et al. (2019)
Neopestalotiopsis rhododendri	GUCC 21504^{T}	China	MW979577	MW980444	MW980443	Yang et al. (2021)
Neopestalotiopsis rosae	CBS 101057^{T}	Zealand New	KM199359	KM199523	KM199429	Maharachchikumbura et al.(2014b)
Neopestalotiopsis rosicola	CFCC 51992^{T}	China	KY885239	KY885243	KY885245	Norphanphoun et al. (2019)
Neopestalotiopsis samarangensis	MFLUCC 12-0233^{T}	Thailand	JQ968609	JQ968611	JQ968610	Maharachchikumbura et al.(2014b)
Neopestalotiopsis saprophytica	MFLUCC 12-0282^{T}	China	JX398982	JX399048	JX399017	Maharachchikumbura et al.(2014b)
Neopestalotiopsis scalabiensis	CAA1029^{T}	Portugal	MW969748	MW959100	MW934611	Santos et al. (2022)
Neopestalotiopsis siciliana	AC46^{T}	Italy	ON117813	ON107273	ON209162	Fiorenza et al. (2022)
Neopestalotiopsis sichuanensis	CFCC 54338^{T}	China	MW166231	MW199750	MW218524	Jiang et al. (2021)
Neopestalotiopsis sonneratiae	MFLUCC 17-1745^{T}	Thailand	MK764280	MK764324	MK764346	Norphanphoun et al. (2019)
Neopestalotiopsis steyaertii	IMI 192475^{T}	Australia	KF582796	KF582792	KF582794	Maharachchikumbura et al.(2014a)
Neopestalotiopsis subepidermalis	CFCC 55160^{T}	China	OK560699	OM622425	OM117690	Peng et al. (2022)
Neopestalotiopsis suphanburiensis	MFLUCC 22-0126^{T}	Thailand	OP497994	OP753372	OP752135	Sun et al. (2023)
Neopestalotiopsis surinamensis	CBS 450.74^{T}	Suriname	KM199351	KM199518	KM199465	Maharachchikumbura et al.(2014b)
Neopestalotiopsis terricola	CGMCC 3.23553^{T}	China	OP082294	OP204796	OP235982	Li et al. (2022)
Neopestalotiopsis thailandica	MFLUCC 17-1730^{T}	Thailand	MK764281	MK764325	MK764347	Norphanphoun et al. (2019)
Neopestalotiopsis vacciniicola	CAA1055^{T}	Portugal	MW969751	MW959103	MW934614	Santos et al. (2022)
Neopestalotiopsis umbrinospora	MFLUCC 12-0285^{T}	China	JX398984	JX399050	JX399019	Maharachchikumbura et al. (2012)
Neopestalotiopsis vaccinii	CAA1059 ^{T}	Portugal	MW969747	MW959099	MW934610	Santos et al. (2022)
Neopestalotiopsis vheenae	BRIP 72293a^{T}	Australia	MZ303792	MZ344177	MZ312685	Prasannath et al. (2021)
Neopestalotiopsis vitis	MFLUCC 15-1265^{T}	China	KU140694	KU140676	KU140685	Jayawardena et al. (2016)
Neopestalotiopsis zakeelii	BRIP 72282a^{T}	Australia	MZ303789	MZ344174	MZ312682	Prasannath et al. (2021)
Neopestalotiopsis zimbabwana	CBS 111495^{T}	Zimbabwe	N/A	KM199545	KM199456	Maharachchikumbura et al.(2014b)
Neopestalotiopsis sp.	MEAN 1325	Portugal	MW794102	MW805414	MW802835	Diogo et al. (2021)
Neopestalotiopsis sp.	MEAN 1327	Portugal	MW794105	MW805416	MW802838	Diogo et al. (2021)
Neopestalotiopsis sp.	MEAN 1328	Spain	MW794115	MW805417	MW802848	Diogo et al. (2021)
Neopestalotiopsis sp.	PPS14	Peru	MK860757	MN000341	MN000344	Rodríguez-Gálvez et al. (2022)
Neopestalotiopsis sp.	PAK10	Peru	MK860755	MN000339	MN000342	Rodríguez-Gálvez et al. (2022)
Neopestalotiopsis sp.	PPS3	Peru	MK860756	MN000340	MN000343	Rodríguez-Gálvez et al. (2022)
Neopestalotiopsis sp.	CBS 664.94	Netherlands	KM199354	KM199525	KM199449	Maharachchikumbura et al.(2014b)
Neopestalotiopsis sp.	CBS 177.25	Unknown	KM199370	KM199533	KM199445	Maharachchikumbura et al.(2014b)
Neopestalotiopsis sp.	CFCC 54340	China	MW166235	MW199754	MW218528	Jiang et al. (2021)
Neopestalotiopsis sp.	ZX22B	China	MW166236	MW199755	MW218529	Jiang et al. (2021)
Pestalotiopsis colombiensis	CBS 118553^{T}	Colombia	KM199307	KM199488	KM199421	Maharachchikumbura et al.(2014b)
Pestalotiopsis diversiseta	MFLUCC 12-0287^{T}	China	NR_120187	JX399073	JX399040	Maharachchikumbura et al. (2012)
Robillarda Africana	CBS 122.75^{T}	South Africa	KR873253	MH554414	MH554656	Crous et al. (2015a); Liu et al. (2019)
Robillarda aquatic	MFLUCC 21–0217^{T}	Thailand	OL504777	N/A	N/A	Manawasinghe et al. (2022)
Robillarda australiana	CBS 143882^{T}	Australia	MH554091	MH554525	MH554764	Liu et al. (2019)
Robillarda khodaparastii	**UJFCC2116^{T}**	**Iran**	**PP038123**	**PP053743**	**PP053737**	**This study**
Robillarda khodaparastii	**UJFCC2117**	**Iran**	**PP038124**	**PP053744**	**PP053738**	**This study**
Robillarda khodaparastii	**UJFCC2118**	**Iran**	**PP038125**	**PP053745**	**PP053739**	**This study**
Robillarda mangiferae	KUMCC 18-0180^{T}	China	OL504777	N/A	N/A	Phookamsak et al. (2019)
Robillarda roystoneae	CBS 115445^{T}	Hong Kong	KR873254	KR873310	KR873317	Crous et al. (2015a)
Robillarda sessilis	CBS 114312^{T}	Germany	KR873256	KR873312	KR873319	Crous et al. (2015a)
Robillarda terrae	CBS 587.71^{T}	India	KJ710484	MH554493	MH554734	Crous et al. (2014); Liu et al. (2019)
Robillarda sp.	CPC 25020	N/A	KR873259	KR873315	KR873322	Crous et al. (2015a)

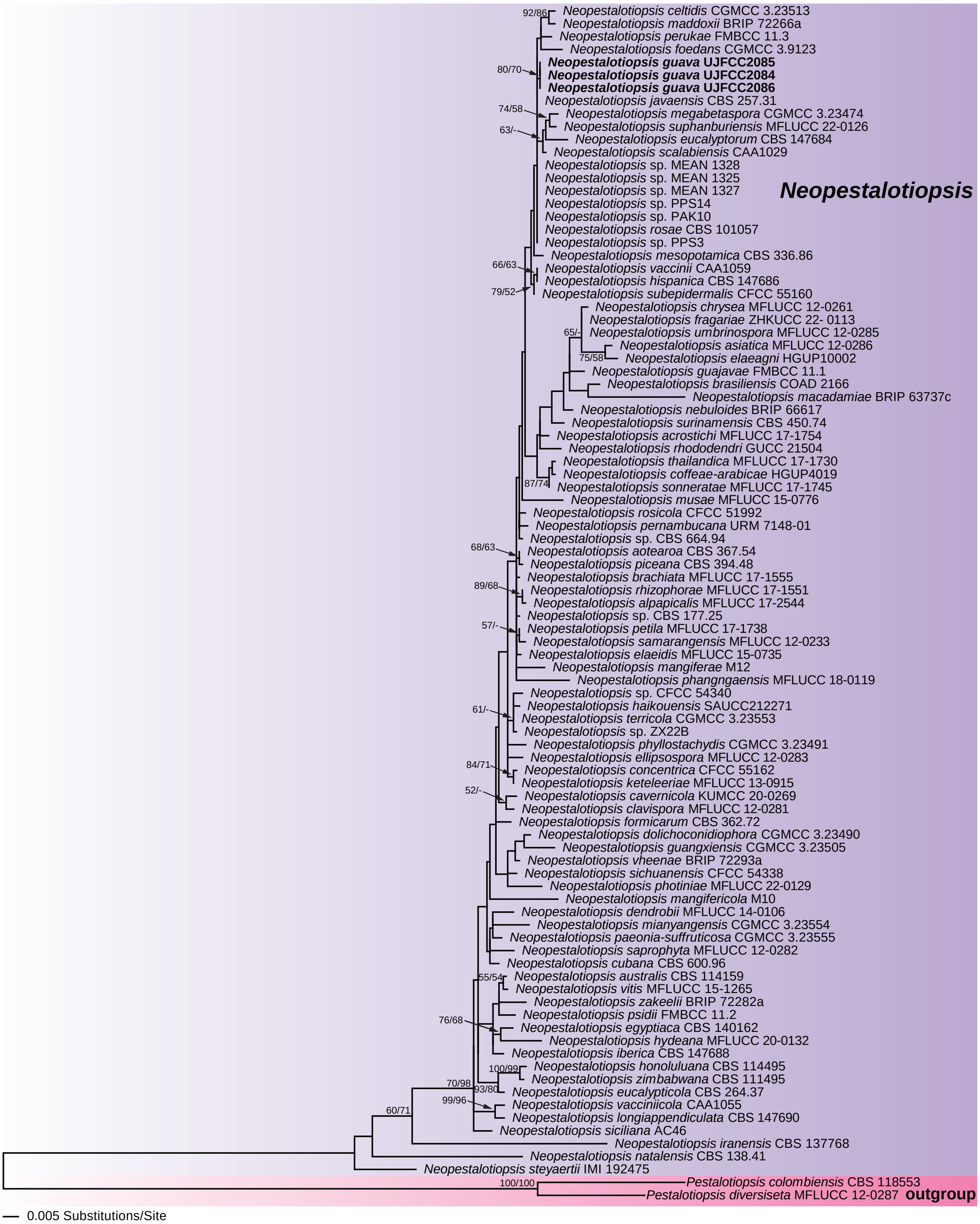

Figure 1. Phylogram of the best ML trees (lnL = −6,428.7652) revealed by RAxML from an analysis of the combined ITS–*tef1*–*tub2* matrix of selected *Neopestalotiopsis*. Strains in bold were sequenced in the current study. ML and MP bootstrap support above 50% are given at the first and second positions, respectively, above or below the branches.

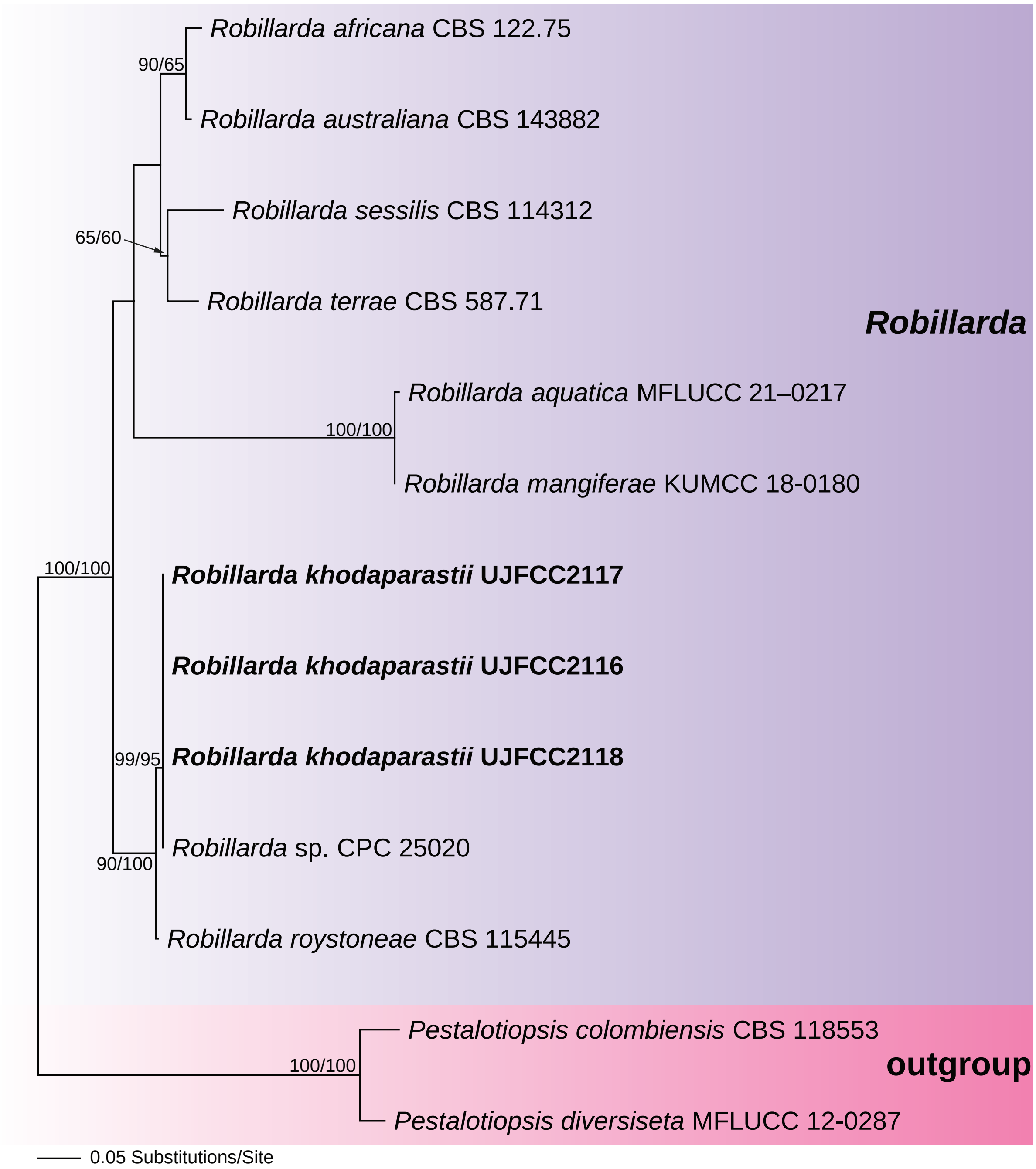

Figure 2. Phylogram of the best ML trees (lnL = −3,732.5074) revealed by RAxML from an analysis of the combined ITS–*tef1*–*tub2* matrix of selected *Robillarda* spp. Strains in bold were sequenced in the current study. ML and MP bootstrap support above 50% are given at the first and second positions, respectively, above or below the branches.

Robillarda isolates from the current study were grouped within a highly supported ML and MP bootstrap-supported clade, along with an unnamed isolate (CPC 25020). Analysis of these sequence data revealed identical sequences across all loci. This clade is a sister group of *R. roystoneae* (CBS 115445) with maximum ML and MP BS support. Molecularly, *R. khodaparastii* differs from *R. roystoneae* by 1 bp difference out of 532 bp in ITS, 2 bp differences out of 284 bp in *tef1* and 2 bp differences out of 237 bp in *tub2*. Based on these findings, we conclude that members of *Neopestalotiopsis* and *Robillarda* represent two independent, so far undescribed species.

Table 2 Base pair differences between *Neopestalotiopsis guava* to related species in this study.

Species	Gene region		
	ITS	*tef1*	*tub2*
Neopestalotiopsis celtidis	4/434	10/432	5/371
Neopestalotiopsis eucalyptorum	1/505	10/475	1/340
Neopestalotiopsis foedans	5/505	6/475	0/340
Neopestalotiopsis hispanica	3/505	8/475	3/340
Neopestalotiopsis javaensis	2/505	3/475	0/340
Neopestalotiopsis maddoxii	6/505	7/475	1/340
Neopestalotiopsis megabetaspora	2/434	11/432	2/371
Neopestalotiopsis mesopotamica	2/505	9/475	1/340
Neopestalotiopsis perukae	5/505	1/475	1/340
Neopestalotiopsis rosae	2/505	7/475	0/340
Neopestalotiopsis scalabiensis	2/505	8/475	0/340
Neopestalotiopsis subepidermalis	3/456	8/432	3/371
Neopestalotiopsis suphanburiensis	2/434	8/411	2/371
Neopestalotiopsis vaccinii	2/505	8/475	3/340

Taxonomy

Neopestalotiopsis guava **A.R. Amirmijani, A. Pordel, & K. Dehghani, sp. nov.**

MycoBank No: 85286
Fig. 3

Holotype. Iran • Sistan and Baluchestan Province, Zar Abad region, from the infected leaves of *Psidium guava*, 5 November 2021, leg. A. Pordel and A.R. Amirmijani (holotype: CUJ0100; ex-type culture: UJFCC2084).

Etymology. Named after the host plant, *Psidium guava*.

Description. Conidiomata, solitary, black, and (300–)500–300(–700) m diam., and glistening conidial masses (Fig. 3E). Conidiogenous cells 6–10 × 2.5–4 µm, discrete, cylindrical, hyaline, smooth, thin-walled, simple, holoblastic-annelidic, percurrently, with collarette present. Conidia 18–30 × 5–7 µm, fusoid, four-septate, smooth, and slightly constricted at the septa; the basal cell thin walled, hyaline, 5–8 µm long; three median cells cylindrical, 15–18 µm long, smooth-walled, with septa darker than the rest of cell; the second cell from the base pale brown and 4–5 µm long; the third cell medium brown and 5 µm long; the fourth cell medium brown and 5 µm long; with septum between the third and fourth cell more distinct, broader, and darker brown than the other septa; the apical cell conic with a subacute apex, thin-walled, smooth, hyaline, 4–6 µm long, and with 2–3(–4) apical appendages (mostly 2) arising from the apical adage; apical appendages unbranched and straight, 11–24 µm long and up to 1 µm wide (n = 100); basal appendage single, filiform, unbranched, centric, 3–5 µm long, and up to 0.5 µm wide (n = 80).

Culture characteristics. Colony on PDA attaining 70 mm diameter after 7 d at 25 °C, surface white and reverse pale cream (Fig. 3A, B), with fluffy white aerial mycelium, conidiomata scattered.

Other specimens examined. Iran • Sistan and Baluchestan Province, Zar Abad region, from the infected leaves of *Psidium guava*, 5 November 2021, leg. A. Pordel and A.R. Amirmijani (cultures UJFCC2084 and UJFCC2086).

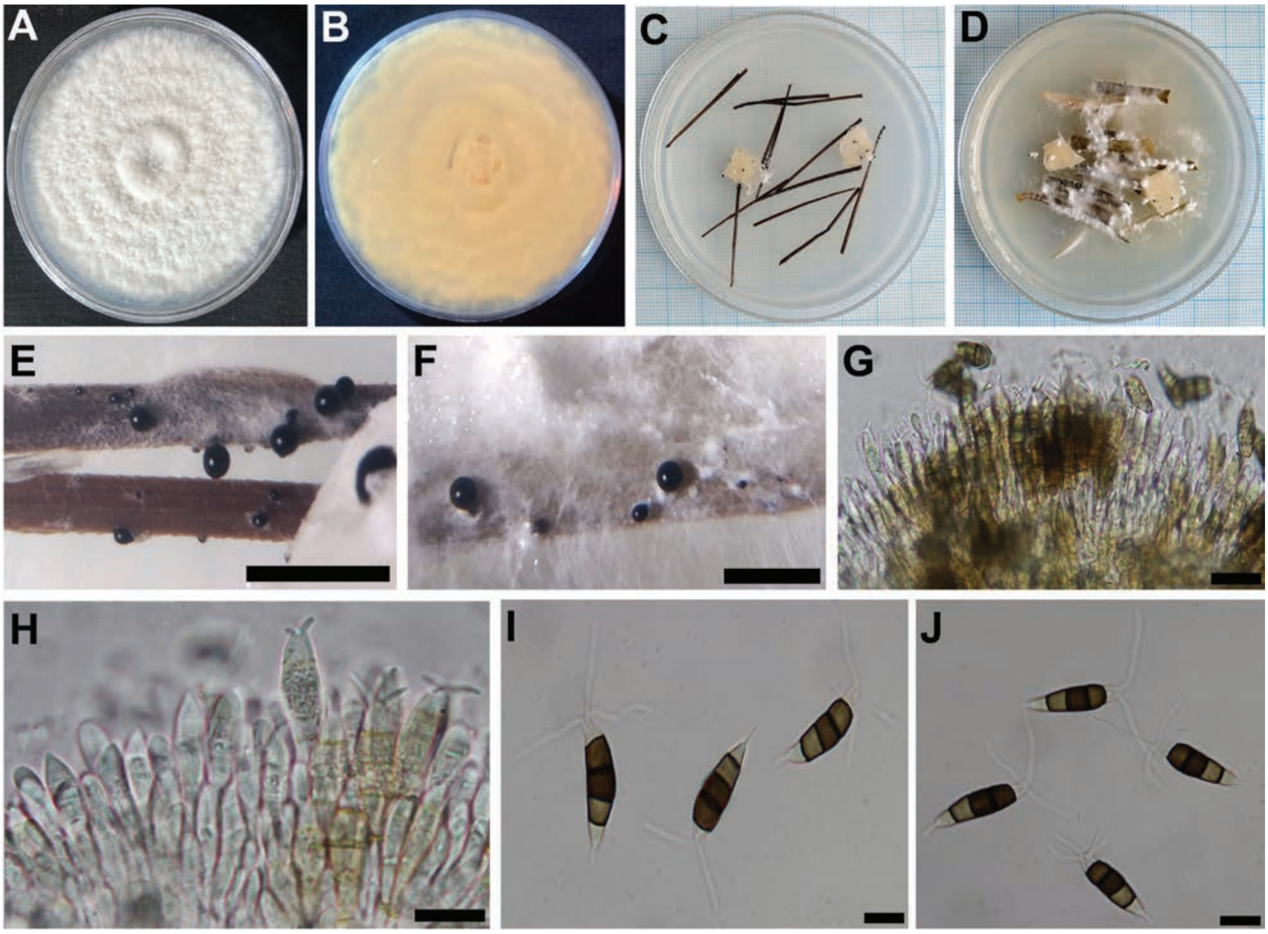

Figure 3. *Neopestalotiopsis guava* (Holotype UJFCC2084) **A, B** surface and reverse of colony after 7 days on PDA **C** colonies on PNA after 7 days **D** colonies on CLA after 7 days **E** conidiomata with black sporulation on PNA **F** conidiomata with black sporulation on CLA **G, H** conidiogenous cells **I, J** conidia with apical and basal appendage. Scale bars: 2 mm (**E, F**); 20 µm (**G, H**); 10 µm (**I, J**).

Notes. *Neopestalotiopsis guava* is phylogenetically closely related to a large clade containing *N. celtidis*, *N. ellipsospora*, *N. eucalyptorum*, *N. foedans*, *N. hispanica*, *N. javaensis*, *N. maddoxii*, *N. megabetaspora*, *N. mesopotamica*, *N. perukae*, *N. rosae*, *N. scalabiensis*, *N. subepidermalis*, *N. suphanburiensis* and *N. vaccinii*. However, distinct morphological differences distinguish it from all these species (Table 3).

Robillarda khodaparastii A.R. Amirmijani, A. Pordel & K. Dehghani, sp. nov.

MycoBank No: 852862
Fig. 4

Holotype. Iran • Sistan and Baluchestan Province, Ghasreghand Abad region, from the infected leaves of *Mangifera indica*, 15 December 2021, leg. A. Pordel and A.R. Amirmijani (holotype: CUJ0103; ex-type culture: UJFCC2116).

Etymology. The species name is suggested as a tribute to our professor, Dr. Seyed Akbar Khodaparast, in recognition of his significant contributions to the progress of mycology in Iran.

Table 3 Morphological comparison of *Neopestalotiopsis* species related to this study.

Species	Conidial size (µm)	Apical appendages		Basal appendage	References
		Number	Length (µm)	Length (µm)	
N. celtidis	17.5–23.5 × 6–8	2–3(–4)	(7.5–)11.5–21(–25)	2–6	Razaghi et al. (2024)
N. ellipsospora	19–25 × 5–6.5	1–3	5–12	3–4	Maharachchikumbura et al. (2012)
N. eucalyptorum	(22.6)27.5–29.2(33.2) × (6.4)7.6–8.1(9.5)	3–4	(12.7)16.2–18.8(27.7)	(3.4)5.4–6.2(8.1)	Diogo et al. (2021)
N. foedans	19–24 × 5.7–6.9	2–3	6–18	3–6	Maharachchikumbura et al. (2012)
N. guava	**18–30 × 5–7**	**2–3(–4)**	**11–24 × 1–1.2**	**3–5 × 0.4–0.5**	**This study**
N. hispanica	(21.4) 22.9–24.1 (29.4) × (7.2)8.2–8.7(9.8)	2–3	(13)18.2–20.3(24.6)	(3.1)5.2–6.1(8.8)	Diogo et al. (2021)
N. javaensis	(24–)25–30(–31) × (6.5–)7–8.5(–9)	1–3	2–10(–18)	2–4	Maharachchikumbura et al. (2014b)
N. maddoxii	25–30 × 7–11	3	15–27	N/A	Prasannath et al. (2021)
N. megabetaspora	(19–)22–28 × 5.5–9	2–4	20–37	(2.5–)4.5–13	Razaghi et al. (2024)
N. mesopotamica	(25–)26–32(–34) × (7–)7.5–9(–9.5)	3–4	(25–)28–38(–41)	4–6.5	Maharachchikumbura et al. (2014b)
N. perukae	19.7 ± 1.4 × 6.4 ± 0.8	2	22.2 ± 5.8	3.8 ± 1.9	Ul Haq et al. (2021)
N. rosae	(20–)22–37(–29) × (7–)7.5–9.5(–10.5)	3–5	(22–)24–31(–33)	5–8	Maharachchikumbura et al. (2014b)
N. scalabiensis	(10.3–)13.8–15.1(–23.3) × (3.7–)4.8–6.6(–5.3)	2–3	5.9–31.8	N/A	Santos et al. (2022)
N. subepidermalis	(19.5–)20–25(–26) × 7.5–9(–9.5)	2–4	(26.5–)27–32.5(–33.5)	(6.5–)7–7.5(–8)	Peng et al. (2022)
N. suphanburiensis	19–29 × 4–7	2–3	9–21	2–11	Sun et al. (2023)
N. vaccinii	(11.0–)13.4–13.8(–15.2) × (4.9–)6.3–6.6(–7.5)	2–3	8.9–25.3	N/A	Santos et al. (2022)

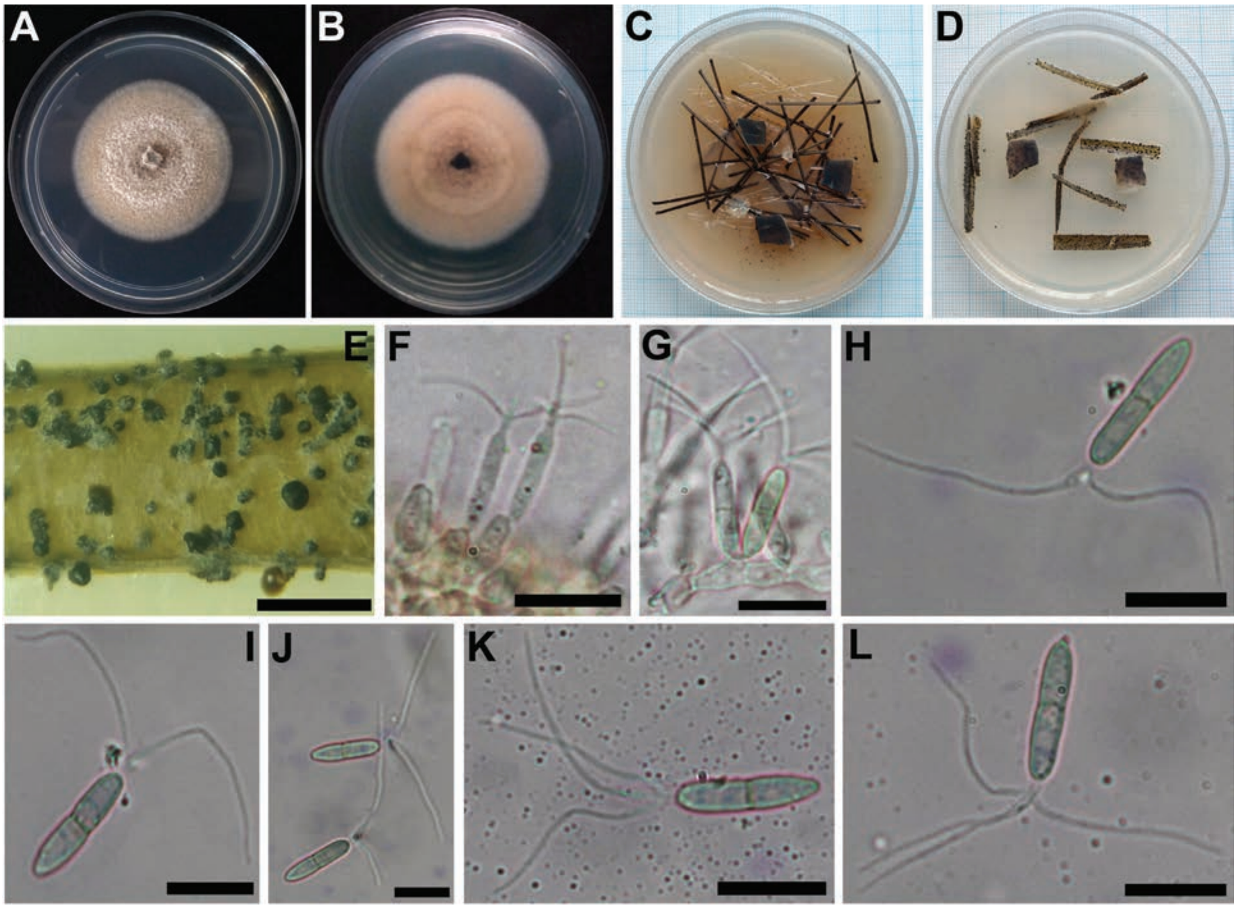

Figure 4. *Robillarda khodaparastii* (Holotype UJFCC2116) **A, B** surface and reverse of colony after 7 days on PDA **C** colonies on PNA after 7 days **D** colonies on CLA after 7 days **E** conidiomata with brown sporulation on CLA **F, G** conidiogenous cells **H–L** conidia with apical appendage. Scale bars: 2 mm (**E**); 10 µm (**F–L**).

Description. Sexual morph undetermined. Asexual morph coelomycetous. Conidiomata 300–340 mm diam., black, semi-immersed, solitary, scattered, irregular shape, glabrous, minutely ostiolate. Conidiophores are reduced to conidiogenous cells. Conidiogenous cells 13–20 × 3–6 μm, holoblastic, proliferation percurrent 1–3 times, discrete, subcylindrical to ampulliform, hyaline, aseptate, smooth-walled. Conidia 12–13 × 2–3 μm (n = 50), hyaline, cylindrical, straight, 1-septate, thin and smooth-walled, apical cell developed into a branched appendage; appendages 12–20 × 1–2.5 μm (n = 50), dividing into 2 branches, straight, non- flexuous, broadly tubular, narrower towards the apex.

Culture characteristics. Colony on PDA and MEA are similar, attaining 75 to 78 mm diameter after 7 d at 25 °C, surface and reverse white to cream (Fig. 4A, B), with fluffy white aerial mycelium, conidiomata scattered.

Other specimen examined. Iran • Sistan and Baluchestan Province, Ghasreghand Abad region, from the infected leaves of *Mangifera indica*, 15 December 2021, leg. A. Pordel and A.R. Amirmijani (cultures UJFCC2117 and UJFCC2118).

Notes. A comparison of sequence data revealed complete identities among the *Robillarda* isolates. This clade was determined as a sister group of *R. roystoneae* (CBS 115445) with maximum ML and MP bootstrap support. *R. khodaparastii* is morphologically and phylogenetically near to *R. roystoneae*, but our species can be easily distinguished from the latter species by producing longer conidiogenous cells [13–20 × 3–6 vs. 7–12 × 2–3 μm] and shorter conidia [12–13 × 2–3 vs. (13–)14–15(–16) × 2.5–3(–3.5) μm].

Discussion

Mango (*Mangifera indica* L.) and Guava (*Psidium guava* L.) are popular fruits in tropical and subtropical regions due to their delicious taste, high nutritional value, and economic importance in international markets (Kumar et al. 2021). The cultivation of mango has expanded beyond traditional and non-traditional production countries like the United Arab Emirates (UAE) (Saeed et al. 2017). Iran's diverse climates, characterized by significant temperature variations between the northern and southern regions, allow for the production of various agricultural products (Saboki et al. 2012).

Several pestalotioid fungi have been reported from diverse hosts in Iran, including: *Pestalotia disseminate*, *Pestalotiopsis acacia*, *P. biciliata*, *P. funereal*, *P. longiseta*, *P. longisetula*, *P. neglecta*, *P. nattrassii*, *P. trachycarpicola*, *P. vismiae*, *P. uvicola*, *Pseudopestalotiopsis theae*, and *Neopestalotiopsis asiatica*, *N. iranensis*, *N. mesopotamica* (Khodaparast and Hedjaroude 1994; Borhani and Mousazadeh 2004; Arzanlou et al. 2012; Naeimi et al. 2015; Ayoubi and Soleimani 2016a, 2016b; Atashi Khalilabad and Fotouhifar 2022; Bakhshi et al. 2022; Amirmijani et al. 2024).

According to Maharachchikumbura et al. (2011, 2013), many species of Pestalotioid fungi have been named based on their host associations due to the lack of reliable distinctive features. However, recent research has demonstrated that many introduced phylogenetic species within Pestalotioid fungi can be distinguished using combined sequence data from ITS-rDNA, β-tubulin (*tub2*), and tef-1α genes. In this study, we employed these gene sequences, along with morphological features, for phylogenetic analysis and species identification. As a result, we described two new species of pestalotioid fungi from Iran. These novel species contribute to a deeper understanding of the taxonomy and diversity of *Neopestalotiopsis* and *Robillarda* in Iran. However, it is likely that our findings represent only the tip of the iceberg.

These fungi were found on leaf spots of mango and guava in southern Iran. Generally, these genera are regarded as insignificant pathogens, however, they have been observed to cause diseases in various crops (Maharachchikumbura et al. 2012). These fungi often act as endophytes or saprobes, and their pathogenic roles still remain little studied and, therefore, inadequately understood. Although these species were isolated from leaf spots, we were unable to conduct pathogenicity tests in this study. Consequently, further research is necessary to evaluate their potential aggressiveness and negative effects on tropical fruits. Accurate species identification of plant-pathogenic genera (Jayawardena et al. 2015), such as Pestalotiopsis-like fungi, is crucial for plant pathologists in managing and controlling plant diseases. Ongoing studies aim to clarify the environmental factors contributing to leaf spot disease to develop effective control measures.

Acknowledgements

The authors thank the Research Deputy of the University of Jiroft, Kerman, Iran, and the Plant Protection Research Department, Baluchestan Agricultural and Natural Resources Research and Education Center, AREEO, Iranshahr, Iran for financial support. We also extend our gratitude to Prof. Sajeewa S. N. Maharachchikumbura, Prof. Ning Jiang, and the other reviewers for reviewing the manuscript and providing insightful suggestions for its improvement.

Additional information

Conflict of interest

The authors have declared that no competing interests exist.

Ethical statement

No ethical statement was reported.

Funding

This work was supported by the Research Deputy of the University of Jiroft, Kerman, Iran, and the Plant Protection Research Department, Baluchestan Agricultural and Natural Resources Research and Education Center, AREEO, Iranshahr, Iran. The study was also supported by the Biodiversa+ Project FUNACTION of the German Science foundation (GR1540/47-1) provided to HPG.

Author contributions

AA, AP: conceptualization, isolation and identification of the producer strain, writing - original draft preparation, review and editing; KS: isolation of the strains; MJP: phylogenetic analysis, writing - review and editing; HM, H-PG: revision and funding.

Author ORCIDs

Amirreza Amirmijani https://orcid.org/0000-0002-4529-4415
Adel Pordel https://orcid.org/0000-0001-5999-9443
Kowsar Dehghani https://orcid.org/0009-0004-2930-3491

Mohammad Javad Pourmoghaddam https://orcid.org/0000-0001-6055-7503
Hans-Peter Grossart https://orcid.org/0000-0002-9141-0325

Data availability

The data that support the findings of this study are available in GenBank (https://www.ncbi.nlm.nih.gov/genbank/) and in culture collections and fungal herbarium, as shown in Table 1 and the text.

References

Akinsanmi OA, Nisa S, Jeff-Ego OS, Shivas RG, Drenth A (2017) Dry flower disease of macadamia in australia caused by *Neopestalotiopsis macadamiae* sp. nov. and *Pestalotiopsis macadamiae* sp. nov. Plant Disease 101(1): 45–53. https://doi.org/10.1094/PDIS-05-16-0630-RE

Amirmijani A, Fotouhifar K, Atashi Khalilabd A, Seyedi N (2024) *Pestalotiopsis biciliata*, a new record for funga of Iran. Mycologia Iranica 11(1): 67–73. https://doi.org/10.22043/MI.2024.365761.1282

Arzanlou M, Torbati M, Khodaei S, Bakhshi M (2012) Contribution to the knowledge of Pestalotioid fungi of Iran. Mycosphere 3(5): 871–878. https://doi.org/10.5943/mycosphere/3/5/12

Atashi Khalilabad A, Fotouhifar K (2022) Morphological and molecular characterization of a novel *Pestalotiopsis trachycarpicola*, causing Garden Croton leaf spot in Iran. Mycologia Iranica 9: 59–66. https://doi.org/10.22043/MI.2022.360270.1236

Ayoubi N, Soleimani MJ (2016a) Strawberry fruit rot caused by *Neopestalotiopsis iranensis* sp. nov., and *N. mesopotamica*. Current Microbiology 72: 329–336. https://doi.org/10.1007/s00284-015-0955-y

Ayoubi N, Soleimani MJ (2016b) Morphological and molecular identification of *Neopestalotiopsis asiatica* causing leaf spot on sweet almond. Journal of Plant Pathology 98(2): 321–325. https://doi.org/10.4454/JPP.V98I2.030

Bakhshi M, Zare R, Ershad D (2022) A detailed account on the statistics of the Fungi and fungus-like taxa of Iran. Mycologia Iranica 9: 1–96. https://doi.org/10.22043/MI.2023.360819.1244

Bezerra JDP, Machado AR, Firmino AL, Rosado AWC, Souza CAF, Souza-Motta CM, Freire KTLS, Paiva LM, Magalhães OMC, Pereira OL, Crous PW, Oliveira TGL, Abreu VP, Fan X (2018) Mycological diversity description I. Acta Botanica Brasílica 32(4): 656–666. https://doi.org/10.1590/0102-33062018abb0154

Borhani A, Mousazadeh S (2004) Study on the hosts and pathogenicity of *Pestalotiopsis funerea* (Desm.) Steyaert on some soft wood species in Mazandaran Province. Proceedings of the 16th Iranian Plant Protection Congress, Vol. II, 28 Aug.–1 Sept., Tabriz, Iran, 441 pp.

Carbone I, Kohn LM (1999) A method for designing primer sets for speciation studies in filamentous ascomycetes. Mycologia 91: 553–556. https://doi.org/10.1080/00275514.1999.12061051

Crous PW, Giraldo A, Hawksworth DL, Robert V, Kirk PM, Guarro J, Robbertse B, Schoch CL, Damm U, Trakunyingcharoen T, Groenewald JZ (2014) The Genera of Fungi: Fixing the application of type species of generic names. IMA Fungus 5(1): 141–160. https://doi.org/10.5598/imafungus.2014.05.01.14

Crous PW, Carris LM, Giraldo A, Groenewald JZ, Hawksworth DL, Hemández-Restrepo M, Jaklitsch WM, Lebrun M-H, Schumacher RK, Stielow JB, van der Linde EJ, Vilcāne

J, Voglmayr H, Wood AR (2015a) The genera of fungi-fixing the application of the type species of generic names–G 2: *Allantophomopsis*, *Latorua*, *Macrodiplodiopsis*, *Macrohilum*, *Milospium*, *Protostegia*, *Pyricularia*, *Robillarda*, *Rotula*, *Septoriella*, *Torula*, and *Wojnowicia*. IMA Fungus 6(1): 163–198. https://doi.org/10.5598/imafungus.2015.06.01.11

Crous PW, Wingfield MJ, Roux JJ le, Richardson DM, Strasberg D, Shivas RG, Alvarado P, Edwards J, Moreno G, Sharma R, Sonawane MS, Tan YP, Altés A, Barasubiye T, Barnes CW, Blanchette RA, Boertmann D, Bogo A, Carlavilla JR, Cheewangkoon R, Daniel R, de Beer ZW, Yáñez-Morales M de Jesús; Duong TA, Fernández-Vicente J, Geering ADW, Guest DI, Held BW, Heykoop M, Hubka V, Ismail AM, Kajale SC, Khemmuk W, Kolařík M, Kurli R, Lebeuf R, Lévesque CA, Lombard L, Magista D, Manjón JL, Marincowitz S, Mohedano JM, Nováková A, Oberlies NH, Otto EC, Paguigan ND, Pascoe IG, Pérez-Butrón JL, Perrone G, Rahi P, Raja HA, Rintoul T, Sanhueza RMV, Scarlett K, Shouche YS, Shuttleworth LA, Taylor PWJ, Thorn RG, Vawdrey LL, Solano-Vidal R, Voitk A, Wong PTW, Wood AR, Zamora JC, Groenewald JZ (2015b) Fungal planet description sheets: 371–399. Persoonia 35(1): 264–327. https://doi.org/10.3767/003158515X690269

Crous PW, Wingfield MJ, Chooi YH, Gilchrist CLM, Lacey E, Pitt JI, Roets F, Swart WJ, Cano-Lira JF, Valenzuela-Lopez N, Hubka V, Shivas RG, Stchigel AM, Holdom DG, Jurjević Ž, Kachalkin AV, Lebel T, Lock C, Martín MP, Tan YP, Tomashevskaya MA, Vitelli JS, Baseia IG, Bhatt VK, Brandrud TE, De Souza JT, Dima B, Lacey HJ, Lombard L, Johnston PR, Morte A, Papp V, Rodríguez A, Rodríguez-Andrade E, Semwal KC, Tegart L, Abad ZG, Akulov A, Alvarado P, Alves A, Andrade JP, Arenas F, Asenjo C, Ballarà J, Barrett MD, Berná LM, Berraf-Tebbal A, Bianchinotti MV, Bransgrove K, Burgess TI, Carmo FS, Chávez R, Čmoková A, Dearnaley JDW, Santiago ALCM de A, Freitas-Neto JF, Denman S, Douglas B, Dovana F, Eichmeier A, Esteve-Raventós F, Farid A, Fedosova AG, Ferisin G, Ferreira RJ, Ferrer A, Figueiredo CN, Figueiredo YF, Reinoso-Fuentealba CG, Garrido-Benavent I, Cañete-Gibas CF, Gil-Durán C, Glushakova AM, Gonçalves MFM, González M, Gorczak M, Gorton C, Guard FE, Guarnizo AL, Guarro J, Gutiérrez M, Hamal P, Hien LT, Hocking AD, Houbraken J, Hunter GC, Inácio CA, Jourdan M, Kapitonov VI, Kelly L, Khanh TN, Kisło K, Kiss L, Kiyashko A, Kolařík M, Kruse J, Kubátová A, Kučera V, Kučerová I, Kušan I, Lee HB, Levicán G, Lewis A, Liem NV, Liimatainen K, Lim HJ, Lyons MN, Maciá-Vicente JG, Magaña-Dueñas V, Mahiques R, Malysheva EF, Marbach PAS, Marinho P, Matočec N, McTaggart AR, Mešić A, Morin L, Muñoz-Mohedano JM, Navarro-Ródenas A, Nicolli CP, Oliveira RL, Otsing E, Ovrebo CL, Pankratov TA, Paños A, Paz-Conde A, Pérez-Sierra A, Phosri C, Pintos Á, Pošta A, Prencipe S, Rubio E, Saitta A, Sales LS, Sanhueza L, Shuttleworth LA, Smith J, Smith ME, Spadaro D, Spetik M, Sochor M, Sochorová Z, Sousa JO, Suwannasai N, Tedersoo L, Thanh HM, Thao LD, Tkalčec Z, Vaghefi N, Venzhik AS, Verbeken A, Vizzini A, Voyron S, Wainhouse M, Whalley AJS, Wrzosek M, Zapata M, Zeil-Rolfe I, Groenewald JZ (2020) Fungal planet description sheets: 1042–1111. Persoonia - Molecular Phylogeny and Evolution Fungi 44: 301–459. https://doi.org/10.3767/persoonia.2020.44.11

Diogo E, Gonçalves CI, Silva AC, Valente C, Bragança H, Phillips AJ (2021) Five new species of *Neopestalotiopsis* associated with diseased *Eucalyptus* spp. in Portugal. Mycological Progress 20(11): 1441–1456. https://doi.org/10.1007/s11557-021-01741-5

FAO (2020) Major Tropical Fruits Market Review 2019. Rome.

FAO (2024) Major Tropical Fruits Market Review. Preliminary Results 2023. Rome.

Fiorenza A, Gusella G, Aiello D, Polizzi G, Voglmayr H (2022) *Neopestalotiopsis siciliana* sp. nov. and *N. rosae* causing stem lesion and dieback on avocado plants in Italy. Journal of Fungi 8(6): 562. https://doi.org/10.3390/jof8060562

Glass NL, Donaldson GC (1995) Development of primer sets designed for use with the PCR to amplify conserved genes from filamentous ascomycetes. Applied and Environmental Microbiology 61(4):1323–1330. https://doi.org/10.1128/aem.61.4.1323-1330.1995

He YK, Yang Q, Sun YR, Zeng XY, Jayawardena RS, Hyde KD, Wang Y (2022) Additions to *Neopestalotiopsis* (Amphisphaeriales, Sporocadaceae) fungi: Two new species and one new host record from China. Biodiversity Data Journal 10: e90709. https://doi.org/10.3897/BDJ.10.e90709

Hsu SY, Xu YC, Lin YC, Chuang WY, Lin SR, Stadler M, Tangthirasunun N, Cheewangkoon R, AL-Shwaiman HA, Elgorban AM, Ariyawansa HA (2024) Hidden diversity of *Pestalotiopsis* and *Neopestalotiopsis* (Amphisphaeriales, Sporocadaceae) species allied with the stromata of entomopathogenic fungi in Taiwan. MycoKeys 101: 275–312. https://doi.org/10.3897/mycokeys.101.113090

Huanlauek N, Jayawardena RS, Maharachchikumbura SSN, Harishchandra DL (2021) Additions to pestalotioid fungi in Thailand: *Neopestalotiopsis hydeana* sp. nov., *Pestalotiopsis hydei* sp. nov. Phytotaxa 479(1): 23–43. https://doi.org/10.11646/phytotaxa.479.1.2

Jayawardena RS, Zhang W, Liu M, Maharachchikumbura SSN, Zhou Y, Huang JB, Nilthong S, Wang ZY, Li XH, Yan JY, Hyde KD (2015) Identification and characterization of *Pestalotiopsis*-like fungi related to grapevine diseases in China. Fungal Biology 119(5): 348–361. https://doi.org/10.1016/j.funbio.2014.11.001

Jayawardena RS, Liu M, Maharachchikumbura SSN, Zhang W, Xing QK, Hyde KD, Nilthong S, Li XH, Yan JY (2016) *Neopestalotiopsis vitis* sp. nov. causing grapevine leaf spot in China. Phytotaxa 258(1): 63–74. https://doi.org/10.11646/phytotaxa.258.1.4

Jiang N, Fan X, Tian C (2021) Identification and characterization of leaf-inhabiting fungi from *Castanea plantations* in China. Journal of Fungi 7(1): 64. https://doi.org/10.3390/jof7010064

Jiang N, Voglmayr H, Xue H, Piao CG, Li Y (2022) Morphology and Phylogeny of *Pestalotiopsis* (Sporocadaceae, Amphisphaeriales) from Fagaceae Leaves in China. Microbiology Spectrum 10(6): 1–28. https://doi.org/10.1128/spectrum.03272-22

Katoh K, Rozewicki J, Yamada KD (2019) MAFFT online service: Multiple sequence alignment, interactive sequence choice and visualization. Briefings in Bioinformatics 20(4): 1160–1166. https://doi.org/10.1093/bib/bbx108

Khodaparast SA, Hedjaroude GhA (1994) Incidence of a new *Pestalotiopsis* species in association with grey blight of tea in Guilan. Iranian Journal of Plant Pathology 30: 79–80 [in Persian], 33 [in English].

Konta S, Tibpromma S, Karunarathna SC, Samarakoon MC, Steven LS, Mapook A, Boonmee S, Senwanna C, Balasuriya A, Eungwanichayapant PD, Hyde KD (2023) Morphology and multigene phylogeny reveal ten novel taxa in Ascomycota from terrestrial palm substrates (Arecaceae) in Thailand. Mycosphere 14(1): 107–152. https://doi.org/10.5943/mycosphere/14/1/2

Kumar S, Stecher G, Tamura K (2016) MEGA7: Molecular Evolutionary Genetics Analysis version 7.0 for bigger datasets. Molecular Biology and Evolution 33(7): 1870–1874. https://doi.org/10.1093/molbev/msw054

Kumar V, Cheewangkoon R, Gentekaki E, Maharachchikumbura SSN, Brahmanage RS, Hyde KD (2019) *Neopestalotiopsis alpapicalis* sp. nov. a new endophyte from tropical mangrove trees in Krabi Province (Thailand). Phytotaxa 393(3): 251–262. https://doi.org/10.11646/phytotaxa.393.3.2

Kumar M, Tomar M, Amarowicz R, Saurabh V, Nair MS, Maheshwari C, Sasi M, Prajapati U, Hasan M, Singh S, Changan S, Prajapat RK, Berwal MK, Satankar V (2021)

Guava (*Psidium guajava* L.) leaves: Nutritional composition, phytochemical profile, and health-promoting bioactivities. Foods 10(4): 752. https://doi.org/10.3390/foods10040752

Li WL, Dissanayake AJ, Zhang T, Maharachchikumbura SSN, Liu JK (2022) Identification and pathogenicity of Pestalotiod Fungi associated with woody oil plants in Sichuan Province, China. Journal of Fungi 8(11): 1175. https://doi.org/10.3390/jof8111175

Liu F, Bonthond G, Groenewald JZ, Cai L, Crous PW (2019) Sporocadaceae, a family of coelomycetous fungi with appendage-bearing conidia. Studies in Mycology 92(1): 287–415. https://doi.org/10.1016/j.simyco.2018.11.001

Liu X, Tibpromma S, Zhang F, Xu J, Chethana KWT, Karunarathna SC, Mortimer PE (2021) *Neopestalotiopsis cavernicola* sp. nov. from Gem Cave in Yunnan Province, China. Phytotaxa 512(1): 1–27. https://doi.org/10.11646/phytotaxa.512.1.1

Ma XY, Maharachchikumbura SSN, Chen BW, Hyde KD, McKenzie EHC, Chomnunti P, Kang J-C (2019) Endophytic pestalotiod taxa in *Dendrobium* orchids. Phytotaxa 419(3): 268–286. https://doi.org/10.11646/phytotaxa.419.3.2

Maharachchikumbura SSN, Guo LD, Chukeatirote E, Bahkali AH, Hyde KD (2011) *Pestalotiopsis*—Morphology, phylogeny, biochemistry and diversity. Fungal Diversity 50(1): 167–187. https://doi.org/10.1007/s13225-011-0125-x

Maharachchikumbura SSN, Guo LD, Cai L, Chukeatirote E, Wu WP, Sun X, Crous PW, Bhat DJ, McKenzie EHC, Bahkali AH, Hyde KD (2012) A multilocus backbone tree for *Pestalotiopsis*, with a polyphasic characterization of 14 new species. Fungal Diversity 56(1): 95–129. https://doi.org/10.1007/s13225-012-0198-1

Maharachchikumbura SSN, Guo LD, Chukeatirote E, McKenzie EHC, Hyde KD (2013) A destructive new disease of *Syzygium samarangense* in Thailand caused by the new species *Pestalotiopsis samarangensis*. Tropical Plant Pathology 38(3): 227–235. https://doi.org/10.1590/S1982-56762013005000002

Maharachchikumbura SSN, Guo LD, Chukeatirote E, Hyde KD (2014a) Improving the backbone tree for the genus *Pestalotiopsis*; addition of *P. steyaertii* and *P. magna* sp. nov. Mycological Progress 13(3): 617–624. https://doi.org/10.1007/s11557-013-0944-0

Maharachchikumbura SSN, Hyde KD, Groenewald JZ, Xu J, Crous PW (2014b) *Pestalotiopsis* revisited. Studies in Mycology 79(1): 121–186. https://doi.org/10.1016/j.simyco.2014.09.005

Maharachchikumbura SSN, Larignon P, Hyde KD, Al-Sadi AM, Liu ZY (2016) Characterization of *Neopestalotiopsis*, *Pestalotiopsis* and *Truncatella* species associated with grapevine trunk diseases in France. Phytopathologia Mediterranea 55(3): 380–390. https://doi.org/10.14601/Phytopathol_Mediterr-18298

Manawasinghe IS, Calabon MS, Jones EBG, Zhang YX, Liao CF, Xiong YR, Chaiwan N, Kularathnage ND, Liu NG, Tang SM, Sysouphanthong P, Du TY, Luo M, Pasouvang P, Pem D, Phonemany M, Ishaq M, Chen JW, Karunarathna SC, Mai ZL, Rathnayaka AR, Samarakoon MC, Tennakoon DS, Wijesinghe SN, Yang YH, Zhao HJ, Fiaz M, Doilom M, Dutta AK, Khalid AN, Liu JW, Thongklang N, Senanayake IC, Tibpromma S, You LQ, Camporesi E, Gafforov YS, Hyde KD KD (2022) Mycosphere notes 345–386. Mycosphere 13(1): 454–557. https://doi.org/10.5943/mycosphere/13/1/3

Marin-Felix Y, Hernández-Restrepo M, Iturrieta-González I, García D, Gené J, Groenewald JZ, Cai L, Chen Q, Quaedvlieg W, Schumacher RK, Taylor PWJ, Ambers C, Bonthond G, Edwards J, Krueger-Hadfield SA, Luangsa-Ard JJ, Morton L, Moslemi A, Sandoval-Denis M, Tan YP, Thangavel R, Vaghefi N, Cheewangkoon R, Crous PW (2019) Genera of phytopathogenic fungi: GOPHY 3. Studies in Mycology 94: 1–124. https://doi.org/10.1016/j.simyco.2019.05.001

Naeimi S, Javadi L, Javadi AR (2015) First report of *Pestalotia disseminata*, the causal agent of feijoa fruit rot in Iran. Mycologia Iranica 2(1): 75–76. https://doi.org/10.22043/mi.2015.14228

Norphanphoun C, Jayawardena RS, Chen Y, et al. (2019) Morphological and phylogenetic characterization of novel pestalotioid species associated with mangroves in Thailand. Mycosphere 10(1): 531–578. https://doi.org/10.5943/mycosphere/10/1/9

O'Donnell K, Kistler HC, Cigelnik E, Ploetz RC (1998) Multiple evolutionary origins of the fungus causing Panama disease of banana: Concordant evidence from nuclear and mitochondrial gene genealogies. Proceedings of the National Academy of Sciences of the United States of America 95(5): 2044–2049. https://doi.org/10.1073/pnas.95.5.2044

Peng C, Crous PW, Jiang N, Fan XL, Liang YM, Tian CM (2022) Diversity of Sporocadaceae (pestalotioid fungi) from Rosa in China. Persoonia 49(1): 201–260. https://doi.org/10.3767/persoonia.2022.49.07

Phookamsak R, Hyde KD, Jeewon R, Bhat DJ, Jones EBG, Maharachchikumbura SSN, Raspé O, Karunarathna SC, Wanasinghe DN, Hongsanan S, Doilom M, Tennakoon DS, Machado AR, Firmino AL, Ghosh A, Karunarathna A, Mešić A, Dutta AK, Thongbai B, Devadatha B, Norphanphoun C, Senwanna C, Wei D, Pem D, Ackah FK, Wang G-N, Jiang H-B, Madrid H, Lee HB, Goonasekara ID, Manawasinghe IS, Kušan I, Cano J, Gené J, Li J, Das K, Acharya K, Raj KNA, Latha KPD, Chethana KWT, He M-Q, Dueñas M, Jadan M, Martín MP, Samarakoon MC, Dayarathne MC, Raza M, Park MS, Telleria MT, Chaiwan N, Matočec N, de Silva NI, Pereira OL, Singh PN, Manimohan P, Uniyal P, Shang Q-J, Bhatt RP, Perera RH, Alvarenga RLM, Nogal-Prata S, Singh SK, Vadthanarat S, Oh S-Y, Huang S-K, Rana S, Konta S, Paloi S, Jayasiri SC, Jeon SJ, Mehmood T, Gibertoni TB, Nguyen TTT, Singh U, Thiyagaraja V, Sarma VV, Dong W, Yu X-D, Lu Y-Z, Lim YW, Chen Y, Tkalčec Z, Zhang Z-F, Luo Z-L, Daranagama DA, Thambugala KM, Tibpromma S, Camporesi E, Bulgakov TS, Dissanayake AJ, Senanayake IC, Dai DQ, Tang L-Z, Khan S, Zhang H, Promputtha I, Cai L, Chomnunti P, Zhao R-L, Lumyong S, Boonmee S, Wen T-C, Mortimer PE, Xu J (2019) Fungal diversity notes 929–1035: Taxonomic and phylogenetic contributions on genera and species of fungi. Fungal Diversity 95(1): 1–273. https://doi.org/10.1007/s13225-019-00421-w

Prasannath K, Shivas RG, Galea VJ, Akinsanmi OA (2021) *Neopestalotiopsis* species associated with flower diseases of *Macadamia integrifolia* in Australia. Journal of Fungi 7(9): 771. https://doi.org/10.3390/jof7090771

Prematunga CJ, You LQ, Gomdola D, Balasuriya A, Yang YH, Jayawardena RS, Luo M (2022) An addition to pestalotioid fungi in China: *Neopestalotiopsis fragariae* sp. nov. causing leaf spots on *Fragaria ananassa.* Asian Journal of Mycology 5(2): 220–238. https://doi.org/10.5943/ajom/5/2/10

Razaghi P, Raza M, Han SL, Ma ZY, Cai L, Zhao P, Chen Q, Phurbu D, Liu F (2024) Sporocadaceae revisited. Studies in Mycology 109: 155–272. https://doi.org/10.3114/sim.2024.109.03

Refaei J, Jones EBG, Sakayaroj J, Santhanam J (2011) Endophytic fungi from *Rafflesia cantleyi*: Species diversity and antimicrobial activity. Mycosphere 2: 429–447.

Rodríguez-Gálvez E, Hilário S, Lopes A, Alves A (2022) Diversity and pathogenicity of *Lasiodiplodia* and *Neopestalotiopsis* species associated with stem blight and dieback of blueberry plants in Peru. European Journal of Plant Pathology 157(1): 89–102. https://doi.org/10.1007/s10658-020-01983-1

Saboki E, Usha K, Singh B (2012) Plant architectural traits and their role in defense mechanism against malformation in mango (*Mangifera Indica* L.). Scientia Horticulturae 139: 25–31. https://doi.org/10.1016/j.scienta.2012.02.025

Saboki E, Usha K, Singh B (2014) Screening for resistance to malformation in mango (*Mangifera indica* L.). Progressive Horticulture 46: 209–216.

Saccardo PA (1880) Conspectus generum fungorum italiae inferiorum nempe ad Sphaeropsideas, Melanconieas et Hyphomyceteas pertinentium, systemate sporologico dispositu. Michelia 2: 1–38.

Saeed EE, Sham A, AbuZarqa A, A. Al Shurafa K, S. Al Naqbi T, Iratni R, El-Tarabily K, F. AbuQamar S (2017) Detection and Management of Mango Dieback Disease in the United Arab Emirates. International Journal of Molecular Sciences 18(10): 2086. https://doi.org/10.3390/ijms18102086

Santos J, Hilário S, Pinto G, Alves A (2022) Diversity and pathogenicity of pestalotioid fungi associated with blueberry plants in Portugal, with description of three novel species of *Neopestalotiopsis*. European Journal of Plant Pathology 162(3): 539–555. https://doi.org/10.1007/s10658-021-02419-0

Shu J, Yu Z, Sun W, Zhao J, Li Q, Tang L, Guo T, Huang S, Mo J, Hsiang T, Luo S (2020) Identification and characterization of pestalotioid fungi causing leaf spots on mango in southern China. Plant Disease 104(4): 1207–1213. https://doi.org/10.1094/PDIS-03-19-0438-RE

Silvério ML, de Cavalcanti MA, Q, Silva GA da, et al. (2016) A new epifoliar species of *Neopestalotiopsis* from Brazil. Agrotópica 28(2): 151–158. https://doi.org/10.21757/0103-3816.2016v28n2p151-158

Silvestro D, Michalak I (2012) raxmlGUI: A graphical front-end for RAxML. Organisms, Diversity & Evolution 12(4): 335–337. https://doi.org/10.1007/s13127-011-0056-0

Song YU, Geng KUN, Hyde KD, Zhao W-S, Wei J-G, Kang J-C, Wang Y (2013) Two new species of *Pestalotiopsis* from Southern China. Phytotaxa 126(1): 22–32. https://doi.org/10.11646/phytotaxa.126.1.2

Song Y, Maharachchikumbura SS, Jiang YL, Hyde KD, Wang Y (2014) *Pestalotiopsis keteleeria* sp. nov., isolated from *Keteleeria pubescens* in China. Warasan Khana Witthayasat Maha Witthayalai Chiang Mai 41: 885–893.

Stamatakis A (2006) RAxML-VI-HPC: Maximum likelihood-based phylogenetic analyses with thousands of taxa and mixed models. Bioinformatics 22(21): 2688–2690. https://doi.org/10.1093/bioinformatics/btl446

Sun YR, Jayawardena RS, Sun JE, Wang Y (2023) Pestalotioid species associated with medicinal plants in southwest China and Thailand. Microbiology Spectrum 11(1): e03987–22. https://doi.org/10.1128/spectrum.03987-22

Sutton BC (1980) The Coelomycetes: Fungi Imperfecti with Pycnidia Acervuli and Stromata. Commonwealth Mycological Institute, Kew, 696 pp.

Swofford DL (2002) PAUP* 4.0b10: phylogenetic analysis using parsimony (*and other methods). Sinauer Associates, Sunderland.

Tibpromma S, Hyde KD, McKenzie EHC, Bhat DJ, Phillips AJL, Wanasinghe DN, Samarakoon MC, Jayawardena RS, Dissanayake AJ, Tennakoon DS, Doilom M, Phookamsak R, Tang AMC, Xu J, Mortimer PE, Promputtha I, Maharachchikumbura SSN, Khan S, Karunarathna SC (2018) Fungal diversity notes 840–928: Micro-fungi associated with Pandanaceae. Fungal Diversity 93(1): 1–160. https://doi.org/10.1007/s13225-018-0408-6

Ul Haq I, Ijaz S, Khan NA (2021) Genealogical concordance of phylogenetic species recognition-based delimitation of *Neopestalotiopsis* species associated with leaf spots and fruit canker disease affected guava plants. Pakistan Journal of Agricultural Sciences 58(4): 1301–1313. https://doi.org/10.21162/PAKJAS/21.1045

White TJ, Bruns TD, Lee S, Taylor S (1990) Amplification and direct sequencing of fungal ribosomal RNA genes for phylogenetics. In: Innis MA, Gelfand DH, Sninsky JJ, White

TJ (Eds) PCR - Protocols and Applications - A Laboratory Manual, Academic Press, New York, 315–322. https://doi.org/10.1016/B978-0-12-372180-8.50042-1

Yang Q, Zeng XY, Yuan J, Zhang Q, He YK, Wang Y (2021) Two new species of *Neopestalotiopsis* from southern China. Biodiversity Data Journal 9: e70446. https://doi.org/10.3897/BDJ.9.e70446

Zhong S, Steffenson BJ (2001) Virulence and molecular diversity in *Cochliobolus sativus.* Phytopathology 91(5): 469–476. https://doi.org/10.1094/PHYTO.2001.91.5.469

Supplementary material 1

Phylogenetic trees

Authors: Amirreza Amirmijani, Adel Pordel, Kowsar Dehghani, Mohammad Javad Pourmoghaddam, Hossein Masigol, Hans-Peter Grossart

Data type: rar

Explanation note: Single gene trees for all loci for both genera.

Link: https://doi.org/10.3897/mycokeys.115.136469.suppl1

MycoKeys

MycoKeys 115: 241–271 (2025)
DOI: 10.3897/mycokeys.115.148914

Research Article

Three new species of *Fusarium* (Nectriaceae, Hypocreales) isolated from Eastern Cape dairy pastures in South Africa

Claudette Dewing[1], Cobus M. Visagie[1], Emma T. Steenkamp[1], Brenda D. Wingfield[1], Neriman Yilmaz[1]

1 Department of Biochemistry, Genetics and Microbiology, Forestry and Agricultural Biotechnology Institute (FABI), Faculty of Natural and Agricultural Sciences, University of Pretoria, Pretoria, South Africa
Corresponding author: Neriman Yilmaz (neriman.yilmaz@fabi.up.ac.za)

Abstract

A survey of the fungal diversity associated with mixed pastures from Eastern Cape dairy farms in South Africa led to the isolation of 155 *Fusarium* strains that belong to the *Fusarium incarnatum-equiseti* species complex (FIESC). Using single and multigene phylogenies based on partial sequences of the translation elongation factor 1-alpha (*TEF*), calmodulin (*CaM*), and the partial RNA polymerase second largest subunit (*RPB2*) genes, we identified 11 species. They included *F. brevicaudatum*, *F. clavus*, *F. coffeatum*, *F. croceum*, *F. goeppertmayerae*, and *F. heslopiae*, with five species that were found to be new. Based on morphological and phylogenetic data, three new species are formally described here as *F. cumulatum*, *F. mariecurieae*, and *F. pascuum*. We also provided a description for *F. goeppertmayerae*, as the authors who identified and named this species did not include one. We have chosen to not describe the remaining species, as our cultures lack proper morphological structure development. This study shows that mixed pastures harbour a diverse range of *Fusarium* species and highlights the need for further studies into their potential to impact animal health.

Key words: *Fusarium camptoceras*, GCPSR, molecular phylogenetics, morphology, mycotoxins

Academic editor: Rajesh Jeewon
Received: 6 February 2025
Accepted: 3 March 2025
Published: 20 March 2025

Citation: Dewing C, Visagie CM, Steenkamp ET, Wingfield BD, Yilmaz N (2025) Three new species of *Fusarium* (Nectriaceae, Hypocreales) isolated from Eastern Cape dairy pastures in South Africa. MycoKeys 115: 241–271. https://doi.org/10.3897/mycokeys.115.148914

Introduction

Well-maintained pastures are important for promoting the well-being of cattle, as they directly impact the animals' nutrition, overall health and productivity (Marais 2001; Neal et al. 2007; Botha et al. 2008a, 2008b; Doxey 2014; van der Colf et al. 2015). Several grass species from Poaceae are used for grazing worldwide (Charlton and Stewart 1999; Lowe 2009; Truter et al. 2015). In South Africa the preferred species are *Cenchrus clandestinus* (formerly known as *Pennisetum clandestinum*; kikuyu), *Lolium multiflorum* (annual ryegrass) and *L. perenne* (perennial ryegrass) (Truter et al. 2015). Despite the obvious nutritional value of pastures, they can also pose health risks to grazing animals under certain circumstances, e.g., kikuyu poisoning in cattle (Bryson and Newsholme 1978; Newsholme et al. 1983; Wong et al. 1987; Bourke 2007; Ryley et al. 2007; Botha et al. 2014) or when the growth of mycotoxigenic fungi leads to mycotoxin build-up in pastures (Golinski et al. 2003; Driehuis et al. 2008; Skládanka et al. 2011; Penagos-Tabares et al. 2021).

Among the various factors that could affect the health of grazing cattle, *Fusarium* species and their mycotoxins pose a significant risk. The genus *Fusarium* comprises a diverse group of filamentous fungi that play significant roles in various ecological and agricultural contexts because of the range of lifestyles they exhibit, including saprotrophic and endophytic modes, often associated with various grass hosts (Leslie et al. 2004; Bentley et al. 2007; Summerell et al. 2010; Nor Azliza et al. 2014; Laurence et al. 2016). Some *Fusarium* species are also well-known pathogens to animals, humans and plants, and are important producers of mycotoxins (Desjardins 2006; Leslie and Summerell 2006; O'Donnell et al. 2013; Gallo et al. 2022). *Fusarium* mycotoxins that are particularly important from a toxicological standpoint include deoxynivalenol (Reed and Moore 2009; Skládanka et al. 2011; Burkin and Kononenko 2015; Penagos-Tabares et al. 2021), fumonisins (Reed and Moore 2009; Gott et al. 2017) and zearalenone (di Menna et al. 1987; Reed et al. 2004; Reed and Moore 2009; Skládanka et al. 2011; Burkin and Kononenko 2015; Nichea et al. 2015; Penagos-Tabares et al. 2021). These toxins can cause severe health issues in animals, including abnormal foetal development, disruptions in cell division and membrane function, reduced feed intake leading to body weight loss, fertility problems, immunosuppression, inhibition of protein synthesis, impaired mitochondrial function and, in severe cases, death (Trenholm et al. 1985; Weaver et al. 1986; Smith et al. 1990; Edrington et al. 1995; Moretti et al. 2013; Eskola et al. 2018; Aranega and Oliveira 2022). Furthermore, certain *Fusarium* species and their associated mycotoxins have been suggested as potential contributors to kikuyu poisoning cases in South Africa and Australia (Ryley et al. 2007; Botha et al. 2014). However, this connection remains hypothetical and unconfirmed due to limited availability of supporting data.

In 2020, cattle in the Eastern Cape province of South Africa showed symptoms of facial eczema, a type of hepatogenous photosensitivity caused by the mycotoxin sporidesmin A, produced by the fungus *Pseudopithomyces chartarum* (= *Pithomyces chartarum*) (Brook 1963; di Menna et al. 1970; Marasas and Schumann 1972; Kellerman et al. 1980; Kellerman and Coetzer 1985; Davis et al. 2021). A fungal survey was subsequently conducted at 14 dairy farms to first determine whether *P. chartarum* was present in affected pastures and second to identify other culturable fungi that may also be present (Dewing et al. 2025). The survey revealed *Fusarium* as the most commonly isolated genus, particularly species within the *Fusarium incarnatum-equiseti* species complex (FIESC). However, some strains in the complex could not be satisfactorily identified to species level. Here we report on the FIESC species present in Eastern Cape dairy pastures and describe three new species using macro- and micro-morphological characterisation with the support of multigene phylogenetic approaches. We also supply *F. goeppertmayerae* with the necessary macro- and micro-morphological characterisation information, as this was not supplied by Tan and Shivas (2023), who identified and named this species.

Materials and methods

Sampling and isolations

A total of 95 mixed pasture grass samples (primarily a mixture of kikuyu and ryegrass) were collected from 14 dairy farms in the Eastern Cape province of South Africa in May 2020, with a specific focus on identifying *Fusarium* species (Table 1). These pastures were potentially associated with a facial eczema outbreak in cattle. Plant material was cut into small pieces (±4 mm) and plated onto potato dextrose agar (PDA; Becton, Dickinson and Company (BD), Franklin Lakes, USA) and water agar (WA). Both were supplemented with chloramphenicol (100 ppm). The plates were incubated for 7–10 d at 25 °C and checked regularly for fungal growth. Colonies were transferred to pure cultures onto ¼PDA supplemented with chloramphenicol (100 ppm). Single spore cultures were prepared for all *Fusarium* strains following Leslie and Summerell (2006). Strains were accessioned and preserved in cryovials containing 10% glycerol and stored at -80 °C in the Applied Mycology working culture collection (CN) housed at the Forestry and Agricultural Biotechnology Institute (FABI) at the University of Pretoria, South Africa. Additionally, representative strains were deposited in the culture collections of FABI (Collection Mike Wingfield (CMW) and Collection Mike Wingfield at Innovation Africa (CMW-IA)) and the Westerdijk Fungal Biodiversity Institute (CBS) in Utrecht, the Netherlands (Table 1).

DNA extraction, PCR, and sequencing

Genomic DNA was extracted from 7-d-old fungal cultures grown on ¼PDA and incubated at 25 °C, using the PrepMan Ultra Sample Preparation Reagent (Thermo Fisher Scientific, Waltham, USA) following the manufacturer's instructions. PCR amplification of the translation elongation factor 1-alpha (*TEF*), calmodulin (*CaM*), RNA polymerase largest subunit (*RPB1*) and RNA polymerase second largest subunit (*RPB2*) loci was conducted using primer pairs and thermal cycle conditions as described in Table 2. The PCR reactions were set up in 25 µL volumes using 17.3 µL Milli-Q water (Millipore Corporation, Burlington, USA), 2.5 µL 10 × FastStart Taq PCR reaction buffer containing 20 mM $MgCl_2$ (Sigma-Aldrich, Roche Diagnostics, Manheim, Germany), 2.5 µL of 100 mM of each deoxynucleotide (New England Biolabs, Inc., Ipswich, USA), 0.5 µL forward primer (10 µM), 0.5 µL reverse primer (10 µM), 0.5 µL 25 mM $MgCl_2$ (Sigma-Aldrich, Roche Diagnostics), 0.2 µL of 5 U/µL FastStart Taq DNA Polymerase (Sigma-Aldrich, Roche Diagnostics, Manheim, Germany), and 1 µL template DNA. PCR products were prepared for sequencing using 2 µL ExoSAP-IT PCR clean-up reagent (1 U/µL FastAP Thermosensitive Alkaline Phosphatase, 20 U/µL Exonuclease I (Thermo Fisher Scientific, Waltham, USA)) and 5 µL PCR product. Sequencing was done bi-directionally using the BigDye terminator sequencing kit v. 3.1 (Applied Biosystems, Foster City, USA) with the same primers used for PCR amplification. Reactions were analysed on an ABI PRISM 3100 DNA sequencer (Applied Biosystems, Foster City, USA). Contigs were assembled and edited in Geneious Prime v. 2019.2.1 (BioMatters Ltd., Auckland, New Zealand). All sequences generated in this study were deposited in GenBank, with accession numbers provided in Table 1.

Phylogenetic analyses

Initial identifications of all *Fusarium* strains relied on BLAST search comparisons against the *Fusarium*-MLST database (https://fusarium.mycobank.org). These results were then used to produce a reference dataset for the

FIESC using previously deposited sequences obtained from the NCBI nucleotide database, largely based on O'Donnell et al. (2009) and Xia et al. (2019) (Suppl. material 5). Several phylogenetic trees were computed. The first included selected reference and newly generated sequences, using *TEF*, *CaM* and *RPB2*. Multi- and single-gene trees were calculated from these datasets, with final identifications being based on these trees. We also computed a phylogeny using a more comprehensive dataset based on *TEF*. This phylogeny included all strains obtained from our study, as well as those strains from Avila et al. (2019), Botha et al. (2014), Crous et al. (2021), Lombard et al. (2022), O'Donnell et al. (2009), O'Donnell et al. (2012), Tan and Shivas (2023), Tan and Shivas (2024) and Xia et al. (2019) that contained highly similar identities to ours. The datasets were aligned using MAFFT v. 7.427 (Katoh and Standley 2013) with the G-INS-I option selected in Geneious Prime. For the concatenated dataset, each gene region was treated as a separate partition. Maximum Likelihood (ML) trees were calculated in IQ-TREE v. 2.1.2 (Nguyen et al. 2015) with the General Time Reversible nucleotide substitution model with gamma distribution with invariant sites (GTR+G+I) applied to each partition. Support of nodes was calculated with a standard nonparametric bootstrap analysis with 1,000 replicates (Felsenstein 1985). The resulting trees were visualised using Figtree v. 1.4.4 and edited in Affinity Designer v. 1.7.3 (Serif (Europe) Ltd, Nottingham, UK).

Morphological characterisation

Fusarium strains were characterised based on macro- and micromorphological features (Leslie and Summerell 2006; Aoki et al. 2013; Sandoval-Denis et al. 2018; Yilmaz et al. 2021). After a 7 d incubation on synthetic nutrient-poor agar (SNA) (Nirenberg 1976) at 25 °C, agar plugs were removed from the colony edges with a 5 mm diameter cork borer and transferred to PDA, oatmeal agar (OA) and SNA for colony morphology and pigmentation assessment. The plates containing the agar plugs were incubated under different light conditions for 7 d, which included 24 h darkness, 24 h near-ultraviolet (nUV) light and a 12/12 h dark/nUV light cycle. Colony colour and codes used in descriptions followed the Methuen Handbook of Colour (Kornerup and Wanscher 1978). Colony growth rates were evaluated on PDA incubated for 7 d at 10–35 °C with 5 °C intervals in 24 h darkness. Colony measurements were recorded daily in four perpendicular directions. Colony images were captured with a Sony Alpha a7 III camera equipped with a Sony FE 90 mm f/2.8 Macro G OSS lens (Tokyo, Japan). Sporodochial formation was evaluated after a 7 d incubation period at 25 °C under a 12/12 h dark/nUV light cycle on SNA and WA, both supplemented with sterilised pieces of carnation leaves. Micromorphological characteristics were examined with a Zeiss AXIO Imager.A2 compound and AXIO Zoom.V16 microscope equipped with an AxioCaM 512 colour camera driven by Zen Blue 3.2 software (Carl Zeiss CMP, Göttingen, Germany). Conidia and other morphological structures were measured using up to 50 measurements each in NIS-Elements Basic Research software v. 4.30.00 (Nikon Europe B.V.). Photographic plates were prepared using Affinity Designer v. 1.7.3 (Serif (Europe) Ltd, Nottingham, UK).

Table 1. *Fusarium* strains from the *Fusarium incarnatum-equiseti* species complex (FIESC) isolated from mixed dairy pastures from the Eastern Cape, South Africa.

Species	Strain	*TEF*	*CaM*	*RPB1*	*RPB2*
***Camptoceras*-clade (FIESC; Han et al. (2023) = orginally the FCAMSC)**					
F. pascuum sp. nov.	CMW-IA 003320 = CMW 61364 = CN056A8	OR670986	OR669177	PP187127	PP235233
F. pascuum sp. nov.	CMW 58649 = CN070E7	PP187098	–	PP187129	PQ467747
F. pascuum sp. nov.	CMW 58650 = CN070F7	OR670991	OR669181	PP187132	PP158160
F. pascuum sp. nov.	CMW-IA 002133 = CMW 60931 = CN070I3	PP187102	PP187122	–	PQ467748
F. pascuum sp. nov.	CMW 58651 = CN070I4	OR671007	OR669194	PP187144	PQ467749
F. pascuum sp. nov.	CMW 58652 = CN071B8	OR671025	OR669210	PP187152	PP158176
F. pascuum sp. nov.	CBS 151772 = CMW 58653 = CN159G4 = CN071C4	OR671027	OR669212	PP187155	PP158178
F. pascuum sp. nov.	CMW 58654 = CN071D3	OR671033	OR669216	PP187158	PQ467750
F. pascuum sp. nov.	CMW 58655 = CN071E9	OR671039	OR669221	PP187161	PP158183
F. pascuum sp. nov.	CMW 58656 = CN071F9	OR671044	OR669225	PP187166	PP235238
F. pascuum sp. nov.	CMW 58657 = CN071G8	OR671051	OR669229	PP187168	PQ467751
F. pascuum sp. nov.	CMW 58658 = CN071I3	OR671057	OR669233	PP187173	PQ467752
F. pascuum sp. nov.	CMW 58659 = CN071I5	OR671058	OR669234	PP187175	PP158189
F. pascuum sp. nov.	CMW 58660 = CN071I9	OR671061	OR669237	PP187179	PQ467753
F. pascuum sp. nov.	CMW 58661 = CN072A1	OR671062	OR669238	PP187180	PP158191
F. pascuum sp. nov.	CMW 58662 = CN104D6	OR671090	OR669265	PP187190	PP158199
F. pascuum sp. nov.	CMW 58663 = CN104D7	OR671091	OR669266	PP187191	PQ467754
***Equiseti*-clade (FIESC)**					
F. brevicaudatum	CMW-IA 003335 = CMW 61379 = CN071C6	OR671028	–	–	–
F. brevicaudatum	CMW-IA 003765 = CMW 61537 = CN110E5	OR671114	–	–	–
F. clavus	CMW-IA 001930 = CMW 60748 = CN041D2	OR670983	–	–	–
F. clavus	CMW-IA 003330 = CMW 61374 = CN070H4	OR671001	OR669189	–	–
F. clavus	CN070H7	PP187101	PP187121	–	–
F. clavus	CN070I8	OR671010	OR669197	–	PP158167
F. clavus	CN071A3	OR671013	OR669200	–	–
F. clavus	CN071A4	OR671014	OR669201	–	–
F. clavus	CN071B3	OR671020	OR669205	–	–
F. clavus	CN071B4	OR671021	OR669206	–	PP158174
F. clavus	CN071D1	OR671031	OR669215	–	–
F. clavus	CN071D2	OR671032	–	–	–
F. clavus	CN071D8	OR671034	OR669217	–	–
F. clavus	CN071E1	OR671035	OR669218	–	–
F. clavus	CN071E2	OR671036	–	–	PP158180
F. clavus	CN071G5	OR671049	OR669227	–	PP158187
F. clavus	CN071G6	OR671050	OR669228	–	–
F. clavus	CN071H6	OR671054	-	–	–
F. clavus	CN072A6	OR671066	OR669241	–	PP158193
F. clavus	CN072A9	OR671069	OR669244	–	PP158195
F. clavus	CN072E4	OR671076	OR669251	–	PP158196
F. croceum	CMW-IA 001923 = CMW 60732 = CN040I7	OR670982	–	–	–
F. croceum	CMW-IA 001934 = CMW 60752 = CN041D9	OR670984	–	–	–
F. croceum	CN048C3	OR670985	–	–	–
F. croceum	CN070F6	OR670990	–	–	–
F. croceum	CMW-IA 003326 = CMW 61370 = CN070F8	OR670992	–	–	–
F. croceum	CN070F9	PP187099	–	–	PQ467755
F. croceum	CN070G4	OR670995	OR669184	PP187135	PP158162
F. croceum	CN070G6	OR670997	–	PP187137	PQ467756
F. croceum	CN070G7	OR670998	OR669186	PP187138	PQ467757
F. croceum	CN070H1	OR671000	OR669188	–	–

Species	Strain	*TEF*	*CaM*	*RPB1*	*RPB2*
F. croceum	CN070H5	OR671002	OR669190	—	—
F. croceum	CN070I1	OR671005	OR669193	PP187143	PQ467758
F. croceum	CN070I2	OR671006	—	—	—
F. croceum	CN070I5	OR671008	OR669195	PP187145	PP158165
F. croceum	CN070I9	OR671011	OR669198	PP187147	PP158168
F. croceum	CN071B1	OR671018	OR669203	PP187148	PP158173
F. croceum	CN071C7	OR671029	OR669213	PP187156	PQ467759
F. croceum	CN071F1	OR671040	OR669222	PP187162	PP158184
F. croceum	CN071G1	OR671045	—	—	—
F. croceum	CN071G2	OR671046	—	—	—
F. croceum	CN071G3	OR671047	—	PP187167	—
F. croceum	CN071H3	PP187104	—	PP187170	PQ467760
F. croceum	CN071H7	OR671055	OR669231	PP187171	PP158188
F. croceum	CN071I4	PP187105	PP187124	PP187174	PP235239
F. croceum	CN072A5	OR671065	OR669240	—	—
F. croceum	CN072A8	OR671068	OR669243	PP187182	PP158194
F. croceum	CN072B1	OR671070	OR669245	PP187183	PQ467761
F. croceum	CN072B4	OR671072	OR669247	—	—
F. croceum	CN072B8	OR671074	OR669249	—	PP235242
F. croceum	CN103E5	OR671077	OR669252	—	—
F. croceum	CN103E6	OR671078	OR669253	—	—
F. croceum	CN104B9	OR671079	OR669254	—	—
F. croceum	CN104C1	OR671080	OR669255	—	—
F. croceum	CN104C3	OR671082	OR669257	—	—
F. croceum	CN104C4	OR671083	OR669258	—	—
F. croceum	CN104C5	OR671084	OR669259	—	—
F. croceum	CN104C7	OR671085	OR669260	—	—
F. croceum	CN104C9	OR671086	OR669261	—	—
F. croceum	CN104D5	OR671089	OR669264	—	—
F. croceum	CN104D8	OR671092	OR669267	—	—
F. croceum	CN104E4	OR671094	—	—	—
F. croceum	CN104E8	OR671095	—	—	—
F. croceum	CN106E9	OR671096	—	—	—
F. croceum	CN110D4	OR671107	—	—	—
F. croceum	CN110D6	OR671109	—	—	—
F. croceum	CN110D8	OR671110	—	—	—
F. croceum	CN110E1	OR671112	—	—	—
F. croceum	CN115A2	PP187108	—	—	—
F. croceum	CN115A3	PP187109	—	—	—
F. croceum	CN115A4	PP187110	—	—	—
F. croceum	CN115B2	PP187111	—	—	—
F. croceum	CN115B6	PP187112	—	—	—
F. croceum	CN115C8	PP187114	—	—	—
F. croceum	CN115D9	PP187117	—	—	—
F. croceum	CN119E7	PP187119	—	—	—
F. cumulatum sp. nov.	CMW 58686 = CN071B9	OR671026	OR669211	PP187153	PP158177
F. cumulatum sp. nov.	CMW 58687 = CN071E5	OR671038	OR669220	PP187160	PP158182
F. cumulatum sp. nov.	CMW-IA 002138 = CMW 60936 = CN071G4	OR671048	OR669226	—	PP158186
F. cumulatum sp. nov.	CBS 151773 = CMW 58688 = CN104D3	OR671087	OR669262	PP187188	PP158197
F. heslopiae	CN071C8	OR671030	OR669214	PP187157	PP158179
***Incarnatum*-clade (FIESC)**					
F. coffeatum	CMW-IA 003332 = CMW 61376 = CN071A2	OR671012	OR669199	—	PP158169
F. coffeatum	CN071A5	OR671015	OR669202	—	PP158170
F. coffeatum	CN071A6	OR671016	—	—	PP158171

Species	Strain	*TEF*	*CaM*	*RPB1*	*RPB2*
F. coffeatum	CN071A7	OR671017	–	–	PP158172
F. coffeatum	CMW-IA 003334 = CMW 61378 = CN071B5	OR671022	OR669207	–	PP158175
F. coffeatum	CMW-IA 003341 = CMW 61385 = CN072A4	OR671064	–	–	–
F. coffeatum	CN072A7	OR671067	OR669242	–	–
F. goeppertmayerae	CBS 151775 = CMW 58689 = CN040I5	OR670981	OR669176	PP187126	PP158159
F. goeppertmayerae	CMW 58690 = CN070F3	OR670988	OR669179	PP187130	PP235234
F. goeppertmayerae	CMW 58691 = CN070G8	OR670999	OR669187	PP187139	PP158163
F. goeppertmayerae	CMW 58692 = CN070G9	PP187100	PP187120	PP187140	PP235236
F. goeppertmayerae	CMW-IA 002132 = CMW 60930 = CN070H9	OR671004	OR669192	PP187142	PP158164
F. goeppertmayerae	CMW-IA 003340 = CMW 61384 = CN071H2	OR671053	–	–	–
F. goeppertmayerae	CMW 58693 = CN071H8	OR671056	OR669232	PP187172	PQ467762
F. goeppertmayerae	CMW 58694 = CN071I6	OR671059	OR669235	PP187176	PP158190
F. goeppertmayerae	CMW 58695 = CN071I7	PP187106	PP187125	PP187177	PQ467763
F. goeppertmayerae	CMW 58696 = CN071I8	OR671060	OR669236	PP187178	PP235240
F. goeppertmayerae	CMW 58697 = CN104D4	OR671088	OR669263	PP187189	PP158198
F. goeppertmayerae	CMW 58698 = CN106F2	OR671098	OR669270	PP187194	PP158201
F. goeppertmayerae	CMW 58699 = CN106F3	OR671099	OR669271	PP187195	PP235244
F. goeppertmayerae	CMW 58700 = CN106F4	OR671100	OR669272	PP187196	PP158202
F. mariecurieae sp. nov.	CMW 58664 = CN070E5	OR670987	OR669178	PP187128	PQ467764
F. mariecurieae sp. nov.	CMW-IA 002131 = CMW 60929 = CN070F5	OR670989	OR669180	PP187131	–
F. mariecurieae sp. nov.	CMW 58665 = CN070G2	OR670994	OR669183	PP187134	PP158161
F. mariecurieae sp. nov.	CMW-IA 003328 = CMW 61372 = CN070G5	OR670996	OR669185	PP187136	PP235235
F. mariecurieae sp. nov.	CMW 58666 = CN070H6	OR671003	OR669191	PP187141	PQ467765
F. mariecurieae sp. nov.	CBS 151774 = CMW 58667 = CN070I7	OR671009	OR669196	PP187146	PP158166
F. mariecurieae sp. nov.	CMW 58668 = CN071B2	OR671019	OR669204	PP187149	PQ467746
F. mariecurieae sp. nov.	CMW 58669 = CN071C1	PP187103	PP187123	PP187154	PQ467766
F. mariecurieae sp. nov.	CMW 58670 = CN071E4	OR671037	OR669219	PP187159	PP158181
F. mariecurieae sp. nov.	CMW-IA 002136 = CMW 60934 = CN071F2	OR671041	–	PP187163	PP235237
F. mariecurieae sp. nov.	CMW-IA 002137 = CMW 60935 = CN071F3	OR671042	OR669223	PP187164	PQ467767
F. mariecurieae sp. nov.	CMW 58671 = CN071F4	OR671043	OR669224	PP187165	PP158185
F. mariecurieae sp. nov.	CMW 58672 = CN071H1	OR671052	OR669230	PP187169	PQ467768
F. mariecurieae sp. nov.	CBS 152079 = CMW 58673 = CN072A3	OR671063	OR669239	PP187181	PP158192
F. mariecurieae sp. nov.	CMW 58674 = CN072B2	OR671071	OR669246	PP187184	PP235241
F. mariecurieae sp. nov.	CMW 58675 = CN072B6	OR671073	OR669248	PP187185	PQ467769
F. mariecurieae sp. nov.	CMW 58676 = CN072E2	OR671075	OR669250	PP187186	PQ467770
F. mariecurieae sp. nov.	CMW 58677 = CN104C2	OR671081	OR669256	PP187187	PP235243
F. mariecurieae sp. nov.	CMW 58678 = CN104E1	OR671093	OR669268	PP187192	PQ467771
F. mariecurieae sp. nov.	CMW 58679 = CN106F1	OR671097	OR669269	PP187193	PP158200
F. mariecurieae sp. nov.	CMW 58680 = CN106F8	PP187107	–	–	–
F. mariecurieae sp. nov.	CMW-IA 003763 = CMW 61535 = CN106F9	OR671101	OR669273	PP187197	PP235245
F. mariecurieae sp. nov.	CMW 58681 = CN106G1	OR671102	OR669274	PP187198	PP158203
F. mariecurieae sp. nov.	CMW 58682 = CN106G2	OR671103	–	PP187199	PQ467772
F. mariecurieae sp. nov.	CMW 58683 = CN106G3	OR671104	–	PP187200	–
F. mariecurieae sp. nov.	CMW 58684 = CN106G4	OR671105	–	–	–
F. mariecurieae sp. nov.	CN106G5	OR671106	OR669275	PP187201	PP235246
F. mariecurieae sp. nov.	CMW-IA 003764 = CMW 61536 = CN110D9	OR671111	OR669277	PP187202	PP235247
F. mariecurieae sp. nov.	CMW 58685 = CN110E2	OR671113	OR669278	PP187203	PP158204
F. mariecurieae sp. nov.	CN115C6	PP187113	–	–	–
F. mariecurieae sp. nov.	CN115C9	PP187115	–	–	–
F. mariecurieae sp. nov.	CN115D4	PP187116	–	–	–
F. mariecurieae sp. nov.	CN115E8	PP187118	–	–	–
Fusarium FIESC 27	CMW-IA 003327 = CMW 61371 = CN070G1	OR670993	OR669182	PP187133	PQ276899
Fusarium sp. nov. 1	CMW-IA 002134 = CMW 60932 = CN071B6	OR671023	OR669208	PP187150	PQ467773
Fusarium sp. nov. 1	CMW-IA 002135 = CMW 60933 = CN071B7	OR671024	OR669209	PP187151	PQ467774

Table 2. Primer pairs and PCR conditions used in this study.

Locus	PCR amplification procedure	Primer	Primer sequence (5′-3′)*	Reference
TEF	95 °C 5 min; 35 cycles of 95 °C 45 s, 52 °C 45 s, 72 °C 90 s; 72 °C 8 min; 10 °C soak	EF1	ATGGGTAAGGARGACAAGAC	O'Donnell et al. (1998)
		EF2	GGARGTACCAGTSATCATG	O'Donnell et al. (1998)
CaM	94 °C 90 s; 35 cycles of 94 °C 45 s, 50 °C 45 s, 72 °C 1 min; 72 °C 10 min; 10 °C soak	CL1	GARTWCAAGGAGGCCTTCTC	O'Donnell et al. (2000)
		CL2A	TTTTTGCATCATGAGTTGGAC	O'Donnell et al. (2000)
RPB1	94 °C 90 s; 5 cycles of 94 °C 45 s, 54 °C 45 s, 72 °C 2 min; 5 cycles of 94 °C 45 s, 53 °C 45 s, 72 °C 2 min; 35 cycles of 94 °C 45 s, 52 °C 45s, 72 °C 2 min; 72 °C 10 min; 10 °C soak	Fa	CAYAARGARTCYATGATGGGWC	Hofstetter et al. (2007)
		R8	CAATGAGACCTTCTCGACCAGC	O'Donnell et al. (2010)
	94 °C 90 s; 5 cycles of 94 °C 45 s, 56 °C 45 s, 72 °C 2 min; 5 cycles of 94 °C 45 s, 55 °C 45 s, 72 °C 2 min; 35 cycles of 94 °C 45 s, 54 °C 45s, 72 °C 2 min; 72 °C 10 min; 10 °C soak	F8	TTCTTCCACGCCATGGCTGGTCG	O'Donnell et al. (2010)
		G2R	GTCATYTGDGTDGCDGGYTCDCC	O'Donnell et al. (2010)
RPB2	95 °C 5 min; 40 cycles of 94 °C 30 s, 51 °C 90 s, 68 °C 2 min; 68 °C 5 min; 10 °C soak	5F2	GGGGWGAYCAGAAGAAGGC	Reeb et al. (2004)
		7Cr	CCCATRGCTTGYTTRCCCAT	Liu et al. (1999)
	95 °C 5 min; 40 cycles of 94 °C 30 s, 51 °C 90 s, 68 °C 2 min; 68 °C 5 min; 10 °C soak	7Cf	ATGGGYAARCAAGCYATGGG	Liu et al. (1999)
		11ar	GCRTGGATCTTRTCRTCSACC	Liu et al. (1999)

* R = A or G; S = C or G; W = A or T; Y = C or T.

Results

Identifications and phylogenetic analyses

Isolations from the 95 mixed pasture grass samples collected in the Eastern Cape resulted in 708 strains isolated, with 55 genera and 133 species identified (Dewing et al. 2025). Of the 207 strains identified as *Fusarium* isolated from 12 of the 14 farms, 155 belonged to the *Fusarium incarnatum-equiseti* species complex (FIESC) (Table 1). The aligned concatenated dataset included 120 taxa and was 2,954 bp long (*CaM*: 1–644; *RPB2_1*: 645–1,471; *RPB2_2*: 1,471–2,334; *TEF*: 2,335–2,954). *Fusarium concolor* (NRRL 13459^{T}) was selected as the outgroup. The obtained ML tree resolved strains into three main clades, including the *Incarnatum*-clade, *Equiseti*-clade and *Camptoceras*-clade (O'Donnell et al. 2009; Xia et al. 2019; Han et al. 2023) (Fig. 1). Strains isolated from pastures represented 11 species, with five well-supported clades representing new species. Individual gene phylogenies for *CaM*, *RPB2* and *TEF* were used to assess these clades, applying genealogical concordance phylogenetic species recognition (GCPSR: Taylor et al. (2000)) (Suppl. materials 1–3). In all analyses, strains of the new species showed no discordance, noting that the branches holding *F. mariecurieae* did not have support in the *CaM* and *RPB2* phylogenies.

Incarnatum-clade—We identified five species in the *Incarnatum*-clade, including *F. coffeatum* (FIESC 28; n = 7), *F. goeppertmayerae* (n = 14) and the clade we introduce as *F. mariecurieae* (n = 33) below (Fig. 1, Suppl. materials 1–3). Strains CMW 58691 and CMW 60930 showed variation in *TEF* by at least 11 bp but had similar *CaM* and *RPB2* sequences from other *F. goeppertmayerae* strains. *Fusarium goeppertmayerae* was described based on a single isolate (BRIP 64547d^{T}), and capturing this type of infraspecies variation is important to better establish its species boundaries. We provide a description of the species below in the Taxonomy section because Tan and Shivas (2023) did not provide this when naming their species. Two additional new species were isolated,

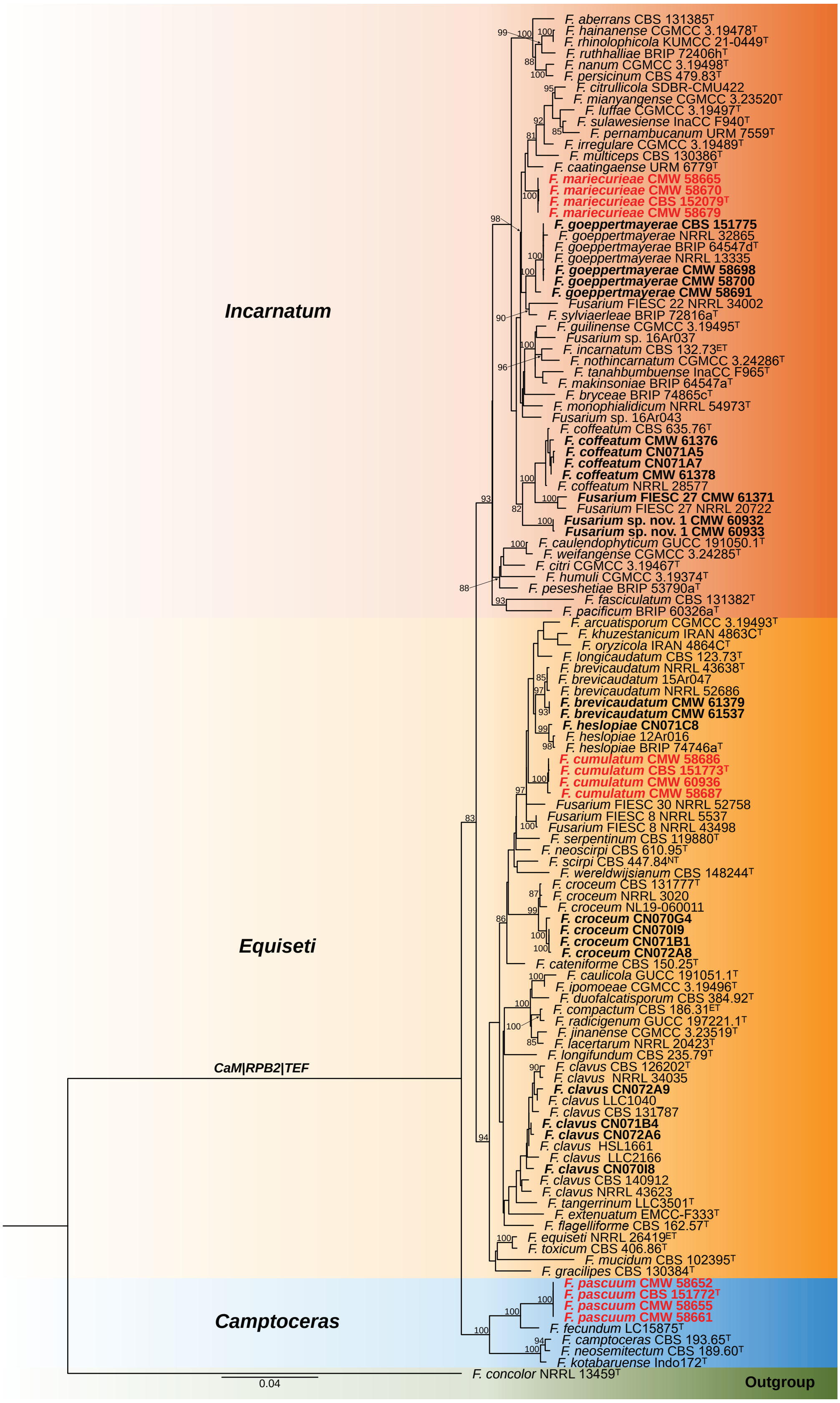

Figure 1. Maximum likelihood phylogenetic tree of the *Fusarium incarnatum-equiseti* species complex based on a concatenated dataset, *CaM, RPB2* and *TEF*. Strains of species isolated from this study are shown in black bold text; strains of new species are indicated in red bold text. The tree was rooted to *Fusarium concolor*. Branch support in nodes higher than 80% are indicated at relevant branches (^{T} = ex-type, ^{ET} = epitype, ^{NT} = neotype).

including *Fusarium* FIESC 27 (O'Donnell et al. 2009) (n = 1) and *Fusarium* sp. nov. 1 (n = 2). However, due to the absence of key microscopic characteristics, we opted to not introduce names for these until additional strains are collected.

Equiseti-clade—Five of our species were resolved in the *Equiseti*-clade, from which *F. brevicaudatum* (FIESC 6; n = 2), *F. clavus* (FIESC 5; n = 19), *F. croceum* (FIESC 10; n = 55) and *F. heslopiae* (n = 1) are known species, while *F. cumulatum* (n = 4) is described below as a new species (Fig. 1, Suppl. materials 1–3). The *F. clavus* clade contains a lot of variation. In the *TEF* phylogeny, *F. clavus* strains form a unique group with *F. tangerrinum*, its closest relative. However, in *RPB2*, both *F. tangerrinum* and *F. extenuatum* resolve inside the broader *F. clavus* clade. In the *CaM* phylogeny, *F. tangerrinum* also resolves inside *F. clavus*, but *F. extenuatum* is a distant relative. Future work is needed on this group. Our *F. croceum* strains consistently formed a distinct clade closely related to other *F. croceum* strains (including the ex-type CBS 131777^{T}), with ours differing by at least 9, 8 and 27 bp for *CaM*, *RPB2* and *TEF*, respectively. Based on these findings, we could introduce a new species for the clade. However, at present we propose that our strains represent new genotypes of *F. croceum* with additional strains that will be needed in the future. Finally, we identify strain CN071C8 as *F. heslopiae*, a species originally introduced based solely on a *TEF* sequence, with no morphological description provided (Tan and Shivas 2024).

Camptoceras-clade—We identified a new species in the *Camptoceras*-clade, which we introduce below as *F. pascuum* (n = 17) (Fig. 1, Suppl. materials 1–3). The new species is a close relative of *F. fecundum*.

Taxonomy

***Fusarium cumulatum* Dewing, Visagie & Yilmaz, sp. nov.**
MycoBank No: 855721
Fig. 2

Etymology. Latin, *cumulatum*, meaning to accumulate or heap up, named for its abundant chlamydospore formation.

Type. South Africa • Eastern Cape, from mixed pasture samples, May 2020, collected by A. Davis (***holotype*:** PRU(M) 4601, dried specimen in a metabolically inactive state); (***ex-type strain*:** CBS 151773 = CMW 58688 = CN104D3).

Description. ***Conidiophores*** borne on aerial mycelium scarce, 13–71 µm tall, unbranched, bearing terminal phialides, often reduced to single phialides; ***aerial phialides*** scarce, monophialidic, subulate to subcylindrical, proliferating percurrently, smooth- and thin-walled, 2.5–20 × 2–4 µm, with inconspicuous thickening; ***aerial conidia*** absent. ***Sporodochia*** orange, present on the surface of carnation leaves and on agar. ***Sporodochial conidiophores*** densely and irregularly branched, bearing apical whorls of 2–5 phialides; ***sporodochial phialides*** monophialidic, subulate to subcylindrical, 7–16.5 × 2–4 µm, smooth, thin-walled, with inconspicuous periclinal thickening; ***sporodochial conidia*** falcate, sometimes becoming sinuate, slender, curved dorsiventrally, tapering towards both ends, with an elongated or whip-like curved apical cell and a barely notched to prominently extended basal cell, 1–5-septate, hyaline, smooth- and thin-walled; 1-septate conidia 16 × 4 µm (n = 1); 2-septate conidia 18–30 × 3–4 µm (av. 25.2 × 3.6 µm) (n = 3), 3-septate conidia 23–42 × 2.5–4 µm (av. 25.2 × 3.5 µm) (n = 15), 4-septate conidia 25.5–54.5 × 2.5–4 µm (av. 43.0 × 3.4 µm) (n = 14), 5-septate conidia 38–57 × 3–4.5 µm (av. 49.1 × 3.8 µm) (n = 17). ***Chlamydospores*** abundant, globose to subglobose, subhyaline, smooth- to slightly rough-walled, terminal or intercalary, solitary or in pairs forming chains, 8–19 µm diam.

Culture characteristics. Colonies on PDA incubated at 25 °C in the dark with an average radial growth rate of 2–8 mm/d, reaching 44–46 mm diam at 25 °C; surface white, flat, felty to velvety, radiate, with abundant aerial mycelium, margin irregular. Additional colony diam (after 7 d, in mm): PDA 10 °C 13–15; PDA at 15 °C 22–26; PDA at 20 °C 27–32; PDA at 30 °C 64–75; PDA at 35 °C 0–2. Odour absent. Reverse yellowish white (2A2). Diffusible pigments absent. On OA in the dark, occupying an entire 90 mm Petri dish in 7 d; surface white to pale yellow, flat, felty to velvety, radiate, with abundant aerial mycelium, margin irregular, filiform. Reverse yellowish white (4A2). Diffusible pigments absent. On SNA with sparse aerial mycelium, sporulation moderate on the surface of the medium.

Additional materials examined. South Africa • Eastern Cape, from mixed pasture samples, May 2020, collected by A. Davis, isolated by C. Dewing, Humansdorp area: CMW 58686 = CN071B9, CMW 58687 = CN071E5, close to Villa Fonte: CMW-IA 002138 = CMW 60936 = CN071G4.

Notes. *Fusarium cumulatum* belongs to the *Equiseti*-clade and is closely related to *F. arcuatisporum* (FIESC 7) (Wang et al. 2019), *F. brevicaudatum* (FIESC 6) (Xia et al. 2019), *F. heslopiae* (Tan and Shivas 2024), *F. longicaudatum* (Xia et al. 2019), *F. khuzestanicum* and *F. oryzicola* (Afzalinia et al. 2024). No aerial phialides or conidia were observed for the closely related species (Wang et al. 2019; Xia et al. 2019; Afzalinia et al. 2024) compared to the few scarce monophialides we recorded for *F. cumulatum*. Sporodochia and chlamydospores were present in *F. cumulatum* and its closely related species, whereas *F. oryzicola* lacked chlamydospore formation (Wang et al. 2019; Xia et al. 2019; Afzalinia et al. 2024). Sporodochial conidia of *F. cumulatum* (1–5-septate; 16–57 × 2.5–4 µm) are similar in length to *F. arcuatisporum* (5-septate; 29–49.5 × 4–6 µm) (Wang et al. 2019) and *F. brevicaudatum* (1–5-septate; 8–64 × 3–5 µm) (Xia et al. 2019), while generally being shorter than those observed in *F. khuzestanicum* (4–7(–9)-septate; 48.5–82 × 2.7–4.3 µm) (Afzalinia et al. 2024), *F. longicaudatum* ((3–)5–6(–7)-septate; 45–81 × 4–5 µm) (Xia et al. 2019) and *F. oryzicola* (4–7-septate; 33.5–77.9 × 3–4 µm) (Afzalinia et al. 2024). Colony colour on PDA differs between *F. cumulatum* and closely related species (Wang et al. 2019; Xia et al. 2019; Afzalinia et al. 2024) as other species show more colour across the surface and reverse compared to the white surface and yellowish white (2A2) reverse of *F. cumulatum*, whereas the colony colour of *F. khuzestanicum* and *F. oryzicola* is white to pale grey. The growth rate after 7 d on PDA for *F. cumulatum* (44–46 mm) is slower than that of *F. arcuatisporum* (48–53 mm) (Wang et al. 2019), *F. brevicaudatum* (50–58 mm) (Xia et al. 2019) and *F. longicaudatum* (full 90 mm plate) (Xia et al. 2019). The growth rate for *F. khuzestanicum* (74–76 mm) (Afzalinia et al. 2024) and *F. oryzicola* (74 mm) (Afzalinia et al. 2024) was measured after 5 d on PDA but appears to be faster than that of *F. cumulatum*. No morphological data is currently available for *F. heslopiae* to compare with. Pairwise comparisons revealed that *F. cumulatum* differs from other species by at least 3, 6 and 16 bp for *CaM*, *RPB2* and *TEF*, respectively.

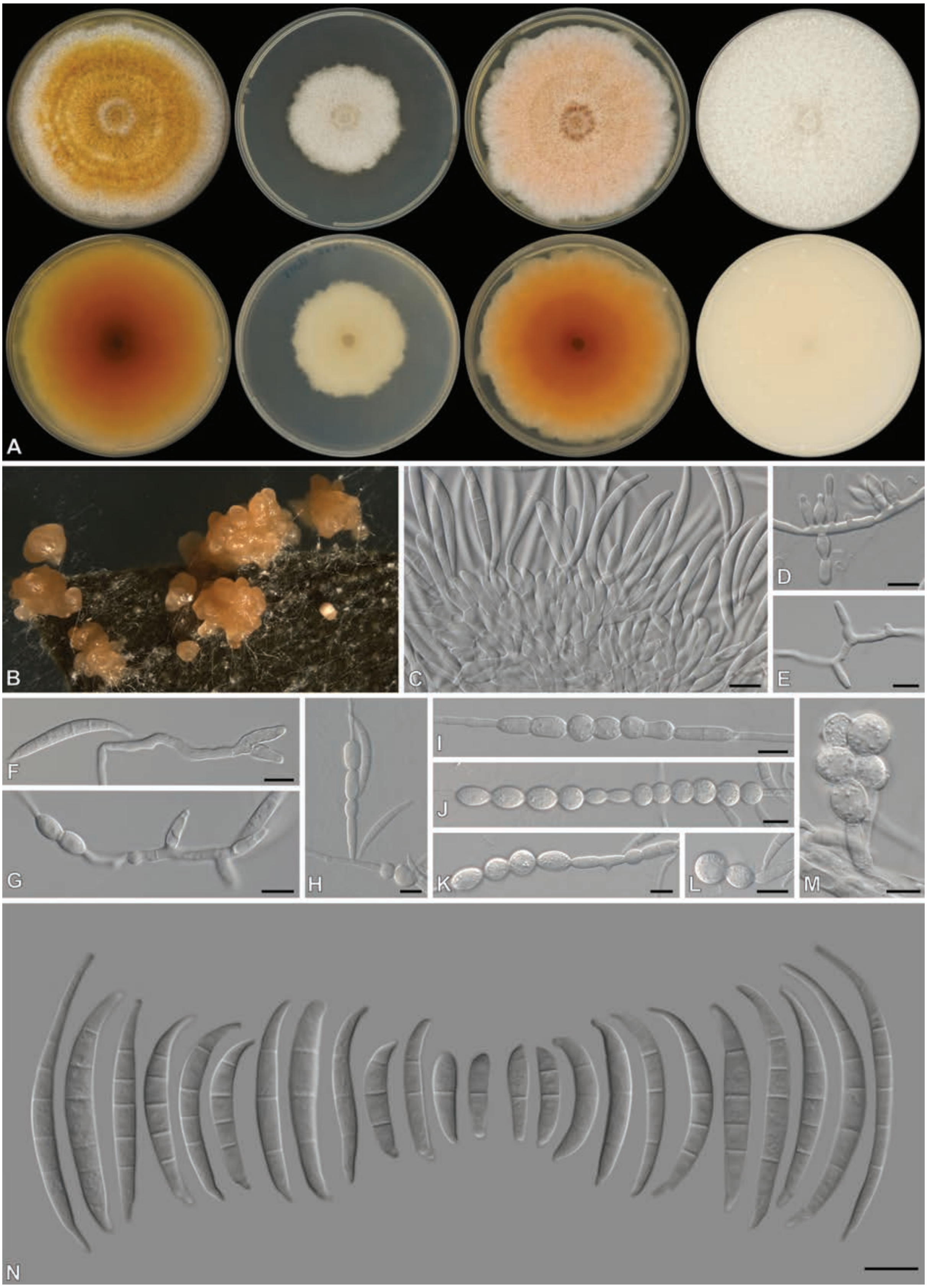

Figure 2. *Fusarium cumulatum* (CBS 151773, ex-type culture) **A** colonies front (top row) and reverse (bottom row) on PDA after 7 d at 25 °C light, dark and nUV and OA after 7 d at 25 °C dark (from left to right), respectively **B** sporodochial formation on the surface of carnation leaves **C, D** sporodochial conidiophores and phialides **E–G** aerial conidiophores and phialides **H–M** intercalary and terminal chlamydospores **N** sporodochial conidia. Scale bars: 10 µm.

Fusarium goeppertmayerae Y.P. Tan & R.G. Shivas, Index of Australian Fungi 5: 7. 2023.

MycoBank No: 900363
Fig. 3

Type. Australia • Queensland, Bongeen, from the peduncle of *Zea mays* (Poaceae), 25 Feb. 2016, B. Thrift (***holotype*****:** BRIP 64547d, ***ex-type*****:** CBS 150772).

Description. ***Conidiophores*** borne on aerial mycelium, 8.5–98 um tall, unbranched, sympodial, bearing terminal or lateral phialides, often reduced to single phialides; ***aerial phialides*** mono- and polyphialidic, subulate to subcylindrical, proliferating percurrently, smooth- and thin-walled, 4–22 × 1.5–5 μm, with inconspicuous thickening; ***aerial conidia*** mostly fusiform, slender, curved dorsiventrally, no apparent tapering observed at ends, blunt to conical and straight to slightly curved apical cell and a blunt to papillate basal cell, 0–3-septate, 0-septate conidia: 7–22 × 2–5 μm (av. 15.0 × 3.4 μm) (n = 9); 1-septate conidia: 12–19 × 2.5–4 μm (av. 15.6 × 3.4 μm) (n = 13); 2-septate conidia: 16–20 × 3.5–4 μm (av. 18.2 × 3.8 μm) (n = 2); 3-septate conidia: 21–31 × 3.5–4 μm (av. 23.9 × 3.9 μm) (n = 6). ***Sporodochia*** pale yellow to white, formed between aerial mycelia around the carnation leaves. ***Sporodochial conidiophores*** densely and irregularly branched, bearing apical whorls of 2–3 phialides; ***sporodochial phialides*** monophialidic, subulate to subcylindrical, 6–12 × 1.5–4 μm, smooth, thin-walled, with inconspicuous periclinal thickening; ***sporodochial conidia*** falcate, curved dorsiventrally, tapering towards both ends, with a slightly curved apical cell and a blunt to foot-like basal cell, (1–)3–5-septate, hyaline, smooth- and thin-walled; 1-septate conidia: 12–17 × 3 μm (av. 14.4 × 3.2 μm) (n = 2); 3-septate conidia: 19–36 × 3 × 4 μm (av. 30.0 × 3.8 μm) (n = 23); 4-septate conidia: 30.5–36 × 4–5 μm (av. 33.2 × 4.3 μm) (n = 4); 5-septate conidia: 30 × 5 μm (n = 1). ***Chlamydospores*** not observed.

Culture characteristics. Colonies on PDA incubated at 25 °C in the dark with an average radial growth rate of 1–15 mm/d and occupying an entire 90 mm Petri dish in 7 d; surface white, radiate, aerial mycelium felty to velvety, margin irregular, filiform. Additional colony diam (after 7 d, in mm): PDA at 10 °C 14–19; PDA at 15 °C 37–43; PDA at 20 °C 63–70; PDA at 30 °C 40–75; PDA at 35 °C 0–2. Odour absent. Reverse pale yellow. Diffusible pigments absent. On OA in the dark, occupying an entire 90 mm Petri dish in 7 d; surface white, flat, slightly felty to velvety, aerial mycelium scant, margin irregular, filiform. Reverse pale luteous, without diffusible pigments. On SNA with sparse aerial mycelium, sporulation moderate on the surface of the medium.

Materials examined. South Africa • Eastern Cape, from mixed pasture samples, May 2020, collected by A. Davis, isolated by C. Dewing, close to Gamtoos River Mouth: CBS 151775 = CMW 58689 = CN040I5, Outside Humansdorp, close to Clarkson: CMW 58690 = CN070F3, CMW 58696 = CN071I8, CMW-IA 003340 = CMW 61384 = CN071H2, CMW 58693 = CN071H8, Humansdorp area: CMW 58691 = CN070G8, CMW 58692 = CN070G9, CMW-IA 002132 = CMW 60930 = CN070H9, CMW 58697 = CN104D4, CMW 58698 = CN106F2, CMW 58699 = CN106F3, CMW 58700 = CN106F4, close to Tsitsikamma on Sea: CMW 58694 = CN071I6, CMW 58695 = CN071I7, CMW 58696 = CN071I8.

Notes. *Fusarium goeppertmayerae* belongs to the *Incarnatum*-clade and is closely related to the undescribed *Fusarium* FIESC 22 isolated from the human sinus cavity (O'Donnell et al. 2009) and *F. sylviaearleae* isolated from a leaf

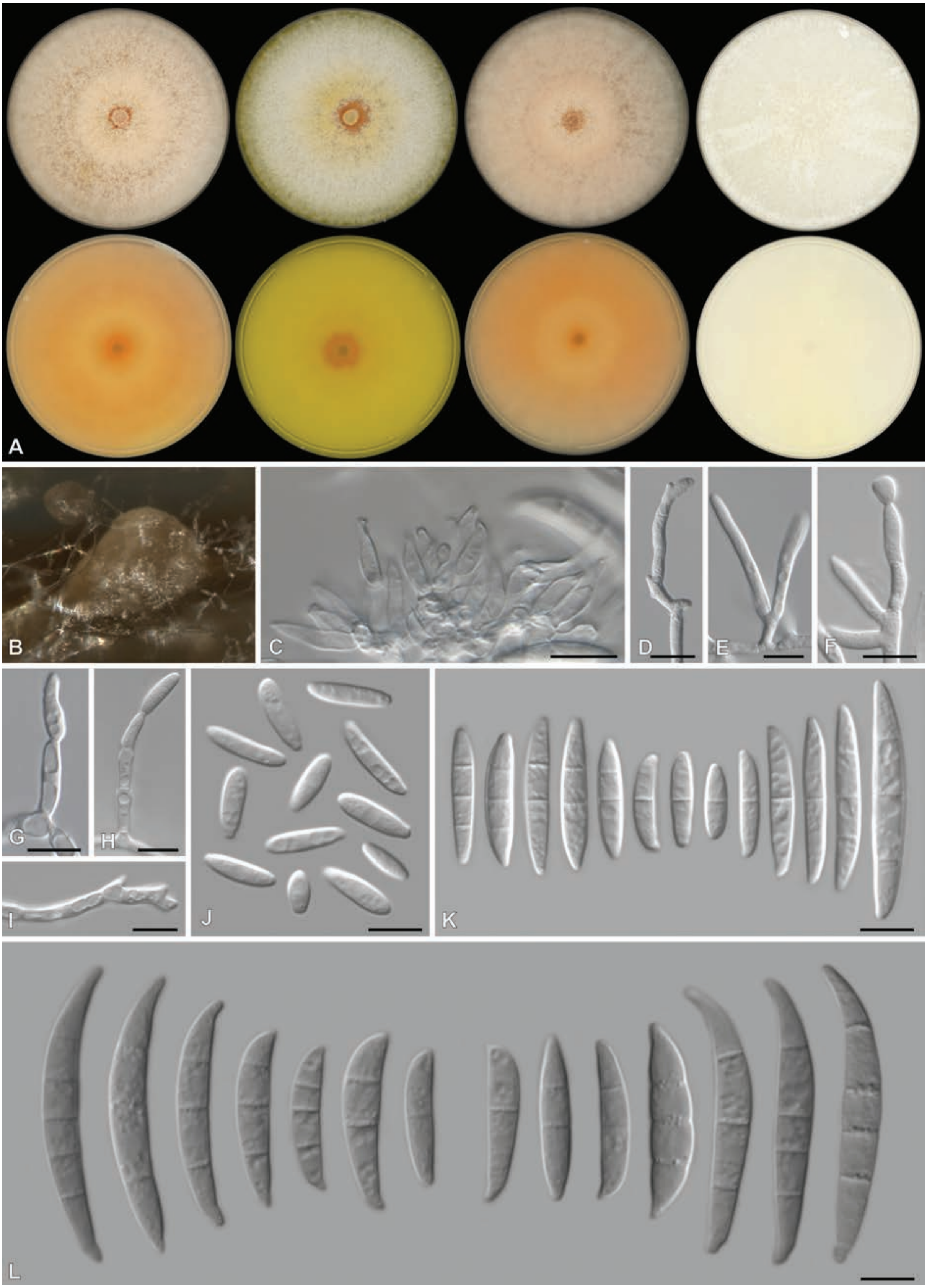

Figure 3. *Fusarium goeppertmayerae* (CBS 151775) **A** colonies front (top row) and reverse (bottom row) on PDA after 7 d at 25 °C light, dark and nUV and OA after 7 d at 25 °C dark (from left to right), respectively **B** sporodochial formation on the surface of carnation leaves **C** sporodochial conidiophores **D–I** aerial mono- and polyphialides **J–K** aerial conidia **L** sporodochial conidia. Scale bars: 10 μm.

lesion of *Sporobolus natalensis* (Poaceae) (Tan and Shivas 2023). No morphological data are available for *Fusarium* FIESC 22 or *F. sylviaearleae*. Furthermore, we demonstrate that strains NRRL 32865 and NRRL 13335, previously considered to belong to *F. guilinense*, belong to *F. goeppertmayerae*, with *F. guilinense* (LC12160^T) a distant relative.

Fusarium mariecurieae **Dewing, Visagie & Yilmaz, sp. nov.**

MycoBank No: 855722
Fig. 4

Etymology. Latin, *mariecurieae*, named after Maria Salomea Skłodowska-Curie (known simply as Marie Curie) (1867–1934), who was a renowned physicist and chemist known for her pioneering research on radioactivity. We also chose this name, as this study was supported by the Marie Skłodowska-Curie Actions (MSCA) grant (number 101008129), project acronym "Mycobiomics".

Type. South Africa • Eastern Cape, from mixed pasture samples, May 2020, collected by A. Davis (***holotype*****:** PRU(M) 4611, dried specimen in a metabolically inactive state; ***ex-type strain*****:** CBS 152079 = CMW 58673 = CN072A3).

Description. ***Conidiophores*** borne on aerial mycelium, 13–106 μm tall, unbranched, sympodial or irregularly branched, bearing terminal or lateral phialides, often reduced to single phialides; ***aerial phialides*** mono- and polyphialidic, subulate to subcylindrical, proliferating percurrently, smooth- and thin-walled, 3.5–28.5 × 1.5–4 μm, with inconspicuous thickening; ***aerial conidia*** ellipsoidal, fusiform, slightly allantoid to falcate, slender, curved dorsiventrally and more pronounced on the apical half, tapering towards both ends, with a blunt to conical and straight to slightly curved apical cell and a blunt to papillate basal cell, 0–3(–5)-septate; 0-septate conidia: 8–11 × 2.5–3 μm (av. 9.6 × 2.6 μm) (n = 2); 1-septate conidia: 11–20 × 3–4 μm (av. 15.6 × 3.3 μm) (n = 11); 2-septate conidia: 15–23 × 3–4 μm (av. 18.7 × 3.6 μm) (n = 6); 3-septate conidia: 18.5–30.5 × 3–5 μm (av. 23.2 × 3.8 μm) (n = 26); 5-septate conidia: 33 × 5 μm (n = 1). ***Sporodochia*** peach to pale straw, formed abundantly on carnation leaves. ***Sporodochial conidiophores*** densely and irregularly branched, bearing apical whorls of 2–3 phialides; ***sporodochial phialides*** monophialidic, subulate to subcylindrical, 6–22 × 2–4 μm, smooth, thin-walled, with inconspicuous periclinal thickening; ***sporodochial conidia*** falcate, curved dorsiventrally, tapering towards both ends, with a slightly curved apical cell and a blunt to foot-like basal cell, (1–)3–5-septate, hyaline, smooth- and thin-walled; 1-septate conidia: 12–17 × 3 μm (av. 14.4 × 3.2 μm) (n = 2); 3-septate conidia: 19–36 × 3–4 μm (av. 30.0 × 3.8 μm) (n = 23); 4-septate conidia: 31–36 × 4–5 μm (av. 33.2 × 4.3 μm) (n = 4); 5-septate conidia: 30 × 5 μm (n = 1). ***Chlamydospores*** not observed.

Culture characteristics. Colonies on PDA incubated at 25 °C in the dark with an average radial growth rate of 5–9 mm/d, occupying an entire 90 mm Petri dish in 7 d; surface white, flat, felty to velvety around the centre, floccose towards the margins, radiate, with abundant aerial mycelium, margin irregular, filiform. Additional colony diam (after 7 d): PDA 10 °C 12–17; PDA at 15 °C 29–40; PDA at 20 °C 48–70; PDA at 30 °C 68–76; PDA at 35 °C 4–6. Odour absent. Reverse yellowish white (3A2). Diffusible pigments absent. On OA in the dark, occupying an entire 90 mm Petri dish in 7 d; surface white, floccose around the centre, flat, felty to velvety towards the margin, radiate, with abundant aerial mycelium, margin irregular, filiform. Reverse yellowish white (2A2). Diffusible pigments absent. On SNA with sparse aerial mycelium, sporulation moderate on the surface of the medium.

Additional materials examined. South Africa • Eastern Cape, from mixed pasture samples, May 2020, collected by A. Davis, isolated by C. Dewing, Humansdorp area: CMW 58664 = CN070E5, CMW-IA 002131 = CMW 60929 = CN070F5, CMW-IA 003328 = CMW 61372 = CN070G5, CMW 58666 = CN070H6, CBS 151774 = CMW 58667 = CN070I7, CMW 58668 = CN071B2, CMW 58669 = CN071C1, CMW 58670 = CN071E4, CMW-IA 002136 = CMW 60934 = CN071F2, CMW-IA 002137 = CMW 60935 = CN071F3, CMW 58671 = CN071F4, CMW 58676 = CN072E2, CMW 58677 = CN104C2, CMW 58678 = CN104E1, CMW 58679 = CN106F1, CMW 58680 = CN106F8, CMW-IA 003763 = CMW 61535 = CN106F9, CMW 58681 = CN106G1, CMW 58682 = CN106G2, CMW 58683 = CN106G3, CMW 58684 = CN106G4, CN106G5, CMW-IA 003764 = CMW 61536 = CN110D9, CMW 58685 = CN110E2, CN115C6, CN115C9, CN115D4, CN115E8, CMW 61371 = CN070G1, Outside Humansdorp, close to Clarkson: CMW 58665 = CN070G2, CMW 58672 = CN071H1, CMW 58674 = CN072B2, close to Villa Fonte: CMW 58675 = CN072B6.

Notes. *Fusarium mariecurieae* belongs to the *Incarnatum*-clade and is most similar to an unsupported clade containing the following species: *F. caatingaense* (FIESC 20) (Santos et al. 2019), *F. citrullicola* (nom. inval.) (Khuna et al. 2022), *F. irregulare* (FIESC 15) (Wang et al. 2019), *F. luffae* (FIESC 18) (Wang et al. 2019), *F. mianyagense* (Han et al. 2023), *F. multiceps* (FIESC 19) (Xia et al. 2019), *F. pernambucanum* (FIESC 17) (Santos et al. 2019) and *F. sulawesiense* (FIESC 16) (Maryani et al. 2019). *Fusarium mariecurieae* produces both aerial mono- and polyphialides compared to *F. irregulare* that only produces monophialides (Wang et al. 2019), *F. luffae* that produces only polyphialides (Wang et al. 2019) and *F. mianyagense* that lacks aerial phialides (Han et al. 2023). Aerial conidia from *F. mariecurieae* (0–3(–5)-septate; 8–30.5 × 3–5 µm) are smaller than that of *F. irregulare* (mostly 3-septate; 16–38.5 × 3–5 µm) (Wang et al. 2019), *F. luffae* (3–5)-septate; 26.5–46 × 4–5 µm) (Wang et al. 2019), *F. multiceps* (1–)3–4(–5)-septate; 16–37 × 3–4 µm) (Xia et al. 2019), *F. pernambucanum* (1–7)-septate; 7–57 × 2.5–5 µm) (Santos et al. 2019) and *F. sulawesiense* (3–5(–9)-septate; 20.5–67 × 3.5–6 µm) (Maryani et al. 2019). Aerial conidia from *F. caatingaense* (0–6-septate; 6–45 × 2.5–5 µm) (Santos et al. 2019) and *F. citrullicola* (1–5-septate; 8–39 × 2–4.9 µm) (Khuna et al. 2022) were, at their largest, bigger than those of *F. mariecurieae*, while aerial conidia were absent from *F. mianyagense* (Han et al. 2023). Sporodochia were absent from *F. citrullicola*, *F. irregulare* and *F. luffae* (Wang et al. 2019), while chlamydospores were absent from *F. irregulare*, *F. luffae*, *F. mianyagense*, *F. multiceps* and *F. sulawesiense* (Maryani et al. 2019; Wang et al. 2019; Xia et al. 2019; Han et al. 2023). Sporodochial conidia from *F. mariecurieae* (1–3(–5)-septate; 12–36 × 3–5 µm) were smaller than that of *F. caatingaense* (1–5-septate; 15–50 × 2–4.5 µm) (Santos et al. 2019), *F. mianyagense* (3(–5)-septate; 24.5–36.6 × 2.5–4.9 µm) (Han et al. 2023), *F. multiceps* ((1–)2–5-septate; 16–46 × 3–4 µm) (Xia et al. 2019) and *F. sulawesiense* ((3–)5(–6)-septate; 29.5–43.5 × 4–5.5 µm) (Maryani et al. 2019). Colony colour on PDA differs between *F. mariecurieae* and closely related species (Maryani et al. 2019; Santos et al. 2019; Wang et al. 2019; Xia et al. 2019; Han et al. 2023) as most other species show more colour across the surface and reverse compared to the white surface and yellowish white (3A2) reverse of *F. mariecurieae*. The growth rate after 7 d on PDA for *F. mariecurieae*

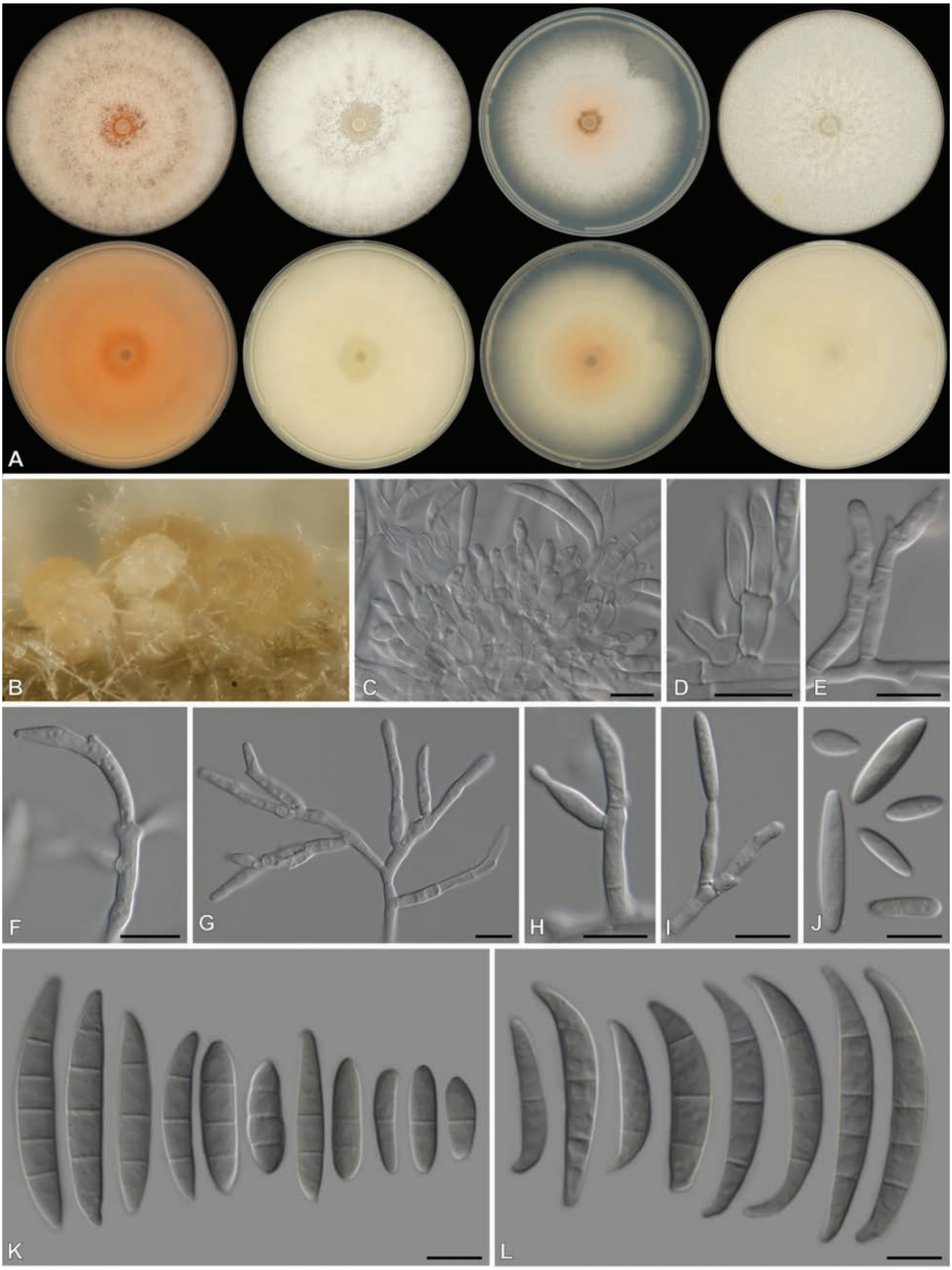

Figure 4. *Fusarium mariecurieae* (CBS 152079, ex-type culture) **A** colonies front (top row) and reverse (bottom row) on PDA after 7 d at 25 °C light, dark and nUV and OA after 7 d at 25 °C dark (from left to right), respectively **B** sporodochial formation on the surface of carnation leaves **C, D** sporodochial conidiophores and phialides **E–G** aerial conidiophores **H–I** mono- and polyphialides **J–K** aerial conidia **L** sporodochial conidia. Scale bars: 10 μm.

is faster (>90 mm plate) than that of *F. citrullicola* (68–74.5 mm) (Khuna et al. 2022), *F. irregulare* (53–59 mm) (Wang et al. 2019), *F. luffae* (53–57 mm) (Wang et al. 2019) and *F. mianyagense* (74–80 mm) (Han et al. 2023). The growth of *F. multiceps* (>90 mm plate) (Xia et al. 2019) is similar to that of *F. mariecurieae*, while the growth rate in terms of diameter was not reported for *F. caatingaense*, *F. pernambucanum* and *F. sulawesiense* (Maryani et al. 2019; Santos et al. 2019). Pairwise comparisons revealed that *F. mariecurieae* differs from other species by at least 1, 4 and 12 bp for *CaM*, *RPB2* and *TEF*, respectively.

Fusarium pascuum **Dewing, Visagie & Yilmaz, sp. nov.**

MycoBank No: 855720
Fig. 5

Etymology. Latin, *pascuum*, meaning pasture, referring to the species isolated from grass pastures.

Type. South Africa • Eastern Cape, from mixed pasture samples, May 2020, collected by A. Davis (***holotype*:** PRU(M) 4600, dried specimen in a metabolically inactive state; ***ex-type strain*:** CBS 151772 = CMW 58653 = CN159G4 = CN071C4).

Description. ***Conidiophores*** borne on aerial mycelium, 15.5–101 µm tall, unbranched, sympodial or irregularly branched, bearing terminal or lateral phialides, often reduced to single phialides; ***aerial phialides*** mono- and polyphialidic, subulate to subcylindrical, proliferating percurrently, smooth- and thin-walled, 4–43 × 1–4.5 µm, with inconspicuous periclinal thickening; ***aerial conidia*** fusiform, falcate, slender, curved dorsiventrally and more pronounced on the apical half, tapering towards both ends, with a blunt to conical and straight to slightly curved apical cell and a blunt to papillate basal cell, 0–3-septate conidia; 0-septate conidia: 7–17 × 2–5 µm (av. 11.7 × 3.2 µm) (n = 34); 1-septate conidia: 12–26 × 3–6 µm (av. 19.2 × 3.8 µm) (n = 14); 2-septate conidia: 23–32 × 4–6 µm (av. 26.9 × 4.5 µm) (n = 7); 3-septate conidia: 27–32 × 3–5 µm (av. 29.5 × 4.4 µm) (n = 2). ***Sporodochia*** and ***chlamydospores*** not observed.

Culture characteristics. Colonies on PDA incubated at 25 °C in the dark with an average radial growth rate of 3–10 mm/d, reaching 80 mm diam at 25 °C; surface white, flat, felty to velvety, radiate, with abundant aerial mycelium, margin irregular, filiform. Additional colony diam (after 7 d, in mm): PDA at 10 °C 13–15; PDA at 15 °C 36–42; PDA at 20 °C 63–65; PDA at 30 °C 34–39; PDA at 35 °C no growth. Odour absent. Reverse yellowish white (3A2). Diffusible pigments absent. On OA in the dark, occupying an entire 90 mm Petri dish in 7 d; surface white, flat, felty to velvety, radiate, with abundant aerial mycelium, margin irregular, filiform. Reverse yellowish white (3A2). Diffusible pigments absent. On SNA with sparse aerial mycelium, sporulation moderate on the surface of the medium.

Additional materials examined. South Africa • Eastern Cape, from mixed pasture samples, May 2020, collected by A. Davis, isolated by C. Dewing, Humansdorp area: CMW-IA 003320 = CMW 61364 = CN056A8, CMW 58649 = CN070E7, CMW 58650 = CN070F7, CMW-IA 002133 = CMW 60931 = CN070I3, CMW 58651 = CN070I4, CMW 58652 = CN071B8, CMW 58654 = CN071D3, CMW 58655 = CN071E9, CMW 58662 = CN104D6, CMW 58663 = CN104D7, close to Kou-Kamma: CMW 58656 = CN071F9, Outside Humansdorp, close to Clarkson:

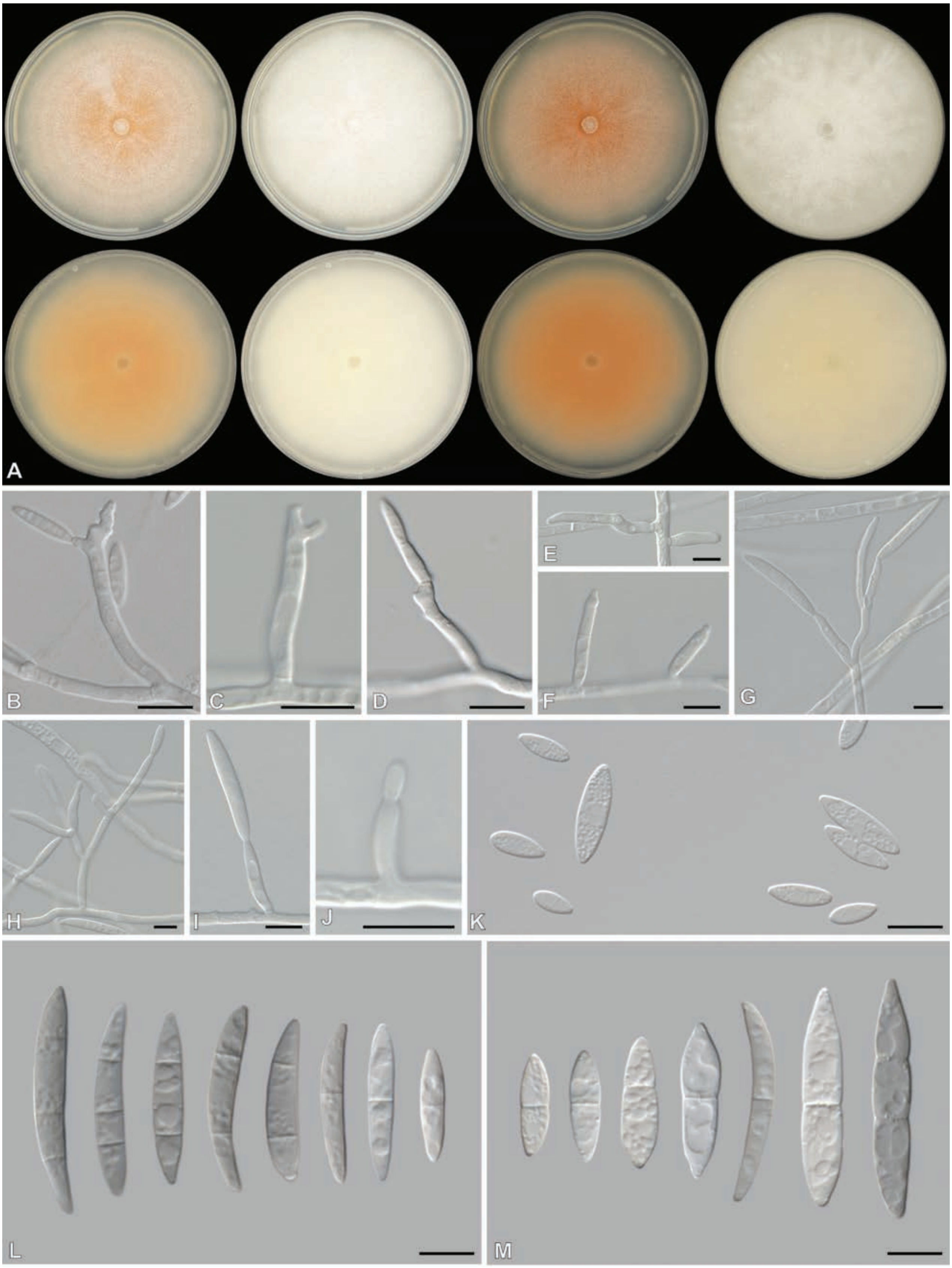

Figure 5. *Fusarium pascuum* (CBS 151772, ex-type culture) **A** colonies front (top row) and reverse (bottom row) on PDA after 7 d at 25 °C light, dark and nUV and OA after 7 d at 25 °C dark (from left to right), respectively **B–J** aerial conidiophores and phialides **K** aerial microconidia **L, M** aerial macroconidia. Scale bars: 10 µm.

CMW 58657 = CN071G8, CMW 58660 = CN071I9, CMW 58661 = CN072A1, close to Tsitsikamma on Sea: CMW 58658 = CN071I3, CMW 58659 = CN071I5.

Notes. *Fusarium pascuum* belongs to the *Camptoceras*-clade (as introduced by Han et al. (2023)) and is closely related to *F. fecundum*. Both *F. pascuum* and *F. fecundum* produce aerial mono- and polyphialides. Aerial conidia from *F. pascuum* (0–3-septate; 7–32 × 2–6 µm) are comparably smaller than those of *F. fecundum* ((1–)2–4(–6)-septate; 3.6–35.8 × 3.6–6.8 µm) (Han et al. 2023). Sporodochia and chlamydospores are absent in both *F. pascuum* and *F. fecundum*. Colony colour on PDA differs between *F. pascuum* and *F. fecundum*, where the former is completely white across the surface and the latter is greyish yellow in the centre, while the reverse of *F. pascuum* is yellowish white and *F. fecundum* is just white (Han et al. 2023). The growth rate after 7 d on PDA in *F. pascuum* (reaching 80 mm) is slightly slower than that of *F. fecundum* (84–90 mm) (Han et al. 2023). Pairwise comparisons revealed that *F. pascuum* differs from other species by at least 8, 8 and 23 bp for *CaM*, *RPB2* and *TEF*, respectively.

Discussion

In a 2020 survey exploring fungal diversity in dairy pastures, 95 mixed pasture samples were collected across 14 dairy farms in the Eastern Cape of South Africa. A total of 155 *Fusarium* strains, belonging to the *Fusarium incarnatum-equiseti* species complex (FIESC), were isolated from 12/14 dairy farms. Strains were analysed using a multigene phylogenetic approach, leading to the identification of 11 species, including five that are new. Of these, we opted to formally describe and name *F. cumulatum*, *F. mariecurieae* and *F. pascuum*. *Fusarium croceum* (n = 55) and *F. mariecurieae* (n = 33) were the most commonly isolated species, followed by *F. clavus* (n = 19), *F. pascuum* (n = 17), *F. goeppertmayerae* (n = 14), *F. coffeatum* (n = 7), *F. cumulatum* (n = 4), *F. brevicaudatum* (n = 2), *Fusarium* sp. nov. 1 (n = 2), *F. heslopiae* (n = 1) and *Fusarium* FIESC 27 (n = 1). Due to a lack of morphological character development in our strains, two of the new species were not described (e.g., *Fusarium* FIESC 27, *Fusarium* sp. nov. 1). In the future, it will be important to obtain additional isolates of the species and name them. Several recently FIESC-introduced species did not include morphological descriptions. This includes *F. goeppertmayerae* that was introduced based on sequence differences of a *TEF* sequence in a single isolate (Tan and Shivas 2023). We found several new isolates of this species in pasture samples, and here we provided a morphological description for the species and capture infraspecies variation in its DNA sequences.

Fusarium species are well-known for their frequent association with Poaceae (grasses), but of the 11 species identified, only five had previously been reported from this plant family. *Fusarium clavus* was reported from *Phalaris minor* (little seed canary grass), *Leucopoa sclerophylla*, *Secale montanum* (wild perennial rye) and *Triticum* (wheat) from Iran (Xia et al. 2019). *Fusarium coffeatum* and *F. heslopiae* were reported from *Cynodon nlemfuensis* (African Bermuda-grass) and *Sporobolus creber* (Western Rat-Tail grass), respectively (Lombard et al. 2019; Tan and Shivas 2024), while *F. croceum* has been isolated from wheat (*Triticum* sp.) from Iran (Xia et al. 2019). *Fusarium goeppertmayerae* has not previously been reported from grass species but was reported from maize peduncles from Australia (Tan and Shivas 2023). Given the diverse impacts of FIESC species, especially with regard to their ability to cause plant and animal diseases and produce mycotoxins (Kosiak et al. 2005; Desjardins 2006; O'Donnell et al. 2013; Villani et al. 2016; Munkvold 2017; O'Donnell et al. 2018; Gallo et al. 2022), it is crucial to investigate the potential implications that species present in our dairy pastures could have for animal health. This is especially relevant considering the growing evidence of *Fusarium* species contributing to toxic effects in livestock grazing on certain grasses (Kellerman et al. 2005; Bourke 2007).

Species previously implicated in kikuyu poisoning were identified in our study. Previous studies have identified *Fusarium* species as potential causal agents of kikuyu poisoning, a condition characterised by toxic effects in livestock, like cattle, that consume kikuyu grass (*Pennisetum clandestinum*) (Kellerman et al. 2005; Bourke 2007). Reports of kikuyu poisoning are sporadic in South Africa and Australia and pose significant economic concerns in dairy farming due to high cattle mortality rates (Kellerman et al. 2005; Bourke 2007). While the exact cause of kikuyu poisoning remains uncertain, Ryley et al. (2007) hypothesised that mycotoxins like wortmannin and butenolide produced by species like *F. torulosum* (*Fusarium tricinctum* species complex (FTSC)) may be involved. Botha et al. (2014) studied the *Fusarium* present in Eastern Cape (South Africa) dairy pastures where cattle intoxication outbreaks occurred. Strains were identified based on *TEF* sequences, and similar to our survey (Dewing et al. 2025), they mostly detected FIESC species and did not detect *F. torulosum*. Both studies, Botha et al. (2014) and Dewing et al. (2025), detected *F. brevicaudatum*, *F. clavu*s, *F. croceum* and the two species we describe above as *F. pascuum* and *F. mariecurieae* (Suppl. material 4). Additionally, our study identified *F. cumulatum*, *F. heslopiae*, *Fusarium* FIESC 27 and *Fusarium* sp. nov. 1, which were not detected in the study by Botha et al. (2014). Conversely, Botha et al. (2014) identified *F. tangerrinum* and *Fusarium* FIESC 34 (undescribed), which were not found in our survey.

Although the mycotoxigenic potential of the species described in this study is unknown, members of the FIESC have been reported to produce various mycotoxins (Phillips et al. 1989; Logrieco et al. 1998; Hestbjerg et al. 2002; Kosiak et al. 2005; Villani et al. 2016; O'Donnell et al. 2018). Many of these, especially deoxynivalenol, fumonisins and zearalenone, can adversely affect cattle health, leading to symptoms such as decreased conception rates, reproductive disorders, feed refusal, gastrointestinal problems, immunosuppression, reduced animal performance, tremors, weight loss and even death (Trenholm et al. 1985; European Food Safety Authority 2004; Morgavi and Riley 2007; Fink-Gremmels 2008). However, toxicological information and their effects on animals for some commonly produced secondary metabolites, such as beauvericin, remain unavailable (de Felice et al. 2023; Hasuda and Bracarense 2024). This lack of information is often due to the absence of regulations for these mycotoxins, resulting in a lack of standardised testing methods, as well as limited monitoring and reporting requirements. It is also crucial to consider the potential synergistic, additive, or antagonistic interactions between emerging mycotoxins and other toxins in animal feed, as these combinations could pose unexpected health risks (Křížová et al. 2021). This is particularly true for FIESC that has only occasionally been linked to cattle poisoning, possibly due to a lack of sufficient studies on pasture fungal diversity. Therefore, the presence of the FIESC species in dairy pasture still poses a potential risk of mycotoxin contamination when these grasses are used for animal feed (Botha et al. 2014), and research into their mycotoxins is urgently needed.

Our study provides a valuable insight into the diversity of the FIESC in dairy pastures in the Eastern Cape. The presence of *Fusarium* species, seemingly in a consistent community in this environment, underscores the importance of further studying these species. Further research must focus on what secondary metabolites, including mycotoxins, these species produce. This will provide insights into their potential impact on cattle health in dairy pastures.

Acknowledgements

We acknowledge Konstanze Bensch (MycoBank curator) for her help regarding Latin names. We are thankful to Anthony Davis and Jan Myburgh for providing the grass samples analysed in this study.

Additional information

Conflict of interest

The authors have declared that no competing interests exist.

Ethical statement

No ethical statement was reported.

Funding

We are grateful for funding supported by the National Research Foundation (NRF) of South Africa (grant number: 137791) and the Future Leaders – African Independent Research fellowship programme (FLAIR, FLR\R1\201831). The FLAIR fellowship programme is a partnership between the African Academy of Sciences and the Royal Society funded by the UK Government's Global Challenges Research Fund. This project is partially funded by the European Union's Horizon 2020 research and innovation programme (RISE) through the Marie Skłodowska-Curie grant agreement No. 101008129, with the project acronym "Mycobiomics" (the lead beneficiaries are Cobus Visagie and Neriman Yilmaz). The authors would like to acknowledge the financial support of MycoKeys and the International Mycological Association. At IMC12 in Maastricht, the Netherlands, on 11 August 2024, the corresponding author, Neriman Yilmaz, was awarded the Young Mycologist Presentation Award, which included a publication prize covering the article processing charges for this manuscript.

Author contributions

Investigation and conceptualisation, C.V., E.S., B.W. and N.Y.; writing—original draft preparation, C.D.; formal analysis, C.D.; resources, C.V., E.S., B.W. and N.Y.; methodology, C.D., C.V. and N.Y.; supervision, C.V., E.S., B.W. and N.Y. All authors have read and agreed to the published version of the manuscript.

Author ORCIDs

Claudette Dewing https://orcid.org/0000-0001-6208-1721
Cobus M. Visagie https://orcid.org/0000-0003-2367-5353
Emma T. Steenkamp https://orcid.org/0000-0003-0217-8219
Brenda D. Wingfield https://orcid.org/0000-0002-6189-1519
Neriman Yilmaz https://orcid.org/0000-0002-4396-4630

Data availability

All sequence data generated for this work can be accessed via GenBank: https://www.ncbi.nlm.nih.gov/genbank/.

References

Afzalinia S, Mehrabi-Koushki M, Farokhinejad R (2024) Two new species of *Fusarium* in the *F. incarnatum-equiseti* species complex from *Oryza sativa* in Iran. Antonie van Leeuwenhoek 118: 5. https://doi.org/10.1007/s10482-024-02019-y

Aoki T, Smith JA, Mount LL, Geiser DM, O'Donnell K (2013) *Fusarium torreyae* sp. nov., a pathogen causing canker disease of Florida torreya (*Torreya taxifolia*), a critically endangered conifer restricted to northern Florida and southwestern Georgia. Mycologia 105: 312–319. https://doi.org/10.3852/12-262

Aranega J, Oliveira C (2022) Occurrence of mycotoxins in pastures: A systematic review. Quality Assurance and Safety of Crops and Foods 14: 135–144. https://doi.org/10.15586/qas.v14i3.1079

Avila CF, Moreira GM, Nicolli CP, Gomes LB, Abreu LM, Pfenning LH, Haidukowski M, Moretti A, Logrieco A, del Ponte EM (2019) *Fusarium incarnatum-equiseti* species complex associated with Brazilian rice: Phylogeny, morphology and toxigenic potential. International Journal of Food Microbiology 306: 108267. https://doi.org/10.1016/j.ijfoodmicro.2019.108267

Bentley AR, Petrovic T, Griffiths SP, Burgess LW, Summerell BA (2007) Crop pathogens and other *Fusarium* species associated with *Austrostipa aristiglumis*. Australasian Plant Pathology 36: 434–438. https://doi.org/10.1071/AP07047

Botha PR, Meeske R, Snyman HA (2008a) Kikuyu over-sown with ryegrass and clover: Dry matter production, botanical composition and nutritional value. African Journal of Range and Forage Science 25: 93–101. https://doi.org/10.2989/AJRF.2008.25.3.1.598

Botha PR, Meeske R, Snyman HA (2008b) Kikuyu over-sown with ryegrass and clover: Grazing capacity, milk production and milk composition. African Journal of Range and Forage Science 25: 103–110. https://doi.org/10.2989/AJRF.2008.25.3.2.599

Botha CJ, Truter M, Jacobs A (2014) *Fusarium* species isolated from *Pennisetum clandestinum* collected during outbreaks of kikuyu poisoning in cattle in South Africa. Onderstepoort Journal of Veterinary Research 81: e1–e8. https://doi.org/10.4102/ojvr.v81i1.803

Bourke CA (2007) A review of kikuyu grass (*Pennisetum clandestinum*) poisoning in cattle. Australian Veterinary Journal 85: 261–267. https://doi.org/10.1111/j.1751-0813.2007.00168.x

Brook PJ (1963) Ecology of the fungus *Pithomyces chartarum* (Berk. & Curt.) M. B. Ellis in pasture in relation to facial eczema disease of sheep. New Zealand Journal of Agricultural Research 6: 147–228. https://doi.org/10.1080/00288233.1963.10418130

Bryson SJ, Newsholme RW (1978) Kikuyu grass poisoning of cattle in Natal. Journal of the South African Veterinary Association 49: 19–21. https://doi.org/10.10520/AJA00382809_4112

Burkin AA, Kononenko G (2015) Mycotoxin contamination of meadow grasses in European Russia. Sel'skokhozyaistvennaya Biologiya 50: 503–512. https://doi.org/10.15389/agrobiology.2015.4.503eng

Charlton JFL, Stewart AV (1999) Pasture species and cultivars used in New Zealand – A list. Proceedings of the New Zealand Grassland Association 61: 147–166. https://doi.org/10.33584/jnzg.1999.61.2328

Crous PW, Lombard L, Sandoval-Denis M, Seifert KA, Schroers HJ, Chaverri P, Gené J, Guarro J, Hirooka Y, Bensch K, Kema GHJ, Lamprecht SC, Cai L, Rossman AY, Stadler M, Summerbell RC, Taylor JW, Ploch S, Visagie CM, Yilmaz N, Frisvad JC, Abdel-Azeem AM, Abdollahzadeh J, Abdolrasouli A, Akulov A, Alberts JF, Araújo JPM, Ariyawansa HA, Bakhshi M, Bendiksby M, Ben Hadj Amor A, Bezerra JDP, Boekhout T, Câmara MPS, Carbia M, Cardinali G, Castañeda-Ruiz RF, Celis A, Chaturvedi V, Collemare J, Croll D, Damm U, Decock CA, de Vries RP, Ezekiel CN, Fan XL, Fernández NB, Gaya E, González CD, Gramaje D, Groenewald JZ, Grube M, Guevara-Suarez M, Gupta VK, Guarnaccia V, Haddaji A, Hagen F, Haelewaters D, Hansen K, Hashimoto A, Hernández-Restrepo M, Houbraken J, Hubka V, Hyde KD, Iturriaga T, Jeewon R, Johnston PR, Jurjević Ž, Karalti I, Korsten L, Kuramae EE, Kušan I, Labuda R, Lawrence DP, Lee HB, Lechat C, Li HY, Litovka YA, Maharachchikumbura SSN, Marin-Felix Y, Matio Kemkuignou B, Matočec N, McTaggart AR, Mlčoch P, Mugnai L, Nakashima C, Nilsson RH, Noumeur SR, Pavlov IN, Peralta MP, Phillips AJL, Pitt JI, Polizzi G, Quaedvlieg W, Rajeshkumar KC, Restrepo S, Rhaiem A, Robert J, Robert V, Rodrigues AM et al. (2021) *Fusarium*: More than a node or a foot-shaped basal cell. Studies in Mycology 98: 100116. https://doi.org/10.1016/j.simyco.2021.100116

Davis AJ, Collett MG, Steyl JCA, Myburgh JG (2021) Hepatogenous photosensitisation in cows grazing turnips (*Brassica rapa*) in South Africa. Journal of South African Veterinary Association 92: e1–e6. https://doi.org/10.4102/jsava.v92i0.2106

de Felice B, Spicer LJ, Caloni F (2023) Enniatin B1: Emerging mycotoxin and emerging issues. Toxins 15: 683. https://doi.org/10.3390/toxins15060383

Desjardins AE (2006) *Fusarium* mycotoxins: Chemistry, genetics, and biology. American Phytopathological Society, 260 pp.

Dewing C, Yilmaz N, Steenkamp ET, Wingfield BD, Visagie CM (2025) [submitted for review] Capturing the fungal diversity hidden in Eastern Cape dairy pastures. Mycological Progress.

di Menna ME, Campbell J, Mortimer PH (1970) Sporidesmin production and sporulation in *Pithomyces chartarum*. Journal of General Microbiology 61: 87–96. https://doi.org/10.1099/00221287-61-1-87

di Menna ME, Lauren DR, Poole PR, Mortimer PH, Hill RA, Agnew MP (1987) Zearalenone in New Zealand pasture herbage and the mycotoxin-producing potential of *Fusarium* species from pasture. New Zealand Journal of Agricultural Research 30: 499–504. https://doi.org/10.1080/00288233.1987.10417963

Doxey J (2014) Pastures for cows and calves. https://www.kzndard.gov.za/images/Documents/Research%20and%20Technology%20Development%20Services/Publications/RESEARCH%20REPORTS/PasturesforCowsandCalves.pdf [Accessed 08 August 2023]

Driehuis F, Spanjer MC, Scholten JM, te Giffel MC (2008) Occurrence of mycotoxins in feedstuffs of dairy cows and sstimation of total dietary intakes. Journal of Dairy Science 91: 4261–4271. https://doi.org/10.3168/jds.2008-1093

Edrington T, Kamps-Holtzapple C, Harvey R, Kubena L, Elissalde M, Rottinghaus G (1995) Acute hepatic and renal toxicity in lambs dosed with fumonisin-containing culture material. Journal of Animal Science 73: 508–515. https://doi.org/10.2527/1995.732508x

Eskola M, Altieri A, Galobart J (2018) Overview of the activities of the European Food Safety Authority on mycotoxins in food and feed. World Mycotoxin Journal 11: 277–289. https://doi.org/10.3920/WMJ2017.2270

EFSA [European Food Safety Authority] (2004) Opinion of the Scientific Panel on contaminants in the food chain [CONTAM] related to Deoxynivalenol (DON) as undesirable substance in animal feed. EFSA Journal 73: 1–42. https://doi.org/10.2903/j.efsa.2004.73

Felsenstein J (1985) Confidence limits on phylogenies: An approach using the bootstrap. Evolution 39: 783–791. https://doi.org/10.2307/2408678

Fink-Gremmels J (2008) The role of mycotoxins in the health and performance of dairy cows. Veterinary Journal 176: 84–92. https://doi.org/10.1016/j.tvjl.2007.12.034

Gallo A, Mosconi M, Trevisi E, Santos RR (2022) Adverse effects of *Fusarium* toxins in ruminants: A review of in vivo and in vitro studies. Dairy 3: 474–499. https://doi.org/10.3390/dairy3030035

Golinski P, Kostechi M, Golinska BT, Golinsky PK (2003) Accumulation of mycotoxins in forage for winter pasture during prolonged utilisation of sward. Polish Journal of Veterinary Sciences 6: 81–88.

Gott PN, Stam A, Johns A, Miller BG, Bell B, Jenkins T, Murugesan GR (2017) Mycotoxin survey of common Bermudagrass in south-central Florida. Journal of Animal Science 95: 19–20. https://doi.org/10.2527/asasann.2017.039

Han SL, Wang MM, Ma ZY, Raza M, Zhao P, Liang JM, Gao M, Li YJ, Wang JW, Hu DM, Cai L (2023) *Fusarium* diversity associated with diseased cereals in China, with an updated phylogenomic assessment of the genus. Studies in Mycology 104: 87–148. https://doi.org/10.3114/sim.2022.104.02

Hasuda AL, Bracarense APFRL (2024) Toxicity of the emerging mycotoxins beauvericin and enniatins: A mini-review. Toxicon 239: 107534. https://doi.org/10.1016/j.toxicon.2023.107534

Hestbjerg H, Nielsen KF, Thrane U, Elmholt S (2002) Production of trichothecenes and other secondary metabolites by *Fusarium culmorum* and *Fusarium equiseti* on common laboratory media and a soil organic matter agar: An ecological interpretation. Journal of Agriculture and Food Chemistry 50: 7593–7599. https://doi.org/10.1021/jf020432o

Hofstetter V, Miadlikowska J, Kauff F, Lutzoni F (2007) Phylogenetic comparison of protein-coding versus ribosomal RNA-coding sequence data: A case study of the Lecanoromycetes (Ascomycota). Molecular Phylogenetics and Evolution 44: 412–426. https://doi.org/10.1016/j.ympev.2006.10.016

Katoh K, Standley DM (2013) MAFFT multiple sequence alignment software version 7: Improvements in performance and usability. Molecular Biology and Evolution 30: 772–780. https://doi.org/10.1093/molbev/mst010

Kellerman TS, Coetzer JA (1985) Hepatogenous photosensitivity diseases in South Africa. Onderstepoort Journal of Veterinary Research 52: 157–173.

Kellerman TS, van der Westhuizen GC, Coetzer JA, Roux C, Marasas WF, Minne JA, Bath GF, Basson PA (1980) Photosensitivity in South Africa. II. The experimental production of the ovine hepatogenous photosensitivity disease geeldikkop (*Tribulosis ovis*) by the simultaneous ingestion of *Tribulus terrestris* plants and cultures of *Pithomyces chartarum* containing the mycotoxin sporidesmin. Onderstepoort Journal of Veterinary Research 47: 231–261.

Kellerman TS, Coetzer JAW, Naudé TW, Botha CJ (2005) Plant poisonings and mycotoxicoses of livestock in Southern Africa. Oxford University Press, Cape Town.

Khuna S, Kumla J, Thitla T, Nuangmek W, Lumyong S, Suwannarach N (2022) Morphology, molecular identification, and pathogenicity of two novel *Fusarium* species associated with postharvest fruit rot of Cucurbits in Northern Thailand. Journal of Fungi 8: 1135. https://doi.org/10.3390/jof8111135

Kornerup A, Wanscher J (1978) Metheun Hand Book of Colour. Metheun London Ltd, London.

Kosiak EB, Holst-Jensen A, Rundberget T, Gonzalez Jaen MT, Torp M (2005) Morphological, chemical and molecular differentiation of *Fusarium equiseti* isolated from Norwegian cereals. International Journal of Food Microbiology 99: 195–206. https://doi.org/10.1016/j.ijfoodmicro.2004.08.015

Křížová L, Dadáková K, Dvořáčková M, Kašparovský T (2021) Feedborne mycotoxins beauvericin and enniatins and livestock animals. Toxins 13: 32. https://doi.org/10.3390/toxins13010032

Laurence MH, Walsh JL, Shuttleworth LA, Robinson DM, Johansen RM, Petrovic T, Vu TTH, Burgess LW, Summerell BA, Liew ECY (2016) Six novel species of *Fusarium* from natural ecosystems in Australia. Fungal Diversity 77: 349–366. https://doi.org/10.1007/s13225-015-0337-6

Leslie JF, Summerell BA (2006) The *Fusarium* Laboratory Manual. Blackwell Publishing. https://doi.org/10.1002/9780470278376

Leslie JF, Zeller KA, Logrieco A, Mulè G, Moretti A, Ritieni A (2004) Species diversity of and toxin production by *Gibberella fujikuroi* species complex strains isolated from native prairie grasses in Kansas. Applied and Environmental Microbiology 70: 2254–2262. https://doi.org/10.1128/AEM.70.4.2254-2262.2004

Liu YJ, Whelen S, Hall BD (1999) Phylogenetic relationships among ascomycetes: Evidence from an RNA polymerse II subunit. Molecular Biology and Evolution 16: 1799–1808. https://doi.org/10.1093/oxfordjournals.molbev.a026092

Logrieco A, Moretti A, Castella G, Kostecki M, Golinski P, Ritieni A, Chelkowski J (1998) Beauvericin production by *Fusarium* species. Applied and Environmental Microbiology 64: 3084–3088. https://doi.org/10.1128/AEM.64.8.3084-3088.1998

Lombard L, van Doorn R, Crous P (2019) Neotypification of *Fusarium chlamydosporum*-a reappraisal of a clinically important species complex. Fungal Systematics and Evolution 4: 183–200. https://doi.org/10.3114/fuse.2019.04.10

Lombard L, van Doorn R, Groenewald JZ, Tessema T, Kuramae EE, Etolo DW, Raaijmakers JM, Crous PW (2022) *Fusarium* diversity associated with the Sorghum-Striga interaction in Ethiopia. Fungal Systematics and Evolution 10: 177–215. https://doi.org/10.3114/fuse.2022.10.08

Lowe KF (2009) The use of temperate species in the Australian subtropics. Proceedings of the New Zealand Grassland Association 71: 9–15. https://doi.org/10.33584/jnzg.2009.71.2763

Marais JP (2001) Factors affecting the nutritive value of kikuyu grass (*Pennisetum clandestinum*) - A review. Tropical Grasslands 35: 65–84.

Marasas WFO, Schumann IH (1972) The Genus *Pithomyces* in South Africa. Bothalia 10: 8. https://doi.org/10.4102/abc.v10i4.1556

Maryani N, Sandoval-Denis M, Lombard L, Crous PW, Kema GHJ (2019) New endemic *Fusarium* species hitch-hiking with pathogenic *Fusarium* strains causing Panama disease in small-holder banana plots in Indonesia. Persoonia 43: 48–69. https://doi.org/10.3767/persoonia.2019.43.02

Moretti A, Susca A, Mulé G, Logrieco A, Proctor R (2013) Molecular biodiversity of mycotoxigenic fungi that threaten food safety. International Journal of Food Microbiology 167: 57–66. https://doi.org/10.1016/j.ijfoodmicro.2013.06.033

Morgavi DP, Riley RT (2007) An historical overview of field disease outbreaks known or suspected to be caused by consumption of feeds contaminated with *Fusarium* toxins. Animal Feed Science and Technology 137: 201–212. https://doi.org/10.1016/j.anifeedsci.2007.06.002

Munkvold G (2017) *Fusarium* species and their associated mycotoxins. Methods in Molecular Biology 1542: 51–106. https://doi.org/10.1007/978-1-4939-6707-0_4

Neal M, Neal J, Fulkerson WJ (2007) Optimal choice of dairy forages in eastern Australia. Journal of Dairy Science 90: 3044–3059. https://doi.org/10.3168/jds.2006-645

Newsholme SJ, Kellerman TS, van der Westhuizen GCA, Soley JT (1983) Intoxication of cattle on kikuyu grass following army worm (*Spodoptera exempta*) invasion. Onderstepoort Journal of Veterinary Research 50: 157–167.

Nguyen LT, Schmidt HA, von Haeseler A, Minh BQ (2015) IQ-TREE: A fast and effective stochastic algorithm for estimating maximum-likelihood phylogenies. Molecular Biology and Evolution 32: 268–274. https://doi.org/10.1093/molbev/msu300

Nichea MJ, Palacios SA, Chiacchiera SM, Sulyok M, Krska R, Chulze SN, Torres AM, Ramirez ML (2015) Presence of multiple mycotoxins and other fungal metabolites in native grasses from a wetland ecosystem in Argentina intended for grazing cattle. Toxins 7: 3309–3329. https://doi.org/10.3390/toxins7083309

Nirenberg H (1976) Untersuchungen über die morphologische und biologische Differenzierung in der *Fusarium*-Sektion Liseola. Technische Universität Berlin, Fachbereich Internationale Agrarentwicklung.

Nor Azliza I, Hafizi R, Nurhazrati M, Salleh B (2014) Production of major mycotoxins by *Fusarium* species isolated from wild grasses in peninsular Malaysia. Sains Malaysiana 43: 89–94.

O'Donnell K, Cigelnik E, Nirenberg HI (1998) Molecular systematics and phylogeography of the *Gibberella fujikuroi* species complex. Mycologia 90: 465–493. https://doi.org/10.1080/00275514.1998.12026933

O'Donnell K, Nirenberg HI, Aoki T, Cigelnik E (2000) A multigene phylogeny of the *Gibberella fujikuroi* species complex: Detection of additional phylogenetically distinct species. Mycoscience 41: 61–78. https://doi.org/10.1007/BF02464387

O'Donnell K, Sutton DA, Rinaldi MG, Gueidan C, Crous PW, Geiser DM (2009) Novel multilocus sequence typing scheme reveals high genetic diversity of human pathogenic members of the *Fusarium incarnatum-F. equiseti* and *F. chlamydosporum* species complexes within the United States. Journal of Clinical Microbiology 47: 3851–3861. https://doi.org/10.1128/JCM.01616-09

O'Donnell K, Sutton DA, Rinaldi MG, Sarver BA, Balajee SA, Schroers H-J, Summerbell RC, Robert VA, Crous PW, Zhang N (2010) Internet-accessible DNA sequence database for identifying fusaria from human and animal infections. Journal of Clinical Microbiology 48: 3708–3718. https://doi.org/10.1128/JCM.00989-10

O'Donnell K, Humber RA, Geiser DM, Kang S, Park B, Robert VA, Crous PW, Johnston PR, Aoki T, Rooney AP, Rehner SA (2012) Phylogenetic diversity of insecticolous fusaria inferred from multilocus DNA sequence data and their molecular identification via FUSARIUM-ID and *Fusarium* MLST. Mycologia 104: 427–445. https://doi.org/10.3852/11-179

O'Donnell K, Rooney AP, Proctor RH, Brown DW, McCormick SP, Ward TJ, Frandsen RJ, Lysøe E, Rehner SA, Aoki T, Robert VA, Crous PW, Groenewald JZ, Kang S, Geiser DM (2013) Phylogenetic analyses of *RPB1* and *RPB2* support a middle Cretaceous origin for a clade comprising all agriculturally and medically important fusaria. Fungal Genetics and Biology 52: 20–31. https://doi.org/10.1016/j.fgb.2012.12.004

O'Donnell K, McCormick SP, Busman M, Proctor RH, Ward TJ, Doehring G, Geiser DM, Alberts JF, Rheeder JP (2018) Marasas et al. 1984 "Toxigenic *Fusarium* Species: Identity and mycotoxicology" revisited. Mycologia 110: 1058–1080. https://doi.org/10.1080/00275514.2018.1519773

Penagos-Tabares F, Khiaosa-Ard R, Nagl V, Faas J, Jenkins T, Sulyok M, Zebeli Q (2021) Mycotoxins, phytoestrogens and other secondary metabolites in Austrian pastures:

Occurrences, contamination levels and implications of geo-climatic factors. Toxins 13: 460. https://doi.org/10.3390/toxins13070460

Phillips N, Goodwin J, Fraiman A, Cole R, Lynn D (1989) Characterization of the *Fusarium* toxin equisetin: The use of phenylboronates in structure assignment. Journal of the American Chemical Society 111: 8223–8231. https://doi.org/10.1021/ja00203a025

Reeb V, Lutzoni F, Roux C (2004) Contribution of *RPB2* to multilocus phylogenetic studies of the euascomycetes (Pezizomycotina, Fungi) with special emphasis on the lichen-forming Acarosporaceae and evolution of polyspory. Molecular Phylogenetics and Evolution 32: 1036–1060. https://doi.org/10.1016/j.ympev.2004.04.012

Reed KFM, Moore DD (2009) A preliminary survey of zearalenone and other mycotoxins in Australian silage and pasture. Animal Production Science 49: 696–703. https://doi.org/10.1071/EA08164

Reed KFM, Sprague M, McFarlane NM, Walsh JR (2004) Zearalenone and its presence in pasture. Science Access 1: 140–143. https://doi.org/10.1071/SA0401036

Ryley M, Bourke C, Liew ECY, Summerell B (2007) Is *Fusarium torulosum* the causal agent of kikuyu poisoning in Australia? Australasian Plant Disease Notes 2: 133–135. https://doi.org/10.1071/DN07053

Sandoval-Denis M, Guarnaccia V, Polizzi G, Crous PW (2018) Symptomatic citrus trees reveal a new pathogenic lineage in *Fusarium* and two new *Neocosmospora* species. Persoonia 40: 1–25. https://doi.org/10.3767/persoonia.2018.40.01

Santos A, Trindade JVC, Lima CS, Barbosa RDN, da Costa AF, Tiago PV, de Oliveira NT (2019) Morphology, phylogeny, and sexual stage of *Fusarium caatingaense* and *Fusarium pernambucanum*, new species of the *Fusarium incarnatum-equiseti* species complex associated with insects in Brazil. Mycologia 111: 244–259. https://doi.org/10.1080/00275514.2019.1573047

Skládanka J, Nedělník J, Adam V, Doležal P, Moravcová H, Dohnal V (2011) Forage as a primary source of mycotoxins in animal diets. International Journal of Environmental Research and Public Health 8: 37–50. https://doi.org/10.3390/ijerph8010037

Smith JF, di Menna ME, McGowan LT (1990) Reproductive performance of Coopworth ewes following oral doses of zearalenone before and after mating. Journal of Reproduction and Fertility 89: 99–106. https://doi.org/10.1530/jrf.0.0890099

Summerell BA, Laurence MH, Liew ECY, Leslie JF (2010) Biogeography and phylogeography of *Fusarium*: A review. Fungal Diversity 44: 3–13. https://doi.org/10.1007/s13225-010-0060-2

Tan YP, Shivas RG (2023) Nomenclatural novelties. Index of Australian Fungi 5: 1–12. https://doi.org/10.5281/zenodo.776516

Tan YP, Shivas RG (2024) Nomenclatural novelties. Index of Australian Fungi 29: 1–10. https://doi.org/10.5281/zenodo.10602835

Taylor JW, Jacobson DJ, Kroken S, Kasuga T, Geiser DM, Hibbett DS, Fisher MC (2000) Phylogenetic species recognition and species concepts in fungi. Fungal Genetics and Biology 31: 21–32. https://doi.org/10.1006/fgbi.2000.1228

Trenholm HL, Thompson BK, Hartin KE, Greenhalgh R, McAllister AJ (1985) Ingestion of vomitoxin (deoxynivalenol)-contaminated wheat by nonlactating dairy cows. Journal of Dairy Science 68: 1000–1005. https://doi.org/10.3168/jds.S0022-0302(85)80921-8

Truter WF, Botha PR, Dannhauser CS, Maasdorp BV, Miles N, Smith A, Snyman HA, Tainton NM (2015) Southern African pasture and forage science entering the 21st century: Past to present. African Journal of Range and Forage Science 32: 73–89. https://doi.org/10.2989/10220119.2015.1054429

van der Colf J, Botha PR, Meeske R, Truter WF (2015) Grazing capacity, milk production and milk composition of kikuyu over-sown with annual or perennial ryegrass. African Journal of Range and Forage Science 32: 143–151. https://doi.org/10.2989/10220119.2015.1052096

Villani A, Moretti A, de Saeger S, Han Z, di Mavungu JD, Soares CMG, Proctor RH, Venâncio A, Lima N, Stea G, Paciolla C, Logrieco AF, Susca A (2016) A polyphasic approach for characterization of a collection of cereal isolates of the *Fusarium incarnatum-equiseti* species complex. International Journal of Food Microbiology 234: 24–35. https://doi.org/10.1016/j.ijfoodmicro.2016.06.023

Wang MM, Chen Q, Diao YZ, Duan WJ, Cai L (2019) *Fusarium incarnatum-equiseti* complex from China. Persoonia 43: 70–89. https://doi.org/10.3767/persoonia.2019.43.03

Weaver G, Kurtz H, Behrens J, Robison T, Seguin B, Bates F, Mirocha C (1986) Effect of zearalenone on the fertility of virgin dairy heifers. American Journal of Veterinary Research 47: 1395–1397. https://doi.org/10.2460/ajvr.1986.47.06.1395

Wong PT, Roth IJ, Jackson AR (1987) Kikuyu poisoning of cattle in New South Wales and its relationship to pasture fungi on kikuyu grass (*Pennisetum clandestinum*). Austrian Veterinary Journal 64: 229–232. https://doi.org/10.1111/j.1751-0813.1987.tb09688.x

Xia JW, Sandoval-Denis M, Crous PW, Zhang XG, Lombard L (2019) Numbers to names - Restyling the *Fusarium incarnatum-equiseti* species complex. Persoonia 43: 186–221. https://doi.org/10.3767/persoonia.2019.43.05

Yilmaz N, Sandoval-Denis M, Lombard L, Visagie CM, Wingfield BD, Crous PW (2021) Redefining species limits in the *Fusarium fujikuroi* species complex. Persoonia 46: 129–162. https://doi.org/10.3767/persoonia.2021.46.05

Supplementary material 1

Maximum likelihood phylogenetic tree of *the Fusarium incarnatum-equiseti* species complex based on the *CaM* dataset

Authors: Claudette Dewing, Cobus M. Visagie, Emma T. Steenkamp, Brenda D. Wingfield, Neriman Yilmaz

Data type: pdf

Explanation note: Strains of species isolated from this study are shown in black bold text; strains of newly described species are indicated in red bold text. The tree was rooted to *Fusarium concolor*. Branch support in nodes higher than 80% are indicated at relevant branches (^{T} = ex-type, ^{ET} = epitype, ^{NT} = neotype).

Link: https://doi.org/10.3897/mycokeys.115.148914.suppl1

Supplementary material 2

Maximum likelihood phylogenetic tree of *the Fusarium incarnatum-equiseti* species complex based on the *RPB2* dataset

Authors: Claudette Dewing, Cobus M. Visagie, Emma T. Steenkamp, Brenda D. Wingfield, Neriman Yilmaz

Data type: pdf

Explanation note: Strains of species isolated from this study are shown in black bold text; strains of newly described species are indicated in red bold text. The tree was rooted to *Fusarium concolor*. Branch support in nodes higher than 80% are indicated at relevant branches (^{T} = ex-type, ^{ET} = epitype, ^{NT} = neotype).

Link: https://doi.org/10.3897/mycokeys.115.148914.suppl2

Supplementary material 3

Maximum likelihood phylogenetic tree of *the Fusarium incarnatum-equiseti* species complex based on the *TEF* dataset

Authors: Claudette Dewing, Cobus M. Visagie, Emma T. Steenkamp, Brenda D. Wingfield, Neriman Yilmaz

Data type: pdf

Explanation note: Strains of species isolated from this study are shown in black bold text; strains of newly described species are indicated in red bold text. The tree was rooted to *Fusarium concolor*. Branch support in nodes higher than 80% are indicated at relevant branches (^{T} = ex-type, ^{ET} = epitype, ^{NT} = neotype).

Link: https://doi.org/10.3897/mycokeys.115.148914.suppl3

Supplementary material 4

Maximum likelihood phylogenetic tree of the *Fusarium incarnatum*-equiseti species complex based on the *TEF* dataset obtained from Botha et al. (2014) and relevant reference sequences

Authors: Claudette Dewing, Cobus M. Visagie, Emma T. Steenkamp, Brenda D. Wingfield, Neriman Yilmaz

Data type: pdf

Explanation note: Strains of species isolated from this study are shown in black bold text; strains of newly described species are indicated in red bold text. The tree was rooted to *Fusarium concolor*. Branch support in nodes higher than 80% are indicated at relevant branches (^{T} = ex-type, ^{ET} = epitype, ^{NT} = neotype).

Link: https://doi.org/10.3897/mycokeys.115.148914.suppl4

Supplementary material 5

Strains examined in this study, with information about substrate, country and GenBank accessions of sequences

Authors: Claudette Dewing, Cobus M. Visagie, Emma T. Steenkamp, Brenda D. Wingfield, Neriman Yilmaz

Data type: xlsx

Link: https://doi.org/10.3897/mycokeys.115.148914.suppl5

MycoKeys 115: 273–308 (2025)
DOI: 10.3897/mycokeys.115.147044

Research Article

Additions to the coriaceous families Peniophoraceae and Stereaceae (Russulales): Six novel wood-inhabiting taxa in the genera *Conferticium*, *Gloeocystidiellum*, and *Peniophora* from southwest China

Lu Wang[1,2], Yonggao Zhu[2], Siyuan He[2], Sana Jabeen[3], Changlin Zhao[1,2,4]

1 *The Key Laboratory of Forest Resources Conservation and Utilization in the Southwest Mountains of China Ministry of Education, Key Laboratory of National Forestry and Grassland Administration on Biodiversity Conservation in Southwest China, Yunnan Provincial Key Laboratory for Conservation and Utilization of In-forest Resource, Southwest Forestry University, Kunming 650224, China*
2 *College of Forestry, Southwest Forestry University, Kunming 650224, China*
3 *Department of Botany, Division of Science and Technology, University of Education, Lahore, Punjab, Pakistan*
4 *Yunnan Academy of Biodiversity, Southwest Forestry University, Kunming 650224, China*
Corresponding author: Changlin Zhao (fungi@swfu.edu.cn)

This article is part of:
Exploring the Hidden Fungal Diversity: Biodiversity, Taxonomy, and Phylogeny of Saprobic Fungi
Edited by Samantha C. Karunarathna, Danushka Sandaruwan Tennakoon, Ajay Kumar Gautam

OPEN ACCESS

Academic editor:
Samantha C. Karunarathna
Received: 17 January 2025
Accepted: 7 March 2025
Published: 21 March 2025

Citation: Wang L, Zhu Y, He S, Jabeen S, Zhao C (2025) Additions to the coriaceous families Peniophoraceae and Stereaceae (Russulales): Six novel wood-inhabiting taxa in the genera *Conferticium*, *Gloeocystidiellum*, and *Peniophora* from southwest China. MycoKeys 115: 273–308. https://doi.org/10.3897/mycokeys.115.147044

Abstract

Russulales comprises a highly diverse group of species with respect to basidiomata morphology and hymenophore configuration, in which this order is highly heterogeneous, that can be classified as resupinate, effused-reflexed, discoid, clavarioid, pileate, or stipitate, and with varied hymenophores such as smooth, hydnoid, poroid, and lamellate in different russuloid species. Species in Russulales have been considered to have significant economic value. Six new wood-inhabiting fungi belonging to the genera *Conferticium*, *Gloeocystidiellum*, and *Peniophora* of two families, Peniophoraceae and Stereaceae (Russulales), were found in southwest China. Sequences of ITS+nLSU loci of six new taxa were generated, and phylogenetic analyses were performed with the maximum likelihood, maximum parsimony, and Bayesian inference methods with an emphasis on the phylogeny of wood-inhabiting smooth species in this order. The combined ITS+nLSU loci analysis showed that the six new species grouped within the order Russulales, in which *Conferticium tuberculatum*, *Gloeocystidiellum cremeum*, and *G. fissuratum* grouped into the family Stereaceae, and *Peniophora albohymenia*, *P. hengduanensis*, and *P. punctata* grouped into the family Peniophoraceae. The morphology and multi-gene phylogenetic analyses confirmed the novelty and placement of the six new taxa. Descriptions, illustrations, and phylogenetic analysis results of the new taxa are provided.

Key words: Biodiversity, corticioid fungi, molecular systematics, taxonomy, Yunnan Province

Introduction

The order Russulales Kreisel ex P.M. Kirk, P.F. Cannon & J.C. David is a highly diverse group of the class Agaricomycetes, which includes around 4,436 described species in 98 genera and 11 families (Hyde et al. 2017; Caboň et al. 2019; Vidal et al. 2019; He et al. 2024). Russulales contains not only the lamellate species like *Russula* Pers. and *Lactarius* Pers. (Herrera et al. 2018; Caboň et al. 2019) but also the poroid, hydnoid, and corticioid representatives like *Asterostroma* Massee, *Hericium* Pers., *Heterobasidion* Bref., and *Peniophora* Cooke (Miller et al. 2006; Chen et al. 2016a; Wu et al. 2020; Yuan et al. 2021; Zhou et al. 2024). In the past few decades, a lot of the new taxa of Russulales have been gathered through both morphological characteristics and DNA sequence phylogenetic analyses (Zhou and Dai 2013; Chen et al. 2015, 2016b; Wu et al. 2020; Zou et al. 2022; Bhunjun et al. 2024; Deng et al. 2024b; Dong et al. 2024; Zhou et al. 2024). Resupinate basidiomata are common in the families Echinodontiaceae, Peniophoraceae, Stereaceae, Terrestriporiaceae, and Xenasmataceae (He et al. 2024; Liu et al. 2024).

The genus *Conferticium* Hallenb. 1980 (Stereaceae, Russulales), typified by *C. insidiosum* (Bourdot & Galzin) Hallenb. (Bernicchia and Gorjón 2010), is characterized by the resupinate basidiomata with membranaceous to ceraceous, smooth to tuberculate hymenophore, a monomitic hyphal system with simple-septate, and numerous cylindrical, sinuous gloeocystidia (Bernicchia and Gorjón 2010). Based on the MycoBank database (http://www.mycobank.org, accessed on 26 February 2025) and the Index Fungorum (http://www.indexfungorum.org, accessed on 26 February 2025), *Conferticium* has registered six specific and infraspecific names; however, only five species are widely recognized (Larsson and Larsson 2003; Bernicchia and Gorjón 2010).

Donk (1931) described *Gloeocystidiellum* (Stereaceae, Russulales), typified by *G. porosum* (Berk. and M.A. Curtis) Donk, as characterized by their resupinate basidiomata with membranaceous to ceraceous, smooth, rarely grandinioid or odontioid hymenophore, a monomitic hyphal system with simple-septate or clamped generative hyphae, and the gloeocystidia numerous, verrucose or aculeate basidiospores (Wu 1996; Bernicchia and Gorjón 2010; Zhao and Zhao 2023). Based on the MycoBank database (http://www.mycobank.org, accessed on 26 February 2025) and the Index Fungorum (http://www.indexfungorum.org, accessed on 26 February 2025), *Gloeocystidiellum* has registered 86 specific and infraspecific names, and the actual number of species is 37 (Zhao and Zhao 2023).

The genus *Peniophora* Cooke (Peniophoraceae, Russulales) was introduced in 1879, typified by *P. quercina* Pers. ex Fr., and it is characterized by the resupinate basidiomata with a smooth hymenophore, a monomitic hyphal system, thin- to thick-walled simple-septate or clamped generative hyphae, dendrohyphidia, lamprocystidia, and gloeocystidia present or absent, and thin-walled, smooth, ellipsoid, cylindrical to allantoid basidiospores negative in Melzer's reagents (Bernicchia and Gorjón 2010; Zou et al. 2022; Xu et al. 2023). Species of the genus prefer to grow on small branches of trees, especially dead but still attached ones in exposed and dry environments (Xu et al. 2023). Based on the MycoBank database (http://www.mycobank.org, accessed on 26 February 2025) and the Index Fungorum (http://www.indexfungorum.org, accessed on 26 February 2025), *Peniophora* was registered with 657 specific and infraspecific names, and the actual number of the species is 211, in which most species have been moved to other genera, and the morphological circumscription of *Peniophora* has been narrowed (Xu et al. 2023). Currently, they occur mainly in the tropical and subtropical areas of the world (Zou et al. 2022; Xu et al. 2023).

Recently, the analysis of DNA sequences has emerged as a common method for deducing fungal phylogenies and enhancing higher classification frameworks through the integration of genetic traits (Wijayawardene et al. 2022, 2024; Dong et al. 2024; He et al. 2022, 2024; Zhang et al. 2023b; Zhao et al. 2023; Zhou et al. 2023; 2025). According to recent research on molecular systematics and divergence times, Basidiomycota is classified into 127 families belonging to 47 orders under 14 classes (He et al. 2024). The family Stereaceae included nineteen genera: *Acanthobasidium*, *Acanthofungus*, *Acanthophysellum*, *Aleurobotrys*, *Aleurodiscus*, *Amylohyphus*, *Amylosporomyces*, *Coniophorafomes*, *Dextrinocystidium*, *Gloeocystidiellum*, *Gloeocystidiopsis*, *Gloeomyces*, *Gloeosoma*, *Megalocystidium*, *Neoaleurodiscus*, *Scotoderma*, *Stereodiscus*, *Stereum*, and *Xylobolus* (Larsson 2007; Vu et al. 2019; He et al. 2024). According to recent research on molecular systematics, the genus *Conferticium* has been reported to have one new taxon, *C. fissuratum* Xin Yang & C.L. Zhao, which is from Yunnan Province, China (Bernicchia and Gorjón 2010; Shen et al. 2024). In the previous study, the phylogenetic relationships among russuloid basidiomycetes were investigated using sequence data from the nuclear 5.8S, ITS2, and large-subunit rDNA genes and elucidated evolutionary relationships within some species of the genus *Gloeocystidiellum* (Larsson and Larsson 2003). The high phylogenetic diversity among corticioid homobasidiomycetes indicated that the species *G. subasperisporum* (Litsch.) J. Erikss. & Ryvarden grouped into the russuloid clade and grouped with the close species *Gloeodontia discolor* (Berk. & M.A. Curtis) Boidin (Larsson et al. 2004). Several morphological and molecular studies as well as cultural studies and intercompatibility tests have analyzed species delimitation in the *Gloeocystidiellum porosum-clavuligerum* group, which revealed that the clade corresponded with two well-distinguished species, *G. kenyense* and *G. clavuligerum* (Telleria et al. 2012). The molecular research carried out on the genus *Gloeocystidiellum*, in which the species *G. granulatum* (Sheng H. Wu) E. Larss. & K.H. Larss and *G. permixtum* (Boidin, Lanq. & Gilles) E. Larss. & K.H. Larss are proposed as new combinations (Larsson et al. 2020). Recently, molecular studies involving *Gloeocystidiellum* based on single-locus or multi-locus datasets have introduced two new taxa, viz. *G. lojanense* A. Jaram., D. Cruz & Decock, and *G. yunnanense* Y.L. Zhao & C.L. Zhao (Jaramillo-Riofrío et al. 2023; Zhao and Zhao 2023).

The genus *Peniophora* Cooke is a large genus of corticioid fungi, which is a cosmopolitan genus with a wide distribution from boreal to tropical areas, causing a white rot on both angiosperms and gymnosperms (Yurchenko 2010; Zou et al. 2022; Xu et al. 2023). Many new lineages and taxa were found and described, and some morphologically dissimilar taxa were proved to be closely related in the phylogeny of *Peniophora* in recent years (Harrington et al. 2021; Lambevska-Hristova 2022; Zou et al. 2022; Xu et al. 2023). The ITS and nLSU sequences of *Peniophora* species, including some from type specimens, were released in GenBank in recent studies and thus made it possible to deeply study the phylogeny of this group (Vu et al. 2019; Zou et al. 2022). The researchers performed the most comprehensive phylogenetic studies using ITS+nLSU datasets, including most of the *Peniophora* species described worldwide (Zou et al. 2022; Xu et al. 2023). Most clades in *Peniophora* are far too resolved, at least considering only ITS or nLSU rDNA regions, and probably a genome full of phylogenetic reconstruction is needed to establish with certitude groups or patterns in the evolution of the different species (Xu et al. 2023; Dong et al. 2024).

Many wood-inhabiting specimens were collected during investigations on wood-inhabiting fungi in the Yunnan-Guizhou Plateau, China. To clarify the placement and relationships of these specimens, we carried out a phylogenetic and taxonomic study based on the ITS+nLSU sequences. These specimens were assigned to the genera *Conferticium*, *Gloeocystidiellum*, and *Peniophora* of the order Russulales. Therefore, six new species, *Conferticium tuberculatum*, *Gloeocystidiellum cremeum*, *G. fissuratum*, *Peniophora albohymenia*, *P. hengduanensis*, and *P. punctata*, are proposed with descriptions and illustrations based on the morphological characteristics and phylogenetic analyses.

Materials and methods

Sample collection and herbarium specimen preparation

Fresh basidiomata of the wood-inhabiting fungi growing on angiosperm branches were collected from the Zhaotong and Diqing of Yunnan Province, China. The samples were photographed *in situ*, and fresh macroscopic details and collection information (Rathnayaka et al. 2024) were recorded. Photographs were taken by a Jianeng 80D camera (Tokyo, Japan). All photos were stacked and merged using Helicon Focus Pro 7.7.5 software. Specimens were dried in an electric food dehydrator at 40 °C, then sealed and stored in an envelope bag and deposited in the herbarium of the Southwest Forestry University (SWFC), Kunming, Yunnan Province, China.

Morphology

Macromorphological descriptions are based on field notes and photos captured in the field and laboratory and follow the color terminology of Petersen (1996). Micromorphological data were obtained from the dried specimens following observation under a light microscope (Zhao et al. 2023a; Dong et al. 2024). The following abbreviations were used: KOH = 5% potassium hydroxide water solution, CB+ = cyanophilous, CB = cotton clue, CB– = acyanophilous, IKI = Melzer's reagent, IKI+ = amyloid, IKI– = both inamyloid and indextrinoid, L = means spore length (arithmetic average for all spores), W = means spore width (arithmetic average for all spores), Q = variation in the L/W ratios between the specimens studied, and n = a/b (number of spores (a) measured from a given number (b) of specimens).

DNA extraction, amplification, and sequencing

The CTAB rapid plant genome extraction kit-DN14 (Aidlab Biotechnologies Co., Ltd., Beijing, China) was used to obtain genomic DNA from dried specimens, according to the previous study (Zhao and Wu 2017). The ITS region was amplified with the primer pair ITS5 and ITS4 (White et al. 1990). The nuclear nLSU region was amplified with primer pair LR0R and LR7 (Vilgalys and Hester 1990). The PCR procedure for ITS was as follows: initial denaturation at 95 °C for 3 min, followed by 35 cycles at 94 °C for 40 s, 54 °C for 45 s, and 72 °C for 1 min; and a final extension at 72 °C for 10 min. The PCR procedure for nLSU was as follows: initial denaturation at 94 °C for 1 min, followed by 35 cycles at 94 °C for 30 s, 50 °C for 1 min, and 72 °C for 1.5 min, and a final extension at 72 °C for 10 min. The PCR products were purified and sequenced at Kunming Tsingke Biological Technology Limited Company, Kunming, Yunnan Province, P.R. China. All newly generated sequences were deposited in GenBank (Table 1).

Phylogenetic analyses

Sequences were aligned using MAFFT version 7, adjusting the direction of nucleotide sequences according to the first sequence and selecting the G-INS-i iterative refinement method (Katoh et al. 2019). The alignment was adjusted manually using AliView version 1.27 (Larsson 2014). A dataset of concatenated ITS and nLSU sequences was used to determine the phylogenetic position of the six new species. (1) *Vararia tropica* A.L. Welden and *V. yaoshanensis* Y.L. Deng & C.L. Zhao were assigned as outgroups to root trees in the ITS+nLSU analysis (Fig. 1) (Deng et al. 2024b); (2) *Stereum complicatum* (Fr.) Fr. and *S. hirsutum* (Willd.) Pers. were assigned as outgroups to root trees following the ITS+nLSU analysis (Fig. 2) (Maekawa et al. 2023); (3) *Gloeocystidiellum yunnanense* Y.L. Zhao & C.L. Zhao and *G. porosum* Berk. & M.A. Curtis) Donk were assigned as outgroups to root trees following the ITS+nLSU analysis (Fig. 3) (Zhao and Zhao 2023); (4) *Asterostroma rhizomorpharum* H.M. Zhou & C.L. Zhao and *A. yunnanense* Y.L. Deng & C.L. Zhao were assigned as outgroups to root trees following the ITS+nLSU analysis (Fig. 4) (Zhou et al. 2024).

Maximum parsimony (MP), maximum likelihood (ML), and Bayesian inference (BI) analyses were applied to the combined three datasets following the methods outlined in a previous study (Zhao and Wu 2017), and the tree construction procedure was performed in PAUP* version 4.0b10 (Swofford 2002). All characters were equally weighted, and gaps were treated as missing data. Trees were inferred using the heuristic search option with TBR branch swapping and 1,000 random sequence additions. Max-trees were set to 5000, branches of zero length were collapsed, and all parsimonious trees were saved. Clade robustness was assessed using bootstrap (BT) analysis with 1,000 replicates (Felsenstein 1985). Descriptive tree statistics—tree length (TL), consistency index (CI), retention index (RI), rescaled consistency index (RC), and homoplasy index (HI)—were calculated for each maximum parsimonious tree generated. Additionally, the multiple sequence alignment was also analyzed using maximum likelihood (ML) in RAxML-HPC2 through the Cipres Science Gateway (Miller et al. 2012). Branch support (BS) for ML analysis was determined by 1000 bootstrap replicates. jModelTest v2 (Darriba et al. 2012) was used to determine the best-fit evolutionary model for each data set for Bayesian inference (BI), which was performed using MrBayes 3.2.7a (Ronquist et al. 2012). The first one-fourth of all generations was discarded as burn-in. The majority rule consensus tree of all remaining trees was calculated. Branches were considered as significantly supported if they received a maximum likelihood bootstrap value (BS) ≥ 70%, a maximum parsimony bootstrap value (BT) ≥ 50%, or Bayesian posterior probabilities (BPP) ≥ 0.95.

Table 1. Names, voucher numbers, references, and corresponding GenBank accession numbers of the taxa used in the phylogenetic analyses.

Taxa	Voucher	Locality	GenBank accession		Reference
			ITS	nLSU	
Acanthobasidium bambusicola	He2357	China	KU559343	KU574833	Dai and He 2016
Acanthobasidium penicillatum	HHB13223	USA	—	KU574816	Maekawa et al. 2023
Acanthofungus rimosus	Wu 9601-1	China	MF043521	AY039333	Maekawa et al. 2023
Acanthophysellum cerussatum	He 20120920—3	China	KU559339	KU574830	Maekawa et al. 2023
Acanthophysium bisporum	T614	USA	—	AY039327	Maekawa et al. 2023
Acanthophysium lividocaeruleum	FP-100292	USA	—	AY039319	Maekawa et al. 2023
Aleurobotrys botryosus	He2712	China	KX306877	KY450788	Maekawa et al. 2023
Aleurobotrys botryosus	Wu 9302-61	China	—	AY039331	Maekawa et al. 2023
Aleurodiscus bambusinus	He4261	China	KY706207	KY706219	Yan et al. 2018
Aleurodiscus canadensis	Wu1207-90	China	KY706203	KY706225	Yan et al. 2018
Aleurodiscus mirabilis	Dai 13281	China	KU559350	KU574839	Yan et al. 2018
Asterostroma laxum	EL33-99	Estonia	AF506410	AF506410	Larsson and Larsson 2003
Asterostroma muscicola	KHL9537	Puerto Rico	AF506409	AF506409	Larsson and Larsson 2003
Asterostroma rhizomorpharum	CLZhao 31212	China	OR672732	OR879302	Zhou et al. 2024
Asterostroma yunnanense	CLZhao 22781	China	OR048809	OR506285	Deng et al. 2024a
Baltazaria octopodites	FLOR 56449	Brazil	MH260025	MH260047	Leal-Dutra et al. 2018
Conferticium heimii	CBS321.66	African	MH858805	MH858805	Tian et al. 2018
Conferticium ochraceum	CLZhao 21515	China	ON211619	—	Present study
Conferticium ochraceum	G07_P24A	Switzerland	KT943933	—	Stroheker et al. 2018
Conferticium ravum	CBS:125849	Estonia	MH863805	MH875269	Vu et al. 2019
Conferticium ravum	NH13291	USA	AF506382	AF506382	Larsson and Larsson 2003
Conferticium tuberculatum	CLZhao 29376*	China	PQ166602	PQ295861	Present study
Conferticium tuberculatum	CLZhao 29390	China	PQ166603	PQ295862	Present study
Dichostereum effuscatum	GG930915	France	AF506390	AF506390	Larsson and Larsson 2003
Dichostereum pallescens	NH7046/673	Canada	AF506392	AF506392	Larsson and Larsson 2003
Entomocorticium cobbii	B720	USA	MT741707	MT741692	Harrington et al. 2021
Entomocorticium whitneyi	B1069	USA	MT741713	MT741698	Harrington et al. 2021
Gloeocystidiellum aspellum	He4262	China	—	KY860460	Jaramillo-Riofrío et al. 2023
Gloeocystidiellum aspellum	LIN 625	China	AF506432	AF506432	Yan et al. 2018
Gloeocystidiellum bisporum	CBS/961.96	Sweden	AY048875	AY048875	Jaramillo-Riofrío et al. 2023
Gloeocystidiellum bisporum	KHL11135	Norway	AY048877	AY048877	Larsson and Larsson 2003
Gloeocystidiellum clavuligerum	GB/NH11185	Spain	AF310088	AF310088	Jaramillo-Riofrío et al. 2023
Gloeocystidiellum clavuligerum	NH13159/2731	Russia	AF310083	AF310083	Larsson and Larsson 2003
Gloeocystidiellum compactum	Wu880615-21	China	AF506434	AF506434	Maekawa et al. 2023
Gloeocystidiellum cremeum	CLZhao 29477*	China	PQ287846	PQ295863	Present study
Gloeocystidiellum cremeum	CLZhao 33623	China	PQ287847	PQ295864	Present study
Gloeocystidiellum cremeum	CLZhao 33690	China	PQ287848	—	Present study
Gloeocystidiellum fissuratum	CLZhao 32247	China	PQ287849	PQ295865	Present study
Gloeocystidiellum fissuratum	CLZhao 32303	China	PQ287850	PQ295866	Present study
Gloeocystidiellum fissuratum	CLZhao 32498*	China	PQ287851	—	Present study
Gloeocystidiellum formosanum	Wu9404-19	China	AF506439	AF506439	Maekawa et al. 2023
Gloeocystidiellum heimii	LY/CBS321.66	African	AF506381	AF506381	Jaramillo-Riofrío et al. 2023
Gloeocystidiellum kenyense	TFC/15278	Portugal	FR878082	—	Jaramillo-Riofrío et al. 2023
Gloeocystidiellum kenyense	TFC/15309	Portugal	FR878083	—	Jaramillo-Riofrío et al. 2023
Gloeocystidiellum lojanense	HUTPL(F)/2181	Ecuador	OP377059	OP377059	Jaramillo-Riofrío et al. 2023
Gloeocystidiellum lojanense	HUTPL(F)/550	Ecuador	OP377083	OP377083	Jaramillo-Riofrío et al. 2023
Gloeocystidiellum luridum	HK9808	Germany	AF506421	AF506421	Maekawa et al. 2023

Taxa	Voucher	Locality	GenBank accession		Reference
			ITS	nLSU	
Gloeocystidiellum porosum	CBS/51085	Netherlands	AF310097	AF310097	Jaramillo-Riofrío et al. 2023
Gloeocystidiellum porosum	NH 10434	Denmark	AF310094	AF310094	Larsson and Hallenberg 2001
Gloeocystidiellum purpureum	Wu9310-45	China	AF441338	AF441338	Larsson and Hallenberg 2001
Gloeocystidiellum rajchenbergii	GB/NH16348	Chile	JQ734555	—	Jaramillo-Riofrío et al. 2023
Gloeocystidiellum rajchenbergii	GB/NH16358	Chile	JQ734554	—	Jaramillo-Riofrío et al. 2023
Gloeocystidiellum triste	KHL10334	Sweden	AF506442	AF506442	Maekawa et al. 2023
Gloeocystidiellum yunnanense	CLZhao 7165	China	MZ710569	MZ710571	Zhao and Zhao 2023
Gloeocystidiellum yunnanense	CLZhao 7202	China	MZ710570	MZ710572	Zhao and Zhao 2023
Gloeocystidiopsis flammea	CBS:324.66	African	AF506437	AF506437	Larsson and Larsson 2003
Gloeocystidiopsis heimii	CBS:321.66	Sweden	AF506381	AF506381	Larsson and Larsson 2003
Gloiothele lactescens	EL8-98	Sweden	AF506453	AF506453	Larsson and Larsson 2003
Gloiothele lamellosa	KHL11031	Venezuela	AF506454	AF506454	Larsson and Larsson 2003
Lachnocladium schweinfurthianum	KM 49740	Cameroon	MH260033	MH260051	Leal-Dutra et al. 2018
Megalocystidium chelidonium	LodgeSJ110.1	USA	AF506441	AF506441	Larsson and Larsson 2003
Megalocystidium diffissum	V.Spirin4244	Sweden	MT477147	MT477147	Maekawa et al. 2023
Megalocystidium leucoxanthum	HK9808	Sweden	AF506420	AF506420	Maekawa et al. 2023
Metulodontia nivea	NH13108	Russia	AF506423	AF506423	Larsson and Larsson 2003
Neoaleurodiscus fujii	He2921	China	KU559357	KU574845	Dai et al. 2017
Neoaleurodiscus fujii	Wu0807-41	Japan	—	FJ799924	Dai et al. 2017
Parapterulicium subarbusculum	FLOR 56456	Brazil	MH260026	MH260048	Leal-Dutra et al. 2018
Peniophora albobadia	CBS:329.66	France	MH858809	MH870448	Vu et al. 2019
Peniophora albobadia	He2159	USA	MK588755	MK588795	Xu et al. 2023
Peniophora albohymenia	CLZhao 23473*	China	PQ066419	PQ295867	Present study
Peniophora aurantiaca	CBS:396.50	France	MH856678	MH868195	Vu et al. 2019
Peniophora aurantiaca	UBCF:19732	Canada	HQ604854	HQ604854	Xu et al. 2023
Peniophora bicornis	He3609	China	MK588763	MK588803	Xu et al. 2023
Peniophora bicornis	He4767	China	MK588764	MK588804	Xu et al. 2023
Peniophora borbonica	He4597	China	MK588766	MK588806	Xu et al. 2023
Peniophora borbonica	He4606	China	MK588765	MK588805	Xu et al. 2023
Peniophora cinerea	CLZhao 23390	China	PQ166604	PQ295868	Present study
Peniophora cinerea	He3725	China	MK588769	MK588809	Xu et al. 2023
Peniophora crassitunicata	CLZhao 29461	China	PQ166605	PQ295869	Present study
Peniophora crassitunicata	He3814	China	MK588770	MK588810	Xu et al. 2023
Peniophora cremicolor	He5380	China	MK588791	MK588831	Xu et al. 2023
Peniophora duplex	CBS:286.58	Canada	MH857787	MH869321	Vu et al. 2019
Peniophora duplex	TPDuB1022	USA	AF119519	—	Harrington and Hsaiu 2003
Peniophora erikssonii	CBS:287.58	France	MH857788	MH869322	Vu et al. 2019
Peniophora erikssonii	Cui 11871	China	MK588771	MK588811	Xu et al. 2023
Peniophora exima	T-523	USA	MK588772	MK588812	Xu et al. 2023
Peniophora fasticata	CBS:942.96	Ethiopia	MH862624	—	Vu et al. 2019
Peniophora fissilis	CBS:681.91	Reunion	MH862298	MH873975	Vu et al. 2019
Peniophora fissilis	CBS:684.91	Mascarene Islands	MH862299	MH873976	Vu et al. 2019
Peniophora gilbertsonii	CBS:357.95	USA	MH862528	MH874164	Vu et al. 2019
Peniophora gilbertsonii	CBS:360.95	USA	MH862530	MH874165	Vu et al. 2019
Peniophora guadelupensis	CBS:715.91	Guadeloupe	MH862304	MH873977	Vu et al. 2019
Peniophora halimi	CBS:863.84	France	MH861844	MH873532	Vu et al. 2019
Peniophora halimi	CBS:864.84	France	MH861845	MH873533	Vu et al. 2019
Peniophora hengduanensis	CLZhao 34697*	China	PQ066422	PQ295870	Present study
Peniophora incarnata	CBS:398.50	France	MH856680	MH868197	Vu et al. 2019
Peniophora incarnata	CBS:399.50	France	MH856681	MH868198	Vu et al. 2019

Taxa	Voucher	Locality	GenBank accession		Reference
			ITS	nLSU	
Peniophora junipericola	CBS:349.54	Sweden	MH857354	—	Vu et al. 2019
Peniophora junipericola	He2462	China	MK588773	MK588813	Xu et al. 2023
Peniophora kuehneri	CBS:719.91	Mascarene Islands	MH862307	MH873980	Vu et al. 2019
Peniophora kuehneri	He4745	China	MK588757	MK588797	Xu et al. 2023
Peniophora kuehneroides	CBS:731.91	Mascarene Islands	MH862317	MH873989	Vu et al. 2019
Peniophora kuehneroides	CBS:732.91	Mascarene Islands	MH862318	MH873990	Vu et al. 2019
Peniophora laete	CBS:256.56	France	MH857617	MH869165	Vu et al. 2019
Peniophora lassa	He3052	China	MK588758	MK588798	Xu et al. 2023
Peniophora lassa	SP6129	Russia	KJ509191	—	Spirin and Kout 2015
Peniophora laxitexta	BAFC 3309	Argentina	FJ882040	—	Robles et al. 2011
Peniophora laxitexta	LGMF1159	Argentina	JX559580	—	Xu et al. 2023
Peniophora lilacea	CBS:337.66	Armenia	MH858813	MH870452	Vu et al. 2019
Peniophora limitata	olrim 963	Lithuania	AY787678	—	Lygis et al. 2005
Peniophora lycii	Boid-437	France	MK588774	MK588814	Xu et al. 2023
Peniophora lycii	CBS:264.56	France	MH857624	MH869169	Vu et al. 2019
Peniophora major	He5528	China	MK588792	MK588832	Xu et al. 2023
Peniophora malaiensis	CBS:679.91	Singapore	MH862297	MH873974	Vu et al. 2019
Peniophora malaiensis	CLZhao 23595	China	PQ166607	PQ295871	Present study
Peniophora manshurica	He2956	China	MK588776	MK588816	Xu et al. 2023
Peniophora manshurica	He3729	China	MK588777	MK588817	Xu et al. 2023
Peniophora meridionalis	CBS:289.58	France	MH857789	MH869323	Vu et al. 2019
Peniophora molesta	CBS:676.91	Gabon	MH862294	MH873973	Vu et al. 2019
Peniophora molesta	CBS:677.91	Gabon	MH862295	—	Vu et al. 2019
Peniophora monticola	CBS:649.91	Reunion	MH862289	MH873970	Vu et al. 2019
Peniophora nuda	CLZhao 23406	China	PQ166608	PQ295872	Present study
Peniophora nuda	He5280	China	MK588778	MK588818	Xu et al. 2023
Peniophora ovalispora	CBS:653.91	Mascarene Islands	MH862290	MH873971	Vu et al. 2019
Peniophora parvocystidiata	CBS:716.91	Guadeloupe	MH862305	MH873978	Vu et al. 2019
Peniophora piceae	209	Russia	JX507718	—	Grum-Grzhimaylo et al. 2016
Peniophora piceae	olrim10	Sweden	AY781264	—	Vasiliauskas et al. 2005
Peniophora pilatiana	CBS:265.56	France	MH857625	MH869170	Vu et al. 2019
Peniophora pilatiana	CBS -A1/A2	China	MK588780	MK588820	Xu et al. 2023
Peniophora pini	CBS:274.56	France	MH857632	MH869177	Vu et al. 2019
Peniophora pini	Hjm 18143	Sweden	EU118651	EU118651	Larsson 2007
Peniophora pithya	CBS:277.56	France	MH857635	MH869180	Vu et al. 2019
Peniophora pithya	He3107	China	MK588781	MK588821	Xu et al. 2023
Peniophora polygonia	CBS:404.50	France	MH856684	MH868201	Vu et al. 2019
Peniophora polygonia	He4651	China	MK588782	MK588822	Xu et al. 2023
Peniophora proxima	CBS:405.50	France	MH856685	MH868202	Vu et al. 2019
Peniophora proxima	He5498	China	MK588783	MK588823	Xu et al. 2023
Peniophora pseudopini	DAOM-30124-Sp	Canada	MK588784	MK588824	Xu et al. 2023
Peniophora pseudopini	TPPpB1007	USA	AF119514	—	Leal-Dutra et al. 2018
Peniophora punctata	CLZhao 33769*	China	PQ066418	—	Present study
Peniophora quercina	CBS:408.50	France	MH856688	MH868205	Vu et al. 2019
Peniophora quercina	CBS:407.50	France	MH856687	MH868204	Vu et al. 2019
Peniophora reidii	CBS:397.83	France	MH861616	MH873334	Vu et al. 2019
Peniophora rhoica	CBS:943.96	Ethiopia	MH862625	MH874246	Vu et al. 2019
Peniophora roseoalba	CLZhao 31523	China	PQ166609	PQ295873	Present study

Taxa	Voucher	Locality	GenBank accession		Reference
			ITS	nLSU	
Peniophora roseoalba	CLZhao 3513	China	ON786559	OP380690	Zou et al. 2022
Peniophora rufa	CBS:351.59	Canada	MH857891	MH869432	Vu et al. 2019
Peniophora rufa	He2788	China	MK588786	MK588826	Xu et al. 2023
Peniophora rufomarginata	CBS:281.56	France	MH857639	MH869183	Vu et al. 2019
Peniophora rufomarginata	CBS:282.56	France	MH857640	MH869184	Vu et al. 2019
Peniophora septentrionalis	CBS:294.58	Canada	MH857791	MH869325	Vu et al. 2019
Peniophora shenghuae	CLZhao 23654	China	PQ066420	—	Present study
Peniophora shenghuae	CLZhao 35044	China	PQ066421	—	Present study
Peniophora shenghuae	He3507	China	MK588788	MK588828	Xu et al. 2023
Peniophora shenghuae	He5447	China	MK588790	MK588830	Xu et al. 2023
Peniophora simulans	CBS:874.84	France	MH861849	MH873537	Vu et al. 2019
Peniophora simulans	CBS:875.84	France	MH861850	MH873538	Vu et al. 2019
Peniophora sphaerocystidiata	HHB-8827-Sp	USA	MK588787	MK588827	Xu et al. 2023
Peniophora subsalmonea	CBS:696.91	Mascarene Islands	MH862302	—	Vu et al. 2019
Peniophora subsalmonea	CBS:697.91	Mascarene Islands	MH862303	—	Vu et al. 2019
Peniophora taiwanensis	Wu9206-28	China	MK588793	MK588833	Xu et al. 2023
Peniophora taiwanensis	Wu9209-14	China	MK588794	MK588834	Xu et al. 2023
Peniophora tamaricicola	CBS:438.62	Morocco	MH858203	MH869802	Vu et al. 2019
Peniophora tamaricicola	CBS:439.62	Morocco	MH858204	MH869803	Vu et al. 2019
Peniophora trigonosperma	CBS:402.83	France	MH861618	MH873335	Vu et al. 2019
Peniophora trigonosperma	He3602	China	MK588762	MK588802	Xu et al. 2023
Peniophora tristicula	CBS:210.63	Pakistan	MH858266	—	Vu et al. 2019
Peniophora tristicula	He4775	China	MH669235	MH669239	Liu and He 2018
Peniophora versicolor	CBS:358.61	Morocco	MH858082	MH869651	Vu et al. 2019
Peniophora versiformis	CBS:358.54	France	MH857360	MH868902	Vu et al. 2019
Peniophora versiformis	He3029	China	MK588756	MK588796	Xu et al. 2023
Peniophora vietnamensis	He5242	Vietnam	MK588761	MK588801	Xu et al. 2023
Peniophora vietnamensis	He5252	Vietnam	MK588761	MK588801	Xu et al. 2023
Peniophora violaceolivida	CBS:348.52	France	MH857077	MH868613	Vu et al. 2019
Peniophora yunnanensis	CLZhao 7347	China	OP380616	—	Zou et al. 2022
Peniophora yunnanensis	CLZhao 3978	China	OP380617	OP380689	Zou et al. 2022
Scytinostroma acystidiatum	CLZhao 32022	China	PQ166610	PQ295874	Present study
Scytinostroma acystidiatum	Dai 24608	China	OQ689127	OQ629351	Zhang et al. 2023
Scytinostroma bambusinum	CLZhao 32789	China	PQ166599	PQ295875	Present study
Scytinostroma bambusinum	JXH 643	China	OR510627	PP660872	Ji et al. 2024
Scytinostroma macrospermum	Dai 24606	China	OQ689126	OQ629350	Wang et al. 2020
Scytinostroma portentosum	EL11-99	Sweden	AF506470	AF506470	Larsson and Larsson 2003
Stereodiscus limonisporus	CBS:125846	New Zealand	—	MH875266	Maekawa et al. 2023
Stereum complicatum	He2234	China	KU559368	KU574828	Maekawa et al. 2023
Stereum hirsutum	Wu1109—127	China	LC430906	LC430909	Maekawa et al. 2023
Stereum sanguinolentum	He2111	China	KU559367	KU574827	Maekawa et al. 2023
Vararia fissurata	CLZhao 8171	China	OQ025219	OR539503	Deng et al. 2024b
Vararia investiens	TAA164122	Norway	AF506484	AF506484	Larsson and Larsson 2003
Vararia tropica	CBS:704.81	France	MH861447	MH873189	Vu et al. 2019
Vararia yaoshanensis	CLZhao 20693	China	PP091665	PP091684	Deng et al. 2024b
Vesiculomyces citrinus	EL53-97	Sweden	AF506486	AF506486	Deng et al. 2024b
Xylobolus frustulatus	He2231	USA	KU881905	KU574825	Maekawa et al. 2023
Xylobolus subpileatus	FP-106735	USA	—	AY039309	Maekawa et al. 2023

* indicates type materials; — indicates sequence unavailability.

Result

The phylogeny of Stereaceae

The dataset based on ITS+nLSU (Fig. 1) comprises sequences from 44 fungal specimens representing 35 species from GenBank. The dataset had an aligned length of 2,136 characters, of which 1,324 characters are constant, 250 are variable and parsimony-uninformative, and 562 are parsimony-informative. Maximum parsimony analysis yielded five equally parsimonious trees (TL = 2,504, CI = 0.5112, HI = 0.4888, RI = 0.6001, RC = 0.3068). The best model for the ITS+nLSU dataset estimated and applied in the Bayesian analysis was GTR+I+G. The phylogenetic tree (Fig. 1) inferred from ITS+nLSU sequences revealed that *Conferticium tuberculatum*, *Gloeocystidiellum cremeum*, and *G. fissuratum* grouped into the family Stereaceae.

The phylogeny of *Gloeocystidiellum*

The dataset based on ITS+nLSU (Fig. 2) comprises sequences from 31 fungal specimens representing 18 species from GenBank. The dataset had an aligned length of 2,154 characters, of which 1,605 characters are constant, 131 are variable and parsimony-uninformative, and 418 are parsimony-informative. Maximum parsimony analysis yielded five equally parsimonious trees (TL = 1,039, CI = 0.7372, HI = 0.2628, RI = 0.8640, RC = 0.6370). The best model for the ITS+nLSU dataset estimated and applied in the Bayesian analysis was GTR+I+G. The phylogenetic tree (Fig. 2) inferred from ITS+nLSU sequences revealed that *Gloeocystidiellum cremeum* and *G. fissuratum* grouped into the genus *Gloeocystidiellum*.

The phylogeny of Peniophoraceae

The dataset based on ITS+nLSU (Fig. 3) comprises sequences from 36 fungal specimens representing 34 species from GenBank. The dataset had an aligned length of 2,375 characters, of which 1,345 characters are constant, 304 are variable and parsimony-uninformative, and 726 are parsimony-informative. Maximum parsimony analysis yielded five equally parsimonious trees (TL = 3,317, CI = 0.5246, HI = 0.4754, RI = 0.6349, RC = 0.3330). The best model for the ITS+nLSU dataset estimated and applied in the Bayesian analysis was GTR+I+G. The phylogenetic tree (Fig. 3) inferred from ITS+nLSU sequences revealed that *Peniophora albohymenia*, *P. hengduanensis*, and *P. punctata* grouped into the family Peniophoraceae.

The phylogeny of *Peniophora*

The dataset based on ITS+nLSU (Fig. 4) comprises sequences from 110 fungal specimens representing 66 species from GenBank. The dataset had an aligned length of 2,006 characters, of which 1,389 characters are constant, 194 are variable and parsimony-uninformative, and 423 are parsimony-informative. Maximum parsimony analysis yielded five equally parsimonious trees (TL = 2,470, CI = 0.3441, HI = 0.6559, RI = 0.6067, RC = 0.2088). The best model for the ITS+nLSU dataset estimated and applied in the Bayesian analysis was SYM+I+G. The phylogenetic tree (Fig. 4) inferred from ITS+nLSU sequences revealed that *Peniophora albohymenia*, *P. hengduanensis*, and *P. punctata* grouped into the genus *Peniophora*.

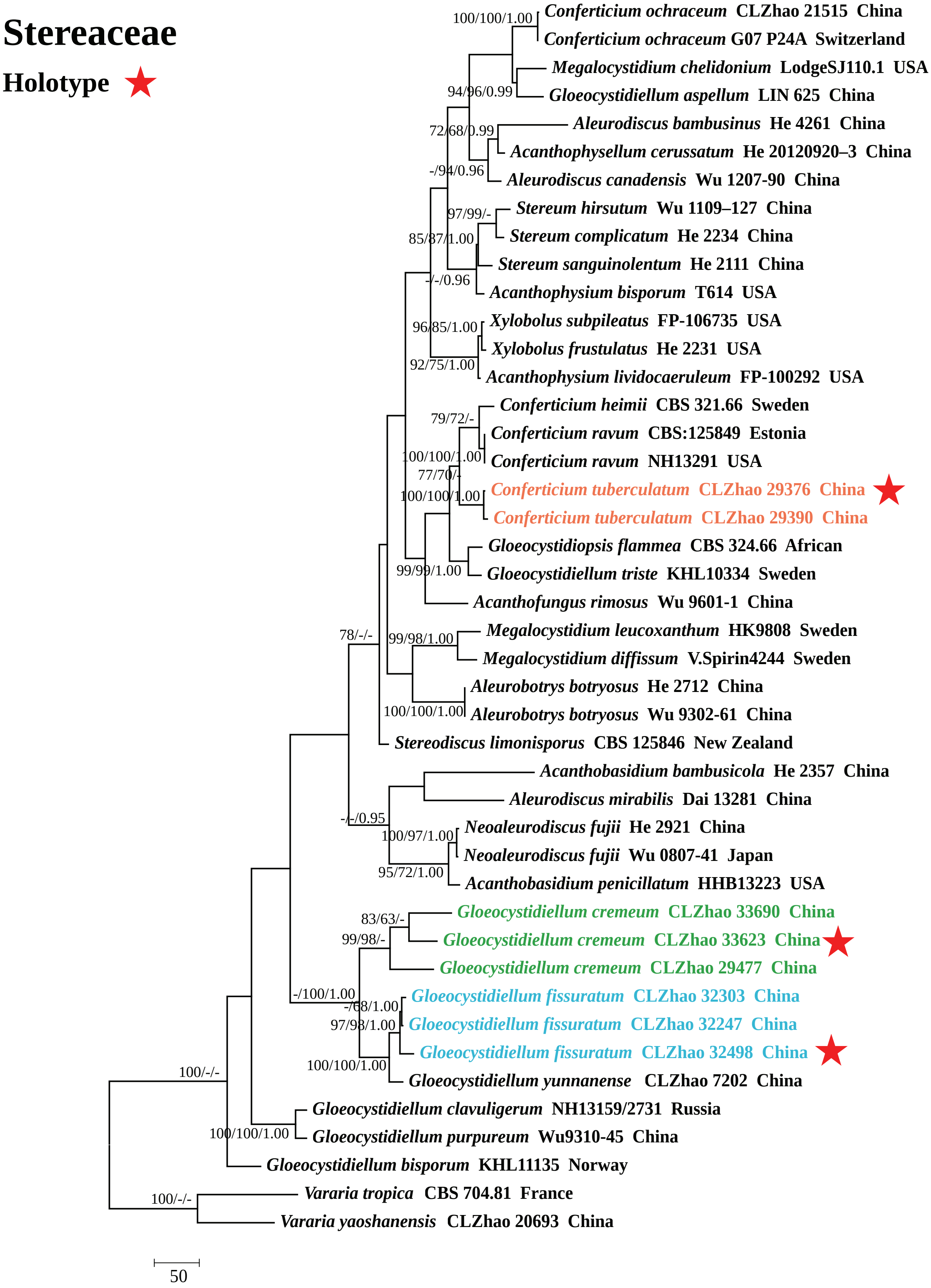

Figure 1. Maximum parsimony strict consensus tree illustrating the phylogeny of *Conferticium* and *Gloeocystidiellum* and related genera in the family Stereaceae, based on ITS+nLSU sequences; branches are labeled with maximum likelihood bootstrap value ≥ 70%, parsimony bootstrap value ≥ 50%, and Bayesian posterior probabilities ≥ 0.95.

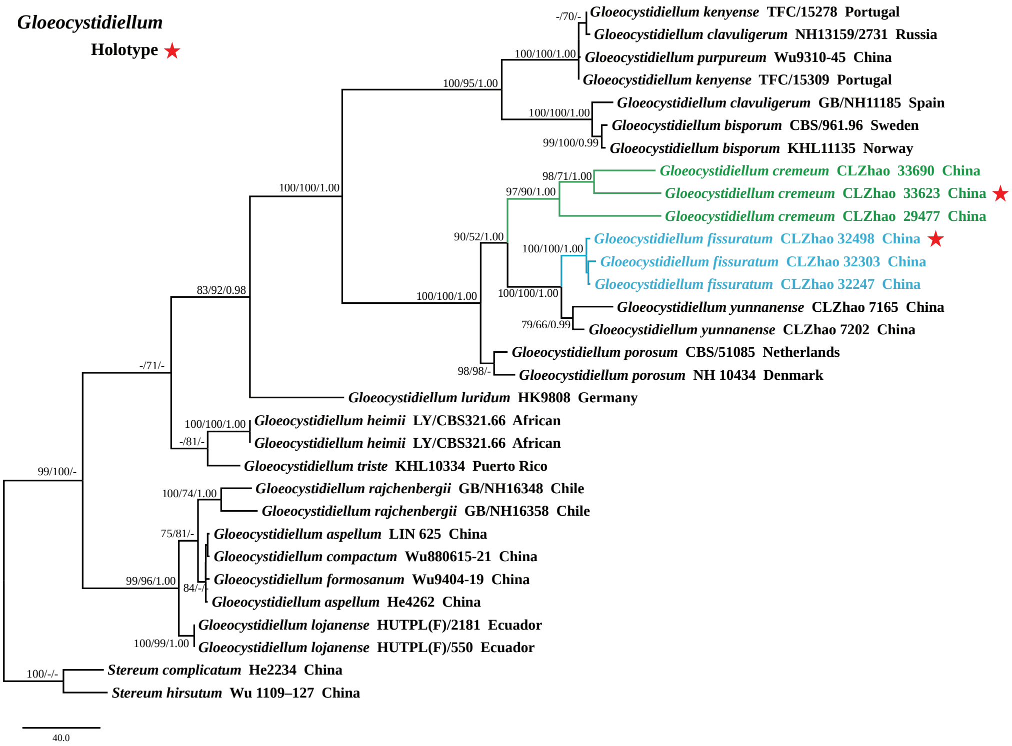

Figure 2. Maximum parsimony strict consensus tree illustrating the phylogeny of two new species and related species in the genus *Gloeocystidiellum*, based on ITS+nLSU sequences; branches are labeled with maximum likelihood bootstrap value ≥ 70%, parsimony bootstrap value ≥ 50%, and Bayesian posterior probabilities ≥ 0.95.

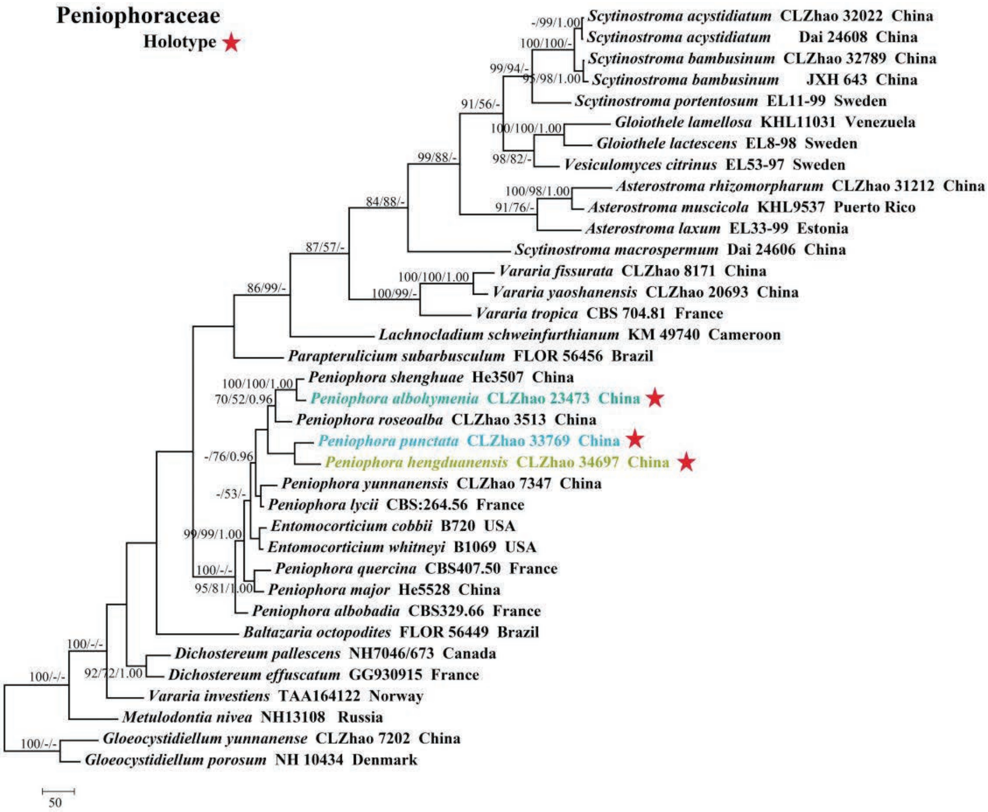

Figure 3. Maximum parsimony strict consensus tree illustrating the phylogeny of *Peniophora* and related genera in the family Peniophoraceae, based on ITS+nLSU sequences; branches are labeled with maximum likelihood bootstrap value ≥ 70%, parsimony bootstrap value ≥ 50%, and Bayesian posterior probabilities ≥ 0.95.

Figure 4. Maximum parsimony strict consensus tree illustrating the phylogeny of three new species and related species in the genus *Peniophora*, based on ITS+nLSU sequences; branches are labeled with maximum likelihood bootstrap value ≥ 70%, parsimony bootstrap value ≥ 50%, and Bayesian posterior probabilities ≥ 0.95.

Taxonomy

Conferticium tuberculatum **L. Wang & C.L. Zhao, sp. nov.**
MycoBank No: 855872
Figs 5, 6

Typification. China. • Yunnan Province: Zhaotong, Daguan County, Huanglianhe Scenic Spot, GPS coordinates: 27°72'N, 103°92'E, altitude: 1480 m asl., on the fallen angiosperm branch, leg. C.L. Zhao, 3 Jul 2023, CLZhao 29376, GenBank: ITS = PQ166602, nLSU = PQ295861 (SWFC!).

Diagnosis. It is characterized by coriaceous basidiomata with tuberculate hymenophore surface, a monomitic hyphal system with simple-septa generative hyphae, and ellipsoid to broadly ellipsoid basidiospores.

Etymology. *Tuberculatum* (Lat.): refers to the species having the tuberculate basidiomata.

Description. ***Basidiomata*.** Annual, resupinate, closely adnate, coriaceous, without odor or taste when fresh, up to 10 cm long, 3 cm wide, and 400 µm thick. Hymenophore tuberculate, white when fresh, white to cream upon drying. Sterile margin narrow, white to cream, up to 1 mm.

***Hyphal system*.** Monomitic; generative hyphae simple-septate, colorless, thin-walled, smooth, rarely branched, interwoven, 3–3.5 µm in diameter, IKI+, CB–; tissues unchanged in KOH.

***Hymenium*.** Gloeocystidia of two types: (1) fusiform, often with an apical appendix, flexuous, colorless, thin-walled, smooth, 34–46 × 7–9 µm; (2) clavate, colorless, thin-walled, smooth, 36–39 × 7–8 µm. Basidia subcylindrical to subclavate, slightly flexuous, with a basal simple septum and four sterigmata, 33.5–43 × 8–10 µm; basidioles numerous, in shape similar to basidia but smaller.

***Spores*.** Basidiospores ellipsoid to broadly ellipsoid, colorless, thin-walled, smooth, IKI+, CB–, (8–)8.5–11 × (5.5–)6–7.5 µm, L = 9.69 µm, W = 6.66 µm, Q = 1.46–1.58 (n = 60/2).

Additional specimen examined (paratype). China. • Yunnan Province: Zhaotong, Daguan County, Huanglianhe Scenic Spot, GPS coordinates: 27°72'N, 103°92'E, altitude: 1480 m asl., on the fallen angiosperm branch, leg. C.L. Zhao, 3 Jul 2023, CLZhao 29390, GenBank: ITS = PQ166603, nLSU = PQ295862 (SWFC!).

Gloeocystidiellum cremeum **L. Wang & C.L. Zhao, sp. nov.**
MycoBank No: 855873
Figs 7, 8

Holotype. China. • Yunnan Province: Zhaotong, Wumengshan National Nature Reserve, GPS coordinates: 27°77'N, 104°25'E, altitude: 1900 m asl., on the fallen angiosperm branch, leg. C.L. Zhao, 20 Sep 2023, CLZhao 33623, GenBank: ITS = PQ287847, nLSU = PQ295864 (SWFC!).

Diagnosis. It is characterized by cream membranaceous basidiomata, a monomitic hyphal system with clamped generative hyphae, thick-walled, subcylindrical to obclavate gloeocystidia, and ellipsoid to subglobose basidiospores.

Etymology. *Cremeum* (Lat.): refers to the species having a cream color of the hymenial surface.

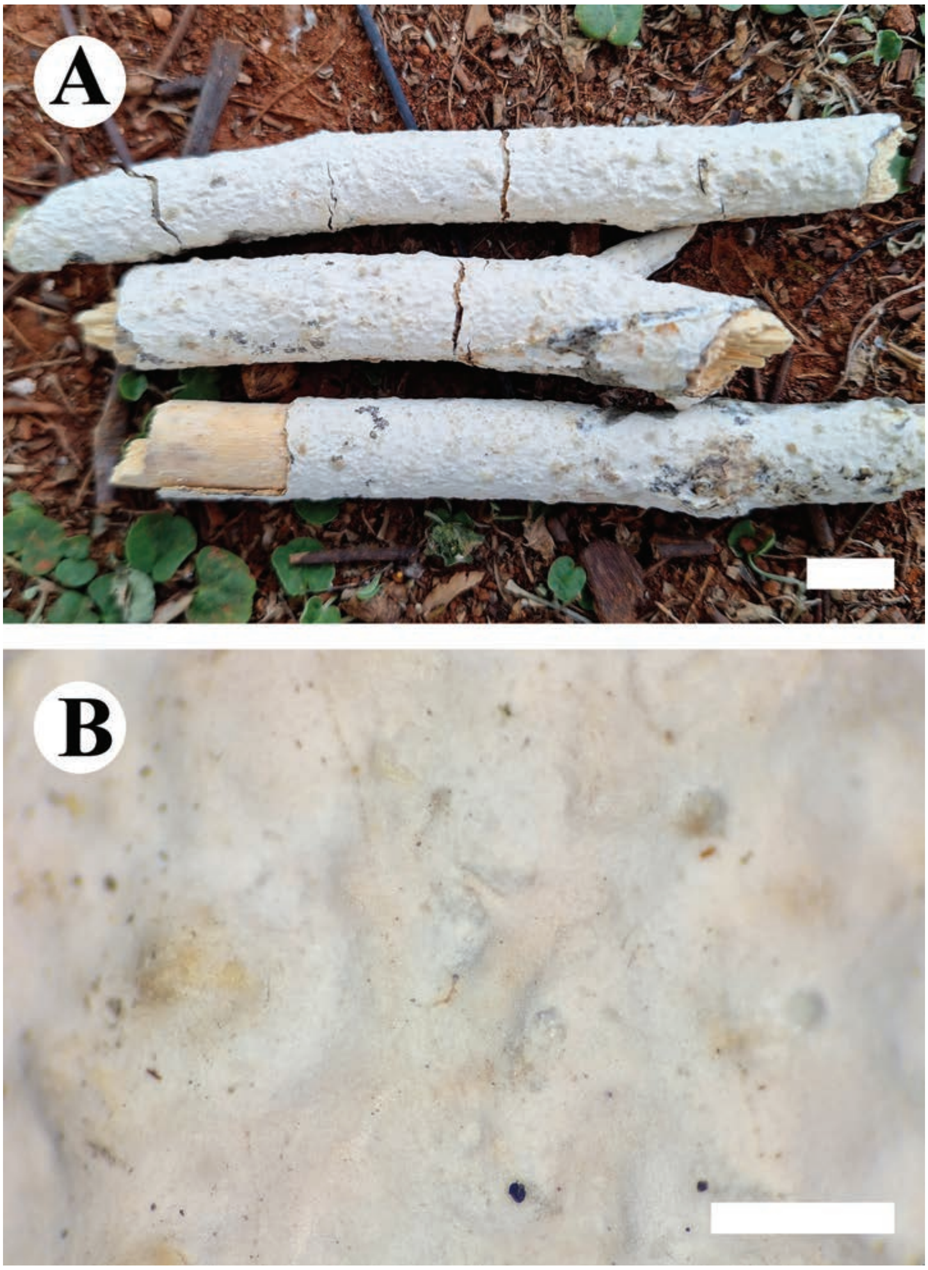

Figure 5. Basidiomata of *Conferticium tuberculatum* (holotype CLZhao 29376). Scale bars: 1 cm (**A**); 1 mm (**B**).

Description. ***Basidiomata*.** Annual, resupinate, closely adnate, membranaceous, without odor or taste when fresh, up to 8.5 cm long, 2 cm wide, and 300 µm thick. Hymenophore smooth, white when fresh, white to cream upon drying. Sterile margin cream, up to 1 mm.

***Hyphal system*.** Monomitic; generative hyphae with clamp connections, colorless, thin-walled, smooth, branched, interwoven, 2–3 µm in diameter, IKI–, CB–; tissues unchanged in KOH.

***Hymenium*.** Gloeocystidia numerous, variable in size and shape, subcylindrical to obclavate, colorless, slightly thick-walled, smooth, mostly 70–77 × 7.5–10.5 µm. Basidia subcylindrical to subclavate, slightly flexuous, with a basal clamp connection and four sterigmata, 19–24 × 3–4.5 µm; basidioles numerous, in shape similar to basidia but smaller.

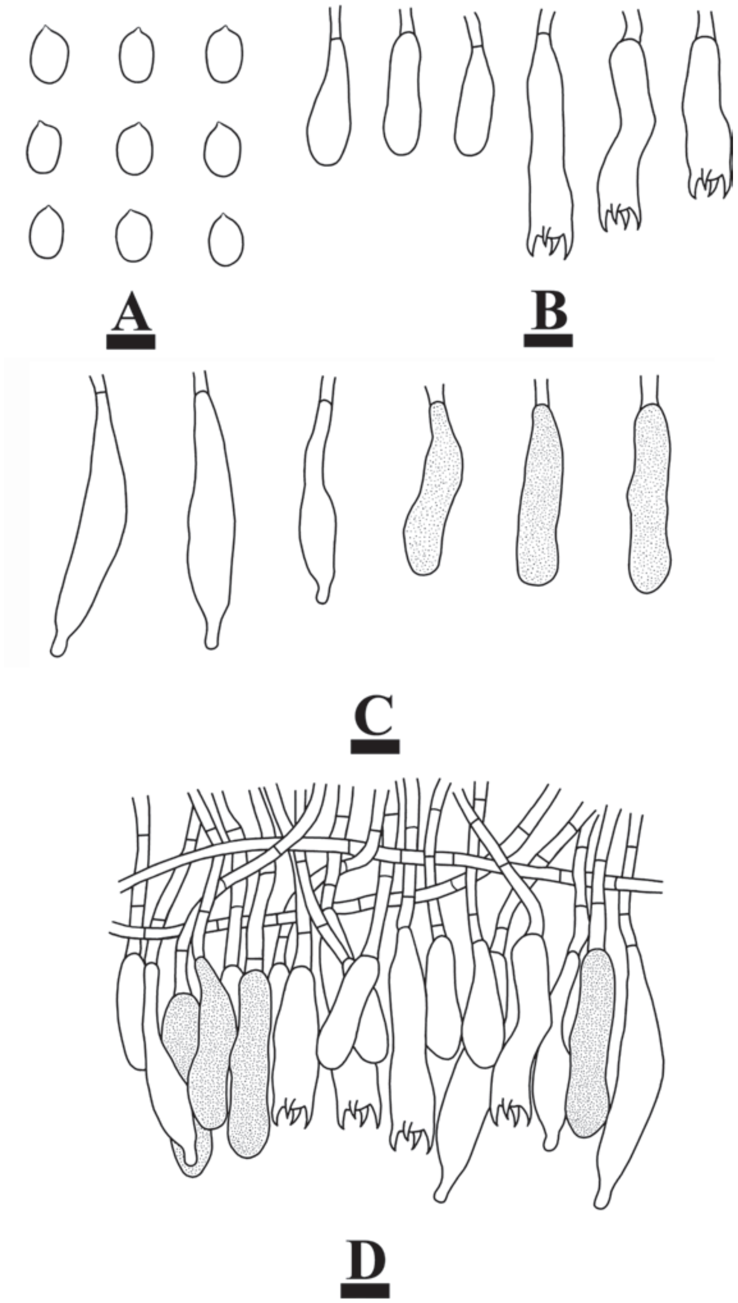

Figure 6. Microscopic structures of *Conferticium tuberculatum* (holotype CLZhao 29376): basidiospores (**A**); basidia and basidioles (**B**); gloeocystidia (**C**); a section of the hymenium (**D**). Scale bars: 10 µm (**A–D**).

***Spores*.** Basidiospores ellipsoid to subglobose, colorless, thin-walled, smooth, IKI+, CB–, (3.5–)4–5 × (2–)2.5–3.5 µm, L = 4.41 µm, W = 2.97 µm, Q = 1.39–1.51 (n = 90/3).

Additional specimens examined (paratypes). China. • Yunnan Province: Zhaotong, Weixin County, Tianxing National Forest Park, GPS coordinates: 28°05'N, 105°09'E, altitude: 900 m asl., on the fallen angiosperm branch, leg. C.L. Zhao, 5 Jul 2023, CLZhao 29477, GenBank: ITS = PQ287846, nLSU = PQ295863; • Zhaotong, Wumengshan National Nature Reserve, GPS coordinates: 27°77'N, 104°25'E, altitude: 1900 m asl., on the fallen angiosperm branch, leg. C.L. Zhao, 20 Sep 2023, CLZhao 33690, GenBank: ITS = PQ287848 (SWFC!).

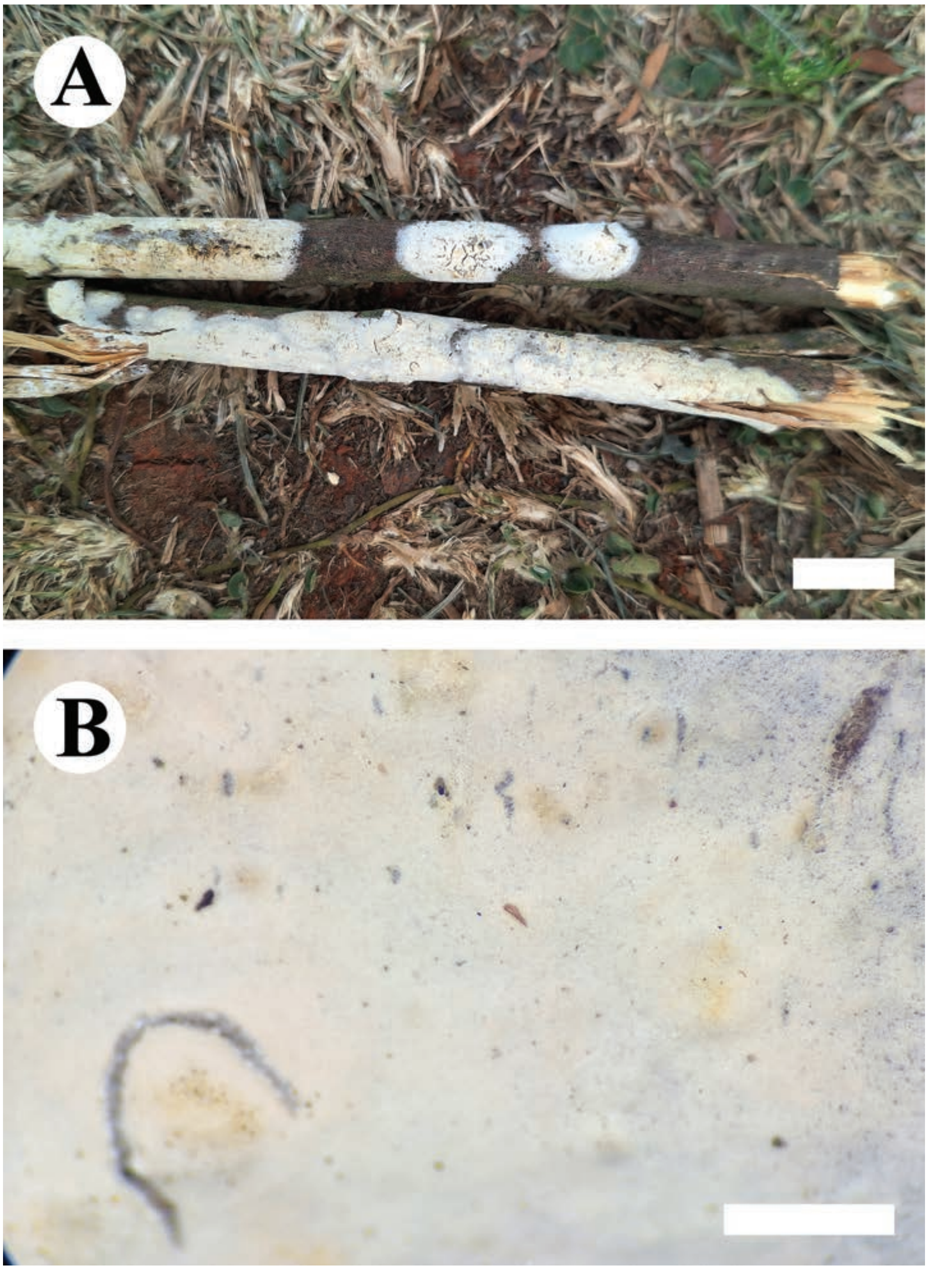

Figure 7. Basidiomata of *Gloeocystidiellum cremeum* (holotype CLZhao 33623). Scale bars: 1 cm (**A**); 1 mm (**B**).

Gloeocystidiellum fissuratum **L. Wang & C.L. Zhao, sp. nov.**
MycoBank No: 855874
Figs 9, 10

Holotype. China. • Yunnan Province: Zhaotong, Wumengshan National Nature Reserve, GPS coordinates: 27°77'N, 104°25'E, altitude: 1900 m asl., on the fallen angiosperm branch, leg. C.L. Zhao, 28 Aug 2023, CLZhao 32498, GenBank: ITS = PQ287851 (SWFC!).

Diagnosis. It is characterized by white to cinnamon-buff, membranaceous basidiomata with grandinioid and cracking hymenophore surfaces, a monomitic hyphal system with clamped generative hyphae, numerous, variable in size and shape gloeocystidia, and subglobose basidiospores.

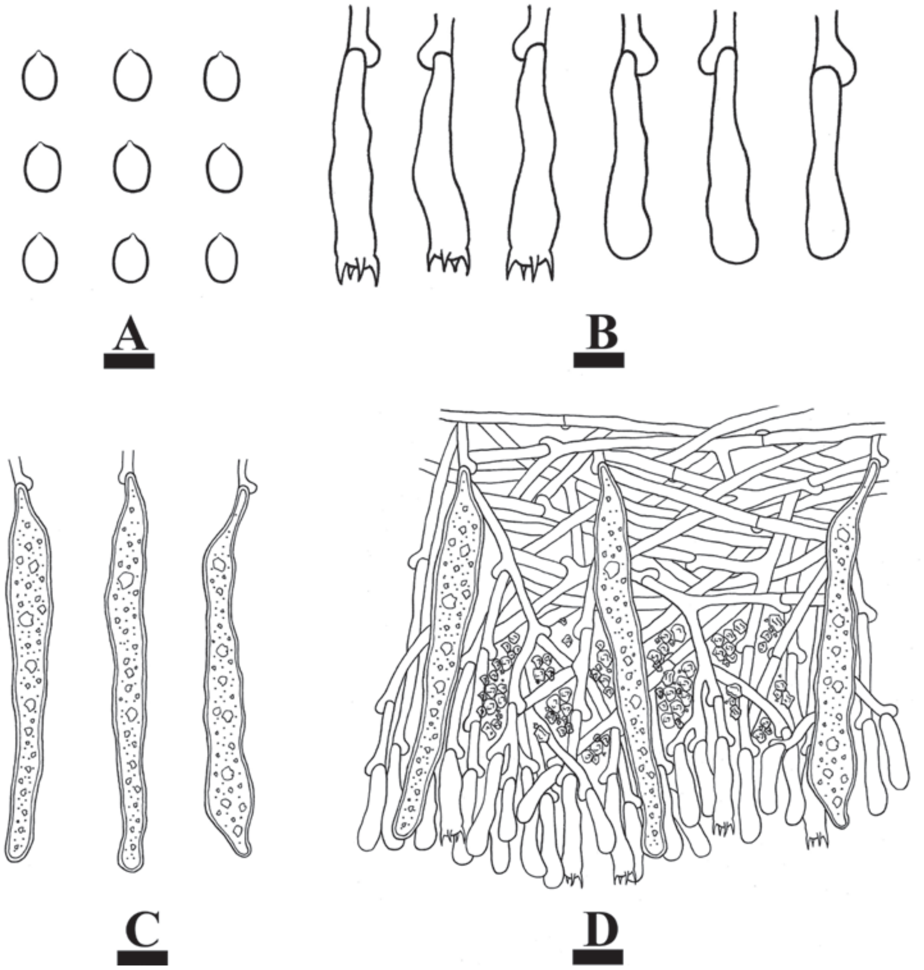

Figure 8. Microscopic structures of *Gloeocystidiellum cremeum* (holotype CLZhao 33623): basidiospores (**A**); basidia and basidioles (**B**); gloeocystidia (**C**); a section of the hymenium (**D**). Scale bars: 5 µm (**A, B**); 10 µm (**C, D**).

Etymology. *Fissuratum* (Lat.): refers to the species having a cracking hymenial surface.

Description. *Basidiomata*. Annual, resupinate, closely adnate, membranaceous, without odor or taste when fresh, up to 8.5 cm long, 2 cm wide, and 300 µm thick. Hymenophore grandinioid, cracking, white to cinnamon-buff when fresh, cinnamon-buff upon drying. Sterile margin cream, up to 2 mm.

***Hyphal system*.** Monomitic; generative hyphae with clamp connections, colorless, thin-walled, smooth, branched, interwoven, 2–3 µm in diameter, IKI–, CB–; tissues unchanged in KOH.

***Hymenium*.** Gloeocystidia numerous, variable in size and shape, subclavate to obclavate, colorless, thin-walled, smooth, mostly 57–88 × 9–10 µm. Basidia subcylindrical to subclavate, slightly flexuous, with a basal clamp connection and four sterigmata, 13–16 × 4–5 µm; basidioles numerous, in shape similar to basidia but smaller.

***Spores*.** Basidiospores subglobose, colorless, thin-walled, verrucose, IKI+, CB–, (3–)3.5–4.5(–5) × 2.5–3.5(–4) µm, L = 4.04 µm, W = 3.06 µm, Q = 1.26–1.32 (n = 90/3).

Additional specimens examined (paratypes). China. • Yunnan Province: Zhaotong, Wumengshan National Nature Reserve, GPS coordinates: 27°77'N, 104°25'E, altitude: 1900 m asl., on angiosperm stump, leg. C.L. Zhao, 28 Aug

Figure 9. Basidiomata of *Gloeocystidiellum fissuratum* (holotype CLZhao 32498). Scale bars: 1 cm (**A**); 1 mm (**B**).

2023, CLZhao 32247, GenBank: ITS = PQ287849; nLSU = PQ295865; on the fallen branch of *Picea*, leg. C.L. Zhao, 28 Aug 2023, CLZhao 32303, GenBank: ITS = PQ287850, nLSU = PQ295866 (SWFC!).

Peniophora albohymenia **L. Wang & C.L. Zhao, sp. nov.**

MycoBank No: 855875
Figs 11, 12

Holotype. China. • Yunnan Province: Zhaotong, Fenghuangshan National Forest Park, GPS coordinates: 27°30'N, 103°70'E, altitude: 1950 m asl., on the fallen angiosperm branch, leg. C.L. Zhao, 24 Aug 2022, CLZhao 23473, GenBank: ITS = PQ066419, nLSU = PQ295867 (SWFC!).

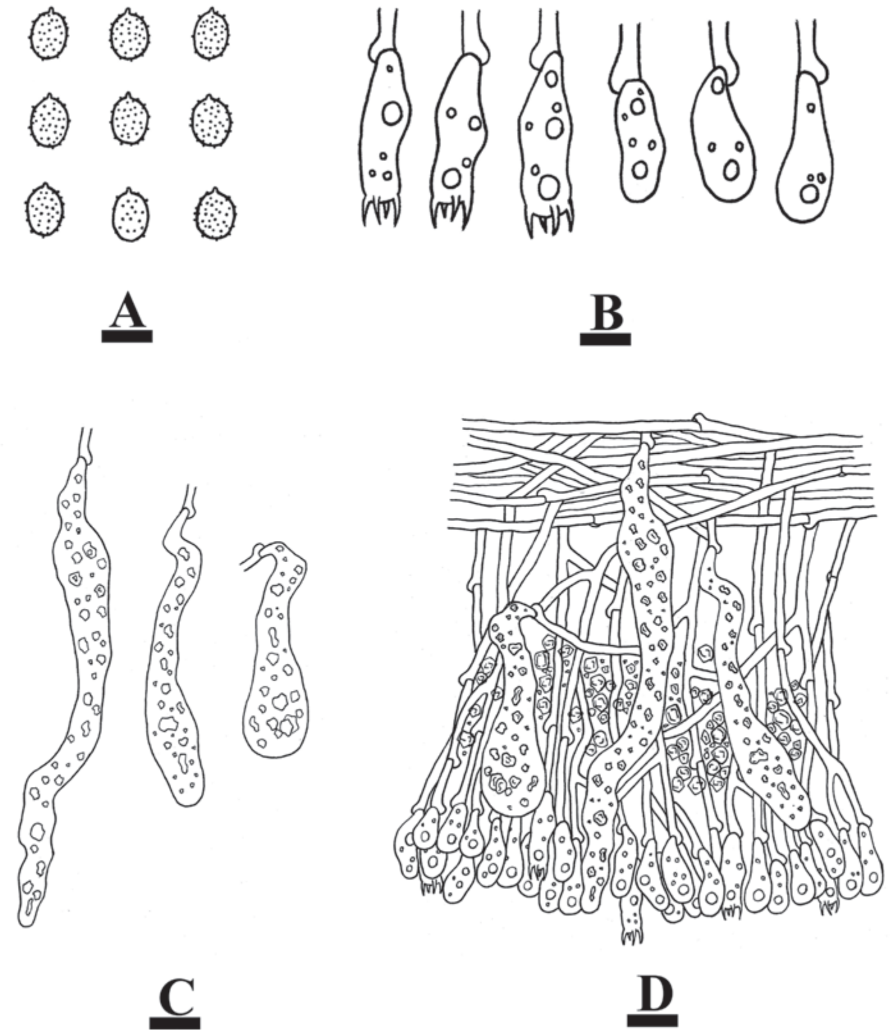

Figure 10. Microscopic structures of *Gloeocystidiellum fissuratum* (holotype CLZhao 32498): basidiospores (**A**); basidia and basidioles (**B**); gloeocystidia (**C**); a section of the hymenium (**D**). Scale bars: 5 µm (**A, B**); 10 µm (**C, D**).

Diagnosis. It is characterized by white to pale pink, smooth membranaceous basidiomata, a monomitic hyphal system with simple-septa generative hyphae, and allantoid to cylindrical basidiospores.

Etymology. *Albohymenia* (Lat.): refers to the species having white basidiomata.

Description. ***Basidiomata*.** Annual, resupinate, closely adnate, membranaceous, without odor or taste when fresh, up to 9 cm long, 3.5 cm wide, and 300 µm thick. Hymenophore smooth, white when fresh, white to pale pink upon drying. Sterile margin narrow, white, up to 1 mm.

***Hyphal system*.** Monomitic; generative hyphae with simple-septa, colorless, slightly thick-walled, smooth, rarely branched and septate, more or less parallel to substrate, 4–4.5 µm in diameter, IKI–, CB–; tissues unchanged in KOH.

***Hymenium*.** Cystidia of two types: (1) Gloeocystidia fusiform, flexuous, colorless, thin-walled, smooth, 31.5–35.5 × 6–7 µm; (2) Lamprocystidia abundant, subulate to subcylindrical, heavily encrusted with crystals in the middle and upper parts, thin-walled, colorless, embedded or projecting beyond the hymenium, with a basal simple-septum, 31–42 × 10–13.5 µm. Basidia subcylindrical to subclavate, slightly flexuous, with a basal simple septum and four

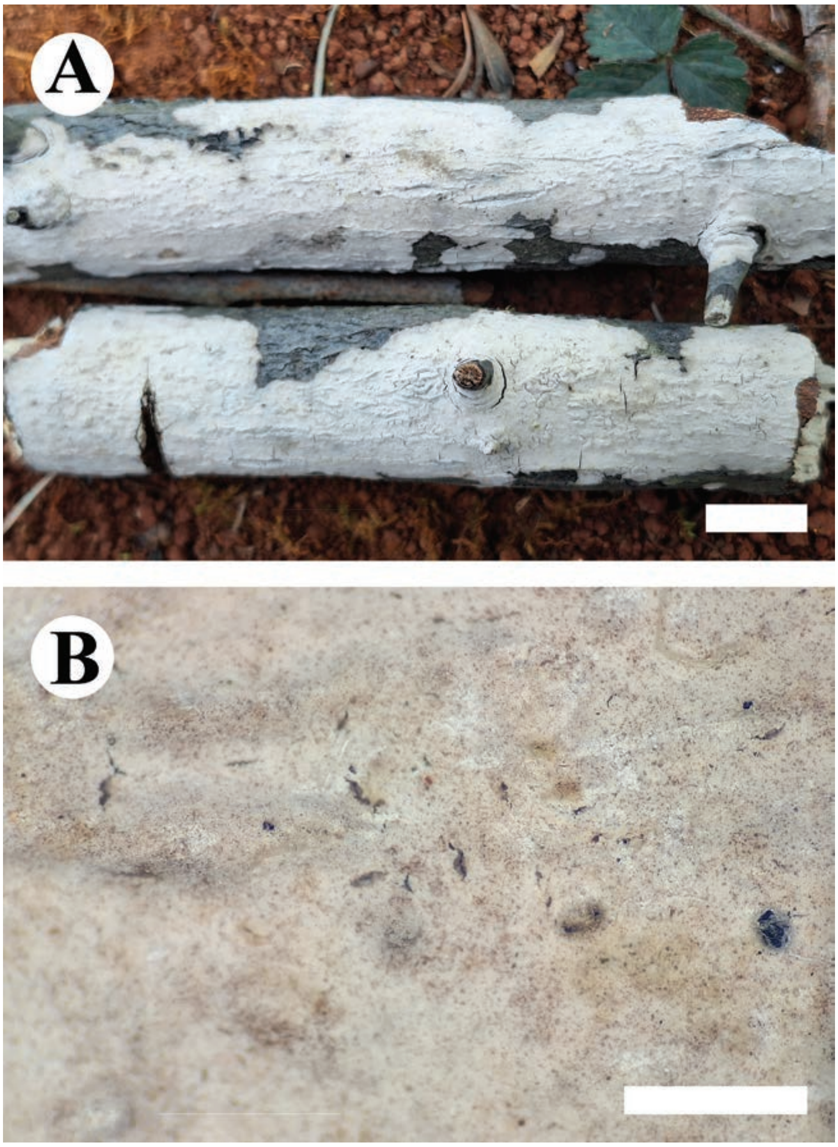

Figure 11. Basidiomata of *Peniophora albohymenia* (holotype CLZhao 23473). Scale bars: 1 cm (**A**); 1 mm (**B**).

sterigmata, 23.5–26 × 4.5–6 µm; basidioles numerous, in shape similar to basidia but slightly smaller.

***Spores*.** Basidiospores allantoid to cylindrical, colorless, thin-walled, smooth, IKI–, CB–, (7–)8.5–11(–11.5) × 3–4.5(–5) µm, L = 9.65 µm, W = 3.93 µm, Q = 2.46 (n = 30/1).

***Peniophora hengduanensis* L. Wang & C.L. Zhao, sp. nov.**
MycoBank No: 855876
Figs 13, 14

Holotype. China. • Yunnan Province: Diqing, Weixi County, Zhonglu Town, GPS coordinates: 27°16'N, 99°15'E, altitude: 2250 m asl., on the fallen angiosperm branch, leg. C.L. Zhao, 14 Oct 2022, CLZhao 34697, GenBank: ITS = PQ066422, nLSU = PQ295870 (SWFC!).

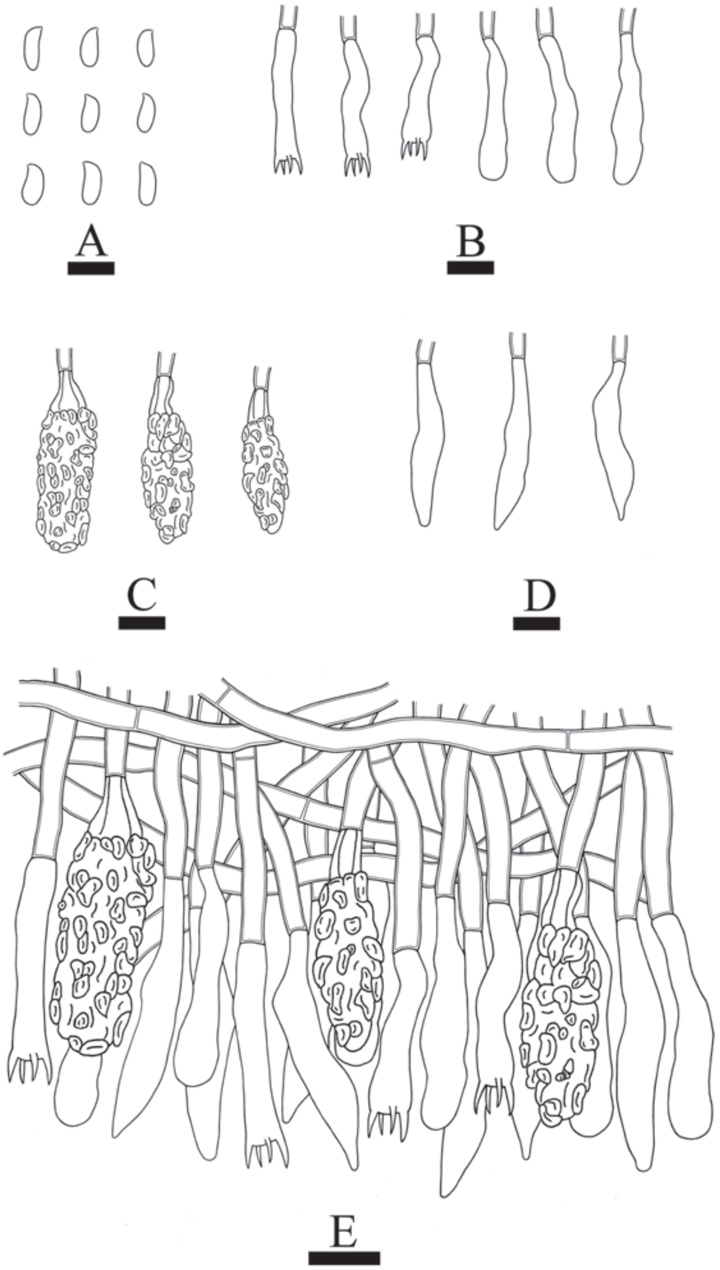

Figure 12. Microscopic structures of *Peniophora albohymenia* (holotype CLZhao 23473): basidiospores (**A**); basidia and basidioles (**B**); lamprocystidia (**C**); gloeocystidia (**D**); a section of the hymenium (**E**). Scale bars: 10 µm (**A–E**).

Diagnosis. It is characterized by pink to vinaceous, smooth membranaceous basidiomata, a monomitic hyphal system with simple-septa, and allantoid to subcylindrical basidiospores.

Etymology. *Hengduanensis* (Lat.): refers to the locality (Hengduan Mountains) of the type specimen.

Description. ***Basidiomata***. Annual, resupinate, closely adnate, membranaceous, without odor or taste when fresh, up to 7.5 cm long, 4 cm wide, and 400 µm thick. Hymenophore smooth, pale pink when fresh, pink to vinaceous upon drying. Sterile margin narrow, white to vinaceous, up to 1 mm.

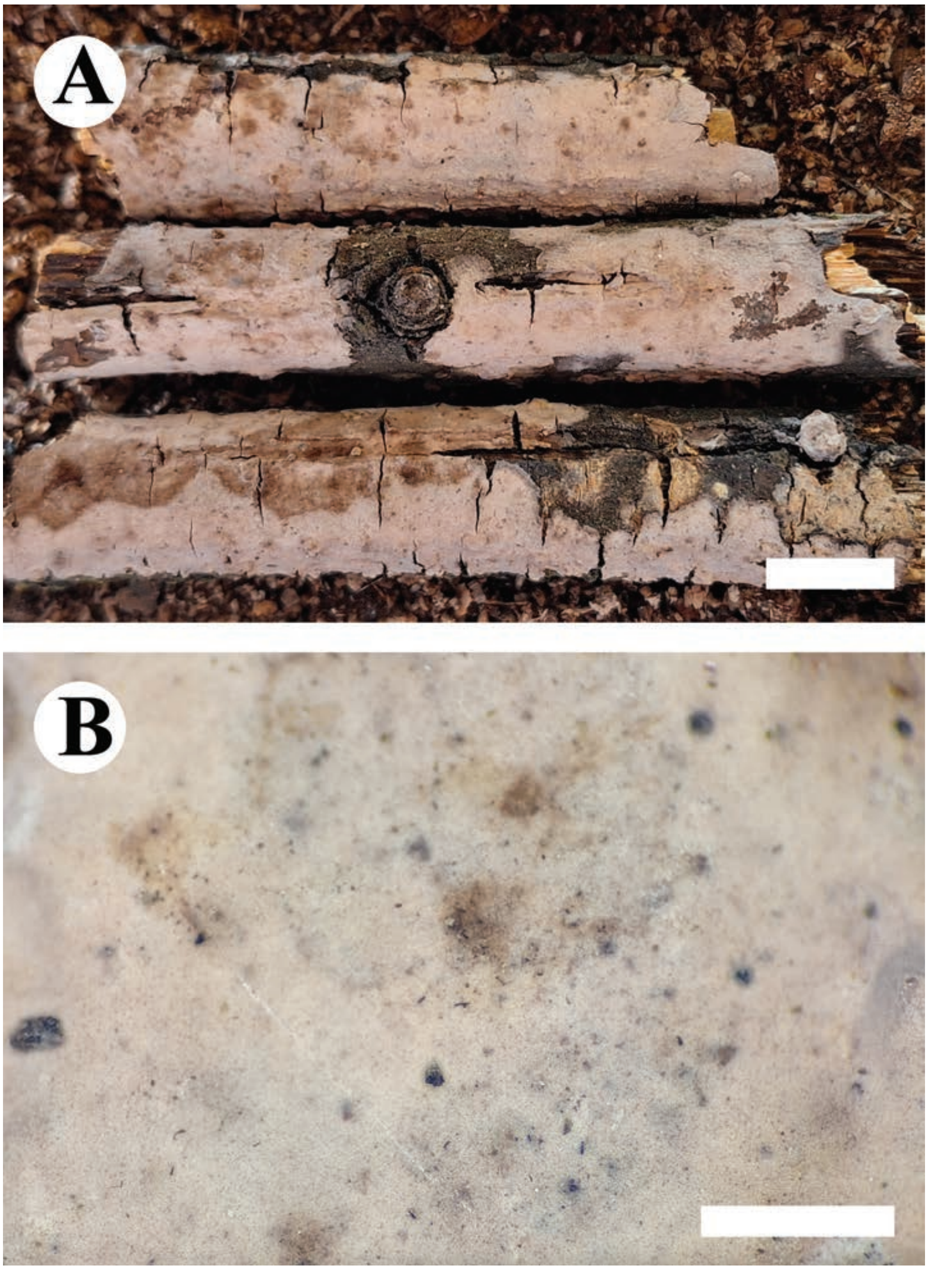

Figure 13. Basidiomata of *Peniophora hengduanensis* (holotype CLZhao 34697). Scale bars: 1 cm (**A**); 1 mm (**B**).

***Hyphal system*.** Monomitic; generative hyphae with simple-septa, colorless, thin-walled, smooth, rarely branched, rarely septate, more or less parallel to substrate, 3.5–4.5 µm in diameter, IKI–, CB–; tissues unchanged in KOH.

***Hymenium*.** Cystidia of two types: (1) Gloeocystidia obclavate, colorless, slightly thick-walled, smooth, 50.5–66 × 11–14.5 µm; (2) Lamprocystidia abundant, subulate to subcylindrical, heavily encrusted with crystals in the middle and upper parts, thin-walled, colorless, embedded or projecting beyond the hymenium, with a basal simple septum, 21.5–25 × 9.5–11 µm. Basidia subcylindrical to subclavate, slightly flexuous, with a basal simple septum and four sterigmata, 20–32.5 × 4.5–6 µm; basidioles numerous, in shape similar to basidia but slightly smaller.

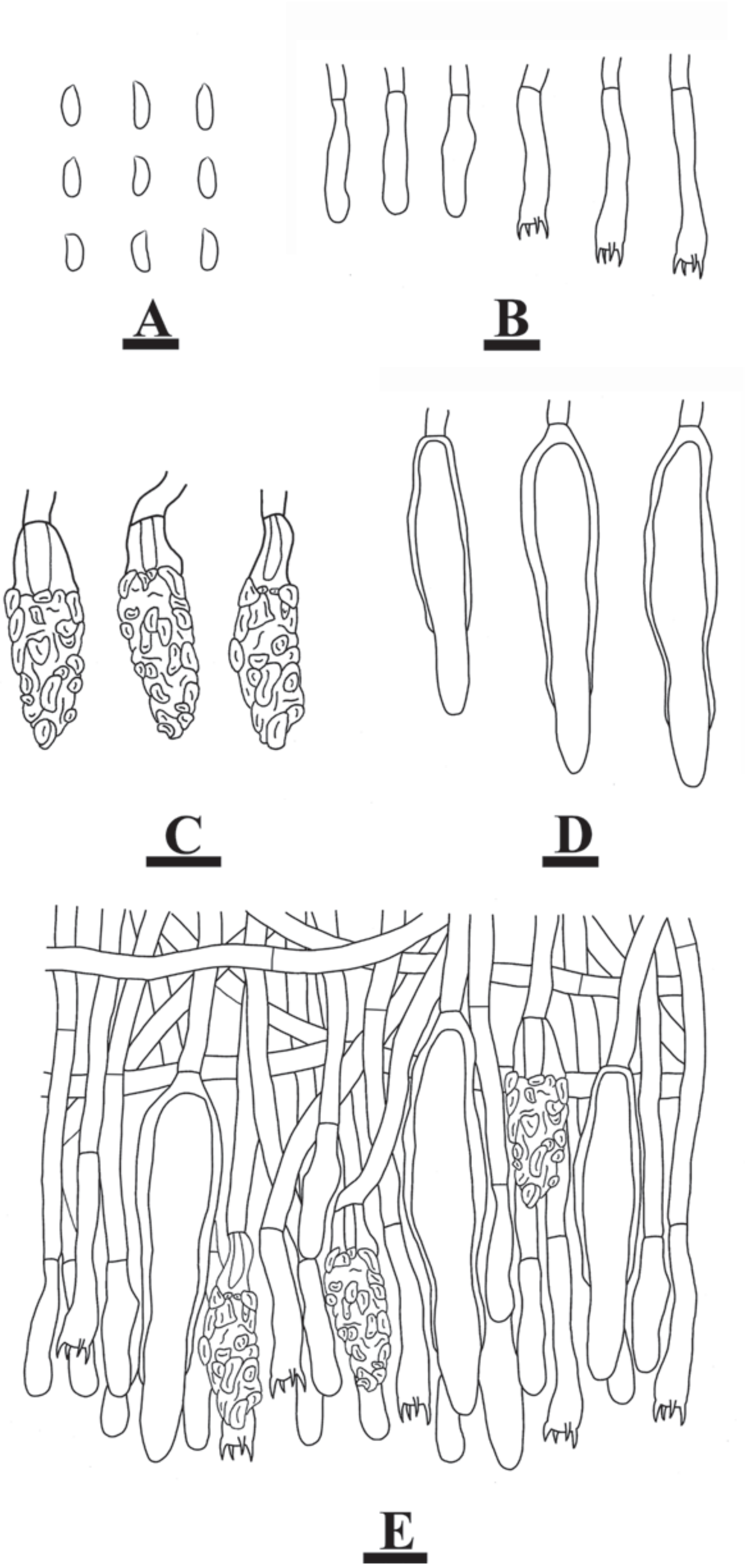

Figure 14. Microscopic structures of *Peniophora hengduanensis* (holotype CLZhao 34697): basidiospores (**A**); basidia and basidioles (**B**); lamprocystidia (**C**); gloeocystidia (**D**); a section of the hymenium (**E**). Scale bars: 10 µm (**A–E**).

***Spores*.** Basidiospores allantoid to subcylindrical, colorless, thin-walled, smooth, IKI–, CB–, (6–)6.5–8.5(–9) × 2.5–3.5(–4) µm, L = 7.35 µm, W = 3.15 µm, Q = 2.33 (n = 30/1).

Peniophora punctata L. Wang & C.L. Zhao, sp. nov.
MycoBank No: 855877
Figs 15, 16

Holotype. China. • Yunnan Province: Zhaotong, Xiaocaoba, Wumengshan National Nature Reserve, GPS coordinates: 27°77'N, 104°25'E, altitude: 1900 m asl., on the fallen angiosperm branch, leg. C.L. Zhao, 21 Sep 2023, CLZhao 33769, GenBank: ITS = PQ066418 (SWFC!).

Diagnosis. It is characterized by pink to slightly purple, cushion-shaped, smooth membranaceous basidiomata, a monomitic hyphal system with simple-septa, thick-walled generative hyphae, and allantoid basidiospores.

Etymology. *Punctata* (Lat.): refers to the species having cushion-shaped basidiomata.

Description. *Basidiomata*. Annual, resupinate, closely adnate, cushion-shaped, membranaceous, without odor or taste when fresh, up to 3 cm long, 1.5 cm wide, and 300 µm thick. Hymenophore smooth, pink to slightly purple when fresh, purple upon drying. Sterile margin narrow, white to vinaceous, up to 1 mm.

***Hyphal system*.** Monomitic; generative hyphae with simple-septa, colorless, slightly thick-walled, smooth, rarely branched, rarely septate, more or less parallel to substrate, 2.5–3.5 µm in diameter, IKI–, CB–; tissues unchanged in KOH.

***Hymenium*.** Cystidia of two types: (1) Gloeocystidia fusiform or subclavate, slightly flexuous, colorless, slightly thick-walled, smooth, 31.5–51.5 × 6–8 µm; (2) Lamprocystidia abundant, subulate to subcylindrical, heavily encrusted with crystals in the middle and upper parts, thin-walled, colorless, embedded or projecting beyond the hymenium, with a basal simple septum, 36–39 × 8.5–12.5 µm. Basidia subcylindrical to subclavate, slightly flexuous, with a basal simple septum and four sterigmata, 18–21.5 × 3–4.5 µm; basidioles numerous, in shape similar to basidia but slightly smaller.

***Spores*.** Basidiospores allantoid, colorless, thin-walled, smooth, IKI–, CB–, 5–7(–7.5) × 1.5–2.5 µm, L = 6.08 µm, W = 2.22 µm, Q = 2.73 (n = 30/1).

Discussion

A large number of studies were focused on the taxonomy and phylogeny of Russulales taxa in the last ten years (He et al. 2019; Wijayawardene et al. 2022; Wu et al. 2020; Zou et al. 2022; Li et al. 2023; Deng et al. 2024b; Dong et al. 2024; Liu et al. 2024; Zhou et al. 2024). Both families, Peniophoraceae and Stereaceae, are well-supported large groups in Russulales, and most species have resupinate and effused-reflexed basidiomata growing on fallen twigs, branches, or trunks of woody plants or bamboos (Larsson and Larsson 2003; Miller et al. 2006; Zhou and Dai 2013; De Crop et al. 2016; He et al. 2024). Molecular analyses have elucidated the evolutionary relationships, in which the findings demonstrate significant morphological changes occurring at both the levels of family and genus (Larsson and Larsson 2003; Miller et al. 2006; Zhao et al. 2017; He et al. 2019; Wu et al. 2020). Elucidating morphological differences for its overall appearance, structure, colors, spore characters, and hyphal structure, as well as its habitat, this distinction holds significant importance for making phylogenetic and systematic conclusions (Miller et al. 2006; Dong et al. 2024; He et al. 2024).

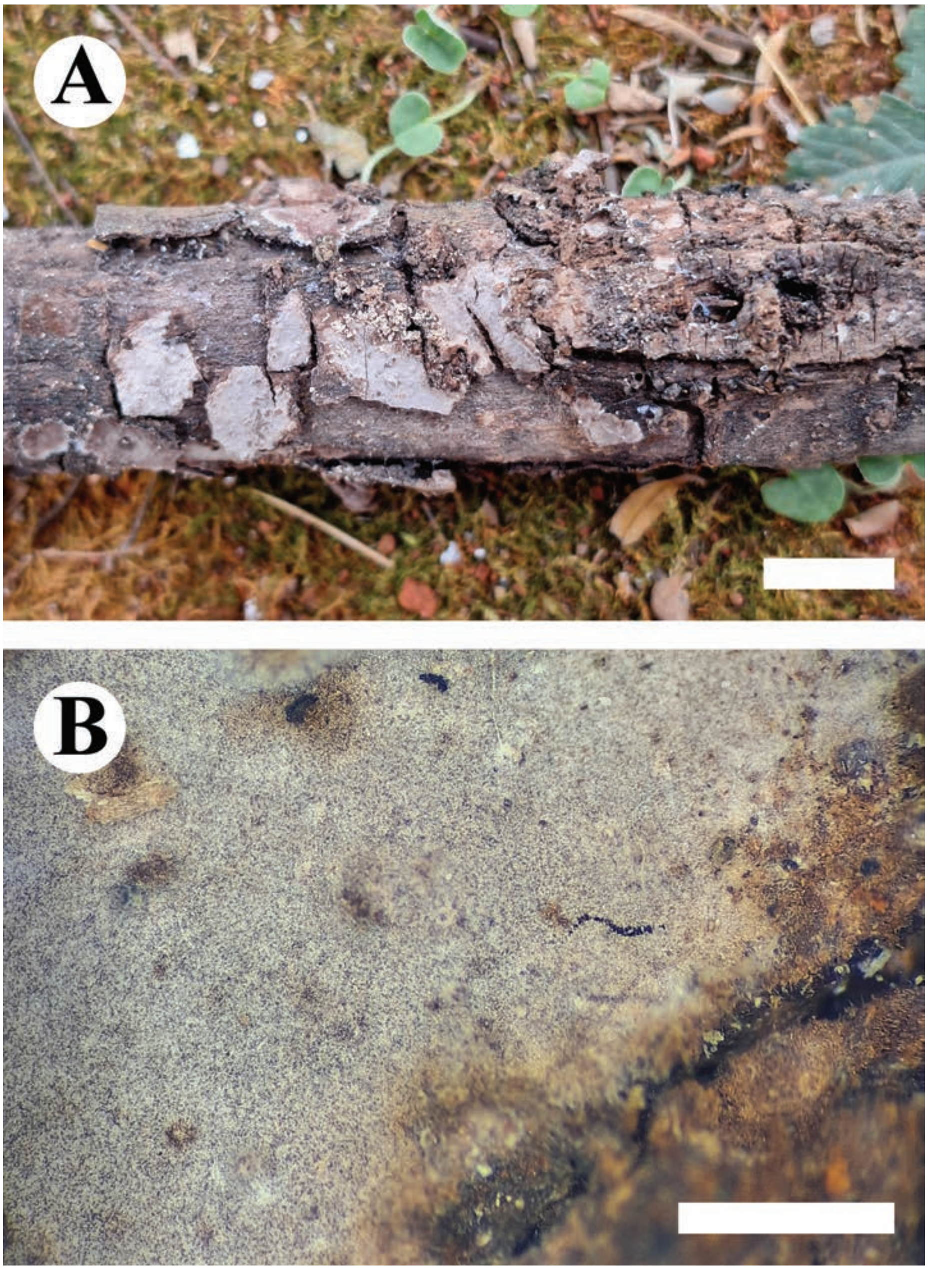

Figure 15. Basidiomata of *Peniophora punctata* (holotype CLZhao 33769). Scale bars: 1 cm (**A**); 1 mm (**B**).

Phylogenetically, the multiple genes with ITS+nLSU analysis showed that the six new species grouped within the order Russulales, in which *Conferticium tuberculatum*, *Gloeocystidiellum cremeum*, and *G. fissuratum* grouped into the family Stereaceae. *Conferticium tuberculatum* is separated from closely related species *C. ravum*, which can be delimited from *C. tuberculatum* by its smooth, yellowish to isabelline hymenophore, shorter basidia (20–30 × 4–6 µm), and ellipsoid to ovoid, verrucose basidiospores (6–7 × 4–4.5 µm; Bernicchia and Gorjón 2010). Based on the ITS+nLSU sequence data (Fig. 2), *Gloeocystidiellum cremeum* is grouped with *G. fissuratum* L. Wang & C.L. Zhao and *G. yunnanense* Y.L. Zhao & C.L. Zhao in the *Gloeocystidiellum* clade. However, *G. fissuratum* differs from *G. cremeum* by its white to cinnamon-buff, grandinioid, and cracking hymenophore and smaller basidia (13–16 × 4–5 µm); *G. yunnanense*

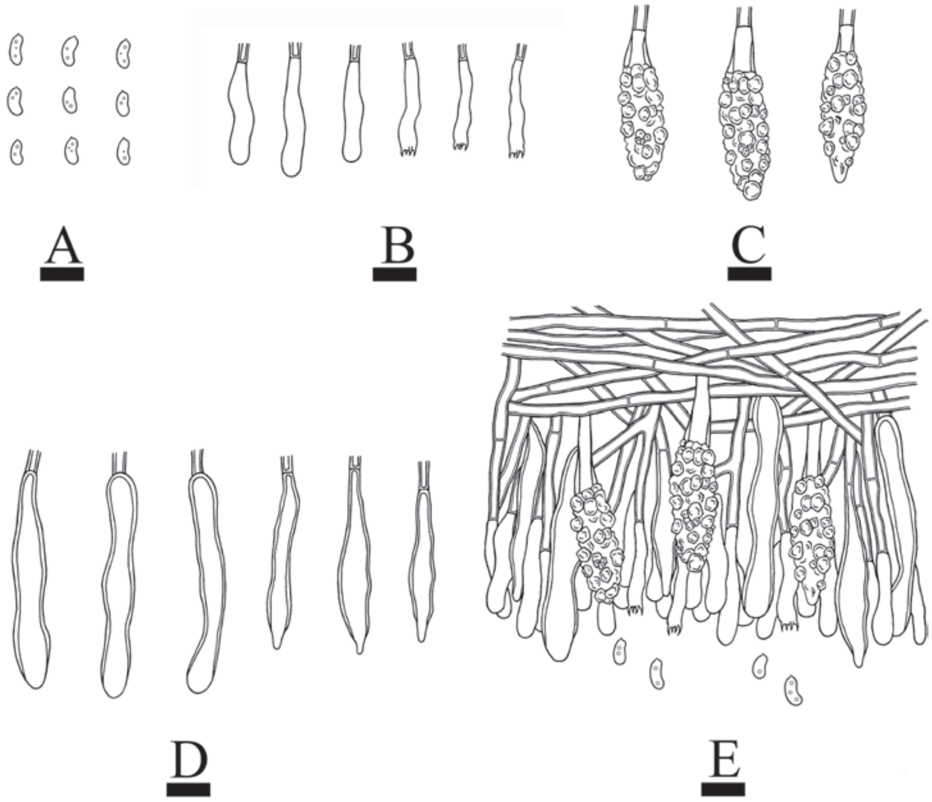

Figure 16. Microscopic structures of *Peniophora punctata* (holotype CLZhao 33769): basidiospores (**A**); basidia and basidioles (**B**); lamprocystidia (**C**); gloeocystidia (**D**); a section of the hymenium (**E**). Scale bars: 10 µm (**A–E**).

is distinguished from *G. cremeum* by its cream, ceraceous, and grandinioid hymenophore, smaller basidia (12.5–14.5 × 3.5–4.5 µm), and slightly thick-walled, aculeate, ellipsoid basidiospores (Zhao and Zhao 2023). *Gloeocystidiellum fissuratum* is distinguished from *G. yunnanense* by cream, ceraceous, and grandinioid hymenophore, smaller basidia (12.5–14.5 × 3.5–4.5 µm), and slightly thick-walled, aculeate, ellipsoid basidiospores (Zhao and Zhao 2023).

Based on the ITS+nLSU analysis, three new taxa, *Peniophora albohymenia*, *P. hengduanensis*, and *P. punctata*, were grouped into the family Peniophoraceae. As inferred from the sequence data (Fig. 4), *Peniophora albohymenia* is a sister of *P. reidii* Boidin & Lanq. However, *P. reidii* is distinguished from *P. albohymenia* by its pinkish gray to gray basidiomata and longer gloeocystidia (25–75 × 5.5–7.5 µm; Boidin and Lanquetin 1983). Based on the ITS+nLSU sequence data (Fig. 4), *Peniophora hengduanensis* formed a sister group with *P. crassitunicata* Boidin, Lanq. However, *P. crassitunicata* is distinguished from *P. hengduanensis* by its pinkish gray to grayish violaceous basidiomata, thick-walled generative hyphae, and bigger, very thick-walled (2–3 µm) gloeocystidia (60–115 × 8–15 µm) (Boidin and Lanquetin 1983). *Peniophora punctata* is a closely related species, viz., *P. borbonica* Boidin, Lanq, and *P. laxitexta* C.E. Gómez. However, *P. borbonica* is delimited from *P. punctata* by its smooth, purplish gray or gray hymenophore, longer gloeocystidia (30–60 × 7–12 µm), and suballantoid to cylindrical, bigger basidiospores (8–10.5 × 2.7–3.5 µm; Boidin and Gilles 2000); *P. laxitexta* can be distinguished from *P. punctata* by its longer basidia (27–35 × 4.5–6 µm) and bigger lamprocystidia (30–60 × 10–22 µm; Gómez and Loewenbaum 1976).

Morphologically, *Conferticium ochraceum* (Fr.) Hallenb. is similar to *C. tuberculatum* by having smooth ceraceous basidiomata. However, *C. ochraceum* differs in its coriaceous basidiomata with pale yellowish hymenophore surface and subcylindrical to subovate basidiospores (4–6.5 × 2.5–3.5 µm; Bernicchia and Gorjón 2010). *Gloeocystidiellum clavuligerum* (Höhn. and Litsch.) Nakasone and *G. porosum* (Berk. and M.A. Curtis) Donk are similar to *G. cremeum* by both having ellipsoid to subglobose basidiospores. However, *G. clavuligerum* differs in its gloeocystidia with a more or less constricted to moniliform apex (50–80 × 8–12 µm; Bernicchia and Gorjón 2010); *G. porosum* differs in its bigger gloeocystidia (80–200 × 8–15 µm, Bernicchia and Gorjón 2010). *Gloeocystidiellum clavuligerum* and *G. porosum* are similar to *G. fissuratum* by both having verrucose, thin-walled basidiospores. However, *G. clavuligerum* differs in its longer basidia (25–30 × 4–5 µm; Bernicchia and Gorjón 2010); *G. porosum* differs in its bigger gloeocystidia (80–200 × 8–15 µm; Bernicchia and Gorjón 2010).

Morphologically, *Peniophora roseoalba* L. Zou & C.L. Zhao and *P. shenghuae* Y.L. Xu, Yan Tian & S.H. He are similar to *P. albohymenia* by both having fusiform, flexuous gloeocystidia. However, *P. roseoalba* differs in its ellipsoid basidiospores (4–6.5 × 3–5 µm; Zou et al. 2022); *P. shenghuae* differs in its coriaceous basidiomata with a brownish-orange hymenophore surface (Xu et al. 2023). *Peniophora vietnamensis* Y.L. Xu, Y. Tian & S.H. He, and *P. pini* (Schleich. ex DC.) Boidin are similar to *P. hengduanensis* by having subcylindrical basidia. However, *P. vietnamensis* differs in its oblong cylindrical basidiospores (14–17 × 4–6 µm; Xu et al. 2023); *P. pini* differs in its clamped generative hyphae and longer lamprocystidia (25–40 × 5–8 µm; Bernicchia and Gorjón 2010). *Peniophora crassitunicata* Boidin, Lanq. & Gilles, and *P. pithya* (Pers.) J. Erikss. are similar to *P. punctata* by having allantoid basidiospores. However, *P. crassitunicata* differs in its clamped generative hyphae and longer subcylindrical basidia (25–40 × 4.5–6 µm; Andreasen and Hallenberg 2009); *P. pithya* differs in its clamped generative hyphae and longer lamprocystidia (30–70 × 8–15 µm; Bernicchia and Gorjón 2010).

Ecological functions performed by members of the order Russulales include mycorrhizal symbiosis and wood decay, which play an important role in nutrient cycling and decomposition within forest ecosystems (Cui et al. 2019; Wu et al. 2019, 2022; Liu et al. 2023; Dai et al. 2021; Deng et al. 2024b; Hyde et al. 2024; Wang et al. 2024a, b; Zhao et al. 2024). Although in the Basidiomycota, there has been a clear evolutionary trend in the development of different types of basidiomata, the taxonomy and phylogeny of some taxa in the order Russulales are still unresolved (Larsson and Larsson 2003; Miller et al. 2006; He et al. 2019, 2024; Wijayawardene et al. 2022, 2024; Wu et al. 2020; Bhunjun et al. 2024; Dong et al. 2024; Liu et al. 2024). In the present study, these data are also crucial as a supplement to the global knowledge of wood-inhabiting of the order Russulales.

Additional information

Conflict of interest

The authors have declared that no competing interests exist.

Ethical statement

No ethical statement was reported.

Funding

The research was supported by the National Natural Science Foundation of China (Project Nos. 32170004, U2102220) and the High-level Talents Program of Yunnan Province (YNQR-QNRC-2018-111).

Author contributions

Contribution, CZ and LW; methodology, CZ and LW; software, LW, Sana J and CZ; validation, CZ and Sana J; formal analysis, CZ, SH, and LW; investigation, CZ and LW; resources CZ; writing—original draft preparation, LW, SH, YZ, and CZ; writing—review and editing, CZ and LW; visualization, CZ and LW; supervision, CZ; project administration, CZ; funding acquisition, CZ. All authors have read and agreed to the published version of the manuscript.

Author ORCIDs

Lu Wang https://orcid.org/0009-0004-6274-5953
Yonggao Zhu https://orcid.org/0009-0008-5341-3798
Yonggao Zhu https://orcid.org/0009-0005-2478-0624
Sana Jabeen https://orcid.org/0000-0001-8839-7716
Changlin Zhao https://orcid.org/0000-0002-8668-1075

Data availability

All of the data that support the findings of this study are available in the main text.

References

Andreasen M, Hallenberg N (2009) A taxonomic survey of the Peniophoraceae. Synop Fungorum 26: 56–119.

Bernicchia A, Gorjón SP (2010) Fungi Europaei 12: Corticiaceae s.l. Edizioni Candusso, Italia.

Bhunjun CS, Chen YJ, Phukhamsakda C, Boekhout T, Groenewald JZ, McKenzie EHC, Francisco EC, Frisvad JC, Groenewald M, Hurdeal VG, Luangsa-ard J, Perrone G, Visagie CM, Bai FY, Błaszkowski J, Braun U, de Souza FA, de Queiroz MB, Dutta AK, Gonkhom D, Goto BT, Guarnaccia V, Hagen F, Houbraken J, Lachance MA, Li JJ, Luo KY, Magurno F, Mongkolsamrit S, Robert V, Roy N, Tibpromma S, Wanasinghe DN, Wang DQ, Wei DP, Zhao CL, Aiphuk W, Ajayi-Oyetunde O, Arantes TD, Araujo JC, Begerow D, Bakhshi M, Barbosa RN, Behrens FH, Bensch K, Bezerra JDP, Bilański P, Bradley CA, Bubner B, Burgess TI, Buyck B, Čadež N, Cai L, Calaça FJS, Campbell LJ, Chaverri P, Chen YY, Chethana KWT, Coetzee B, Costa MM, Chen Q, Custódio FA, Dai YC, Damm U, de Azevedo SALCM, De Miccolis Angelini RM, Dijksterhuis J, Dissanayake AJ, Doilom M, Dong W, Alvarez-Duarte E, Fischer M, Gajanayake AJ, Gené J, Gomdola D, Gomes AAM, Hausner G, He MQ, Hou L, Iturrieta González I, Jami F, Jankowiak R, Jayawardena RS, Kandemir H, Kiss L, Kobmoo N, Kowalski T, Landi L, Lin CG, Liu JK, Liu XB, Loizides M, Luangharn T, Maharachchikumbura SSN, Makhathini Mkhwanazi GJ, Manawasinghe IS, Marin-Felix Y, McTaggart AR, Moreau PA, Morozova OV, Mostert L, Osiewacz HD, Pem D, Phookamsak R, Pollastro S, Pordel A, Poyntner C, Phillips AJL, Phonemany M, Promputtha I, Rathnayaka AR, Rodrigues AM, Romanazzi G, Rothmann L, Salgado-Salazar C, Sandoval-Denis M, Saupe SJ, Scholler M, Scott P, Shivas RG, Silar P, Souza-Motta CM, Silva-Filho AGS, Spies CFJ, Stchigel AM, Sterfinger K, Summerbell RC, Svetasheva TY, Takamatsu S, Theelen B, Theodoro RC, Thines M, Thongklang N, Torres R, Turchetti B, van den Brule T, Wang XW, Wartchow F, Welti S, Wijesinghe SN, Wu F, Xu R, Yang ZL, Yilmaz N, Yurkov A, Zhao L, Zhao RL, Zhou N, Hyde KD, Crous PW (2024) What are the 100 most cited fungal genera? Studies in Mycology 108: 1–411. https://doi.org/10.3114/sim.2024.108.01

Boidin J, Gilles G (2000) Basidiomycètes Aphyllophorales de l'ile de La Reunion. XXI–Suite. Mycotaxon 75: 357–387.

Boidin J, Lanquetin P (1983) Two new species of *Peniophora* without clamp-connexions. Transactions of the British Mycological Society 81(2): 279–284. https://doi.org/10.1016/S0007-1536(83)80080-1

Boidin J, Lanquetin P, Gilles, G (1991) Les Peniophoraceae de la zone intertropicale (Basidiomycetes, Aphyllophorales). Bulletin de la Société Mycologique de France 107(3): 91–156.

Caboň M, Li GJ, Saba M, Kolařík M, Jančovičová S, Khalid AN, Moreau PA, Wen HA, Pfister DH, Adamčík S (2019) Phylogenetic study documents different speciation mechanisms within the *Russula globispora* lineage in boreal and arctic environments of the Northern Hemisphere. IMA Fungus 1(5): 1–16. https://doi.org/10.1186/s43008-019-0003-9

Chen JJ, Cui BK, Zhou LW, Korhonen K, Dai YC (2015) Phylogeny, divergence time estimation, and biogeography of the genus *Heterobasidion* (Basidiomycota, Russulales). Fungal Diversity 71: 185–200. https://doi.org/10.1007/s13225-014-0317-2

Chen JJ, Cui BK, Dai YC (2016a) Global diversity and molecular systematics of *Wrightoporia* s.l. (Russulales, Basidiomycota). Persoonia 37: 21–36. https://doi.org/10.3767/003158516X689666

Chen JJ, Cui BK, He SH, Cooper JA, Barrett MD, Chen JL, Dai YC (2016b) Molecular phylogeny and global diversity of the remarkable genus *Bondarzewia* (Basidiomycota, Russulales). Mycologia 108: 697–708. https://doi.org/10.3852/14-216

Cui BK, Li HJ, Ji X, Zhou JL, Song J, Si J, Yang ZL, Dai YC (2019) Species diversity, taxonomy and phylogeny of Polyporaceae (Basidiomycota) in China. Fungal Diversity 97: 137–392. https://doi.org/10.1007/s13225-019-00427-4

Dai LD, He SH. (2016) New species and new records of *Aleurodiscus* s.l. (Basidiomycota) in China. Mycological Progress 15: 717–730. https://doi.org/10.1007/s11557-016-1202-z

Dai LD, Wu SH, Nakasone KK, Burdsall HH, He SH (2017) Two new species of *Aleurodiscus* s.l. (Russulales, Basidiomycota) on bamboo from tropics. Mycoscience 58(3): 213–220. https://doi.org/10.1016/j.myc.2017.02.001

Dai YC, Yang ZL, Cui BK, Wu G, Yuan HS, Zhou LW, He SH, Ge ZW, Wu F, Wei YL, Yuan Y, Si J (2021) Diversity and systematics of the important macrofungi in Chinese forests. Mycosystema 40(4): 770–805. https://doi.org/10.13346/j.mycosystema.210036

Darriba D, Taboada GL, Doallo R, Posada D (2012) jModelTest 2: More models, new heuristics and parallel computing. Nature Methods 9(8): 772. https://doi.org/10.1038/nmeth.2109

De Crop E, Nuytinck J, Van de Putte K, Wisitrassameewong K, Hackel J, Stubbe D, Hyde KD, Roy M, Halling RE, Moreau PA, Eberhardt U, Verbeken A (2016) A multi-gene phylogeny of *Lactifluus* (Basidiomycota, Russulales) translated into a new infrageneric classification of the genus. Persoonia 38(1): 58–80. https://doi.org/10.3767/003158517X693255

Deng YL, Li JF, Zhao CL, Zhao J. (2024a) Four new fungal species in forest ecological system from southwestern China. Journal of Fungi 10: 194. https://doi.org/10.3390/jof10030194

Deng YL, Jabeen S, Zhao CL (2024b) Species diversity and taxonomy of *Vararia* (Russulales, Basidiomycota) with descriptions of six species from Southwestern China. Mycokeys 103: 97–128. https://doi.org/10.3897/mycokeys.103.118980

Dong JH, Li Q, Yuan Q, Luo YX, Zhang XC, Dai YF, Zhou Q, Liu XF, Deng YL, Zhou HM, Zhao CL, Akmal M (2024) Species diversity, taxonomy, molecular systematics and divergence time of wood-inhabiting fungi in Yunnan-Guizhou Plateau, Asia. Mycosphere 15(1): 1110–1293. https://doi.org/10.5943/mycosphere/15/1/10

Donk MA (1931) Revisie van de Nederlandse Heterobasidiomycetae en Homobasidiomycetae - Aphyllophoraceae I. Mededelingen van de Nederlandse Mycologische Vereeniging 18–20: 67–200.

Felsenstein J (1985) Confidence intervals on phylogenetics: an approach using bootstrap. Evolution 39(4): 783–791. https://doi.org/10.2307/2408678

Gómez CE, Loewenbaum M (1976) El genero *Peniopgoa* (Cooke) Donk (Basidiomycetes-Aphyllophorales) de los alrededores de Buenos Aires. Darwiniana 20: 189–209.

Grum-Grzhimaylo OA, Debets AJ, Bilanenko EN (2016) The diversity of microfungi in peatlands originated from the White Sea. Mycologia 108(2): 233–254. https://doi.org/10.3852/14-346

Harrington T, Hsaiu P (2003) Phylogenetics and adaptations of basidiomycetous fungi fed upon by bark beetles (Coleoptera:Scolytidae). Symbiosis 34(2): 111–131.

Harrington T, Batzer JC, Mcnew D (2021) Corticioid basidiomycetes associated with bark beetles, including seven new *Entomocorticium* species from North America and *Cylindrobasidium ipidophilum*, comb. nov. Antonie van Leeuwenhoek 114(5): 1–19. https://doi.org/10.1007/s10482-021-01541-7

He MQ, Zhao RL, Hyde KD, Begerow D, Kemler M, Yurkov A, McKenzie EHC, Raspe O, Kakishima M, Sánchez-Ramírez S, Vellinga CE, Halling R, Papp V, Zmitrovich IV, Buyck B, Ertz D, Wijayawardene NN, Cui BK, Schoutteten N, Liu XZ, Li TH, Yao YJ, Zhu XY, Liu AQ, Li GJ, Zhang MZ, Ling ZL, Cao B, Antonín V, Boekhout T, da Silva BDB, De Crop E, Decock C, Dima B, Dutta AK, Fell WJ, Geml J, Ghobad-Nejhad M, Giachini AJ, Gibertoni TB, Gorjón SP, Haelewaters D, He SH, Hodkinson BP, Horak E, Hoshino T, Justo A, Lim YW, Menolli Jr. N, Mešić A, Moncalvo JM, Mueller GM, Nagy L, Nilsson RH, Noordeloos M, Nuytinck J, Orihara T, Ratchadawan C, Rajchenberg M, Silva-Filho AGS, Sulzbacher MA, Tkalčec Z, Valenzuela R, Verbeken A, Vizzini A, Wartchow F, Wei TZ, Weiß M, Zhao CL, Kirk PM (2019) Notes, outline and divergence times of Basidiomycota. Fungal Diversity 99: 105–367. https://doi.org/10.1007/s13225-019-00435-4

He MQ, Zhao RL, Liu MD, Denchev TT, Begerow D, Yurkov A, Kemler M, Millanes AM,Wedin M, McTaggart AR, Shivas RG, Buyck B, Chen J, Vizzini A, Papp V, Zmitrovich IV, Davoodian N, Hyde KD (2022) Species diversity of Basidiomycota. Fungal Diversity 114(1): 1–45. https://doi.org/10.1007/s13225-021-00497-3

He MQ, Cao B, Liu F, Boekhout T, Denchev TT, Power N, Denchev CM, Kemler M, Gorjón SP, Begerow D, Valenzuela R, Davoodian N, Niskanen T, Vizzini A, Redhead SA, Ramírez Cruz V, Papp V, Dudka VA, Dutta AK, García-Sandoval R, Liu XZ, Kijpornyongpan T, Savchenko A, Tedersoo L, Theelen B, Trierveiler-Pereira L, Wu F, Zamora JC, Zeng XY, Zhou LW, Liu SL, Ghobad-Nejhad M, Giachini AJ, Li GJ, Kakishima M, Olariaga I, Haelewaters D, Sulistyo B, Sugiyama J, Svantesson S, Yurkov A, Alvarado P, Antonín V, da Silva AF, Druzhinina I, Gibertoni TB, Guzmán Davalos L, Justo A, Karunarathna SC, Galappaththi MCA, Toome-Heller M, Hosoya T, Liimatainen K, Márquez R, Mešić A, Moncalvo JM, Nagy LC, Varga T, Orihara T, Raymundo T, Salcedo I, Silva-Filho AGS, Tkalčec Z, Wartchow F, Zhao CL, Bau T, Cabarroi-Hernández M, CortésPérez A, Decock C, De Lange R, Weiss M, Menolli N, Nilsson RH, Fan YG, Verbeken A, Gaforov Y, Meiras-Ottoni A, Mendes-Alvarenga RL, Zeng NK, Wu Q, Hyde KD, Kirk PM, Zhao RL (2024) Phylogenomics, divergence times and notes of orders in Basidiomycota. Fungal Diversity 126(3): 1–280. https://doi.org/10.1007/s13225-024-00535-w

Herrera M, Montoya L, Bandala VM (2018) Two *Lactarius* species (subgenus Plinthogalus) in ectomycorrhizal association with tropical *Quercus* trees in eastern Mexico. Mycologia 110: 1033–1046. https://doi.org/10.1080/00275514.2018.1521685

Hyde KD, Norphanphoun C, Abreu VP, Bazzicalupo A, Thilini Chethana KW, Clericuzio M, Dayarathne MC, Dissanayake AJ, Ekanayaka AH, He MQ, Hongsanan S, Huang SK, Jayasiri SC, Jayawardena RS, Karunarathna A, Konta S, Kušan L, Lee H, Li JF, Lin CG, Liu GN, Lu YZ, Luo ZL, Manawasinghe IS, Mapook A, Perera RH, Phookamsak R, Phukhamsakda C, Siedlecki L, Soares AM, Tennakoon DS, Tian Q, Tibpromma S, Wanasinghe DN, Xiao YP, Yang J, Zeng XY, Abdel-Aziz FA, Li WJ, Senanayake IC, Shang JQ, Daranagama DA, de Silva NI, Thambugala KM, Abdel-Wahab MA, Bahkali AH, Berbee ML, Boonmee S, Bhat DJ, Bulgakov TS, Buyck B, Camporesi E, Castaneda-Ruiz RF, Chomnunti P, Doilom M, Dovana F, Gibertoni TB, Jadan M, Jeewon R, Jones GEB, Kang JC, Karunarathna SC, Lim YW, Liu JK, Liu ZY, Plautz Jr HL, Lumyong S, Maharachchikumbura SSN, Matočec N, McKenzie EHC, Mešic A, Miller D, Pawłowska J, Pereira OL, Promputtha I, Romero AI, Ryvarden L, Su HY, Suetrong S, Tkalčec Z, Vizzini A, Wen TC, Wisitrassameewong K, Wrzosek M, Xu JC, Zhao Q, Zhao RL, Mortimer PE (2017) Fungal diversity notes 603–708: taxonomic and phylogenetic notes on genera and species. Fungal Diversity 87: 1–235. https://doi.org/10.1007/s13225-017-0391-3

Hyde KD, Baldrian P, Chen Y, Chethana KWT, De Hoog S, Doilom M, Gomes de Farias AR, Gonçalves MFM, Gonkhom D, Gui H, Hilário S, Hu Y, Jayawardena RS, Khyaju S, Kirk PM, Kohout P, Luangharn T, Maharachchikumbura SSN, Manawasinghe IS, Mortimer PE, Niego AGT, Phonemany M, Sandargo B, Senanayake IC, Stadler M, Surup F, Thongklang N, Wanasinghe DN, Bahkali AH, Walker A (2024) Current trends, limitations and future research in the fungi? Fungal Diversity 125(1): 1–71. https://doi.org/10.1007/s13225-023-00532-5

Jaramillo-Riofrío A, Decock C. Suárez JP, Benítez Á, Castillo G, Cruz D (2023) Screening of antibacterial activity of some resupinate fungi, reveal *Gloeocystidiellum lojanense* sp. nov. (Russulales) against *E. coli* from Ecuador. Journal of Fungi 9: 54. https://doi.org/10.3390/jof9010054

Ji XH, Sun B, He G, Sun QB (2024) *Scytinostroma bambusinum* sp. nov. (Russulales, Basidiomycota) in China evidenced by morphological characteristics and phylogenetic analyses. Biodiversity Data Journal 12: e115975. https://doi.org/10.3897/BDJ.12.e115975

Katoh K, Rozewicki J, Yamada KD (2019) MAFFT online service: multiple sequence alignment, interactive sequence choice and visualization. Brief Bioinform 20: 1160–1166. https://doi.org/10.1093/bib/bbx108

Lambevska-Hristova A (2022) New Records of *Peniophora* Species (Basidiomycota) for the Bulgarian Mycota. Ecologia Balkanica 14(1): 23–30

Larsson KH (2007) Re-thinking the classification of corticioid fungi. Mycological Research 111: 1040–1063. https://doi.org/10.1016/j.mycres.2007.08.001

Larsson A (2014) AliView: a fast and lightweight alignment viewer and editor for large datasets. Bioinformatics. 30(22): 3276–3278. https://doi.org/10.1093/bioinformatics/btu531

Larsson E, Hallenberg N (2001) Species delimitation in the *Gloeocystidiellum porosum-clavuligerum* complex inferred from compatibility studies and nuclear rDNA sequence data. Mycologia 93: 907–914. https://doi.org/10.1080/00275514.2001.12063225

Larsson E, Larsson KH (2003) Phylogenetic relationships of russuloid basidiomycetes with emphasis on aphyllophoralean taxa. Mycologia 95(6): 1037–1065. https://doi.org/10.1080/15572536.2004.11833020

Larsson KH, Larsson E, Kõljalg U (2004) High phylogenetic diversity among corticioid homobasidiomycetes. Mycological Research 108: 983–1002. https://doi.org/10.1017/S0953756204000851

Larsson KH, Larsson E, Ryvarden L, Spirin V (2020) Some new combinations of corticioid fungi (Basidiomycota. Agaricomycetes). Synopsis Fungorum 40: 113–117.

Leal-Dutra CA, Neves MA, Griffith GW, Reck MA, Clasen LA. Dentinger BT (2018) Reclassification of *Parapterulicium* Corner (Pterulaceae, Agaricales), contributions to Lachnocladiaceae and Peniophoraceae (Russulales) and introduction of *Baltazaria* gen. nov. MycoKeys 37: 39–56. https://doi.org/10.3897/mycokeys.37.26303

Li Y, Xu WQ, Liu SL, Yang N, He SH (2023) Species diversity and taxonomy of *Scytinostroma* sensu stricto (Russulales, Basidiomycota) with descriptions of four new species from China. MycoKeys 98: 133–152. https://doi.org/10.3897/mycokeys.98.105632

Liu SL, He SH (2018) Taxonomy and phylogeny of *Dichostereum* (Russulales), with descriptions of three new species from southern China. MycoKeys 40(40): 111–126. https://doi.org/10.3897/mycokeys.40.28700

Liu S, Shen LL, Xu TM, Song CG, Gao N, Wu DM, Sun YF, Cui BK (2023) Global diversity, molecular phylogeny and divergence times of the brown-rot fungi within the Polyporales. Mycosphere 14(1): 1564–1664. https://doi.org/10.5943/mycosphere/14/1/18

Liu SL, Wei XW, Li GJ, Deng CY, Rossi W, Leonardi M, Liimatainen K, Kekki T, Niskanen T, Smith ME, Ammirati J, Bojantchev D, Abdel-Wahab MA, Zhang M, Tian E, Lu YZ, Zhang JY, Ma J, Dutta AK, Acharya K, Du TY, Xu J, Kim JS, Lim YW, Gerlach A, Zeng NK, Han YX, Razaghi P, Raza M, Cai L, Calabon M, Jones EBG, Saha R, Kumar TKA, Krishnapriya K, Thomas A, Kaliyaperumal M, Kezo K, Gunaseelan S, Singh SK, Singh PN, Lagashetti AC, Pawar KS, Jiang SH, Zhang C, Zhang H, Qing Y, Bau T, Peng XC, Wen TC, Ramirez NA, Niveiro N, Li MX, Yang ZL, Wu G, Tarafder E, Tennakoon DS, Kuo CH, Silva TM, Souza-Motta CM, Bezerra JDP, He G, Ji XH, Suwannarach N, Kumla J, Lumyong S, Wannathes N, Rana S, Hyde KD, Zhou LW 2024. Fungal diversity notes 1717–1817: taxonomic and phylogenetic contributions on genera and species of fungal taxa. Fungal Diversity 124(6): 1–216. https://doi.org/10.1007/s13225-023-00529-0

Lygis V, Vasiliauskas R, Larsson KH, Stenlid J (2005) Wood-inhabiting fungi in stems of *Fraxinus excelsior* in declining ash stands of northern Lithuania, with particular reference to *Armillaria cepistipes*. Scandinavian Journal of Forest Research 20(4): 337–346. https://doi.org/10.1080/02827580510036238

Maekawa N, Sugawara R, Nakano R, Shino R, Sotome K, Nakagiri K, Oba Y (2023) A new species of the genus *Aleurodiscus* sensu lato (Russulales, Basidiomycota) from Hachijo Island, Japan. Mycoscience 64: 109–115. https://doi.org/10.47371/mycosci.2023.06.001

Miller S, Larsson E, Larsson KH, Verbeken M, Nuytinck J (2006) Perspectives in the new Russulales. Mycologia 98(6): 960–970. https://doi.org/10.1080/15572536.2006.11832625

Miller MA, Pfeiffer W, Schwartz T (2012) The CIPRES science gateway. Proceedings of the 1st Conference of the extreme Science and engineering Discovery environment: Bridging from the extreme to the Campus and Beyond. Chicago, IL, 39 pp. https://doi.org/10.1145/2335755.2335836

Petersen JH (1996) Farvekort. The Danish Mycological Society’s Colour-Chart. Foreningen til Svampekundskabens Fremme, Greve, Denmark, 1–6.

Rathnayaka AR, Tennakoon DS, Jones GE, Wanasinghe DN, Bhat DJ, Priyashantha, AH, Stephenson SL, Tibpromma S, Karunarathna SC (2024) Significance of precise documentation of hosts and geospatial data of fungal collections, with an emphasis on plant-associated fungi. New Zealand Journal of Botany, 1–28. https://doi.org/10.1080/0028825X.2024.2381734

Robles CA, Carmarán CC, Lopez SE (2011) Screening of xylophagous fungi associated with *Platanus acerifolia* in urban landscapes: Biodiversity and potential biodeterioration. Landscape and Urban Planning 100(1): 129–135. https://doi.org/10.1016/j.landurbplan.2010.12.003

Ronquist F, Teslenko M, van der Mark P, Ayres DL, Darling A, Hohna S, Larget B, Liu L, Suchard MA, Huelsenbeck JP (2012) Mrbayes 3.2: Efficient bayesian phylogenetic inference and model choice across a large model space. Systematic Biology 61(3): 539–542. https://doi.org/10.1093/sysbio/sys029

Shen LL, Wang KY, Xia H, Lang SL, Yao L, Yang X (2024) Molecular phylogeny and morphology reveal a new wood-inhabiting fungal species of *Conferticium* (Stereaceae, Basidiomycota) from southwest China. Phytotaxa 677(1): 077–086. https://doi.org/10.11646/phytotaxa.677.1.4

Spirin V, Kout J (2015) *Duportella lassa* sp. nov. from Northeast Asia. Mycotaxon 130(2): 483–488. https://doi.org/10.5248/130.483

Stroheker S, Weiss M, Sieber TN, Bugmann H (2018) Ecological factors influencing norway spruce regeneration on Nurse Logs in a Subalpine Virgin Forest. Forests 9(3): 120. https://doi.org/10.3390/f9030120

Swofford DL (2002) PAUP*: Phylogenetic analysis using parsimony (*and Other Methods), Version 4.0b10, Sinauer Associates, Sunderland, MA, USA.

Telleria MT, Dueñas M, Melo I, Beltrán-Tejera E, Rodríguez-Armas JL, Salcedo I, Martín MP (2012) *Gloeocystidiellum kenyense hjortstam* in Azores and Madeira. Mycotaxon 119(1): 337–343. https://doi.org/10.5248/119.337

Tian Y, Ghobad-Nejhad M, He SH, Dai YC (2018) Three new species of *Aleurodiscus* s.l. (Russulales, Basidiomycota) from southern China. MycoKeys 37: 93–107. https://doi.org/10.3897/mycokeys.37.25901

Vasiliauskas R, Larsson E, Larsson KH, Stenlid J (2005) Persistence and long-term impact of Rotstop biological control agent on mycodiversity in *Picea abies* stumps. Biological Control 32(2): 295–304. https://doi.org/10.1016/j.biocontrol.2004.10.008

Vidal JM, Alvarado P, Loizides M, Konstantinidis G, Chachuła P, Mleczko P, Moreno G, Vizzini A, Krakhmalnyi M, Paz A, CaberoJ, Kaounas V, Slavova M, Moreno-Arroyo B, Llistosella J (2019) A phylogenetic and taxonomic revision of sequestrate Russulaceae in Mediterranean and temperate Europe. Persoonia 42: 127–185. https://doi.org/10.3767/persoonia.2019.42.06

Vilgalys R, Hester M (1990) Rapid genetic identification and mapping of enzymatically amplified ribosomal DNA from several *Cryptococcus* species. Journal of Bacteriology 172(8): 4238–4246. https://doi.org/10.1128/jb.172.8.4238-4246.1990

Vu D, Groenewald M, de Vries M, Gehrmann T, Stielow B, Eberhardt U, Al-Hatmi A, Groenewald JZ, Cardinali G, Houbraken J, Boekhout T, Crous PW, Robert V, Verkley GJM (2019) Large-scale generation and analysis of filamentous fungal DNA barcodes boosts coverage for kingdom fungi and reveals thresholds for fungal species and higher taxon delimitation. Studies in Mycology 92(1): 135–154. https://doi.org/10.1016/j.simyco.2018.05.001

Wang H, He X, Zhao CL (2020) *Scytinostroma yunnanense* sp. nov. (Russulales,basidiomycota) evidenced by morphological characteristics and phylogenetic analyses in China. Phytotaxa 451(2): 145–153. https://doi.org/10.11646/phytotaxa.451.2.4

Wang CG, Dai YC, Kout J, Gates GM, Liu HG, Yuan Y, Vlasák J (2024a) Multi-gene phylogeny and taxonomy of *Physisporinus* (Polyporales, Basidiomycota). Mycosphere 15: 1455–1521. https://doi.org/10.5943/mycosphere/15/1/12

Wang L, Yang X, Zhao CL (2024b) The wood-decaying fungal diversity unveiled by morphology and phylogeny in Ailaoshan Mountain, Yunnan, China. Phytotaxa 661(1): 001–030. https://doi.org/10.11646/phytotaxa.661.1.1

White TJ, Bruns T, Lee S, Taylor J (1990) Amplification and direct sequencing of fungal ribosomal RNA genes for phylogenetics. PCR Protocols: A Guide to Methods and Applications. Academic Press, San Diego, 315–322. https://doi.org/10.1016/B978-0-12-372180-8.50042-1

Wijayawardene NN, Hyde KD, Dai DQ, Sánchez-García M, Goto BT, Saxena RK, Erdoğdu M, Selçuk F, Rajeshkumar KC, Aptroot A, Błaszkowski J, Boonyuen N, da Silva GA, de Souza FA, Dong W, Ertz D, Haelewaters D, Jones EBG, Karunarathna SC, Kirk PM, Kukwa M, Kumla J, Leontyev DV, Lumbsch HT, Maharachchikumbura SSN, Marguno F, Martínez-Rodríguez P, Mešić A, Monteiro JS, Oehl F, Pawłowska J, Pem D, Pfiegler WP, Phillips AJL, Pošta A, He MQ, Li JX, Raza M, Sruthi OP, Suetrong S, Suwannarach N, Tedersoo L, Thiyagaraja V, Tibpromma S, Tkalčec Z, Tokarev YS, Wanasinghe DN, Wijesundara DSA, Wimalaseana SDMK, Madrid H, Zhang GQ, Gao Y, Sánchez Castro I, Tang LZ, Stadler M, Yurkov A, Thines M (2022) Outline of Fungi and fungus-like taxa – 2021. Mycosphere 13: 53–453. https://doi.org/10.5943/mycosphere/13/1/2

Wijayawardene NN, Hyde KD, Mikhailov KV, Péter G, Aptroot A,Pires-Zottarelli CLA, Goto BT, Tokarev YS, Haelewaters D, Karunarathna SC, Kirk PM, Santiago ALCMA, Saxena RK, Schoutteten N, Wimalasena MK, Aleoshin VV, Al-Hatmi AMS, Ariyawansa KGSU, Assunção AR, Bamunuarachchige TC, Baral HO, Bhat DJ, Blaszkowski J, Boekhout T, Boonyuen N, Brysch-Herzberg M, Cao B, Cazabonne J, Chen XM, Coleine C, Dai DQ, Daniel HM, Silva SBG, Souza FA, Dolatabadi S, Dubey MK, Dutta AK, Ediriweera A, Egidi E, Elshahed MS, Fan XL, Felix JRB, Galappaththi MCA, Groenewald M, Li-Su Han, Bo Huang, Hurdeal VG, Ignatieva AN, Jerônimo GH, Jesus AL, Kondratyuk S, Kumla J, Kukwa M, Li QR, Lima JLR, Liu XY, Lu WH, Lumbsch HT, Madrid H, Magurno F, Marson G, McKenzie EHC, Menkis A, Mešić A, Nascimento ECR, Nassonova ES, Nie Y, Oliveira NVL, Ossowska EA, Pawtowska J, Peintner U, Pozdnyakov LR, Premarathne BM, Priyashantha AKH, Quandt CA, Queiroz MB, Rajeshkuma KC, Raza M, Roy N, Samarakoon MC, Santos AA, Santos LA, Schumm F, Selbmann L, Selçuk F, Simmons DR, Simakova AV, Smith MT, Sruthi OP, Suwannarach N, Tanaka K, Tibpromma S, Tomás EO, Ulukapı M, Vooren NV, Wanasinghe DN, Weber E, Wu QZ, Yang EF, Yoshioka R, Youssef NH, Zandijk A, Zhang GQ, Zhang JY, Zhao H, Zhao RL, Zverkov OA, Thines M, Karpov SA (2024) Classes and phyla of the kingdom Fungi. Fungal Diversity 127(1): 1–165. https://doi.org/10.1007/s13225-024-00540-z

Wu SH (1996) Studies on *Gloeocystidiellum* sensu lato (Basidiomycotina) in Taiwan. Mycotaxon 58: 1–68.

Wu F, Zhou LW, Yang ZL, Bau T, Li TH, Dai YC (2019) Resource diversity of Chinese macrofungi: edible, medicinal and poisonous species. Fungal Diversity 98: 1–76. https://doi.org/10.1007/s13225-019-00432-7

Wu F, Yuan Y, Chen JJ, Cui BK, Zhou M, Dai YC (2020) Terrestriporiaceae fam. nov., a new family of Russulales (Basidiomycota). Mycosphere 11(1): 2755–2766. https://doi.org/10.5943/mycosphere/11/1/21

Wu F, Man XW, Tohtirjap A, Dai YC (2022) A comparison of polypore funga and species composition in forest ecosystems of China, North America, and Europe. Forest Ecosystems 9: 100051. https://doi.org/10.1016/j.fecs.2022.100051

Xu YL, Tian Y, He SH (2023) Taxonomy and phylogeny of *Peniophora* sensu lato (Russulales, Basidiomycota). Journal of Fungi 9: 93. https://doi.org/10.3390/jof9010093

Yuan Y, Chen JJ, Korhonen K, Martin F, Dai YC (2021) An updated global species diversity and phylogeny in the forest pathogenic genus *Heterobasidion* (Basidiomycota, Russulales). Frontiers in Microbiology 11: 596393. https://doi.org/10.3389/fmicb.2020.596393

Yurchenko E (2010) The genus *Peniophora* (Basidiomycota) of Eastern Europe: morphology, taxonomy, ecology, distribution. National Academy of Sciences of Belarus, VF Kuprevich Insitute of Experimental Botany, Minsk.

Zhang QY, Liu HG, Bian LS, Chen Q (2023a) Two new species of *Scytinostroma* (Russulales, Basidiomycota) in Southwest China. Frontiers in Cellular and Infection Microbiology 13: 1189600. https://doi.org/10.3389/fcimb.2023.1189600

Zhang QY, Liu HG, Papp V, Zhou M, Dai YC, Yuan Y (2023b) New insights into the classification and evolution of *Favolaschia* (Agaricales, Basidiomycota) and its potential distribution, with descriptions of eight new species. Mycosphere 14: 777–814. https://doi.org/10.5943/mycosphere/14/1/10

Zhao H, Nie Y, Zong TK, Wang K, Lv ML, Cui YJ, Tohtirjap A, Chen JJ, Zhao CL, Wu F, Cui BK, Yuan Y, Dai YC, Liu XY (2023) Species diversity, updated classification and divergence times of the phylum Mucoromycota. Fungal Diversity123: 49–157. https://doi.org/10.1007/s13225-023-00525-4

Zhao CL, Wu ZQ (2017) *Ceriporiopsis kunmingensis* sp. nov. (Polyporales, Basidiomycota) evidenced by morphological characters and phylogenetic analysis. Mycological Progress 16: 93–100. https://doi.org/10.1007/s11557-016-1259-8

Zhao YL, Zhao CL (2023) A corticioid fungus, *Gloeocystidiellum yunnanense* sp. nov. (Russulales) with characteristic gloeocystidia from southern China. Nova Hedwigia 116: (1–2). https://doi.org/10.1127/nova_hedwigia/2023/0725

Zhao RL, Li GJ, Sánchez-Ramírez S, Stata M, Yang ZL, Wu G, Dai YC, He SH, Cui BK, Zhou JL, Wu F, He MQ, Moncalvo JC, Hyde KD (2017) A six-gene phylogenetic overview of Basidiomycota and allied phyla with estimated divergence times of higher taxa and a phyloproteomics perspective. Fungal Diversity 84: 43–74. https://doi.org/10.1007/s13225-017-0381-5

Zhao CL, Qu MH, Huang RX, Karunarathna SC (2023a) Multi-gene phylogeny and taxonomy of the wood-rotting fungal genus *Phlebia* sensu lato (Polyporales, Basidiomycota). Journal of Fungi 9: 320. https://doi.org/10.3390/jof9030320

Zhao H, Wu YD, Yang ZR, Liu HG, Wu F, Dai YC, Yuan Y (2024) Polypore funga and species diversity in tropical forest ecosystems of Africa, America and Asia, and a comparison with temperate and boreal regions of the Northern Hemisphere. Forest Ecosystems 11: 100200. https://doi.org/10.1016/j.fecs.2024.100200

Zhou LW, Dai, YC (2013) Taxonomy and phylogeny of wood-inhabiting hydnoid species in Russulales: two new genera, three new species and two new combinations. Mycologia 105(3): 636–649. https://doi.org/10.3852/12-011

Zhou M, Dai YC, Vlasák J, Liu HG, Yuan Y (2023) Updated systematics of *Trichaptum* s.l. (Hymenochaetales, Basidiomycota). Mycosphere 14(1): 815–917. https://doi.org/10.5943/mycosphere/14/1/11

Zhou HM, Gu ZR, Zhao CL (2024) Molecular phylogeny and morphology reveal a new species of *Asterostroma* from Guizhou Province, China. Phytotaxa 635(2): 173–181. https://doi.org/10.11646/phytotaxa.635.2.7

Zhou HM, Dai YC, Bian LS, Liu HG, Vlasák J, Yuan Y (2025) Diversity, divergence time, and biogeography of the genus *Albatrellus* (Agaricomycetes, Russulales). Mycology, 1–39. https://doi.org/10.1080/21501203.2024.2386021

Zou L, Zhang XL, Deng YL, Zhao CL (2022) Four new wood-inhabiting fungal species of Peniophoraceae (Russulales, Basidiomycota) from the Yunnan-Guizhou Plateau, China. Journal of Fungi 8: 1227. https://doi.org/10.3390/jof8111227

MycoKeys 115: 309–326 (2025)
DOI: 10.3897/mycokeys.115.146604

Research Article

Unveiling new species of Phragmidiaceae (Basidiomycota, Pucciniales) on rosaceous plants from Guizhou, China

Qinfang Zhang[1,2], Qianzhen Wu[1,2], Peng Zhao[3], Kamran Habib[1], Yao Wang[2], Dexiang Tang[1], Muhammad Aijaz Ahmad[1], Yulin Ren[1,4], Xiangchun Shen[1], Qingde Long[1,2], Lili Liu[1], Qirui Li[1,2]

1 *State Key Laboratory of Discovery and Utilization of Functional Components in Traditional Chinese Medicine & School of Pharmaceutical Sciences, Guizhou Medical University, Guian New District, Guizhou 550004, China*
2 *The High Efficacy Application of Natural Medicinal Resources Engineering Center of Guizhou Province (The Key Laboratory of Optimal Utilization of Natural Medicine Resources), School of Pharmaceutical Sciences, Guizhou Medical University, University Town, Guian New District, Guizhou 550004, China*
3 *State Key Laboratory of Mycology, Institute of Microbiology, Chinese Academy of Sciences (CAS), Beijing 100101, China*
4 *Immune Cells and Antibody Engineering Research Center of Guizhou Province, Guizhou Medical University, Guiyang 550004, China*
Corresponding authors: Qirui Li (lqrnd2008@163.com); Lili Liu (lililiu550025@163.com)

Abstract

Rust fungi associated with *Rubus* were collected across diverse locations in Guizhou Province, and three new species – *Gerwasia amphidasydis* on *Rubus amphidasys*, *Phragmidium coreanicola* on *Rubus coreanus*, and *Phragmidium parvifolius* on *Rubus parvifolius* are introduced. These novel species are described based on morphological characteristics and phylogenetic analysis of the ITS and LSU loci. Additionally, *Gerwasia rubi-setchuenensis* is introduced as a new host record on *Rubus buergeri*. The study includes comprehensive morpho-anatomical descriptions, detailed illustrations, and a phylogenetic tree, providing insights into the taxonomic placement and relationships of these novel taxa within their respective lineages.

Key words: ITS, LSU, Phragmidiaceae, phylogeny, rust disease, taxonomy

Academic editor: Samantha C. Karunarathna
Received: 13 January 2025
Accepted: 2 March 2025
Published: 28 March 2025

Citation: Zhang Q, Wu Q, Zhao P, Habib K, Wang Y, Tang D, Ahmad MA, Ren Y, Shen X, Long Q, Liu L, Li Q (2025) Unveiling new species of Phragmidiaceae (Basidiomycota, Pucciniales) on rosaceous plants from Guizhou, China. MycoKeys 115: 309–326. https://doi.org/10.3897/mycokeys.115.146604

Introduction

Pucciniales (Basidiomycota, Pucciniomycetes) represents approximately 25% of basidiomycete fungi and constitutes one of the most prevalent fungal groups, parasitizing leaves, fruits, and branches of plants, thereby inhibiting normal growth and development of plants and impacting yield and quality (Aime and McTaggart 2021; Zhao et al. 2022a). To date, seven suborders (i.e., Araucariomycetineae, Melampsorineae, Mikronegeriineae, Raveneliineae, Rogerpetersonineae, Skierkineae, and Uredinineae) and 18 families (i.e., Araucariomycetaceae, Coleosporiaceae, Crossopsoraceae, Gymnosporangiaceae, Melampsoraceae, Milesinaceae, Ochropsoraceae, Phakopsoraceae, Phragmidiaceae, Pileolariaceae, Pucciniaceae, Pucciniastraceae, Raveneliaceae, Rogerpetersoniaceae, Skierkaceae, Sphaerophragmiaceae, Tranzscheliaceae, and Zaghouaniaceae) have been reported (Aime et al. 2017; Aime and McTaggart 2021; Zhao et al. 2022b).

According to estimations, there are approximately 35,000 higher plant species in China, which are categorized into 454 families and 3,818 genera (Wang et al. 2015). It is further estimated that between 1,700 and 8,800 species of rust fungi may exist within the country, posing a significant threat to the health and productivity of these plant species (Zhao et al. 2021). More than 8,400 rust taxa have been documented worldwide (Zhao et al. 2021; Sun et al. 2022). Based on their morphological characteristics and host associations, 1,200 species from 71 genera across 15 families have been documented in China. Among them, more than 70 species of *Phragmidium* have been identified. (Dai 1979; Zhuang et al. 1998, 2003, 2005, 2012, 2021; Ji et al. 2019, 2020; Zhao et al. 2021; Sun et al. 2022, 2024). Plants are susceptible to Coleosporiaceae, Melampsoraceae, Phragmidiaceae, and Pucciniaceae, which are the dominant families of rust taxa in China (Zhao et al. 2021; Zhao et al. 2022b; Sun et al. 2024).

The genus *Phragmidium* (Pucciniales: Phragmidiaceae) was established by Link (1816). Phragmidiaceae comprises a diverse array of species, encompassing 14 genera and an estimated 200 species, primarily targeting the economically vital family Rosaceae (examples of hosts in Rosaceae: *Rosa*, *Rubus*, *Potentilla*, *Sanguisorba*, *Duchesnea*, and *Acaena*) (Zhao et al. 2021; Sun et al. 2024). A total of 115 *Phragmidium* species have been described (Cummins 1931; Arthur 1934; Wahyuno et al. 2001; Cummins and Hiratsuka 2003; Zhuang et al. 2012; Yang et al. 2015; Ali et al. 2017; Zhao et al. 2021; Sun et al. 2022; Ya 2024). Among these, 38 species specifically target and parasitize members of the genus *Rosa* (Ya 2024), and at least 39 *Phragmidium* species have been reported in China (Wei 1988; Zhuang et al. 2003, 2012; Yang et al. 2015; Liu et al. 2018).

The susceptibility of Rosaceae plants to Phragmidiaceae infections underscores the importance of understanding the biology, ecology, and management strategies of these fungal pathogens (Dietel 1905; Yun et al. 2011; Sun et al. 2022). During the field investigation of rust fungi on medicinal plants in Guizhou Province, China, three potential new species were found belonging to the genera *Gerwasia* and *Phragmidium* of Phragmidiaceae, which infect the members of Rosaceae, as well as one species that infects a new host. We conducted a phylogenetic analysis using multi-locus (ITS and LSU) phylogeny and morphological characteristics to better understand their taxonomic position. Descriptions, illustrations, and phylogenetic analysis results of all the novel species and the new host record are provided.

Materials and methods

Sample collection and preservation

Rust-infected specimens were collected in Guizhou Province, China, from August to November of each year from 2021 to 2023. All host and habitat information of specimens was recorded (Rathnayaka et al. 2024). Photographs of the infected plants were taken using a camera (Canon G15, Corporation, Tokyo, Japan). The samples were kept in blotting papers and were brought to the laboratory for examination. The collected specimens were partly kept in a refrigerator at 4 °C for spare parts and partly pressed and air-dried to make pressed specimens (Wei and Wang 2011; Wu et al. 2023). All specimens were deposited at the herbarium of Guizhou Medical University (**GMB**) and Kunming Institute of Botany, Chinese Academy of Sciences (**KUN-HKAS**).

Morphological characterization

Macroscopic characteristics were observed under a stereomicroscope (Olympus SZ61), and photographs were taken with a digital camera (Canon 700D) fitted with a light microscope (Nikon Ni). The infected portions were examined, and photographs were taken as described by Wu et al. (2023). More than 30 measurements were noted for each type of teliospores, urediniospores, and paraphyses for each sample using the Tarosoft (R) Image Frame Work v. 0.9.0.7. The images were arranged using Adobe Photoshop CS6 (Adobe Systems, the USA).

DNA extraction and PCR amplification

The infected portion of the rust fungus was scraped using a sterilized scalpel. DNA extraction was carried out following the manufacturer's protocols for the Biomiga Fungal gDNA Kit. The DNA samples were kept at –20 °C. The rust-specific primer pairs Rust2inv (Aime 2006) and ITS4rust (Pfunder et al. 2001) were used for the PCR amplification of the regions of internal transcribed spacer (ITS), whereas the universal primer pairs LR0R (Hopple and Vilgalys 1999) and LR6 (Vilgalys and Hester 1990) were used for the large subunit ribosomal (LSU). The composition of a 25 μL PCR mixture comprised the following: 9.5 μL of double-distilled water, 12.5 μL of PCR Master Mix, 1 μL of each primer, as well as 1 μL of template DNA. The qualified PCR products were verified through 1.5% agarose gel electrophoresis, stained with GoldenView, and subsequently submitted to Sangon Co. China for sequencing (Zhao et al. 2016).

Phylogenetic analyses

All sequences were obtained in ABI file format and deposited in the GenBank (Table 1). The consensus sequences were blasted in GenBank using the BLAST algorithm. The similar sequences were retrieved from the GenBank database. The molecular phylogeny was inferred from a combined dataset of ITS and LSU sequences. The reference sequences retrieved from open databases originated from recently published literature (Zhao et al. 2021; Wu et al. 2023; Sun et al. 2024). All the ambiguous nucleotides were trimmed using BioEdit software v.7.0.5.3 and TrimAL (Hall 1999). Sequences were aligned using the MAFFT v.7.110 online tool (Katoh and Standley 2013). The alignments are available in TreeBASE (www.treebase.org/treebase-web/home.html) under ID31754 for LSU and ITS rDNA sequences. The maximum likelihood (ML) analysis was implemented in RAxML v.8.2.12 using the GTRGAMMA substitution model with 1,000 bootstrap replicates (Stamatakis 2015). The phylogenetic analyses were also performed using Bayesian inference in MrBayes v.3.2.1 (Ronquist et al. 2015) online. The Markov chain Monte Carlo (MCMC) sampling in MrBayes v.3.2.2 (Ronquist et al. 2015) was used to determine the Bayesian posterior probabilities (BYPP). Six simultaneous Markov chains were run for 3,000,000 generations, and trees were sampled every 1,000th generation. All analyses were run on the CIPRES Science Gateway v.3.3 web portal (Miller et al. 2010; Huelsenbeck and Ronquist 2001). The phylogenetic tree was visualized by FigTree v.1.4.3 (Rambaut 2012).

Table 1. Taxa information and corresponding GenBank accession numbers of the sequences used in the phylogenetic analyses.

Species	Specimen No.	Host	Province, Country	GenBank Accession No.		References
				ITS	LSU	
Gerwasia chinensis	HMAS249978 (ZP-R5)	*Rubus parkeri*	Yunnan, China	MK519039	MK518737	Zhao et al. 2021
G. chinensis	HMAS249980 (ZP-R295)	*Rubus parkeri*	Yunnan, China	MK519038	MK518540	Zhao et al. 2021
G. pittieriana	BPI 843556	*Rubus* sp.	USA	KY764065	KY764065	Zhao et al. 2021
G. rubi	(ZP-R345)	*Rubus setchuenensis*	Sichuan, China	–	MK518735	Zhao et al. 2021
G. amphidasydis	GMB4047*	*Rubus amphidasys*	Guizhou, China	PQ472136	PQ456450	This study
G. amphidasydis	GMB4076	*Rubus amphidasys*	Guizhou, China	PQ472137	PQ456451	This study
G. rubi-setchuenensise	GMB4052	*Rubus buergeri*	Guizhou, China	PQ472135	PQ456449	This study
G. rubi-setchuenensise	GMB4075	*Rubus buergeri*	Guizhou, China	PQ472134	PQ456448	This study
G. rubi-setchuenensis	HGUP21168*	*Rubus setchuenensis*	Guizhou, China	OR470045	OR528540	Sun et al. 2024
G. rubus-playfairianus	HMAS249840 (ZP-R 1374)	*Rubus playfairianus*	Guangxi, China	MK518976	MK518674	Sun et al. 2024
Gymnosporangium asiaticum	CUP-0016*	*Juniperus chinensis*	Japan	MN642593	MN642617	Zhao et al. 2020
Gymnosporangium sabinae	TNM F0030477	*Pyrus communis*	Bulgaria: Sofia	KY964764	KY964764	Shen et al. 2017
Hamaspora acutissima	BRIP:55606	*Rubus rolfei*	Philippines	–	KT199398	McTaggart et al. 2016
H. sinica	ZP-R1	*Rubus setchuenensis*	Guangdong, China	MK519049	MK518636	Zhao et al. 2020
H. longissima	BPI 871506	*Rubus rigidu*	South Africa	–	MW049262	Aime and McTaggart 2021
H. rubi-lambertianuse	HGUP21164*	*Rubus lambertianus*	Guizhou, China	OR470053	OR528547	Sun et al. 2024
H. rubi-parkerii	HGUP21159*	*Rubus parkeri*	Guizhou, China	OR470055	OR528543	Sun et al. 2024
H. rubi-alceifolii	GMB0109*	*Rubus alceifolius*	Guizhou, China	OQ067094	OQ067532	Wu et al. 2023
H. rubi-alceifolii	GMB0116	*Rubus alceaefolius*	Guizhou, China	OQ067095	OQ067533	Wu et al. 2023
Kuehneola uredinis	LD1029	*Rubus* sp.	New York, America	GU058013	GU058013	Dixon et al. 2018
Phragmidium barnardii	HGUP21035	*Rubus parvifolius*	Guizhou, China	OL684828	OL684839	Sun et al. 2022
P. charyuensis	BJFC: R02532*	*Rosa duplicata*	China	MH128374	NG_064492	Liu et al. 2018
P. cibanum	BJFC: R02528	*Rubus niceus*	China	MH128370	NG_064491	Liu et al. 2018
P. cymosum	GMB0115	*Rosa cymosa*	Guizhou, China	OQ067097	OQ067531	Wu et al. 2023
P. cymosum	GMB0108*	*Rosa cymosa*	Guizhou, China	OQ067096	OQ067530	Wu et al. 2023
P. coreanicola	GMB0101*	*Rubus coreanus*	Guizhou, China	PQ472133	PQ456447	This study
P. coreanicola	GMB4071	*Rubus coreanus*	Guizhou, China	PQ472132	PQ456448	This study
P. griseum	HMAS56906	*Rubus crataegifoliu*	Beijing, China	MH128377	MG669115	Liu et al. 2018
P. griseum	BJFCR 03451	–	Beijing, China	MN264713	MN264731	Liu et al. 2020
P. griseum	BJFCR03449	*Rubus crataegifoliu*	Beijing, China	MN264712	MN264730	Liu et al. 2020
P. japonicum	HMAS41585	*Rosa laecigata*	Fujian, China	MN264716	MN264734	Liu et al. 2020
P. jiangxiense	BJFCR 03453*	*Rosa laecigata*	Jiangxi, China	MN264715	MN264733	Liu et al. 2020
P. kanasense	ZP-R1382	*Phoenix acaulis*	Yunnan, China	MK518980	MK518678	Zhao et al. 2021
P. kanasense	ZP-R491	*Rosa fedtschenkoana*	Xinjiang, China	–	MK518748	Zhao et al. 2021
P. leucoaecium	BJFCR 02118*	*Rosa* sp.	Yunnan, China	MN264719	MN264737	Liu et al. 2020
P. mexicanum	E14_5_1	*Potentilla indica*	Slovenia, Forestry	LN795901	LN795901	Piškur and Jurc 2017
P. octoloculare	HMAS140416	*Rubus biflorus*	China	MH128376	MG669119	Liu et al. 2018
P. pauciloculare	ZP-R318	*Rubus corchorifolius*	Guangxi, China	MK518874	MK518542	Zhao et al. 2021
P. potentillae	HGUP21034	*Acaena novae-zelandiae*	Tasmania, Australia	OL684827	OL684838	Sun et al. 2022
P. potentillae	HMJAU8609	*Potentilla chinensis*	China	MK296538	MK296520	Ji et al. 2019
P. potentillae	BJFCR 00961	*Potentilla chinensis*	Beijing, China	MN264720	MN264738	Liu et al. 2020

Species	Specimen No.	Host	Province, Country	GenBank Accession No.		References
				ITS	LSU	
P. potentillae	TJ-1F	*Potentilla chinensis*	China	PP272995	PP266810	Liu et al. 2020
P. potentillae	GMB4048	*Potentilla chinensis*	Guizhou, China	PQ472142	PQ456456	This study
P. potentillae	GMB4072	*Potentilla chinensis*.	Guizhou, China	PQ472143	PQ456457	This study
P. rosae-multiflorae	HGUP21158	*Rosa multiflora*	Guizhou, China	OR470059	OR528548	Sun et al. 2024
P. rosae-multiflorae	BIFCR 03454	*Rosa multiflora*	Jiangxi, China	MN264721	MN264739	Liu et al. 2020
P. rosae-multiflorae	HMAS94924	*Rosa multiflora*	Zhejiang, China	–	KU059175	Sun et al. 2022
P. rosae-multiflorae	GMB4044	*Rosa multiflora*	Guizhou, China	PQ472144	PQ456459	This study
P. rosae-multiflorae	GMB4073	*Rosa multiflora*	Guizhou, China	PQ472145	PQ456458	This study
P. rosae-roxburghii	HGUP21025*	*Rosa roxburghii*	Guizhou, China	OL684818	OL684831	Liu et al. 2018
P. rosae-roxburghii	GMB0104	*Rosa xanthina*	Guizhou, China	OQ067092	–	Wu et al. 2023
P.rosae-kwangtungensise	HGUP21154*	*Rosa kwangtungensis*	Guizhou, China	OR470067	–	Sun et al. 2024
P. rosae-cymosaii	HGUP21147	*Rosa cymosa*	Guizhou, China	OR470062	OR528551	Sun et al. 2024
P. rubi-idaei	HMUT100470	*Rubus saxatilis*	Chongqing, China	OQ613354	OQ606768	–
P. rubi-oldhami	KSNUH1322	*Rubus pungens*	South Korea	ON180674	ON170371	Kim et al. 2022
Phragmidium sp.	HMJAU8613	–	Changchun, China	MK398297	MK398296	Ji et al. 2019
P. parvifolius	GMB4054*	*Rubus parvifolius*	Guizhou, China	PQ472140	PQ456454	This study
P. parvifolius	GMB4070	*Rubus parvifolius*	Guizhou, China	PQ472141	PQ456455	This study
P. tormentillae	GMB00114	*Potentilla simulatrix*	Guizhou, China	OQ067093	–	Wu et al. 2023
P. tormentillae	BPI 843392	*Duchesnea* sp.	USA: Maryland	–	DQ354553	Yun et al. 2011
P. violaceum	KRM 0035511	*Rubus* sp.	Germany	ON063390	ON063390	Bradshaw et al. 2023
P. violaceum	ZP-R1384	*Duchesnea indica*	Yunnan, China	MK518982	MK518680	Zhao et al. 2021
P. yangii	BJFCR 00338	*Rosa lichiangensis*	Beijing, China	MN264725	MN264743	Yang et al. 2015
P. zangdongi	BJFC: R02447*	*Rosa tibetica*	Tibet, China	MH128372	NG064490	Liu et al. 2018
P. zhouquensis	BJFCR01516	*Rosa omeiensis*	Yunnan, China	MN264728	MN264746	Yang et al. 2015
P. zhouquensis	BJFCR01529	*Rosa omeiensis*	Yunnan, China	MN264729	MN264747	Liu et al. 2020
Trachyspora alchemillae	BPI 843828	*Alchemilla vulgari*	Switzerland	DQ354550	DQ354550	Aime 2006

Notes: –: no data available; *: type specimens or strains.

Results

Phylogeny

In this study, 14 samples from twelve host plant species were collected in Guizhou Province. Through morphological and molecular systematic studies, a total of 6 species were identified, including three new species, one new host species, and two known species.

For the final phylogenetic analyses, taxa were selected based on their morphological and phylogenetic affinities, largely following the approach of Zhao et al. (2021). Both the RAxML and BYPP analyses produced similar overall tree topologies with no significant differences. The alignment includes 67 species (comprising one family: Phragmidiaceae, six genera: *Phragmidium*, *Gerwasia*, *Hamaspora*, *Kuehneola*, *Trachyspora*, and the outgroup genus *Gymnosporangium*) and contains 1245 characters, including gaps (ITS: 398 bp, LSU: 847 bp). Among these, three novel species have been identified (*Gerwasia amphidasydis* sp. nov., *Phragmidium parvifolius* sp. nov., and *P. coreanicola* sp. nov.). Additionally, one species (*G. rubi-setchuenensise*) was reported for the first time on *Rubus buergeri*.

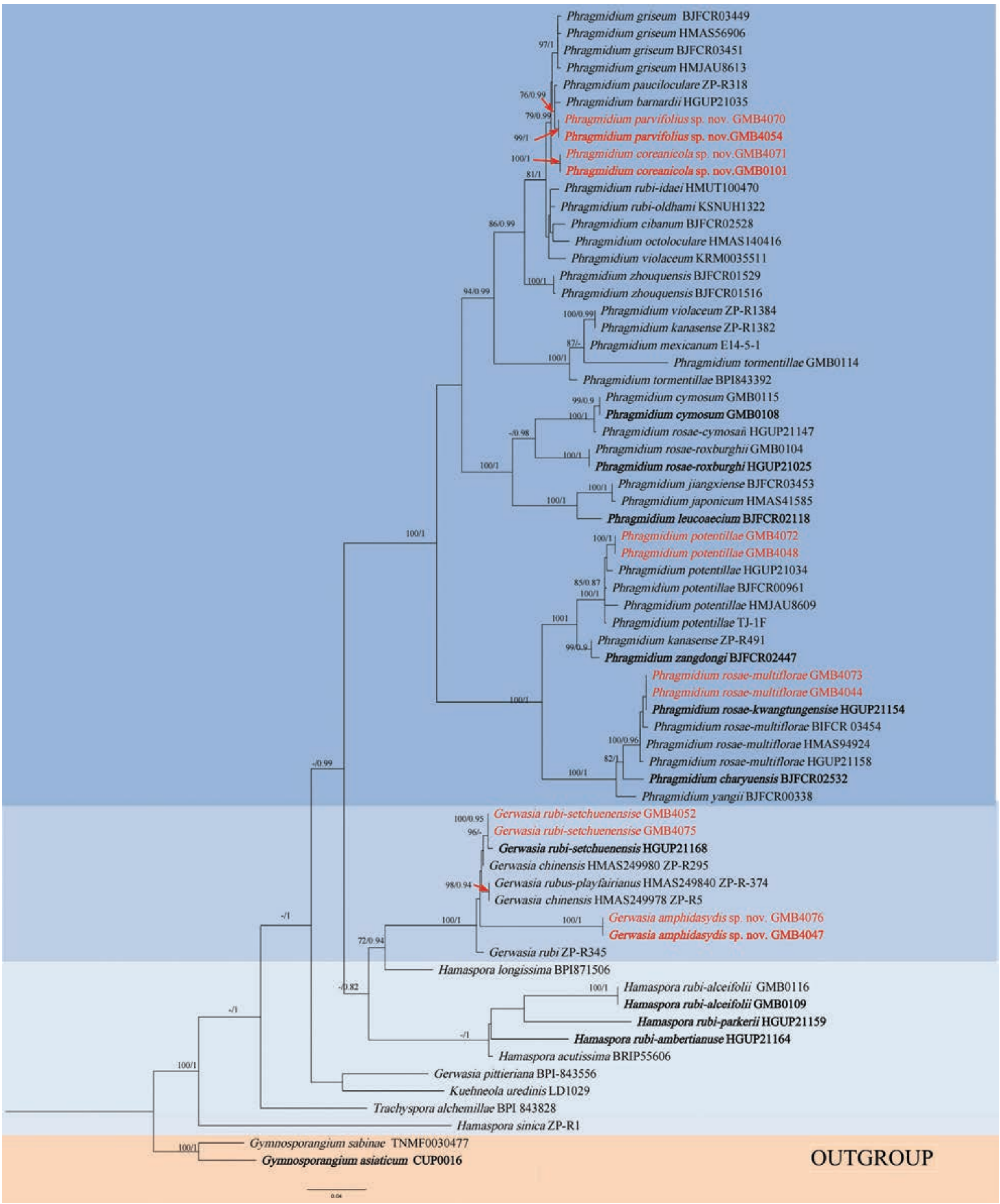

Figure 1. RAxML tree of the family Phragmidiaceae based on rDNA ITS and LSU sequences. ML bootstrap supports (≥75%) and Bayesian posterior probability (≥0.90) are indicated as ML/BYPP. The tree is rooted to *G. sabinae* and *G. asiaticum* (Yang et al. 2015; Aime et al. 2018). All species newly studied are indicated in red, with novel species highlighted in bold red. Type materials were highlighted in bold.

Taxonomy

Family Phragmidiaceae Corda, Icon. Fung. (Prague) 1: 6. 1837

Genus *Gerwasia* Racib. Bull. Acad. Sci. Lett. Cracovie, Cl. Sci. Math. Nat. Sér. B, Sci. Nat. 3: 270. 1909

Gerwasia amphidasydis Q. F. Zhang, Q. Z. Wu & Q. R. Li, sp. nov.

MycoBank No: 854995
Fig. 2

Type. China • Guizhou Province, Zunyi City, Kuangkuoshui Nature Reserve (28°12'40"N, 107°10'22"E), 2227 m a.s.l., on leaves of *Rubus amphidasys*. 1 November 2022, Q. Z. Wu and Q. F. Zhang (holotype GMB4047, isotype KUN-HKAS144247);

Etymology. The epithet refers to the host species, *Rubus amphidasys* Focke ex Diels., from which the holotype was collected.

Description. ***Spermogonia***, ***Aecia***, and ***Telia*** not found. ***Uredinia*** 0.2–0.8 mm diam. produced on the abaxial leaf surface, scattered to gregarious, hypophyllous, covered by peridium, small, rounded, light yellow, or orange-yellow. Urediniospores 29–41 × 22–29 µm (av. = 34 × 26 µm, n = 30), globose to subglobose or ovoid, golden, yellow-brown, wall 1.2–2.5 µm thick at sides, hyaline, prominent sparsely echinulate, markings elongated longitudinally, 1.3–3.1 µm in distance, pore obscure, germ pores inconspicuous. Pedicel broken; paraphyses not seen.

Additional material examined. China • Guizhou Province, Zunyi City, Kuangkuoshui Nature Reserve, (28°12'38"N, 107°10'21"E) 2214 m a.s.l., on the leaves of *Rubus amphidasys* (Rosaceae). 1 November 2022, Q. Z. Wu and Q. F. Zhang (GMB4076).

Notes. *Gerwasia amphidasydis* was the first species of *Gerwasia* described on *Rubus amphidasys*. Our phylogenetic analyses showed that *G. amphidasydis* formed a separate branch (Fig. 1). Morphologically, *G. amphidasydis* and *G. rubi* exhibit similar spines. Moreover, the difference between *G. amphidasydis* and *G. rubi* is that the former has bigger urediniospores (29–41 × 22–29 µm vs. 22–33 × 16–26 µm) (Ito 1950; Hiratsuka et al. 1992). *Gerwasia amphidasydis* and *G. guanganensis* have similar *uredinia* and *urediniospores*; however, *G. guanganensis* has longer spine distances compared to *G. amphidasydis* (4.0–6.0 µm vs. 1.3–3.1 µm) (Zhao et al. 2021). *Gerwasia amphidasydis* is distinguishable from *G. rubi-setchuenensise* by having larger urediniospores (29–41 × 22–29 µm vs. 18–29 × 15–22 µm) and a thinner wall (1.2–2.5 µm vs. 2.1–3.2 µm) (Sun et al. 2024).

Additionally, the LSU sequences of *Gerwasia amphidasydis* also differ from that of *G. rubi* with 93.74% similarity and from *G. rubi-setchuenensis* with 90.56% similarity. The ITS sequence for *Gerwasia rubi* is not available in the NCBI database, whereas the ITS sequence similarity between *Gerwasia amphidasydis* and *G. rubi-setchuenensis* is 98.56%.

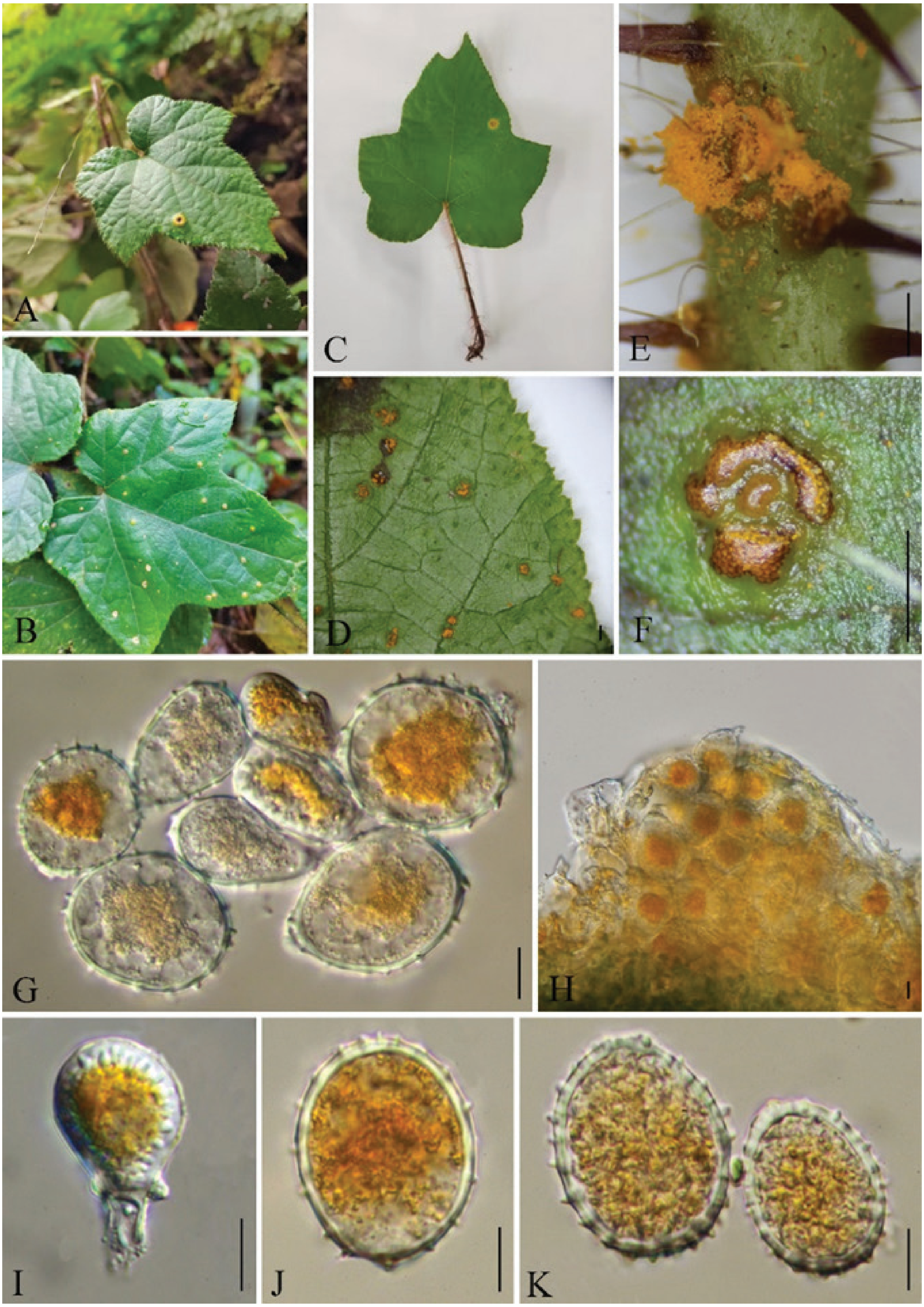

Figure 2. *Gerwasia amphidasydis* (Holotype GMB4047) **A–D** host and its habitat **E–F** uredinia under a stereomicroscope **G–K** urediniospores. Scale bars: 1 mm (**D, F**); 0.5 mm **(E)**; 10 μm (**G–K**).

Genus *Phragmidium* Link, Mag. Gesell. Naturf. Freunde, Berlin 7: 30. 1816

Phragmidium coreanicola Q. F. Zhang, Q. Z. Wu & Q. R. Li, sp. nov.

MycoBank No: 855005
Fig. 3

Type. China • Guizhou Province, Guiyang City, Campus of Guizhou Medical University (26°22'48"N, 106°37'30"E), 1911 m a.s.l., on leaves of *Rubus coreanus* (Rosaceae), 7 October 2021, Q. Z. Wu (holotype GMB0101, isotype KUN-HKAS144249).

Etymology. The epithet refers to the host species, *Rubus coreanus* Miq. var. *coreanus*, from which the holotype was collected.

Description. ***Spermogonia*** and ***Aecia*** not found. ***Uredinia*** 0.1–0.7 mm diam., produced on the abaxial leaf surface, scattered to gregarious, hypophyllous, yellow spots, scattered, irregular patches. Urediniospores 20–29 × 14–25 μm (av. = 24 × 21 μm, n = 30), globose to subglobose or broadly elliptical to ellipsoidal, wall 0.8–2.1 μm thick (av. = 1.4 μm, n = 30), inconspicuous or smooth at the base; inclusions orange-yellow or pale-yellow; germ pores 2–3, sub-equatorial. ***Telia*** 0.1–0.9 mm diam., hypophyllous, dark brown to black, clustered or scattered, bacilliform. Teliospores 107–167 × 25–35 μm (av. = 134 × 30 μm, n = 30), cylindrical, 5–7 cells, often 6, reddish-brown to opaque, rounded at the apex, rounded or somewhat attenuate at the base, not or slightly constricted at the septum, pedicels sub-hyaline, persistent, 47–96 × 12–19 μm (av. = 68 × 16 μm, n = 30), with a swollen base that gradually shows orange-yellow contents towards the lower end. Pedicel broken; paraphyses not seen.

Additional material examined. China • Guizhou Province, Qingzhen City (26°34'58"N, 106°28'28"E), 1972 m a.s.l., on leaves of *Rubus coreanus* (Rosaceae), 7 October 2021, Q.Z. Wu (GMB4071).

Notes. *Phragmidium coreanicola* formed a separate branch in our phylogenetic analyses (Fig. 1). Morphologically, *P. coreanicola* differs from *P. griseum* in having slightly wider urediniospores (14–25 μm vs. 13–21 μm) and larger teliospores (107–167 × 25–35 μm vs. 50–125 × 18–28 μm) (Liu et al. 2018). Additionally, *P. coreanicola* is reported on *Rubus coreanus*, whereas *P. griseum* was found on *Rubus crataegifolius*. *Phragmidium coreanicola* differs from *P. cibanum*, which is reported on *Rubus niveus*, by having bigger urediniospores (20–29 × 14–25 μm vs. 17–20 × 18–19 μm) and larger teliospores (107–167 × 25–35 μm vs. 80–100 × 20–30 μm) (Wei 1988; Hiratsuka et al.1992; Liu et al. 2018). *Phragmidium coreanicola* has the same host species as *P. rubi-coreani* in Guiyang City. However, *P. coreanicola* has larger teliospores (107–167 × 25–35 μm vs. 29–74 ×14–37 μm) (Sun et al. 2022). The morphological comparison between *P. coreanicola* and *P. pauciloculare* shows that the *uredinia* of *P. coreanicola* are larger than those of *P. pauciloculare* (0.1–0.7 mm diam vs. 0.2–0.3 mm diam), and teliospores of *P. coreanicola* are also larger than those of *P. pauciloculare* (107–167 × 25–35 μm vs. 35–111 × 18–27 μm) (Wei 1988).

Furthermore, the ITS sequences of *P. coreanicola* and *P. griseum* exhibit significant differences, with a similarity of 87.33%. However, the LSU sequences of *P. coreanicola* and *P. griseum* have little variation, sharing a similarity of 99.38%.

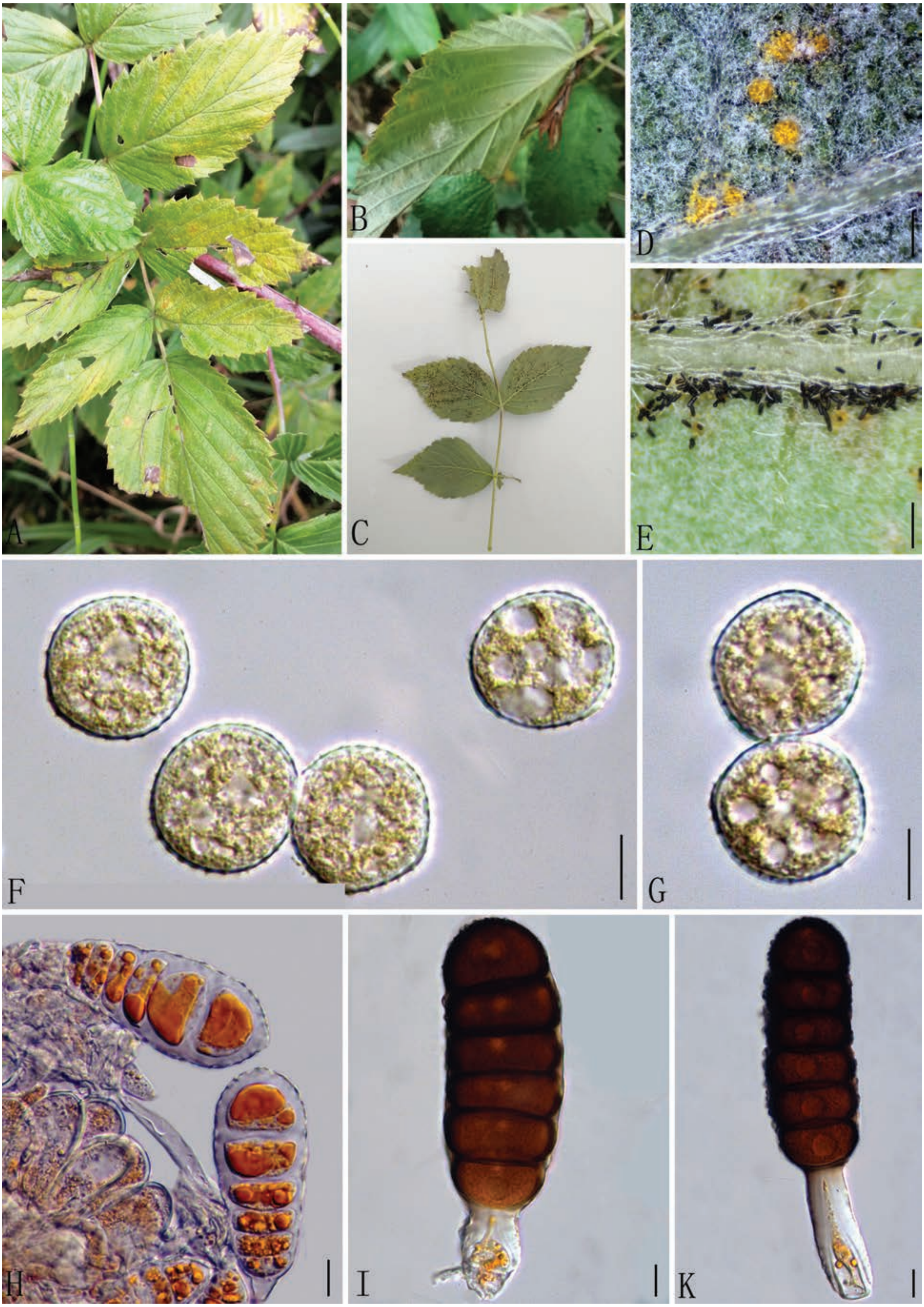

Figure 3. *Phragmidium coreanicola* (Holotype, GMB0101) **A–C** host and its habitat **D–E** uredinia and telia **F, G** urediniospores **H–K** teliospores. Scale bars: 0.5 mm **(D, E)**; 10 μm (**F–K**).

Phragmidium parvifolius **Q. F. Zhang, Q. Z. Wu & Q. R. Li, sp. nov.**

MycoBank No: 855006
Fig. 4

Type. China • Guizhou Province, Guiyang City, Huaxi District (26°43'27.3"N, 106°67'14.4"E), 1,114 m a.s.l., on leaves of *Rubus parvifolius* (Rosaceae), 3 November 2022, Q. Z. Wu and Q. F. Zhang (holotype GMB4054, isotype KUN-HKAS144250).

Etymology. The epithet refers to the host species, *Rubus parvifolius* L., from which the holotype was collected.

Description. ***Spermogonia***, ***Aecia*** and ***Telia*** not found. ***Uredinia*** 0.3–0.8 mm diam., produced on the abaxial leaf surface, scattered to gregarious, hypophyllous, rounded to irregular, powdery, orange, pulverulent, at first covered by the epidermis, later, not surrounded by host epidermis; Urediniospores 18–32 × 12–24 μm (av. = 22 × 18 μm, n = 30), globose, oblong, orange, wall 1.1–1.7 μm thick (av. = 1.3 μm, n = 30) at sides, regularly echinulate with stout spines; germ pores 2–3, supra-equatorial. Paraphyses 49–83 × 10–19 μm (av. = 65 × 15 μm, n = 30), hyaline, curved.

Additional material examined. China • Guizhou Province, Guiyang City, Huaxi District (26°43'59.7"N, 106°67'66.5"E), 1114 m a.s.l., on leaves of *Rubus parvifolius* (Rosaceae), 3 November 2022, Q. Z. Wu and Q. F. Zhang (GMB4070).

Notes. Phylogenetically, *P. parvifolius* formed a sister branch to *P. barnardii* Plowr. & G. Winter (HGU21035), which was also reported on *Rubus parvifolius* (Fig. 1). Morphologically, *P. parvifolius* can be easily differentiated from *P. barnardii* by its larger urediniospores (18–32 × 12–24 μm vs. 16–19 × 15–18 μm) and larger paraphyses (49–83 × 10–19 μm vs. 26–39 × 10–13 μm) (Winter 1886; McTaggart et al. 2016; Sun et al. 2022). In terms of urediniospore size, *P. parvifolius* is similar to *P. griseum* (Dietel) Syd. However, *P. parvifolius* differs from *P. griseum* by having relatively larger paraphyses (49–83 × 10–19 μm vs. 34–70 × 7–16 μm) and by its host, *Rubus parvifolius* vs. *Rubus crataegifolius* (Wei 1988; Hiratsuka et al. 1992; Liu et al. 2018; Sun et al. 2024). Additionally, *P. parvifolius* differs from *P. pauciloculare* by its larger urediniospores (18–32 μm vs. 13–20 μm) (Wei 1988; Hiratsuka et al. 1992). *Phragmidium parvifolius* and *P. kanas* have the same urediniospores and paraphyses, but *P. parvifolius* has no teliospores, whereas *P. kanas* has them (Zhao et al. 2021).

Furthermore, the morphological comparison between *P. parvifolius* and *P. coreanicola* (this study) shows that the urediniospores of *P. parvifolius* are larger than those of *P. coreanicola* (18–32 μm vs. 20–29 μm), and *P. parvifolius* has no teliospores, whereas *P. coreanicola* has them. The ITS and LSU sequence similarities of *P. parvifolius* with *P. coreanicola* are 97.57% and 99.22%.

Gerwasia rubi-setchuenensis **J.E. Sun, Yong Wang bis & K.D. Hyde, (2024)**

Fig. 5

Host. *Rubus buergeri* Miq.

Description. ***Spermogonia***, ***aecia***, and ***telia*** unknown. ***Uredinia*** 0.4–1.0 mm diam., hypophyllous, pulverulent, golden, scattered, irregular, surrounded by host epidermis. *Urediniospores* 24–30 × 19–25 μm (av. = 27.2 × 22.3 μm, n = 30), subglobose or fusiform, inclusions golden or bright yellow; wall 1.4–2.9 μm thick (av. = 2.0 μm, n = 30), colorless, irregularly elongated verrucae.

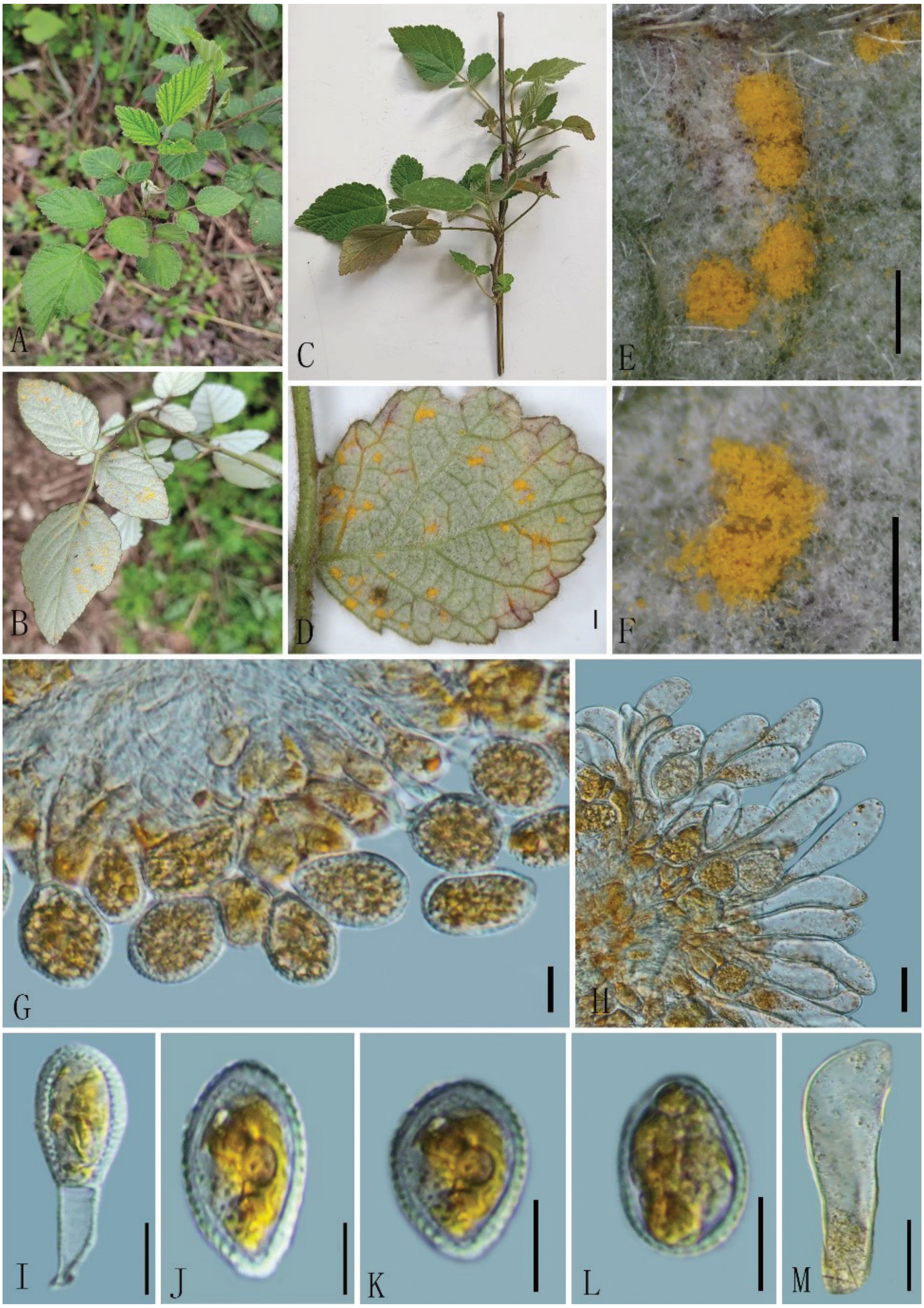

Figure 4. *Phragmidium parvifolius* (Holotype, GMB4054) **A–D** host and its habitat **E, F** uredinia under a stereomicroscope **G, H** urediniospores and paraphyses **I–L** urediniospores **M** paraphyses. Scale bars: 1 mm (**D**); 0.5 mm (**E, F**); 10 μm (**G–M**).

Materials examined. China • Guizhou Province, Zunyi City, Xishui County (28°49'38"N, 106°41'23"E), 1223 m a.s.l., on the leaves of *Rubus buergeri* Miq. (Rosaceae), 3 November, 2022, Q. Z. Wu and Q. F. Zhang (GMB4052); China • Guizhou Province, Zunyi City, Xishui County (28°33'43"N, 106°24'3"E), 1997 m a.s.l., on *Rubus buergeri* (Rosaceae), 3 November 2022, Q. Z. Wu and Q. F. Zhang (GMB4075).

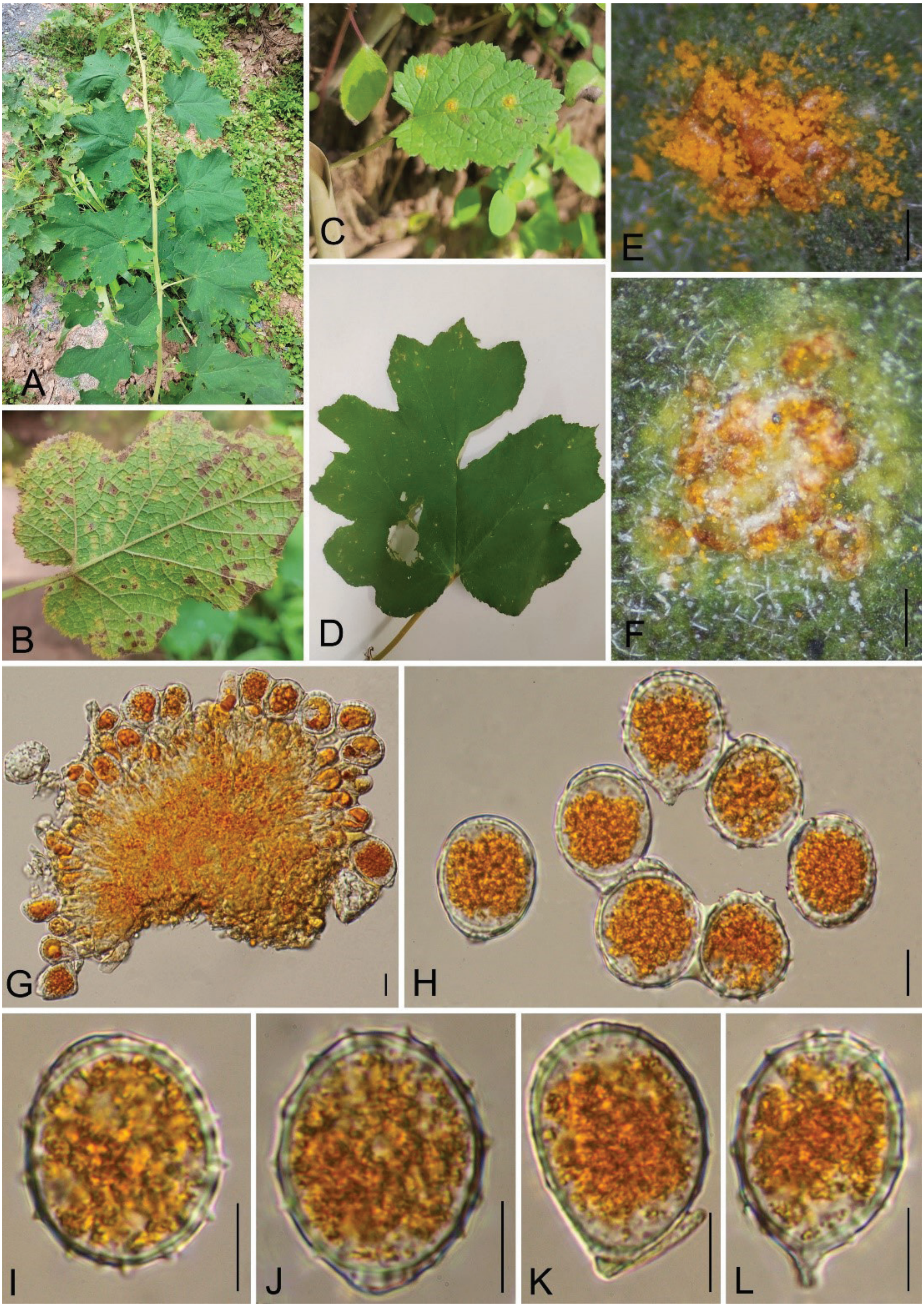

Figure 5. *Gerwasia rubi-setchuenensis* (GMB4052) **A–D** host and its habitat **E–F** uredinia under the stereomicroscope **G–K** urediniospores. Scale bars: 0.5 mm (**E–F**); 10 μm (**G–L**).

Notes. In the phylogram (Fig. 1), our collections (GMB4052 and GMB4075) clustered with *G. rubi-setchuenensis* (HGUP21168). The morphological characteristics of our specimen are consistent with the original description of *G. rubi-setchuenensis*, and the DNA sequence aligns with that of *G. rubi-setchuenensis* HGUP21168 (ITS 100%; LSU 99.67%) (Sun et al. 2024). The only difference observed between the descriptions and figure of *G. rubi-setchuenensis* in Sun et al. (2024) is the size of the urediniospores. The urediniospores of *G. rubi-setchuenensis* (GMB4075) are slightly wider than those of *G. rubi-setchuenensis* (HGUP21168) (19–25 μm vs. 15–22 μm). This study identifies *Rubus buergeri* as a new host for this fungus.

Discussion

The exploration of rust fungi in China began in the mid-19th century, and to date, over 1200 rust taxa have been documented (Zhuang et al. 1998, 2005, 2021; Zhao et al. 2022a, b; Sun et al. 2024). Molecular techniques have significantly advanced fungal species identification, but accurately identifying rust fungi remains challenging, necessitating a comprehensive approach incorporating morphology, host specificity, and phylogenetic analyses (Sun et al. 2024). In China, over 70 species of *Phragmidium* have been described, although numerous species remain without molecular data. According to our literature review, approximately 22 species of *Phragmidium* have been reported in Guizhou (Cummins 1931; Zhuang et al. 2012; Aime et al. 2018; Aime and McTaggart 2021; Zhao et al. 2021; Sun et al. 2022, 2024). These studies emphasize the critical role of integrating morphological data, host specificity, and phylogenetic insights for a comprehensive understanding and accurate identification of rust fungi.

In our investigation, three new species of Phragmidiaceae belonging to the genera *Gerwasia* and *Phragmidium* are introduced based on phylogenetic analysis of the ITS and LSU regions and morphological features. *amphidasydis* sp. nov., *Phragmidium coreanicola* sp. nov., and *P. parvifolius* sp. nov. infected *Rubus amphidasys*, *Rubus coreanus*, and *Rubus parvifolius*, respectively. The host of the *P. coreanicola* is the same as that of *P. rubi-coreani*; however, *P. coreanicola* has larger teliospores (107–167 × 25–35 μm vs. 29–74 ×14–37 μm), and *P. rubi-coreani* possesses aeciospores (Sun et al. 2022). In addition, *Rubus buergeri* was identified as a new host plant for *Gerwasia rubi-setchuenensis*. Previously, it was known only on *Rubus setchuenensis* (Sun et al. 2024). At the same time, we discovered some samples of *Phragmidium rosae-multiflorae* Dietel, and *Phragmidium potentillae* (Pers.) P. Karst. Here, we provide their sequences.

The hosts of *Phragmidium* discussed in this study are mainly from the genus *Rubus* within the Rosaceae family, yet *P. coreanicola* represents a new species on a previously reported host, while *Gerwasia rubi-setchuenensis* originates from a different host. This demonstrates the host specificity and species diversity of rust fungi (Wei 1988; Zhuang et al. 2012; Yang et al. 2015; Liu et al. 2018). Investigations into the interaction between plant hosts and pathogens suggest that the variety of pathogenic fungi may stem from host-switching or cooperative coevolutionary processes. These findings prompt inquiries concerning the linkage between plant hosts and *Phragmidium*, as well as the evolutionary dynamics at play (Zhao et al. 2016; McTaggart et al. 2015, 2016). Addressing these inquiries necessitates further research into *Phragmidium* in the future.

Additional information

Conflict of interest

The authors have declared that no competing interests exist.

Ethical statement

No ethical statement was reported.

Funding

This research was supported by the Guizhou Province Ordinary Colleges and Universities Youth Science and Technology Talent Growth Project (2021)154; the Guizhou Medical University High Level Talent Launch Fund Project (2023-058); and the National Natural Science Foundation of China (31960005, 32000009).

Author contributions

Conceptualization: Qinfang Zhang, Qirui Li, and Lili Liu. Collection and morphological examinations: Qinfang Zhang, Qianzhen Wu, Yulin Ren. Molecular sequencing and phylogenetic analyses: Qinfang Zhang, Kamran Habib, Lili Liu. Specimen identification: Peng Zhao, Qirui Li. Plant identification: Qingde Long. Original draft preparation: Qinfang Zhang, Qirui Li. Review and editing, supervision: Muhammad Aijaz Ahmad, Peng Zhao, Yao Wang, Dexiang Tang, Xiangchun Shen, Qirui Li. All authors have read and agreed to the published version of the manuscript.

Author ORCIDs

Qinfang Zhang https://orcid.org/0009-0003-9408-4988
Kamran Habib https://orcid.org/0000-0003-2572-0306
Yao Wang https://orcid.org/0000-0002-1262-6700
Muhammad AIjaz Ahmad https://orcid.org/0000-0003-2798-5500
Yulin Ren https://orcid.org/0009-0003-9063-425X
Xiangchun Shen https://orcid.org/0000-0002-4333-9106
Qirui Li https://orcid.org/0000-0001-8735-2890

Data availability

All the specimens are deposited in the Herbaria of Guizhou Medical University (GMB) and Kunming Institute of Botany, Chinese Academy of Sciences (KUN-HKAS). Sequences have been deposited in the GenBank. The alignment file can be obtained from the corresponding author.

References

Aime MC (2006) Toward resolving family–level relationships in rust fungi (Uredinales). Mycoscience 47(3): 112–122. https://doi.org/10.1007/S10267-006-0281-0

Aime MC, Bell CD, Wilson AW (2018) Deconstructing the evolutionary complexity between rust fungi (Pucciniales) and their plant hosts. Studies in Mycology 89: 143–152. https://doi.org/10.1016/j.simyco.2018.02.002

Aime MC, McTaggart AR (2021) A higher-rank classification for rust fungi, with notes on genera. Fungal Systematics and Evolution 7(1): 21–47. https://doi.org/10.3114/fuse.2021.07.02

Aime MC, McTaggart AR, Mondo SJ, Duplessis S (2017) Phylogenetics and phylogenomics of rust fungi. Advances in Genetics 100: 267–307. https://doi.org/10.1016/bs.adgen.2017.09.011

Ali B, Sohail Y, Mumtaz AS, Berndt R (2017) *Phragmidium punjabense*, a new species of rust fungus on *Rosa brunonii* in the outer Himalayan ranges of Murree, Pakistan. Nova Hedwigia 105(3–4): 385–396. https://doi.org/10.1127/nova_hedwigia/2017/0418

Arthur JC (1934) Manual of the rust in United States and Canada, Hafner Publishing Company, New York, USA.

Bradshaw MJ, Carey J, Liu M, Bartholomew HP, Jurick WM II, Hambleton S, Hendricks D, Schnittler M, Scholler M (2023) Genetic time traveling: Sequencing old herbarium specimens, including the oldest herbarium specimen sequenced from kingdom Fungi, reveals the population structure of an agriculturally significant rust. The New Phytologist 237(4): 1463–1473. https://doi.org/10.1111/nph.18622

Cummins GB (1931) *Phragmidium* species of North America: Differential teliospore and aecial characters. Mycologia 23(6): 433–445. https://doi.org/10.1080/00275514.1931.12017054

Cummins GB, Hiratsuka Y (2003) Illustrated genera of rust fungi. 3rd Edn. American Phytopathological Society Press: 222–223.

Dai FL (1979) China fungus confluence. Science Press, Beijing, China 1527.

Dietel P (1905) Über die arten der Gattung *Phragmidium.* Hedwigia 44: 112–132.

Dixon LJ, Castlebury LA, Aime MC, Glynn NC, Comstock JC (2018) Phylogenetic relationships of sugarcane rust fungi. Mycological Progress 9(4): 459–468. https://doi.org/10.1007/s11557-009-0649-6

Hall TA (1999) BioEdit: A user-friendly biological sequence alignment editor and analysis program for Windows 95/98/NT. Nucleic Acids Symposium Series 41: 95–98.

Hiratsuka N, Sato S, Katsuya K, Kakishima M, Hiratsuka Y, Kaneko S, Ono Y, Sato T, Harada Y, Hiratsuka T, Nakayama K (1992) The rust flora of Japan. Tsukuba Shuppankai 41: 127–151.

Hopple Jr JS, Vilgalys R (1999) Phylogenetic relationships in the mushroom genus Coprinus and dark-spored allies based on sequence data from the nuclear gene coding for the large ribosomal subunit RNA: Divergent domains, outgroups, and monophyly. Molecular Phylogenetics and Evolution 13(1): 1–19. https://doi.org/10.1006/mpev.1999.0634

Huelsenbeck JP, Ronquist F (2001) MRBAYES: Bayesian inference of phylogenetic trees. Bioinformatics (Oxford, England) 17(8): 754–755. https://doi.org/10.1093/bioinformatics/17.8.754

Ito S (1950) Basidiomycetes, no. 3. Uredinales-Pucciniaceae, Uredinales Imperfecti. Mycological flora of Japan 2.

Ji JX, Li Z, Li Y, Kakishima M (2019) Two new species of *Pucciniastrum* producing dimorphic sori and spores from northeast of China. Mycological Progress 18(4): 529–540. https://doi.org/10.1007/s11557-018-1460-z

Ji JX, Li Z, Li Y, Kakishima M (2020) Life cycle and taxonomy of *Chrysomyxa succinea* in China and phylogenetic positions of *Caeoma* species on *Rhododendron*. Forest Pathology 50(2): e12585. https://doi.org/10.1111/efp.12585

Katoh K, Standley DM (2013) MAFFT multiple sequence alignment software version 7: Improvements in performance and usability. Molecular Biology and Evolution 30(4): 772–780. https://doi.org/10.1093/molbev/mst010

Kim BR, Sim JY, Lee SH, Ryu JY, Lee JS, Choi YJ, Kim HJ, Jin HY, Kim YJ (2022) First report of *Phragmidium rubi-oldhami* causing rust disease on *Rubus pungens* in Korea. New Disease Reports 46(1): e12113. https://doi.org/10.1002/ndr2.12112

Link HF (1816) Observations in ordines plantarum naturales. Magazinder Gesellschaft Naturforschenden Freunde Berlin 7: 25–45.

Liu Y, Cao B, Tao S, Tian C, Liang Y (2018) *Phragmidium* species parasitizing species of Rosaceae in Tibet, China, with descriptions of three new species. Mycological Progress 17(8): 967–988. https://doi.org/10.1007/s11557-018-1406-5

Liu Y, Liang YM, Ono Y (2020) Taxonomic revision of species of *Kuehneola* and *Phragmidium* on *Rosa*, including two new species from China. Mycologia 112(4): 742–752. https://doi.org/10.1080/00275514.2020.1753426

McTaggart AR, Doungsa-Ard C, Geering ADW, Aime MC, Shivas RG (2015) A co-evolutionary relationship exists between *Endoraecium* (Pucciniales) and its *Acacia* hosts in Australia. Persoonia 35(1): 50–62. https://doi.org/10.3767/003158515X687588

McTaggart AR, Shivas RG, Nest MA, Roux J, Wingfield BD, Wingfield MJ (2016) Host jumps shaped the diversity of extant rust fungi (Pucciniales). The New Phytologist 209(3): 1149–1158. https://doi.org/10.1111/nph.13686

Miller MA, Pfeiffer W, Schwartz T (2010) Creating the CIPRES Science Gateway for inference of large phylogenetic trees. 2010 Gateway Computing Environments Workshop (GCE), New Orleans, Louisiana, 14 Nov 2010. IEEE, New York, 1–8. https://doi.org/10.1109/GCE.2010.5676129

Pfunder M, Schürch S, Roy BA (2001) Sequence variation and geographic distribution of pseudoflower-forming rust fungi (*Uromyces pisi* s. lat.) on *Euphorbia cyparissias*. Mycological Research 105(1): 57–66. https://doi.org/10.1017/S0953756200003208

Piškur B, Jurc D (2017) New findings of rusts (Pucciniales) on trees and other plants in Slovenia. Proceedings of the Zbornik Predavanj in Referatov 13.

Rambaut A (2012) FigTree: Tree figure drawing tool 2006–2012, version 1.4.0. Edinburgh: Institute of Evolutionary Biology, University of Edinburgh.

Rathnayaka AR, Tennakoon DS, Jones GE, Wanasinghe DN, Bhat DJ, Priyashantha AH, Stephenson SL, Tibpromma S, Karunarathna SC (2024) Significance of precise documentation of hosts and geospatial data of fungal collections, with an emphasis on plant-associated fungi. New Zealand Journal of Botany 63: 462–489. https://doi.org/10.1080/0028825X.2024.2381734

Ronquist F, Nieves-Aldrey JL, Buffington ML, Liu Z, Liljeblad J, Nylander JA (2015) Phylogeny, evolution and classification of gall wasps: The plot thickens. PLoS One 10(5): e0123301. https://doi.org/10.1371/journal.pone.0123301

Shen YM, Chung WH, Huang TC, Rodeva R, Hung TH (2017) Unveiling *Gymnosporangium corniforme*, *G. unicorne*, and *G. niitakayamense* sp. nov. in Taiwan. Mycoscience 59(3): 218–228. https://doi.org/10.1016/j.myc.2017.11.003

Stamatakis A (2015) Using RAxML to infer phylogenies. Current Protocols in Bioinformatics 51(1): 6–14. https://doi.org/10.1002/0471250953.bi0614s51

Sun JE, Fu L, Norphanphoun C, Chen XJ, Yu LF, Hyde KD, McKenzie EHC, Wang Y, Yang ZF, Liu FQ (2024) Study on the diversity of rust pathogens from different hosts in Guizhou Province, China. Mycosphere: Journal of Fungal Biology 15(1): 473–653. https://doi.org/10.5943/mycosphere/15/1/4

Sun JE, Zhang Q, Luo WM, Yang YQ, An HM, Wang Y (2022) Four new *Phragmidium* (Phragmidiaceae, Pucciniomycetes) species from Rosaceae plants in Guizhou Province of China. MycoKeys 93: 193–213. https://doi.org/10.3897/mycokeys.93.90861

Vilgalys R, Hester M (1990) Rapid genetic identification and mapping of enzymatically amplified ribosomal DNA from several Cryptococcus species. Journal of Bacteriology 172(8): 4238–4246. https://doi.org/10.1128/jb.172.8.4238-4246.1990

Wahyuno D, Kakishima M, Ono Y (2001) Morphological analyses of urediniospores and teliospores in seven *Phragmidium* species parasitic on ornamental roses. Mycoscience 42(6): 519–533. https://doi.org/10.1007/BF02460950

Wang L, Jia Y, Zhang X, Qin H (2015) Overview of higher plant diversity in China. Shengwu Duoyangxing 23(2): 217–224. https://doi.org/10.17520/biods.2015049

Wei GR, Wang XJ (2011) Purification and storage of *Puccinia striiformis* f. sp. Tritici. Henan Nongye Kexue 40: 90–92.

Wei SX (1988) A taxonomic study of the genus *Phragmidium* of China. Junwu Xuebao 1: 179–210.

Winter G (1886) Fungi australienses. Revue Mycologique Toulouse 8: 207–213.

Wu QZ, He MH, Liu TZ, Hu HM, Liu LL, Zhao P, Li QR (2023) Rust fungi on medicinal plants in Guizhou province with descriptions of three new species. Journal of Fungi (Basel, Switzerland) 9(9): 953. https://doi.org/10.3390/jof9090953

Ya TY (2024) Species of the genus *Phragmidium* (Pucciniales) as parasites of roses (*Rosa*, Rosaceae) in Ukraine. Ukrains'kyi Botanichnyi Zhurnal. Ukrains'ke Botanichne Tovarystvo 81(3): 214–228. https://doi.org/10.15407/ukrbotj81.03.214

Yang T, Chang W, Cao B, Tian C, Zhao L, Liang Y (2015) Two new *Phragmidium* species identified on *Rosa* plants native to China. Phytotaxa 217(2): 182–190. https://doi.org/10.11646/phytotaxa.217.2.8

Yun HY, Minnis AM, Kim YH, Castlebury LA, Aime MC (2011) The rust genus *Frommeëlla* revisited: A later synonym of *Phragmidium* after all. Mycologia 103(6): 1451–1463. https://doi.org/10.3852/11-120

Zhao P, Qi XH, Crous PW, Duan W, Cai L (2020) *Gymnosporangium* species on Malus: species delineation, diversity and host alternation. Persoonia-Molecular Phylogeny and Evolution of Fungi 45(1): 68–100. https://doi.org/10.3767/persoonia.2020.45.03

Zhao P, Li Y, Liu F, Liang J, Zhou X, Cai L (2022a) Applying early divergent characters in higher rank taxonomy of Melampsorineae (Basidiomycota, Pucciniales). Mycology 14(1): 11–36. https://doi.org/10.1080/21501203.2022.2089262

Zhao P, Liu F, Huang JE, Zhou X, Duan WJ, Cai L (2022b) *Cronartium* rust (Pucciniales, Cronartiaceae): Species delineation, diversity and host alternation. Mycosphere: Journal of Fungal Biology 13(1): 672–723. https://doi.org/10.5943/mycosphere/13/1/7

Zhao P, Liu F, Li YM, Cai L (2016) Inferring phylogeny and speciation of *Gymnosporangium* species, and their coevolution with host plants. Scientific Reports 6(1): 29339. https://doi.org/10.1038/srep29339

Zhao P, Zhang ZF, Hu DM, Tsui KM, Qi XH, Phurbu D, Gafforov Y, Cai L (2021) Contribution to rust flora in China I, tremendous diversity from natural reserves and parks. Fungal Diversity 110(1): 1–58. https://doi.org/10.1007/s13225-021-00482-w

Zhuang JY, Wei SX, Wang YC (1998) Flora Fungorum Sinicorum. Vol 10. Uredinales (I). Science Press, Beijing, China.

Zhuang JY, Wei SX, Wang YC (2003) Flora Fungorum Sinicorum. Vol 19. Uredinales (II). Science Press, Beijing, China.

Zhuang JY, Wei SX, Wang YC (2005) Flora Fungorum Sinicorum. Vol 25. Uredinales (III). Science Press, Beijing, China.

Zhuang JY, Wei SX, Wang YC (2012) Flora Fungorum Sinicorum. Vol 41. Uredinales (IV). Science Press, Beijing.

Zhuang JY, Wei SX, Wang YC (2021) Flora Fungorum Sinicorum. Vol 62. Uredinales (V). Science Press, Beijing, China.

MycoKeys 115: 327–362 (2025)
DOI: 10.3897/mycokeys.115.144137

Research Article

Additions to the genus *Mycena* (Mycenaceae, Agaricales): Descriptions of five new taxa in Hunan Province, China

Ying Xin Xiao[1*], Li Na Liu[2*], Zhu Ming Tan[2], Ai Rong Shen[2], Bao Ming Shen[2], Yun Tan[2], Sai Nan Li[2], Li Guo Feng[3], Jing Bo Long[4], Zhu Xiang Liu[1]

1 *College of Biology and Environmental Sciences, Jishou University, Jishou 416000, China*
2 *Institute of Biodiversity Studies, Hunan Academy of Forestry, Changsha 410004, China*
3 *Hunan Edible Fungi Research Institute, Changsha 410004, China*
4 *Huangsang National Nature Reserve Management Office, Shaoyang 422000, China*
Corresponding author: Zhu Xiang Liu (liuzhuxiang@126.com)

This article is part of:
Exploring the Hidden Fungal Diversity: Biodiversity, Taxonomy, and Phylogeny of Saprobic Fungi
Edited by Samantha C. Karunarathna, Danushka Sandaruwan Tennakoon, Ajay Kumar Gautam

Academic editor:
Samantha C. Karunarathna
Received: 11 December 2024
Accepted: 5 March 2025
Published: 28 March 2025

Citation: Xiao YX, Liu LN, Tan ZM, Shen AR, Shen BM, Tan Y, Li SN, Feng LG, Long JB, Liu ZX (2025) Additions to the genus *Mycena* (Mycenaceae, Agaricales): Descriptions of five new taxa in Hunan Province, China. MycoKeys 115: 327–362. https://doi.org/10.3897/mycokeys.115.144137

Abstract

Few studies have been conducted on *Mycena* species in Hunan Province, China. During our research on the species diversity of *Mycena* in Hunan Province, we identified approximately 30 *Mycena* species based on morphological and molecular evidence. Five species are recognized herein as new to science, namely, *M. fulvomarginata*, *M. huangsangensis*, *M. hongfengensis*, *M. subroriduliformis*, and *M. roseolamellata*. The phylogenetic analyses of a combined ITS and LSU sequence dataset revealed that five new species each formed an independent lineage that could separate phenotypically similar and phylogenetically related species. Descriptions, photographs, and phylogenetic analysis results are provided for the five new species, along with the comparisons with related species. A key to all *Mycena* species found in Hunan is also provided.

Key words: Basidiomycota, biodiversity, five new species, phylogenetic analysis, taxonomy

Introduction

Hunan Province is located in the southern middle reaches of the Yangtze River, China, and covers an area of approximately 211,800 km^2 (Gao and Dou 1981). The province is surrounded by mountains and hills in the east, west, and south, basins in the center, and plains in the north. This area has a subtropical humid monsoon climate with four distinct seasons, sufficient sunshine, and abundant rainfall, which benefits vegetation (Qing 1990). The people's government of Hunan Province reported that there are 17 national nature reserves, including 16 focused on preserving forest ecological systems (https://www.hunan.gov.cn/). The unique topography and good forest ecological systems make Hunan home to macrofungi (Liu et al. 2024), among which the members of *Mycena* (Pers.) Roussel are prominent in Agaricales (Liu et al. 2022a, 2022b).

Mycena is one of the largest genera in the Mycenaceae family of Agaricales, including at least 600 species worldwide (Kirk et al. 2008; Fan et al. 2024; Zhang

---

[*] These authors contributed equally to this work.

et al. 2024). *Mycena* plays an important role in ecosystems, which depend on the strong decomposition abilities of fungi to promote material circulation, forest metabolism, and natural renewal (Fukasawa et al. 2009; Guerreiro et al. 2023). Some *Mycena* are symbiotic fungi with *Gastrodia elata* seeds (Lee et al. 2017; Liu et al. 2022b, 2025). Moreover, approximately 60 *Mycena* species are reported to be bioluminescent worldwide (Chew et al. 2014, 2015; Cortés-Pérez et al. 2019, 2023; Lu et al. 2024).

Mycena was first moved to the genus level by Roussel in 1806, but this change was not widely accepted by the majority of mycologists until the 20th century (Roussel 1806). It is a widely studied genus despite many species in the genus having small basidiomata (Aronsen and Læssøe 2016). Many important contributions about taxonomic studies of *Mycena* have been made to temperate regions, and several monographs have been published (Smith 1947; Robich 2003, 2016; Aronsen and Læssøe 2016). For subtropical and tropical areas, the study of local floras has contributed to the early reporting of *Mycena* species (Métrod 1949; Singer and Digilio 1951; Pegler 1977, 1983, 1986, 1987), and those studies made substantial contributions to more important papers and related monographs on *Mycena* (Singer 1989; Corner 1994; Grgurinovic 1998, 2003; Perry 2002; Cooper et al. 2018; Bau et al. 2021).

Some classifications have been proposed based on the morphological characteristics of *Mycena* (Fries 1821; Lange 1914; Kühner 1926, 1931, 1938; Singer and Digilio 1951; Singer 1986; Maas Geesteranus 1992a, 1992b; Maas Geesteranus and Horak 1995; Bau et al. 2021). Currently, mycologists tend to accept, use, and update the infrageneric classification, which was proposed by Maas Geesteranus (Grgurinovic 1998, 2003; Robich 2003, 2016; Cooper et al. 2018). Species are classified into 44 sections based on a combination of macroscopic and microscopic features. With the development of molecular biology research, the phylogenetic positions of *Mycena* have become increasingly apparent (Moncalvo et al. 2002; Matheny et al. 2006; Wei et al. 2024). As a part of the subtropical area of China, studies on *Mycena* have been conducted in Hunan Province. The book Hunan Macrofungi was specially written in 1997 to document the fungi in the region and described two *Mycena* species (Li et al. 1993). Five *Mycena* species from Hupingshan, Hunan, are described in the Atlas of Macrofungi (Zhang et al. 2005). Seven *Mycena* species were recorded in the Atlas of Macrofungi in Hunan (Chen and Zhang 2019). A species in China, *M. heteracantha* (Singer) Desjardin, which was collected from Hunan Province, was described by Na Q and Bau T in 2019 (Na and Bau 2019a). *Mycena subpiligera* L.N. Liu, a new species collected in Hunan Province that can significantly enhance the germination efficiency of *Gastrodia elata* seeds, was reported in 2022 (Liu et al. 2022b). *Mycena chlorocyanea* L.N. Liu, another new species whose type was collected in Hunan Province, was reported in recent years (Liu et al. 2022a). As a region that is rich in natural resources, further studies on *Mycena* in Hunan Province are needed.

Aiming to explore the diversity of *Mycena* in the region, we conducted literature reviews and field investigations in Hunan Province from 2020 to 2024. Through macroscopic comparison and phylogenetic analysis, we found 30 *Mycena* species collected from Hunan Province, including five new species that are described in this paper.

Materials and methods

Sample collection and morphological description

Approximately 400 *Mycena* specimens belonging to 30 taxa were collected from Hunan Province (Table 1). During fieldwork, the collected samples were photographed, and additional information, such as elevation, habitat, and collection date, was recorded (Rathnayaka et al. 2024). Detailed morphological features, including basidiomata size, color and shape, odor, taste, and viscosity, were also documented from fresh specimens. The specimens were dried with silica gel and deposited in the Herbarium of Hunan Institute of Forestry (HUIF) and the Herbarium of Jishou University (JSU). The macromorphological characteristics of the samples were determined based on field notes and photographs. The color codes followed Kornerup & Wanscher (Kornerup and Wanscher 1978). Micromorphological characters of dry specimens were observed under light microscopy (Olympus BX51). To measure the sizes of related tissues, basidiospores, basidia, pileipellis, stipitipellis, and other tissues were mounted in pure water, 5% KOH solution, or 1% Congo Red solution. Melzer's reagent was used to test the amyloid reaction of the spores. At least 30 basidiospores were measured in each sample. The Q value refers to the length/width ratio of the basidiospores. Q ± av represents the average Q of all basidiospores ± the sample standard deviation. The ranges of the basidiospores are presented as (a–) b–c (–d): the range 'b–c' represents 90% of the measured values, while 'a' and 'd' represent extreme values. The measurements of other microscopic structures were based on 20 measurements per specimen.

DNA extraction, PCR amplification, and sequencing

Genomic DNA was extracted from fresh or dried specimens using the NuClean Plant Genomic DNA kit (Kangwei Century Biotechnology Co., Beijing, China) following the manufacturer's protocols. The ITS rDNA region (ITS1–5.8S–ITS2) was amplified using the primer pair ITS1 and ITS4 (White et al. 1990). The LSU region was amplified with the primers LR0R and LR7 (Vilgalys and Hester 1990). PCR was performed in a total volume of 25 μL containing 1 μL template DNA, 9.5 μL distilled water, 1 μL of each primer, and 12.5 μL 2x Taq PCR Master Mix with blue dye (Sangon Biotech, Shanghai, China). The PCR conditions were as follows: initial denaturation at 95 °C for 5 min, followed by 35 cycles of 94 °C for 45 s, 45 s at 52 °C, and 1 min at 72 °C for ITS (Liu et al. 2022a). For the LSU conditions: initial denaturation at 95 °C for 4 min, followed by 35 cycles of 95 °C for 1 min, 1 min at 53 °C, and 80 s at 72 °C (Zhang et al. 2024). The amplified products were determined by electrophoresis on a 1% agarose gel against a known standard DNA marker and directly sequenced at Sangon Biotech. Newly generated sequences in this study have been submitted to the NCBI GenBank database.

Molecular phylogeny

Details of the sequences used for phylogenetic analysis were obtained from this study and downloaded from GenBank (Table 2). DNA sequences were checked using Bioedit v7.0.9 to ensure sequencing quality (Hall 1999). SeqMan 7.1.0 was used for splicing and manual editing (Swindell and Plasterer 1997).

Table 1. Summary of the collection of *Mycena* species and their distributions and seasons in Hunan.

Species name	Ecology and location (in Hunan)	Occurrence time (in Hunan)	Geographical compositions	References
M. abramsii	Solitary, in small groups or subfasciculate on dead twigs or woody debris of deciduous trees; also occurs occasionally on dead twigs of coniferous trees. Widespread in Hunan.	May to July	Worldwide distribution	(Singer and Digilio 1951; Hintikka 1963; Watling 1984; Maas Geesteranus 1988; Emmett 1992; Marra 2000; Tholl et al. 2000; Veerkamp 2001; Laganà et al. 2002; Perry 2002; Robich 2003; Afyon et al. 2005; Bronckers and Kelderman 2011; Senn-Irlet et al. 2012; Gierczyk et al. 2015; Aronsen and Læssøe 2016; Rudolf et al. 2016; Vishwakarma et al. 2017; Bau et al. 2021)
M. adnexa	In small groups on dead twigs of deciduous trees. Widespread in Hunan.	May to June	Worldwide distribution	(Bau et al. 2021)
M. algeriensis	Subfasciculate on rotten stumps in deciduous forests. Collected only in western areas of Hunan.	April to May	Temperate-subtropical and tropical distribution	(Hintikka 1963; Laganà et al. 2002; Gierczyk et al. 2015; Aronsen and Læssøe 2016; Bau et al. 2021)
M. bicystidiata	Scattered on rotten wood in mixed forests. Collected in western and eastern areas of Hunan.	April to June	Only found in China	(Bau et al. 2021)
M. castaneicola	Scattered or gregarious on *Castanea mollissima* fruits. Collected only in western areas of Hunan.	June to July	Only found in China	(Bau et al. 2021)
M. chlorocyanea	Gregarious in leaf humus under deciduous trees. Collected only in western areas of Hunan.	April to May	Only found in China	(Liu et al. 2022a)
M. citrinomarginata	Gregarious in leaf humus under deciduous trees. Collected in western and eastern areas of Hunan.	May to June	Temperate-subtropical and tropical distribution	(Smith 1935; Hintikka 1963; Watling 1984; Senn-Irlet 1987; Emmett 1992; Laganà et al. 2002; Perry 2002; Kalamees and Raitviir 2006; Senn-Irlet et al. 2012; Gierczyk et al. 2015; Gáperová et al. 2015; Na and Bau 2018; Lee et al. 2021)
M. corynephora	Gregarious on bark of living deciduous trees. Widely distributed in Hunan.	April to May	Worldwide distribution	(Desjardin 1995; Laganà et al. 2002; Aronsen and Læssøe 2016; Bau et al. 2021)
M. deeptha	Gregarious on rotten wood of living deciduous trees. Collected in western and southern areas of Hunan.	April to July	Temperate-subtropical and tropical distribution	(Aravindakshan et al. 2012)
M. digitifurcata	Gregarious on bark of living deciduous trees. Collected only in Changsha.	June	Only found in China	(Wei et al. 2024)
M. filopes	Solitary on dead twigs of deciduous trees. Collected only in western areas of Hunan.	October	Worldwide distribution	(Beardslee and Coker 1924; Watling 1984; Kalamees and Raitviir 2006; Bronckers and Kelderman 2011; Senn-Irlet et al. 2012; Aronsen and Læssøe 2016; Bau et al. 2021; Cho and Chung 2023)
M. fulvomarginata	Gregarious on moss-covered bark of living deciduous trees. Collected only in western areas of Hunan.	June to July	Only found in China	This study
M. galericulata	Solitary to fasciculate on branches, trunks and stumps of deciduous trees. Collected only in western areas of Hunan.	October to November	Worldwide distribution	(Beardslee and Coker 1924; Swartz 1933; Imai 1938; Hintikka 1963; Ballesteros 1984; Watling 1984; Maas Geesteranus 1992c; Nauta and Vellinga 1992; Marra 2000; Tholl et al. 2000; Laganà et al. 2002; Perry 2002; Robich 2003; Senn-Irlet et al. 2012; Gáperová et al. 2015; Aronsen and Læssøe 2016; Gyosheva et al. 2016; Vishwakarma et al. 2017; Cho and Chung 2020, 2023; Bau et al. 2021; Lee et al. 2021; Łuszczyński et al. 2022)
M. haematopus	In small groups or fasciculate on twigs and trunks of deciduous trees. Distributed in eastern, western and southern areas of Hunan.	May, June, October, November	Worldwide distribution	(Beardslee and Coker 1924; Swartz 1933; Imai 1938; Hintikka 1963; Watling 1984; Emmett 1992; Grgurinovic 1998; Laganà et al. 2002; Perry 2002; Robich 2003; Bronckers and Kelderman 2011; Senn-Irlet et al. 2012; Aravindakshan and Manimohan 2013b; Aronsen and Læssøe 2016; Mustafabayli and Aghayeva 2019; Bau et al. 2021; Cho and Chung 2023)

Species name	Ecology and location (in Hunan)	Occurrence time (in Hunan)	Geographical compositions	References
M. heteracantha	Gregarious on decaying leaves and twigs of deciduous trees. Collected only in southwestern areas of Hunan.	May	Temperate-subtropical and tropical distribution	(Desjardin 1995; Bau et al. 2021)
M. hongfengensis	Gregarious on decaying leaves of deciduous trees. Collected only in western areas of Hunan.	April	Only found in China	This study
M. huangsangensis	Gregarious on decaying leaves of deciduous trees. Collected only in southwestern areas of Hunan.	April to May	Only found in China	This study
M. laevigata	In small groups or fasciculate on twigs and trunks of deciduous trees. Collected in western and southern areas of Hunan.	June to September	Temperate-subtropical and tropical distribution	(Chen and Zhang 2019)
M. leaiana	Fasciculate on rotten wood of deciduous trees. Collected in western and southern areas of Hunan.	July	Temperate-subtropical and tropical distribution	(Chen and Zhang 2019)
M. leptocephala	Gregarious on moss-covered hardwood or on branches. Collected in western and southern areas of Hunan.	April to May	Worldwide distribution	(Beardslee and Coker 1924; Smith 1935; Hintikka 1963; Watling 1984; Senn-Irlet 1987; Laganà et al. 2002; Kalamees and Raitviir 2006; Bronckers and Kelderman 2011; Senn-Irlet et al. 2012; Gierczyk et al. 2015; Aronsen and Læssøe 2016; Baldrian et al. 2016; Bau et al. 2021; Łuszczyński et al. 2022)
M. maculata	Solitary to fasciculate on branches, trunks and stumps of deciduous trees. Collected in western areas of Hunan.	October to November	Temperate distribution	(Marra 2000; Tholl et al. 2000; Laganà et al. 2002; Perry 2002; Bau et al. 2021)
M. meliigena/ juniperina	Gregarious on moss-covered bark of living deciduous trees. Widespread.	November to June	Temperate distribution	(Aronsen 1996; Doğan and Karadelev 2006; Halama et al. 2014)
M. pearsoniana	Scattered in leaf humus in deciduous trees. Collected only in western areas of Hunan.	May to June	Worldwide distribution	(Hintikka 1963; Watling 1984; Moreno and Albertó 1996; Robich 2003; Senn-Irlet et al. 2012; Aronsen and Læssøe 2016; Türkekul 2017; Vishwakarma et al. 2017; Kwon et al. 2020; Bau et al. 2021)
M. picta	Scattered on decaying leaves of deciduous trees. Collected only in some parks of Changsha.	April to May	Temperate-subtropical and tropical distribution	(Miyamoto et al. 1996; Halama and Romański 2010; Shiryaeva 2018; Retnowati et al. 2020; Bau et al. 2021)
M. pluteoides	Solitary or gregarious on rotten wood of deciduous trees. Collected in western and southern areas of Hunan.	May, June	Only found in China	(Bau et al. 2021)
M. pura	Scattered in leaf humus and on needles or in grasslands, on both deciduous and coniferous trees. Widely distributed in Hunan.	November, March to June	Worldwide distribution	(Beardslee and Coker 1924; Swartz 1933; Imai 1938; Hintikka 1963; Watling 1984; Senn-Irlet 1987; Emmett 1992; Maas Geesteranus 1992c; Marra 2000; Laganà et al. 2002; Perry 2002; Robich 2003; Kalamees and Raitviir 2006; Senn-Irlet et al. 2012; Casabón 2015; Gáperová et al. 2015; Aronsen and Læssøe 2016; Gyosheva et al. 2016; Mustafabayli and Aghayeva 2019; Bau et al. 2021; Lee et al. 2021)
M. roseolamellata	Gregarious on decayed twigs of bamboo or woody debris of deciduous trees. Ningxiang, Hunan.	November, December and March	Only found in China	This study
M. subpiligera	Longshan and Suining Counties, Hunan.	April to July	Only found in China	(Liu et al. 2022b)
M. subroriduliformis	Gregarious on decaying leaves of deciduous trees. Suining County, Hunan.	April to May	Only found in China	This study
M. yuezhuoi	Scattered on the litter layer in *Pinus*, *Quercus*, and *Robinia* mixed forests. Suining County, Hunan.	April to May	Temperate-subtropical and tropical distribution	(Liu et al. 2021; Cho et al. 2024)

Table 2. Names, voucher numbers, locations, and corresponding GenBank accession numbers of the taxa used in the phylogenetic analysis. - refers to the data unavailability.

Species	Voucher	GenBank accession no.		Location	References
		ITS	LSU		
Atheniella adonis	H6036863	MW540691	-	Finland	Unpublished
A. aurantiidisca	UBCF33062	MF908459	-	Canada	Unpublished
Clitocybula intervenosa	BAP 588	MH414560	-	Africa	(Cooper et al. 2018)
C. intervenosa	BAP 613	MH414561	MH385335	Africa	(Cooper et al. 2018)
Hydropus murinus	BAP 657	MH414565	-	Africa	(Cooper et al. 2018)
Mycena abramsii	HUIFS50116	OP604436	OP605596	China	Unpublished
M. abramsii	HUIFS50074	OP604427	-	China	Unpublished
M. abramsii	HUIF50533	PQ406957	-	China	This study
M. adnexa	HMAJU43360	MK733290	MK722345	China	Unpublished
M. adnexa	HMAJU43691	MK733293	MK722346	China	Unpublished
M. adnexa	HUIF50339	PQ406958	-	China	This study
M. adnexa	HUIF60005	PQ465300	-	China	This study
M. albiceps	F27622	MZ303026	-	USA	Unpublished
M. albiceps	RA705-6	MK234177	-	USA	Unpublished
M. algeriensis	HMAS 291753	OR236986	-	China	Unpublished
M. algeriensis	HUIF50368	PQ406959	-	China	This study
M. alniphila	904	JF908482	-	Italy	Unpublished
M. amicta	CBS:254.53	MH857183	-	France	(Vu et al. 2019)
M. amicta	CBS:352.50	MH856655	MH868170	France	(Vu et al. 2019)
M. arcangeliana	252b	JF908401	-	Spain	(Osmundson et al. 2013)
M. arcangeliana	252f	JF908402	-	Spain	(Osmundson et al. 2013)
M. bicystidiata	HMJAU43648	MK309773	MK629359	China	(Na and Bau 2019b)
M. bicystidiata	HUIF50044	PQ406952	-	China	This study
M. bicystidiata	HUIF50583	PQ406953	-	China	This study
M. breviseta	BAP 633	MH414551	MH385327	Africa	(Cooper et al. 2018)
M. brunnescens	JSU125	ON778578	OP360941	China	(Zhang et al. 2024)
M. brunnescens	JSU126	ON778579	OP360942	China	(Zhang et al. 2024)
M. brunnescens	JSU127	PP152232	-	China	(Zhang et al. 2024)
M. bulliformis	SFSU:BAP 547	KX513844	KX513848	USA	(Perry and Desjardin 2016)
M. caeruleomarginata	FFAAS0358	OL711670	OL711665	China	(Na et al. 2022)
M. caeruleomarginata	FFAAS0357	OL711669	OL711664	China	(Na et al. 2022)
M. capillaripes	HRL2854	PQ811198	-	USA	Unpublished
M. castaneicola	JSU138	PQ406949	-	China	This study
M. castaneicola	JSU263	PQ406950	-	China	This study
M. castaneicola	HMJAU43581	MH136827	-	China	(Na and Bau 2019a)
M. cf. *cinerella*	173	MF926553	-	Russia	(Malysheva et al. 2017)
M. chlorocyanea	HUIF50234	OP358280	OP360937	China	(Liu et al. 2022a)
M. chlorocyanea	HUIF50238	OP358281	OP360938	China	(Liu et al. 2022a)
M. chlorophos	CT15101401	MH400938	-	China	Unpublished
M. cinerella	Aronsen051014	KT900146	-	Norway	Unpublished
M. citrinomarginata	SHXG	OM228755	OM228763	China	Unpublished
M. citrinomarginata	HMJAU 43563	MG654739	-	China	(Na and Bau 2018)
M. confinationis	MO362993	PP831662	-	USA	Unpublished
M. confinationis	PAMP-fungi-41	MT764847	MT764850	Spain	Unpublished
M. corynephora	JSU145	PQ406951	-	China	This study
M. corynephora	SJiao	OP604434	-	China	Unpublished
M. cristinae	JS347	MT921381	MT921384	Brazil	(Oliveira et al. 2021)
M. cristinae	JS767	MT921382	-	Brazil	(Oliveira et al. 2021)
M. crocea	S.D. Russell iNaturalist #16588497	OM473679	-	USA	Unpublished
M. crocea	OMDL K. Canan iNaturalist 182892200	PP436589	-	USA	Unpublished
M. cyanorhiza	J24082010	MW540696	-	Finland	Unpublished
M. cyanorhiza	120b	JF908385	-	Italy	(Osmundson et al. 2013)

Species	Voucher	GenBank accession no.		Location	References
		ITS	LSU		
M. deeptha	DM334g (K(M)178333)	JX481737	-	India	(Aravindakshan et al. 2012)
M. deeptha	HUIF50518	PQ406962	-	China	This study
M. digitifurcata	HUIF60006	PQ406940	-	China	(Wei et al. 2024)
M. digitifurcata	FFAAS1055	PP706100	PP704700	China	(Wei et al. 2024)
M. entolomoides	HMJAU 43126	MG654738	-	China	(Na and Bau 2018)
M. entolomoides	HMJAU 43052	MG654737	-	China	(Na and Bau 2018)
M. entolomoides	HMJAU 43048	MG654736	-	China	(Na and Bau 2018)
M. filopes	HUIF50198	OP604441	OP605599	China	Unpublished
M. filopes	HMAS 291835	OR236988	-	China	Unpublished
M. flosoides	HUIF50128	OP358282	OP360939	China	(Liu et al. 2022a)
M. flosoides	HUIF50129	OP358283	OP360940	China	(Liu et al. 2022a)
M. flosoides	HUIF50128-R	OP745013	-	China	(Liu et al. 2022a)
M. fulgoris	ACP1690	MG926694	-	Mexico	(Cortés-Pérez et al. 2019)
M. fulgoris	ACP1785	MG926693	-	Mexico	(Cortés-Pérez et al. 2019)
M. fulvomarginata	**HUIF50088 Holotype**	**PQ406943**	**-**	**China**	**This study**
M. fulvomarginata	**HUIF50089**	**PQ406944**	**PQ406964**	**China**	**This study**
M. galericulata	TFB14675	MN088380	-	USA	(Hughes et al. 2020)
M. galericulata	TFB14649	MN088382	-	USA	(Hughes et al. 2020)
M. galericulata	HUIF50196	OP604439	-	China	Unpublished
M. haematopus	HUIF50203	OP604443	OP605601	China	Unpublished
M. haematopus	HMJAU43662	MK733299	MK722353	China	Unpublished
M. huangsangensis	**HUIF50526 Holotype**	**PQ406935**	**-**	**China**	**This study**
M. huangsangensis	**HUIF50528**	**PQ406936**	**PQ406965**	**China**	**This study**
M. interrupta	HMJAU43849	MK733301	-	China	Unpublished
M. interrupta	HMJAU43791	MK733300	-	China	Unpublished
M. juniperina	869	JF908478	-	Italy	(Osmundson et al. 2013)
M. laevigata	HMJAU43618	MK733304	MK722355	China	Unpublished
M. laevigata	MHHNU 8626	MK453048	-	China	Unpublished
M. leaiana	MHHNU 30544	MK250916	-	China	Unpublished
M. leaiana	HKAS126400	OQ025147		China	Unpublished
M. leptocephala	HUIF50005	PQ406956	-	China	This study
M. leptocephala	CA FUNDIS iNaturalist #160824125	OR778420	-	USA	Unpublished
M. longinqua	BAP 648	MH414552	MH385328	Africa	(Cooper et al. 2018)
M. maculata	HUIFS50209	OP604446	-	China	Unpublished
M. maculata	HMJAU43009	MK309791	MK629347	China	Unpublished
M. meliigena	39c	JF908428	-	Italy	(Osmundson et al. 2013)
M. meliigena	39	JF908423	-	Italy	(Osmundson et al. 2013)
M. meliigena/ juniperina	HUIF60003	PQ406954	-	China	This study
M. meliigena/ juniperina	HUIF60004	PQ406955	-	China	This study
M. metata	313b	JF908412	-	Italy	(Osmundson et al. 2013)
M. metata	HMJAU43625	MH396636	-	China	Unpublished
M. hongfengensis	**JSU114 Holotype**	**PQ406945**	**PQ406967**	**China**	**This study**
M. hongfengensis	**JSU121**	**PQ406946**	**PQ406968**	**China**	**This study**
M. oryzifluens	FFAAS1051	PP706096	PP704696	China	(Wei et al. 2024)
M. pasvikensis	AAronsen50-13	KU861558	-	Norway	Unpublished
M. pasvikensis	AAronsen86-12	KU861556	-	Norway	Unpublished
M. pearsoniana	TENN61384	JN182200	-	USA	(Harder et al. 2012)
M. pearsoniana	TENN61544	JN182199	-	USA	(Harder et al. 2012)
M. pearsoniana	HUIF50392	PQ406948	-	China	This study
M. picta	CA FUNDIS iNaturalist 171114596	OR858681	-	USA	Unpublished
M. picta	TUR194167	MW540717	-	Finland	Unpublished
M. pluteoides	HMJAU43771	MK733307	MK722357	China	Unpublished
M. pluteoides	HMJAU43765	MK733306	-	China	Unpublished
M. pluteoides	HUIF50584	PQ406961	-	China	This study
M. pluteoides	HUIF50591	PQ406960	-	China	This study

Species	Voucher	GenBank accession no.		Location	References
		ITS	LSU		
M. polygramma	CBS:240.47	MH856235	MH867764	France	(Vu et al. 2019)
M. polygramma	439b	JF908433	-	Italy	(Osmundson et al. 2013)
M. pura	HUIF50006	OP604419	OP605597	China	Unpublished
M. pura	TENN60139	EU517505	-	Russia	(Petersen et al. 2008)
M. purpureofusca	HMJAU 43554	MG654740	-	China	(Na and Bau 2018)
M. purpureofusca	HMJAU 43624	MG654741	-	China	(Na and Bau 2018)
M. rosella	73h	JF908471	-	Italy	(Osmundson et al. 2013)
M. rosella	53	MW576937	-	Norway	Unpublished
M. roseolamellata	**HUIF60001 Holotype**	**PQ406941**	**PQ406969**	**China**	**This study**
M. roseolamellata	**HUIF60002**	**PQ406942**	**-**	**China**	**This study**
M. rubromarginata	CBS:265.48	MH856335	MH867890	France	(Vu et al. 2019)
M. rubromarginata	CBS:268.48	MH856338	MH867891	France	(Vu et al. 2019)
M. sanguinolenta	TENN59879	FJ596764	-	USA	(Hughes et al. 2009)
M. seynesii	71h	JF908470	-	Italy	(Osmundson et al. 2013)
M. seynesii	71I	JF908469	-	Italy	(Osmundson et al. 2013)
Mycena sp.	JSU008	PQ465299	-	China	Unpublished
Mycena sp.	JSU132	PQ406963	-	China	This stufy
Mycena sp.	080108	LC504829	-	Japan	This study
M. silvaenigrae	HMJAU43815	MK733310	MK722359	China	Unpublished
M. subcaerulea	TENN-F-051121	OL711671	OL711666	USA	(Na et al. 2022)
M. subcaerulea	TENN-F-057919	OL711672	OL711667	USA	(Na et al. 2022)
M. subpiligera	HUIF50036	OM228758	-	China	(Liu et al. 2022b)
M. subpiligera	HUIFS50007	OM228759	-	China	(Liu et al. 2022b)
M. subroriduliformis	**HUIF50540 Holotype**	**PQ406937**	**PQ406970**	**China**	**This study**
M. subroriduliformis	**HUIF50546**	**PQ406938**	**-**	**China**	**This study**
M. substylobates	HMJAU43444	MH216190	-	China	(Na and Bau 2019a)
M. substylobates	HMJAU43418	MH216189	-	China	(Na and Bau 2019a)
M. tenax	OSC 113746	EU846251	-	USA	Unpublished
M. tenax	OSC 113728	EU669224	-	USA	Unpublished
M. vulgaris	447h	JF908435	-	Italy	Unpublished
M. vulgaris	CBS:248.47	MH856240	MH867770	France	(Vu et al. 2019)
M. xantholeuca	CBS370.50	MH856663	MH868180	France	(Vu et al. 2019)
M. xantholeuca	CBS371.50	MH856664	MH868181	France	(Vu et al. 2019)
M. yuezhuoi	FFAAS0346	MW581492	-	China	(Liu et al. 2021a)
M. yuezhuoi	HUIF50535	PQ406947	-	China	(Liu et al. 2021)
M. zephirus	CBS:270.48	MH856339	MH867892	France	(Liu et al. 2021)
M. zephirus	AH60146	PP868143	-	Spain	(Villarreal et al. 2024)
Phloeomana minutula	H6036841	MW540684	-	Finland	Unpublished
P. speirea	iNAT: 100003394	ON206666	-	USA	Unpublished

The final datasets were aligned using MAFFT v.7.310 (Katoh and Standley 2013). The sequences were concatenated into one multi-loci dataset with SequenceMatrix 1.7.8 (Vaidya et al. 2011). The ALTER (Alignment Transformation EnviRonment) online tool was used for the final conversion of the FASTA format to the NEXUS format (Glez-Penñ et al. 2010). The best-fit evolutionary model was selected using MrModelTest v.2.3 under the Akaike information criterion (AIC) (Nylander 2004). A phylogenetic tree was constructed based on maximum likelihood and Bayesian inference methods. Maximum likelihood (ML) analyses were performed with RAxML-NG v.0.9.0 (Kozlov et al. 2019), and bootstrap values were calculated from 1,000 replicates. Bayesian inference analysis was performed using the Metropolis-coupled Markov chain Monte Carlo method with MrBayes v3.2.5 under the GTR +I+G model (Ronquist and Huelsenbeck 2003). Analyses were run with 4 chains of 2,000,000 generations, and trees were sampled every 100th generation. The first 25% of the sample trees were discarded as burn-in. Gaps were treated as missing data. Phylogenetic trees were visualized with FigTree v1.4.3 (http://tree.bio.ed.ac.uk/software/figtree/).

Results

Phylogenetic analysis

The two-locus dataset (ITS + LSU) consisted of 191 sequences and 1,680 nucleotide sites in total, which are shown in Table 2. It includes sequences of 28 *Mycena* taxa except for *M. picta* (Fr.) Harmaja and *M. heteracantha*, which are present in Hunan. Sequences of closely related species with high homology and morphologically similar species were also downloaded from GenBank. *Atheniella adonis* (Bull.) Redhead, Moncalvo, Vilgalys, Desjardin, & B.A. Perry, *A. aurantiidisca* (Murrill) Redhead, Moncalvo, Vilgalys, Desjardin, & B.A. Perry; *Clitocybula intervenosa* A.C. Cooper, Desjardin, & B.A. Perry (BAP 588, BAP 613), *Phloeomana minutula* (Sacc.) Redhead; *P. speirea* (Fr.) Redhead, and *Hydropus murinus* A.C. Cooper, Desjardin, & B.A. Perry were chosen as the outgroup (Liu et al. 2022a). The topologies generated from maximum likelihood (ML) and Bayesian inference (BI) analyses were identical, although statistical support for some branches showed slight differences. The BI tree with branch lengths inferred from the ITS and LSU datasets is shown in Fig. 1.

The phylogeny inferred from the combined dataset revealed that the *Mycena* split into two well-supported clades, and all new taxa formed a well-supported monophyletic lineage. *Mycena hongfengensis* formed a small branch and grouped with an unidentified *Mycena* sp. in clade 1 (BS/BP = 100/1.00). *Mycena roseolamellata*, *M. fulvomarginata*, *M. huangsangensis*, and *M. subroriduliformis* were members of clade 2. *Mycena roseolamellata* and *M. entolomoides* T. Bau formed a supported branch in the tree (BS/BP = 100/1.00), and their genetic distance is substantial enough to distinguish between the two species. *Mycena fulvomarginata* is most related to *M. capillaripes* Peck. They grouped together with BS/BP = 83/1.00 statistical support, and they were distinct. *Mycena albiceps* (Peck) Gilliam, *M. flosoides* L.N. Liu, *M. brunnescens* L.N. Liu, and our specimens (*M. huangsangensis* and *M. subroriduliformis*) formed a separate branch with strong statistical support (BS/BP = 86/1.00).

Taxonomy

***Mycena huangsangensis* L.N. Liu, sp. nov.**
MycoBank No: 856016
Figs 2, 3

Diagnosis. Differs from the most similar species, *M. alniphila*, by its decurrent lamellae and longer basidiospores.

Holotype. China • Hunan Province, Shaoyang City, Suining County, Hunan Huangsang National Nature Reserve, 26°24'18"N, 110°05'37"E, elev. 644 m, 24 April 2024, LiNa Liu, *HUIF50526* (collection number NN526).

Etymology. Refers to the Huangsang National Nature Reserve, from where the holotype was collected.

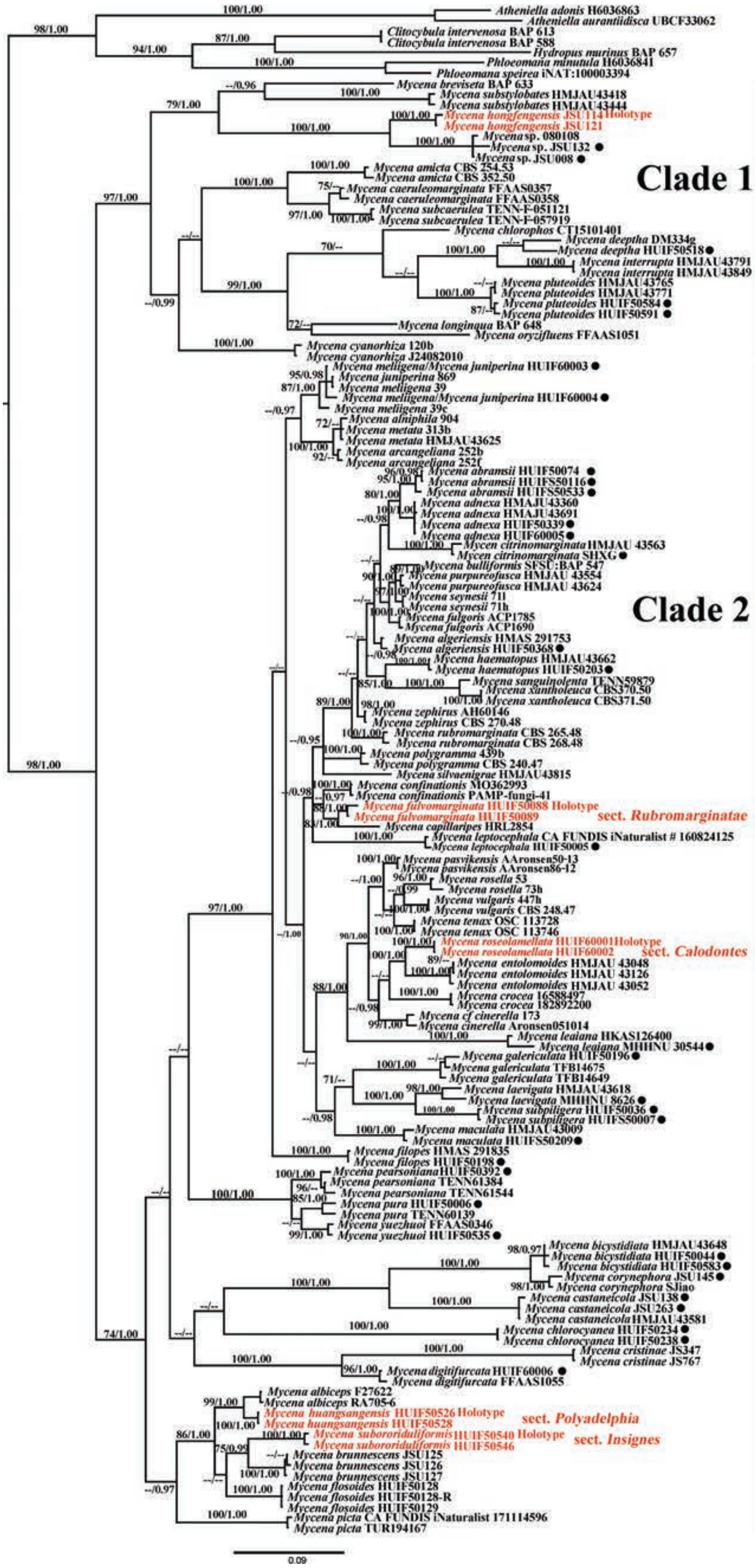

Figure 1. Phylogenetic relationships of *Mycena* species in Hunan Province inferred from the combined dataset (ITS and nrLSU) using Bayesian posterior probabilities (BP) ≥ 0.95; Bootstrap support (BS) ≥ 70% are reported on the branches. Red text represents new taxa. The black dots indicate the *Mycena* species collected from Hunan Province.

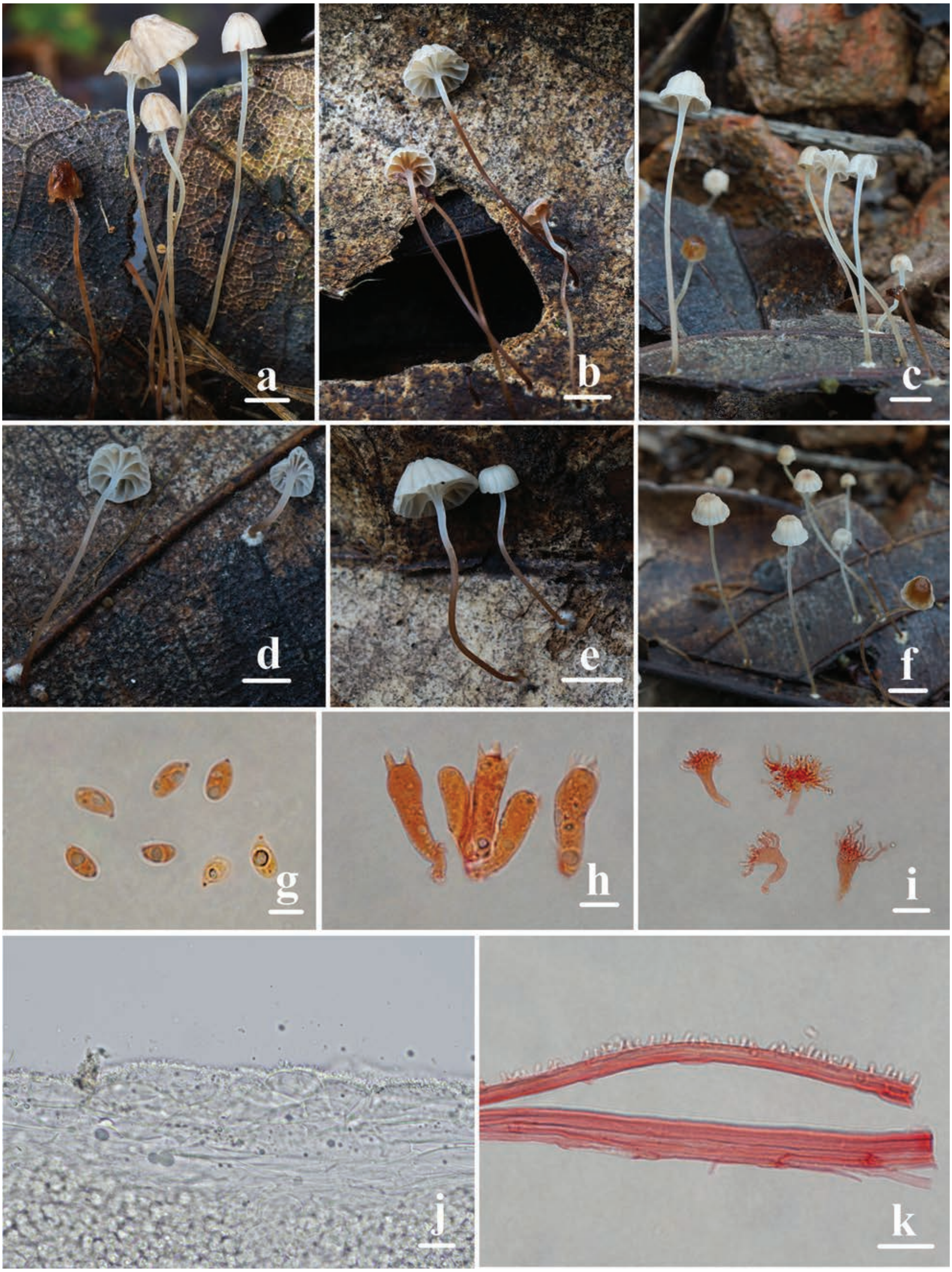

Figure 2. Basidiomata and microscopic features of *Mycena huangsangensis* **a–f** basidiomata **g** basidiospores **h** basidia **i** cheilocystidia **j** pileipellis **k** stipitipellis. Structures (**g–i, k**) were stained in 1% Congo red solution and **j** were rehydrated in 5% KOH solution. Scale bars: 5 mm (**a–f**); 5 µm (**g**); 10 µm (**h–k**).

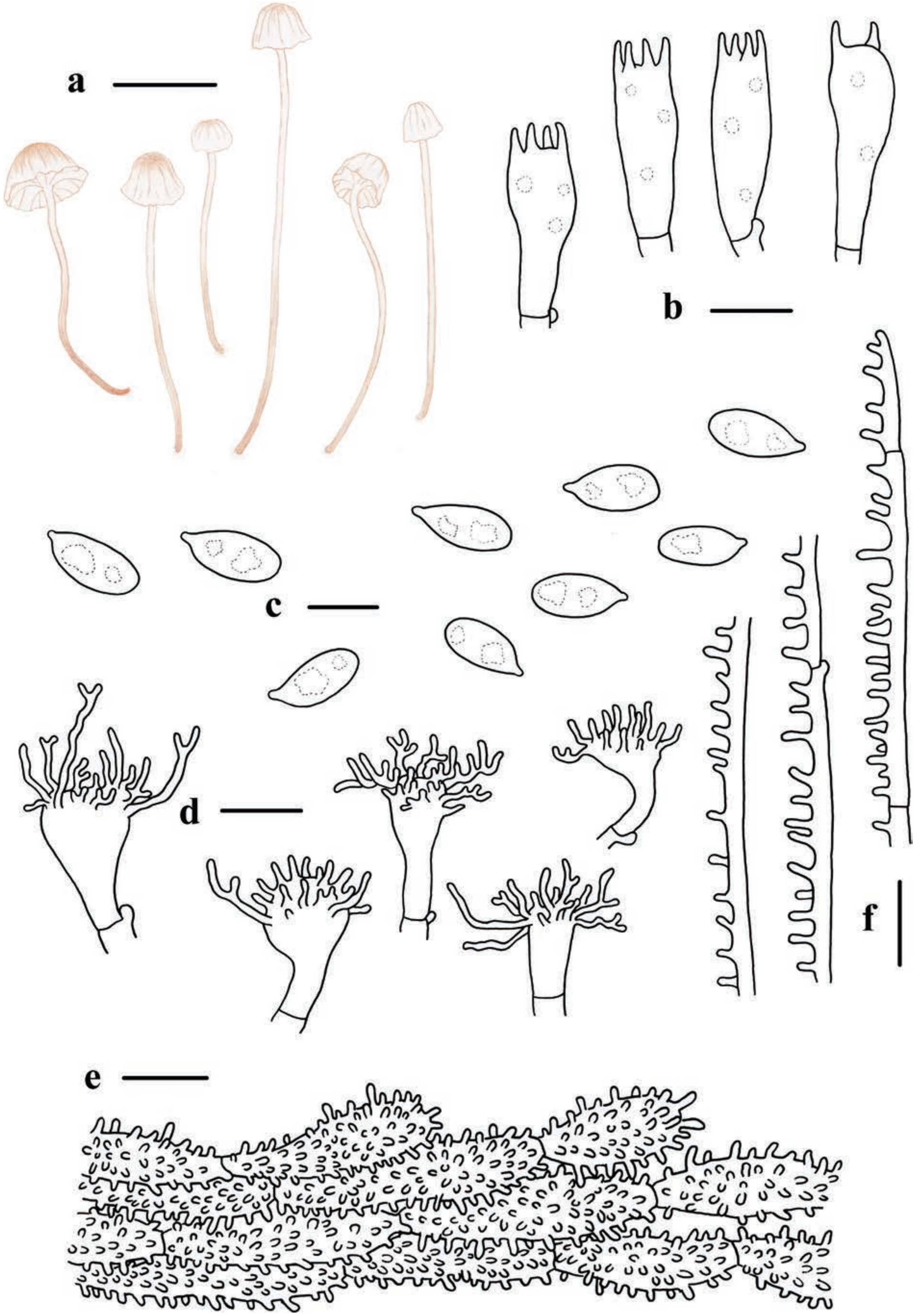

Figure 3. Morphological features of *Mycena huangsangensis* **a** basidiomata **b** basidia **c** basidiospores **d** cheilocystidia **e** pileipellis **f** hyphae of stipitipellis. Scale bars: 1 cm (**a**); 5 µm (**c**); 10 µm (**b, d–f**).

Description. Pileus 1–5 mm diam., hemispherical to obtusely conical, expanding with age, umbilicate or depressed center, sulcate, translucent-striate, pruinose and pubescent, light brown (6B4–6B7) to dark brown (6E7–6E8), or brownish-pink (7A4–7B4), paler brown towards margin. Context white, thin, fragile. Lamellae 9–11 reach the stipe, with 1–2 tiers of lamellulae, decurrent, white (4A1) to brown (7D7), edge concolorous with face. Stipe 6–25 × 1–2 mm, cylindrical, hollow, fragile, light brown (6B4–6B7) to brown (6E5–6E8) at the base, gradually becoming paler to white (4A1) towards the apex. Base covered with white fibrils. Odor and taste indistinctive.

Basidiospores 6.0–7.4 (7.8) × (3.2) 3.4–4.2 (4.3) μm, Q = 1.4–2.1, Q = 1.8 ± 0.2, pip-shaped, elongated, hyaline, smooth, thin-walled, amyloid. Basidia 15.4–20.9 × 6.2–9.0 μm, 4-spored, clavate. Cheilocystidia 13.2–25.0 × 8.5–19.9 μm, abundant, clavate to obpyriform, covered with fairly numerous, simple to furcate, cylindrical excrescences. 1.2–9.5 × 0.5–1.4 μm. Pleurocystidia absent. Hyphae of the pileipellis 12–27 μm wide, densely covered with warts or short cylindrical excrescences. Hyphae of the stipitipellis 1.0–3.0 μm wide, densely covered with simple, cylindrical excrescences 1.0–3.2 × 0.8–1.5 μm. Clamp connections are present in the basidia, pileipellis, and stipitipellis hyphae.

Habitat. Gregarious on decaying leaves of deciduous trees.

Known distribution. Shaoyang City, Hunan Province.

Additional materials examined. CHINA• Hunan Province, Shaoyang City, Suining County, Hunan Huangsang National Nature Reserve, 26°24'21"N, 110°05'36"E, elev. 675 m, 24 April 2024, LiNa Liu, *HUIF50528* (collection number NN528).

Notes. *Mycena huangsangensis* can be considered to be a member of sect. *Polyadelphia* owing to very small basidiomata, a small number of lamellae, and a slender stipe and hyphae of the pileipellis, which are ornamented with short warts. *Mycena huangsangensis* belongs to the section with a brownish pileus, while *M. alniphila* Robich shows the most significant morphological similarity to *M. huangsangensis*. They have similar basidiomata color and shape of cheilocystidia, pileipellis hyphae densely covered with cylindrical excrescences, and diverticulate stipitipellis hyphae. However, *M. alniphila* differs in having adnate lamellae, slightly longer spores measuring 8.5–11.0 × (3.5) 4.0–5.5 μm, simple cheilocystidia without branching, and caulocystidia present (Robich 2003). *Mycena albiceps* and *M. catalaunica* Robich are somewhat similar to the new species; in particular, they share the same basidiomata shape and similar habitats. *Mycena albiceps* differs in the white colors of the pileus and black stipe (Gilliam 1976; Maas Geesteranus 1986). The latter, *M. catalaunica*, has a pale violaceous pink to pale vinaceous pink pileus, subglobose spores, and caulocystidia; the clamp connection is absent in all tissues, and cheilocystidia are subglobose (Robich 2003).

Mycena fulvomarginata **L.N. Liu, sp. nov.**

MycoBank No: 856027
Figs 4, 5

Diagnosis. Differs from the closest species, *M. rubromarginata*, in having yellow lamellae edges and light-yellow contents in cheilocystidia, hyphae of the pileipellis, and stipitipellis.

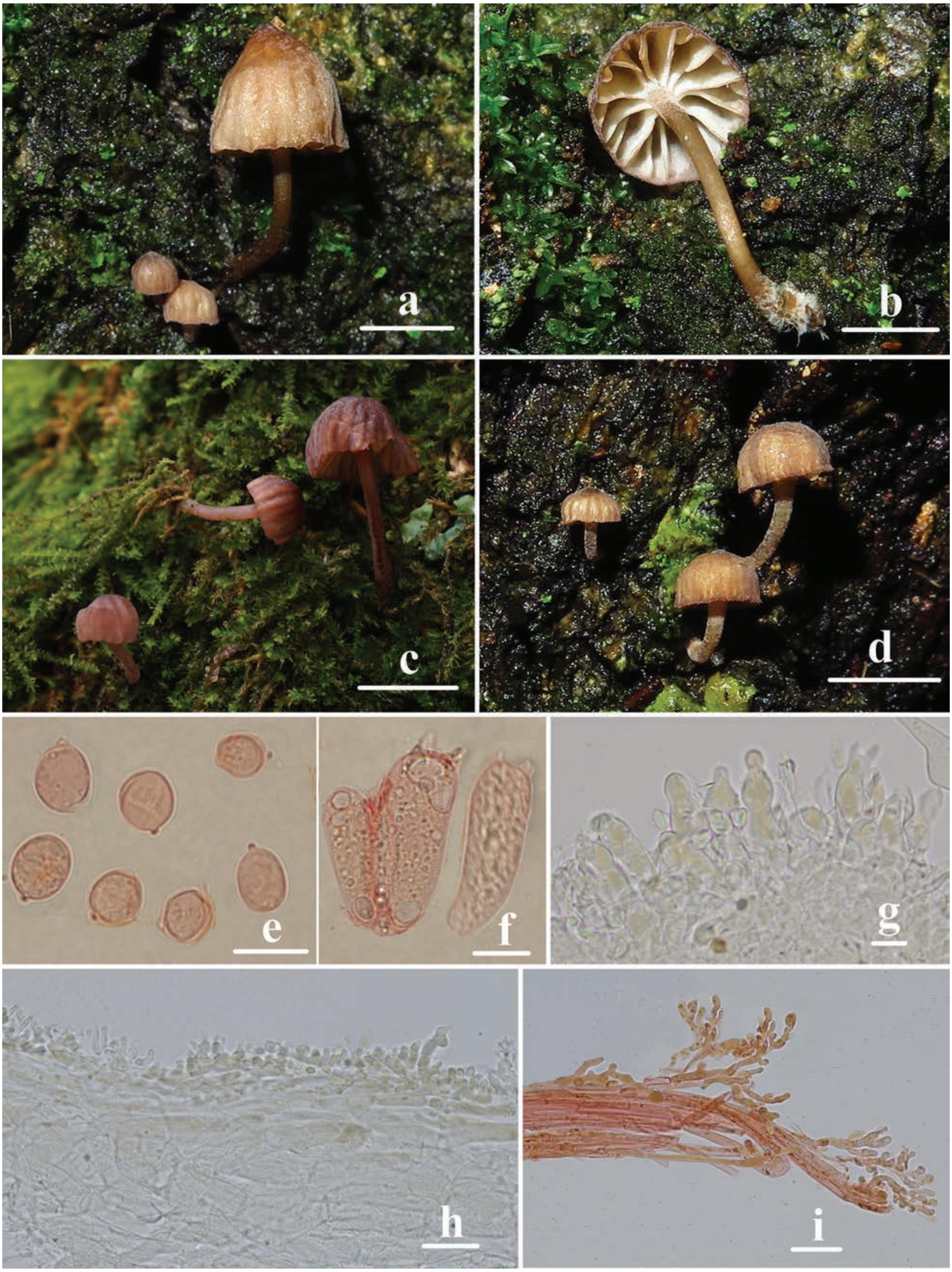

Figure 4. Basidiomata and microscopic features of *Mycena fulvomarginata* **a–d** basidiomata **e** basidiospores **f** basidia and basidioles **g** cheilocystidia **h** pileipellis **i** stipitipellis. Structures (**e, f, i**) were stained in a 1% Congo red solution, and **g, h** were rehydrated in a 5% KOH solution. Scale bars: 5 mm (**a–d**); 10 µm (**e–i**).

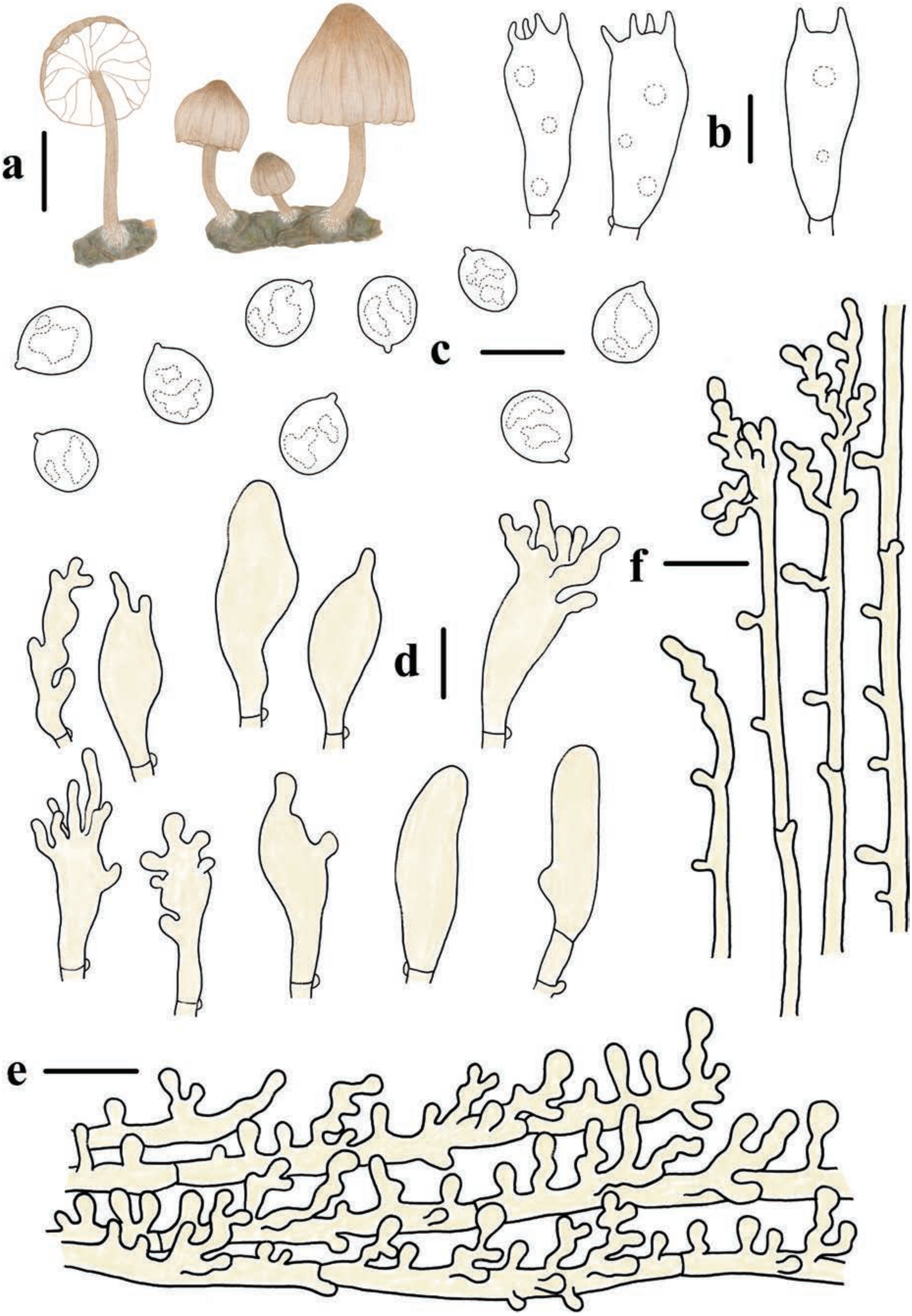

Figure 5. Morphological features of *Mycena fulvomarginata* **a** basidiomata **b** basidia **c** basidiospores **d** cheilocystidia **e** pileipellis **f** hyphae of stipitipellis. Scale bars: 5 mm (**a**); 10 µm (**b–f**).

Holotype. China• Hunan Province, Suining County, Hunan Huangsang National Nature Reserve, Shaoyang City, 26°25'41"N, 110°03'27"E, elev. 1075 m, 26 June 2021, LiNa Liu, *HUIF50088* (collection number NN88).

Etymology. Refers to the yellow color of the lamellae edges.

Description. Pileus 4–8 mm diam., hemispherical when young, paraboloid or campanulate with age, sulcate, pellucid-striate, pruinose, apex with obtuse umbo, the margin infrequently out of flatness, dark reddish brown (7C8) at center, gradually becoming paler towards the margin to light brown (7A6), turning purple (12B5) with age. Context white, thin, fragile. Lamellae 10–12 reach the stipe, with 1 tier of lamellulae, adnexed, white (4A1), edge yellow (5B7), stipe 6.0–12.0 × 0.5–1.0 mm, central, cylindrical, hollow, fragile, finely white pruinose and pubescent, pale brown (6D7) to brown (6F7), fading to purple (12B5). Base slightly bulbous, covered with white fibrils. Odor and taste indistinctive.

Basidiospores (7.8) 7.9–9.9 (10.0) × (4.5) 5.7–8.0 (8.2) µm, Q = 1.2–1.7, Q = 1.3 ± 0.1, subglobose to broadly ellipsoid, hyaline, smooth, thin-walled, amyloid. Basidia 24.8–33.5 × 8.2–13.5 µm, 4-spored, clavate. Cheilocystidia 22.6–45.8 × 7.7–17.8 µm, abundant, fusiform to ventricose, clavate, subcylindrical, or somewhat irregularly shaped, smooth or covered with one or more apical simple to furcate excrescences, with light yellow contents. Pleurocystidia absent. Hyphae of the pileipellis 3.0–9.0 µm wide, covered with simple to much-branched excrescences, 2.0–6.0 × 2.0–4.0 µm, with light yellow contents. Hyphae of the stipitipellis 2.0–5.0 µm wide, covered with numerous simple to furcate cylindrical excrescences, 2.0–11.0 × 2.0–8.0 µm, with light yellow contents. Clamp connections are present in the basidia, pileipellis, and stipitipellis hyphae.

Habitat. Gregarious on moss-covered bark of living deciduous trees.

Known distribution. Hunan Province and Guangxi Zhuang Autonomous Region, China.

Additional materials examined. China • Guangxi Zhuang Autonomous Region, Baise City, Leye County, Yachang Orchid National Nature Reserve, 24°46'29"N, 106°20'09"E, elev. 1080 m, 24 April 2024, LiNa Liu, *HUIF50089* (collection number NN89).

Notes. *Mycena fulvomarginata* belongs to sect. *Rubromarginatae* Singer ex. Maas Geest. due to the very small basidiomata, yellow lamellar edges, cheilocystidia with colored contents, diverticular pileipellis, and stipitipellis hyphae, along with exhibiting a growth habit on decaying wood. *Mycena fulvomarginata* is similar to the species described in this section: *M. rubromarginata* (Fr.) P. Kumm., *M. seynii* Quél., and *M. bulliformis* B.A. Perry & Desjardin. They resemble *M. fulvomarginata* in the shape of their cheilocystidia, are covered with excrescences on the pileipellis and stipe cortical hyphae, and have a similar brown pileus. However, *M. rubromarginata* differs in that it has longer pileipellis excrescences, up to 36 µm, and cheilocystidia that are 20–65 (up to 90) µm long, with reddish-brown contents (Robich 2003; Aronsen and Læssøe 2016). *Mycena seynii* should be easy to separate from the new species by its medium basidiomata, larger basidiospores measuring 10.5–15.0 × 6.0–7.5 µm, reddish-purple edge, larger cheilocystidia measuring 30–85 × 8–16 µm, pileipellis, and stipitipellis hyphae with brown to dark red granular contents (Robich 2003; Aronsen and Læssøe 2016). In addition, *M. bulliformis* differs from *M. fulvomarginata* by its violet to violet-brown edges, ellipsoid to broadly ellipsoid spores, and some smooth pileipellis hyphae (Perry and Desjardin 2016).

Mycena hongfengensis **L.N. Liu, sp. nov.**

MycoBank No: 856029
Figs 6, 7

Diagnosis. Differs from *M. castaneicola* in having smooth cheilocystidia, dermatocysts present in the pileipellis, and stipitipellis hyphae.

Holotype. China • Hunan Province, Xiangxi Tujia-Miao Autonomous Prefecture, Jishou City, Hongfeng Forest Park, 28°16'23"N, 109°40'45"E, elev. 230 m, 22 April 2024, ZhuXiang Liu, *JSU114* (collection number JD114).

Etymology. Refers to the Hongfeng Forest Park, from where the holotype was collected.

Description. Pileus 2–5 mm diam., hemispherical when young, becoming nearly campanulate or plano-convex with age, with a centrally flattened depression, margin smooth, sulcate, translucently striate, pure white (4A1), white pubescent. Context pure white, thin, fragile. Lamellae 16–18 reach the stipe, with 1–2 tiers of lamellulae, narrowly free, pure white (4A1), concolorous with the sides. Stipe 15–40 × 0.1–0.5 mm, almost equal or slightly expanding towards the base, hollow, white (4A1) to greyish-white (4B1), pubescent or puberulous, base swollen. With a not well-developed basal disc, covered with white hirsute. Odor and taste not distinctive.

Basidiospores (6.2) 6.3–7.6 (7.7) × (3.4) 3.5–4.9 (5.2) μm, Q = 1.4–2.0, Qm = 1.7 ± 0.2, oblong or pip-shaped, hyaline, thin-walled, amyloid. Basidia 8–16 × 4–8 μm, two- and four-spored, clavate, hyaline. Cheilocystidia 11–43 × 5–9 μm, obpyriform, fusiform, ventricose, filiform, with a long neck, up to 25 μm, with an acute and occasionally branched apex, hyaline. Pleurocystidia absent. Pileipellis hyphae 2–13 μm wide, hyphae cylindrical, densely covered with warts and cylindrical excrescences, 1.0–6.0 × 1.0–2.0 μm, with irregularly cylindric to strangulated dermatocysts, 63–200 × 7–20 μm, walls 1.0–2.0 μm, greenish grey (1C2). Hyphae of the stipitipellis 1.0–6.0 μm wide, smooth, dermatocysts numerous, clavate to pyriform, 50–320 × 5–20 μm, long, flexuous, filiform, simple, and tapering towards the apex. Clamp connections are absent in the basidia, pileipellis, and stipitipellis hyphae.

Habitat. Gregarious on decaying leaves of deciduous trees.

Known distribution. Xiangxi Tujia-Miao Autonomous Prefecture, Hunan Province.

Additional materials examined. China• Hunan Province, Xiangxi Tujia-Miao Autonomous Prefecture, Jishou City, Hongfeng Forest Park, 28°16'26"N, 109°40'48"E, elev. 255 m, 22 April 2024, ZhuXiang Liu, *JSU121* (collection number JD121).

Notes. *Mycena hongfengensis* is characterized by its pure white basidiomata, free lamellae, oblong to pip-shaped spores, and the presence of dermatocysts in the pileipellis and stipitipellis. According to the Maas Geesteranus classification, the new species could belong to an uncertain position. When we first found this specimen in the field, we thought it might be a member of either sect. *Saccharifera* or sect. *Amparoina*. All species in two sections have a white basidiomata, pubescent pileus and stipe, and stipe with a basic disc (Maas Geesteranus 1983; Desjardin 1995; Na and Bau 2019b). However, *M. hongfengensis* can be clearly distinguished from other species through microscopic characteristics. The presence of dermatocysts in the pileipellis and stipitipellis is the most important characteristic for separating *M. hongfengensis* from species of sect. *Sacchariferae* and sect. *Amparoina*. *Mycena castaneicola* T. Bau & Q. Na is the most similar to the new species in the macroscopic characteristics, but the microscopic features differ significantly. Sequences labeled as *Mycena* sp., which were extracted from

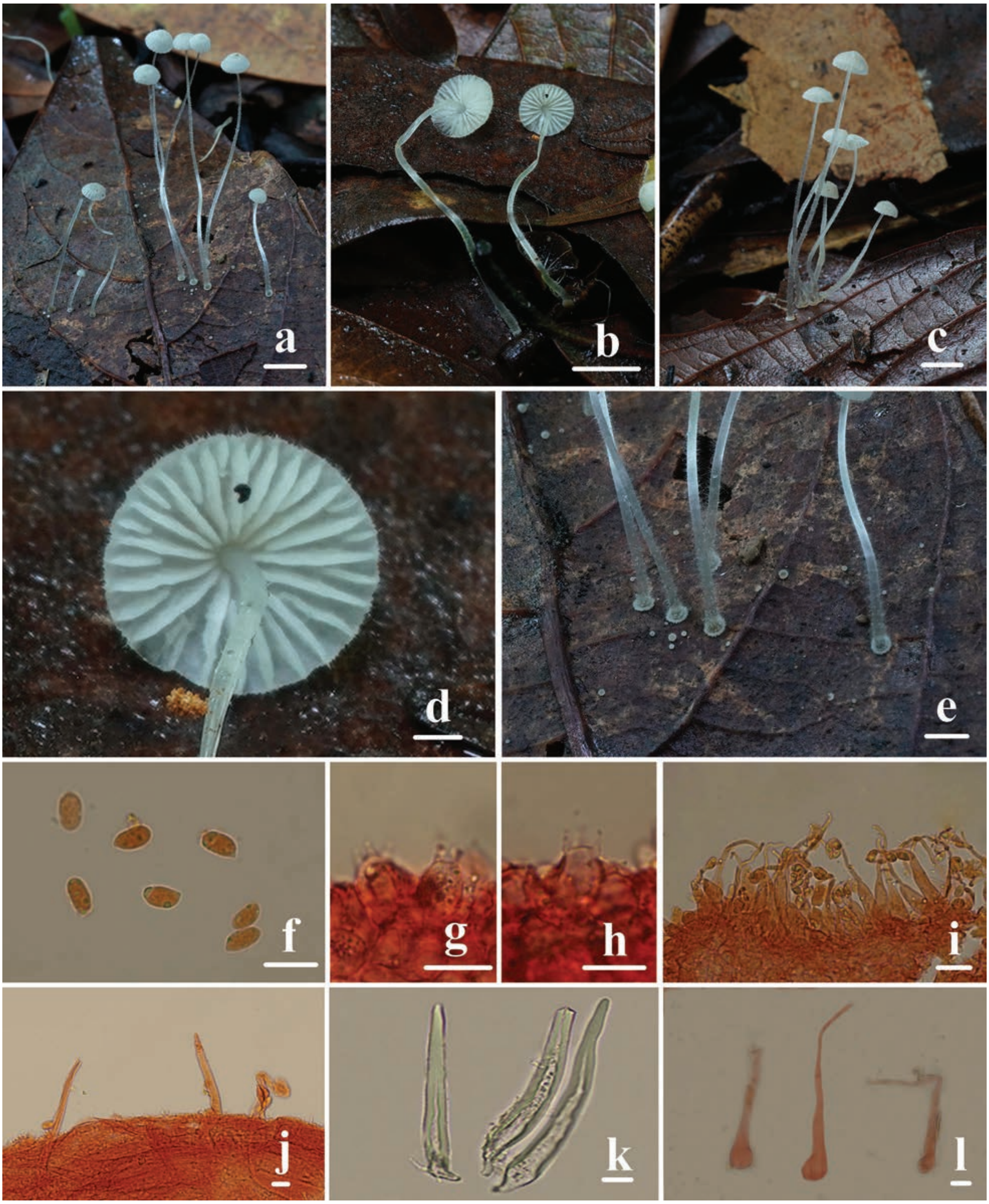

Figure 6. Basidiomata and microscopic features of *Mycena hongfengensis* **a–e** basidiomata **f** basidiospores **g, h** basidia **i** cheilocystidia **j, k** dermatocysts in the pileipellis **l** dermatocysts in the stipitipellis. Structures (**f–j, l**) were stained in a 1% Congo red solution and **k** were rehydrated in a 5% KOH solution. Scale bars: 5 mm (**a–c, e**); 1 mm (**d**); 5 μm (**f**); 10 μm (**g–l**).

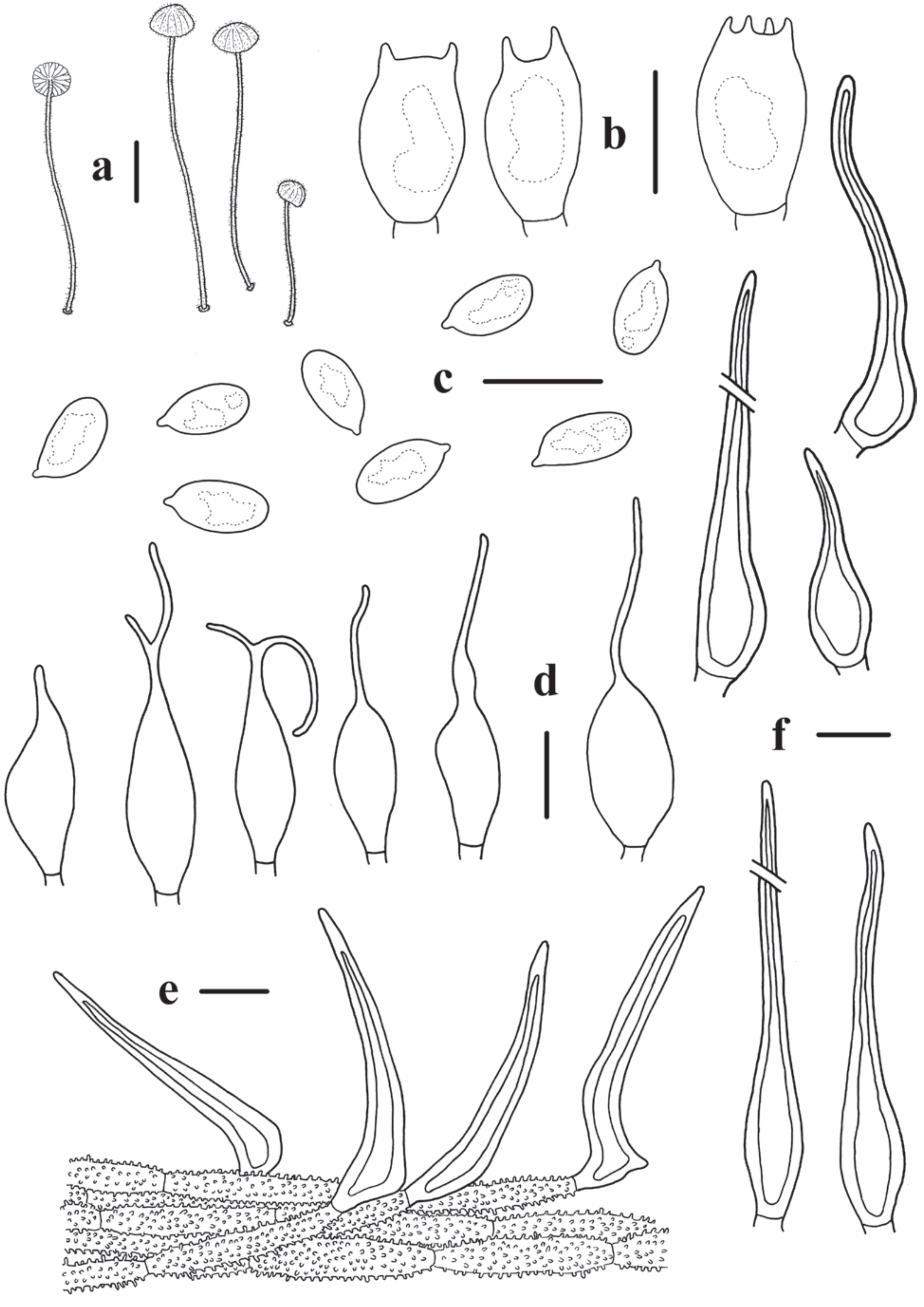

Figure 7. Morphological features of *Mycena hongfengensis* **a** basidiomata **b** basidia **c** basidiospores **d** cheilocystidia **e** dermatocysts in the pileipellis **f** dermatocysts in the stipitipellis. Scale bars: 1 cm (**a**); 10 µm (**b–f**).

the host *Myrica rubra* (Lour.) Siebold & Zucc. and originated from Japan, along with the sequence of *M. hongfengensis*, formed a well-supported lineage in the phylogenetic analysis (BS/BP = 100/1.00). We are very fortunate to have collected *Mycena* sp. in the field. However, we only collected one tiny basidioma; the microscopic structures we observed are not comprehensive. Both taxa have white pileus and pubescent pileus and stipe. The uncertain *Mycena* species differs in pileipellis, which has "acanthocysts" that are spherical or vesicular and covered with spines. These features can be used to easily differentiate the two species.

Mycena subroriduliformis **L.N. Liu, sp. nov.**

MycoBank No: 856045
Figs 8, 9

Diagnosis. Differs from *M. surculosa* in having a viscid pileus and stipe.

Holotype. China • Hunan Province, Suining County, Hunan Huangsang National Nature Reserve, Shaoyang City, 26°24'47"N, 110°05'20"E, elev. 542 m, 25 April 2024, LiNa Liu, *HUIF50540* (collection number NN540).

Etymology. Refers to the viscid pileus and stipe of the new species.

Description. Pileus 2–8 mm diam., hemispherical when young, campanulate with age, with obvious depression at the center, sulcate, translucent-striate, surface wet, glabrous, brownish white (7A1), light brown (7C3), brownish grey (7D1–6D2) when old. Context white, thin, and fragile. Lamellae 18–20 reach the stipe, with 1–2 tiers of lamellulae, decurrent, white (4A1), concolorous with the sides. Stipe 2–45 × 1–2 mm, cylindrical, hollow, fragile, surface glutinous, white (4A1) to brownish grey (5A1–5D3) towards the apex, light brown to brown (5D6–6D6) towards the base, base swollen. Odor and taste indistinctive.

Basidiospores (6.2) 6.6–8.5 (9.0) × (3.6) 3.8–5.2 (5.3) μm, Q = 1.5–2.1, Q = 1.7 ± 0.1, pip-shaped, cylindrical, hyaline, amyloid, smooth. Basidia 19.3–26.9 × 5.6–8.0 μm, 4-spored, clavate, hyaline. Cheilocystidia 16.8–26.9 × 6.3–17.1 μm, abundant and variably shaped, clavate to cylindrical with short, more or less branched projections, 1.0–6.0 × 1.0–2.0 μm, thin-walled, hyaline. Pleurocystidia absent. Pileipellis hyphae somewhat gelatinized, 2.0–5.0 μm wide, with irregular simple to branched warts or cylindrical excrescences, 1.0–4.0 × 1.0–2.0 μm. Hyphae of the stipitipellis 1.0–6.0 μm wide, covered with cylindrical excrescences. 1.0–4.0 × 1.0–2.0 μm. Clamp connections are present in the basidia, pileipellis, and stipitipellis hyphae.

Habitat. Gregarious on decaying leaves of deciduous trees.

Known distribution. Shaoyang City, Hunan Province.

Additional materials examined. China• Hunan Province, Suining County, Hunan Huangsang National Nature Reserve, Shaoyang City, 26°24'39"N, 110°05'25"E, elev. 588 m, 25 April 2024, LiNa Liu, *HUIF50546* (collection number NN546).

Notes. The following characteristics placed this new species in the sect. *Insignes* Maas G. due to the viscid pileus and stipe, decurrent lamellae, pip-shaped spores, clavate cheilocystidia with coarse excrescences, hyphae of the pileipellis embedded in gelatinous matter, and diverticulate (Maas Geesteranus 1989). The three other similar species in sect. *Insignes* are *M. surculosa* Maas G. & de Meijer, *M. odorifera* (Peck) Sacc., and *M. calceata* Robich. All are differentiated from *M. subroriduliformis* as follows: *M. surculosa* has a dry pileus, with only

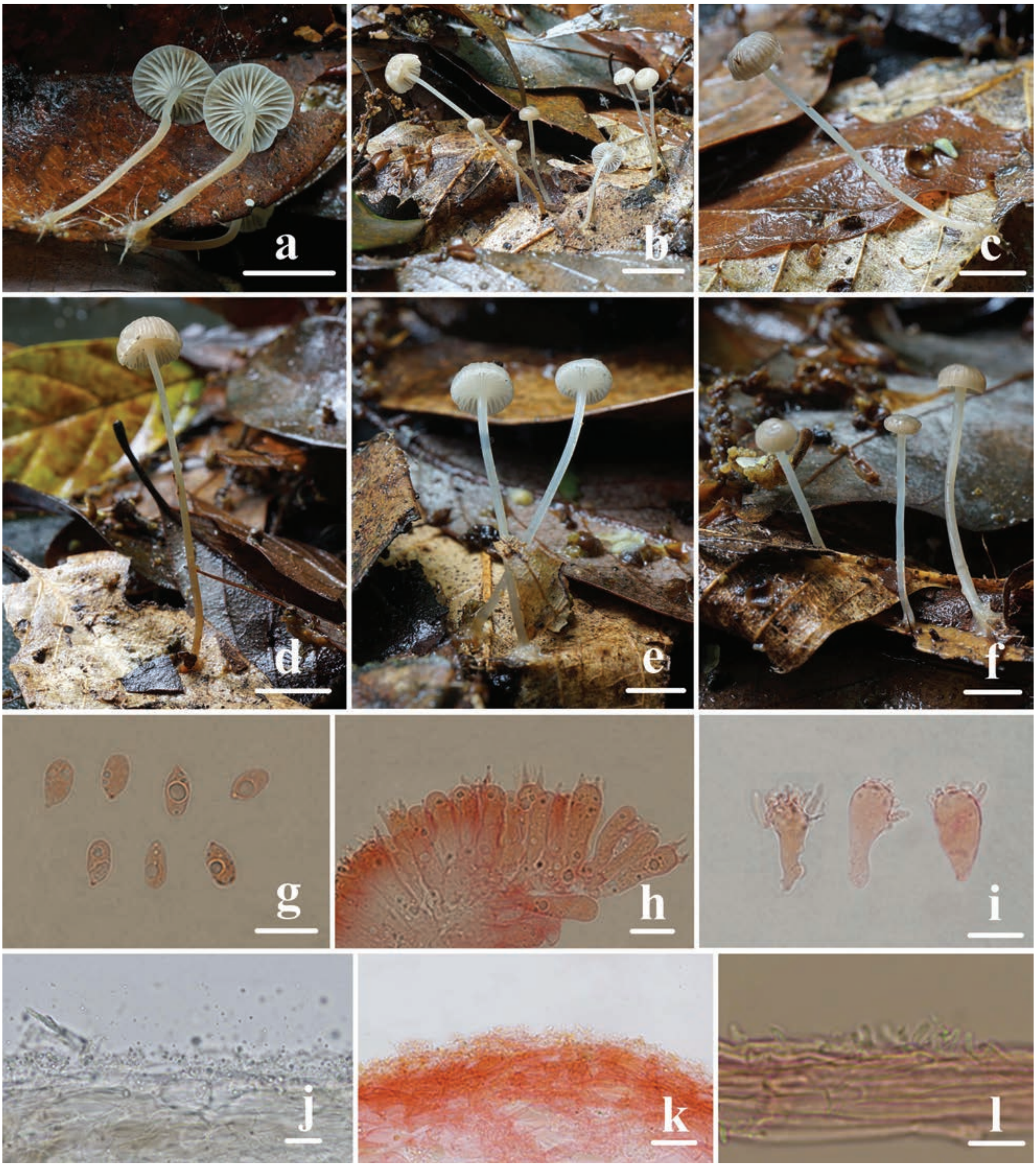

Figure 8. Basidiomata and microscopic features of *Mycena subroriduliformis* **a–f** basidiomata **g** basidiospores **h** basidia **i** cheilocystidia **j, k** pileipellis **l** stipitipellis. Structures (**g–i, k, l**) were stained in a 1% Congo red solution and **j** were rehydrated in a 5% KOH solution. Scale bars: 1 cm (**a–f**); 10 μm (**g–l**).

the stipe being viscid. The apical side branches of the pileipellis are densely covered and simple to forked, with cylindrical excrescences. The stipitipellis is somewhat gelatinized (Maas Geesteranus and De Meijer 1997). *Mycena odorifera* has a distinctive alkaline-like odor, a pruinose stipe, pubescence, and cheilocystidia occasionally with forked apices (Smith 1935). *Mycena calceata* has dark brown basidiomata and relatively large spores (11.0–13.5 × 5.5–8.0 μm), smooth cheilocystidia, or one or two branches at the apex (Robich 2003).

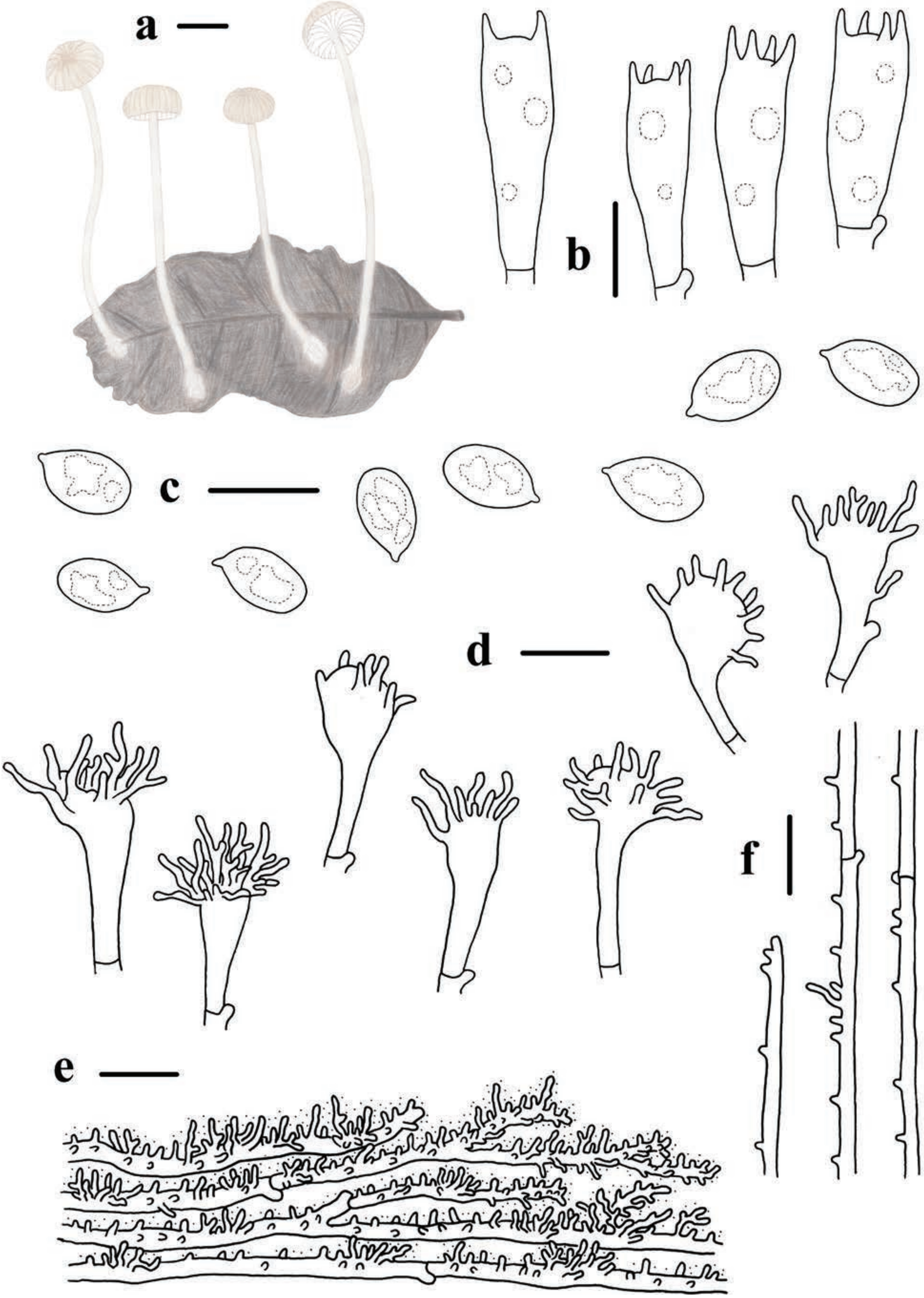

Figure 9. Morphological features of *Mycena subroriduliformis* **a** basidiomata **b** basidia **c** basidiospores **d** cheilocystidia **e** pileipellis **f** hyphae of stipitipellis. Scale bars: 5 mm (**a**); 10 µm (**b–f**).

Mycena roseolamellata **L.N. Liu, sp. nov.**

MycoBank No: 856026
Figs 10, 11

Diagnosis. Differs from *M. pura* in having a brown pileus and pink lamellae.

Holotype. China• Hunan Province, Ningxiang City, Biandan'ao, Lijingpu Subdistrict, 28°12'07"N, 112°32'43"E, elev. 110 m, 28 November 2023, ShengQiang Liu, *HUIF60001* (collection number NN601).

Etymology. Refers to the pink colors of lamellae.

Description. Pileus 7–17 mm diam., parabolic when young, then campanulate or broadly conical with age, apex with an obtuse umbo, sulcate, translucent-striate, glabrous, dark brown (6F5–6F8) at first, then turning pale brownish yellow (6A4) to pale brown (6E4) with age, margin brownish white (6A2) to pale brown (6D4–6D6). Context white, fragile, thin. Lamellae 24–26 reach the stipe, with 1–2 tiers of lamellulae, adnate or slightly adnex, white (4A1) when young, pinkish to light pink (9A3–9A2) at maturity, concolorous with faces. Stipe 29–30 × 2.0–3.0 mm, central, cylindrical, hollow, dark brown (6F5-6F8), pale brownish yellow (6A4) to pale brown (6D7) with age, base covered with long, dense, white fibrils. Odor and taste indistinctive.

Basidiospores (8.3) 8.6–10.8 (11.5) × (5.3) 5.4–6.3 (6.4) µm, Q = 1.5–2.0, Q = 1.7 ± 0.1, ellipsoid to elongated, hyaline, smooth, thin-walled, amyloid. Basidia 21.7–30.8 × 6.8–8.9 µm, 2-spored, clavate. Cheilocystidia 26.7–84.9 × 8.6–18.7 µm, abundant, fusiform, ventricose-rostrate, obtuse apex, base tapered, with short to long stalk, smooth, hyaline, amyloid, thin-walled. Pleurocystidia similar to cheilocystidia, 52.3–105.7 × 12.3–20.9 µm. Pileipellis 1.0–6.0 µm wide, smooth, terminal hyphae sometimes diverticulate, 1.0–6.0 × 1.0–2.0 µm. Stipitipellis 2.0–5.0 µm, smooth, terminal hyphae sometimes diverticulate, 1.0–4.0 × 1.0–2.0 µm. Clamp connections are absent in the basidia, pileipellis, and stipitipellis hyphae.

Habitat. Gregarious on decayed twigs of bamboo or woody debris of deciduous trees.

Known distribution. Ningxiang City, Hunan Province.

Additional materials examined. China • Hunan Province, Ningxiang City, Biandan'ao, Lijingpu Subdistrict, 28°12'07"N, 112°32'43"E, elev. 110 m, 22 December 2023, ShengQiang Liu, *HUIF60002* (collection number NN602).

Notes. *Mycena roseolamellata* is classified into sect. *Calodontes* based on the smooth cheilocystidia and stipitipellis. Microscopically, *M. pura* (Pers.) P. Kumm. is the most similar to *M. roseolamellata*; however, *M. pura* is distinguished from *M. roseolamellata* by its purple pileus with pinkish or brown tints, lamellae interveined with age, the presence of clamp connections in all tissues, and the absence of a root-like, pruinose stipe (Robich 2003; Aronsen and Læssøe 2016). *Mycena rosea* Gramberg is somewhat similar to *M. roseolamellata*; they have pink lamellae, smooth cheilocystidia, and pleurocystidia. *Mycena rosea* can be distinguished from *M. roseolamellata* by having a pink pileus with a dull yellow center, a white or pink stipe, and the presence of clamp connections in all tissues (Robich 2003; Aronsen and Læssøe 2016). *Mycena roseolamellata* is very different from any species of sect. *Calodontes*, owing to its brown pileus. *Mycena galericulata* (Scop.) Gray shares some similarities with *M. roseolamellata* in terms of pileus color, but *M. galericulata* is differentiated by the presence of non-smooth cheilocystidia, pileipellis, and stipitipellis (Maas Geesteranus 1992a, 1992b).

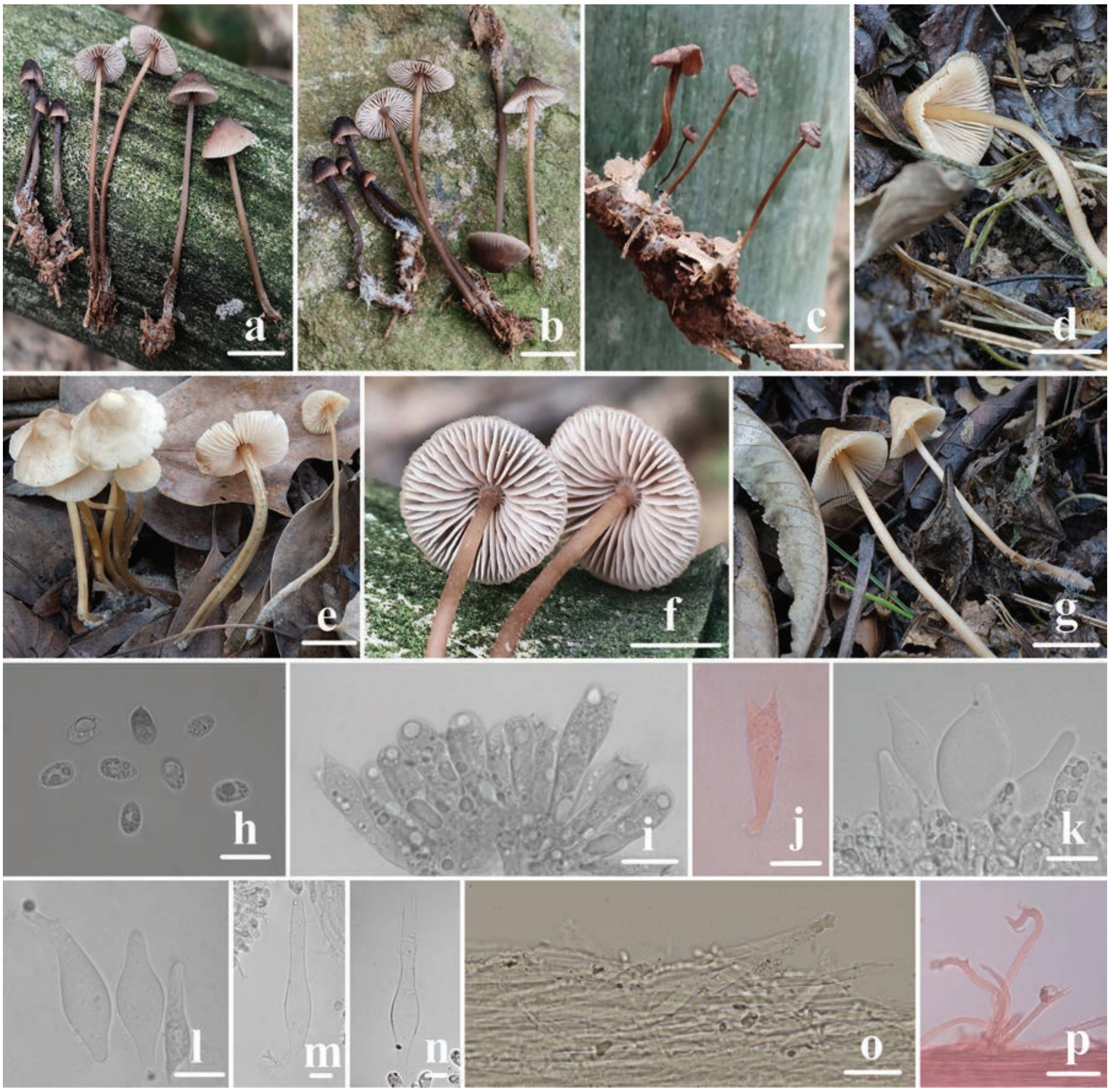

Figure 10. Basidiomata and microscopic features of *Mycena roseolamellata* **a–g** basidiomata **h** basidiospores **i, j** basidia **k, l** cheilocystidia **m, n** pleurocystidia **o** pileipellis **p** stipitipellis. Structures (**j, p**) were stained in 1% Congo red solution, and **h, i, k–o** were rehydrated in 5% KOH solution. Scale bars: 1 cm (**a–g**); 10 μm (**h–p**).

Discussion

The combination of morphological features and phylogenetic analyses revealed the presence of 30 species in Hunan Province, including five new species. In the Maas Geesteranus classification, the new species *M. fulvomarginata*, *M. huangsangensis*, *M. subroriduliformis*, and *M. roseolamellata* are classified into sect. *Rubromarginatae*, sect. *Polyadelphia*, sect. *Insignes*, and sect. *Calodontes*, respectively (Maas Geesteranus 1980, 1992a, 1992b; Maas Geesteranus and De Meijer 1997; Robich 2003, 2016). However, we could not place the new species *M. hongfengensis* in any section at present due to its special characteristics. The taxonomy of *Mycena* is overly complex, and infrageneric classification generally relies on the reported morphology of *Mycena*, and the characteristics of some species are not consistent with the common features shared by species of the numerous sections. Therefore, we need to increase the number of related species to identify the common characteristics of those species and further improve the taxonomy of *Mycena*.

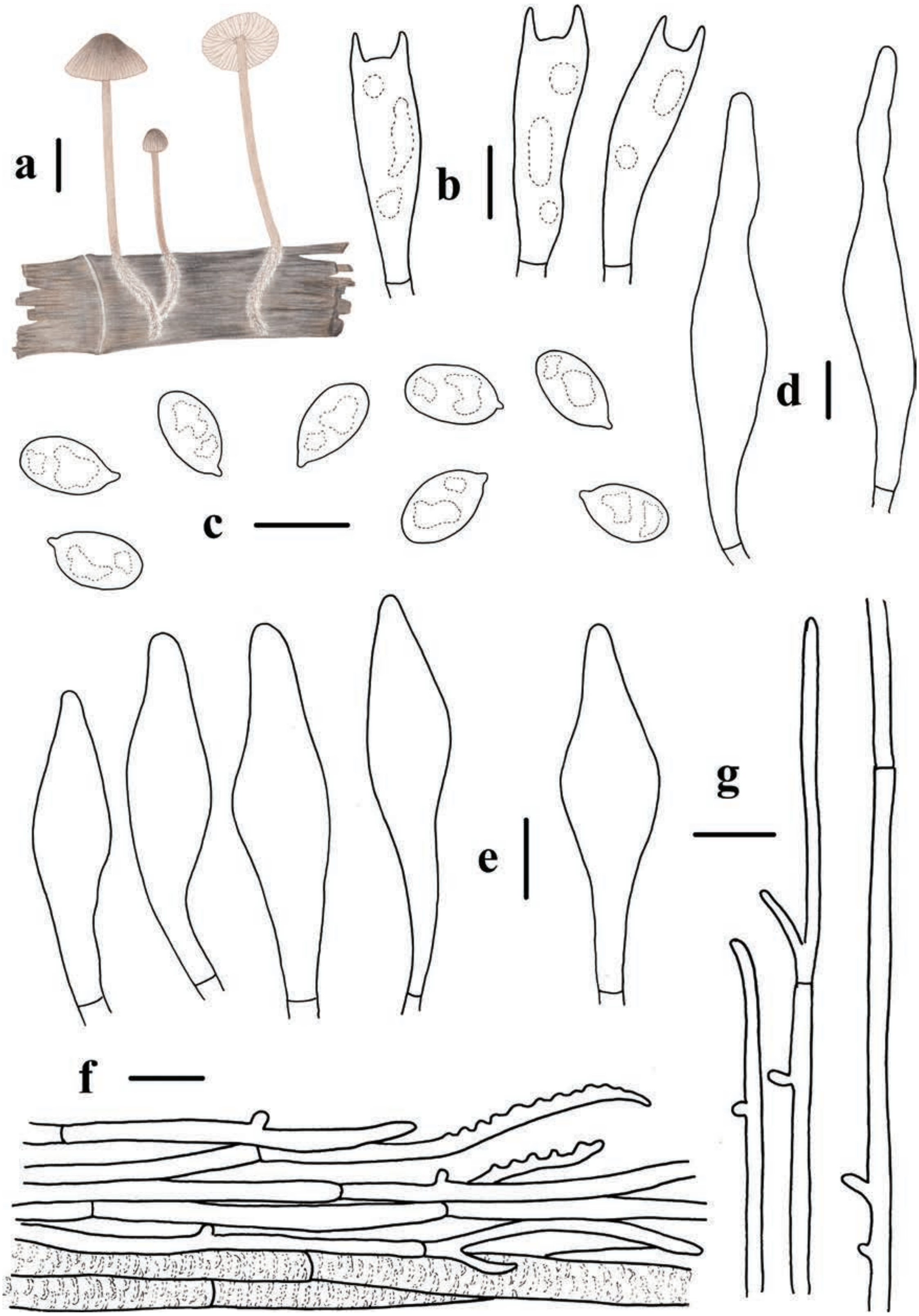

Figure 11. Morphological features of *Mycena roseolamellata* **a** basidiomata **b** basidia **c** basidiospores **d** pleurocystidia **e** cheilocystidia **f** pileipellis **g** hyphae of stipitipellis. Scale bars: 1 cm (**a**); 10 μm (**b–g**).

Among the 30 *Mycena* species collected in Hunan, we found *M. picta* (Fr.) Harmaja on Yuelu Mountain, Hunan. As we obtained only one basidiomata in the field, sequences of *M. picta* could not be obtained for phylogenetic analysis.

However, we can confirm that the specimen is *M. picta* based on its distinct macroscopic and microscopic characteristics (Aronsen and Læssøe 2016; Bau et al. 2021). And *M. heteracantha* was also collected in Yuelu Mountain (Na and Bau 2019a). We are uncertain of the classification of *M. juniperina* Aronsen and *M. meliigena* (Berk. & Cooke) Sacc. Distinguishing the 8 related specimens we collected in Hunan was difficult because of their similar microcharacteristics and the limited number of sequences available for downloading from GenBank, although the color of their basidiomata varies. Therefore, we identified all the related specimens we collected as *M. juniperina/meliigena*, as we did not obtain type specimens. Additional studies are needed.

Among the phylogenetic trees, *M. hongfengensis*, *M. deeptha* Aravind. & Manim. and *M. pluteoides* T. Bau & Q. Na were grouped into clade 1. Interestingly, all species have a non-smooth pileipellis hyphae. Most species collected from Hunan are mainly concentrated in clade 2. Four new species are grouped in clade 2; all *Mycena* species in this clade have a stipe or a stipe base that is covered with white fibrils.

The distinct topography, climate, and flora of Hunan Province have produced abundant and distinctive *Mycena* specimens. We conducted a comparative analysis of the geographical compositions of the 30 *Mycena* species we collected and preliminarily divided the distribution of the genus *Mycena* in Hunan Province into the following four types (Table 1). The analysis of the floristic components of the species reveals that *Mycena* in Hunan Province is cosmopolitan, exhibiting tropical-subtropical floristic characteristics as well as a certain proportion of northern temperate characteristics, indicating that *Mycena* species in Hunan possess diverse and transitional features.

Although *Mycena* was widely distributed in the world, the earliest and most detailed research was conducted in Europe and North America (Singer and Digilio 1951; Robich 2003, 2016). The morphological and microscopic characteristics of the *Mycena* species collected in Hunan Province are basically consistent with those of materials from Europe. However, the sizes of the basidiomata, basidiospores, basidia, cheilocystidia, and caulocystidia occasionally vary subtly. This may be due to the geographical location and environmental changes in the species at that time. From a geographical point of view, the *Mycena* species we collected show some differences compared with those documented in monographs from Europe and North America. Free lamellae are important for diagnosing these species in *Mycena*. We found that *Mycena* with free lamellae are more commonly collected in Hunan Province than in temperate regions in China; for example, *M. deeptha* and *M. pluteoides*, belonging to sect. *Exornatae* Maas Geest, are widely distributed in the western and southern areas of Hunan. And members of the sect. *Exornatae* are most commonly found in subtropical regions of Asia (Desjardin et al. 2010; Aravindakshan et al. 2012; Aravindakshan and Manimohan 2013a; Bau et al. 2021). These findings also indirectly suggest that sect. *Exornatae* has a certain preference for geographical location. Our research may contribute to the exploration of the origin and evolution of *Mycena*.

Key to the known species of *Mycena* in Hunan Province

1 Stipe arising from a basal disc **2**
– Stipe not arising from a basal disc.. **3**

2 Dermatocysts present in the pileipellis and stipitipellis .... ***M. hongfengensis***
– Dermatocysts absent in the pileipellis and stipitipellis **4**
3 Fresh and young basidiomata exude colored fluid when damaged .... ***M. haematopus***
– Basidiomata do not exude colored fluid when damaged **7**
4 Pileus glabrous, viscid, white, with a pale brown center, depressed at the center **5**
– Pileus dry, pubescent, pure white, not depressed at center **6**
5 Cheilocystidia vesiculose, smooth .... ***M. deeptha***
– Cheilocystidia densely covered with projections .... ***M. pluteoides***
6 Basidiomata growing on *Castanea* burs, pileus slightly pubescent .... ***M. castaneicola***
– Basidiomata growing on dead wood or humus layer, pileus with bran-like covering .... ***M. heteracantha***
7 Lamellae not white, or occasionally white when young **8**
– Lamellae white **9**
8 Lamellae faces pink, occasionally white when young, cheilocystidia hyaline .... ***M. roseolamellata***
– Lamellae faces orange-yellow, cheilocystidia with yellow contents .... ***M. leaiana***
9 Cheilocystidia smooth **10**
– Cheilocystidia with simple to branched excrescences **21**
10 Lamellae faces not concolorous with the sides **11**
– Lamellae faces concolorous with the sides **12**
11 Lamellae edges light yellow .... ***M. citrinomarginata***
– Lamellae edges light brown to yellowish-brown .... ***M. fulvomarginata***
12 Hyphae of the pileipellis smooth **13**
– Hyphae of the pileipellis diverticulate **16**
13 Pileus brown .... ***M. algeriensis***
– Pileus violet **14**
14 Pleurocystidia absent **15**
– Pleurocystidia present .... ***M. pura***
15 Pileipellis not gelatinized .... ***M. yuezhuoi***
– Pileipellis gelatinized .... ***M. pearsoniana***
16 Lamellae adnate or adnexed **17**
– Lamellae decurrent **18**
17 Pileus grey brown **19**
– Pilues white **20**
18 Cheilocystidia thick-walled .... ***M. subpiligera***
– Cheilocystidia thin-walled .... ***M. digitifurcata***
19 Hyphae of the stipitipellis smooth, caulocystidia present .... ***M. leptocephala***
– Hyphae of the stipitipellis covered with warty or diverticulae, caulocystidia absent .... ***M. abramsii***
20 Pileipellis and stipitipellis gelatinized .... ***M. laevigata***
– Pileipellis and stipitipellis not gelatinized .... ***M. adnexa***
21 Basidiomata sticky .... ***M. subroriduliformis***
– Basidiomata dry **22**
22 Pileus with yellow tone **23**
– Pileus without yellow tone **24**

23 Pileus bucket-shaped, lamellae broader than the length................ ***M. picta***
– Pileus hemispherical, parabolical to convex, lamellae broad..***M. meliigena*/*M. juniperina***
24 Basidiospores globose ....***M. corynephora***
– Basidiospores broadly ellipsoid to ellipsoid **25**
25 Pileus and lamella with red spots when old .... ***M. maculata***
– Pileus and lamella without red spots when old..**26**
26 Rhizomorphs present .... ***M. chlorocyanea***
– Rhizomorphs absent **27**
27 Clamp connections absent in all tissues ....***M. galericulata***
– Clamp connections present in all tissues...**28**
28 Acanthocysts present, acanthocysts of two types, pyriform to vesicular... ***M. bicystidiata***
– Acanthocysts absent **29**
29 Pileus and stipe pruninose, iodoform when dry .... ***M. filopes***
– Pileus and stipe glabrous, odor indistinctive................ ***M. huangsangensis***

Acknowledgements

Thanks to Prof. Zuo Hong Chen of Hunan Normal University for providing help in fieldwork. Thanks to Prof. Xun Lin Yu from the Central South University of Forestry and Technology for his help in plant identification. Thanks to Ms. Shuang Qu and Ms. Chang Zhuo Liu for helping with the article layout design and specimen collection and to Mr. Sheng Qiang Liu and Mr. Wu Ping Luo for providing the specimens in this study.

Additional information

Conflict of interest

The authors have declared that no competing interests exist.

Ethical statement

No ethical statement was reported.

Funding

This study was supported by the Hunan Natural Science Foundation (2023JJ50073) and the Graduate Scientific Research Innovation Project of Jishou University (Jdy22072).

Author contributions

Data curation: YT. Investigation: SNL, YT. Resources: JBL, LGF. Validation: SNL, ARS, BMS. Writing - original draft: YXX. Writing - review and editing: ZXL, ZMT, LNL.

Author ORCIDs

Ying Xin Xiao https://orcid.org/0009-0008-7041-503X
Li Na Liu https://orcid.org/0000-0003-3241-4016
Zhu Ming Tan https://orcid.org/0000-0001-6696-1179
Ai Rong Shen https://orcid.org/0000-0003-4543-0250
Bao Ming Shen https://orcid.org/0000-0003-0110-3370

Yun Tan https://orcid.org/0000-0002-8129-0163
Sai Nan Li https://orcid.org/0000-0002-8818-446X
Zhu Xiang Liu https://orcid.org/0000-0001-6014-3554

Data availability

All of the data that support the findings of this study are available in the main text.

References

Afyon A, Konuk M, Yağiz D, Helfer S (2005) A study of wood decaying macrofungi of the western Black Sea region, Turkey. Mycotaxon 93: 319–322.

Aravindakshan DM, Manimohan P (2013a) A new species of *Mycena* sect. *Exornatae* and some taxonomic observations. Mycosphere 4(1): 146–150. https://doi.org/10.5943/mycosphere/4/1/9

Aravindakshan DM, Manimohan P (2013b) *Mycena* sect. *Galactopoda*: Two new species, a key to the known species and a note on the circumscription of the section. Mycosphere 4(4): 653–659. https://doi.org/10.5943/mycosphere/4/4/1

Aravindakshan DM, Kumar TKA, Manimohan P (2012) A new bioluminescent species of *Mycena* sect. *Exornatae* from Kerala State, India. Mycosphere 3(5): 556–561. https://doi.org/10.5943/mycosphere/3/5/4

Aronsen A (1996) *Mycena juniperina*, a new member of section *Supinae* from Norway. Persoonia-Molecular Phylogeny and Evolution of Fungi 16(2): 257–259.

Aronsen A, Læssøe T (2016) The genus *Mycena* s.l. Fungi of Northern Europe 5. Narayana Press, Gylling, Denmark, 373 pp.

Baldrian P, Zrůstová P, Tláskal V, Davidová A, Merhautová V, Vrška T (2016) Fungi associated with decomposing deadwood in a natural beech-dominated forest. Fungal Ecology 23: 109–122. https://doi.org/10.1016/j.funeco.2016.07.001

Ballesteros E (1984) Primera contribució al coneixement dels macromicets del Massís de Cadiretes (La Selva). Butlletí de la Institució Catalana d'Història Natural 51(Sec. Bot., 5): 67–76. https://digital.csic.es/bitstream/10261/97720/1/primera%20contribuci%C3%B3.pdf

Bau T, Na Q, Liu LN (2021) A monograph of Mycenaceae (Agaricales) in China. Science press, Beijing, 326 pp.

Beardslee HC, Coker WC (1924) The Mycenas of North Carolina. Journal of the Elisha Mitchell Scientific Society 40(1/2): 49–91. https://dc.lib.unc.edu/cdm/ref/collection/jncas/id/1348

Bronckers R, Kelderman PH (2011) Paddenstoelen in Groeve't Rooth: een voorlopig resultaat van tien jaar inventariseren. Natuurhistorisch Maandblad 100(8): 121–128. https://natuurtijdschriften.nl/pub/1003301

Casabón JCC (2015) El Género Lactarius En El Sur De Europa. Introducción Al Conocimiento De Algunas Especies Mediterráneas. Annali del XXI Giornate della Conferenza Europea di Micologia Mediterranea 21: 67–72. https://www.micobotanicajaen.com/AsoJaen/Actividades/Actividades2013/03CEMM2013/Anales.pdf

Chen ZH, Zhang P (2019) Atlas of Macrofungi in Hunan. Hunan Science and Technology Press, Changsha, 426 pp.

Chew ALC, Tan YS, Desjardin DE, Musa MY, Sabaratnam V (2014) Four new bioluminescent taxa of *Mycena* sect. *Calodontes* from Peninsular Malaysia. Mycologia 106(5): 976–988. https://doi.org/10.3852/13-274

Chew ALC, Desjardin DE, Tan YS, Musa MY, Sabaratnam V (2015) Bioluminescent fungi from Peninsular Malaysia—a taxonomic and phylogenetic overview. Fungal Diversity 70(1): 149–187. https://doi.org/10.1007/s13225-014-0302-9

Cho DH, Chung JY (2020) Study of fungal diversity of Mt. Cheonggye. Korean Journal of Nature Conservation 19(1): 29–60. https://doi.org/10.30960/kjnc.2020.19.1.29

Cho DH, Chung JY (2023) Study of fungal diversity and fungal resources in Mt. Gwangdeok. Korean Journal of Nature Conservation 22(1): 1–26. https://doi.org/10.30960/kjnc.2023.22.1.1

Cho M, Kwon SL, Jang S, Yoo Y, Lee SH, Kwon DY, Kim C, Lim YW, Kim JJ (2024) Notes of 15 unrecorded macrofungi in Korea. Journal of Species Research 13(1): 67–88. https://doi.org/10.12651/JSR.2024.13.1.067

Cooper AC, Desjardin DE, Perry BA (2018) The genus *Mycena* (Basidiomycota, Agaricales, Mycenaceae) and allied genera from Republic of São Tomé and Príncipe, West Africa. Phytotaxa 383(1): 1–47. https://doi.org/10.11646/phytotaxa.383.1.1

Corner EJH (1994) Agarics in Malesia. II Mycenoid. Beih. Nova Hedwig 109: 165–271.

Cortés-Pérez A, Desjardin DE, Perry BA, Cruz V, Ramírez F, Villalobos-Arámbula AR, Rockefeller A (2019) New species and records of bioluminescent *Mycena* from Mexico. Mycologia 111(2): 1–20. https://doi.org/10.1080/00275514.2018.1554172

Cortés-Pérez A, Guzmán-Dávalos L, Ramírez-Cruz V, Villalobos-Arámbula AR, Ruiz-Sanchez E, Ramírez-Guillén F (2023) New species of bioluminescent *Mycena* sect. *Calodontes* (Agaricales, Mycenaceae) from Mexico. Journal of Fungi 9(9): 902. https://doi.org/10.3390/jof9090902

Desjardin DE (1995) A preliminary accounting of the worldwide members of *Mycena* sect. *Sacchariferae.* Bibliotheca Mycologica 159: 1–89.

Desjardin DE, Perry BA, Lodge DJ, Stevani CV, Nagasawa E (2010) Luminescent *Mycena*: New and noteworthy species. Mycologia 102(2): 459–477. https://doi.org/10.3852/09-197

Doğan HH, Karadelev M (2006) First record of *Mycena juniperina* from Turkey on a new host. Mycologia Balcanica 3: 77–79. https://doi.org/10.5281/zenodo.2547358

Emmett EE (1992) British *Mycena* species—3. Mycologist 6(4): 165–173. https://doi.org/10.1016/S0269-915X(09)80559-4

Fan LF, Wang BY, Ma TF, Li B, Ma JW, Lei XT, Bao NH (2024) Three new species of *Gymnopus* and *Mycena* (Agaricales, Basidiomycota) from Northwestern China. Frontiers in Microbiology 15: 1487598. https://doi.org/10.3389/fmicb.2024.1487598

Fries EM (1821) Systema mycologicum, 3 Vols. Office Berlingiana, Lund, Greifswald, 202 pp.

Fukasawa Y, Osono T, Takeda H (2009) Effects of attack of saprobic fungi on twig litter decomposition by endophytic fungi. Ecological Research 24(5): 1067–1073. https://doi.org/10.1007/s11284-009-0582-9

Gao GM, Dou XY (1981) Hunan Physical Geography. Hunan People's Publishing House, Changsha, 204 pp.

Gáperová S, Náplavová K, Gáper J (2015) Ectomycorrhizal and saprotrophic macrofungi associated with woody plants in the borova hora arboretum. Thaiszia Journal of Botany 25(1): 163–170.

Gierczyk B, Kujawa A, Szczepkowski A, Ślusarczyk T, Kozak M, Mleczko P (2015) XXI Wystawa Grzybów Puszczy Białowieskiej: materiały do poznania mykobioty Puszczy Białowieskiej. Przegląd Przyrodniczy 26(3): 10–50.

Gilliam MS (1976) The genus *Marasmius* in the northeastern United States and adjacent Canada. Mycotaxon 4(1): 1–144.

Glez-Penñ D, Gómez-Blanco D, Reboiro-Jato M, Fdez-Riverola F, Posada D (2010) ALTER: Program-oriented conversion of DNA and protein alignments. Nucleic Acids Research 38(suppl_2): W14–W18. https://doi.org/10.1093/nar/gkq321

Grgurinovic CA (1998) *Mycena* in Australia: Section *Lactipedes*. Botanical Journal of Scotland 50(2): 199–208. https://doi.org/10.1080/03746609808684917

Grgurinovic CA (2003) The Genus *Mycena* in South-Eastern Australia. Fungal Diversity Press, Hong Kong, 329 pp.

Guerreiro MA, Kambach S, Stoll R, Brachmann A, Senker J, Begerow D, Peršoh D (2023) Linking processes to community functions—insights into litter decomposition combining fungal metatranscriptomics and environmental NMR profiling. Mycological Progress 22(2): 10. https://doi.org/10.1007/s11557-022-01859-0

Gyosheva MM, Stoykov DY, Marinov YA (2016) Data on the fungal diversity of Balgarka Nature Park (Central Balkan, Bulgaria). Phytologia Balcanica 22(3): 309–322.

Halama M, Romański M (2010) A new record of *Mycena picta* (Fr.: Fr.) Harmaja (Agaricales, Basidiomycota) from the Wigierski National Park (NE Poland). Opole Scientific Society Nature Journal 43: 29–36.

Halama M, Chachuła P, Rutkowski R (2014) *Mycena Juniperina* (Agaricales, Basidiomycota), new for the polish and central European Mycobiota. Polish Botanical Journal 59(1): 109–116. https://doi.org/10.2478/pbj-2014-0008

Hall TA (1999) BioEdit: A user-friendly biological sequence alignment editor and analysis program for Windows 95/98/NT. Nuclc Acids Symposium Series 41(41): 95–98. https://doi.org/10.12691/ajidm-4-3-3

Harder CB, Lodge DJ, Petersen RH, Hughes KW, Blanco JC, Frøslev TG, Læssøe T (2012) Amyloidity is not diagnostic for species in the *Mycena pearsoniana* complex (*Mycena* section *Calodontes*). Mycological Progress 11: 725–732. https://doi.org/10.1007/s11557-011-0782-x

Hintikka V (1963) Studies in the genus *Mycena* in Finland. Karstenia 6(7): 77–87. https://doi.org/10.29203/ka.1963.39

Hughes KW, Petersen RH, Lickey EB (2009) Using heterozygosity to estimate a percentage DNA sequence similarity for environmental species' delimitation across basidiomycete fungi. New Phytologist 795–798. https://doi.org/10.1111/j.1469-8137.2009.02802.x

Hughes KW, Matheny PB, Miller AN, Petersen RH, Iturriaga TM, Johnson KD, Methven AS, Raudabaugh DB, Swenie RA, Bruns TD (2020) Pyrophilous fungi detected after wildfires in the Great Smoky Mountains National Park expand known species ranges and biodiversity estimates. Mycologia 112(4): 677–698. https://doi.org/10.1080/00275514.2020.1740381

Imai S (1938) Studies on the Agaricaceae of Hokkaido. I. Journal of the Faculty of Agriculture. Hokkaido Imperial University 43(1): 1–178.

Kalamees K, Raitviir A (2006) Macromycetes on Ainovy islands (Murmansk region, Russia). Meddelelser om Grønland. Bioscience 56: 139–147. https://doi.org/10.7146/mogbiosci.v56.142877

Katoh K, Standley DM (2013) MAFFT multiple sequence alignment software version 7: Improvements in performance and usability. Molecular Biology and Evolution 30(4): 772–780. https://doi.org/10.1093/molbev/mst010

Kirk PM, Cannon P, Stalpers J, Minter DW (2008) Dictionary of the Fungi. 10th edn. Centre for Agriculture and Bioscience International, Wallingford, UK, 771 pp.

Kornerup A, Wanscher JH (1978) Methuen handbook of colour. Eyre Methuen, London, 252 pp.

Kozlov AM, Darriba D, Flouri T, Morel B, Stamatakis A (2019) RAxML-NG: A fast, scalable, and user-friendly tool for maximum likelihood phylogenetic inference. Bioinformatics 35(21): 4453–4455. https://doi.org/10.1093/bioinformatics/btz305

Kühner R (1926) Contribution à l'étude des Hyménomycètes et spécialement des Agaricacés. Le Botaniste 17: 1–215.

Kühner R (1931) Utilisation de la réaction iodée dans la classification des *Mycena*. Bulletin Mensuel de la Societe Linneenne de Lyon 8: 122–127.

Kühner R (1938) Le genre *Mycena*. Encyclopedie Mycologique 10: 1–710.

Kwon SL, Jang S, Kim C, Lim YW, Kim JJ (2020) Note of five unrecorded mushrooms including three rare species on Mount Juwang in Korea. Mycobiology 48(3): 157–168. https://doi.org/10.1080/12298093.2020.1759348

Laganà A, Salerni E, Barluzzi C, De Dominics V, Perini C (2002) Fungi (macromycetes) in various types of Mediterranean forest ecosystems (Tuscany, Italy). Polish Botanical Journal 47(2): 143–165.

Lange JE (1914) Studies in the agarics of Denmark I. Dansk botanisk arkiv udgivet af Dansk botanisk forenin 1(5): 1–40.

Lee HR, Han M, Choi MN, Lee H, Lee SW, Park EJ (2017) Enhancement of the germination efficiency of *Gastrodia elata* seeds using a new *Mycena* species. Journal of Plant Biotechnology 44(1): 56–60. https://doi.org/10.5010/JPB.2017.44.1.056

Lee JK, Kim DH, Nguyen MH, Bae YJ, Manilak P (2021) A checklist of mushrooms of Dong Hua Sao National Biodiversity Conservation Area (DHSNBCA) of Lao-PDR. Journal of Forest and Environmental Science 37(2): 163–167. https://doi.org/10.7747/JFES.2021.37.2.163

Li JZ, Hu XW, Peng YB (1993) Macrofungi of Hunan. Hunan Normal University Press, Changsha, 418 pp.

Liu ZW, Na Q, Cheng XH, Wu XM, Ge YP (2021) *Mycena yuezhuoi* sp. nov. (Mycenaceae, Agaricales), a purple species from the peninsula areas of China. Phytotaxa 511(2): 148–162. https://doi.org/10.11646/phytotaxa.511.2.3

Liu LN, Zhou GY, Tan ZM, Tian YX (2022a) Two new *Mycena* (Mycenaceae, Agaricales) species with rhizomorphs from subtropical areas of China. Phytotaxa 576(1): 75–88. https://doi.org/10.11646/phytotaxa.576.1.4

Liu LN, Zhou GY, Shen AR, Shen BM, Tan Y, Tan ZM (2022b) *Mycena subpiligera* sp. nov., a symbiotic species from china associated with the seed germination of *Gastrodia elata*. Mycobiology 50(5): 294–301. https://doi.org/10.1080/12298093.2022.2132001

Liu XF, Deng PT, Wang XY, Zhang P (2024) A new edible *Clavulina* species from Hunan Province, China. Phytotaxa 661(2): 169–180. https://doi.org/10.11646/phytotaxa.661.2.4

Liu LN, Shen AR, Shen BM, Tan Y, Li SN, Tan ZM (2025) Preliminary study on species diversity of symbiotic *Mycena* sensu lato promoting *gastrodia elata* seed germination. Acta Edulis Fungi 32(1): 65–76.

Lu W, Priyashantha AKH, Galappaththi MC, Tibpromma S, Dai DQ, Patabendige NM, Premarathne BM, Kulasuriya DM, Ediriweera AN, Nimalrathna TS, Suwannarach N, Lumyong S, Tang A, Shao SC, Karunarathna SC (2024) Fungal bioluminescence: Past, present, and future. Diversity 16(9): 539. https://doi.org/10.3390/d16090539

Łuszczyński J, Adamska E, Wojciechowska A, Czerwik-Marcinkowska J (2022) Diversity patterns of macrofungi in Xerothermic Grasslands from the Nida Basin (Małopolska Upland, Southern Poland): A case study. Biology 11(4): 531. https://doi.org/10.3390/biology11040531

Maas Geesteranus RA (1980) Studies in Mycenas—15. A tentative subdivision of the genus *Mycena* in the northern Hemisphere. Persoonia-Molecular Phylogeny and Evolution of Fungi 11(1): 93–120. https://repository.naturalis.nl/pub/531705

Maas Geesteranus RA (1983) Conspectus of the Mycenas of the Northern Hemisphere. 1. Sections *sacchariferae*, *basipedes*, *bulbosae*, *clavulares*, *exiguae*, and *longisetae*. Proceedings of the Koninklijke Nederlandse Akademie van Wetenschappen. Series C. Biological and Medical Sciences 86: 401–421.

Maas Geesteranus RA (1986) Conspectus of the Mycenas of the Northern Hemisphere 6. Sections *Polyadelphia* and *Saetulipedes*. Koninklijke Nederlandse Akademie van Wetenschappen, Proceedings, Series C 89(2): 159–182.

Maas Geesteranus RA (1988) Conspectus of the Mycenas of the Northern Hemisphere 9. Section *Fragilipedes*, species AG. Koninklijke Nederlandse Akademie van Wetenschappen, Proceedings, Series C 91: 43–83.

Maas Geesteranus RA (1989) Conspectus of the Mycenas of the Northern Hemisphere, 12. Sections *Fuliginellae*, *Insignes*, *Ingratae*, *Euspeireae*, and *Caespitosae*. Koninklijke Nederlandse Akademie van Wetenschappen, Proceedings, Series C 92: 331–365.

Maas Geesteranus RA (1992a) Mycenas of the Northern Hemisphere I. Studies in Mycenas and other papers. Koninklijke Nederlandse Akademie van Wetenschappen, Amsterdam, 493 pp.

Maas Geesteranus RA (1992b) Mycenas of the Northern Hemisphere(II, Conspectus of the Mycenas of the Northern Hemisphere). Koninklijke Nederlandse Akademie van Wetenschappen, Amsterdam, 904 pp.

Maas Geesteranus RA (1992c) Some Myceneae of the Himalayan foothills. Persoonia-Molecular Phylogeny and Evolution of Fungi 15(1): 33–53. https://archive.org/details/persoonia531739

Maas Geesteranus RA, De Meijer AAR (1997) Mycenae paranaenses. Proceedings van de Koninklijke Nederlandse Akademie van Wetenschappen (Ser C), Amsterdam, North-Holland, 164 pp.

Maas Geesteranus RA, Horak E (1995) *Mycena* and related genera from Papua new Guinea and new Caledonia. Bibliography. Mycology 159: 143–229.

Malysheva V, Malysheva E, Voronina EY, Fedosova A, Bibikov N, Kiseleva D, Tiunov A, Kovalenko A (2017) Mycorrhiza of pyroloids (*Pyrola rotundifolia*, *P. media* and *Orthilia secunda*): Species composition of symbionts and trophic status of plants. Mikologiâ i Fitopatologiâ 51(6): 350–364.

Marra D (2000) Osservazioni sui macromiceti nella Riserva Naturale Regionale del Lago di Villa (Challand St. Victor, Valle d'Aosta). Revue Valdôtaine d'Histoire Naturelle 54: 37–56.

Matheny PB, Curtis JM, Hofstetter V, Aime MC, Moncalvo JM, Ge ZW, Yang ZL, Slot JC, Ammirati JF, Baroni TJ, Bougher NL, Hughes KW, Lodge DJ, Kerrigan RW, Seidl MT, Aanen DK, DeNitis M, Daniele GM, Desjardin DE, Kropp BR, Norvell LL, Parker A, Vellinga EC, Vilgalys R, Hibbett DS (2006) Major clades of Agaricales: A multilocus phylogenetic overview. Mycologia 98(6): 982–995. https://doi.org/10.1080/15572536.2006.11832627

Métrod G (1949) Les Mycènes de Madagascar: (*Mycena*, *Corrugaria*, *Pterospora*). Prodrome à une flore mycologique de Madagascar 3: 1–146.

Miyamoto T, Cha JY, Igarashi T (1996) A new record of *Mycena picta* from Japan. Mycoscience 37(4): 463–466. https://doi.org/10.1007/BF02461005

Moncalvo JM, Vilgalys R, Redhead SA, Johnson JE, James TY, Aime MC, Valerie H, Verduin SJW, Larsson E, Baroni TJ, Thorn RG, Jacobsson S, Clémençon H, Miller OK (2002) One hundred and seventeen clades of euagarics. Molecular Phylogenetics and Evolution 23(3): 357–400. https://doi.org/10.1016/S1055-7903(02)00027-1

Moreno G, Albertó E (1996) Agaricales sensu lato de Argentina. I. Cryptogamie Mycologie 17(2): 61–84. https://doi.org/10.5962/p.354462

Mustafabayli EH, Aghayeva DN (2019) Mushroom diversity in Shaki district of Azerbaijan. Plant & Fungal Research 2(1): 23–31. https://doi.org/10.29228/plantfungalres.45

Na Q, Bau T (2018) New species of *Mycena* (Mycenaceae, Agaricales) with colored lamellae and three new species records from China. Phytotaxa 361(3): 266–278. https://doi.org/10.11646/phytotaxa.361.3.2

Na Q, Bau T (2019a) *Mycena* section *Sacchariferae*: Three new species with basal discs from China. Mycological Progress 18: 483–493. https://doi.org/10.1007/s11557-018-1456-8

Na Q, Bau T (2019b) Recognition of *Mycena* sect. *Amparoina* sp. nov. (Mycenaceae, Agaricales), including four new species and revision of the limits of sect. *Sacchariferae*. MycoKeys 52: 103–124. https://doi.org/10.3897/mycokeys.52.34647

Na Q, Liu ZW, Zeng H, Ke BR, Song ZZ, Cheng XH, Ge YP (2022) Taxonomic studies of bluish *Mycena* (Mycenaceae, Agaricales) with two new species from northern China. MycoKeys 90: 119. https://doi.org/10.3897/mycokeys.90.78880

Nauta M, Vellinga EC (1992) Towards a distribution atlas of macrofungi in the Netherlands. Mycologist 6(1): 6–10. https://doi.org/10.1016/S0269-915X(09)80506-5

Nylander J (2004) MrModeltest 2.3, Computer program and documentation distributed by the author. Evolutionary Biology Centre, Uppsala University, Uppsala.

Oliveira JJ, Vargas-Isla R, Cabral TS, Cardoso JS, Andriolli FS, Rodrigues DP, Ikeda T, Clement CR, Ishikawa NK (2021) The Amazonian luminescent *Mycena cristinae* sp. nov. from Brazil. Mycoscience 62(6): 395–405. https://doi.org/10.47371/mycosci.2021.05.004

Osmundson TW, Robert VA, Schoch CL, Baker LJ, Smith A, Robich G, Mizzan L, Garbelotto MM (2013) Filling gaps in biodiversity knowledge for macrofungi: Contributions and assessment of an herbarium collection DNA barcode sequencing project. PLoS ONE 8(4): e62419. https://doi.org/10.1371/journal.pone.0062419

Pegler DN (1977) A preliminary agaric flora of East Africa. Kew Bulletin Additional Series 6: 1–615.

Pegler DN (1983) Agaric flora of the Lesser Antilles. Kew Bulletin Additional Series 9: 1–668.

Pegler DN (1986) Agaric Flora of Sri Lanka. Kew Bulletin Additional Series 12: 1–519.

Pegler DN (1987) A revision of the Agaricales of Cuba 1. Species described by Berkeley & Curtis. Kew Bulletin 42(3): 501–585. https://doi.org/10.2307/4110064

Perry BA (2002) A taxonomic investigation of *Mycena* in California. Doctoral dissertation, San Francisco State University, California, USA

Perry BA, Desjardin DE (2016) New species of *Mycena* (Basidiomycota, Agaricales) from California. Phytotaxa 269(1): 33–40. https://doi.org/10.11646/phytotaxa.269.1.4

Petersen RH, Hughes KW, Lickey EB, Kovalenko AE, Morozova OV, Psurtseva NV, Morosova O (2008) A new genus, *Cruentomycena*, with *Mycena viscidocruenta* as the type species. Mycotaxon 105(4): 119–136.

Qing CJ (1990) Hunan vegetation. Hunan Science and Technology Press, Changsha, 420 pp.

Rathnayaka AR, Tennakoon DS, Jones GE, Wanasinghe DN, Bhat DJ, Priyashantha AH, Stephenson SL, Tibpromma S, Karunarathna SC (2024) Significance of precise documentation of hosts and geospatial data of fungal collections, with an emphasis on plant-associated fungi. New Zealand Journal of Botany 63(2–3): 462–489 [1–28]. https://doi.org/10.1080/0028825X.2024.2381734

Retnowati A, Kusumawaty A, Apandi I, Haryadi A (2020) Two newly recorded species of Agaricales (Basidiomycota) from Banggai Kepulauan, Sulawesi, Indonesia. Biodiversitas Journal of Biological Diversity 21(12): 5615–5621. https://doi.org/10.13057/biodiv/d211217

Robich G (2003) *Mycena* d'Europa Vol. 1. Associazione Micologica Bresadola, Trento, Italy, 728 pp.

Robich G (2016) *Mycena* d'Europa Vol. 2. Associazione Micologica Bresadola, Trento, 796 pp.

Ronquist F, Huelsenbeck JP (2003) MrBayes 3: Bayesian phylogenetic inference under mixed models. Bioinformatics 19(12): 1572–1574. https://doi.org/10.1093/bioinformatics/btg180

Roussel HFA (1806) Flore du Calvades et des terreins adjacens. 2nd edn. Caen, 252 pp.

Rudolf K, Pál-Fám F, Morschhauser T (2016) Macrofungi records from a wood pasture in the Belső-Cserehát (NE Hungary). Studia Botanica Hungarica 47(1): 29–40. https://doi.org/10.17110/StudBot.2016.47.1.29

Senn-Irlet B (1987) Pilze aus der alpinen stufe des Val d'Anniviers (Wallis). Bulletin de la Murithienne 105: 87–106. https://core.ac.uk/reader/20655250

Senn-Irlet B, Mürner R, Martini E, Küffer N, Marchi RD, Bieri G (2012) Saprobic fungi on wood and litter of Alnus alnobetula in the Swiss Alps. Mycotaxon 120(506): 1–34.

Shiryaeva OS (2018) New records of agaricoid fungi from Sverdlovsk Region, Russia. Botanica Lithuanica 24(2): 150–161. https://doi.org/10.2478/botlit-2018-0015

Singer R (1986) The Agaricales in modern taxonomy. Koeltz Scientific Books, Koenigstein, 1609 pp.

Singer R (1989) New taxa and new combinations of Agaricales (diagnoses fungorum novorum Agaricalium IV). Fieldiana: Botany New Series 21: 1–133. https://doi.org/10.5962/bhl.title.2537

Singer R, Digilio AP (1951) Pródromo de la flora agaricina Argentina. Lilloa 25: 1–461.

Smith AH (1935) Studies in the genus *Mycena*. I. American Journal of Botany 22(10): 858–877. https://doi.org/10.1002/j.1537-2197.1935.tb05071.x

Smith AH (1947) North American Species of *Mycena*. University of Michigan Press, Ann Arbor, Michigan, 521 pp.

Swartz D (1933) Studies of Arkansas Fungi. I. Basidiomycetes. American Midland Naturalist 14(6): 714–719. https://doi.org/10.2307/2420128

Swindell SR, Plasterer TN (1997) Sequence data analysis guidebook. Humana Press, Totowa.

Tholl MT, Baral HO, Schultheis B, Marson G, Diederich P (2000) Journées luxembourgeoises de mycologie vernale 1998. Bulletin de la Société des Naturalistes Luxembourgeois 100: 39–62. http://lichenology.info/pdf/Tholl2000.pdf

Türkekul İ (2017) New *Calbovista*, *Mycena*, *Rhizopogon*, *Stictis*, and *Symphyosirinia* records from Turkey. Mycotaxon 132(3): 503–512. https://doi.org/10.5248/132.503

Vaidya G, Lohman DJ, Meier R (2011) SequenceMatrix: Concatenation software for the fast assembly of multi-gene datasets with character set and codon information. Cladistics 27(2): 171–180. https://doi.org/10.1111/j.1096-0031.2010.00329.x

Veerkamp MT (2001) Paddestoelen in acht bosreservaten; Stille Eenzaamheid, Kremboong, Tongerense Hei, Norgerholt, Zwarte Bulten, Mattemburgh, Hollandse Hout en Houtribbos. Alterra, Wageningen, 101 pp.

Vilgalys R, Hester M (1990) Rapid genetic identification and mapping of enzymatically amplified ribosomal DNA from several *Cryptococcus* species. Journal of Bacteriology 172(8): 4238–4246. https://doi.org/10.1128/jb.172.8.4238-4246.1990

Villarreal M, Couceiro A, Sos C, Mateos J, Rodrigues H (2024) *Mycena dasypus* (Agaricales, Mycenaceae), Primer Registro En La Península Ibérica. Boletin de la Sociedad Micologica de Madrid 48: 63–70.

Vishwakarma P, Tripathi NN, Singh P (2017) A checklist of macrofungi of Gorakhpur District, UP India. Current Research in Environmental & Applied Mycology 7(2): 109–120. https://doi.org/10.5943/cream/7/2/8

Vu D, Groenewald M, De Vries M, Gehrmann T, Stielow B, Eberhardt U, Al-Hatmi A, Groenewald JZ, Cardinali G, Houbraken J, Boekhout T, Crous PW, Robert V, Verkley GJM (2019) Large-scale generation and analysis of filamentous fungal DNA barcodes boosts coverage for kingdom fungi and reveals thresholds for fungal species and higher taxon delimitation. Studies in Mycology 92(1): 135–154. https://doi.org/10.1016/j.simyco.2018.05.001

Watling R (1984) Larger fungi around Kindrogan, Perthshire. Transactions of the Botanical Society of Edinburgh 44(3): 237–259. https://doi.org/10.1080/03746608408685391

Wei RX, Ge YP, Qi LL, Han MH, Zeng H, Hu YP, Zou L, Cheng XH, Wu XM, Na Q (2024) Revealing brownish *Mycena* diversity in China: new discoveries and taxonomic insights. Journal of Fungi 10(6): 439. https://doi.org/10.3390/jof10060439

White T, Bruns T, Lee S, Taylor J (1990) Amplification and direct sequencing of fungal ribosomal RNA genes for phylogenetics. In: Innis M, Gelfand D, Shinsky J, White T (Eds) PCR protocols: a guide to methods and applications, 315–322. https://doi.org/10.1016/B978-0-12-372180-8.50042-1

Zhang P, Deng HZ, Chen ZH, Li JZ (2005) Atlas of Macrofungi in Hupingshan, Hunan. Hunan Science and Technology Press, Changsha, 325 pp.

Zhang H, Xiao YX, Tan ZM, Shen AR, Shen BM, Tan Y, Li SN, Feng LG, Liu ZX, Liu LN (2024) *Mycena brunnescens* (Basidiomycota, Mycenaceae), a new species of *Mycena* sect. *Pterigenae* from China. Biodiversity Data Journal 12: e125570. https://doi.org/10.3897/BDJ.12.e125570

MycoKeys 115: 363–381 (2025)
DOI: 10.3897/mycokeys.115.144522

Research Article

Two new species of *Colletotrichum* (Glomerellales, Glomerellaceae) causing anthracnose on *Epimedium sagittatum*

Kaiyun Jiang[1], Zhong Li[1], Xiangyu Zeng[1], Xiangsheng Chen[1], Shuang Liang[1], Wensong Zhang[1]

1 *Key Laboratory of Agricultural Microbiology, College of Agriculture, Guizhou University, Guiyang, 550025 China*
Corresponding authors: Zhong Li (zli2@gzu.edu.cn); Xiangyu Zeng (xyzeng3@gzu.edu.cn)

Abstract

Epimedium sagittatum (Sieb. et Zucc.) Maxim, a perennial herb belonging to the Berberidaceae family, is widely used in traditional Chinese medicine for its beneficial role in enhancing kidney function, strengthening bones and muscles, and dispelling wind-dampness. Clinically, it is commonly used to treat osteoporosis, rheumatism, hypertension, and cardiovascular diseases. During 2023 to 2024, a disease suspected to be anthracnose was observed to be infecting the bases of *Epimedium* seedlings in Bibo Town, Kaili City, Guizhou Province. In the fall, the disease incidence reached 90%, with severe infection resulting in total desiccation and foliage death. Tissue isolation and single-conidium methods were used to identify and isolate the pathogens, which were determined to be two anthracnose strains. Multi-locus phylogenetic analysis using ITS, *gapdh*, *act*, *tub2*, *chs-1*, *his3*, and *cal*, and morphological observations of representative isolates indicated that the two isolated fungal strains were new species belonging to the genus *Colletotrichum*, namely *Colletotrichum epimedii* and *Colletotrichum sagittati*. Pathogenicity tests, adhering to Koch's postulates, confirmed that both fungi could infect *E. sagittatum*; *C. epimedii* exhibited a higher pathogenicity than *C. sagittati*. The present study provides valuable information regarding the prevention of *E. sagittatum* anthracnose.

Key words: *Epimedium sagittatum*, *Boninense* complex, new species, *Spaethianum* complex, pathogenicity test

OPEN ACCESS

Academic editor:
Chayanard Phukhamsakda
Received: 16 December 2024
Accepted: 13 March 2025
Published: 3 April 2025

Citation: Jiang K, Li Z, Zeng X, Chen X, Liang S, Zhang W (2025) Two new species of *Colletotrichum* (Glomerellales, Glomerellaceae) causing anthracnose on *Epimedium sagittatum*. MycoKeys 115: 363–381. https://doi.org/10.3897/mycokeys.115.144522

Introduction

Epimedium sagittatum (Sieb. et Zucc.) Maxim is a perennial medicinal plant endemic to China, primarily distributed in northern, central, and southeastern regions (He et al. 2003). Its roots and leaves are traditionally used to treat rheumatism and kidney disorders (Shen et al. 2020; Yang et al. 2020; Zheng et al. 2024). Recent studies highlight its pharmacological potential, including anti-tumour, anti-inflammatory, anti-hepatic fibrosis, and anti-osteoporosis properties. (Deng et al. 2022; Gao and Zhang 2022; Huong and Son 2023).

In October 2023, a novel leaf disease (incidence ~25%) was observed on *E. sagittatum* seedlings in Bibo Town, Guizhou Province. Initial symptoms included light brown leaf spots that expanded into greyish-white lesions with dark brown margins and yellow halos. Advanced lesions exhibited tissue thinning and saprophytic mycelial proliferation. Currently, major diseases affecting *E. sagittatum* include anthracnose, grey mould, leaf blight, and root rot (Chu et al. 2024; Hou et al. 2024a, 2024b; Zhou et al. 2024). However, research on these diseases is limited; thus, further studies are required to elucidate the diseases affecting *E. sagittatum*.

Anthracnose is a significant pathogen and endophyte widely distributed globally, which affects various hosts. Anthracnose causes substantial crop yield losses and even total crop failure annually, mainly affecting the leaves, fruits, and stems (Cannon et al. 2012; Liu et al. 2020; Stutts and Vermerris 2020). A single host plant can be infected by multiple anthrax fungi (Liu et al. 2022), whereas a single anthrax fungus can infect multiple host plants. (Damm et al. 2012; Jayawardena et al. 2021). Identification of *Colletotrichum* species is complicated by inconsistencies in morphological characteristics and host associations (Hyde et al. 2009; Jayawardena et al. 2021). However, an increasing number of *Colletotrichum* species have been identified and classified into different species complexes, such as the *Orchidearum* and *Boninense* complexes (Damm et al. 2019; Liu et al. 2022).

Therefore, accurate identification of *Colletotrichum* species is crucial for the control and prevention of anthracnose. Currently, research regarding anthracnose in *E. sagittatum* is limited. In 2024, Hou et al. (2024b) reported that *C. fructicola* caused anthracnose in *E. sagittatum* in the Henan Province. However, the specific pathogen species causing anthracnose in *E. sagittatum* in the Guizhou Province remains unknown. Thus, this study aimed to identify the pathogens responsible for *E. sagittatum* anthracnose in the Guizhou Province using a systematic classification combining morphological and multi-locus phylogenetic analyses. This research provides a theoretical basis for accurate diagnosis and effective management of the disease.

Materials and methods

Isolation and culturing of the pathogenic fungi

Samples of leaves exhibiting disease symptoms were collected from *E. sagittatum* in Bibo Town, Kaili City, Guizhou Province (26°30'38"N, 107°37'23"E). Pathogenic fungi were isolated from symptomatic leaves using single-spore and tissue isolation methods. If visible conidial masses were observed on the leaves, the conidia were retrieved under a microscope and transferred to sterile water to create a conidial suspension, which was then evenly spread on PDA plates in a laminar flow hood (Senanayake et al. 2020). After 24 h, the mycelium was transferred to fresh PDA plates to obtain pure cultures.

For leaves without visible conidial masses, the tissue isolation method was used to isolate the pathogenic strains. Leaf tissue pieces of approximately 0.5 × 0.5 cm were excised from the margin between healthy and diseased areas. The tissue pieces were immersed in 75% ethanol for 30 s for disinfection, followed by three washes with sterile water for a total of 30 s. The leaf pieces were then placed on sterile filter paper to dry before being transferred to PDA plates (Yao et al. 2024). All PDA plates were incubated in the dark at 28 °C for 1–2 days. Once colonies emerged, a small amount of mycelium was picked from the colony edge and transferred to fresh PDA medium for further cultivation. Colonies were purified at least twice until pure cultures were obtained.

Type specimens were deposited in the Herbarium of the Department of Plant Pathology, Agricultural College, Guizhou University (HGUP). Ex-type cultures were deposited in the Culture Collection at the Department of Plant Pathology, Agriculture College, Guizhou University, P.R. China (GUCC).

Morphological observations

The purified pathogenic fungi were inoculated onto PDA plates and incubated at 28 °C for 7 days. The colony morphology, including shape and colour, was observed and recorded according to the colour map of Rayner (1970). A small amount of mycelium from the colonies was sampled and examined using a Carl Zeiss AGAxiomo microscope to record structural details such as conidia, setae, and asci. Appressoria germination was induced by slide culture, and the conidial masses from PDA plates were transferred to sterile water to prepare a conidial suspension. A drop of this suspension was placed on a microscope slide and incubated at 28 °C for 12–24 h (Cai et al. 2009). Subsequently, the slides were observed using a Carl Zeiss AGAxiomo microscope to document appressoria shape, colour, and size. Thirty conidia and appressoria were selected randomly to measure their lengths and widths.

DNA extraction and amplification

DNA extraction: After culturing the pathogenic fungi on PDA for 10 days, the mycelium was scraped from the plates using a sterile surgical scalpel and placed into a 2 mL centrifuge tube for storage. DNA of pathogenic fungi was extracted using a Fungal DNA (Biomiga) reagent kit and stored at -20 °C for future use.

Polymerase chain reaction (PCR) amplification was performed using the extracted DNA samples as templates. The gene sequences of the following genomic regions were amplified: rDNA internal transcribed spacer (ITS), actin (*act*), chitin synthase (*chs-1*), β-tubulin (*tub2*), glyceraldehyde-3-phosphate dehydrogenase (*gapdh*), histone H3 (*his3*), and calmodulin (*cal*). Primers used for the amplification are listed in Table 1. Each PCR reaction mixture had a total volume of 25 μL, comprising 1 μL each of forward and reverse primer, 12.5 μL of 2× PCR Master Mix, 9.5 μL of deionised water (ddH$_2$O), and 1.0 μL of the DNA template (Liu 2023).

Table 1. Polymerase chain reaction and sequencing primers.

Target	Primer	Primer sequence (5'-3')	Reference
ITS	ITS1	CTTGGTCATTTAGAGGAAGTAA	(Gardes and Bruns 1993; White 1994)
	ITS4	TCCTCCGCTTATTGATATGC	
act	ACT-512F	ATGTGCAAGGCCGGTTTCGC	(Carbone and Kohn 1999)
	ACT-783R	TACGAGTCCTTCTGGCCCAT	
tub2	TI	AACATGCGTGAGATTGTAAGT	(Glass and Donaldson 1995; O'Donnell and Cigelnik 1997)
	Bt2b	ACCCTCAGTGTAGTGACCCTTGGC	
chs-1	CHS-79F	TGGGGCAAGGATGCTTGGAAGAAG	(Carbone and Kohn 1999)
	CHS-354R	TGGAAGAACCATCTGTGAGAGTTG	
his3	CYLH-3F	AGGTCCACTGGTGGCAAG	(Crous et al. 2006)
	CYLH-3R	AGCTGGATGTCCTTGGACTG	
gapdh	GDF	GCCGTCAACGACCCCTTCATT	(Guerber et al. 2003)
	GDR	GGGTGGAGTCGTACTTGAGCATGT	
cal	CL1C	GAATTCAAGGAGGCCTTCTC	(Weir et al. 2012)
	CL2C	CTTCTGCATCATGAGCTGGAC	

The amplification protocol for the ITS region was as follows (Woudenberg et al. 2009): first, initial denaturation at 95 °C for 4 min; second, 35 denaturation cycles at 95 °C for 30 s, annealing at 52 °C for 30 s, and extension at 72 °C for 45 s; lastly, single extension at 72 °C for 10 min. The annealing temperatures for the other genes were as follows: 58 °C for *act*, *his3*, and *chs-1*; 55 °C for *tub2*; 59 °C for *gapdh*; and 57 °C for *cal*.

A 1.2% agarose gel was used for electrophoresis, which was stained with 0.5 g/mL ethidium bromide for 10 min. Visualisation was performed using a BIO-RAD gel imaging system. Subsequently, PCR products were sent to the Shanghai Bioengineering Company for sequencing.

Phylogenetic analysis

Phylogenetic analysis was performed using DNA sequence data obtained from GenBank (https://www.ncbi.nlm.nih.gov/, accessed on 23 October 2024) (Tables 2, 3) and following previous publications (Liu et al. 2022; Zhang et al. 2023; Li et al. 2024). Multiple sequence alignments were performed using MAFFT (Miller et al. 2010); aligned sequences were manually adjusted using BioEdit v7.0.5 software (Rambaut 2009); using SequenceMatrix 1.8 to assemble multiple gene sequences (Vaidya et al. 2011). Phylogenetic trees were constructed using MrBayes and RAxML on the CIPRES Science Gateway V.3.3 website (https://www.phylo.org/portal2/login.action) (Miller et al. 2010; Weir et al. 2012). For the maximum likelihood (ML) analysis, RAxML-HPC2 on XSEDE v.8.2.12 was employed with a PHYLIP-formatted sequence alignment file under the GTR+GAMMA nucleotide substitution model. Branch support values were estimated through 1,000 bootstrap replicates, and the final ML tree retained branch lengths. For the Bayesian inference (BI) analysis, MrBayes v.3.2.6 was executed using a NEXUS-formatted alignment file. The optimal nucleotide substitution model was selected via MrModeltest v.2.3. Markov Chain Monte Carlo (MCMC) simulations were run with sampling every 1,000 generations. To ensure convergence, the first 25% of samples were discarded as burn-in, and a majority-rule consensus tree was generated from the remaining post-burn-in samples. Branch credibility was assessed using posterior probabilities (PP). The resulting tree files were visualised and resized using FigTree v1.4.0 (Rambaut et al. 2018) and then edited with Adobe Illustrator CS5.

Pathogenicity assay

The pathogenic fungus was isolated and purified from diseased *Epimedium* plants before performing a Koch's postulate reinoculation experiment. The strains were cultured in a 28 °C incubator for 10–25 days until conidia were produced. Using a punch, fungal cakes were harvested and transferred to conical flasks containing potato dextrose broth (PDB). These flasks were then placed on a shaker set to 220 rpm at 28 °C and cultured for 5 days to prepare a conidial suspension. The conidia concentration was determined using a hemocytometer, and the conidial suspension was adjusted to 1×10^6 conidia/mL using sterile water (Guo 2023). Subsequently, this conidial suspension was sprayed onto the leaves of healthy, injured, and uninjured *Epimedium*

Table 2. Sequence information for the strains used in *C. spaethianum* for multigene phylogenetic analysis. T = Type.

Species	Strain No.	Gene Bank Accession Number					
		ITS	*gapdh*	*act*	*tub2*	*chs-1*	*his3*
C. bletillum	CGMCC3.5117 T	JX625178	KC843506	KC843542	JX625207	MZ799322	MZ673854
C.guizhouensis	CGMCC3.15112 T	JX625158	KC843507	KC843536	JX625185	MZ799321	MZ673850
C.guizhouensis	CGMCC3.15113	JX625164	KC843508	KC843537	JX625192		
C.incanum	ATCC 64682 T	KC110789	KC110807	KC110825	KC110816		KC110798
C.incanum	CBS133485	KC110787	KC110805	KC110823	KC110814		KC110796
C.incanum	YYH-2	OL457651	OL439729	OL539406	OL439728	OL539407	
C.incanum	CBS130835	KR003337	KR003362	KR003347	KR003342	KR003357	KR003352
C.incanum	JZB330312	OL377888	OL471265	OL471267	OL471271	OL471269	
C.incanum	IL9A	KC110788	KC110806	KC110824	KC110815		KC110797
C.incanum	CAUCT34	KP145641	KP145573	KP145505	KP145675	KP145539	KP145607
C.lilii	CBS109214	GU227810	GU228202	GU227908	GU228104	GU228300	GU228006
C.liriopes	CBS122747	GU227805	GU228197	GU227903	GU228099	GU228295	GU228001
C.liriopes	CBS119444 T	GU227804	GU228196	GU227902	GU228098	GU228294	GU228000
C.liriopes	NN071073	MZ595908	MZ664093	MZ664206	MZ674026	MZ799326	MZ673928
C.liriopes	LC11287	MZ595843	MZ664092	MZ664141	MZ673964	MZ799325	MZ673863
C.liriopes	LC7623	MZ595842	MZ664091	MZ664140	MZ673963	MZ799324	MZ673862
C.liriopes	BZG101	MH291212	MH291256	MH292787		MH291234	MH292815
C.liriopes	DHJGF-Z5170	KC244167	KC843505	KC843543	KC244160		
C.kingianum	DHJGF-ZY	MW537100	MW537070	MW537088	MW537094	MW537076	MW537082
C.kingianum	DHJGF-P	MW537103	MW537075	MW537093	MW537099	MW537081	MW537087
C.disporopsis	GUCC12152	OP723106	OP784050	OP740146	OP761917		OP784175
C.disporopsis	GUCC12153	OP723107	OP784051	OP740147	OP761918		OP784176
C. riograndense	COAD928 T	KM655299	KM655298	KM655295	KM655300	KM655297	
C. spaethianum	CCPO34	MH020771	MH020772	MH045677	MH045678	MH020773	
C. spaethianum	CBS167.49 T	GU227807	GU228199	GU227905	GU228101	GU228297	GU228003
C. spaethianum	AJ006	KT122847	KT122856	KT122853		KT122850	MF362664
C. spaethianum	CLHJY4-3	MH453905	MH456883	MH456881	MH456884	MH456882	
C. spaethianum	CFCC57499	OP437705	OP455897	OP455891	OP455900	OP455894	
C. tofieldiae	CBS495.85	GU227801	GU228193	GU227899	GU228095	GU228291	GU227997
C. tofieldiae	CBS168.49	GU227802	GU228194	GU227900	GU228096	GU228292	GU227998
C. verruculosum	IMI45525 T	GU227806	GU228198	GU227904	GU228100	GU228296	GU228002
C. iris	LC3697*	MZ595837	MZ664090	MZ664135	MZ673958	MZ799323	MZ673856
C. bicoloratum	NN055229 T	MZ595899	MZ664100	MZ664197	MZ674017	MZ799332	MZ673919
C.kingianum	DHJGF-ML	MW537101	MW537071	MW537089	MW537095	MW537077	MW537083
C. destmctivum	KACC 47639	OR31676	OR449456	OR449427	OR449416	OR449433	OR449494
C. destmctivum	CBS136228	KM105207	KM105561	KM105417	KM105487	KM105277	KM105347
C. epimedii	**GUCC 24-0190**	**PQ555629**	**PQ650625**	**PQ650629**	**PQ650626**	**PQ650632**	**PQ650622**
C. epimedii	**GUCC 24-0191**	**PQ555630**	**PQ655137**	**PQ650630**	**PQ650628**	**PQ650633**	**PQ650623**
C. epimedii	**GUCC 24-0192**	**PQ555631**	**PQ655138**	**PQ650631**	**PQ650627**	**PQ650634**	**PQ650624**

plants for pathogenicity assessment (Than et al. 2008; Cai et al. 2009), with three replicates per treatment and spraying plants with sterile water as controls. The inoculated plants were covered with plastic bags to maintain humidity and placed in a controlled environment chamber (28 °C, 12 h light/12 h dark, 80% humidity) for observation. Regular assessments of disease development were conducted, and the results were recorded. After disease onset, the pathogen was isolated and purified from the diseased tissue.

Table 3. Sequence information for the strains used in *C. boninense* for multigene phylogenetic analysis. T = Type.

Species	Strain No.	Gene Bank Accession Number						
		ITS	*gapdh*	*act*	*tub2*	*chs-1*	*his3*	*cal*
C. boninense	CBS 123755 T	MH863323	JQ005240	JQ005501	JQ005588	JQ005327	JQ005414	JQ005674
C. watphraense	MFLUCC14-0123T	MF448523	MH049479	MH376384	MH351276			
Colletotrichum sp.	CBS 123921	JQ005163	JQ005250	JQ005511	JQ005597	JQ005337	JQ005424	JQ005684
C. torulosum	CBS 128544 T	JQ005164	JQ005251	JQ005512	JQ005598	JQ005338	JQ005425	JQ005685
C. torulosum	CBS 102667	JQ005165	JQ005252	JQ005513	JQ005599	JQ005339	JQ005426	JQ005686
C. doitungense	MFLUCC 14-0128 T	MF448524	MH049480	MH376385	MH351277			
C. cymbidlicola	IMI 347923 T	JQ005166	JQ005253	JQ005514	JQ005600	JQ005340	JQ005427	JQ005687
C. cymbidlicola	CBS 128543	JQ005167	JQ005254	JQ005515	JQ005601	JQ005341	JQ005428	JQ005688
C. oncidii	CBS 129828 T	JQ005169	JQ005256	JQ005517	JQ005603	JQ005343	JQ005430	JQ005690
C. oncidii	CBS 130242	JQ005170	JQ005257	JQ005518	JQ005604	JQ005344	JQ005431	JQ005691
C. diversum	LC11292 T	MZ595844	MZ664081	MZ664142	MZ673965	MZ799272	MZ673864	
C. beeveri	CBS 128527 T	JQ005171	JQ005258	JQ005519	JQ005605	JQ005345	JQ005432	JQ005692
C. beeveri	NN004142	MZ595881	MZ664082	MZ664179		MZ799277	MZ673901	
C. colombiense	CBS 129818 T	JQ005174	JQ005261	JQ005522	JQ005608	JQ005348	JQ005435	JQ005695
C. karstii	CBS127597 T	JQ005204	JQ005291	JQ005552	JQ005638	JQ005378	JQ005465	JQ005725
C. karsti	CBS 110779	JQ005198	JQ005285	JQ005546	JQ005632	JQ005372	JQ005459	JQ005719
C. annellatum	CBS 129826 T	JQ005222	JQ005309	JQ005570	JQ005656	JQ005396	JQ005483	JQ005743
C. citricola	ACCC 35478	OR240824	OR251061	OR251089	OR251096	OR251075	OR251082	OR251103
C. citricola	CBS 134228 T	KC293576	KC293736	KC293616	KC293656	KC293792		
C. camelliae-japonicae	CGMCC 38118 T	KX853165	KX893584	KX893576	KX893580	MZ799271	MZ673859	
C. phyllanthi	CBS 175.67 T	JQ005221	JQ005308	JQ005569	JQ005655	JQ005395	JQ005482	JQ005742
C. petchii	CBS 125957	JQ005226	JQ005313	JQ005574	JQ005660	JQ005400	JQ005487	JQ005747
C. petchii	CBS 378.94 T	JQ005223	JQ005310	JQ005571	JQ005657	JQ005397	JQ005484	JQ005744
C. feijoicola	CBS 144633 T	MK876413	MK876475	MK876466	MK876507			
C. feijoicola	CPC 34245	MK876414	K876474	MK876465	MK876506	MK876471	MK876477	
C. limonicola	CPC 27861	KY856471	KY856295	KY856044	KY856553		KY856387	
C. limonicola	CBS 142410 T	KY856472	KY856296	KY856045	KY856554	KY856213	KY856388	
C. novae zelandiae	CBS 130240	JQ005229	JQ005316	JQ005577	JQ005663	JQ005403	JQ005490	JQ005750
C. parsonsiae	CGMCC 35126	JX625181	KC843500	KC843561	JX625210			
C. condaoense	CBS 134299 T	MH229914	MH229920		MH229923	MH229926	MH229927	
C. condaoense	CBS 135989	MH229916	MH229922		MH229925			
C. condaoense	CBS 135823	MH229915	MH229921		MH229924			
C. brasiliense	CBS 128501 T	JQ005235	JQ005322	JQ005583	JQ005669	JQ005409	JQ005496	JQ005756
C. brasiliense	CBS 128528	JQ005234	JQ005321	JQ005582	JQ005668	JQ005408	JQ005495	JQ005755
C. brasiliense	TFL33.2	PP291938		PP318622	PP318621	PP318624	PP318625	PP318623
C. hippeastri	CBS 125376 T	JQ005231	JQ005318	JQ005579	JQ005665	JQ005405	JQ005492	JQ005752
C. hippeastri	CBS 125377	JQ005230	JQ005317	JQ005578	JQ005664	JQ005404	JQ005491	JQ005751
C. hippeastri	CBS 241.78	JQ005232	JQ005319	JQ005580	JQ005666	JQ005406	JQ005493	
C. constrictum	CBS 128503	JQ005237	JQ005324	JQ005585	JQ005671	JQ005411	JQ005498	JQ005758
C. constrictum	CBS 128504 T	JQ005238	JQ005325	JQ005586	JQ005672	JQ005412	JQ005499	JQ005759
C. constrictum	BXG-1	MW828148	MW855886	MW855882	MW855888	MW855884.		
C. dacrycarpi	CBS 130241 T	JQ005236	JQ005323	JQ005584	JQ005670	JQ005410	JQ005497	JQ005757
C. bromeliacearum	LC13854	MZ595833	MZ664078	MZ664131		MZ799268		
C. bromeliacearum	LC13855	MZ595834	MZ664079	MZ664132		MZ799269		
C. bromeliacearum	LC0951 T	MZ595832	MZ664077	MZ664130	MZ673956	MZ799267	MZ673843	MZ799233
C. araujiae	BBB:GR3504 T	OP035058	OP067659		OP067660			
C. cliviigenum	CBS 146825 T	MZ064415	MZ078178	MZ078143	MZ078260	MZ078161	MZ078180	

Species	Strain No.	Gene Bank Accession Number						
		ITS	*gapdh*	*act*	*tub2*	*chs-1*	*his3*	*cal*
C. chongqingense	CS0612 T	MG602060	MG602022	MT976107	MG602044	MT976117		
C. spicati	CGMCC 38942 T	OL842171	OL981266	OL981240	OL981226	OL981292		
C. celtidis	GUCC 12014	OP723045	OP784060	OP740155	OP761926	OP730613	OP784180	
C. chamaedoreae	NN052884		MZ664083	MZ664187	MZ674007	MZ799273	MZ673909	
C. chamaedoreae	NN052885 T		MZ664084	MZ664188	MZ674008	MZ799274	MZ673910	
C. catinaense	CBS 142417 T	KY856400	KY856224	KY855971	KY856482	KY856136	KY856307	
C. parsonsiae	CBS 128525 T	JQ005233	JQ005320	JQ005581	JQ005667	JQ005407	JQ005494	JQ005754
C. bromeliacearum	LC13856	MZ595835	MZ664080	MZ664133		MZ799270		
C. brassicicola	CBS 101059 T	JQ005172	JQ005259	JQ005520	JQ005606	JQ005346	JQ005433	JQ005693
C. bromeliacearum	LC13854	MZ595833	MZ664078	MZ664131		MZ799268		
C. palki	CCCT 23.04 T	OR644584	OR644991	OR645097	OR645149	OR645044	OR659722	
C. laurosilvaticum	RGM 3086	OR644581	OR644988	OR645094	OR645146	OR645041	OR659719	
C. laurosilvaticum	RGM 3406	OR644582	OR644989	OR645095	OR645147	OR645042	OR659720	
C. wuxuhaiense	F 34	OL842173	OL981268	OL981242	OL981228	OL981294		
C. wuxuhaiense	YMF1.04951	OL842175	OL981270	OL981244	OL981230	OL981296		
C. orchidophilum	CBS 632.80	JQ948151	JQ948481	JQ949472	JQ949802	JQ948812	JQ949142.1	
C. orchidophilum	Clo-170	OR515649	OR566949	OR589427	OR640720			
C. orchidophilum	COAD 3300	MZ726565	ON512560	ON512556	ON512563	ON512557		
C. sagittati	**GUCC 24-0193**	**PQ555633**	**PQ664909**	**PQ655139**	**PQ655148**	**PQ655142**	**PQ655145**	**PQ655151**
C. sagittati	**GUCC 24-0194**	**PQ555634**	**PQ664910**	**PQ655140**	**PQ655149**	**PQ655143**	**PQ655146**	**PQ655152**
C. sagittati	**GUCC 24-0195**	**PQ555635**	**PQ664911**	**PQ655141**	**PQ655150**	**PQ655144**	**PQ655147**	**PQ655153**

Results

Field symptom observation

The disease typically starts in April, persisting until October, with a peak incidence from June to August, when the disease incidence reaches up to 25%, and in severe cases, up to 90%. Early symptoms manifest as small light brown or brown circular spots on the middle or edges of the leaves. Gradually, these lesions expand into circular, elliptical and irregular shapes, often accompanied by irregular concentric rings. The centre of the lesions eventually turns greyish-white or grey-brown, and the margins turn dark brown and are surrounded by a yellow halo (Fig. 1A, B). In the late stages of the disease, the lesions become thin and prone to cracking, with distinct fruiting bodies; conidial heads can be observed microscopically (Fig. 1C, D).

Pathogenicity assessment

A total of 16 *C. epimedii* and 9 *C. sagittati* isolates were obtained in this study. Three representative strains from each species were selected for pathogenicity re-inoculation experiments. Symptoms began to appear four days after inoculation with *C. epimedii*, characterised by localised leaf yellowing and discolouration and accompanied by irregular brown spots. Over time, the lesions resembled the symptoms observed in the natural fields (Figs 1A, B, 2A, B). Non-treated control plants remained healthy without any symptoms (Fig. 2C). Similarly, *C. sagittati* could infect healthy plants but exhibited weaker pathogenicity, requiring wound inoculation to induce disease development. The resultant symptoms resembled field observations (Fig. 2D, E). Negative controls inoculated with sterile water remained asymptomatic (Fig. 2F).

Figure 1. Symptoms of field anthracnose in *Epimedium sagittatum*.

Following pathogenicity assays, lesion margin tissues from inoculated *E. sagittatum* leaves were subjected to re-isolation of both *Colletotrichum* species. Morphological characterisation of the re-isolated pathogens revealed identical conidial dimensions and colony characteristics to those of the original isolates. These findings were consistent with initial isolation data, confirming *C. epimedii* and *C. sagittati* as the causal agents of anthracnose in *E. sagittatum*.

Phylogenetic analysis

Twenty-five strains of *Colletotrichum*, isolated from leaves of *E. sagittatum*, were identified based on phylogenetic analyses of six or seven loci. In the phylogenetic analysis of the *C. spaethianum* species complex, a total of 2327 characters, including gaps, were identified (ITS: 538, *act*: 237, *chs-1*: 251, *gapdh*: 255, *his3*: 373 and *tub2*: 673). Similarly, the phylogenetic analysis of the *C. boninense* species complex yielded a total of 2583 characters, including gaps (ITS: 554, *act*: 254, *chs-1*: 251, *gapdh*: 242, *his3*: 375, *tub2*: 500, and *cal*: 407). The topology of Bayesian analysis of cascading datasets is almost the same as the ML consistency tree.

In the phylogenetic tree (Figs 3, 4), the isolates from this study formed two distinct, well-supported clades and, thus, were considered to represent two

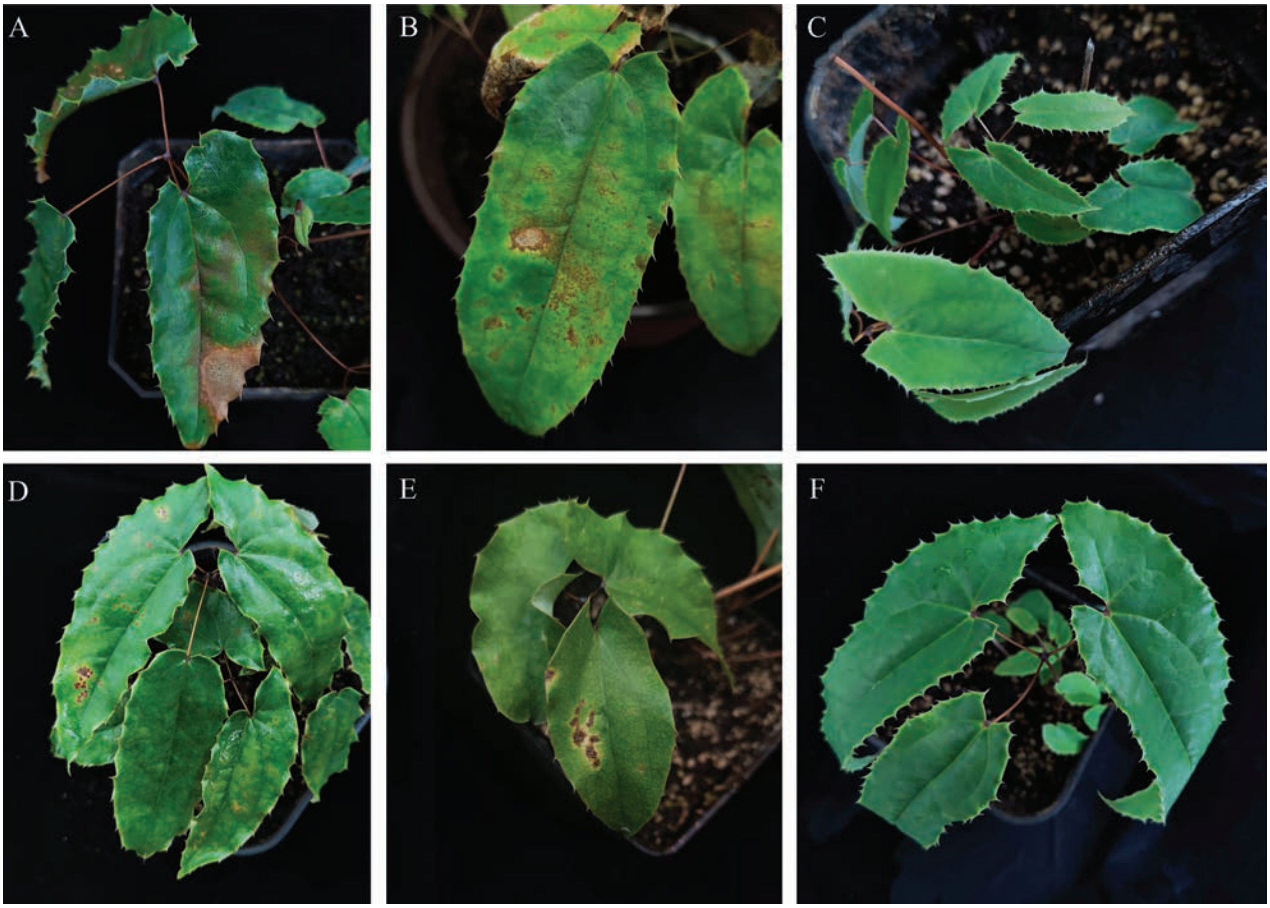

Figure 2. Pathogen inoculation and symptom (10 days) **A, B** symptoms resulting from inoculation with *Colletotrichum epimedii* **C** control **D, E** symptoms resulting from inoculation with *Colletotrichum sagittati* **F** control.

previously unknown species. *C. epimedii* GUCC 24-0190, GUCC 24-0191 and GUCC 24-0192 without the DNA base differences in six loci amongst strains (ITS, *gapdh*, act, *his3*, *chs-1* and *tub2*) form an independent branch with strong support (ML = 95, PP = 1) sister to *C. incanum* (Fig. 3). Similarly, in the phylogenetic tree (Fig. 4), *C. sagittati* GUCC 24-0193, GUCC 24-0194 and GUCC 24-0195 also form an independent branch with strong support (ML = 94, PP = 1).

Taxonomy

Colletotrichum epimedii **K.Y. Jiang & Zhong Li, sp. nov.**
MycoBank No: 856528
Fig. 5

Etymology. Named after the host plant genus, *Epimedium*.

Type. CHINA • Guizhou Province, Kaili City, Bibao Town (26°30'38"N, 107°37'23"E), from leaves of *E. sagittatum*, Apr 12, 2024, KY Jiang (holotype HGUP 21489, ex--holotype culture GUCC 24-0190).

Description. Sexual morph: Not observed. Asexual morph: ***Conidiomata***, globose to irregular, ash black. ***Setae*** and ***conidiophores*** formed on a cushion of dark brown and are non-branched. ***Setae*** medium to dark brown, straight, 81.2–168.5 μm long, 1–2 septate, tip acut. ***Conidiophores*** hyaline, unbranched, upon

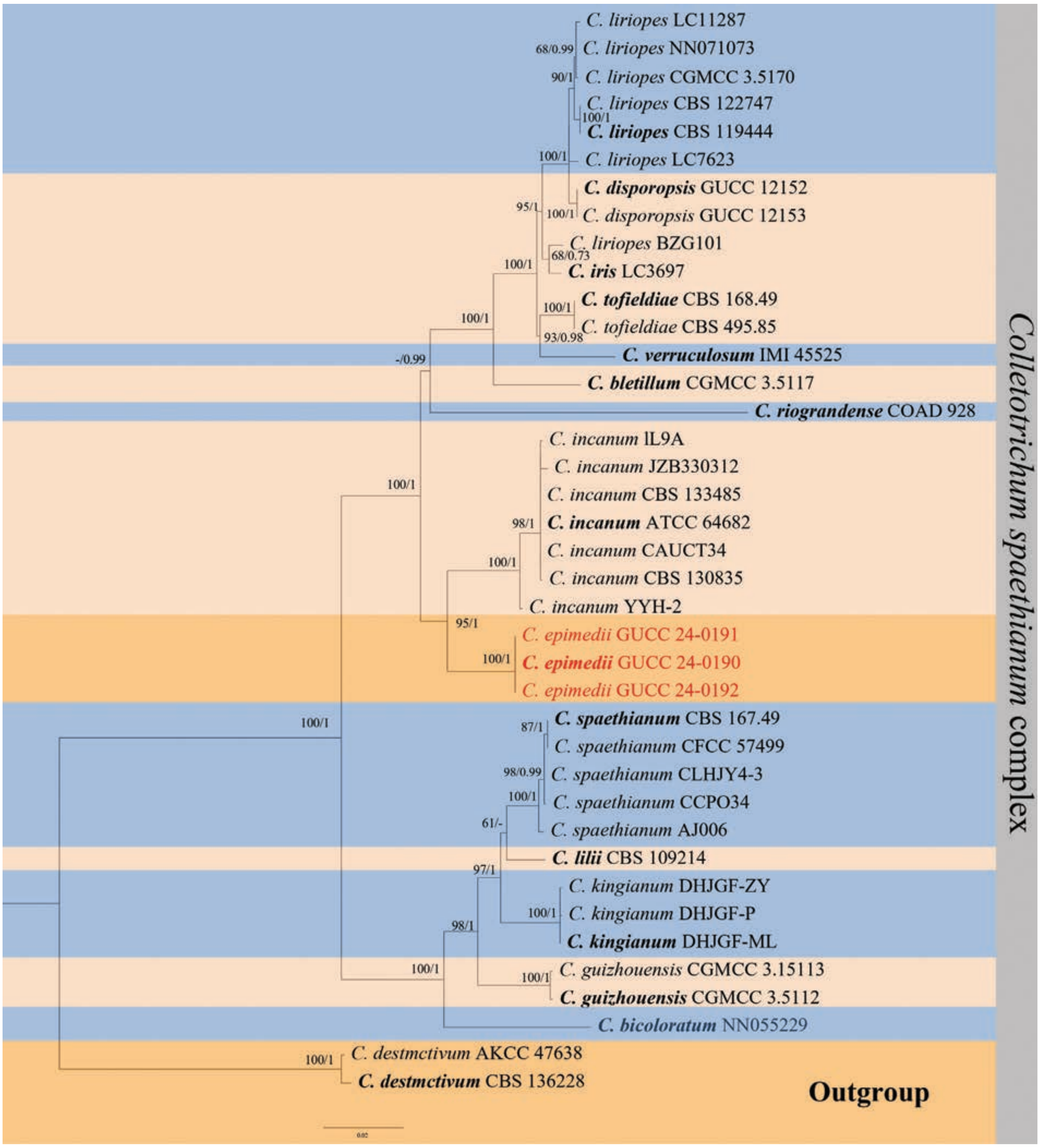

Figure 3. Phylogenetic tree of the *Colletotrichum spaethianum* complex based on multi-gene sequences (ITS, *act*, *tub2*, *gapdh*, *chs-1* and *his3*). Support values at the nodes indicate a maximum likelihood (ML) of > 60% and Bayesian posterior probability (BYPP) of > 0.70. The outgroup is *C. destructivum* CBS 136228 and *C. destructivum* AKCC 47638. The strains used were GUCC 24-0190, GUCC 24-0191 and GUCC 24-0192. The scale bar represents 0.02.

maturation of the ***conidia***, the apical portion undergoes constriction to form an ampulla or bowling pin-shaped structure, followed by subsequent detachment of the developed conidium. ***Conidia*** rough, non-septate, crescent or slightly curved in shape, with a near 1/2 mid-section having a depressed shape or multiple depressions, more towards the round or somewhat acute apex, base truncate, 16.5–18.8 × 4.3–5.4 µm (mean ± SD = 17.9 ± 0.8 × 4.7 ± 0.3 µm, L/W = 3.9). ***Appressoria*** single, grey–brown, irregularly shaped, 5.0–8.2 × 3.4–5.4 µm (mean ± SD = 6.1 ± 1.0 × 4.4 ± 0.4 µm, L/W = 1.4).

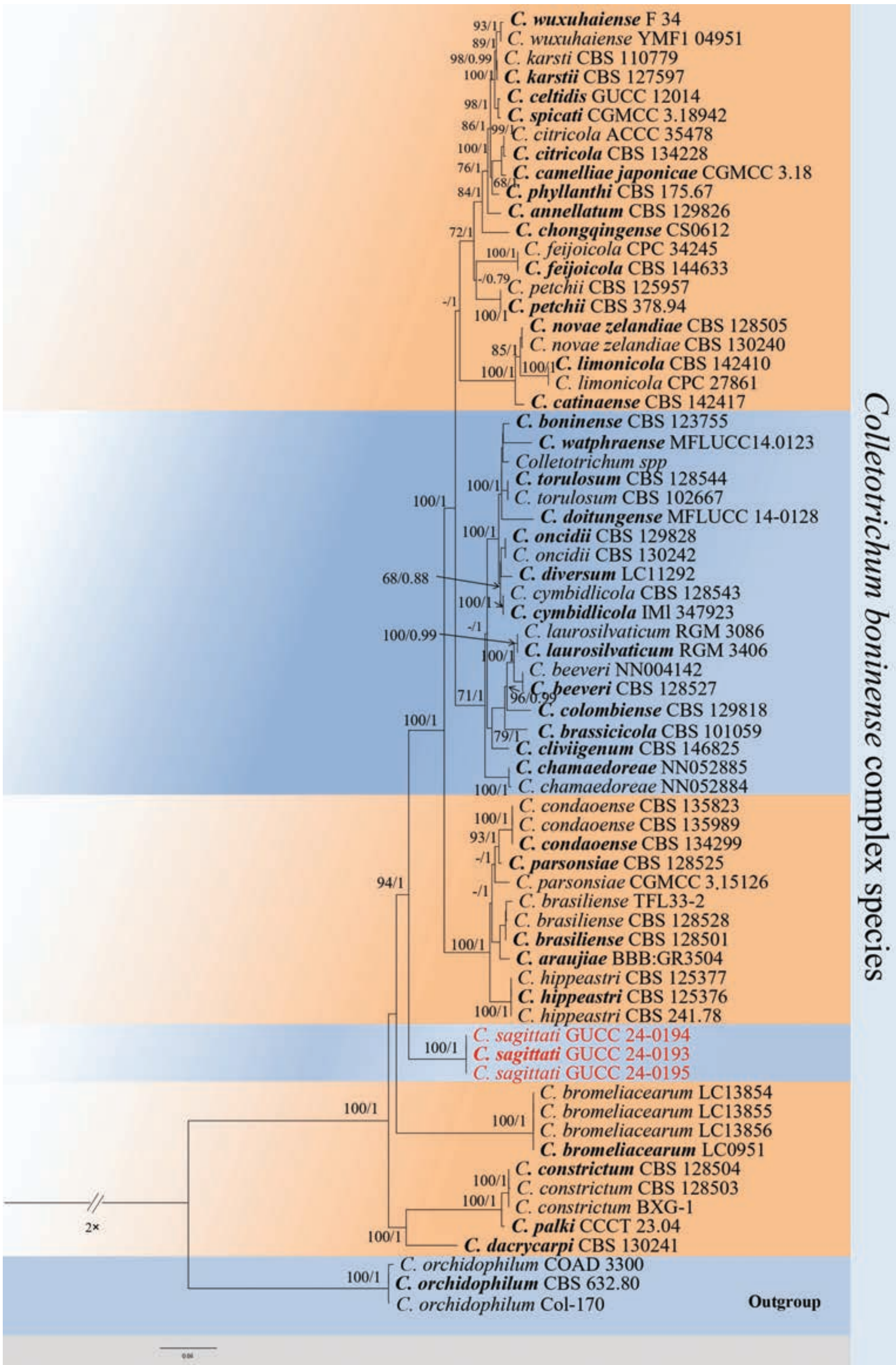

Figure 4. Phylogenetic tree of the *Colletotrichum boninense* complex constructed using multi-gene sequences (ITS, *act*, *tub2*, *gapdh*, *chs-1*, *his3* and *cal*). Support values at the nodes indicate a maximum likelihood (ML) of > 60% and Bayesian posterior probability (BYPP) of > 0.70. The outgroup is *C. euphorbiae* CBS 134752, COAD 3300, and Col-170. The strains used are GUCC 24-0193, GUCC 24-0194 and GUCC 24-0195, with a scale bar of 0.04.

Culture characteristics. Colonies on PDA taupe, rapidly growing to 8 cm within 7 days at 28 °C, with a dense mycelium, covered by a velvety grey–brown aerial mycelium on the surface. The reverse side of the colony is black in the centre, gradually lightening towards the edge and fading to grey.

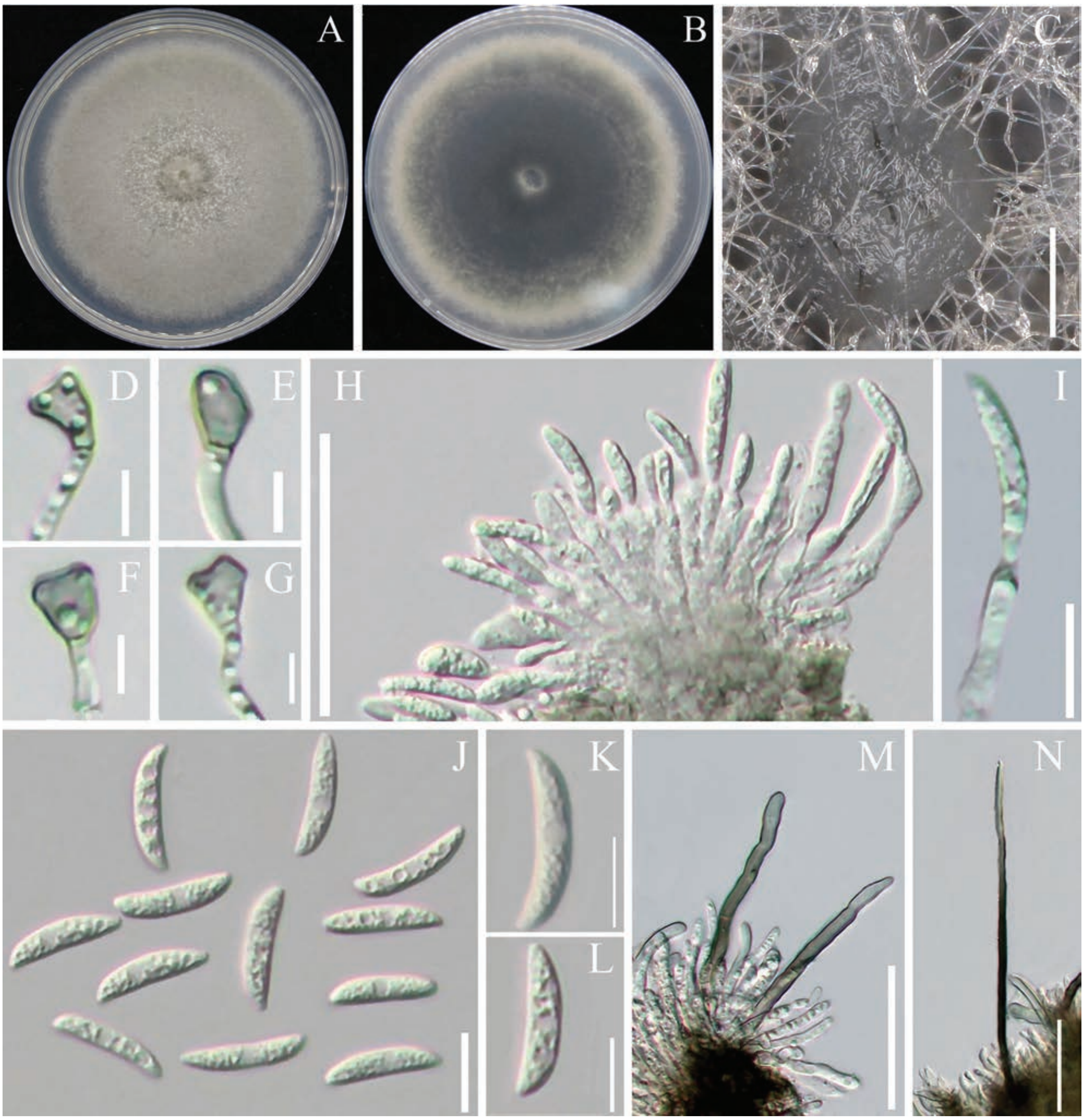

Figure 5. Morphological characteristics of *Colletotrichum epimedii* **A** upper surface of the colony **B** underside of the colony **C** *Conidiomata* **D–G** appressoria **H, I** conidiophores **J–L** conidia **M, N** setae. Scale bars: 100 μm (**C**); 5 μm (**D–J**); 10 μm (**I, J–L**); 50 μm (**H**); 50 μm (**M, N**).

Notes. Multi-locus phylogenetic analysis indicates that the three *C. epimedii* strains form distinct branches; our taxonomic unit *C. epimedii* belongs to the *Spaethianum* complex. It shares low sequence similarity with the phylogenetically related species *C. incanum* at *act* (96%), *chs-1* (98%), *gapdh* (92%), *his3* (94%), *tub2* (98%) and ITS (99%). Morphologically, *C. epimedii* and *C. incanum* had different colony characteristics on PDA. The *C. incanum* colony has fewer mycelia, growing closely against the plate, whereas *C. epimedii* has a dense mycelium. Both strains are dark brown but had different conidia sizes: *C. epimedii* had shorter but wider conidia than *C. incanum*, length (16.5–18.8 μm vs. 17.0–21.9 μm), width (4.3–5.4 μm vs. 2.3–3.7 μm) and L/W ratio (3.9 vs. 6.5).

The setae of *C. epimedii* were also slightly shorter than those of *C. incanum* (81.2–168.4 μm vs. 74–202 μm) (Yang et al. 2014). Considering both molecular phylogenetics and morphological characteristics, *C. epimedii* was identified as a new species.

Colletotrichum sagittati **K.Y. Jiang & Zhong Li, sp. nov.**

MycoBank No: 856529
Fig. 6

Etymology. Named after the host plant species *sagittatum*.

Type. China • Guizhou Province, Kaili City, Bibao Town (26°30'38"N, 107°37'23"E), from leaves of *E. sagittatum*. 12 Nov, 2024, KY Jiang (holotype HGUP 21490, ex-holotype culture GUCC 24-0193).

Description. Asexual morph: *Conidiomata*, irregular, orange. ***Setae*** not observed. ***Conidiophores***, formed directly on hyphae, usually reduced to conidiogenous cells, laterally. ***Conidia*** hyaline, smooth-walled, aseptate, straight, few conidia slightly curved, cylindrical, the apex and base rounded 14.6–17.9 × 4.9–6.8 μm (mean ± SD = 16.0 ± 0.9 × 6.2 ± 0.6 μm, L/W = 2.56). ***Appressoria*** single, dark brown, irregularly, a small amount. **Sexual morph**: ***Ascomata*** perithecia, clustered, superficial, spherical, medium to dark brown, covered with sparse ***Asci*** unitunicate, 8–spored, cylindrical or rod-shaped, smooth-surfaced and slightly pointed at the apex, 38.7–70.5 × 11.0–15.7 μm. ***Ascospores*** single or multiseriately arranged, aseptate, hyaline, smooth-walled, cylindrical, blunt rounded ends or slightly protruding at one end, 16.0–19.4 × 3.7–5.6 μm (mean ± SD = 17.1 ± 1.0 × 4.8 ± 0.4 μm and L/W ratio = 3.6).

Culture characteristics. Colonies on PDA flat, with poorly developed aerial mycelium, closely adhered to the medium surface, with numerous ascomata in the centre. Mycelium white, reverse same colour, growth 7 cm in 14 d.

Notes. Multi-locus phylogenetic analysis indicates that the three strains of *C. sagittati* formed a distinct branch within the *C. boninense* species complex (Fig. 4). Every locus sequenced for these species differed from currently recognised *Colletotrichum* species. A BLASTn search of *C. epimedii* sequences in the NCBI GenBank revealed low similarity to other species. The highest similarities for *cal*, *act*, *chs-1*, *GADPH*, *his3*, ITS and *tub2* were found with *C. hippeastri* CSSG1 (92.01%), *C. karsti* AGMy0178 (92.54%), *C. chamaedorea* LC13867 (98.34%), *C. bromeliacearum* LC13855 (77.78%), *C. liriopes* HZ-1 (91.30%), *C. boninense* INBio-275813 (97.96%) and *C. karsti* BRIP (91.76%). In morphology, they can be distinguished from *Colletotrichum hippeastri* by its smaller conidia (14.6–17.9 × 4.9–6.8 vs. 19–37.5 × 5.5–8.5) (Damm et al. 2012). Additionally, *C. sagittati* produces greater *conidia* than *Colletotrichum bromeliacearum* (14.6–17.9 × 4.9–6.8 vs. 8.5–16 × 5–7.5) (Liu et al. 2022). Based on the integrated molecular phylogenetics and morphology, *C. sagittati* was identified as a new species.

Discussion

In fungal identification, the integrated application of morphological and molecular biological approaches represents the most widely utilised methodology and demonstrates enhanced taxonomic efficacy. (Cai et al. 2009;

Figure 6. Morphological characteristics of *Colletotrichum sagittati* **A** colony surface **B** colony reverse **C** ascomata **D** surface of the ascomata **E–H** asci **I–M** ascospores **N, O** appressoria **P** conidiomata **Q, R** conidiophores and Conidiogenous cells **S** conidia. Scale bars: 2.5 cm (**C**); 25 µm (**D–H, Q**); 10 µm (**I–M, R**); 25 µm (**P**); 5 µm (**N, O**); 20 µm (**S**).

Jayawardena et al. 2016). The genus *Colletotrichum*, commonly known as anthracnose fungi, is an important group of plant pathogens that can infect more than 3,200 plant species, causing substantial harm to various economic crops worldwide. This genus is characterised by its ubiquity and severity (Cannon et al. 2012; Guarnaccia et al. 2017; Fu et al. 2019). The classification of *Colletotrichum* has historically been complex, but the application of multi-locus molecular methods has facilitated the identification and categorisation of numerous *Colletotrichum* species into distinct species complexes (Cannon et al. 2012; Crouch 2014; Damm et al. 2019). Currently, the genus is divided into 16 complexes, with more than 750 new species described based on different host plants (Liu et al. 2022). Many closely related species are difficult to differentiate based solely on morphological characteristics. Therefore, constructing multi-gene phylogenetic trees in conjunction with morphological features is fundamental for identifying species within this genus and serves as a primary basis for describing new species (Cai et al. 2009; Jayawardena et al. 2016). Utilising combined multi-gene sequences from ITS, *gapdh*, *chs-1*, *his3*, *act*, *tub2*, and *cal* yields better results than single-gene analyses. This study constructed a phylogenetic tree based on combined multi-gene sequences of ITS, *gapdh*, *chs-1*, *his3*, *act*, *tub2*, and *cal*. Pathogenicity tests led to the identification of two new *Colletotrichum* species associated with anthracnose disease on *E. sagittatum*, named *C. epimedii* and *C. sagittati*.

In recent years, the cultivation area of *Epimedium* has been increasing to meet growing market demand. However, this trend has also led to issues such as a high incidence of diseases and the rapid spread of diseases within plantations. Therefore, accurate diagnosis and prevention of these diseases are crucial. The current reports of anthracnose on *E. sagittatum* are limited to two cases caused by *C. fructicola* and *C. karstii* (Hou et al. 2024b; Lin et al. 2025). The symptoms of anthracnose observed here are similar to those reported by Hou et al. (2024b). However, the involved pathogens and their respective species complexes differ. Although we isolated *C. fructicola* from *E. sagittatum*, its pathogenicity was weak. Moreover, this variation in pathogenicity among regions may be due to regional adaptation of the pathogens. Thus, we hypothesise that anthracnose in *E. sagittatum* may represent a complex disease. Before implementing effective control and prevention strategies, it is essential to accurately identify and understand the types of pathogens involved. Further identification and classification of the pathogens responsible for anthracnose are warranted.

Conclusion

This study identified two novel species of anthracnose fungi, *C. epimedii* and *C. sagittati*, responsible for anthracnose in *E. sagittatum*. These species belong to the *C. spaethianum* and *C. boninense* complexes. To effectively control the disease, further research is required to elucidate how these two strains respond to climatic conditions, common fungicides and prevalent *Epimedium* genotypes. Such studies will aid in developing more targeted disease management strategies.

Acknowledgements

No data was used for the research described in the article. We have read and understood your journal's policies, and we believe that neither the manuscript nor the study violates any of these. There are no conflicts of interest to declare.

Additional information

Conflict of interest

The authors have declared that no competing interests exist.

Ethical statement

No ethical statement was reported.

Funding

This work was supported by the National Key Research and Development Program under grant number 2021YFD1601001.

Author contributions

Data curation: ZL, XZ, KJ. Formal analysis: XZ, ZL, SL. Funding acquisition: ZL. Investigation: WZ, XC. Writing - original draft: KJ. Writing - review and editing: KJ.

Data availability

All of the data that support the findings of this study are available in the main text.

References

Cai L, Hyde KD, Taylor P, Weir BS, Liu ZY (2009) A polyphasic approach for studying *Colletotrichum.* Fungal Diversity 39(2): 183–204. https://doi.org/10.1016/j.riam.2009.11.001

Cannon PF, Damm U, Johnston PR, Weir BS (2012) *Colletotrichum*–current status and future directions. Studies in Mycology 73(1): 181–213. https://doi.org/10.3114/sim0014

Carbone I, Kohn LM (1999) A method for designing primer sets for speciation studies in filamentous ascomycetes. Mycologia 91(3): 553–556. https://doi.org/10.1080/00275514.1999.12061051

Chu L, Li D, Hou W, Dan Z, Wang X, Dong C (2024) First report of *Fusarium falciforme* causing root and rhizome rot of *Epimedium sagittatum* in China. Plant Disease 108(5): 1400. https://doi.org/10.1094/PDIS-01-24-0185-PDN

Crouch JA (2014) *Colletotrichum caudatum s.l.* Is a species complex. IMA Fungus 5(1): 17–30. https://doi.org/10.5598/imafungus.2014.05.01.03

Crous PW, Groenewald JZ, Risède JM, Simoneau P, Hyde KD (2006) Calonectria species and their Cylindrocladium anamorphs: Species with clavate vesicles. Studies in Mycology 55: 213–226. https://doi.org/10.3114/sim.55.1.213

Damm U, Cannon PF, Woudenberg JHC, Johnston PR, Weir BS, Tan YP, Shivas RG, Crous PW (2012) The *Colletotrichum boninense* species complex. Studise In Mycology 73: 1–36. https://doi.org/10.3114/sim0002

Damm U, Sato T, Alizadeh A, Groenewald JZ, Crous PW (2019) The *Colletotrichum dracaenophilum*, *C. magnum* and *C. orchidearum* species complexes. Studies in Mycology 92(1): 1–46. https://doi.org/10.1016/j.simyco.2018.04.001

Deng D, Li L, Tan X, Sun Y, Wang C, Zhen G, Wang G, Hu J (2022) Study on the mechanism of icariin inhibiting the proliferation of intrahepatic bile duct cancer cells by regulating glycolysis via Akt/mTOR. Chinese Traditional and Herbal Drugs 53(10): 3061–3069.

Fu M, Crous PW, Bai Q, Zhang PF, Xiang J, Guo YS, Zhao FF, Yang MM, Hong N, Xu WX, Wang GP (2019) *Colletotrichum* species associated with anthracnose of *Pyrus* spp. In China. Persoonia 42: 1–35. https://doi.org/10.3767/persoonia.2019.42.01

Gao L, Zhang SQ (2022) Antiosteoporosis effects, pharmacokinetics, and drug delivery systems of icaritin: Advances and prospects. Pharmaceuticals 15(4): 397. https://doi.org/10.3390/ph15040397

Gardes M, Bruns TD (1993) ITS primers with enhanced specificity for basidiomycetes—Application to the identification of mycorrhizae and rusts. Molecular Ecology 2(2): 113–118. https://doi.org/10.1111/j.1365-294X.1993.tb00005.x

Glass NL, Donaldson GC (1995) Development of primer sets designed for use with the PCR to amplify conserved genes from filamentous ascomycetes. Applied and Environmental Microbiology 61(4): 1323–1330. https://doi.org/10.1128/aem.61.4.1323-1330.1995

Guarnaccia V, Groenewald JZ, Polizzi G, Crous PW (2017) High species diversity in *Colletotrichum* associated with citrus diseases in Europe. Persoonia 39: 32–50. https://doi.org/10.3767/persoonia.2017.39.02

Guerber JC, Liu B, Correll JC, Johnston PR (2003) Characterization of diversity in *Colletotrichum* acutatum sensu lato by sequence analysis of two gene introns, mtDNA and intron RFLPs, and mating compatibility. Mycologia 95(5): 872–895. https://doi.org/10.1080/15572536.2004.11833047

Guo Z (2023) Pathogen diversity of watermelon anthracnose and genetic analysis of *Colletotrichum magnum*. Huazhong Agricultural University.

He S, Guo B, Wang X (2003) Taxonomic study of *Epimedium Sagittarius* and its related species. Guizhou Science Z1: 102–106.

Hou W, Chu L, Da Z, Dong N, Yang L, Dong C (2024a) First Report of *Alternaria alternata* Causing Leaf Blight on *Epimedium sagittatum* in China. Plant Disease 108(5): 1394. https://doi.org/10.1094/PDIS-12-23-2621-PDN

Hou W, Chu L, Yang L, Dong N, Dan Z, Zhong H, Dong C (2024b) First report of *Colletotrichum fructicola* causing anthracnose on *Epimedium sagittatum* in China. Plant Disease 108(3): 813. https://doi.org/10.1094/PDIS-11-22-2556-PDN

Huong NT, Son NT (2023) Icaritin: A phytomolecule with enormous pharmacological values. Phytochemistry 213: 113772. https://doi.org/10.1016/j.phytochem.2023.113772

Hyde KD, Cai L, McKenzie EHC, Yang YL, Zhang JZ, Prihastuti H (2009) *Colletotrichum*: A catalogue of confusion. Fungal Diversity 39: 1–17.

Jayawardena RS, Hyde KD, Damm U, Cai L, Liu M, Li XH, Zhang W, Zhao WS, Yan JY (2016) Notes on currently accepted species of *Colletotrichum*. Mycosphere 7(8): 1192–1260. https://doi.org/10.5943/mycosphere/si/2c/9

Jayawardena RS, Bhunjun CS, Hyde KD, Gentekaki E, Itthayakorn P (2021) *Colletotrichum*: Lifestyles, biology, morpho-species, species complexes and accepted species. Mycosphere 12(1): 519–669. https://doi.org/10.5943/mycosphere/12/1/7

Li Y, Lin L, Cao J, Gan M, Fan X (2024) Three new species of *Colletotrichum* (Glomerellales, Glomerellaceae) associated with walnut (Juglans regia) anthracnose from China. MycoKeys 108: 147–167. https://doi.org/10.3897/mycokeys.108.125382

Lin R, Li XY, Wu S, Feng K, He YT, Wang XS, Huang ZX, Li JT, Lou T, Sun L (2025) First Report of Anthracnose Caused by *Colletotrichum karstii* on *Epimedium sagittatum* in China. Plant Disease 109(1): 235. https://doi.org/10.1094/PDIS-06-24-1277-PDN

Liu Y (2023) Identification of the pathogen of anthracnose and preliminary study on its interaction with anthracnose. Guizhou University. https://doi.org/10.27047/d.cnki.ggudu.2023.003037

Liu L, Zhang L, Qiu P, Wang Y, Liu Y, Li Y, Gao J, Hsiang T (2020) Leaf spot of Polygonatum odoratum caused by *Colletotrichum spaethianum*. Journal of General Plant Pathology 86(2): 157–161. https://doi.org/10.1007/s10327-019-00903-4

Liu F, Ma ZY, Hou LW, Diao YZ, Wu WP, Damm U, Song S, Cai L (2022) Updating species diversity of *Colletotrichum*, with a phylogenomic overview. Studies in Mycology 101(1): 1–56. https://doi.org/10.3114/sim.2022.101.01

Miller MA, Pfeiffer WT, Schwartz T (2010) Creating the CIPRES Science Gateway for Inference of Large Phylogenetic Trees. Gateway Computing Environments Workshop (GCE), 2010. https://doi.org/10.1109/GCE.2010.5676129

O'Donnell K, Cigelnik E (1997) Two divergent intragenomic rDNA ITS2 types within a monophyletic lineage of the fungus Fusarium are Nonorthologous. Molecular Phylogenetics and Evolution 7(1): 103–116. https://doi.org/10.1006/mpev.1996.0376

Rambaut A (2009) FigTree, a graphical viewer of phylogenetic trees. http://www.mendeley.com/catalog/figtree-graphical-viewer-phylogenetic-trees

Rambaut A, Drummond AJ, Xie D, Baele G, Suchard MA (2018) Posterior summarization in Bayesian phylogenetics using tracer 1.7. Systematic Biology 67(5): 901–904. https://doi.org/10.1093/sysbio/syy032

Rayner RW (1970) A Mycological Colour Chart. Commonwealth Mycological Institute, Kew, UK.

Senanayake IC, Rathnayake AR, Marasinghe DS, Calabon MS, Gentekaki E, Lee HB, Hurdeal VG, Pem D, Dissanayake LS, Wijesinghe SN, Bundhun D, Nguyen TT, Goonasekara ID, Abeywickrama PD, Bhunjun CS, Jayawardena RS, Wanasinghe DN, Jeewon R, Bhat DJ, Xiang MM (2020) Morphological approaches in studying fungi: Collection, examination, isolation, sporulation and preservation. Mycosphere 11(1): 2678–2754. https://doi.org/10.5943/mycosphere/11/1/20

Shen B, Tan Z, Shen A, Tan Y (2020) Literature review of *Epimedium Sagittarius*. Hunan Forestry Science & Technology 47(5): 96–109.

Stutts LR, Vermerris W (2020) Elucidating anthracnose resistance mechanisms in sorghum-A review. Phytopathology 110(12): 1863–1876. https://doi.org/10.1094/PHYTO-04-20-0132-RVW

Than PP, Jeewon R, Hyde KD, Pongsupasamit S, Mongkolporn O, Taylor PWJ (2008) Characterization and pathogenicity of *Colletotrichum* species associated with anthracnose on chilli (*Capsicum* spp.) in Thailand. Plant Pathology 57(3): 562–572. https://doi.org/10.1111/j.1365-3059.2007.01782.x

Vaidya G, Lohman DJ, Meier R (2011) SequenceMatrix: Concatenation software for the fast assembly of multi-gene datasets with character set and codon information. Cladistics 27(2): 171–180. https://doi.org/10.1111/j.1096-0031.2010.00329.x

Weir BS, Johnston PR, Damm U (2012) The *Colletotrichum gloeosporioides* species complex. Studies in Mycology 73(1): 115–180. https://doi.org/10.3114/sim0011

White TJ (1994) Amplification and direct sequencing of fungal ribosomal RNA genes for phylogenetics. PCR Protocols, 315-322. https://doi.org/10.1016/B978-0-12-372180-8.50042-1

Woudenberg JHC, Aveskamp MM, De Gruyter J, Spiers AG, Crous PW (2009) Multiple *Didymella* teleomorphs are linked to the Phoma clematidina morphotype. Persoonia 22: 56–62. https://doi.org/10.3767/003158509X427808

Yang HC, Haudenshield JS, Hartman GL (2014) *Colletotrichum incanum* sp nov., a curved-conidial species causing soybean anthracnose in USA. Mycologia 106(1): 32–42. https://doi.org/10.3852/13-013

Yang X, Wang J, Gan C, Yang Y (2020) Progress in clinical application and basic research of Epimedium in andrology. Acta Chinese Medicine and Pharmacology 48(12): 70–73. https://doi.org/10.19664/j.cnki.1002-2392.200219

Yao Q, Zhao Q, Jiang K, Li C, Liao M, Chen X, Li Z (2024) Diversity of causal agents of *Pseudostellaria heterophylla* leaf spot from Guizhou Province, China. Journal of Phytopathology 172(4): e13372. https://doi.org/10.1111/jph.13372

Zhang Q, Nizamani M, Feng Y, Yang Y, Jayawardena R, Hyde K, Wang Y, Li C (2023) Genome-scale and multi-gene phylogenetic analyses of *Colletotrichum* spp. Host preference and associated with medicinal plants. Mycosphere 14(si2): 1–106. https://doi.org/10.5943/mycosphere/14/si2/1

Zheng X, Li S, Wang K, Wang Z, Li J, Yang Q, Wu Y, Chen Q, Dou Y, Yao S, Xu J, Zheng X (2024) Comparing the pharmacological effects of the prepared folium of *Epimedium brevicornu* Maxim. And *Epimedium sagittatum* Maxim. On kidney-Yang deficiency syndrome and liver injury complications. Fitoterapia 176: 106006. https://doi.org/10.1016/j.fitote.2024.106006

Zhou S, Gao Y, An J, Qin L, Ou X, Guo L, Jiang W, Zhou T, Yuan QS (2024) *Rhizopus oryzae* causes the leaf rot disease of *Epimedium sagittatum* in guizhou, China. Plant Disease 108(4): 1105. https://doi.org/10.1094/PDIS-10-23-2241-PDN